CONTRIBUTORS TO THIS VOLUME

K. Dehnicke

Russell N. Grimes

A. G. Massey

R. C. Mehrotra

K. K. Pandey

H. W. Roesky

Harald Schäfer

Jean'ne M. Shreeve

Jack M. Williams

Advances in
INORGANIC CHEMISTRY
AND
RADIOCHEMISTRY

EDITORS
H. J. EMELÉUS
A. G. SHARPE
University Chemical Laboratory
Cambridge, England

VOLUME 26

1983

ACADEMIC PRESS
A Subsidiary of Harcourt Brace Jovanovich, Publishers

New York London
Paris San Diego San Francisco São Paulo Sydney Tokyo Toronto

COPYRIGHT © 1983, BY ACADEMIC PRESS, INC.
ALL RIGHTS RESERVED.
NO PART OF THIS PUBLICATION MAY BE REPRODUCED OR TRANSMITTED IN ANY FORM OR BY ANY MEANS, ELECTRONIC OR MECHANICAL, INCLUDING PHOTOCOPY, RECORDING, OR ANY INFORMATION STORAGE AND RETRIEVAL SYSTEM, WITHOUT PERMISSION IN WRITING FROM THE PUBLISHER.

ACADEMIC PRESS, INC.
111 Fifth Avenue, New York, New York 10003

United Kingdom Edition published by
ACADEMIC PRESS, INC. (LONDON) LTD.
24/28 Oval Road, London NW1 7DX

LIBRARY OF CONGRESS CATALOG CARD NUMBER: 59-7692
ISBN 0-12-023626-5

PRINTED IN THE UNITED STATES OF AMERICA

83 84 85 86 9 8 7 6 5 4 3 2 1

CONTRIBUTORS

Numbers in parentheses indicate the pages on which the authors' contributions begin.

K. DEHNICKE (169), *Fachbereich Chemie der Universität Marburg, Marburg, Federal Republic of Germany*

RUSSELL N. GRIMES (55), *Department of Chemistry, University of Virginia, Charlottesville, Virginia 22901*

A. G. MASSEY (1), *Department of Chemistry, University of Technology, Loughborough, Leicestershire LE11 3TU, England*

R. C. MEHROTRA (269), *Department of Chemistry, University of Rajasthan, Jaipur 302004, India*

K. K. PANDEY (337), *Anorganisch-Chemisches Institut der Universität Göttingen, D-3400 Göttingen, Federal Republic of Germany*

H. W. ROESKY (337), *Anorganisch-Chemisches Institut der Universität Göttingen, D-3400 Göttingen, Federal Republic of Germany*

HARALD SCHÄFER (201), *Universität Münster, Münster, Westphalia, Federal Republic of Germany*

JEAN'NE M. SHREEVE (119), *Department of Chemistry, University of Idaho, Moscow, Idaho 83843*

JACK M. WILLIAMS (235), *Chemistry Division, Argonne National Laboratory, Argonne, Illinois 60439*

ADVANCES IN INORGANIC CHEMISTRY AND RADIOCHEMISTRY, VOL. 26

THE SUBHALIDES OF BORON

A. G. MASSEY

Department of Chemistry, University of Technology, Loughborough, Leicestershire, England

I. Introduction

The last major review of the boron subhalides was published in Volume 10 of *Advances* in 1967 (*84*), although several brief discussions (*42, 85, 133*) have appeared in the intervening years. The present article attempts to cover comprehensively the work that has been

Copyright © 1983 by Academic Press, Inc.
All rights of reproduction in any form reserved.
ISBN 0-12-023626-5

published since 1967. Undoubtedly, the most outstanding advance has been Timms' synthesis of BF, from which he has been able to make a variety of new boron fluorides.

A curious facet of boron subhalide chemistry is that fluorine does not appear to support a series of monohalides as do chlorine, bromine, and, probably, iodine. It has been suggested several times that a monofluoride such as B_4F_4 may be less stable than the corresponding chloride because of relatively weak back-bonding from the fluorine p orbitals into cage bonding orbitals. That this is not the whole answer is shown by the preparation of alkyl-substituted cages such as $B_4(t\text{Bu})_4$ and $B_9Br_{9-n}Me_n$, where n can range from 1 to at least 6. Calculations show that B_4F_4 should be at least as stable as B_4Cl_4 relative to four BX units, which suggests that the present nonexistence of B_4F_4, and possibly other B_nF_n derivatives, is due only to a lack of suitable synthetic routes to them. Starting from the monochlorides, what is required is a mild, volatile fluorinating agent that produces a volatile chloride byproduct; diboron tetrafluoride (*56*) and allyl fluoride (*15*) would appear to fulfil these criteria. As a possible incentive to the preparative chemist, intense peaks due to $B_nF_n^+$ fragment ions have been noted in the mass spectra of several boron subfluorides. However, the very low thermal stability of B_3F_5 and B_8F_{12} lends little hope of even their chlorine analogs ever being synthesized when it is remembered that B_2F_4 is so much more stable then either B_2Cl_4 or B_2Br_4.

Two interesting phenomena arising from the interaction of diboron tetrachloride with unsaturated hydrocarbons are worthy of further study. It has been noted a number of times that the thermal decomposition of B_2Cl_4 is arrested in the presence of haloolefins (*15, 110, 112*); NMR (*20*), and infrared (*104*) studies have failed to detect any evidence of interaction between the components of such mixtures but some must surely take place. Striking visual evidence of quite strong interaction between acetylene and B_2Cl_4 can be obtained by mixing them at $-78°C$; a solid mass is formed from which the acetylene can be pumped off intact when the B_2Cl_4 reverts to its normal liquid form (*133*). A further study of both these systems should reveal considerable information about the mechanism involved in the addition of diboron tetrachloride to alkenes and alkynes (see Section V,B).

Table I shows the subhalides that are known to date, including a number that have not been fully characterized. The diboron tetrahalides possess rather daunting properties in that they are pyrophoric in air and water sensitive, they attack both hydrocarbon and silicone greases, and, furthermore, they decompose spontaneously at room temperature. The tetrafluoride, tetrachloride, and tetrabromide (together

TABLE I

THE KNOWN BORON SUBHALIDES[a]

B_2F_4	B_2Cl_4	B_2Br_4	B_2I_4 (pale yellow)
B_3F_5	—	—	—
—	B_4Cl_4 (pale yellow)	—	—
—	—	B_7Br_7 (black?)	—
—	B_8Cl_8 (very dark purple)	B_8Br_8 (dark red-brown)	$(B_8I_8)^b$
B_8F_{12} (yellow)	—	—	—
—	B_9Cl_9 (yellow-orange)	B_9Br_9 (red)	B_9I_9 (dark brown)
—	$B_{10}Cl_{10}$ (orange-brown)	$(B_{10}Br_{10})^b$	—
—	$B_{11}Cl_{11}$ (orange-red)	—	—
—	$(B_{12}Cl_{12})^b$	—	—
$B_{14}F_{18}$	—	—	—

[a] Colorless unless indicated otherwise. The colors of these compounds are worthy of note because the vast majority of boron compounds are colorless. Had the monohalides not been colored they would have been virtually impossible to separate because it is only by observing color changes that one can assess how a separation is progressing. The observed colors are somewhat dependent on the physical state of the halides. For example, B_8Cl_8 forms greenish, thin films, black crystals, and a purple vapor, whereas B_9Br_9 forms dark red crystals but has a bright yellow vapor.

[b] Detected but not isolated.

with B_4Cl_4, B_3F_5, and B_8F_{12}) are sufficiently volatile to be handled in conventional vacuum lines equipped with greaseless taps and may be stored in traps at low temperatures until required.

Mercury manometers and mercury float valves are not recommended for use with the bromides or iodides because of the possibility of hydrogen halides, which attack mercury, being produced by adventitious hydrolysis. New glassware must be thoroughly baked out, first under vacuum and then under a slight pressure of boron trihalide, to drive off adsorbed water and so prevent such hydrolyses.

Ground glass joints that are exposed to the halides for relatively brief periods may be lubricated with halocarbon greases, although even Kel-F grease turns brown after 4 days contact with BCl_3–B_2Cl_4 mixtures (*7*). Diboron tetrabromide rapidly attacked Apiezon W wax used as a window seal for an infrared cell; a mixture of powdered PTFE and fluorocarbon oil was found to make a better sealant, but even this showed signs of attack after several days (*99*).

II. Identification

Conventional analytical techniques are difficult to carry out on all but the diboron tetrahalides. High-temperature decomposition to bo-

ron and boron trifluoride has been used as a means of obtaining the B:F ratio in the lower boron fluorides (*69, 70, 126*).

The high thermal stability and volatility of the monohalides make them suitable subjects for mass-spectral analysis. That boron, chlorine, and bromine all possess two stable isotopes rather complicates the appearance of the mass spectra but at the same time provides a powerful means of "fingerprinting" the various ions present. Even for a simple ion like $B_2Cl_2^+$ there are nine possible isotopic species—isotopomers—although under normal resolution only seven separate peaks are observed due to overlap at *m/e* = 92 and again at *m/e* = 94 (see Table II). By using the known relative abundances of the ^{10}B, ^{11}B, ^{35}Cl, and ^{37}Cl isotopes, it is possible to compute (*79*) the expected intensities of the various peaks making up the $B_2Cl_2^+$ ion cluster—such an intensity pattern is highly characteristic of the ion under study and can be used in conjunction with the *m/e* values estimated from the spectrum to identify positively an unknown ion species. This is demonstrated for the parent ion of $B_{12}Cl_{12}$ in Fig. 1.

A prominent group of peaks found in the mass spectra of all the monohalides represents the loss of BX_3 from the parent ion and is accompanied by the corresponding metastable peak, showing that the process occurs in a single step. Sometimes, a second metastable peak can also be observed for the loss of another BX_3 molecule from the $(P—BX_3)^+$ ion.

$$B_9Cl_9^+ \xrightarrow{-BCl_3} B_8Cl_6^+ \xrightarrow{-BCl_3} B_7Cl_3^+$$

In the case of a mixed halide $B_nCl_{n-x}Br_x$, the boron trihalide molecule lost from the parent ion can be BCl_3, BCl_2Br, $BClBr_2$, or BBr_3.

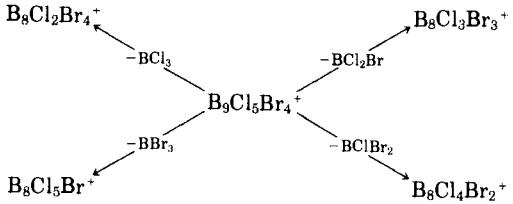

Due to the number of isotopomeric ions involved in these processes, the metastable peaks are very broad indeed and in some cases can span 8–10 mass units. The stability toward loss of BX_3 from $B_9X_9^+$ increases as the halogen is changed from chlorine to iodine, the relative intensity ratios $B_9X_9^+ : B_8X_5^+$ being 0.4(Cl), 1.3(Br), and 8(I); the spectrum of B_9I_9 even shows a group of peaks due to the doubly charged parent ion.

TABLE II

THEORETICAL PEAK INTENSITIES FOR THE ION $B_2Cl_2^+$ (*79*)

$B_2Cl_2^+$ (mass no.)	Probability (%)	
90	2.22	**
91	18.04	******************
92	38.04	**************************************
93	11.77	***********
94	24.11	**********************
95	1.92	**
96	3.89	****
	100.00	

Isotope	Mass	Abundance (%)
^{10}B	10.01294	19.78
^{11}B	11.00931	80.22
^{35}Cl	34.96885	75.53
^{37}Cl	36.96590	24.47

Species produced by $B_2Cl_2^+$ in the mass spectrum	*m/e*		
$^{10}B^{10}B^{35}Cl^{35}Cl$	90		
$^{10}B^{10}B^{35}Cl^{37}Cl$	92	91.96063	
$^{10}B^{10}B^{37}Cl^{37}Cl$	94		93.95768
$^{11}B^{10}B^{35}Cl^{35}Cl$	91		
$^{11}B^{10}B^{35}Cl^{37}Cl$	93		
$^{11}B^{10}B^{37}Cl^{37}Cl$	95		
$^{11}B^{11}B^{35}Cl^{35}Cl$	92	91.95632	
$^{11}B^{11}B^{35}Cl^{37}Cl$	94		93.95337
$^{11}B^{11}B^{37}Cl^{37}Cl$	96		

So facile is the loss of boron trifluoride from the parent ions of the lower boron fluorides that the P^+ ion is often unobservable, as happens in the case of B_8F_{12} (*69*). A major difference between the subfluorides and the other subhalides is that the latter have a B:X ratio of 1 whereas the B:F ratio is apparently variable. It is interesting to note, therefore, that prominent ions noted in the mass spectra of boron subfluorides include $B_9F_9^+$, $B_{11}F_{11}^+$, and $B_{12}F_{12}^+$ (*69*), showing that such clusters are stable under certain conditions, a point that should stimulate attempts to synthesize the parent B_nF_n compounds.

Infrared spectra of the volatile subhalides may be obtained using conventional gas cells to which the windows may be attached with

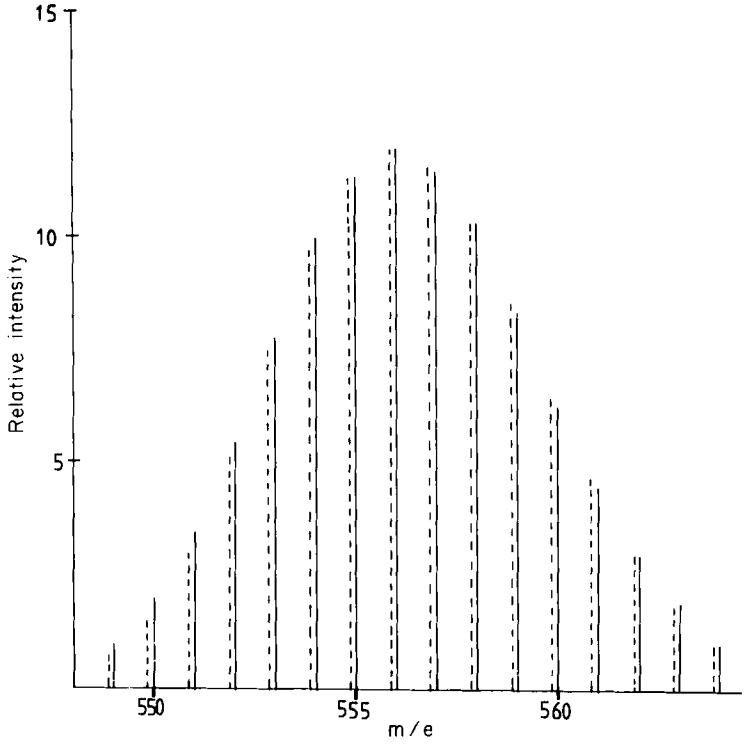

FIG. 1. Comparison of the observed (——) and theoretical (– – –) intensities for the molecular ion of $B_{12}Cl_{12}$.

halocarbon grease or cyanoacrylate resin; an all-metal seal consisting of an amalgamated lead gasket set between a silvered glass cell and rock-salt window has also been found useful in boron halide studies (46). The spectrum of the highly unstable B_8F_{12} has been laboriously recorded in 200-cm^{-1} stages at room temperature, a fresh sample being used for each stage (*70*). Such thermally fragile compounds are better studied using a low-temperature "spray-on" infrared cell (*14, 69, 99, 126*). The greater all-around stability of B_9Cl_9, B_9Br_9, and B_9I_9 allows their infrared spectra to be obtained from either nujol mulls or disks of the respective potassium halide. The spectrum of the very water-sensitive B_8Cl_8 has been obtained from a cyclopentane solution using matched cells (*76*).

Raman and NMR spectra can be recorded either on neat liquids or on solutions in a variety of solvents: B_8F_{12} (B_3F_5; *126*); CCl_4 (B_4Cl_4; *14, 25*); BCl_3 (B_4Cl_4; *25*); BBr_3 (B_9Br_9; *75*); pentane (B_9Br_9, $B_{10}Br_{10}$; *75*).

Visible–ultraviolet spectra have been obtained using gaseous samples or solutions in the solvents BCl_3 (B_8Cl_8; *76*; B_9Cl_9; *77*) and BBr_3 (B_9Br_9; *108*).

III. Preparation

A. Fluorides (BF, B_2F_4, B_3F_5, B_8F_{12})

The original method, involving treatment of B_2Cl_4 with antimony trifluoride (*36, 111*), is still frequently used for small-scale (up to 22 g; *32*) preparations of diboron tetrafluoride, including $^{10}B_2F_4$ (*95*). Titanium tetrafluoride can also be used as the fluorinating agent (*82*).

A more recent synthesis (*126*) involves cocondensation of boron monofluoride and boron trifluoride in an approximate 1 : 1 ratio, when up to 25% of the BF is recovered as diboron tetrafluoride. The monofluoride is produced by passing boron trifluoride over boron heated to 1950–2000°C in the apparatus shown in Fig. 2; the yield of diboron tetrafluoride is very dependent on the amount of BF_3 condensed with the BF.

Cocondensation of B_2F_4 with boron monofluoride results in the formation of the very unstable B_3F_5 (*126*). Boron monofluoride is thus capable of insertion into the B—F bonds of both BF_3 and B_2F_4. When no BF_3 or B_2F_4 is cocondensed with boron monofluoride, then a mixture of B_2F_4, B_3F_5, and higher boron fluorides is obtained, the first two presumably arising from one, and two, BF insertions into boron trifluoride molecules that passed unchanged over the heated boron (under these conditions there would be a high $BF : BF_3$ ratio). No free $B(BF_2)_3$, which would require three BF insertions into an original boron trifluoride molecule, was obtained, but small amounts of its carbon monoxide adduct $OCB(BF_2)_3$ were isolated. The source of the CO was thought to be oxygen-containing impurities in the boron trifluoride starting material that had reacted with the graphite apparatus. Deliberate addition of carbon monoxide to the BF_3 stream increased the relative yield of $OCB(BF_2)_3$ but at the same time reduced the efficienty of BF condensation (CO is noncondensable at −196°C).

Disproportionation of liquid B_3F_5 at −30°C occurs slowly according to the equation

$$4B_3F_5 \rightarrow 2B_2F_4 + B_8F_{12}$$

The yellow compound B_8F_{12} may be separated from the other fluorides by low-temperature fractional distillation. Although the dispropor-

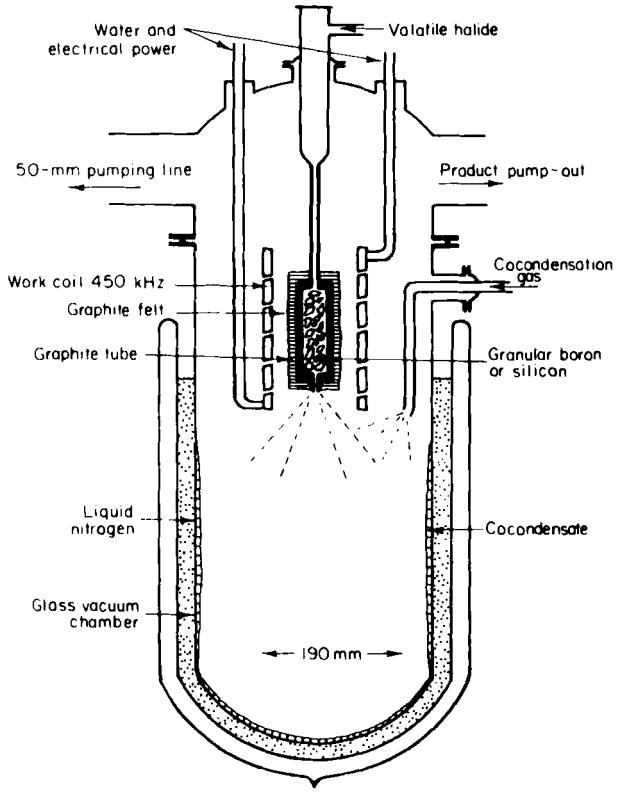

FIG. 2. Apparatus for production of BF and its subsequent reaction with other gases. Reprinted from Timms (*139*, p. 139).

tionation becomes more rapid at high temperatures, it may become violent, resulting in lower yields of B_8F_{12} due to the production of boron trifluoride and yellow, nonvolatile polymers (*126*).

B. CHLORIDES (BCl, B_2Cl_4, B_4Cl_4, B_8Cl_8, B_9Cl_9, $B_{10}Cl_{10}$, $B_{11}Cl_{11}$)

Preparative amounts of boron monochloride may be made by passing B_2Cl_4 vapor rapidly through a narrow-bore quartz tube maintained at 1000°C. Under the optimum conditions an approximately 50% yield of BCl may be obtained to give between 10 and 20 mmol in an hour (*131*, *132*). A competing reaction produces a deposit of elemental boron, which tends to block the quartz tube. Alternatively, the BCl molecules can be made by passing diboron tetrachloride through an ac discharge in the apparatus shown in Fig. 3 (*132*). The direct reduction of boron

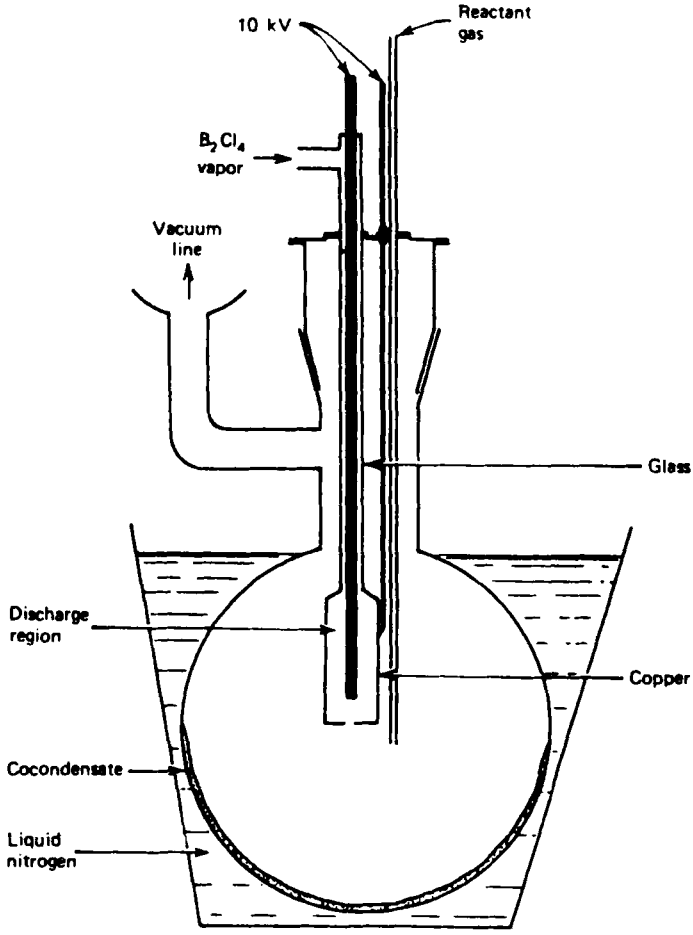

FIG. 3. Apparatus for the formation of BCl and its subsequent reaction with other gaseous species. Reprinted from Timms (*132*, p. 111).

trichloride vapor by heated boron (*74*) is not considered a practical route to BCl (*131*).

The mercury-discharge synthesis of diboron tetrachloride (*11, 90*) is still used for small-scale preparations, including that of $^{10}B_2Cl_4$ (*8*). However, for multigram quantities the copper-atom method of Timms is recommended (*128, 129*). In a typical experiment 10 g of copper are slowly evaporated over about 1 h from an electrically heated crucible contained in the apparatus shown in Fig. 4. The copper vapor and boron trichloride, passed in at the rate of about 2.5 g min^{-1}, are

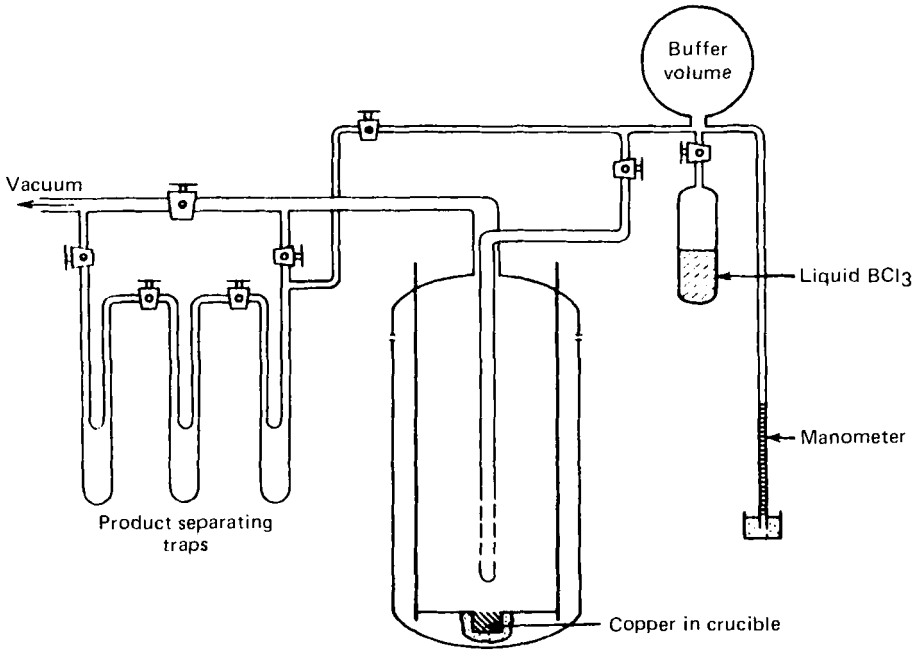

FIG. 4. Apparatus for treating boron trichloride with copper atoms. Reprinted from Timms (*129*, p. 76), *Inorganic Syntheses*, Vol. 19. Copyright 1979 Inorganic Syntheses, Inc. With permission of John Wiley & Sons, Inc.

condensed together at −196°C in the bottom of the reactor. After an hour the BCl_3 flow is stopped, the crucible allowed to cool, and the liquid-nitrogen bath removed from around the reactor, thus allowing it to warm up slowly to room temperature. Fractionation of the issuing vapors yields up to 4 g of diboron tetrachloride, representing a 30% yield based on evaporated copper. The method can be scaled up to produce 10 g of B_2Cl_4 in a 1-h run, starting from 20–30 g of copper. Silver may be used in place of copper, but the yields of diboron tetrachloride obtained are lower; no B_2Cl_4 is formed using nickel (*130*). Separate experiments show that no detectable reaction occurs when copper and B_2Cl_4 are condensed together.

Cocondensation of gaseous B_2O_2 with boron trichloride at −196°C gives a 60% yield of diboron tetrachloride based on the reaction

$$3B_2O_2(g) + 4BCl_3 \rightarrow 2B_2O_3 + 3B_2Cl_4$$

but full details of the system are lacking (*130*). Low yields of B_2X_4 are also formed when either boron trifluoride or boron trichloride is cocon-

densed with boron atoms (*130*). Irradiation of boron trichloride–hydrogen mixtures with the 10.55-μm radiation from a high-power TEA CO_2 pulse laser in the presence of a lead catalyst produced $^{10}B^{11}BCl_4$, $^{11}B^{11}BCl_4$, and HCl, but no $^{10}B^{10}BCl_4$. It was assumed that selective excitation of $^{11}BCl_3$ molecules occurred, and the following mechanism was proposed to account for the observed products (*80*).

$$^{11}BCl_3 + h\nu\ (10.55\ \mu m) \rightarrow {}^{11}BCl_2 + Cl$$

$$^{11}BCl_2 + H_2{---}Pb \rightarrow {}^{11}BCl_2{---}Pb + H_2$$

$$^{11}BCl_2{---}Pb + {}^{10,11}BCl_3 \rightarrow {}^{10,11}B^{11}BCl_4 + Cl$$

$$2Cl + H_2 \rightarrow 2HCl$$

A small amount of diboron tetrachloride is formed when boron trichloride is cocondensed with carbon vapor, the mechanism suggested being that of chlorine abstraction followed by $\cdot BCl_2$ radical coupling (*32*).

Tetraboron tetrachloride, which occurs in tiny amounts as a by-product from the discharge synthesis of B_2Cl_4, can now be made at the rate of about 10 mg h^{-1} by passing diboron tetrachloride vapor through a mercury discharge (*65, 92*). A more convenient synthesis, giving 3–5 mg h^{-1} of product, consists of setting up a radiofrequency discharge in a low-pressure stream of boron trichloride vapor and using mercury as a chlorine "getter" (*25*). Contrary to earlier reports (*121*), B_4Cl_4 is not produced by decomposing diboron tetrachloride (*65*).

Condensation of BCl in the presence of BCl_3 at −196°C gives good yields of tetraboron tetrachloride (*131*), but formidable problems associated with the preparation of BCl would not appear to make this an attractive synthesis.

Diboron tetrachloride decomposes thermally to give a number of boron monochlorides, B_nCl_n. Urry (*135*) described a dark purple, volatile decomposition product melting at 185°C but was unable to identify it fully. It has since been shown to be B_8Cl_8 (*76*), and, along with B_9Cl_9, it may be volatilized from the other decomposition products on gentle warming (it is very slightly volatile under a good vacuum at room temperature); vacuum sublimation up a long tube affords about 95% pure B_8Cl_8, which may be further purified by fractional crystallization from dichloromethane.

Schram and Urry described (*121*) a "non-crystalline yellow solid slightly volatile *in vacuo* at room temperature"; from its description this compound would appear to be B_9Cl_9 (although the latter can be readily induced to crystallize). When isolated from the B_2Cl_4 decompo-

sition products, B_9Cl_9 is contaminated with B_8Cl_8, which may be removed by heating the mixture under vacuum (*77*). A high yield of pure B_9Cl_9 is obtained by heating $B_{10}Cl_{10}$–$B_{11}Cl_{11}$ mixtures with chlorine (*6*).

A breakthrough in the preparative chemistry of the boron monohalides has been achieved by Wong and co-workers. They have shown that it is possible to oxidize $B_9X_9^{2-}$ ions (X = H, Cl, Br, I) to the respective neutral halide B_9X_9. In particular, B_9Cl_9 may be obtained in over 30% yield by treating $(n\text{Bu}_4\text{N})_2B_9H_9$ in CH_2Cl_2 with a large excess of sulfuryl chloride, removing the volatiles and extracting the residue with *n*-hexane (*63*). If $B_9Cl_9^{2-}$ or $B_9Cl_9^-$ is used as starting material, the oxidation can be carried out with thallium(III) trifluoroacetate (*143*).

Removal of B_8Cl_8 and B_9Cl_9 from the decomposition products of diboron tetrachloride leaves a reddish solid, which may be resolved, by warming, into a volatile, red $B_{10}Cl_{10}$–$B_{11}Cl_{11}$ mixture and a white, nonvolatile residue. The volatile, red mixture was originally considered to be a free radical $B_{12}Cl_{11}$ (*121, 135*), on the basis of its elemental analysis and its ESR spectrum; however, after the red solid is sublimed repeatedly it exhibits no ESR spectrum, showing that the paramagnetic properties are due to impurities. The $B_{11}Cl_{11}$ component of the mixture can be removed by heating to 350°C (*109*).

Dilute solutions of diboron tetrachloride in BCl_3 form mainly $B_{11}Cl_{11}$ when allowed to decompose at room temperature for many weeks. After removal of the boron trichloride, $B_{11}Cl_{11}$ may be sublimed carefully from the reaction tube, using a free flame. The product is only about 95–97% pure and is contaminated with $B_{12}Cl_{12}$ (*6*).

C. Bromides (B_2Br_4, B_7Br_7, B_8Br_8, B_9Br_9, $B_{10}Br_{10}$)

When boron tribromide vapor at low pressure is passed through a radiofrequency discharge in the presence of mercury, diboron tetrabromide is produced in yields of 200–300 mg hr^{-1} (*75*). This represents a convenient and relatively simple synthesis, giving about a 70% yield based on BBr_3 consumed. Nöth has described a nondischarge preparation in which tetramethoxydiboron in CH_2Cl_2 is treated with an excess of boron tribromide at room temperature; the yield was 49% after 30 min reaction. The corresponding reaction between $B_2(OMe)_4$ and BCl_3 gave no diboron tetrachloride (*96*). The reaction of copper atoms with boron tribromide has been reported to yield B_2Br_4, but no details were given (*75*).

Diboron tetrabromide decomposes rapidly at room temperature, visi-

bly darkening after 5 min and depositing dark-brown solids after 20 min (*66, 75*). Removal of the product boron tribromide allows separation of highly colored, slightly volatile bromides from the nonvolatile residue; fractional sublimation resolves the mixture of bromides into black B_7Br_7 and dark red B_9Br_9 (*66*). Although B_8Br_8 can be detected among the decomposition products (*66*), it has yet to be isolated from this source and is better made by treating B_8Cl_8 with aluminum bromide at 100°C in BBr_3 solvent (*83*). In the original study of the decomposition of diboron tetrabromide no $B_{10}Br_{10}$ was observed (*66*), but it has since been confirmed as a product (*108*) and has been separated from contaminating B_9Br_9 by precipitating the latter from a strongly cooled pentane solution (*75*).

Pure B_9Br_9 can be prepared from diboron tetrabromide more conveniently than by the fractional sublimation mentioned previously. Passage of diboron tetrabromide through a silent electric discharge produces B_9Br_9 and BBr_3; the latter can be used as a solvent to manipulate the relatively nonvolatile B_9Br_9 into strategically placed sidearms, which are sealed with a torch. It is then a simple matter to remove the BBr_3 and purify the B_9Br_9 by sublimation (*108*). Because diboron tetrabromide is formed by passing BBr_3 through a silent electric discharge the same apparatus may be used both to prepare and decompose the B_2Br_4. However, the rate of production of the tetrabromide is very low, and it is more convenient to prepare B_2Br_4 by other processes before decomposing it in the discharge (*108*). For small-scale syntheses diboron tetrabromide is decomposed at 200°C and the solid residues treated with bromine to give B_9Br_9 in 46% yield, based on the equation (*75*)

$$9B_2Br_4 \rightarrow 9BBr_3 + B_9Br_9$$

D. Iodides (B_2I_4, B_9I_9)

Although B_2I_4 has been mentioned as one of the products when zirconium tetrahydroborate, $Zr(BH_4)_4$, is treated with iodine (*150*), the radiofrequency-discharge synthesis reported many years ago by Schumb, Gamble, and Banus remains the only practical method for the preparation of the tetraiodide (*122*). This yellow solid is relatively stable at room temperature but decomposes very rapidly on melting at 94–95°C. Only two volatile monoiodides appear to be formed during the decomposition at temperatures between 100 and 400°C; these are B_8I_8 and B_9I_9. Heating the discharge apparatus strongly after a synthesis of B_2I_4 has been carried out allows isolation of the same two monoiodides,

which presumably arise from B_2I_4 decomposed in the hot discharge zone, not as primary discharge products (*87*).

B_9I_9 can be made without recourse to discharge procedures. Addition of thallium(III) trifluoroacetate to either $(n\text{Bu}_4\text{N})_2B_9I_9$ or $(n\text{Bu}_4\text{N})B_9I_9$ in CH_2Cl_2 gives a red-purple solution; after solvent removal and extraction with carbon tetrachloride, B_9I_9 is obtained in 30% yield as dark brown crystals (*142*).

E. Possible Intermediates in the Discharge Synthesis of Diboron Tetrahalides

When Schlesinger first prepared B_2Cl_4 by passing BCl_3 vapor through a mercury discharge, he assumed the product arose by simple dimerization of BCl_2 radicals formed by stripping of a chlorine atom from boron trichloride molecules by excited mercury atoms (*136*). It was shown many years later (*13*) that the spectrum of such mercury discharges contains no lines attributable to BCl_2 radicals, whereas strong emission due to the diatomic molecule BCl is present. Similarly, the spectrum of BCl was observed during the microwave excitation of BCl_3 vapor, a system that also produces diboron tetrachloride (and chlorine) (*59*). These results suggest that BCl is a precursor in the formation of diboron tetrachloride. Thermodynamically, the reaction

$$\begin{array}{rccc} & BCl_3 + & BCl & \rightarrow & B_2Cl_4 \\ \Delta G_f^{\ominus} & -92.9 & +28.9 & & -110.11 \text{ kcal mol}^{-1} \text{ (138)} \end{array}$$

is favored ($\Delta G_f^{\ominus} = -46.1$ kcal mol^{-1}) and, presumably, proceeds via the donation of a lone pair of electrons on BCl into the empty 2p orbital of boron trichloride.

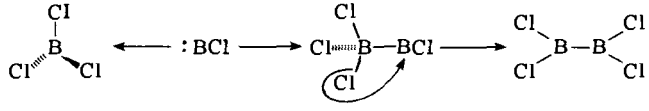

Urry (*133*) has objected to such a mechanism for the mercury-discharge system, mainly on the grounds that mercury(I) chloride is a by-product of reaction [Urry presumably thought mercury(II) chloride would be a more obvious product of stripping two chlorines from a boron trichloride molecule] and because no mixed boron–silicon chlorides were observed when BCl_3 and $SiCl_4$ were passed through the discharge (BCl might be expected to be inserted into silicon tetrachloride: $BCl + SiCl_4 \rightarrow Cl_2BSiCl_3$).

It is well known (*123*) that mercury(II) chloride will react with mercury to form Hg_2Cl_2. Also, the molecule Cl_2BSiCl_3 has been isolated as a by-product in the discharge preparation of diboron tetrachloride (*88*), presumably arising from $SiCl_4$, an impurity in the boron trichloride passing through the discharge (see also *147*). Thus two of Urry's objections can be disregarded. The other objection was that no Cl_2BPCl_2 could be detected (*40*) when a mixture of boron and phosphorus trichlorides was passed through the mercury discharge; perhaps this experiment ought to be repeated.

Whether or not BCl reacts with boron trichloride must depend to some extent on the prevailing conditions, because Timms and Maddren have shown (*132*) that BCl and BCl_3 do not form diboron tetrachloride when these compounds are condensed together at −196°C [under similar conditions BF is inserted into BF_3 to give diboron tetrafluoride (*126*)].

Boron trichloride, when passed at low pressure through a radiofrequency discharge in the presence of mercury, produces diboron tetrachloride and B_4Cl_4 (*25*). The emission spectrum of the discharge contains lines that are due to atomic mercury as well as bands in the region 2660–2880 Å, which are due to the (0,0), (1,0), (0,1), (1,1), (2,0), (2,1), (2,2), (0,3), (4,4), and (5,5) transitions of the BCl molecule (*12*). Thus once again we are led to the conclusion that the production of the two subchlorides B_2Cl_4 and B_4Cl_4 occurs via the BCl intermediate.

For the reaction

$$\begin{array}{ccccc} BBr_3 & + & BBr & \rightarrow & B_2Br_4 \\ \Delta G_f^\ominus\ -\ 57.0 & & +46.7 & -- & \text{kcal mol}^{-1} \end{array}$$

the free energy of formation of diboron tetrabromide, $\Delta G_f^\ominus$ (B_2Br_4), is unknown, but the positive value of $\Delta G_f^\ominus$ (BBr) ensures that $\Delta G^\ominus$ (reaction) = $\Delta G_f^\ominus$ (B_2Br_4) − (−57.0 + 46.7) will be highly negative for any plausible value assigned to $\Delta G_f^\ominus$ (B_2Br_4). It would, therefore, appear reasonable to suggest BBr as a possible intermediate in the formation of diboron tetrabromide from BBr_3. Diener and Pflugmacher (*31*) prepared diboron tetrabromide by passing boron tribromide through an electrical discharge maintained between nickel electrodes; previously, an almost identical system had been used to study the emission spectrum of BBr in the discharge zone (*114*). When boron tribromide is passed at low pressure through a radiofrequency glow discharge, diboron tetrabromide is formed (*75*). Strong bands of the BBr molecule can be observed in the emission spectrum of the discharge; when mercury is added to the system to act as a bromine

getter, the only observable change in the spectrum is that additional lines appear due to atomic mercury (*12*).

Iodine dominates the spectrum of the radiofrequency discharge in boron triiodide vapor, and because of this it was impossible to observe any bands due to BI or any other boron system. Lebreton (*78*) used argon to suppress the iodine spectrum in studies on BI made in a Schuler-type discharge. Even when argon was bled into the radiofrequency discharge at such a pressure just to sustain the glow, iodine still emitted too strongly to allow detection of BI (*12*).

IV. Structure and Bonding

A. Diboron Tetrahalides

Diboron tetrahalides have been fairly extensively studied in recent years as models to test the spectroscopist's art, because their adopted structure depends on the prevailing conditions. X-Ray crystallography has been used to show that diboron tetrafluoride and tetrachloride are planar (**I**) in the crystalline state at low temperatures (*84*). The planar form of B_2Cl_4 is a result of crystal packing forces and not an inherent thermodynamic stability of the D_{2h} rotamer at low temperatures (*33*). However, the anisotropic forces in an argon matrix at 20 K, unlike those in the crystal, must be less than the barrier to rotation because both tetrahalides assume the staggered conformation (**II**) under these conditions (*95*).

D_{2d} (I) D_{2h} (II)

The gas-phase electron-diffraction pattern of diboron tetrafluoride has been interpreted in terms of the planar, D_{2h}, structure (*24*). In particular, the two peaks corresponding to cis and trans F---F distances (3.1 and 3.8 Å) would be a single peak at about 3.4 Å in the pattern given by the staggered, D_{2d}, molecule. The very marked temperature dependence of the shape of these two peaks, which represent rotation-sensitive distances, was thought compatible only with a low rotational barrier in the B_2F_4 molecule; the average value estimated for this barrier was 0.42 ($\pm$0.16) kcal mol^{-1}.

Because five infrared-active fundamentals are expected for both the D_{2h} and D_{2d} forms of diboron tetrafluoride, the infrared technique alone

is incapable of differentiating between them. However, from a combination of infrared and Raman spectroscopy it was concluded that B_2F_4 is planar in all states (*34*), a fact that is at variance with earlier studies (*84, 95*). Ab initio (*37, 43, 60*) and MNDO (*28*) calculations on the diboron tetrafluoride molecule suggest that the D_{2d} model is the more stable, with a barrier to rotation of 0.3–1.1 kcal mol^{-1}. Extended Hückel-theory calculations suggest either that the two ends of the B_2F_4 molecule rotate virtually freely about the B—B axis [although slightly stable in the D_{2d} form; (*93*)] or that the D_{2h} rotamer is lower in energy (*18*).

In contrast to diboron tetrafluoride, B_2Cl_4 appears to adopt the staggered conformation in both the liquid and the gaseous states, as judged by electron diffraction (*54, 116*), vibrational spectroscopy (*8, 84, 95*), and most calculations (*1, 43, 93*); Hückel-type calculations lead to the suggestions that either the planar molecule is the more stable (*18*) or "the rotation about the B—B bond is very easy and that the conversion between the two forms may be carried out without a great hindrance" (*67*). The barrier to rotation determined from the electron-diffraction data (*116*) is 1.85 ± 0.03 kcal mol^{-1}, in good agreement with the value 1.8 ± 0.1 kcal estimated from the torsional mode in the Raman spectrum (*62*); calculations give the slightly lower values of 1.48 (*43*) and 1.67 (*93*) kcal mol^{-1}. The mean amplitudes of vibration and force constants have also been calculated for both B_2F_4 and B_2Cl_4 (*21, 22, 101, 105*).

For the larger halogen bromine there will be increased steric interaction in the planar B_2Br_4 molecule relative to B_2F_4 and B_2Cl_4. It is not too surprising, therefore, to find that vibrational spectra show that the staggered, D_{2d}, conformation is adopted in all three states (*99*).

Table III summarizes the structural data for diboron tetrafluoride and tetrachloride. The boron–fluorine bonds in B_2F_4 are about 0.05 Å

TABLE III

MOLECULAR PARAMETERS FOR DIBORON TETRAFLUORIDE AND TETRACHLORIDE

	B_2F_4		B_2Cl_4	
Species	Gas[a] (*24*)	Crystal (*84*)	Gas (*116*)	Crystal (*84*)
B—X (Å)	1.317 (*2*)	1.32 (*4*)	1.750 (*10*)	1.73 (*2*)
B—B (Å)	1.720 (*4*)	1.67 (*5*)	1.702 (*69*)	1.75 (*5*)
< XBX	117.2(2)°	120(2.5)°	118.65(66)°	120.5(1.3)°

[a] MNDO calculations for the D_{2d} form give B—B and B—F distances of 1.747 and 1.316 Å, respectively (*28*).

shorter than the sum of the single bond radii, corrected for electronegativity differences, which suggests a π-type interaction between the two atoms (*24*), a point apparently verified by calculation (*37, 43*). Less B—X π bonding is thought to occur in diboron tetrachloride (*43, 116*), which is consistent with the assignments made in the photoelectron spectra of the two molecules (*82*).

Electron delocalization in the conjugated π system of bonds in structures **IIIa** and **IIIb** is thought to occur, which would tend to stabilize the planar form of a B_2X_4 molecule. The contrasting gaseous structures

(IIIa) (IIIb)

of B_2F_4 and B_2Cl_4 thus result from a delicate balance between this conjugation and opposing steric effects (*24*). The B—B π-bond order in diboron tetrachloride is calculated to be 0.08 (*1*). It has also been argued that a σ-type 1,4 interaction **(IV)** may be an important factor in the stabilization of a planar B_2X_4, the stabilization being least in B_2F_4, when the small fluorine orbitals are involved (*60*). The B—B bond dissociation energy of B_2F_4 [103 kcal mol^{-1} (*29*)] is larger than that of

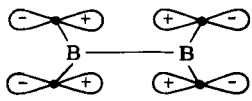

(IV)

B_2Cl_4 [87.6 kcal mol^{-1}, (*30*)]. This may be due, at least in part, to the greater electronegativity difference between B and F than between B and Cl (*41*).

B. B_3F_5 AND B_8F_{12}

Although no diffraction studies have been reported for B_3F_5 and B_8F_{12}, their spectroscopic properties are consistent with structures **V** (*26*) and **VI** (*70*).

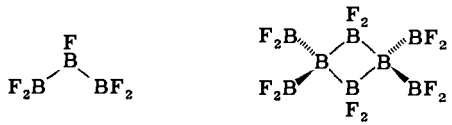

(V) (VI)

C. $B_{14}F_{18}$

The compound $B_5(BF_2)_9$ may be a formal analog of B_5H_9 in which BF_2 groups have replaced both bridging and terminal hydrogen atoms (cf. the analogy between B_2H_6 and B_8F_{12}) (*131*).

D. Tetraboron Tetrahalides

Only tetraboron tetrachloride has so far been isolated. In the solid state, tetraboron tetrachloride has the structure shown in Fig. 5, the molecule deviating only very slightly from T_d symmetry, possibly due to molecular packing in the crystal (*84*). The infrared and Raman spectra of the solid and gaseous phases have been interpreted fully on the basis of T_d symmetry, the slight distortions in the solid producing some splittings in the Raman spectrum (*14*); boron isotopic splitting into three (or four?) of the expected five peaks is clearly visible on the Raman bands at 1302 and 685 cm^{-1}, but the effect of the ^{35}Cl and ^{37}Cl isotopes is smaller and not seen. Although the B—Cl stretching force constant of 4.076 mdyne $Å^{-1}$ is in the middle of the range of values quoted for boron trichloride, the B—B constant (2.3 mdyne $Å^{-1}$) is rather low and suggests that the B—B bonds in B_4Cl_4 are abnormally weak (*14*). There are no features in the spectra that suggested the presence of the planar isomer of B_4Cl_4, which was suggested as a possibility by Lipscomb (*72*).

The bonding in B_4F_4 and B_4Cl_4 has been discussed by numerous authors (*1, 43–45, 68, 89, 125, 137*). Qualitative Hückel-type calculations (*89*), semiempirical CNDO calculations (*1*), and more sophisticated ab initio SCF calculations (*43, 45*) all suggest that B_4Cl_4 is stabilized by a π-type back donation of charge from the chlorine atoms to the B_4 cage orbitals; this appears to be verified by a study of the photoelectron spectrum (*81*). However, there is some dispute as to whether more (*45*) stabilization occurs in B_4F_4 than in B_4Cl_4, or less (*43, 89*). The lower stabilization suggested for B_4F_4 seems to be in agreement with the repeated failures to fluorinate B_4Cl_4 with typical reagents such as PbF_2, SbF_3, and TiF_4 (*86, 92*) and the lack of B_4F_4 when BF is condensed at low temperatures [BCl under similar conditions gives good yields of B_4Cl_4 (*131*)].

Substantial energy barriers exist for the transformations

$$B_4F_4\ (T_d) \rightarrow B_4F_4\ (D_{4h}) \rightarrow B_4F_4\ (T_d)$$

apparently due to a HOMO–LUMO crossing. From this, and the similar energies calculated for the two forms of B_4F_4, it has been suggested

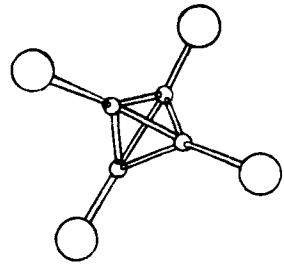

B_4Cl_4

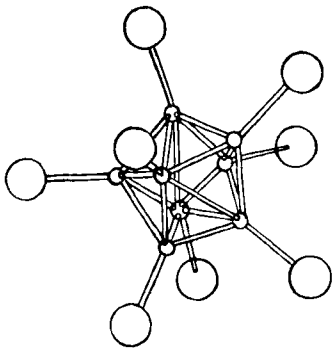

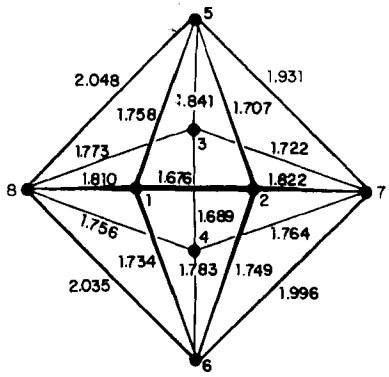

B_8Cl_8

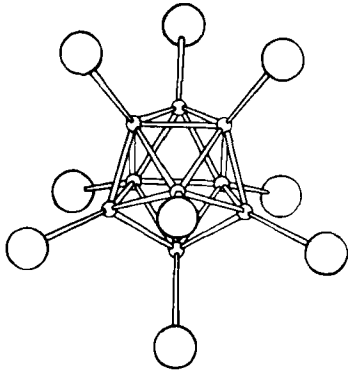

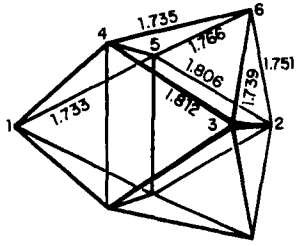

B_9Cl_9

FIG. 5. The structure of, and bond lengths (Å) in B_4Cl_4 (B—B, 1.70 ± 0.04; B—Cl, 1.70 ± 0.04) (*4*), B_8Cl_8 [B(*n*)—Cl: *n* = 1, 1.739; 2, 1.722; 3, 1.720; 4, 1.721; 5, 1.772; 6, 1.748; 7, 1.746; 8, 1.721] (*5*), and B_9Cl_9 [B(*n*)—Cl: *n* = 1, 1.729; 2, 1.748; 3, 1.738; 4, 1.741; 5, 1.746; 6, 1.721] (*61*). ○, B; ○, Cl.

that B_4F_4 (once formed) and B_4Cl_4 could exist under some conditions as either the tetrahedral or the planar isomer, or perhaps a mixture of both (*72*). Under all the conditions so far studied, B_4Cl_4 has been found to adopt the tetrahedral structure (*14*).

E. B_8Cl_8

The B_8Cl_8 molecule has the dodecahedral structure shown in Fig. 5 (*5*). The source of the crystal used in the structure determination was a sample of red solid product arising from the decomposition of diboron tetrachloride and was at that time known only by the formula $(BCl_{0.9})_x$. Later work by Urry (*121*) showed that such red solids contain about 5% of a dark purple subchloride impurity; it is this dark purple subchloride that is B_8Cl_8 (*76*) and not the bulk of the red material (which is mainly a mixture of $B_{10}Cl_{10}$ and $B_{11}Cl_{11}$).

B_8Cl_8 is diamagnetic (*76*), hence the ESR spectrum observed by Urry (*135*) must have been due to the presence of impurities in his "dark purple crystalline solid"; traces of water in systems used to handle B_8Cl_8 produce paramagnetic hydrolysis products (*76*). Theoretical discussions of B_8Cl_8 have been only briefly summarized in the literature (*68, 100, 137*).

F. B_9X_9 (X = Cl, Br, I)

B_9Cl_9 has the tricapped trigonal-prismatic structure shown in Fig. 5 (*61*). The very similar infrared spectra of B_9Cl_9, B_9Br_9, and B_9I_9 (*142*) suggest that all three halides are isostructural. If this is so, it is interesting to note that the ^{11}B-NMR spectrum of B_9Br_9 consists of a single peak, even down to $-60°C$, suggesting that the molecule is fluxional (*75*).

V. Chemical and Physical Properties

A. BF AND BCl

The short-lived species BF and BCl have been studied by cocondensation reactions at low temperatures. As described in Section III,A, the condensation of BF with BF_3 at $-196°C$ yields B_2F_4, B_3F_5, and small amounts of more complex fluorides containing between 10 and 16 boron atoms (*69, 126, 131*). The presence of CO or PF_3 in the system results in the formation of the adducts $OCB(BF_2)_3$ and $F_3PB(BF_2)_3$ (*126*). Although BF is readily inserted into BF_3 and B_2F_4, only traces of

F_3SiBF_2 were obtained when insertion into SiF_4 was attempted (*126*). When silicon tetrafluoride is passed over heated boron, the exit gases contain BF, BF_3, and SiF_2, and when condensed at −196°C these give rise to $F_2Si(BF_2)_2$, possibly via the reaction sequence (*71*)

$$SiF_2 + BF \rightarrow [\cdot\, SiF_2BF \cdot] \xrightarrow{BF_3} F_2Si(BF_2)_2$$

Other products include the known species BF_3, B_2F_4, SiF_4, Si_2F_6, Si_3F_8, and $Si_2F_5BF_2$; an electron-diffraction study has confirmed that the latter compound has the structure $F_3SiSiF_2BF_2$ (*17*).

Condensation of BCl with boron trichloride produces good yields of B_4Cl_4, but no diboron tetrachloride (*132*); similarly, BF is not inserted into $MeBF_2$ to give B_2F_3Me (*69*).

Attempts have been made to use BF as a ligand to transition metals because it is formally isoelectronic with carbon monoxide. Condensation of iron atoms with a mixture of B_2F_4 (as BF precursor) and PF_3 gave two products, one of which was the known $Fe(PF_3)_5$ and the other a very unstable compound of probable formula $Fe(PF_3)_4BF$ (*131*). Similar products were obtained using other transition metals, but attempts to characterize them fully have been frustrated by their extreme thermal instability.

BF and BCl readily add to alkenes and alkynes; propene has been used as the model alkene because C_2H_4 is slightly volatile at −196°C and interferes with the production of BX, by destroying the required high-vacuum conditions. Both types of hydrocarbon are thought to form unstable, three-membered heterocycles as the initial products.

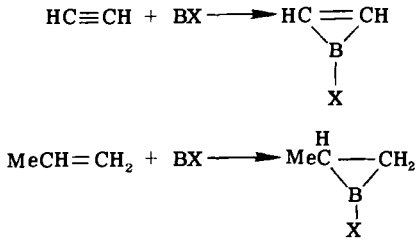

The fate of these heterocycles depends on the halogen X. With the chloride simple dimerization would give the observed products,

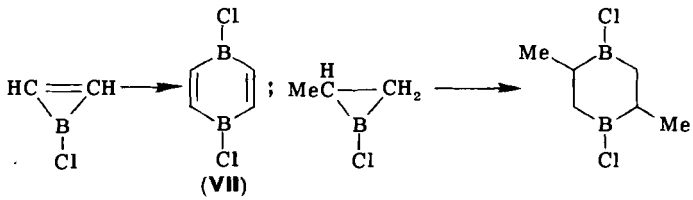

(VII)

whereas interaction with boron trifluoride (always present in the BF system) appears to occur when X = fluorine. When heated to 70°C,

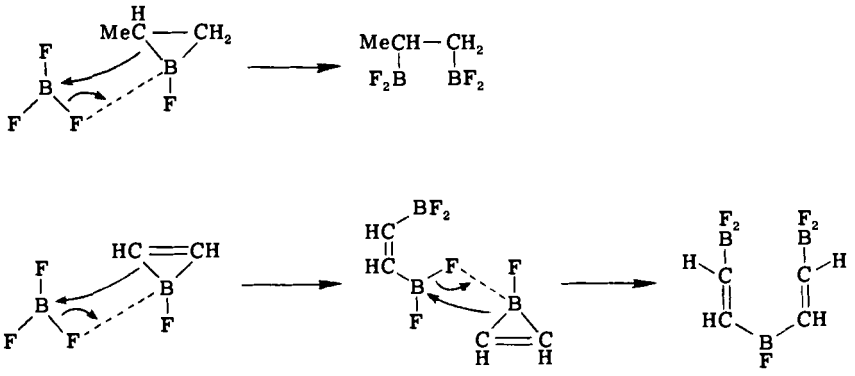

VIII loses boron trifluoride to form the fluorine analog of the boracyclohexadiene **VII** (*131*). Intermediates similar to **VIII** are not formed when BF reacts with methylacetylene or dimethylacetylene (*127*).

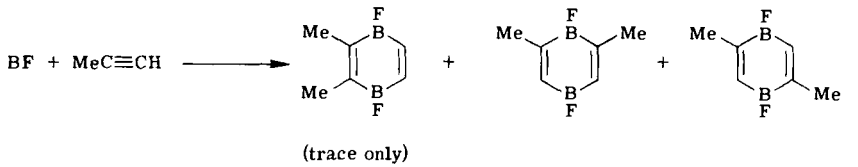

(trace only)

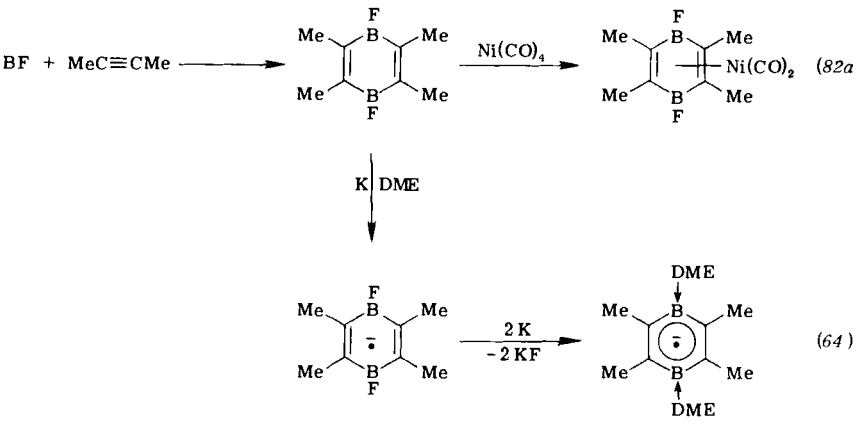

(82a)

(64)

B. Diboron Tetrahalides

The physical properties of the diboron tetrahalides are shown in Table IV. They all spontaneously ignite in air when in the vapor state and are thermally unstable. The fluoride is the most stable, decomposing to the extent of about 40% when held at 200°C for several hours; the products are boron trifluoride and a yellow solid that does not sublime, even at 375°C (*7*). Diboron tetrachloride decomposes to the extent of 13% in 29 h at 25°C, and 32% after 4 h at 155°C; between 138 and 155°C the decomposition data support a second-order heterogeneous reaction that is strongly retarded by products and promoted by systems with a high surface-to-volume ratio (*7*). Colored decomposition products can be detected when diboron tetrabromide is held at room temperature for only 5 min (*75*). Although the tetraiodide appears to be reasonably stable in the solid state at room temperature, dark-colored decomposition products begin to form immediately on melting (*87*).

After liquid B_2Cl_4 and B_2Br_4 have been held at room temperature for several hours, it is possible to detect the presence of long-lived paramagnetic species that give rise to a broad, featureless peak in the ESR spectra (*75, 86*).

The decomposition of diboron tetrachloride has been the most fully studied. Adiabatic flash photolysis shows the initial reaction to be the extrusion of a BCl molecule (*91*)

$$B_2Cl_4 \rightarrow BCl_3 + BCl \tag{1}$$

which is in agreement with McHale's observation that when diboron tetrachloride decomposes, a 1:1 B_2Cl_4:BCl_3 ratio is always obtained (*92*). By passing diboron tetrachloride through a narrow silica tube held at 1100°C, Timms has used the decomposition [Eq. (1)] to form preparative amounts of boron monochloride (*131, 132*); a side reaction, not noted under any other conditions, gives solid boron (which tends to block the silica tube).

$$3B_2Cl_4 \rightarrow 2B + 4BCl_3$$

Under some conditions (Section III,E) BCl will add to BCl_3 to give diboron tetrachloride so that Eq. (1) may well be reversible in the liquid state. The other option open to the BCl molecules is polymerization, forming the observed products B_nCl_n. Contrary to earlier reports, no B_4Cl_4 can be detected among the decomposition products of B_2Cl_4, and, furthermore, deliberately added B_4Cl_4 may be isolated unchanged

TABLE IV

PHYSICAL PROPERTIES OF THE DIBORON TETRAHALIDES[a,b]

Property	B_2F_4	B_2Cl_4	B_2Br_4	B_2I_4
Melting point (°C)	−56.0; −55 (*126*)	−92.6; −92.95	0.5–1.5	94–95 (*87*)
Boiling point (°C)	−34	65.5	—	—
Vapor pressure relation for solid: $\log p_{mm} = A - B/T$ (T in K)	A = 10.82 B = 1856	—	—	Vapor pressure at 60–70°C is 10^{-3} Torr
Vapor pressure relation for liquid: $\log p_{mm} = A - B/T$ (T in K)	A = 9.009 B = 1446	A = 8.057 B = 1753	Vapor pressure at 22.5°C is 5 Torr	—
Trouton constant	28	23.7	—	—
Heat of evaporation (cal mol^{-1})	6700	8029	—	—
Heat capacity	—	Normal from 20 to 220 K	—	—
Heat of fusion (cal mol^{-1})	—	2579 ± 4	—	—
ΔH_f^θ (298 K (kcal mol^{-1}) (l)	—	−125.0 (*138*)	—	—
ΔH_f^θ (298 K) (kcal mol^{-1}) (g)	−344.2 (*138*)	−117.2 (*138*)	—	—
ΔG_f^θ (kcal mol^{-1}) (l)	—	−111.1 (*138*)	—	—
ΔG_f^θ (kcal mol^{-1}) (g)	−337.1 (*138*)	−110.1 (*138*)	—	—
S^θ (cal deg^{-1} mol^{-1}) (l)	—	62.7 (*138*)	—	—
S^θ (cal deg^{-1} mol^{-1}) (g)	75.8 (*138*)	85.4 (*138*)	—	—
D_0 (X_2B—BX_2) (kcal mol^{-1})	103.1 (*29*)	87.6 (*30*)	—	—
$\Delta H_{f0}^\theta(B_2X_4^+)$ (kcal mol^{-1})	−65.2 (*29*)	120.8 (*30*)	—	—

[a] Calculated enthalpies of formation of B_2F_3Cl, B_2FCl_3, F_3BBCl_3, and FClBBFCl are (kcal mol^{-1}): −287.1, −173.5, −230.8, and −229.7, respectively (*35*).

[b] Reference (*84*) unless stated otherwise.

at the end of the experiment, showing that it is not an intermediate necessary for the formation of the other monochlorides (*106*). [On the other hand, very high local concentrations of BCl, which are formed when BCl vapor is condensed at −196°C, produce B_4Cl_4 in good yield (*132*).] If polymerization of the BCl molecules produces the observed B_nCl_n products (n = 8 to 12), there must be open-cage species, which are possibly stabilized by interaction with BCl_3 or B_2Cl_4 molecules, acting as intermediates.

It is possible to exercise some slight control as to which decomposition products are formed. By holding the liquid diboron tetrachloride at about 70°C instead of room temperature, a higher proportion of B_8Cl_8 is obtained (*106, 121*). If dilute solutions of B_2Cl_4 in BCl_3 are allowed to decompose over a period of weeks at room temperature, the product is $B_{11}Cl_{11}$, contaminated with small amounts of $B_{12}Cl_{12}$ (*6*).

When diboron tetrabromide decomposes, the products are BBr_3, involatile solid debris, and a series of monobromides, B_nBr_n (n = 7 to 10) (*66, 75*). The latter have been separated by fractional sublimation (*66*) or fractional precipitation from pentane at low temperatures (*75*). Diboron tetraiodide decomposes to give mainly BI_3, B_8I_8, and B_9I_9 (*87*).

Stabilization of the diboron tetrahalides may be accomplished by complexing them with a suitable donor molecule such as trimethylamine. Cryoscopic measurements on the molecular weight of the adduct $B_2Cl_4 \cdot 2NMe_3$ originally suggested that the compound was tetrameric (*136*), but more recent work shows it to be monomeric in the solid and gaseous phases (*119*). The B—B and B—N bond lengths are 1.72 and 1.75 Å, respectively (*119*). For the solid bisphosphine adducts $B_2Cl_4 \cdot 2PH_3$ and $B_2Cl_4 \cdot 2PD_3$, the vibrational spectra have been interpreted on the basis of a trans (C_{2h}) molecular conformation with a rotation barrier about the B—P bonds of 2.92 ± 0.18 kcal mol^{-1} (*98*).

The diboron tetrahalides are capable of acting as either mono- or dibasic Lewis acids. For example, Schlesinger originally showed that, on pumping, the bis(diethyl ether) adduct $B_2Cl_4 \cdot 2OEt_2$ loses a mole of diethyl ether to give $B_2Cl_4 \cdot OEt_2$ (*136*). When a tensiometric titration is carried out between diboron tetrafluoride and trimethylamine, two breaks are observed in the pressure:mole-ratio curve (Fig. 6), the first representing the formation of $B_2F_4 \cdot NMe_3$ and the second, $B_2F_4 \cdot 2NMe_3$ (*3*). By using this technique to form $B_2F_4 \cdot NMe_3$ and then adding a second mole of triethylamine, it is possible to make the mixed adduct $B_2F_4 \cdot NMe_3NEt_3$ (*3*). Only a single broad peak at +11.7 ppm (relative to $BF_3 \cdot OEt_2$) is observed in the ^{11}B-NMR spectrum of $B_2F_4 \cdot NMe_3$, which implies rapid exchange of trimethylamine between the two boron sites (*3*).

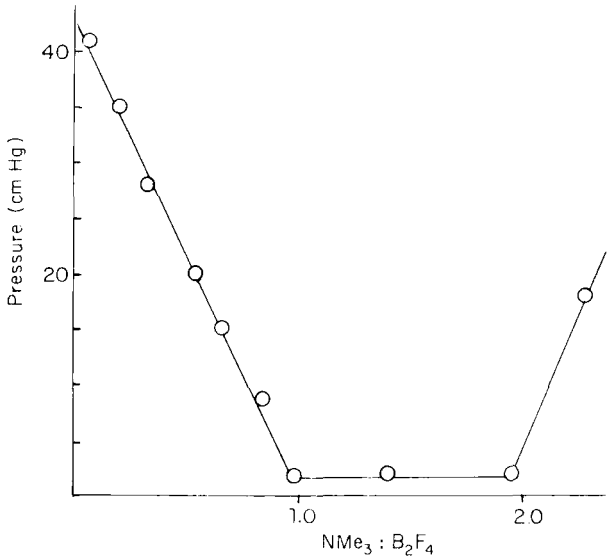

FIG. 6. Tensiometric titration of trimethylamine against diboron tetrafluoride.

Diboron tetrafluoride is liberated by BF_3 from several of its adducts, including $B_2F_4 \cdot 2NMe_3$, showing that the trifluoride is the stronger Lewis acid (*46*).

Bases that contain reactive hydrogens on the donor atom readily evolve hydrogen chloride when treated with diboron tetrachloride

$$4ROH + B_2Cl_4 \rightarrow B_2(OR)_4 + 4HCl \qquad (84)$$

Advantage has been taken of this to form heterocyclic species, starting with difunctional bases such as ethylene glycol, ethanedithiol, 1,3-propanediol, catechol, *sym*-dimethylethylenediamine, and *o*-phenylenediamine (*141*).

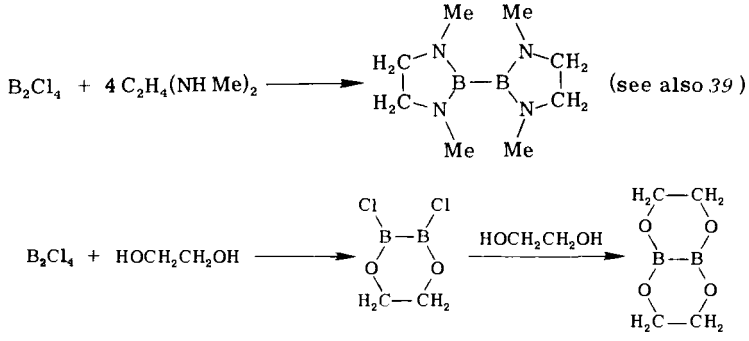

Only polymeric products were obtained with 1,3-propanedithiol, 2-aminophenol, 2-mercaptoethanol, and styrene glycol. It has since been suggested that the NMR data of the oxygen and sulfur heterocycles are more consistent with structures similar to the nitrogen complex (*97*).

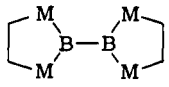

(M = O, S)

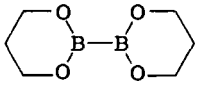

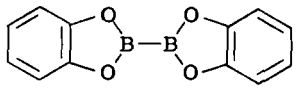

Conductimetric titrations of diboron tetrachloride in liquid hydrogen chloride with either Me_4NCl or PCl_5 indicate the formation of the hexachlorodiborate anion, which may be isolated as the tetramethylammonium or tetrachlorophosphonium salts. The titration curves showed no breaks at mole ratios of 1 : 1, corresponding to the $B_2Cl_5^-$ ion; attempts to prepare tetramethylammonium pentachlorodiborate by mixing stoichiometric amounts of reagents have resulted only in the formation of the hexachlorodiborate. The reactions of diboron tetrafluoride in liquid hydrogen chloride are complicated by the occurrence of partial solvolysis (*103*).

Early attempts to methylate diboron tetrachloride with dimethylcadmium (*136*) or tetramethyllead (*55*) gave BMe_3 as the only volatile, boron-containing product; treatment with dimethylmercury resulted in explosions (*139*). Later work, however, shows that MeB_2Cl_3 is formed, along with methylchloroboranes, when B_2Cl_4 is treated with Me_4Ge, Me_4Sn, or Me_4Pb; unfortunately, it has proven impossible to separate the MeB_2Cl_3 from unchanged diboron tetrachloride (*110*). The thermally unstable 1,2-dimethyldichlorodiboron can be made by treating $MeBCl_2$ with copper atoms (*128*)

$$2MeBCl_2 + 2Cu \xrightarrow{-196°C} Me(Cl)B{-}BMe(Cl)$$

Very slow, partial methylation of $B_2Cl_4 \cdot 2NMe_3$ appears to occur at room temperature with tetramethyllead; presumably, the methylated products are stabilized by coordination to trimethylamine (*55*). No alkylated products containing B—B bonds could be detected when the tetramethylethylenediamine and glyme adducts of B_2F_4 were treated with diethylzinc (*46*).

Although B_2R_4 derivatives have not been prepared from the diboron tetrahalides, thermally stable tetraalkyldiborons containing bulky R groups have been described (*10, 120*). The products do not react at room temperature with methanol, ammonia, hydrazine, or pyridine; **IX** is even stable toward oxygen.

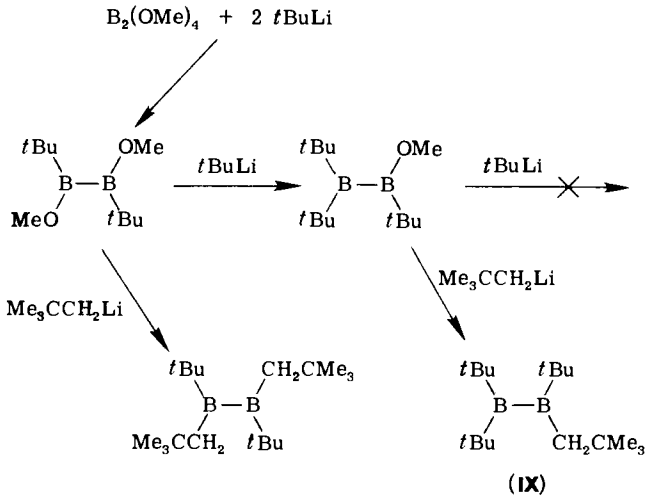

(IX)

Simple cleavage of the B—B bonds in diboron tetrachloride occurs with chlorine and bromine (*84*); however, the slow reaction with iodine at room temperature produces a black, solid monoiodide (*92*).

$$3B_2Cl_4 + 2I_2 \rightarrow 4BCl_3 + BI_3 + (BI)_x$$

Small quantities of mixed chloroiodoboranes were also present, which, presumably, were formed by interaction between the two trihalides.

Chloramines readily cleave the B—B bonds of diboron tetrachloride, the products depending on the temperature and reaction stoichiometry (*53*).

$$B_2Cl_4 + Me_2NCl \xrightarrow{20^\circ C} BCl_3 + Me_2NH \cdot BCl_3 + \text{nonvolatile residue}$$

$$\downarrow 80^\circ C$$

$$Me_2NBCl_2$$

$$B_2Cl_4 + EtNCl_2 \longrightarrow BCl_3 + EtNCl{-}BCl_2$$

$$2B_2Cl_4 + EtNCl_2 \longrightarrow 2BCl_3 + Cl_2B{-}N(Et){-}BCl_2$$

Diboron tetrachloride, when cocondensed with carbon vapor generated in a carbon arc, gives a mixture of $C(BCl_2)_4$, $ClC(BCl_2)_3$, $Cl_2C(BCl_2)_2$, and $(Cl_2B)_2C{=}C(BCl_2)_2$. For example, the process leading to tetrakis(dichloroboryl)methane probably involves a double-insertion reaction (*32, 130*).

$$:C: + Cl_2BBCl_2 \rightarrow Cl_2B\ddot{C}BCl_2 \xrightarrow{B_2Cl_4} C(BCl_2)_4$$

When B_2F_4 is used, rather unstable compounds are isolated that originate from only C_2 and C_3 species (*32*).

$$B_2F_4 \begin{cases} \xrightarrow{C_2} [F_2BC_2BF_2] \xrightarrow{B_2F_4} (F_2B)_2C{=}C(BF_2)_2 \\ \xrightarrow{C_3} [F_2BC_3BF_2] \xrightarrow{B_2F_4} (F_2B)_2C{=}C{=}C(BF_2)_2 \end{cases}$$

Any fluoro derivatives containing single carbon atoms were probably too unstable to be isolated; the chloro analog of tetrakis(difluoroboryl)allene may have been formed, but it was thought too nonvolatile to be removed from the reaction vessel.

The reaction of silicon atoms with diboron tetrafluoride at −196°C is complex, but it has proved possible to isolate the pyrophoric $FSi(BF_2)_3$ in about 2% yield (based on silicon); a trace of $F_2Si(BF_2)_2$ is also formed (*71, 131*). Silicon difluoride and B_2F_4 give a blue solid at −196°C, which on warming evolves BF_3, SiF_4, B_2F_4, Si_2F_6, and a very unstable volatile compound that may be $(F_5Si_2)BFBF_2$; in the presence of phosphorus trifluoride, $(F_5Si_2)_2(BF_2)B \cdot PF_3$ is formed (*131*). In the hope of making $Cl_3SiBClBCl_2$, silicon dichloride and diboron tetrachloride were condensed together at −196°C and then allowed to warm up to room temperature; only nonvolatile solids, $SiCl_4$, and Cl_3SiBCl_2 were obtained (*131*). [The latter compound has also been made at the rate of 12 mg h^{-1} by passing a $SiCl_4$–BCl_3 mixture through a pulsed discharge (*147*).] When carbon monoxide is added to the $SiCl_2$–B_2Cl_4 matrix during warmup to room temperature, a very stable carbonyl adduct $(Cl_3Si)_2(BCl_2)B \cdot CO$ results. Partial halogen exchange occurs when CO is replaced by phosphorus trifluoride, and the product is then $(Cl_3Si)_2(BF_2)B \cdot PF_3$ (*131*).

It appears (*131*) from these silicon dihalide experiments and from a study of B_3F_5 (Section V,D) that compounds of the formula $XBY{-}BY_2$ (X = BF_2, $SiCl_3$, or Si_2F_5) are highly unstable toward disproportionation into B_2Y_4 and $[X_2(BY_2)B]_2$. The CO and PF_3 adducts mentioned previously probably arise via cleavage of the latter dimer (compare B_8F_{12}, Section V,E).

$$[X_2(BY_2)B]_2 + 2CO \rightarrow 2X_2(BY_2)BCO$$

$$\begin{aligned} X &= BF_2, & Y &= F \\ X &= SiCl_3, & Y &= Cl \\ X &= Si_2F_5, & Y &= F \end{aligned}$$

There has been considerable interest shown in the stereochemistry of products formed by addition of B_2F_4 and B_2Cl_4 to alkenes and al-

kynes. With acetylene (*52, 115*), 2-butyne (*145*), *trans*-2-butene (*115, 145*), *cis*-2-butene (*115, 145*), *trans*-2,2,5,5-tetramethyl-3-hexene (*149*), norbornylene (*144*), cyclohexane (*9, 145*), 1,3-cyclohexadiene (*148*), cyclopropene (*113*), cyclobutene (*113*), cyclopentene (*113*), and naphthalene (*144*) cis addition occurs

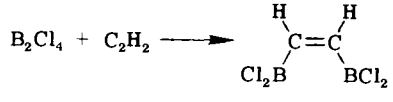

(X)

On standing (*52*) or under the influence of ultraviolet radiation (*19*), **X** changes to the trans isomer. Addition of another mole of diboron tetrachloride to both **X** and its trans isomer can occur.

$$Cl_2BCH{=}CHBCl_2 + B_2Cl_4 \rightarrow (Cl_2B)_2CHCH(BCl_2)_2 \qquad (20, 84)$$

When **X** is used, some *trans*-1,2-bis(dichloroboryl)ethylene is also formed, presumably by isomerization of **X** under the reaction conditions (*19*). Treatment of **X** with CH_3COOD at 80°C gives both *cis*- and *trans*-$C_2H_2D_2$, showing that this cleavage is not entirely sterospecific; alkaline hydrolyses or reductions by ammoniacal silver oxide are recommended as better cleavage systems (*19*). In contrast to C_2H_2, the substituted alkynes propyne, 2-butyne, and di-*t*-butylacetylene only add 1 mol of B_2Cl_4 (*144*).

In apparent contrast to these reactions, addition of B_2Cl_4 to cyclopentene has been claimed to give 1,2-bis(dichloroboryl)cyclopentane, which on cleavage with alkaline peroxide yielded only *trans*-1,2-cyclopentanediol (*117*). However, this work has been repeated under a wide variety of conditions and the reaction shown to give only the expected cis product (*113*).

The formation of only cis products from these addition reactions has been interpreted by most workers in terms of a mechanism involving a four-centered intermediate, which is assumed to arise by interaction of the hydrocarbon's π system with the vacant boron 2p orbitals.

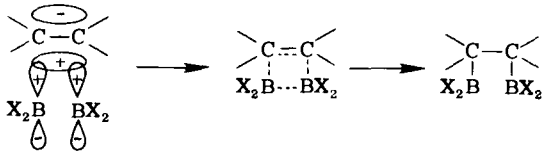

A planar B_2X_4 would clearly be preferred for such an interaction. That $B_2(NMe_2)_4$ and B_2Br_4 (both of which adopt the nonplanar conformation in all phases) do not react with ethylene appears to be in keeping with this mechanism.

However, a theoretical study of the B_2H_4–C_2H_2 reaction suggests that it proceeds in two steps. The first, which is rate determining with an activation energy of 12.8 kcal mol^{-1}, results in the formation of the three-center π complex **XI**; the second step is the attachment of the other BH_2 to the second carbon and involves rotation of the BH_2 group until it comes out of the B_2C_2 plane.

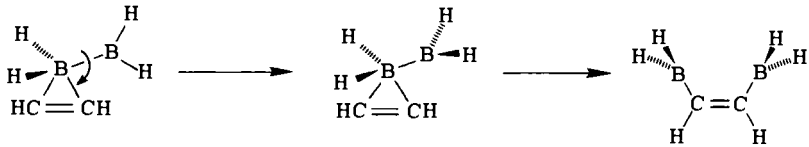

(XI)

Like the previous one, this new mechanism predicts the formation of cis products (*16*). Naturally enough, after their formation by cis addition, saturated products adopt a structure appropriate to the prevailing conditions. Thus the planar "trans" conformation of 1,2-bis(dichloroboryl)ethane is found in the crystal (*94*) and is the main constituent of the liquid and gaseous phases (*124*).

Contrary to earlier reports (*84, 144*), haloolefins slowly add diboron tetrahalides. For example, 2 mol of B_2Cl_4 react with vinyl chloride, yielding 1,1,2-tris(dichloroboryl)ethane and boron trichloride; the reaction sequence is considered to be (*112*)

$$ClCH{=}CH_2 + B_2Cl_4 \rightarrow Cl(BCl_2)CHCH_2(BCl_2) \xrightarrow{-BCl_3} CH_2{=}CHBCl_2 \quad \textbf{(XII)}$$

$$CH_2{=}CHBCl_2 \xrightarrow{B_2Cl_4} (Cl_2B)CH_2CH(BCl_2)_2$$

The rapid addition of B_2Cl_4 to vinyldichloroborane (**XII**) had been demonstrated previously (*20*). Similar reactions occur with *trans*-2-chlorovinyldichloroborane, fluoroethylene, vinyl bromide, and 1-bromopropene, or when B_2F_4 is substituted for diboron tetrachloride (*110, 112*). This work also confirmed earlier observations (*15*) that diboron tetrachloride is stabilized toward decomposition by haloolefins; it is not a simple dilution effect because B_2Cl_4 decomposes normally in either *n*-hexane or ethyl chloride (*112*).

Addition of diboron tetrahalides occurs even when the double bonds

are attached, as vinyl groups, to a variety of elements such as boron, silicon, germanium, and tin.

$$Me_3MCH{=}CH_2 + B_2X_4 \rightarrow Me_3MCH(BX_2)CH_2BX_2 \qquad (20)$$
$$M = C, Si$$

$$Cl_3MCH{=}CH_2 + B_2X_4 \rightarrow Cl_3MCH(BX_2)CH_2BX_2 \qquad (20)$$
$$M = Si, Ge, Sn$$

$$B(CH{=}CH_2)_3 \xrightarrow{B_2Cl_4} (CH_2{=}CH)_2BCH(BCl_2){-}CH_2(BCl_2) \xrightarrow{B_2Cl_4} CH_2{=}CH\,B(CH(BCl_2){-}CH_2(BCl_2))_2 \xrightarrow{B_2Cl_4} \not\rightarrow \qquad (57)$$

As an exception, tetravinyltin does not yield simple addition products with B_2F_4; instead, ethylene, vinyldifluoroborane, and nonvolatile residues are obtained (*58*).

Diboron tetrachloride reacts with cyclopropane and methylcyclopropanes to give ring-cleavage addition products. Deboronation of **XIII** and **XIV** with propionic acid produces *n*-butane and methylpropane, respectively. The ring cleavage has been shown to occur stereospecifically for *cis*- and *trans*-1,2-dimethylcyclopropane (*146*). When the cyclopropane ring is substituted with either a methylene or a vinyl group, addition of diboron tetrahalide takes place only on the exocyclic double bond, even when an excess of halide is used (*50*).

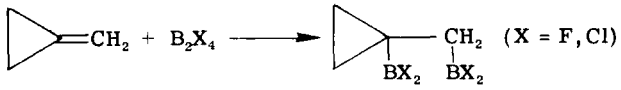

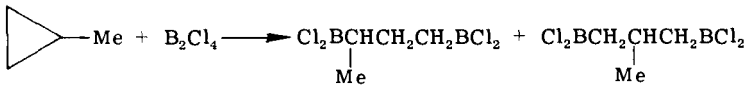

(XIII) **(XIV)**

Addition to the double bond and not ring cleavage also occurs when diboron tetrachloride reacts with cyclopropene; however, when methylcyclopropene is used both types of addition product are formed in competing reactions (*113*).

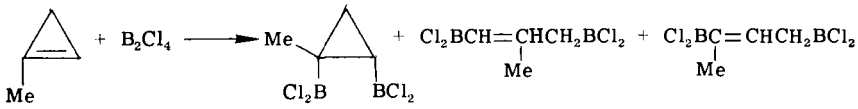

Cyclobutane does not react with diboron tetrachloride (*146*).

One mole of either B_2F_4 or B_2Cl_4 will add to 1,3-butadiene to yield 1,4-bis(dihaloboryl)-2-butene, and, in the case of the tetrachloride, further addition occurs to the butene double bond

$$B_2Cl_4 + CH_2{=}CHCH{=}CH_2 \rightarrow \underset{\textbf{(XV)}}{Cl_2BCH_2CH{=}CHCH_2BCl_2} \xrightarrow{B_2Cl_4} Cl_2BCH_2\underset{Cl_2B}{CH}{-}\underset{BCl_2}{CH}CH_2BCl_2$$

Cautious hydrolysis of **XV** followed by oxidation with H_2O_2 gives wholly *cis*-1,4-dihydroxy-2-butene. Methyl-substituted conjugated or cumulated dienes rapidly polymerize in the presence of diboron tetrahalides (*51*). Allene itself will undergo both 1 : 1 and 2 : 1 addition with diboron tetrachloride (*47*).

$$H_2C{=}C{=}CH_2 + B_2Cl_4 \rightarrow CH_2{=}C(BCl_2)CH_2BCl_2 \xrightarrow{B_2Cl_4} BCl_2CH_2C(BCl_2)_2CH_2BCl_2$$

$$CH_2{=}C(BCl_2)CH_2BCl_2 \xrightarrow[(1\ mol)]{Br_2} CH_2{=}C(BCl_2)CH_2Br$$

$$CH_2{=}C(BCl_2)CH_2BCl_2 \xrightarrow[(excess)]{Br_2} BrCH_2CBr_2CH_2Br$$

With ferrocene, diboron tetrachloride undergoes substitution rather than addition to form ferrocenyldichloroborane, $C_5H_5FeC_5H_4BCl_2$ (**XVI**). The other product, $HBCl_2$, also reacts with ferrocene to give **XVI** and hydrogen; this latter process is cyclic because H_2 gives more dichloroborane with unchanged diboron tetrachloride. A simpler process by which to make **XVI** is to treat boron trichloride with ferrocenyl mercurichloride in hexane (*73*). Diboron tetrafluoride fails to react with ferrocene (*104*).

C. Properties of B_2X_4–Hydrocarbon Addition Products

In the main, B_2X_4–hydrocarbon addition products are thermally stable but water-sensitive, colorless solids or liquids; among the least stable are the products derived from methylenecyclopropane and vinylcyclopropane; they decompose at or around room temperature (*50*). On heating, loss of boron trihalide occurs with, usually, the formation of complex mixtures of products (e.g., *20, 84*); atypically, 1,2-bis(dichloroboryl)-1-trichlorostannylethane decomposes almost quantitatively to three well-defined products at 100°C (*20*).

$$Cl_2BCH_2CH(BCl_2)SnCl_3 \rightarrow CH_2{=}CHBCl_2 + BCl_3 + SnCl_2$$

At 400°C, 1,2-bis(dichloroboryl)ethane undergoes rapid charring, and from among the many products it is possible to isolate low yields of the crystalline hexachlorohexaboroadamantane (*107*).

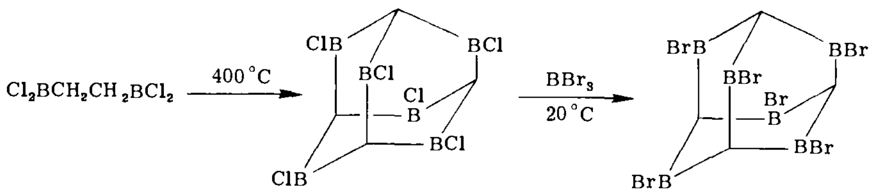

The overall stability of 1,2-bis(dichloroboryl)-1-divinylborylethane allows both vinylic double bonds to be hydrogenated, using a Raney nickel catalyst, and the vinyl groups to be exchanged for chloride or dimethylamino (*57*).

$$(CH_2{=}CH)_2B\underset{\substack{|\\ BCl_2}}{C}HCH_2BCl_2 + BX_3 \rightarrow X_2B\underset{\substack{|\\ BCl_2}}{C}HCH_2BCl_2 + (CH_2{=}CH)_2BX$$

$$X = Cl, NMe_2$$

The addition products contain trigonal boron atoms and thus can be expected to react with Lewis bases such as trimethylamine (*9, 84, 117*) and dimethyl ether (*9*). In some cases, however, simple adducts are not obtained. The decomposition of 1,1,2,2-tetrakis(difluoroboryl)ethane is promoted by trimethylamine, and Me_3NBF_3 is the only identifiable product (*56*). At room temperature 2 mol of trimethylamine are taken up by 1,2-bis(difluoroboryl)-1-divinylborylethane in a typical acid–base reaction

$$(CH_2{=}CH)_2B\underset{\substack{|\\ BF_2}}{C}HCH_2BF_2 + 2NMe_3 \rightarrow (CH_2{=}CH)_2B\underset{\substack{|\\ F_2BNMe_3}}{C}HCH_2BF_2NMe_3$$

But at 80°C in the presence of another mole of base, dehydroboration occurs (*57*).

$$(CH_2{=}CH)_2B\underset{\substack{|\\ F_2BNMe_3}}{C}HCH_2BF_2NMe_3 + NMe_3 \rightarrow$$
$$(CH_2{=}CH)_2BHNMe_3 + Me_3NBF_2CH{=}CHBF_2NMe_3$$

The decomposition is even more complex when 1,2-bis(dichloroboryl)-1-divinylborylethane is used, because the intermediate compound $Cl_2BCH{=}CHBCl_2$, unlike the corresponding fluoride, releases acetylene in the presence of trimethylamine

$$Cl_2BCH{=}CHBCl_2 + 2NMe_3 \xrightarrow{120°C} C_2H_2 + Me_3NBCl_3 + 1/n(Me_3NBCl)_n$$

so that the overall reaction then becomes (*57*)

$$(CH_2{=}CH)_2BCH(BCl_2){-}CH_2BCl_2 + 3Me_3N \rightarrow Me_3NBCl_3 + Me_3NBH(CH{=}CH_2)_2 + C_2H_2 + 1/n(Me_3NBCl)_n$$

The BCl_2 groups of the B_2Cl_4 addition compounds behave normally and undergo typical substitution reactions.

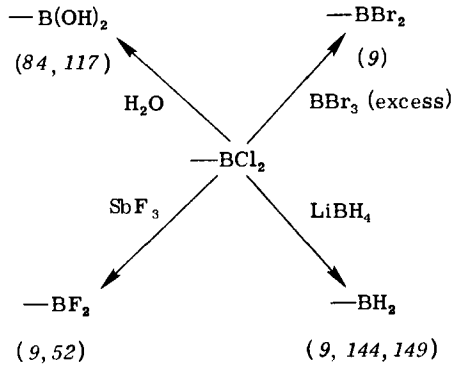

Sometimes when there are several BCl_2 groups to substitute, as in 1,1,2,2-tetrakis(dichloroboryl)ethane, the antimony trifluoride reaction fails and a better fluorinating agent in this case was found to be diboron tetrafluoride (*56*). Attempted methylation of 1,2-bis(dichloroboryl)ethylene with tetramethyllead at room temperature gave trimethylborane as the only identifiable boron compound (*55*).

$$C_2H_2(BCl_2)_4 + 2B_2F_4 \rightarrow C_2H_2(BF_2)_4 + 2B_2Cl_4$$

A typical reaction of dihydroxyborylethanes, formed by hydrolysis of the corresponding chlorides, is that on heating they lose the carbon backbone to form saturated alkanes, sometimes quantitatively. Similarly, some dihydridoboryl derivatives are pyrolyzed with (apparently stereospecific) release of hydrocarbon.

$$2[(HO)_2B]_2CHCH_2B(OH)_2 \xrightarrow{200°C} 3B_2O_3 + 3H_2O + C_2H_6 \quad (57)$$

$$[(HO)_2B]_2CHCH[B(OH)_2]_2 \longrightarrow 2B_2O_3 + 2H_2O + C_2H_6 \quad (56)$$

$$Me_3CCH(BX_2){-}CHMe_3(BX_2) \rightarrow B_2X_6 + \textit{trans}\text{-}Me_2CCH{=}CHCMe_3$$

X = H, D (50–70% yield) (*144, 149*)

Starting with bifunctional trimethylsilyl derivatives, $(Me_3Si)_2X$, and bis(dichloroboryl) compounds, Haubold has succeeded in making a variety of heterocycles by a Me_3SiCl extrusion reaction (*49*).

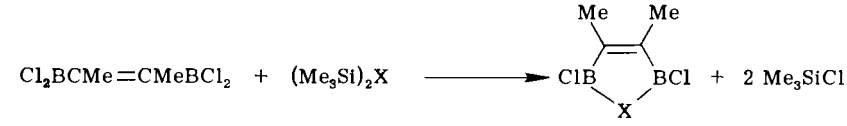

X = S, NMe, MeNNMe

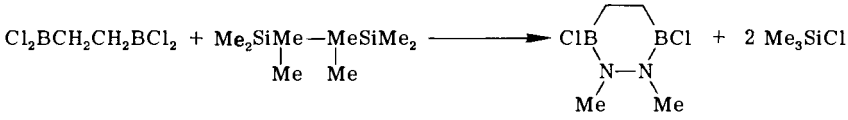

Cleavage of the B—C bonds in dihaloboryl derivatives by either propionic acid or alkaline peroxide is widely used as a diagnostic aid to structure determination. However, the products in a few cases are not always those anticipated.

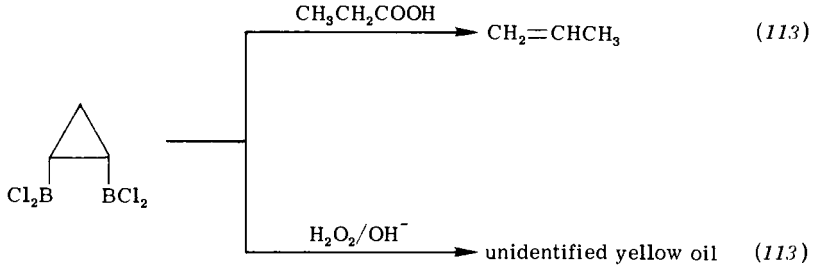

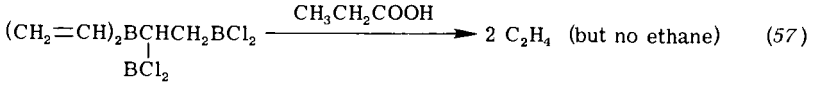

The nonstereospecific nature of the propionic acid reaction, when applied to the cleavage of $Cl_2BCH{=}CHBCl_2$ (*19*), was referred to in Section V,B.

The transformation of *cis*-bis(dichloroboryl)ethylene into the trans isomer on irradiation (*19*) is accompanied by a side reaction that produces about a 15% yield of $HC{\equiv}CBCl_2$; treatment of this chloride with antimony trifluoride gives $HC{\equiv}CBF_2$, which releases acetylene when

heated with propionic acid. A microwave-spectral study of ethynyldifluoroborane gave the following parameters (*110*).

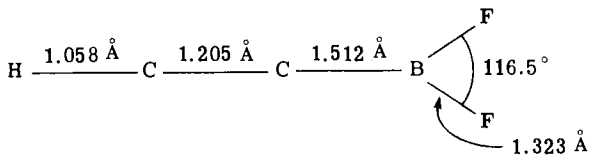

Assignments have been made of the bands in the vibrational spectra of $F_2BCH{=}CHBF_2$ (*52*), $F_2BCH_2CH_2BF_2$ (*124*), $Cl_2BCH{=}CHBCl_2$ (*52, 115*), and $Cl_2BCH_2CH_2BCl_2$ (*124*).

D. Triboron Pentafluoride (B_3F_5)

The air- and water-sensitive compound triboron pentafluoride, the first reported (*126*) to have a simple chain of three boron atoms, melts between −55 and −50°C. Decomposition is very rapid above −30°C and produces mainly B_2F_4 and B_8F_{12}. Carbon monoxide apparently catalyzes this decomposition, because reaction occurs even at temperatures as low as −70°C to form $OCB(BF_2)_3$ and B_2F_4, the carbonyl arising from interaction of CO with B_8F_{12} (see following discussion).

Hydrogen reacts rapidly with B_3F_5 at temperatures from −70°C upward to give a mixture of HBF_2, B_2F_4, and B_2H_6, together with a nonvolatile BF polymer.

A smooth reaction occurs at −100°C with liquid tetrafluoroethylene to produce fair yields of *cis*-1,2-bis(difluoroboryl)difluoroethylene, $CF(BF_2){=}CF(BF_2)$; above −100°C the C_2F_4 is explosively polymerized by triboron pentafluoride. No reaction occurs with hexafluorobenzene.

E. Dodecafluorooctaborane(12) (B_8F_{12})

As found with most boron–fluorine derivatives containing B—B bonds, B_8F_{12} reacts explosively with air and water; the only inert solvents appear to be liquid B_2F_4 or B_3F_5. No crystalline state of B_8F_{12} has yet been obtained; below −90°C the glassy solid is faintly yellow. On warming, a bright yellow liquid is formed, the viscosity of which decreases with increasing temperature until at about −20°C it is fairly mobile; the vapor is intensely yellow-brown. The visible spectrum of the gas shows a broad peak at 345 nm, and then an intense maximum starts at 320 nm and extends well into the ultraviolet region (*70*).

TABLE V

^{11}B-NMR CHEMICAL SHIFTS OF BORON SUBHALIDES AND THEIR DERIVATIVES[a]

Compound	^{11}B-NMR shift (relative to BF_3OEt_2)	Reference	Comments
B_2F_4	−23.0	(*52, 70*)	
B_2Cl_4	−62.4 ± 0.1	(*25, 52*)	
B_2Br_4	−70.0	(*75*)	
MeClBBClMe	−91.0	(*128*)	
B_3F_5	−25	(*70*)	
B_8F_{12}	−25	(*70*)	Peak width, 800 Hz
B_4Cl_4	−85.0 ± 0.3	(*25*)	Temperature range −78 to +118°C; peak width, Hz (°C): 35 (−78°); 16–18 (25°C); 8 (118°C)
$B_4(t\text{-Bu})_4$	−135.1	(*26*)	
B_7Br_7	−69.5	(*75*)	
B_8Br_8	−67.3	(*75*)	
B_9Br_9	−60.4	(*75*)	Peak width ~30 Hz at −60°C
$B_{10}Br_{10}$	−65.2	(*75*)	
$B_9Br_9^{2-}$	−0.77; −8.15	(*143*)	
MeB_9Br_8	−62.2	(*118*)	τ, ^1H = 10.06
$MeEtB_9Br_7$	−62.4	(*118*)	Shoulder slightly to lower field; τ, ^1H = 10.06(Me); 10.10(CH_3, Et); 10.16(CH_2, Et)
$Cl_2BCH{=}CHBCl_2$	−54.0	(*52*)	
$Cl_2BCH_2CH_2BCl_2$	−63.0	(*52*)	
$Cl_2BCMe_3CHCHCMe_3BCl_2$	−64.0	(*144*)	
$Cl_2BCMe_3CHCHMeBCl_2$	−64.9	(*144*)	
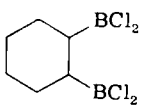	−65.0	(*144*)	

(*continued*)

TABLE V (*continued*)

Compound	^{11}B-NMR shift (relative to BF_3OEt_2)	Reference	Comments
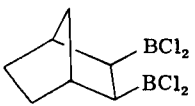	−59.7	(*144*)	
$F_2BCH{=}CHBF_2$	−23.0	(*32*, *52*)	J_{BF} = 64 (*52*); 58 Hz (*32*)
$F_2BCH_2CH_2BF_2$	−29.5	(*52*)	J_{BF} = 76 Hz
$Me_3CC(H)(BH_2)C(H)(BH_2)CMe_3$	−25	(*149*)	
$(Cl_2B)_2CCl_2$	−53.1	(*32*)	
$(Cl_2B)_3CCl$	−54.1	(*32*)	
$(Cl_2B)_4C$	−57.2	(*32*)	
$(BF_2)_2C{=}C{=}C(BF_2)_2$	−23.5	(*32*)	
$FB(CH{=}CHBF_2)_2$	−23.0	(*127*)	Single broad peak
$(BF_2)_2C{=}C(BF_2)_2$	−23.0	(*32*)	
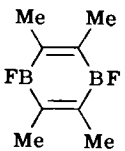	−40.2	(*82a*)	
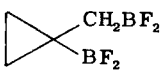	−27.3	(*50*)	1:2:1 triplet, J_{BF} = 68 Hz
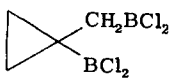	−59.5	(*50*)	

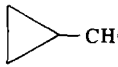	−27.1; −30.5	(*50*)	Relative intensity 1 : 1; broad
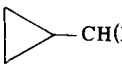	−58.5	(*50*)	Broad
$Cl_2BCH_2CH{=}CHCH_2BCl_2$	−58	(*51*)	
$Cl_2BCH_2CH(BCl_2)CH(BCl_2)CH_2BCl_2$	−59.0	(*51*)	Single broad peak
$B_2(O_2C_2H_4)_2$	−31.5	(*97, 141*)	
$B_2(S_2C_2H_4)_2$	−68.3	(*97, 141*)	
$B_2(O_2C_3H_6)_2$	−28.6	(*97, 141*)	
$B_2(O_2C_6H_4)_2$	−30.7	(*97, 141*)	
$B_2Cl_2(O_2C_2H_4)$	−30.8	(*97, 141*)	
$B_2Cl_2(S_2C_2H_4)$	−67.8	(*97, 141*)	
$B_2[(NMe)_2C_2H_4]_2$	−33.7	(*97, 141*)	
$B_2[(NH)_2C_6H_4]_2$	−27.9	(*97, 141*)	
Cl_3SiBCl_2	−63.0	(*70*)	
F_3SiBF_2	−28.0	(*70*)	
Cl_3SiBCl_2	−63	(*70*)	

	3-Coordinate B	4-Coordinate B	Reference	
$(Cl_3Si)_2(BCl_2)BCO$	−70	+20	(*70*)	
$(Si_2F_5)(SiF_2)(BF_2)BPF_3$	−30	+52	(*70*)	
$(Cl_3Si)_2(BF_2)BPF_3$	−30	+36	(*70*)	
$(BF_2)_3BPF_3$	−32	+49	(*70*)	
$B_2F_4 \cdot 2NMe_3$	—	+ 6.7	(*3*)	
$B_2F_4 \cdot 2NEt_3$	—	+ 8.3	(*3*)	
$B_2F_4 \cdot NMe_3NEt_3$	—	+ 8.4	(3)	Single very broad peak
$B_2F_4 \cdot NMe_3$	+11.7		(*3*)	Single broad peak

[a] For the shifts of other diboron compounds not synthesized from the subhalides, see Table L in Nöth and Wrackmeyer (*97*).

TABLE VI

^{19}F-NMR CHEMICAL SHIFTS OF BORON SUBFLUORIDES AND THEIR DERIVATIVES

Compound	^{19}F-NMR shift (relative to $CFCl_3$ unless specified)	Reference
B_2F_4	+55.7	(70)
B_3F_5	−26.2 (BF); +61.0 (BF_2)	(126)
B_8F_{12}	+44.1	(70)
F_3SiBF_2	+40.9 (BF_2)	(70)
$(Si_2F_5)(SiF_3)(BF_2)BPF_3$	+33.5 (BF_2)	(70)
$(Cl_3Si)_2(BF_2)BPF_3$	+35.2 (BF_2)	(70)
$(BF_2)_3BPF_3$	+37.4 (BF_2)	(70)
$(BF_2)_3BCO$	+38.4	(70)
$(BF_2)_3BPCl_3$	+40.3	(70)
$(BF_2)_3BPH_3$	+43.5	(70)
$(BF_2)_3BSMe_2$	+46.8	(70)
$(BF_2)_3BNMe_3$	+44.0	(48)
$F_3PB(BF_2)_{3-n}(BF_2 \cdot NMe_3)_n$	n = 1: +132.8 (complexed BF_2); +43.5 (free BF_2)	(48)
	n = 2: +133.1 (complexed BF_2); +41.9 (free BF_2)	(48)
	n = 3: +126.8; 130.7 (complexed BF_2)	(48)
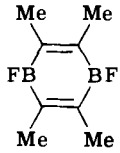	+67.8	(82a)
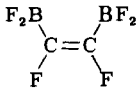	+80.6 (BF_2); +158 (CF)	(126)
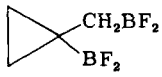	+2.7; −12 (relative to CF_3COOH)	(50)
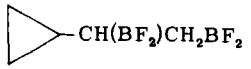	+9.6; −0.5 (relative to CF_3COOH)	(50)

The vapor pressure is about 23 Torr at 0°C, but decomposition is quite rapid at this temperature. Although pure B_8F_{12} shows no ESR spectrum at −50°C, partially decomposed samples contain unidentified paramagnetic species that produce a complex spectrum. There appears to be no dissociation of the vapor to free $B(BF_2)_3$ (70).

The single broad peak observed in the ^{19}F-NMR spectrum between

−80 and 0°C suggests that an exchange process is occurring to make all the BF_2 groups in structure **VI** equivalent on the NMR time scale. The single ^{11}B-NMR peak (800 Hz wide) may result from coincidence between the chemical shifts of the three types of boron atom (*70*).

Only BF_3 adducts are formed when B_8F_{12} is treated with an excess of strong Lewis bases such as diethyl ether, trimethylamine, and acetonitrile (*70*). However, there is some NMR evidence for the formation of the unstable $Me_3N—B(BF_2)_3$ when B_8F_{12} is treated with a deficiency of trimethylamine at low temperatures. A little boron trifluoride is released during the reaction, and this remains uncomplexed, showing that $B(BF_2)_3$ is a stronger Lewis acid than BF_3 toward trimethylamine, a point apparently confirmed by the values of the complexation shifts of the protons in $Me_3N \cdot B(BF_2)_3$ and $Me_3N \cdot BF_3$ relative to those in free NMe_3 [0.81 and 0.45 ppm, respectively (*48*)].

In contrast, "soft" bases such as carbon monoxide symmetrically cleave B_8F_{12} and form thermally stable complexes. Other bases that

$$B_8F_{12} + 2CO \rightarrow 2OCB(BF_2)_3 \qquad (69, 70, 126)$$

react similarly are PF_3 (*126*), PCl_3, PH_3, AsH_3, and SMe_2 (*70*). The complex $F_3PB(BF_2)_3$ has the structure shown in **XVII** (27) (Table VII).

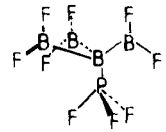

Approximately C_{3v} symmetry; Bond lengths (Å; ± 0.015): B—B = 1.68; B—F = 1.305; B—P = 1.825; P—F = 1.51

(XVII)

Attempts to investigate the relative base strengths of the ligands toward $B(BF_2)_3$ have failed because replacement reactions between an adduct and a different base do not occur; in all cases the original

TABLE VII

PHYSICAL DATA FOR $B(BF_2)_3$ ADDUCTS

Adduct	Vapor pressure[a]	Melting point (°C)	Reference
$(BF_2)_3BCO$	$A = -2078$; $B = 8.742$	40	(*70, 126*)
$(BF_2)_3BPF_3$	$A = -2008$; $B = 8.665$	55	(*70, 126*)
$(BF_2)_3BPCl_3$	10 Torr at 59°C	134	(*70*)
$(BF_2)_3BPH_3$	10 Torr at 53°C	112	(*70*)
$(BF_2)_3BSMe_2$	10 Torr at 43°C	107	(*70*)

[a] Log p (Torr) = $A/T + B$.

adduct was the only one to be recovered (*70*). However, competition reactions between B_8F_{12} and equimolar amounts of CO and PF_3 give the respective adducts in approximately equal amounts (*69*). The range of bases complexing with $B(BF_2)_3$ shows it to be an even stronger acid than BH_3, prompting Timms to call it a *super acid*. The rather large 5.9-ppm shift to high field in the ^{19}F resonance of B_8F_{12} dissolved in CH_2Cl_2, relative to its position in the free liquid or $CFCl_3$ solution, suggests that B_8F_{12} may even interact weakly with the chlorine atoms of dichloromethane (*48*).

The other three boron atoms in $B(BF_2)_3$ can be made to complex with trimethylamine once the acid has been stabilized by coordination of PF_3 to the unique boron. Thus low-temperature NMR studies on the reaction of **XVII** with trimethylamine indicate the formation of all three adducts in the series $F_3PB(BF_2NMe_3)_n(BF_2)_{3-n}$ (n = 1, 2, or 3). The n = 1 adduct is stable, whereas the n = 2 and 3 complexes dissociate on warming; a high NMe_3 : **XVII** ratio is required to shift the equilibrium in favor of the n = 3 complex, even at −90°C. Two ^{19}F-NMR peaks are observed when the n = 3 complex is held at −90°C, but these are found to coalesce at about −85°C. This behavior may be due to the adoption of the preferred conformation **XVIII**, in which the bulky NMe_3 groups coordinate in the "equatorial" positions, giving rise to

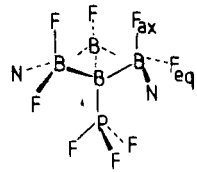

N = NMe_3

(**XVIII**)

two types of fluorine, F_{ax} and F_{eq}; hindered rotation about the B—B bonds is then assumed to be slow on the ^{19}F-NMR time scale at −90°C. The phenomenon was not observed with either the n = 1 and 2 complexes or free B_8F_{12} (*48*).

Tetrafluorohydrazine and B_8F_{12} explode when mixed together at −70°C, giving boron trifluoride and nitrogen; the latter does not react with B_8F_{12} (*69*). Sulfur tetrafluoride forms an explosive, slightly volatile solid of unknown composition when treated with B_8F_{12} (*69, 70*). Nonvolatile solids and small quantities of $PF_3B(BF_2)_3$ are the only products from the reaction between B_8F_{12} and $P(PF_2)_3$ (*70*). Hydrogen and B_8F_{12} give nonvolatile solids, BF_3 and HBF_2 (*70*).

F. Other Boron Fluorides

At least five boron fluorides having molecular weights greater than that of B_8F_{12} have been detected. They are formed in very small amounts as by-products in B_2F_4 and B_3F_5 production or arise from the decomposition of simpler boron fluorides. Their volatilities are similar, all of them condensing in a −40°C trap (*69*). From their ^{19}F-NMR spectra it would appear that none of them possesses any

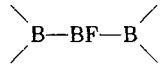

groups, because the only resonances occur between +30 and +45 ppm (relative to $CFCl_3$), the region typical of BF_2 groups (*131*).

1. Compound A

The best characterized (*69*) of the five is a clear, colorless liquid arising from the decomposition of B_8F_{12}. Broad, strong peaks occur in the infrared spectrum at 1160, 1210, 1230, and 1390 cm^{-1}; the highest, but very weak, mass-spectral peak is due to $B_{12}F_{16}^+$, with the base peak corresponding to $B_{10}F_8^+$. At 15 eV, two series of peaks are observed due to the ions $B_8F_6^+$, $B_9F_9^+$, $B_{10}F_{12}^+$, and $B_9F_5^+$, $B_{10}F_8^+$, $B_{11}F_{11}^+$, $B_{12}F_{14}^+$.

The B : F ratio, determined by thermal decomposition into elemental boron and boron trifluoride, is 0.85 ± 0.05. Three broad singlets occur in the ^{19}F-NMR spectrum at +31.9, +37.1, and +45.8 ppm (relative to $CFCl_3$ contained in an internal capillary).

It has been suggested (*131*) that this compound may be $B_{14}F_{18}$, a formal analog of B_5H_9 in which both terminal and bridging hydrogen atoms are replaced by BF_2 groups. (As described in Section II, the boron subfluorides tend not to exhibit a molecular ion in their mass spectra.)

2. Compound B

Compound B (*69*), a liquid, was isolated from the products of cocondensation of BF and B_2F_4 in an all-glass system (only minute amounts were observed when a stainless steel apparatus was used). Relatively sharp peaks occur at 1160, 1230, 1245, 1385, and 1435 cm^{-1} in its infrared spectrum.

The mass spectrum is particularly complex, with 17 ions having a relative intensity above 20% at 30 eV. The 15-eV spectrum shows the

same two series of peaks as compound A plus a third series starting at $B_8F_5^+$ and including $B_9F_8^+$, $B_{10}F_{11}^+$, and $B_{11}F_{14}^+$; the highest mass ion observed is $B_{12}F_{14}^+$, and the B:F ratio is 0.89 ± 0.05.

3. Compound C

The use of a stainless steel apparatus for B_8F_{12} production leads to the formation of compound C (*69*), a yellow solid, as a by-product. Its infrared spectrum is similar to that of A, with broad absorptions centered at 760, 812, and 843 cm^{-1} as weak secondary features. Only very small peaks are observed in the mass spectrum for ions heavier than $B_{10}F_{12}^+$, with $B_{12}F_{17}^+$ being the maximum; the 15-eV spectrum consists of only six peaks, four of them, corresponding to $B_7F_3^+$, $B_8F_6^+$, $B_9F_9^+$, and $B_{10}F_{12}^+$, related by loss of BF_3. This series of ions does not occur in the other fluorides.

4. Compounds D and E

Compounds D and E (*69*) are formed in the glass BF-production apparatus and have not been completely separated. The most volatile fraction shows a set of BF_3-related ions $B_6F_4^+$, $B_7F_7^+$, and $B_8F_{10}^+$, whereas the least volatile component is similar but has an additional series of peaks due to $B_{10}F_6^+$, $B_{11}F_9^+$, and $B_{12}F_{12}^+$. This latter fraction has an intense $B_{12}F_{12}^+$ peak at 15 eV, but the presence of $B_{13}F_{12}^+$ shows that at least 13 boron atoms are present.

The reason why fluorine behaves so differently from the other halogens regarding the formation of these curious subfluorides is not known.

G. Tetraboron Tetrachloride (B_4Cl_4)

Tetraboron tetrachloride melts sharply under vacuum at 95°C (*25, 65*). A redetermination of the vapor pressure between 26.3 and 63.5°C shows that the pressure may be reproduced accurately by the equation

$$\log p \text{ (Torr)} = -3455/T + 11.5398,$$

the values being consistently lower than those previously published. From these data the heat of sublimation has been calculated as 15.81 kcal mol^{-1} (*92*). The vapor pressure of about 1 Torr at room temperature allows B_4Cl_4 to be handled in a conventional vacuum line, provided that greaseless valves are used.

The compound is also much more thermally stable than has previously been supposed. It can be recovered unchanged after many days at 60–65°C (*92*) or 3 days at 154°C (*7*); even at 240–275°C in the gas phase less than 10% decomposition occurs during 10 min (*92*). In the liquid state 10% decomposition occurs after 6 h at 125°C, and 80% after 28 h at 152°C (*25*). After 6 h at 320°C, complete decomposition occurs to give boron trichloride, involatile debris, and a slightly volatile, yellow solid (*7*) (probably B_9Cl_9, judging from its description).

There is no evidence of any fluxionality as measured on the ^{11}B-NMR time scale over a 200°C temperature range (*25*).

Tetraboron tetrachloride is pyrophoric at room temperature. A close study of the oxidation reaction under more controlled conditions in a solvent has shown that the products are boron trichloride, boric oxide, and an unidentified, red boron monochloride; when a deficiency of oxygen is used some diboron tetrachloride also appears to be formed (*92*).

Although hydrogen sulfide does not react with tetraboron tetrachloride between −112°C and room temperature, water rapidly produces hydrogen, hydrogen chloride, boric acid and subboric acid (*92*). Acid hydrolysis gives 3 mol of hydrogen, and alkaline hydrolysis 4 mol (*133*).

A variety of substitution reactions have been attempted on B_4Cl_4, but most have been without much success. Lithium tetrahydroborate gave only about a 3% yield of diborane after 40 h at room temperature (*92*). Trimethylborane does not react below 65°C; trimethylborane was the only identified boron-containing product when trimethylaluminum (*92*), tetramethyllead (*55*), and dimethylzinc (*92*) were used as methylating agents; the latter reagent had previously been claimed to give B_4Cl_3Me (*134*). Substitution of alkyl groups onto the B_4 cage is more readily accomplished using organolithium reagents. Thus ethyllithium gives B_4Cl_3Et and $B_4Cl_2Et_2$, whereas $B_4(CMe_3)_4$ can be achieved using *t*-butyllithium (*26*). No B_4F_4 is formed when tetraboron tetrachloride is treated with BF_3, SbF_3, PbF_2, or TiF_4 (*86, 92*); the latter three reagents produce only boron trifluoride. Boron tribromide gives chlorobromoboranes and much solid debris (*66, 92*) together with tiny amounts of B_4Cl_3Br and $B_4Cl_2Br_2$ (*66*); further substitution by bromine does not appear to be possible.

Cleavage of the B_4 tetrahedron occurs when B_4Cl_4 is treated with the halogens. Controlled reactions with chlorine and bromine give some of the corresponding diboron tetrahalides in addition to the trihalides (*92, 140*). Any diboron tetraiodide formed on iodination apparently decomposes during the 3 weeks of reaction time to give an unidentified black solid thought to be $(BI)_y$ (*92*).

Trimethylamine, triethylamine, pyridine, and tetramethylethylenediamine react with B_4Cl_4 to give solid products, but no meaningful stoichiometries could be established. Although qualitative tests showed that the solids possessed boron–boron bonds, their structures remain in doubt (*92*). No evidence for simple adducts was obtained when B_4Cl_4 was treated with dimethyl or diethyl ethers; methyl or ethyl chloride and glassy, unidentified solids were the major products (*92*).

H. B_8Cl_8, B_9X_9, $B_{10}Cl_{10}$, AND $B_{11}Cl_{11}$

Little is known about the chemistry of B_8Cl_8, B_9X_9, $B_{10}Cl_{10}$, or $B_{11}Cl_{11}$. Complete exchange of chlorine for bromine occurs in B_8Cl_8 and B_9Cl_9 when they are heated with aluminum tribromide at 100 and 265°C, respectively (*83*). A range of mixed chlorobromides, $B_9Br_{9-n}Cl_n$, can be made by heating B_9Br_9 with tin or titanium tetrachlorides, but no halogen exchange occurs with BCl_3, BF_3, SbF_3, or TiF_4 (*108*). About 90% of the boron is recovered as trimethylborane when B_9Br_9 is added to trimethylaluminum at room temperature (*75*); partial methylation of the B_9 cage is possible using $SnMe_4$ or $PbMe_4$ (*75, 83, 108*).

The heated vapor of B_8Cl_8 ignites in air with a mild explosion (*83*). The air sensitivity of the B_9X_9 series decreases markedly from Cl to I, the iodide being stable for months in air (*142*); B_9Br_9 will withstand limited contact with degassed water under vacuum conditions (*108*). Chlorinated hydrocarbons, boron trichloride, and boron tribromide are among the best solvents for all the B_9X_9 derivatives; donor organic solvents produce a characteristic dark blue coloration with B_9I_9, due to the formation of $B_9I_9^-$ (*142*).

Mixtures of $B_{10}Cl_{10}$ and $B_{11}Cl_{11}$ give a variety of B_{10} and B_{11} chlorobromides when treated with aluminum tribromide in BBr_3 at 20°C (*109*). B_8Cl_8 and B_9Cl_9 show no reaction with chlorine at 70 and 250°C, respectively (*6*). When the $B_{10}Cl_{10}$–$B_{11}Cl_{11}$ mixtures are heated with dry chlorine, a contraction in cluster size occurs and high yields of B_9Cl_9 are produced (*6*); bromine and iodine give a number of mixed halides $B_9Cl_{9-n}X_n$ (X = Br, I) (*6*). $B_{10}Cl_{10}$ and $B_{11}Cl_{11}$ undergo a similar reaction with hydrogen to produce B_9Cl_8H and $B_9Cl_7H_2$, respectively (*6, 83*). Pyrolysis of $(H_3O)_2B_{10}Cl_{10}$ is known to give low yields of B_9Cl_8H (*38*); it is possible that this product arises via the initial formation of $B_{10}Cl_{10}$, which then undergoes reduction to B_9Cl_8H with hydrogen present in the system from hydrolysis of some of the boron cages. The mechanism by which B_9Cl_8Me and B_9Br_8Me arise from pyrolysis of either $(Me_4N)_2B_{10}Cl_{10}$ (*83*) or $(Me_4N)_2B_{10}Br_{10}$ (*118*) is less clear.

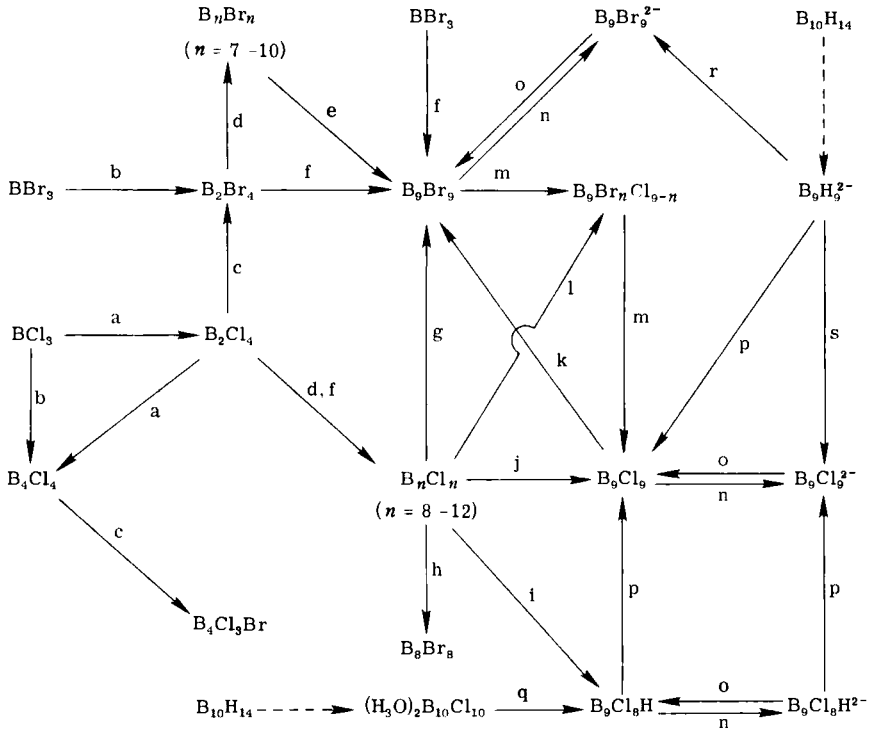

SCHEME 1. Interconversion reactions among the boron subchlorides and subbromides. a, Mercury discharge (*65*, *90*); b, radiofrequency discharge (*25*, *75*); c, BBr_3 at room temperature (*66*, *136*); d, thermal decomposition (*66*, *75*, *84*, *84*); e, pyrolysis at 200°C (*75*, *108*); f, silent electric discharge (*108*); g, BBr_3 at 250°C (*108*); h, $AlBr_3$ at 100°C (n = 8) (*83*); i, H_2 at 150°C (n = 10) (*6*, *83*); j, Cl_2 at 140°C (n = 10, 11) (*6*); k, $AlBr_3$ at 260°C (*83*); l, Br_2 at 115°C (n = 10, 11) (*6*); m, $TiCl_4$ or $SnCl_4$ at 250°C (*108*); n, $(Bu_4N)I$ (*143*); o, $Tl(OOCCF_3)_3$ (*143*); p, SO_2Cl_2 (*63*, *143*); q, pyrolysis at 260°C (*38*); r, *N*-bromosuccinimide (*143*); s, *N*-chlorosuccinimide (*143*).

Reduction of the B_9 halides occurs smoothly with tetrabutylammonium iodide in dichloromethane, giving first $B_9X_9^-$ and then $B_9X_9^{2-}$. Competition reactions of the type

$$B_9X_9 + B_9Y_9^- \rightarrow B_9X_9^- + B_9X_9$$

$$B_9X_9^- + B_9Y_9^{2-} \rightarrow B_9X_9^{2-} + B_9X_9^-$$

reveal that the oxidative power follows the order $B_9I_9 > B_9Br_9 > B_9Cl_9$ and $B_9I_9^- > B_9Br_9^- > B_9Cl_9^-$. Oxidation of the ions with thallium(III) trifluoroacetate releases the neutral boron cluster, thus establishing

the redox sequence (*142*, *143*)

$$B_9X_9^{2-} \rightleftharpoons B_9X_9^{-} \rightleftharpoons B_9X_9$$

The hydrogen-substituted derivative B_9Cl_8H undergoes a similar series of reactions (*143*). The paramagnetic $B_9X_9^{-}$ ions show featureless, broad ESR peaks at g values of 2.018, 2.080, and 2.191 (X = Cl, Br, and I, respectively), the breadth increasing from the chloride to the iodide (*143*).

It appears likely that all the B_9X_9 species have a very similar cage structure, that of a tri-capped trigonal prism (*61*, *108*, *142*, *143*). The HOMO in a B_9^{2-} cage has a_2' symmetry so that the B_9X_9, $B_9X_9^{-}$, and $B_9X_9^{2-}$ sequence will have outer electron configurations $(a_2')^0$, $(a_2')^1$, and $(a_2')^2$, respectively. Although B_9Cl_9, for example, has a closed-shell configuration, it has been pointed out by Wade (*100*) that the skeletal bonding will be greatest when the a_2' orbital is occupied, that is, when there are nine bonding pairs of electrons. In apparent agreement with this, the average B—B bond length in $B_9H_9^{2-}$ is 1.76 Å, compared with 1.81 Å in B_9Cl_9 (*100*). Similarly, the HOMO of dodecahedral B_8^{2-} has b_2 symmetry, so B_8Cl_8 has a closed-shell configuration, $(b_2)^0$; the various B—B bond lengths in $B_8H_8^{2-}$ are consistently shorter than those of B_8Cl_8, in keeping with the extra pair of cage-bonding electrons in the ion (*100*).

The HOMOs of a D_{4d} B_{10}^{2-} cage and an I_h B_{12}^{2-} cage are degenerate (e_1 and g_u, respectively). The neutral clusters $B_{10}X_{10}$ and $B_{12}X_{12}$ would thus be expected either to be paramagnetic or to undergo distortion to achieve spin-paired closed-shell electron configurations. The ^{11}B-NMR spectrum of $B_{10}Br_{10}$ consists of a single peak for sample temperatures down to −60°C; the obvious implication is that the molecule is fluxional, but there is nothing about the spectrum that suggests that the molecule is paramagnetic (*75*). All the cage MOs of B_{11}^{2-} (C_{2v} symmetry) are nondegenerate, hence a neutral $B_{11}X_{11}$ species should be diamagnetic and undistorted (*100*).

The list of possible binary halides is obviously not yet complete because there is mass-spectral evidence (*106*) that $B_{13}Cl_{13}$ and $B_{14}Cl_{14}$ exist among the decomposition products of diboron tetrachloride. Furthermore, there are indications that a dark red chloride of very low volatility (*6*) and a bromide (*75*) may possess structures in which two B_9 cages are linked together as $(B_9X_8)_2$. If such linked cages are generally possible then the theoretical number of halides yet to be found, because of isomers, is large indeed.

REFERENCES

1. Armstrong, D. R., Perkins, P. G., and Stewart, J. J., *J. Chem. Soc. A* p. 3674 (1971).
2. Ashcroft, B. W. C., Thesis, Liverpool University, Liverpool (1969).
3. Ashcroft, B. W. C., and Holliday, A. K., *J. Chem. Soc. A* p. 2581 (1971).
4. Atoji, M., and Lipscomb, W. N., *Acta Crystallogr.* **6,** 547 (1953).
5. Atoji, M., and Lipscomb, W. N., *J. Chem. Phys.* **31,** 601 (1959); Jacobson, R. A., and Lipscomb, W. N., *ibid.* p. 605; *J. Am. Chem. Soc.* **80,** 5571 (1958); Pawley, G. S., *Acta Crystallogr.* **20,** 631 (1966).
6. Awad, S. B., Prest, D. W., and Massey, A. G., *J. Inorg. Nucl. Chem.* **40,** 395 (1978).
7. Barr, J. B., Thesis, Pennsylvania State University, University Park (1961).
8. Becher, H. J., and Schnöckel, H., *Z. Anorg. Allg. Chem.* **379,** 136 (1970).
9. Biallas, M. J., *Inorg. Chem.* **10,** 1320 (1971).
10. Biffar, W., Nöth, H., and Pommerening, H., *Angew. Chem., Int. Ed. Engl.* **19,** 56 (1980).
11. Brennan, J. P., *Inorg. Chem.* **13,** 490 (1974).
12. Briggs, A. G., Massey, A. G., and Portal, P. J., unpublished work.
13. Briggs, A. G., Reason, M. S., and Massey, A. G., *J. Inorg. Nucl. Chem.* **37,** 313 (1975).
14. Brown, F. R., Miller, F. A., and Sourisseau, C., *Spectrochim. Acta, Part A* **32A,** 125 (1976); Miller, F. A., *Appl. Spectrosc.* **29,** 461 (1975).
15. Ceron, P., Finch, A., Frey, J., Kerrigan, J., Parsons, T. D., Urry, G., and Schlesinger, H. I., *J. Am. Chem. Soc.* **81,** 6368 (1959).
16. Chadha, R., and Ray, N. K., *J. Am. Chem. Soc.* (in press).
17. Chang, C. H., Porter, R. F., and Bauer, S. H., *Acta Crystallogr., Sect A* **A25,** S125 (1969); *J. Phys. Chem.* **74,** 1363 (1970).
18. Cowley, A. H., White, W. D., and Damasco, M. C., *J. Am. Chem. Soc.* **91,** 1922 (1969).
19. Coyle, T. D., and Ritter, J. J., *J. Am. Chem. Soc.* **89,** 5739 (1967).
20. Coyle, T. D., and Ritter, J. J., *J. Organomet. Chem.* **12,** 269 (1968).
21. Cyvin, S. J., *Z. Anorg. Allg. Chem.* **378,** 117 (1970).
22. Cyvin, S. J., and Elvebredd, I., *Z. Anorg. Allg. Chem.* **371,** 220 (1969).
23. Danielson, D. D., and Hedberg, K., *J. Am. Chem. Soc.* **101,** 3199 (1979).
24. Danielson, D. D., Patton, J. V., and Hedberg, K., *J. Am. Chem. Soc.* **99,** 6484 (1977).
25. Davan, T., and Morrison, J. A., *Inorg. Chem.* **18,** 3194 (1979).
26. Davan, T., and Morrison, J. A., *J. Chem. Soc., Chem. Commun.* p. 250 (1981).
27. DeBoer, B. G., Zalkin, A., and Templeton, D. H., *Inorg. Chem.* **8,** 836 (1969).
28. Dewar, M. J. S., and Rzepa, H. S., *J. Am. Chem. Soc.* **100,** 58 (1978).
29. Dibeler, V. H., and Liston, S. K., *Inorg. Chem.* **7,** 1742 (1968).
30. Dibeler, V. H., and Walker, J. A., *Inorg. Chem.* **8,** 50 (1969).
31. Diener, W., and Pflugmacher, A., *Angew. Chem.* **69,** 777 (1957).
32. Dobson, J. E., Tucker, P. M., Stone, F. G. A., and Schaeffer, R., *J. Chem. Soc. A* p. 1882 (1969).
33. Durig, J. R., Saunders, J. E., and Odom, J. D., *J. Chem. Phys.* **54,** 5285 (1971).
34. Durig, J. R., Thompson, J. W., Witt, J. D., and Odom, J. D., *J. Chem. Phys.* **58,** 5339 (1973).
35. Elkaim, J. C., Pace, S., and Riess, J. G., *J. Phys. Chem.* **84,** 354 (1980).
36. Finch, A., and Schlesinger, H. I., *J. Am. Chem. Soc.* **80,** 3573 (1958).
37. Fitzpatrick, N. J., *Inorg. Nucl. Chem. Lett.* **9,** 965 (1973).

38. Forstner, J. A., Haas, T. E., and Muetterties, E. L., *Inorg. Chem.* **3,** 155 (1964).
39. Fusstetter, H., Huffman, J. C., Nöth, H., and Schaeffer, R., *Z. Naturforsch., B: Anorg. Chem., Org. Chem.* **31B,** 2441 (1976).
40. Garrett, A. G., and Urry, G., *Inorg. Chem.* **2,** 400 (1963).
41. Gimarc, B. M., Khan, S. A., and Kohn, M. C., *J. Am. Chem. Soc.* **100,** 1996 (1978).
42. Greenwood, N. N., *Compr. Inorg. Chem.* **1,** 987 (1973).
43. Guest, M. F., and Hillier, I. H., *J. Chem. Soc., Faraday Trans.* **70,** 398 (1974).
44. Hall, J. H., Halgren, T. A., Kleier, D. A., and Lipscomb, W. N., *Inorg. Chem.* **13,** 2520 (1974).
45. Hall, J. H., and Lipscomb, W. N., *Inorg. Chem.* **13,** 710 (1974).
46. Hansen, J. D., Thesis, Oregon State University, Corvallis (1965).
47. Harng-Shen, Kuo, Thesis, Pennsylvania State University, University Park (1970).
48. Hartman, S. J., and Timms, P. L., *J. Chem. Soc., Dalton Trans.* p. 1373 (1975).
49. Haubold, W., and Gemmler, A., *Chem. Ber.* **113,** 3352 (1980).
50. Haubold, W., and Stanzl, K., *Chem. Ber.* **111,** 2108 (1978).
51. Haubold, W., and Stanzl, K., *J. Organomet. Chem.* **174,** 141 (1979).
52. Haubold, W., and Weidlein, J., *Z. Anorg. Allg. Chem.* **406,** 171 (1974).
53. Haubold, W., and Zurmühl, K., *Chem. Ber.* **113,** 2333 (1980).
54. Hedberg, K., *Trans. Am. Crystallogr. Assoc.* **2,** 79, (1966).
55. Holliday, A. K., and Jessop, G. N., *J. Chem. Soc. A* p. 889 (1967).
56. Holliday, A. K., Jessop, G. N., and Ottley, R. P., *J. Organomet. Chem.* **14,** 211 (1968).
57. Holliday, A. K., and Ottley, R. P., *Chem. Commun.* p. 336 (1969); *J. Chem. Soc, A* p. 886 (1971).
58. Holliday, A. K., and Taylor, F. B., *J. Chem. Soc.* p. 2731 (1964).
59. Holzmann, R. T., and Morris, W. F., *J. Chem. Phys.* **29,** 677 (1958).
60. Howell, J. M., and van Wazer, J. R., *J. Am. Chem. Soc.* **96,** 7902 (1974).
61. Hursthouse, M. B., Kane, J., and Massey, A. G., *Nature (London)* **228,** 659 (1970).
62. Jones, L. H., and Ryan, R. R., *J. Chem. Phys.* **57,** 1012 (1972).
63. Kabbani, R. M., and Wong, E. H., *J. Chem. Soc., Chem. Commun.* p. 462 (1978).
64. Kaim, W., Bock, H., Hawker, P., and Timms, P. L., *J. Chem. Soc., Chem. Commun.* p. 577 (1980); *Chem. Ber.* **113,** 3196 (1980).
65. Kane, J., and Massey, A. G., *Chem. Commun.* p. 378 (1970).
66. Kane, J., and Massey, A. G., *J. Inorg. Nucl. Chem.* **33,** 1195 (1971).
67. Kato, H., Yamaguichi, K., Yonezawa, T., and Fukui, K., *Bull. Chem. Soc. Jpn.* **38,** 2144 (1965).
68. Kettle, S. F. A., and Tomlinson, V., *J. Chem. Soc. A* p. 2002 (1969).
69. Kirk, R. W., Thesis, University of California, Berkeley (1969).
70. Kirk, R. W., Smith, D. L., Airey, W., and Timms, P. L., *J. Chem. Soc.* p. 1392 (1972).
71. Kirk, R. W., and Timms, P. L., *J. Am. Chem. Soc.* **91,** 6315 (1969).
72. Kleier, D. A., Bicerano, J., and Lipscomb, W. N., *Inorg. Chem.* **19,** 216 (1980).
73. Kotz, J. C., and Post, E. W., *J. Am. Chem. Soc.* **90,** 4503 (1968); *Inorg. Chem.* **9,** 1661 (1970).
74. Krenev, V. A., and Evdokimov, V. I., *Russ. J. Inorg. Chem. (Engl. Transl.)* **17,** 171 (1972).
75. Kutz, N. A., and Morrison, J. A., *Inorg. Chem.* **19,** 3295 (1980).
76. Lanthier, G. F., Kane, J., and Massey, A. G., *J. Inorg. Nucl. Chem.* **33,** 1569 (1971).
77. Lanthier, G. F., and Massey, A. G., *J. Inorg. Nucl. Chem.* **32,** 1807 (1970).
78. Lebreton, J., Ferran, J., Chatalic, A., Iacocca, D., and Marsigny, L., *J. Chim. Phys.* **71,** 587 (1974).

79. Lee, J. D., *Talanta* **20,** 1029 (1973).
80. Lin, C. T., and Atvars, T. D. Z., *J. Chem. Phys.* **68,** 4233 (1978).
81. Lloyd, D. R., and Lynaugh, N., *Chem. Commun.* p. 627 (1971).
82. Lynaugh, N., Lloyd, D. R., Guest, M. F., Hall, M. B., and Hillier, I. H., *J. Chem. Soc., Faraday Trans. 2* **68,** 2192 (1972).
82a. Maddren, P. S., Modinos, A., Timms, P. L., and Woodward, P., *J. Chem. Soc., Dalton Trans* p. 1272 (1975).
83. Markwell, A. J., Massey, A. G., and Portal, P. J., *Polyhedron* **1,** 134 (1982).
84. Massey, A. G., *Adv. Inorg. Chem. Radiochem.* **10,** 1 (1967).
85. Massey, A. G., *Chem. Br.* **16,** 588 (1980).
86. Massey, A. G., unpublishable work.
87. Massey, A. G., and Portal, P. J., *Polyhedron* **1,** 319 (1982).
88. Massey, A. G., and Urch, D. S., *Proc. Chem. Soc., London* p. 284 (1964).
89. Massey, A. G., and Urch, D. S., *J. Chem. Soc.* p. 6180 (1965).
90. Massey, A. G., Urch, D. S., and Holliday, A. K., *J. Inorg. Nucl. Chem.* **28,** 365 (1966).
91. Massey, A. G., and Zwolenik, J. J., *J. Chem. Soc.* p. 5354 (1963).
92. McHale, J. J., Thesis, Pennsylvania State University, University Park (1966).
93. Moore, E. B., *Theor. Chim. Acta* **7,** 144 (1967); *J. Chem. Phys.* **43,** 503 (1965).
94. Moore, E. B., and Lipscomb, W. N., *Acta Crystallogr.* **9,** 668 (1956).
95. Nimon, L. A., Seshadri, K. S., Taylor, R. C., and White, D., *J. Chem. Phys.* **53,** 2416 (1970).
96. Nöth, H., and Pommerening, H., *Chem. Ber.* **114,** 398 (1981).
97. Nöth, H., and Wrackmeyer, B., "Nuclear Magnetic Resonance Spectroscopy of Boron Compounds," p. 62. Springer-Verlag, Berlin and New York, 1978.
98. Odom, J. D., Kalasinsky, V. F., and Durig, J. R., *Inorg. Chem.* **14,** 434 (1975).
99. Odom, J. D., Saunders, J. E., and Durig, J. R., *J. Chem. Phys.* **56,** 1643 (1972).
100. O'Neill, M. E., and Wade, K., *Inorg. Chem.* **21,** 461 (1982).
101. Padmaja, K. M., and Aruldhas, G., *J. Phys. Chem. Solids* **36,** 563 (1975).
102. Patton, J. V., and Hedberg, K., *Bull. Am. Phys. Soc.* [2] **13,** 831 (1968).
103. Peach, M. E., and Waddington, T. C., *J. Chem. Soc. A* p. 180 (1968).
104. Post, E. W., Thesis, Kansas State University, Manhattan (1969).
105. Ramaswamy, K., and Kalyanaraman, S. B., *Indian J. Phys.* **51B,** 309 (1977).
106. Reason, M. S., Thesis, Loughborough University of Technology (1974).
107. Reason, M. S., Briggs, A. G., Lee, J. D., and Massey, A. G., *J. Organomet. Chem.* **77,** C9 (1974).
108. Reason, M. S., and Massey, A. G., *J. Inorg. Nucl. Chem.* **37,** 1593 (1975).
109. Reason, M. S., and Massey, A. G., *J. Inorg. Nucl. Chem.* **38,** 1789 (1976).
110. Ritter, J. J., Thesis, University of Maryland, College Park (1971).
111. Ritter, J. J., and Coyle, T. D., *J. Chem. Soc. A* p. 1303 (1970).
112. Ritter, J. J., Coyle, T. D., and Bellama, J. M., *J. Organomet. Chem.* **29,** 175 (1971).
113. Rosen, A., and Zeldin, M., *J. Organomet. Chem.* **31,** 319 (1971).
114. Rosenthaler, E., *Helv. Phys. Acta* **13,** 355 (1940).
115. Rudolph, R. W., *J. Am. Chem. Soc.* **89,** 4216 (1967).
116. Ryan, R. R., and Hedberg, K., *J. Chem. Phys.* **50,** 4986 (1969).
117. Saha, H. K., Glicenstein, L. J., and Urry, G., *J. Organomet. Chem.* **8,** 37 (1967).
118. Saulys, D., and Morrison, J. A., *Inorg. Chem.* **19,** 3057 (1980).
119. Schaeffer, R., Johnson, Q., and Kane, J., *J. Am. Chem. Soc.* **92,** 7614 (1970).
120. Schlüter, K., and Berndt, A., *Angew. Chem., Int. Ed. Engl.* **19,** 57 (1980).
121. Schram, E. P., and Urry, G., *Inorg. Chem.* **2,** 405 (1963).

122. Schumb, W. C., Gamble, E. L., and Banus, M. D., *J. Am. Chem. Soc.* **71,** 3225 (1949).
123. Sharpe, A. G., "Inorganic Chemistry," p. 641. Longmans, Green, New York, 1981.
124. Shriver, D. F., Jackovitz, J. F., and Biallas, M. J., *Spectrochim. Acta, Part A* **24A,** 1469 (1968).
125. Stone, A. J., *Inorg. Chem.* **20,** 563 (1981).
126. Timms, P. L., *J. Am. Chem. Soc.* **89,** 1629 (1967).
127. Timms, P. L., *J. Am. Chem. Soc.* **90,** 4585 (1968).
128. Timms, P. L., *Chem. Commun.* p. 1525 (1968).
129. Timms, P. L., *J. Chem. Soc., Dalton Trans.* p. 830 (1972); *Inorg. Synth.* **19,** 74 (1979).
130. Timms, P. L., *Adv. Inorg. Chem. Radiochem.* **14,** 145 (1972).
131. Timms, P. L., *Acc. Chem. Res.* **6,** 118 (1973).
132. Timms, P. L., *in* "Cryochemistry" (M. Moskovits, and G. A. Ozin, eds.), p. 61. Wiley (Interscience), New York, 1976.
133. Urry, G., *in* "The Chemistry of Boron and its Compounds" (E. L. Meutterties, ed.), p. 325. Wiley, New York, 1967.
134. Urry, G., Garrett, A. G., and Schlesinger, H. I., *Inorg. Chem.* **2,** 396 (1963).
135. Urry, G., Schram, E. P., and Weissman, S. I., *J. Am. Chem. Soc.* **84,** 2654 (1962).
136. Urry, G., Wartik, T., Moore, R. E. and Schlesinger, H. I., *J. Am. Chem. Soc.* **76,** 5293 (1954).
137. Waddington, T. C., *Trans. Faraday Soc.* **63,** 1313 (1967).
138. Wagman, D. D., Evans, W. H., Parker, V. B., Halow, I., Bailey, S. M., and Schumm, R. H., *NBS Tech. Note (U.S.)* **270-3** (1968).
139. Wartik, T., and Grassenheimer, B., *Inorg. Chem.* **10,** 650 (1971).
140. Wartik, T., and McHale, J. M., *Inorg. Nucl. Chem. Lett.* **1,** 113 (1965).
141. Welch, C. N., and Shore, S. G., *Inorg. Chem.* **7,** 225 (1968).
142. Wong, E. H., *Inorg. Chem.* **20,** 1300 (1981).
143. Wong, E. H., and Kabbani, R. M., *Inorg. Chem.* **19,** 451 (1980).
144. Zeldin, M., Thesis, Pennsylvania State University, University Park (1966).
145. Zeldin, M., Gatti, A. R., and Wartik, T., *J. Am. Chem. Soc.* **89,** 4217 (1967).
146. Zeldin, M., and Rosen, A., *J. Organomet. Chem.* **34,** 259 (1972).
147. Zeldin, M., Solan, D., and Dickman, B., *J. Inorg. Nucl. Chem.* **37,** 25 (1975).
148. Zeldin, M., and Wartik, T., *J. Am. Chem. Soc.* **88,** 1336 (1966).
149. Zeldin, M., and Wartik, T., *Inorg. Chem.* **12,** 1433 (1973).
150. Zhuk, B. V., Domrachev, G. A., and Ob'edkov, A. M., *Izv. Akad. Nauk SSSR, Ser. Khim.* p. 1201 (1977).

CARBON-RICH CARBORANES AND THEIR METAL DERIVATIVES

RUSSELL N. GRIMES

Department of Chemistry, University of Virginia, Charlottesville, Virginia

I. Introduction

Interplay between experiment and theory is a basic feature of science, and the field of boron cluster chemistry since the 1960s provides a

Copyright © 1983 by Academic Press, Inc.
All rights of reproduction in any form reserved.
ISBN 0-12-023626-5

fascinating illustration of this process (*17, 21, 22, 24, 45, 66*). The boron hydrides, with their peculiar, unconventional cage-like structures, have intrigued theorists for years, even as the degree of interest exhibited in them by industry and government has waxed and waned (and recently waxed again). Because boron has four valence orbitals but only three electrons, its binary hydrides have fewer than one electron pair per bonding interaction, yet they hold together very nicely by the trick of electron delocalization; that is, some of the electrons are not constrained to ordinary Lewis-type bonds between pairs of atoms (so-called two-center bonds), but can extend over three atoms (three-center B—B—B and B—H—B bonds). In fact, in some types of boranes electrons are effectively delocalized over the entire cage framework, as in the icosahedral $B_{12}H_{12}^{2-}$ system and its analogous carborane $C_2B_{10}H_{12}$ (*45*).

In order to facilitate this electron delocalization, borane molecules adopt cluster shapes that permit high connectivities between boron atoms and thus make the most efficient use of the available electrons. Hydrocarbons, in contrast, have exactly the right numbers of electrons for *localized* two-center bond networks of carbon and hydrogen atoms. Here, there is no need for clustering; indeed, the most favorable arrangements are chains and rings, which allow each carbon atom to use its four valence orbitals and to acquire a full octet of valence electrons.

Boranes and hydrocarbons thus represent two extremes in network bonding systems. But what happens when carbon is incorporated into a polyhedral borane framework? The answer to this question has been emerging since the early 1960s, during which time vast new areas of synthetic and structural chemistry have been opened for exploration and numerous types of molecular geometry that were not even conceived previously have been shown to have stable existence. An oversimplified summary is as follows. When boron is the dominant structural element and the number of available bonding electrons is not sufficient for a classical hydrocarbon-like chain or ring structure (a so-called electron-deficient condition), the cluster motif is followed; this is the case in the polyhedral carboranes of the $C_2B_{n-2}H_n$ class (known for $5 \leqslant n \leqslant 12$) and their $B_nH_n^{2-}$ counterparts ($6 \leqslant n \leqslant 12$). In many carboranes, such as the extremely stable icosahedral $C_2B_{10}H_{12}$ isomers, carbon often adopts a role quite out of character from the viewpoint of organic chemists, by assuming a coordination number of five or six. On the other hand, cage systems containing mostly carbon with an occasional boron atom or two naturally tend to adopt hydrocarbon-like geometries; examples are boradamantane and borabenzene, which

have the classical (Lewis) structures of their organic namesakes and are properly described as organic heterocycles (*67*).

Is there an intermediate region of composition and structure in which one encounters stable "hybrid" geometries that exhibit both borane-like and hydrocarbon-like features within the same molecular framework? There is, and it is to this class of compounds that the present chapter is directed. In these "carbon-rich" carboranes, most of which have four skeletal carbon atoms in a borane matrix, some truly novel patterns of structure and reactivity have been observed (*18, 19*). This chemistry grew primarily out of a discovery in 1974 in the author's laboratory, by two former postdoctoral associates, Vernon Miller and William Maxwell (*53*), and was subsequently developed by a series of other able postdoctoral and graduate students. This work is far from complete—indeed, it must be regarded as still in an exploratory phase—but it has progressed to a point where a summary appears warranted. The current body of structural and spectroscopic data on four-carbon carboranes and metal complexes, which includes some two dozen X-ray crystal structures, provides a reasonable basis for discerning patterns in bonding and geometry; moreover, the stereochemistry involved is sufficiently different from that in "ordinary" carborane systems as to justify separate treatment.

Before we turn to the subject at hand, some perspective may be helpful. Hundreds of carboranes and metallacarboranes are now known, the vast majority of which (at least 95%) contain two skeletal carbon atoms. The dominance of the dicarbon species reflects primarily the fact that most carboranes are prepared via incorporation of alkynes into borane skeletons; however, a few one-carbon species have also been characterized. In the main, the structures of these one- and two-carbon polyhedral carboranes are reasonably well accounted for by the skeletal electron-count theory (see Section II), which was developed in the 1970s. In nearly all cases the observed cage structures are either closo polyhedra (all faces triangular) or fragments thereof, in accordance with theory. But what would be the structural consequences if, starting with a carborane such as icosahedral $C_2B_{10}H_{12}$, one were successively to replace boron atoms with carbon atoms, forming species such as $C_3B_9H_{12}$, $C_4B_8H_{12}$, $C_5B_7H_{12}$, and so on? According to the general rules of electron counting in clusters, the cage structure would be expected to become progressively more open as the carbon content, and hence the skeletal electron population, increased; however, one could not have said with confidence just what form this cage opening might take. Actually, there is no known way to perform such step-by-step

carbon substitutions, but, in the 1974 work already mentioned, we unexpectedly found a way to make *C*-alkyl derivatives of $C_4B_8H_{12}$ in high yield. Subsequently, Freyberg *et al.*, in our laboratory, determined the structure of $(CH_3)_4C_4B_8H_8$ by X-ray diffraction and found a distorted icosahedral geometry with two open faces (*16*)—a type of cage structure not previously known and certainly not predicted by anyone. Even more unexpectedly, we found that when $(CH_3)_4C_4B_8H_8$ is dissolved in common polar or nonpolar solvents, it partially and reversibly rearranges to a different isomer, as shown in NMR spectra; when the solvent is evaporated, the solid compound reverts to its original structure (*52*).

These discoveries led to numerous others that were scarcely less surprising, many of which have involved metal insertion into tetracarbon carborane polyhedra. In the early part of this work we were confronted with a growing collection of odd structures in which it was difficult to see an underlying pattern, but now, with a considerable body of chemical and spectroscopic data in hand, the dust is gradually clearing. The key point, on which we shall elaborate, is that *local carbon–carbon and carbon–metal interactions within the skeletal framework* profoundly influence cage geometry in these carbon-rich systems. In the dicarbon carboranes, such local effects are much less evident as a rule. For example, isomers of a given dicarbon cage system, such as $(\eta^5\text{-}C_5H_5)CoC_2B_9H_{11}$, normally have the same polyhedral shape and differ only in the location of heteroatoms (in this case, cobalt and carbon) on the cage surface; in contrast, isomers of tetracarbon species often exhibit very dissimilar gross geometries.

The different character of the carbon-rich carboranes, relative to the well-developed dicarbon carborane field, is not restricted to structure alone but is also reflected in some unique chemistry that will be described below. Section II deals with the theory of structure in boron clusters as it applies to the subject of interest here.

II. Structural Patterns in Carboranes: General Considerations

Bonding and molecular structure in borane frameworks have been treated by numerous authors from many different viewpoints, and no attempt will be made here to deal with this subject in detail. Rather, our purpose will be to provide sufficient background to allow rational discussion of the chemistry and geometry of carbon-rich carboranes to be described later.

A. Valence-Bond Descriptions

It will be assumed that readers of this chapter have some familiarity with the localized-bond description of the boron hydrides developed by Lipscomb and co-workers [and which led ultimately to a Nobel award to Lipscomb in 1976; (*45*)]. In this approach, a borane framework is viewed as a collection of BH units bound together by some combination of two-center B—B and three-center B—B—B bonds; the number of each type depends on the number of available valence electrons in the molecule. "Extra" hydrogen atoms are attached either to B—B edges (forming B—H—B three-center bridge bonds), or to individual BH groups, converting them to BH_2 units. Because each boron atom has four valence orbitals and each hydrogen one, the number of allowed bonding descriptions for a given borane is obviously limited, in some cases to a single structure. Further constraints are given by considerations of valence bond angles. These ideas have been formulated quantitatively in the famous *equations of balance* (*45*), which are now found even in some undergraduate inorganic texts.

Figure 1 depicts the localized-bond description of hexaborane(10), B_6H_{10}, together with its actual molecular structure. Note that in drawing the molecular geometry (Fig. 1b) we represent all the bonded connections by single lines, irrespective of the actual electron distribution; this is standard practice and is followed throughout this chapter (except when, as in Fig. 1a, we wish to present explicitly a localized-bond arrangement). In comparing Figures 1a and 1b it will be seen that, although the apex boron atom is six-coordinate, it is only tetravalent, that is, it is involved in only four electron-pair bonds, as indeed it must be because boron, like carbon, has only four valence orbitals.

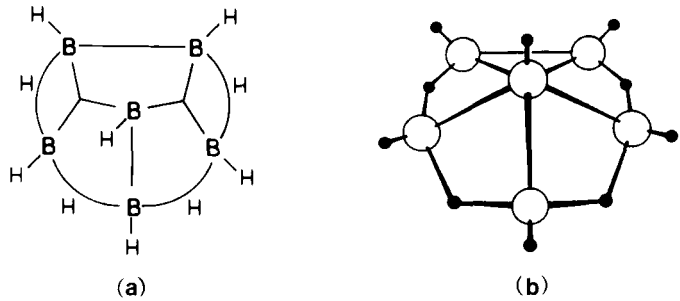

FIG. 1. (a) Localized bonds in B_6H_{10}. (b) Molecular structure of B_6H_{10} (*45*).

It will be noted that the B_6H_{10} structure in Fig. 1a has four B—H—B three-center bonds, two B—B two-center bonds, two B—B—B three-center bonds, and no BH_2 groups; in shorthand form this is referred to as a 4220 structure (*45*). The eight bonds require a total of 16 electrons, which is exactly the number available: of the total of 28 valence electrons in the molecule, 12 are required for the six localized B—H bonds, leaving the remaining 16 to bind the six BH units and the four extra hydrogens together. Other possible bonding schemes could be written, for example, 3311 and 2402 (note that in each instance the total of the digits must equal the number of bonds, in the present case, eight). However, these latter possibilities are eliminated by the known molecular structure (Fig. 1b), which contains four bridging hydrogens and no BH_2 groups; hence the 4220 arrangement (Fig. 1a) is correct.

In many cases, particularly in large or highly symmetric molecules, resonance descriptions involving several different arrangements may be required. Also, in recent years detailed theoretical studies have provided support for the concept of "fractional" three-center bonds (see later discussion), wherein particular groups of atoms may be linked by only part of an electron pair (*8*); such concepts have increased the utility of the localized-bond theory, for example, in calculating charge distributions. However, for present purposes we shall not require these more sophisticated refinements of the theory.

If one replaces a boron atom with carbon in the cage framework, at the same time removing a hydrogen atom to maintain the number of electrons constant, the same type of localized-bond description can in principle be employed. This is illustrated in Fig. 2 for the carborane 2,3-$C_2B_4H_8$, which is an analog of B_6H_{10}. The molecular structure of 2,3-$C_2B_4H_8$ (the prefix numbers of which designate the carbon locations) is shown in Fig. 2a, and it resembles that of B_6H_{10} (Fig. 1b), except that there are only two B—H—B bridges rather than four. This, of course, requires a different localized-bond description from that in

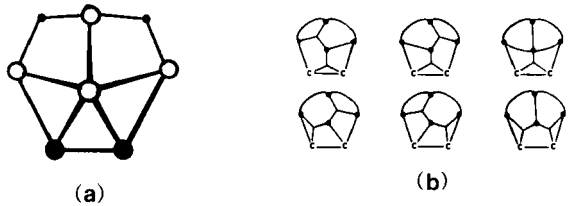

FIG. 2. (a) Molecular structure of 2,3-$C_2B_4H_8$. ○, BH; ●, CH; •, H. (b) Some localized valence structures for 2,3-$C_2B_4H_8$ (*49*). Reprinted from *J. Am. Chem. Soc.* **94**, 8699. Copyright 1972 American Chemical Society.

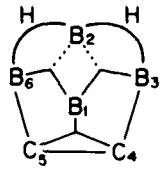

FIG. 3. Fractional three-center bond description of $2,3\text{-}C_2B_4H_8$ (*49*). Reprinted from *J. Am. Chem. Soc.* **94**, 8699. Copyright 1972 American Chemical Society.

Fig. 1a, and several possible structures (*49*) are shown in Fig. 2b. Alternatively, a fractional three-center bond description (*49*), given in Fig. 3, is in reasonable accord with quantitative molecular orbital treatments.

The molecule $2,3\text{-}C_2B_4H_8$ is but one member of a series of isoelectronic molecules analogous to B_6H_{10} (Fig. 4). All of these are known either as parent species or alkyl derivatives, and all can be described in terms of localized bonds, if desired. This group of molecules rather dramatically illustrates the importance of fundamental principles of bonding and structure that provide a common thread linking such apparently unrelated species as B_6H_{10} and $C_6(CH_3)_6^{2+}$.

The placement of carbon atoms in the structures in Fig. 4 is highly significant, as it demonstrates several trends that are well established in carborane structural chemistry. The two most important observations are that *carbon tends to occupy low-coordinate vertices when possible* and that *bridging hydrogen atoms are located between boron atoms only;* no clear examples of discrete B—H—C or C—H—C bridges

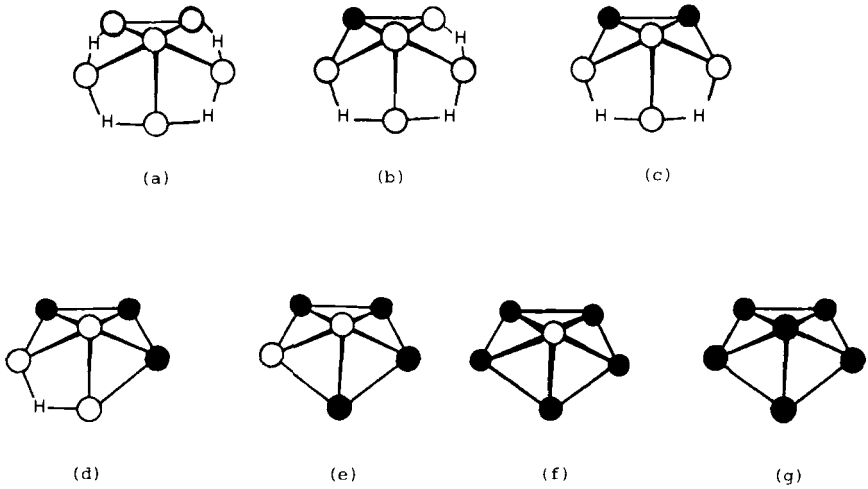

FIG. 4. Isoelectronic series of 6-vertex nido species. (a) B_6H_{10}, (b) CB_5H_9, (c) $C_2B_4H_8$, (d) $C_3B_3H_7$, (e) $C_4B_2H_6$, (f) $C_5BH_6^+$, (g) $(CH_3)_6C_6^{2+}$. ○, BH; ●, CH or CCH_3.

have been found. Other generalizations regarding the structural role of carbon will be presented later.

B. Molecular Orbital Descriptions and Electron-Counting Rules

Localized-bond treatments of the sort illustrated in Section I,A work well for open-cage molecules, particularly small ones where the number of allowed structures is limited. For closo (completely triangulated) cages, however, localized descriptions tend to become cumbersome and make it difficult to gain qualitative insight into the bonding, to rationalize structures, and to see relationships among different molecular species. Consequently, the closo systems, which are regarded in general as highly electron-delocalized, are commonly treated in molecular orbital (MO) terms. Quantitative MO studies have for the most part been centered on the binary borane clusters such as the polyhedral $B_nH_n^{2-}$ ions, but conclusions reached for these systems can usefully be transferred to their carborane (and other heteroborane) counterparts; thus both icosahedral $B_{12}H_{12}^{2-}$ and its analog, $C_2B_{10}H_{12}$, have 13 bonding skeletal molecular orbitals which precisely accommodate the 26 electrons available for cage bonding.

These studies of the $B_nH_n^{2-}$ series and related clusters have established a very important rule: closo n-vertex polyhedra composed of units such as BH and CH, which supply three valence orbitals for framework bonding (the fourth orbital being utilized for linkage to hydrogen) have $n + 1$ skeletal bonding MOs (*46, 65, 79, 88*). If $n + 1$ electron pairs are available to fill these orbitals, a stable closed-shell system should result. Hence, *n-vertex clusters having 2n + 2 electrons for cage bonding are predicted to have closo geometry.* Additional electrons beyond the quota of $2n + 2$ must occupy antibonding orbitals, leading to distortion; normally, this distortion takes the form of cage opening to produce a cluster with one or more open (i.e., nontriangular) faces. An equivalent way of describing this is to observe that, if one removes a vertex from an n-vertex closo system, the *absolute* number of bonding MOs is unchanged, but because the value of n has been reduced, the number of bonding MOs must be given as $n + 2$. Thus both octahedral $C_2B_4H_6$ ($n = 6$) and square-pyramidal $C_2B_3H_7$ ($n = 5$) have 7 skeletal bonding MOs, represented as $n + 1$ in the former case and $n + 2$ in the latter.

Clusters that correspond to closo polyhedra minus one vertex are labeled *nido* (Greek for *nest*); examples are the square pyramid and the pentagonal pyramid. Clusters representing closo polyhedra minus *two*

vertices are classified *arachno* (*web*), and for three missing vertices the term is *hypho* (*net*). Hence the skeletal electron requirements for closo, nido, arachno, and hypho species are $(2n + 2)$, $(2n + 4)$, $(2n + 6)$, and $(2n + 8)$, respectively.

The number of skeletal electrons in the cage is the sum of contributions from all the units, assuming that bonds external to the polyhedron are not involved; thus, BH, CH, and NH groups contribute 2, 3, and 4 electrons, respectively; a "bare" nitrogen atom is a 3-electron donor if the presence of an exopolyhedral lone pair is assumed. Transition metal–ligand units such as $Co(\eta^5\text{-}C_5H_5)$, $Fe(CO)_3$, and $Ni(\eta^5\text{-}C_5H_5)$ contribute, respectively, 2, 2, and 3 electrons; here several things are taken for granted: (1) the metal, like B or C, utilizes three orbitals for bonding to the cage skeleton; (2) the metal acquires an 18-electron configuration; and (3) metal orbitals that are not used for bonding to the cage or to external ligands are nonbonding and are filled with electrons. Because $Co(\eta^5\text{-}C_5H_5)$ and $Fe(CO)_3$ are both 2-electron donors, one expects that they could replace BH in borane frameworks, and indeed this is a very common occurrence; B_5H_9 analogs such as 1- and 2-$(\eta^5\text{-}C_5H_5)CoB_4H_8$ and 1-$(CO)_3FeB_4H_8$, B_6H_{10} analogs such as 1- and 2-$(CO)_3FeB_5H_{10}$ and 1-$(\eta^5\text{-}C_5H_5)CoB_5H_9$, $C_2B_{10}H_{12}$ analogs such as $(\eta^5\text{-}C_5H_5)_2Co_2C_2B_8H_{10}$ and $(\eta^5\text{-}C_5H_5)_2Ni_2B_{10}H_{10}$, and hundreds of other examples have been thoroughly characterized (*17, 22, 66*). These ideas have received considerable support from detailed MO studies and, most importantly, from a large body of experimental evidence.

The skeletal electron-count theory was originated by Wade (*88*) and is based on concepts inherent in the Lipscomb valence-bond treatment of boranes and carboranes (*45, 46*), and it received important contributions from Mingos (*65*) and Rudolph (*79*); in addition, a number of other authors have elaborated on various aspects of cluster bonding (*20, 44, 71, 90*). In recent years it has become clear that the theory is broad in scope and can usefully be applied to metal clusters and other nonboron systems, with some modifications. Nevertheless, major limitations of this approach have become apparent in certain types of boron clusters, including the tetracarbon carboranes. We turn now to a consideration of this problem.

C. Structure and Bonding in Carbon-Rich Cage Systems

The simple closo–nido–arachno classification of clusters, described in Section II,B, works well for boranes, dicarbon carboranes, and their metal derivatives. Most such clusters are readily identifiable as stand-

ard closo polyhedra or polyhedral fragments, and there is a clear correlation between the cage geometry and the skeletal electron population, as was outlined previously. Where "violations" of the electron-counting rules occur, these usually involve heavy metals such as platinum, species of high metal content in which local metal–metal interactions are important [e.g., $(\eta^5\text{-}C_5H_5)_4M_4B_4H_4$ (M = Co, Ni)] or halogenated clusters (halogen substituents tend to donate electron density into the cage and thus alter the skeletal electron population).

The carbon-rich carboranes present an altogether different situation and illustrate three major limitations of the skeletal electron-counting theory as presented: (1) it predicts only thermodynamically favored structures and cannot anticipate kinetically stabilized cage geometries; (2) even when the structural class (e.g., nido) is correctly assigned, the theory may not be able to specify which particular geometry is to be expected; and (3) because the theory assumes electron delocalization over the entire cluster, it cannot easily handle situations involving local bonding interactions in portions of the cluster framework. The extent of this problem varies considerably with cluster size and number of valence electrons. For example, all known 12-vertex, 26-electron clusters are icosahedral (closo), and all 11-vertex, 26-electron clusters have a nido geometry, corresponding to an icosahedron minus one vertex (Fig. 5). These structures are exactly in accord with the presence of $2n + 2$ and $2n + 4$ electrons, respectively, and illustrate the fact that the icosahedron is the overwhelmingly preferred arrangement for 26-electron systems.

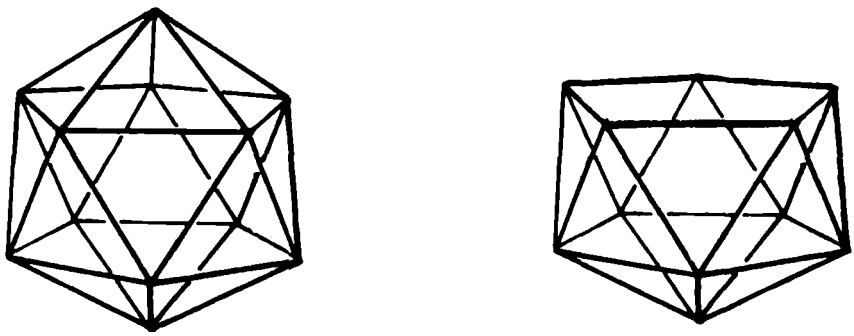

FIG. 5. (a) Icosahedron. (b) Nido icosahedral fragment.

In dramatic contrast, consider the 28-electron, 12-vertex clusters. According to theory, these are $(2n + 4)$-electron systems and formally belong to the nido classification; thus we would expect them to adopt an open-cage geometry derived from a 13-vertex closo polyhedron by removal of one vertex (Fig. 6). What we find, actually, is that the known 12-vertex, 28-electron systems adopt a wide variety of different shapes, comprising at least seven different structural types [Fig. 7; (*59*)]. Of these, all except types 1 and 7 involve four-carbon carboranes or metallacarboranes. The three compounds of type 5 have the "expected" nido geometry, corresponding to Fig. 6b; the others are widely divergent and can be described as distorted icosahedra. Particularly noteworthy is the fact that the three isomers of $(\eta^5\text{-}C_5H_5)Co(CH_3)_4C_4B_7H_7$ fall into three different structural classes (types 4–6). It should be stressed that the classification of structural types in Fig. 7 is based on *distinct differences in connectivity;* formal conversion of any of these geometries to any other requires bond breakage and bond formation, as opposed to mere "distortion."

The species illustrated in Fig. 7 are a somewhat motley collection with diverse origins; some clearly do not represent thermodynamically favored structures, but all are reasonably heat- and air-stable (the two isomers of $R_4C_4B_8H_8$, types 2 and 3, are in equilibrium in solution at room temperature).

We shall defer detailed discussion of the individual structures to a

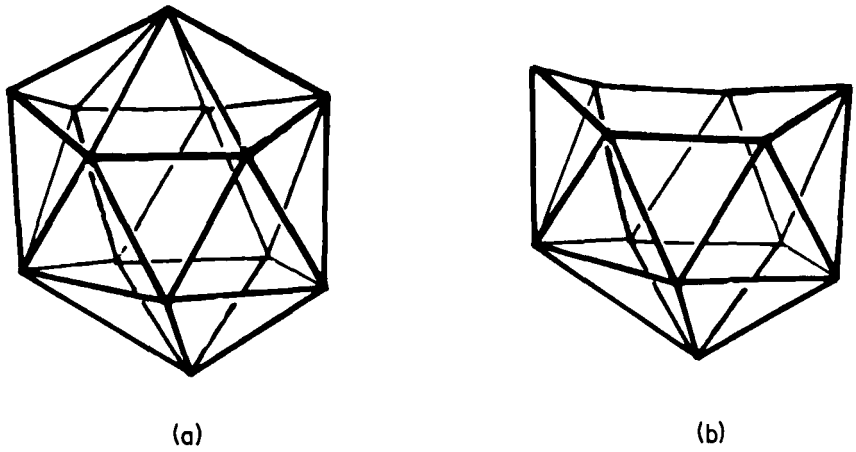

FIG. 6. (a) 13-Vertex closo polyhedron (docosahedron). (b) Nido 12-vertex cage formed by removal of a six-coordinate vertex from a closo 13-vertex polyhedron.

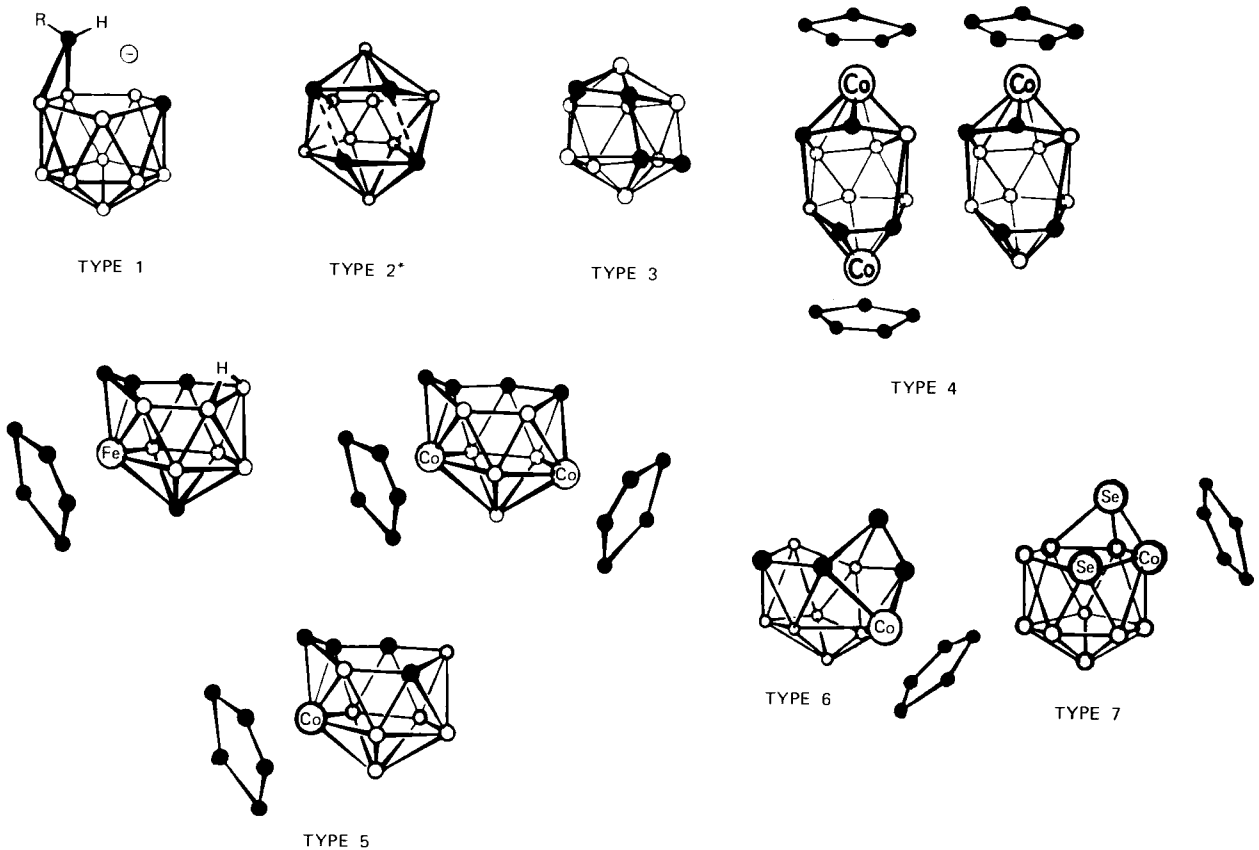

FIG. 7. Structural types of 12-vertex 28-electron cages (*59*). *, NMR only; ○, BH; ●, CH or CCH_3. Reprinted from *Inorg. Chem.* **20,** 1201. Copyright 1981 American Chemical Society.

later point, but several general observations can be made here. First, the observed differences in cage geometry cannot be ascribed solely, or even mainly, to differences in elemental composition; this is shown by the existence of three different structural isomers of $(\eta^5\text{-}C_5H_5)Co(CH_3)_4C_4B_7H_7$, as mentioned previously. Moreover, in the 26-electron, 12-vertex family there is only one observed geometry—icosahedral—despite wide variation in elemental composition. Second, it is clear that a major factor determining structure in these systems (particularly the metal-containing ones) is the *synthetic origin;* we shall have more to say on this. Third, the apparent thermodynamically favored geometry for 12-vertex, 28-electron *metallacarboranes* (but not carboranes) is that shown as type 5 (Fig. 7), which is the nido geometry that would have been expected from electron-counting arguments in the first place. Hence, to this limited degree the structural theory is in accord with observation for the 12-vertex nido case. Finally, an important point: these carbon-rich cage structures are clearly beyond the scope of quantitative MO calculations, and hence this is an area in which understanding can be gained only through a combination of experimental study and shrewd qualitative insight. In this field, the experimentalist unquestionably leads the way.

The 12-vertex, 28-electron systems in Fig. 7 represent only a portion of the four-carbon carborane and metallacarborane structures that have been established, albeit a major portion. With a single exception, $(\eta^5\text{-}C_5H_5)Co(C_6H_5)_4C_4B_3H_3$, an 8-vertex arachno species (see later discussion), all of the structural investigations in this area involve 26-, 28-, or 30-electron cages of 11–14 vertices. Table I classifies these compounds according to electron count and number of vertices and indicates, by code, the coordination numbers of metal and carbon atoms in each of the established structures. In all but a few instances the structures are known with certainty from X-ray diffraction studies; those characterized only by NMR data are enclosed in brackets.

All of the molecules in Table I contain four skeletal carbon atoms and were derived from $(CH_3)_4C_4B_8H_8$ or $(C_2H_5)_4C_4B_8H_8$ by synthetic routes outlined in the following discussion. No significance can be attached to the relative number of species in the various categories, but the table does indicate where the bulk of our structural information lies at the time of this writing. The available structural data reveal some significant patterns with respect to the stereochemistry of metal and carbon atoms in the cage framework, and we shall discuss these in the latter part of the chapter, following a description of synthetic routes and some chemistry of individual clusters.

TABLE I

STRUCTURALLY CHARACTERIZED 11- TO 14-VERTEX CARBON-RICH CARBORANES AND METALLACARBORANES[a,b]

Number of skeletal electrons	11-Vertex systems	12-Vertex systems	13-Vertex systems	14-Vertex systems
30	$2n + 8$ electrons	$2n + 6$ electrons $Me_4C_4B_8H_9^-$ 2444(4,6)[b] (cobaltocenium derivative)	$2n + 4$ electrons $CpCrEt_4C_4B_8H_8$ 6-3445(5)[b] $(Ph_2PCH_2)_2NiMe_4C_4B_8H_8$ [Isomer **I:** 5-4445(5)] $[CpCoMe_4C_4B_8H_8]$ 5-4445(5) $[Me_2C_2B_4H_4]CoMe_4C_4B_8H_7 \cdot$ THF 6-4445(5)	$2n + 2$ electrons $Cp_2Fe_2Me_4C_4B_8H_8$ Isomer **I:** 66-4445(5)[b] Isomer **II:** 66-4445(4) *Isomer **V:** 66-4455(5) *[Isomer **VII:** 66-5555(0)] **[Isomer **VIII:** 66-5555(0)] *Thermal rearrangement product **Final product of thermal rearrangement
28	$2n + 6$ electrons $Me_4C_4B_7H_8Br$ 2444(5,5)	$2n + 4$ electrons $CpCrEt_4C_4B_7H_7$ 6-3444(6) Type 2 (see Fig. 7) $Et_4C_4B_8H_8$ 3344(6) $[Cp_2Co_2C_4B_8H_{10}$, isomer **VI**] 55-4444(4)? Type 3 $Me_4C_4B_8H_8$ 4444(4,4) $Me_4C_4B_8H_7$-C_5H_4FeCp 4444(4,4)	$2n + 2$ electrons	$2n$ electrons

		Type 4 $Cp_2Co_2Me_4C_4B_6H_6$, Isomer **V** 55-3344(6) $CpCoMe_4C_4B_7H_7$, Isomer **I** 5-3344(6) $CpCoMe_4C_4B_7H_6$-OEt, Isomer **I** 5-3344(6) Type 5 $CpFeMe_4C_4B_7H_8$ 6-3445(6) *$CpCoMe_4C_4B_7H_7$, Isomer **III** 6-3444(6) $Cp_2Co_2C_4B_6H_{10}$, Isomer **VII** 56-3444(6) Type 6 $CpCoMe_4C_4B_7H_7$, Isomer **II** 5-3444(4,5) *Thermal rearrangement product		
26	$2n$ + 4 electrons $CpCoMe_4C_4B_6H_6$ Isomer **I:** 5-4444(5) Isomer **II:** 4-4444(5)	$2n$ + 2 electrons	$2n$ electrons	$2n$ − 2 electrons

[a] All species have been characterized by X-ray diffraction, except those enclosed in brackets; structures of bracketed compounds are assigned from NMR evidence. Abbreviations: Cp, η^5-C_5H_5; Me, methyl; Et, ethyl; Ph, phenyl.

[b] Structure Code: Digits represent coordination numbers (with respect to the cage framework only) of nonboron atoms in the skeleton; those to left of hyphen are metals, those to right of hyphen are carbon. Underlined digits indicate location on an open face (double-underlined atoms are on two open faces). Digits in parentheses denote the number of atoms on the open face, or faces, in the cage. Example: for $Cp_2Fe_2Me_4C_4B_8H_8$, isomer **II** (Fig. 31b) 66-4445(4) signifies that the cage has two 6-coordinate metal atoms (one on an open face), three 4-coordinate carbons (two of them on open faces), and a 5-coordinate carbon; the molecule has a single 4-membered open face.

III. Small Three- and Four-Carbon Carborane Systems

As the foregoing discussion makes clear, this chapter is concerned primarily with the large C_4B_8 carboranes and their metallacarborane derivatives. The smaller C_3 and C_4 carboranes fall into a somewhat different category in terms of chemistry and geometry, and very few of them have been structurally characterized by diffraction methods. However, a brief outline of their syntheses is presented in this section.

A. Three-Carbon Carboranes

The reaction of tetraborane(10), B_4H_{10}, with acetylene in the vapor phase at 25–50°C produces small quantities of *C*-methyl and *C,C'*-dimethyl derivatives of 2,3,4-$C_3B_3H_7$, characterized from NMR spectra as a pentagonal pyramid with the three carbons in adjacent basal locations [Fig. 4(d)] (*26*). A kinetic study of this reaction (*15*) indicated that the initial step is formation of the unstable species B_4H_8, which adds four C_2H_2 units in stepwise fashion to form a solid polymer (the main product); side reactions, involving rearrangement of the $B_4H_8(C_2H_2)_x$ intermediates, evidently yield $C_3B_3H_7$ derivatives. The monomethyl compound, 2-$CH_3C_3B_3H_6$, on treatment with NaH loses its B—H—B bridging proton to form the $CH_3C_3B_3H_5^-$ anion, which in turn reacts with bromomanganese pentacarbonyl to form initially a red $(CO)_5Mn—(CH_3)C_3B_3H_5$ intermediate; at 100°C this complex loses CO to produce yellow *closo*-1,2,3,4-$(CO)_3Mn(CH_3)C_3B_3H_5$ (*40*). The same manganacarborane product can be prepared by reaction of neutral 2-$CH_3C_3B_3H_6$ with $Mn_2(CO)_{10}$ at elevated temperature (*40*).

The only other reported example of a three-carbon carborane is the strange species $C_3B_5H_7$, a colorless solid (mp 37°C) obtained in 15–20% yield by pyrolysis of the *nido*-carborane silyl derivatives μ- or 4-$SiH_3C_2B_4H_7$ (*84*). From spectroscopic evidence a fluxional closo cage structure has been proposed for $C_3B_5H_7$, with one of the framework carbon atoms lacking a hydrogen substituent. No further studies of this species have been reported.

Three-carbon metallacarboranes have also been prepared from alkyl derivatives of 1,3-diborolene, $C_3B_2H_6$, a five-membered ring system. Both nido 6-vertex monometallic complexes and closo 7-vertex dimetallic complexes (triple-decker sandwiches) have been characterized. Thus treatment of 1,3,4,5-tetraethyl-2-methyl-1,3-diborolene with nickelocene or $[(\eta^5\text{-}C_5H_5)Ni(CO)]_2$ gives orange-red $(\eta^5\text{-}C_5H_5)Ni(CH_3)(C_2H_5)_2C_3B_2(C_2H_5)_2$, a pentagonal pyramid with the metal in the apex, and green, paramagnetic $(\eta^5\text{-}C_5H_5)_2Ni_2(CH_3)(C_2H_5)_2C_3B_2(C_2H_5)_2$

(*81*). A pyramidal cobalt complex, $(CO)_3Co(CH_3)(C_2H_5)_2C_3B_2(C_2H_5)_2$, has been obtained with $HCo(CO)_4$ or $Co_2(CO)_8$ reagents (*80*).

B. Four-Carbon Carboranes

Pyramidal $C_4B_2H_6$, a 16-electron ($2n + 4$) nido cage system (Fig. 4e), was first prepared, in peralkylated form, by treatment of 1,2-bis-(diethylboryl)-1,2-dialkylethylene with a trace of $(C_2H_5)_2BCl$ at 40°C (*2*). Other alkyl derivatives have been obtained by the reaction of 1,1′-dimethyl-3-diethylboryl-4-ethyl-1-stannacyclopentadiene with CH_3BBr_2 (*1*). The parent $C_4B_2H_6$ was first synthesized (*70*) by pyrolysis of tetramethylene diborane, $(CH_2)_4B_2H_4$, at 550°C, and later by insertion of acetylene into the small *nido*-carborane $C_2B_3H_7$ (*63*). No metal derivatives of the $C_4B_2H_6$ system had been reported by the time of this writing, but a microwave study of the parent molecule (*72*) established the pyramidal cage structure and revealed that the three C—C distances are equal (1.43 Å), supporting an electron-delocalized model of the framework bonding.

A different tetracarbon system, $(CH_3)_4C_4B_4H_4$, has been obtained by reaction of dimethylacetylene with the *nido*-ferraborane $1\text{-}(CO)_3FeB_4H_8$ (*12*). An intermediate in this synthesis is an apparent *closo*-ferracarborane, $(CO)_3Fe(CH_3)_4C_4B_4H_4$. Possible structures for $(CH_3)_4C_4B_4H_4$ and the iron complex, based on NMR observations, are shown in Fig. 8; in both cases the proposed geometry is in accord with the electron-counting rules outlined previously. A different C_4B_4 species, $(C_2H_5)_4C_4B_4(CH_3)_4$, has been prepared by treatment of thiadiborolene, $(C_2H_5)_2C_2(CH_3)_2B_2S$, with potassium metal in THF (*82*). In this

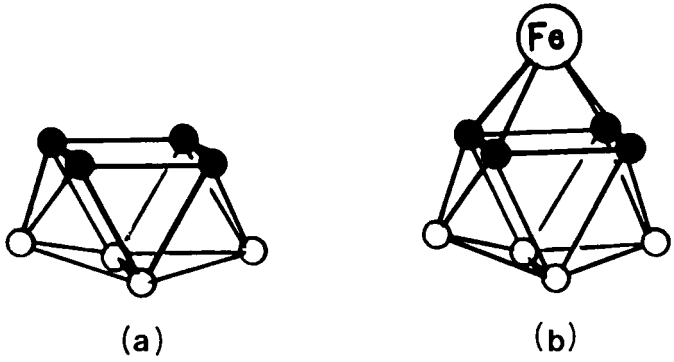

FIG. 8. Proposed structures for (a) $(CH_3)_4C_4B_4H_4$ and (b) $(CO)_3Fe(CH_3)_4C_4B_4H_4$ (*12*). ○, BH; ●, CCH_3.

compound the NMR spectra exhibit two ethyl resonances, showing that the skeletal carbon atoms are present in nonequivalent pairs; thus the cage structure of this derivative cannot be that of Fig. 8a.

At this writing the geometry of these 8-vertex carboranes is an unresolved problem. However, a closely related cobaltacarborane, $(\eta^5\text{-}C_5H_5)Co(C_6H_5)_4C_4B_3H_3$, has been prepared (*92*) and characterized by X-ray diffraction [(*93*); Fig. 9]. This material was obtained in very small quantity by the reaction of B_5H_9, cyclopentadiene, $(C_6H_5)_2C_2$, and cobalt vapor, which also generated dicarbon cobaltacarborane products. The observed geometry is essentially an arachno cage, resembling a 10-vertex closo polyhedron with two missing vertices; this is a more open structure than the nido geometry expected for a $(2n + 4)$-electron system, but it may be a consequence of severe steric repulsion by the four phenyl groups. It is also interesting that the framework C—C bond adjacent to cobalt is significantly shorter [1.379(5) Å] than the other C—C interaction [1.419(5) Å], suggesting that localized carbon–carbon bonding may be important in dictating cluster geometry. Such local effects are dominant features in the large tetracarbon clusters discussed later.

A number of four-carbon metallacarborane clusters have been prepared from derivatives of the cyclic borole system, especially pentaphenylborole, $(C_6H_5)_5C_4B$. Reactions of this compound with $Fe_2(CO)_9$ or $Ni(CO)_4$ yield $(CO)_3Fe(C_6H_5)_5C_4B$ and $(CO)_2Ni(C_6H_5)_5C_4B$, respectively; both species are *nido*-MC_4B pentagonal pyramidal systems with

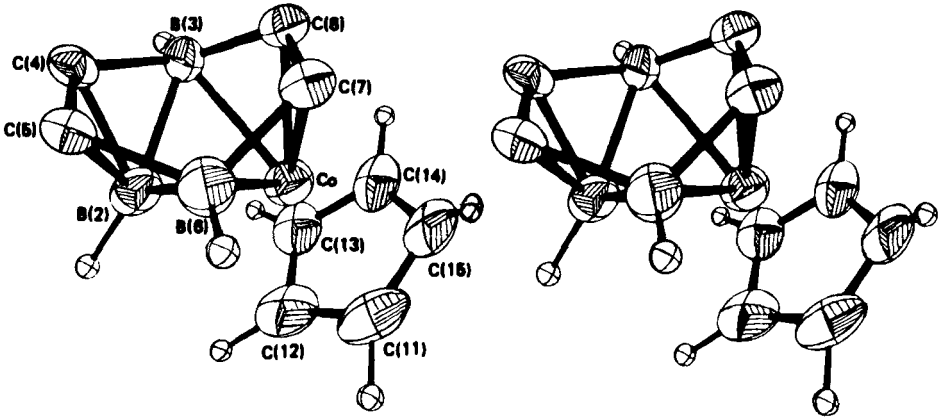

FIG. 9. Stereoview of the structure of $(\eta^5\text{-}C_5H_5)Co(C_6H_5)_4C_4B_3H_3$ (*93*). Phenyl rings are not shown. Reprinted from *Inorg. Chem.* **19**, 3650. Copyright 1980 American Chemical Society.

the metal in the apex position (*34*). Metal–borole complexes have also been obtained from 1-phenyl-4,5-dihydroborepin, a seven-membered boron heterocycle (*34*). Both monometallic (nido) complexes and dimetallic (closo) species have been characterized; an example of the latter is the dimanganese complex 1,7,2,3,4,5-$(CO)_6Mn_2C_4BH_3$-2-C_2H_5-6-C_6H_5, a pentagonal bipyramid with both apices occupied by $Mn(CO)_3$ units (*33*). Still other four-carbon metal complexes have been generated from 1,4-difluoro-1,4-diboracyclohexadiene ($F_2B_2C_4H_4$) derivatives. The cyclic planar $F_2B_2C_4R_4$ species (*85*), with the BF groups occupying para positions in a 2,5-hexadiene-like ring, is *formally* a *B,B'*-difluoro-substituted derivative of the *nido*-carborane $C_4B_2H_6$ mentioned previously (Fig. 4e); that the difluoro derivatives adopt a planar geometry testifies to the considerable influence of electron-rich ligands such as fluorine or ferrocenyl on the skeletal structure (*5*). The planar $F_2B_2C_4(CH_3)_4$ molecule readily forms sandwich complexes such as $[F_2B_2C_4(CH_3)_4]_2Ni$ (*48*), which could be considered metallacarboranes in a broad sense. The closely related 1,4-dimethyl-1,4-diborabenzene ligand, $(CH_3)_2B_2C_4H_4$, also generates sandwich complexes with cobalt and rhodium (*35, 36*).

Still other boron-containing heterocycles capable of coordination to metals are known, (e.g., derivatives of borabenzene, C_5H_5B), and a number of transition metal complexes have been characterized. Such compounds are better described as arene–metal sandwiches rather than cage compounds and are outside the scope of the present chapter, but they have been reviewed elsewhere (*23, 80*).

IV. Large Carbon-Rich Carboranes: Synthesis and Stereochemistry

A. Formation of C_4B_8 Cages via Oxidative Fusion

1. Background

The concept of constructing large cages by low-energy, metal-promoted, face-to-face fusion of smaller cages does not seem to have occurred to anyone prior to its discovery in 1974 (*53*). The principle of oxidative *coupling* to give dimeric products involving single-bond linkages has been well established for some time; processes such as the conversion of polyhedral $B_{10}H_{10}^{2-}$ to $(B_{10}H_9)_2^{2-}$ (*6, 32, 42, 62*) or of $C_2B_9H_{12}^-$ to $(C_2B_9H_{11})_2$ (*41, 78*) require an oxidant but do not involve metal-complex formation. On the other hand, the formation of the bis(carborane) 5,5'-$[(CH_3)_2C_2B_4H_5]_2$ by thermal ejection of mercury

from μ,μ'-$[(CH_3)_2C_2B_4H_5]_2Hg$ (*37*) can be described as a metal-promoted synthesis. All these processes, however, involve linkage of polyhedra rather than fusion into a single cage framework.

The oxidative fusion reaction has been shown to occur with a variety of carborane and metallacarborane species (*18, 39, 52, 54, 58, 75, 76, 91*), but the principal work (and the original discovery) utilized C,C'-disubstituted derivatives of *nido*-2,3-$C_2B_4H_8$ (Fig. 4c). The $R_2C_2B_4H_6$ species are now accessible in bench (multigram) quantities via the base-promoted addition of an alkyne to B_5H_9 (*38*).

$$B_5H_9 + RC{\equiv}CR \xrightarrow[0\text{–}25°C]{Et_3N} 2,3\text{-}R_2C_2B_4H_6 + Et_3NBH_3$$

$$R = CH_3, C_2H_5, C_3H_7, \text{etc.}$$

This method affords the carborane product in a form easily separable by vacuum fractionation, in contrast to the original vapor-phase B_5H_9–alkyne thermal reaction (*68*), which gives complex product mixtures requiring chromatographic separation (hence limiting the scale to a few millimoles). However, for the preparation of parent $C_2B_4H_8$ the vapor-phase reaction of B_5H_9 and C_2H_2 is required.

Bridge deprotonation of $C_2B_4H_8$ and its C-substituted derivatives occurs readily in the presence of alkali-metal hydrides in ethereal solvents (*69*), giving the corresponding $R_2C_2B_4H_5^-$ anions which are versatile ligands for metal complexation and can coordinate in η^1, η^2, or η^5 fashion. Reaction with $FeCl_2$ in cold THF forms the bis(carboranyl) sandwich complex $(R_2C_2B_4H_4)_2Fe^{II}H_2$ (R = alkyl) in high yield, as shown in Fig. 10 (*52*). Similar treatment with $CoCl_2$ generates $(R_2C_2B_4H_4)_2Co^{III}H$ (*54*). Both complexes are red, air-sensitive, diamagnetic solids, which on exposure to oxygen undergo ligand fusion to form, nearly quantitatively, the colorless, air-stable carborane $R_4C_4B_8H_8$ (Fig. 10); because the ligands carry a formal −2 charge, the

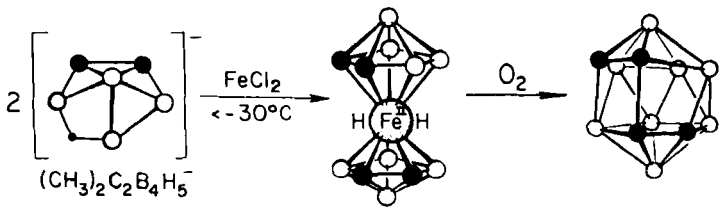

FIG. 10. Synthesis of $[(CH_3)_2C_2B_4H_4]_2FeH_2$ and conversion to $(CH_3)_4C_4B_8H_8$ via oxidative fusion (*18, 52*). ○, BH; ●, CCH_3. Reprinted from *Acc. Chem. Res.* 11, 420. Copyright 1978 American Chemical Society.

net process involves a four-electron oxidation. Crystallographic studies of $[(CH_3)_2C_2B_4H_4]_2FeH_2$ (*75*), $(CH_3)_4C_4B_8H_8$ (*16*), and a *B*-ferrocenyl derivative of the latter species (*27*) have established the solid-state structures depicted in Figs. 11, 12, and 13, respectively. We shall return to these compounds later.

2. *Mechanism*

As this chapter is written, we are far from a detailed understanding of the fusion process. Indeed, there may well be more than one mechanism, depending on the metal, the ligand, the solvent system, or other variables. However, a number of facts have been established concerning the oxidative fusion of $(R_2C_2B_4H_4)_2FeH_2$ and $(R_2C_2B_4H_4)_2CoH$ complexes in THF (R = CH_3, C_2H_5, or C_3H_7). The process in each case is intramolecular and does not involve dissociation of $R_2C_2B_4H_4^{2-}$ ligands from the metal; thus oxidation of mixtures of $(R_2C_2B_4H_4)_2FeH_2$ and $(R'_2C_2B_4H_4)_2FeH_2$ in solution gives only $R_4C_4B_8H_8$ and $R'_4C_4B_8H_8$,

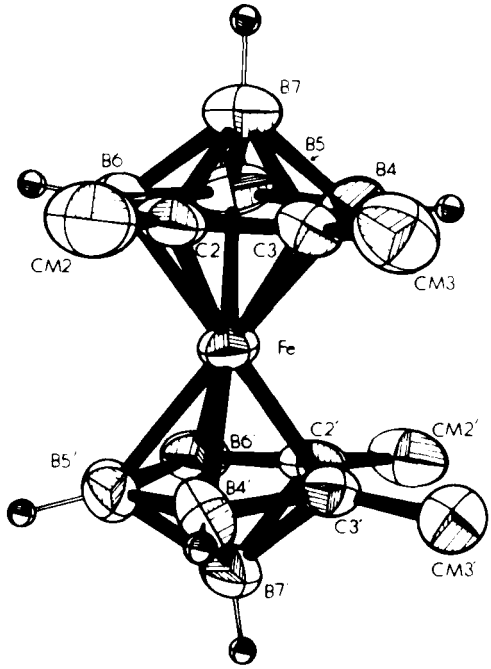

FIG. 11. Structure of $[(CH_3)_2C_2B_4H_4]_2FeH_2$ (*75*). Metal-bound hydrogen locations were not found in the X-ray study. Reprinted from *Inorg. Chem.* **18**, 263. Copyright 1979 American Chemical Society.

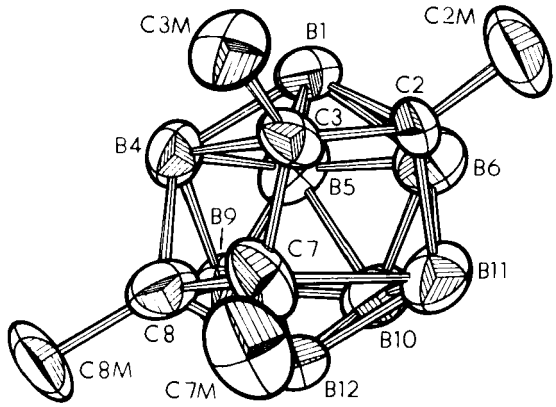

FIG. 12. Solid-state (**A** isomer) structure of $(CH_3)_4C_4B_8H_8$ (*16*) Reprinted from *Inorg. Chem.* **16**, 1847. Copyright 1977 American Chemical Society.

with no mixed-ligand ($R_2R'_2C_4B_8H_8$) products. Moreover, no ligand exchange occurs between the biscarborane metal complexes and free $R'_2C_2B_4H_5^-$ ion (*28*).

In the presence of air, the conversion to carborane occurs instantaneously in all media, but when oxygen is rigorously excluded the process is solvent dependent. No reaction occurs in diethyl ether, but in THF or dimethoxyethane (DME) an extraordinary reaction takes place almost quantitatively over several hours (*28*).

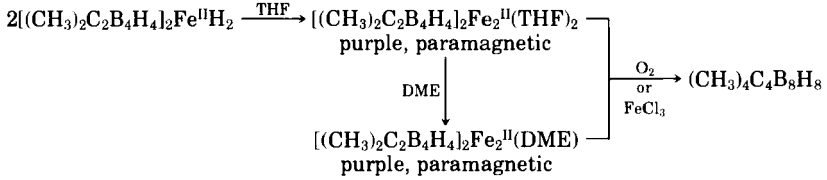

The purple diiron complex has been characterized by X-ray diffraction (as the DME adduct) and has the structure shown in Fig. 14, with an Fe—Fe distance of 2.414(4) Å (*29*). Mössbauer, ESR, and magnetic-susceptibility measurements indicate that both iron atoms are in the +2 oxidation state but that the central Fe^{2+} is low-spin d^6, while the outer Fe^{2+} is high-spin d^6, with four unpaired electrons. This reconciles nicely with a model in which the carborane ligands are more tightly bound to the central iron than to the outer metal atom; thus, the d orbitals of the outer iron are not sufficiently perturbed to produce a high-field, low-spin configuration. The purple THF and DME adducts are evidently stable under anaerobic conditions but rapidly form $(CH_3)_4C_4B_8H_8$ on exposure to air (*28*).

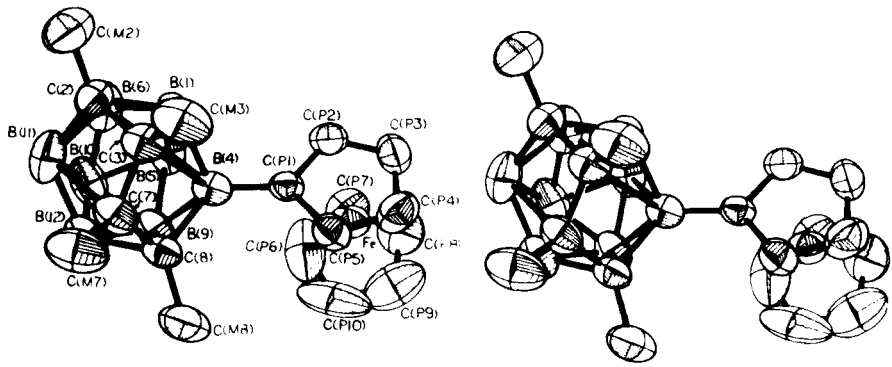

FIG. 13. Stereoview of 4-[(η^5-C_5H_5)Fe(η^5-C_5H_4)]—$(CH_3)_4C_4B_8H_7$ (*27*). Reprinted from *Inorg. Chem.* **19**, 2981. Copyright 1980 American Chemical Society.

If a catalytic quantity of $FeCl_3$ is present, the conversion of red $(R_2C_2B_4H_4)_2Fe^{II}H_2$ (R = CH_3 or C_2H_5) to the purple diiron compound occurs very quickly; an excess of $FeCl_3$ pushes the reaction all the way to $R_4C_4B_8H_8$. However, traces of Fe^{3+} (or other metal ions) may not be required to initiate the conversion, as it occurs even with $(R_2C_2B_4H_4)_2Fe^{II}H_2$ samples that have been rigorously purified by vacuum sublimation (*28*). The mechanistic details of the fusion process have not been uncovered at this writing.

Oxidative fusion appears to have significant potential as a synthetic tool, inasmuch as it has been observed with other carborane ligands and with metallacarborane substrates such as (η^5-C_5H_5)$CoR_2C_2B_4H_5^-$ (see Section V,B). Moreover, several partially fused species we have

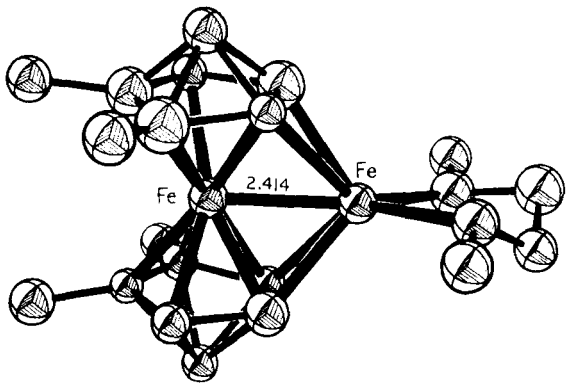

FIG. 14. Structure of $[(CH_3)_2C_2B_4H_4]_2Fe_2(OCH_3)_2C_2H_4$ (*28, 29*). Reprinted from *J. Am. Chem. Soc.* **104**, 5983. Copyright 1982 American Chemical Society.

isolated and structurally characterized may resemble early or intermediate stages in the fusion mechanism. These are discussed in Section VI.

B. Structure and Rearrangement of $R_4C_4B_8H_8$ Carboranes

The oxidative fusion of two $R_2C_2B_4H_4^{2-}$ ligands to generate $R_4C_4B_8H_8$ via metal sandwich complexes, a reaction of some interest in its own right, has led to another area of investigation, namely, the study of the $R_4C_4B_8H_8$ products. The formation of $(CH_3)_4C_4B_8H_8$ and its tetraethyl and tetrapropyl homologs occurs in high yield, and the air-stable products are easily purified by sublimation; hence it has been possible to explore in some detail the novel chemistry based on these carboranes (*18, 19*). In this subsection we outline the nonmetal stereochemistry based on the C_4B_8 system.

1. Solid-State Structure

The tetramethyl compound $(CH_3)_4C_4B_8H_8$ is an air-stable, easily sublimable, white solid (mp 138°C), which has surprising volatility at room temperature in air (in contrast, the icosahedral *o*-carborane $C_2B_{10}H_{12}$ is nonvolatile at room temperature). Its solid-state geometry (Fig. 12) has been established by X-ray crystallography, but the data are not of high quality. More recently, an X-ray study of the 4-ferrocenyl derivative (Fig. 13) confirmed, with much better precision, the same cage structure found for the unsubstituted compound; there are no significant differences in the two skeletal geometries. The C_4B_8 cage is a distorted icosahedron in which the C(2)—C(7) and C(3)—C(8) edges are stretched to nonbinding distances (~2.4 Å), thereby creating two four-sided, open faces. These stretch distortions allow all four skeletal carbon atoms to be low-coordinate, and reflect the presence of 28 (i.e., $2n + 4$) skeletal electrons, two more than a regular closo (icosahedral) cage can accommodate.

The neutral $(CH_3)_4C_4B_8H_8$ molecule is isoelectronic with the $C_2B_{10}H_{12}^{2-}$ dianions; a comparison of their structures would be of interest, but X-ray studies on the dianions have not been reported. However, the structures of two C,C′-disubstituted derivatives of the 1,2-$C_2B_{10}H_{13}^-$ monoanion (obtained by protonation of $C_2B_{10}H_{12}^{2-}$) have been determined (*7, 86*), and the cage geometry is shown in Fig. 7, type 1. This arrangement, in which one of the skeletal carbons accepts the proton and adopts a methylene-like bridging role, is clearly quite different from that of its isoelectronic C_4B_8 counterpart, shown as Fig. 7,

type 3. However, as was just noted, the structure of the nonprotonated $C_2B_{10}H_{12}^{2-}$ dianion is *not* known, and it is entirely possible that significant changes occur on protonation and deprotonation.

2. *Solution Structure*

An unusual type of fluxionality is exhibited by $R_4C_4B_8H_8$ species in solution. Boron-11 and proton pulse Fourier transform NMR studies of the tetramethyl compound in CCl_4, $CDCl_3$, benzene, and toluene (*52, 87*) reveal that a second isomer is formed in a matter of minutes, but the isomerization is only partial, and an equilibrium is established between the solid-state geometry (**A**) and the new isomer (**B**) (see Fig. 15). This behavior is largely solvent independent, and the equilibrium **B**:**A** ratio is approximately 3:5 at room temperature. When the solvent is removed the structure reverts entirely to **A**, as shown by NMR. It has not been possible to isolate the **B** form of $(CH_3)_4C_4B_8H_8$, but NMR evidence suggests a structure having a nonbonding interaction between the central carbon atoms (Fig. 7, type 2). This proposal is supported, in essence, by recent evidence on the tetraethyl carborane, $(C_2H_5)_4C_4B_8H_8$. Remarkably, this species exhibits a stereochemistry that is the *reverse* of that observed for $(CH_3)_4C_4B_8H_8$; that is, the solid-state structure corresponds to the **B** cage geometry, and an equilibrium between **B** and **A** isomers is established in solution. The direct correspondence between the **B** and **A** geometries in $(C_2H_5)_4C_4B_8H_8$ and their counterparts in $(CH_3)_4C_4B_8H_8$ is clear from the high-field ^{11}B- and ^1H- FT NMR spectra, which are closely similar (*87*). An X-ray diffraction study (*87*) has revealed the geometry of the solid-state (**B**) isomer of $(C_2H_5)_4C_4B_8H_8$ to be essentially that proposed for the **B** form of $(CH_3)_4C_4B_8H_8$, with the central carbon atoms well apart; the C(2)—C(7) and C(3)—C(8) distances are also nonbonding (~2.7 Å) so that the actual solid-state **B** structure of the $R_4C_4B_8H_8$ system (Fig. 16) is slightly more open than had been proposed.

The **A** and **B** geometries are nicely reconciled with the NMR observation of a facile, reversible interconversion in solution, because only small atomic motions are required for isomerizatin of **A** to **B** or vice versa. Moreover, the "idealized" (C_{2v}) representation of **B** (Fig. 16) is consistent with the ^1H-NMR spectrum of the **B** isomer of $(CH_3)_4C_4B_8H_8$, which indicates equivalence of all four C—CH_3 units above 40°C. Significantly, the ^1H- and ^{11}B-NMR spectra of **A** *do not* change materially at elevated temperature (*52, 87*).

Figure 16 depicts the proposed rearrangement equilibria for the $(CH_3)_4C_4B_8H_8$ isomers (*30*). Structure **C** is a cube-octahedron, a geome-

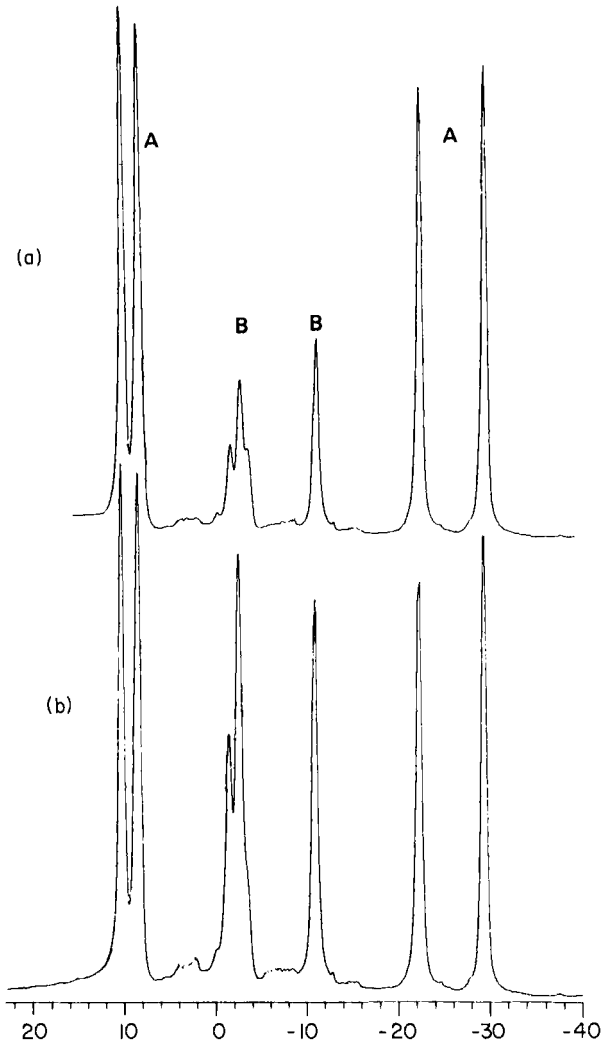

FIG. 15. 115-MHz ^{11}B- FT NMR spectra (proton decoupled) of $(CH_3)_4C_4B_8H_8$ in $CDCl_3$ solution at 25°C. (a) 2 min after dissolving. Peaks A are due to isomer **A** (solid-state structure, Fig. 12); peaks B are due to **B**. (b) Equilibrium mixture of **A** and **B**, observed 1 h 35 min after dissolving. Integrated A : B area ratio is 62 : 38 (*87*). Horizontal scale is chemical shift in parts per million [$BF_3 \cdot O(C_2H_5)_2$ = zero].

try that has been suggested as an intermediate in the isomerization of icosahedral $C_2B_{10}H_{12}$ carboranes (*47*). If **C** represents a time-averaged cage geometry for isomer **B** at 50°C, the C—CH_3 groups would be equivalent, as observed (*30*).

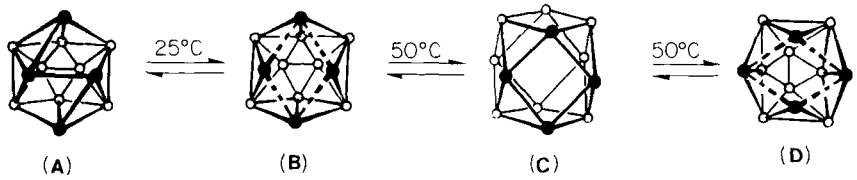

FIG. 16. Proposed fluxional interconversion of $(CH_3)_4C_4B_8H_8$ isomers **A** and **B**, showing postulated reversible thermal rearrangement of **B** at 50°C; **C** is a time-averaged (cube-octahedral) structure (*30*).

C. Formation and Fluxional Behavior of the $R_4C_4B_8H_8^{2-}$ Ion

If neutral $R_4C_4B_8H_8$, a 28-electron nido system, is reduced to the $R_4C_4B_8H_8^{2-}$ dianion, a 30-electron arachno species, one expects the cage structure to open significantly. This does in fact happen, but the stereochemistry is complex, and there seems to be no single preferred cage geometry. Treatment of $(CH_3)_4C_4B_8H_8$ with sodium naphthalenide in THF gives initially a green solution that changes to wine red and finally to yellow; presumably, the wine-colored species is a monoanion intermediate, $(CH_3)_4C_4B_8H_8^-$. The sodium salt of the yellow dianion $(CH_3)_4C_4B_8H_8^{2-}$ exhibits four equal-area ^{11}B-NMR resonances, suggesting C_s or C_2 symmetry (*50*), but the structure has not been established. However, the interaction of the dianion with transition-metal reagents generates an almost bewildering variety of metallacarborane complexes, strongly implying that the dianion exists in solution as a mixture of isomers.

An important clue to the structure of the dianion has been obtained via an X-ray diffraction study (*30*) of a *B*-cobaltocenium derivative of the $(CH_3)_4C_4B_8H_9^-$ monoanion, a species formed on protonation of $(CH_3)_4C_4B_8H_8^{2-}$. This compound, formulated as a σ-$[(C_5H_5)Co(C_5H_4)]^+$—$[(CH_3)_4C_4B_8H_8]^-$ zwitterion, has the structure shown in Fig. 17, in which the "extra" proton is located on one of the framework carbon atoms, which is lifted out of the cage skeleton and adopts a methylenic bridging role. The H—C—CH_3 bridging group is oriented such that the methyl group is located over the open face of the cage and the hydrogen is directed outward. This is reminiscent of the $R_2C_2B_{10}H_{11}^-$ structures shown in Fig. 7, type 1, except that in the latter the orientation of the R—C—H group is reversed; also, in the $R_2C_2B_{10}H_{11}^-$ structures, the bridging carbon spans a *bonded* B—B edge, whereas in the tetracarbon system the bridging carbon connects *nonbonded* boron and carbon atoms (Fig. 17). (It should be remembered, in comparing these species, that $R_2C_2B_{10}H_{11}^-$ is a 28-electron

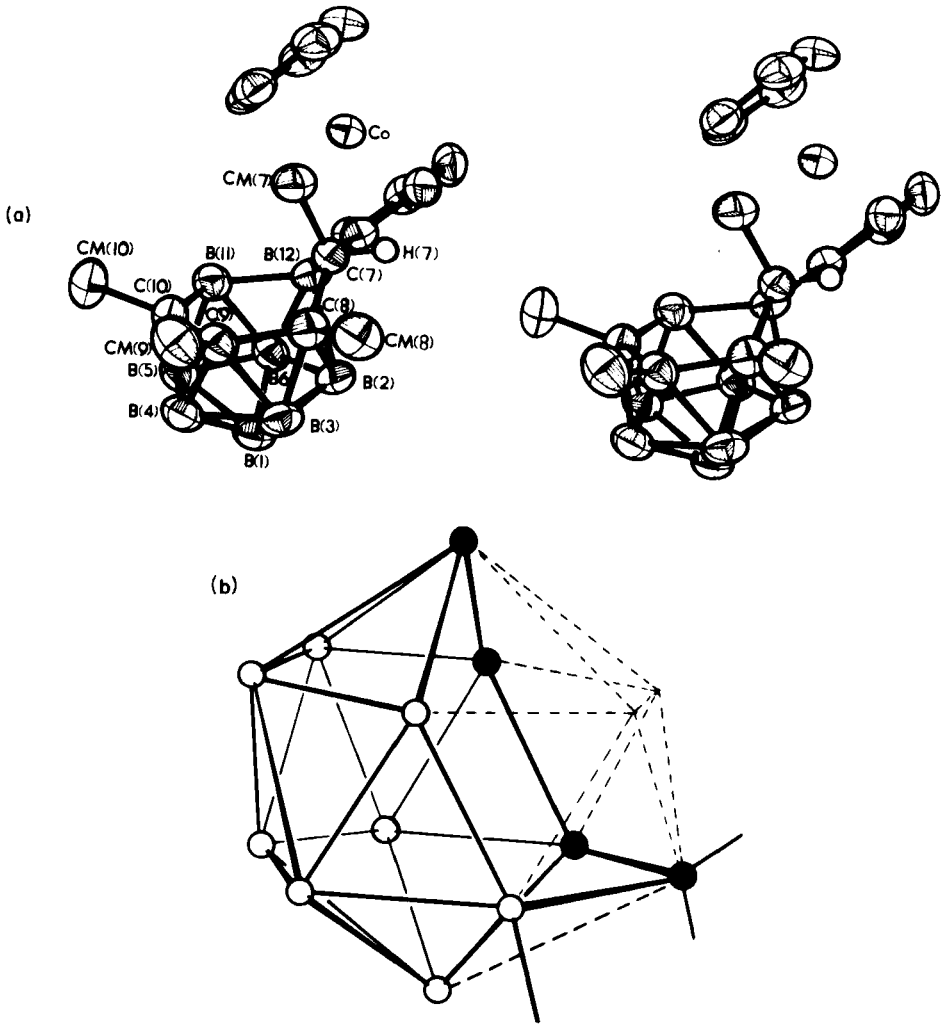

FIG. 17. (a) Stereoview of the 12-cobaltocenium derivative of the $(CH_3)_4C_4B_8H_9^-$ ion (*30*). Hydrogen atoms are omitted except for the unique methylenic hydrogen, H(7). (b) Cage structure of the cobaltocenium carborane, depicted as a fragment of a 14-vertex closo polyhedron (missing "vertices" are shown by dashed lines (*30*). Reprinted from *J. Am. Chem. Soc.* **101**, 4172. Copyright 1979 American Chemical Society.

system, whereas $R_4C_4B_8H_8^{2-}$ and its protonated form are 30-electron cages.)

The formation of $(CH_3)_4C_4B_8H_8^{2-}$ and its protonation to $(CH_3)_4$-$C_4B_8H_9^-$ are depicted in Fig. 18. The structure shown for the

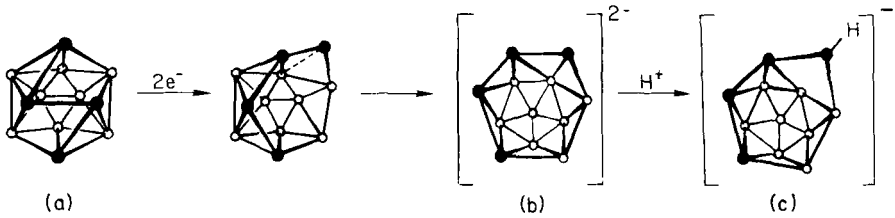

FIG. 18. Proposed scheme for conversion of neutral $(CH_3)_4C_4B_8H_8$ (a) to the $(CH_3)_4C_4B_8H_8^{2-}$ dianion (b) and the $(CH_3)_4C_4B_8H_9^-$ monoanion (c) (*30*).

dianion can be inferred from the known geometry of the monoanion (protonated species) in Fig. 17. In the absence of the extra proton, all four skeletal carbons are assumed to be fully incorporated into the cage, as shown for the dianion in Fig. 18; on protonation the unique low-coordinate carbon atom assumes an sp^3-hybridized bridging function across the open face. Protonation at carbon, rather than at the boron–boron edge on the open face, permits the cage to approach closely icosahedral-fragment geometry and relieves valence angle strain on the bridging carbon.

As mentioned previously, the $(CH_3)_4C_4B_8H_8^{2-}$ dianion gives every indication of being fluxional in solution at room temperature. Direct study of this behavior has been precluded by low solubility of salts of the dianion at low temperatures, but the established structures of transition metal complexes of the dianion provide some useful evidence. If we assume that (1) the attack of transition metal ions on a carborane anion occurs only at an open face and that (2) extensive skeletal rearrangement of metallacarborane products does not occur under the conditions of formation (i.e., room temperature), then the abundance of structural isomers obtained on metal complexation is explainable only in terms of the presence of several different isomers of the $(CH_3)_4C_4B_8H_8^{2-}$ ion in solution. Using the structure of $(CH_3)_4$-$C_4B_8H_8^{2-}$ in Fig. 18 as a model, we have proposed (*30*) that two kinds of reversible processes occur in this system, shown in Fig. 19. In the "fold-out" rearrangement, an atom on the four-membered open face of neutral $(CH_3)_4C_4B_8H_8$ is envisioned as moving away from two of its neighboring atoms, thereby creating an enlarged open face; in Fig. 19, the C—CH_3 unit at position 7 migrates in this fashion and adopts a lower-coordinate vertex on a six-membered C_4B_2 open face (structure **1A**). However, by small atomic motions, for example, stretching the B(2)—B(12) bond and compressing the C(7)—B(6) distance, B(12) can be made to occupy the unique low-coordinate position as in **1B**.

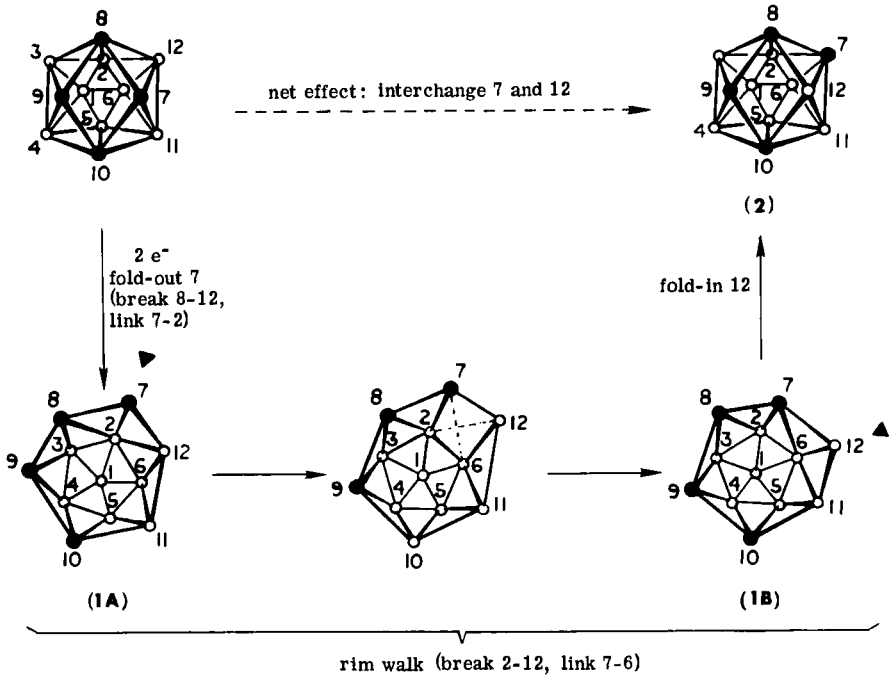

FIG. 19. Proposed scheme for fluxional rearrangement of $(CH_3)_4C_4B_8H_8^{2-}$ framework (*30*). **1A** corresponds to the established cage structure of the derivative shown in Fig. 17a; **1B** has the same geometric shape, but the unique low-coordinate vertex (marked by wedges in each structure) is now occupied by a BH unit. Reprinted from *J. Am. Chem. Soc.* **101**, 4172. Copyright 1979 American Chemical Society.

Clearly, one can in principle conduct the same kind of operation again with respect to B(12) and B(11), thus converting B(11) to a low-coordinate vertex; by extension of this idea, all six atoms on the open rim can, in turn, assume the low-coordinate role. We have labeled this kind of fluxional movement *rim walking* (*30*).

The reverse of the fold-out process depicted at the left of Fig. 19 is, of course, the fold-in, in which the low-coordinate atom (whatever it happens to be) migrates back into the open face to recreate a quasi-icosahedral cage geometry. This is illustrated at the right of Fig. 19, where B(12) is folded in to form bonds with C(8) and C(10) and produce a C(8)—C(9)—C(10)—B(12) open face (**2**). The interesting thing about the geometry of **2** is that it is related to the original geometry (upper left corner) *by interchange of C(7) and B(12)*. Obviously, one could, by a similar sequence, interchange C(7) with B(11), C(9) with B(3), or C(9)

with B(4). Even more generally, because a quasi-icosahedral geometry like that of $(CH_3)_4C_4B_8H_8$ can in principle be achieved by simply stretching *any* of the 30 edges of the icosahedron, it is clear that the fold-out → rim walk → fold-in sequence can, in theory, be used to interchange any two adjacent atoms on the 12-vertex polyhedral surface.

Actually, the preference of carbon for low-coordinate vertices, a well-established principle in carborane chemistry (*90*), is such that C—C and C—B edges are much more likely to be stretched than are the B—B interactions. (Indeed, this is shown by the fact that only two isomers of neutral $R_4C_4B_8H_8$, both involving stretch–distortion along C—C edges, are observed.) Thus the number of $(CH_3)_4C_4B_8H_8^{2-}$ isomers present in significant concentration is likely to be quite limited. Even so, the existence of several different forms of the dianion in fluxional equilibrium sets the stage for a stereochemically complicated interaction with transition-metal ions. This postulated fluxionality provides a reasonable explanation for the observed geometries of metal complexes derived from the $(CH_3)_4C_4B_8H_8^{2-}$ ion, as described in Section V.

Why are neutral $R_4C_4B_8H_8$ and $R_4C_4B_8H_8^{2-}$ ions fluxional in solution? This is a fair question because no such behavior is observed with the icosahedral $C_2B_{10}H_{12}$ isomers, and it is relatively unusual among carboranes in general. A qualitative answer is that there are opposing driving forces, one favoring icosahedral geometry because of its high inherent symmetry and stability, the other being the "electron-rich" condition (relative to the optimal $2n + 2$ electrons for a closo system), which favors cage opening. Moreover, the different forms are accessible by minor alterations in the cage framework, so that activation energies for interconversion are apt to be quite low. In this situation there is no clearly favored geometry, and the result is a highly mobile system in which even small changes, such as replacement of CH_3 by C_2H_5 or other alkyl groups, can affect the equilibria dramatically.

D. Synthesis and Stereochemistry of $(CH_3)_4C_4B_7H_9$

One of the most important properties of the dicarbon carborane 1,2-$C_2B_{10}H_{12}$ is its reaction with Lewis bases, in which the B(6)—H [or the equivalent B(9)—H] unit is selectively removed. The "hole" thus created can be filled by a wide variety of atomic units, including nonmetals, main-group metals, and transition elements. Can the $R_4C_4B_8H_8$ systems be similarly degraded? The answer is yes, but with

unexpected consequences; once again, the chemistry exhibited by the tetracarbon species is remarkably different from that of its dicarbon cousins, opening numerous new synthetic possibilities.

Triethylamine and THF are unreactive with $(CH_3)_4C_4B_8H_8$ in the absence of air, but 95% aqueous ethanol slowly converts the compound to $(CH_3)_4C_4B_7H_9$, a white, air-stable solid (mp 190°C) in yields of 40–60% (*13*). The reaction can be represented as

$$(CH_3)_4C_4B_8H_8 + 3H_2O \rightarrow (CH_3)_4C_4B_7H_9 + B(OH)_3 + H_2$$

although this is oversimplified, because there are other products not identified. The same carborane product can be prepared by the treatment of $Na^+[(CH_3)_2C_2B_4H_5]^-$ with $FeCl_2$ in THF at room temperature [recall that at −30°C these reagents generate $(CH_3)_4C_4B_8H_8$].

The molecular structure of $(CH_3)_4C_4B_7H_9$ was elucidated from an X-ray study of its monobromo derivative, which was obtained by reaction with Br_2 in carbon disulfide over aluminum chloride (*13*). Figure 20 shows the bromo species, which contains an H—C—CH_3 unit bridging the open top of a C_3B_7 basket that is isoelectronic and isostructural with $B_{10}H_{14}$. Thus once again we see the tendency of a framework carbon atom to accept a proton and thereby adopt an exopolyhedral bridging role. In this case a B—H—B hydrogen bridge is also present, as shown.

There is no doubt that the cage structure of the 11-bromo derivative (Fig. 20) is also that of the nonbrominated compound; the ^{1}H-NMR spectra are nearly identical, and the ^{11}B spectra differ, in essence, only in the replacement of a B—H doublet by a singlet resonance due to the brominated boron atom, B(11).

The cage framework can be represented as an arachno system, that is, a 13-vertex polyhedron with two vertices removed (Fig. 20b), in accordance with the presence of 28 ($2n$ + 6) skeletal electrons. The structure can also be described as a distorted 11-vertex polyhedron in which the edges connecting the apex [C(7)] to vertices 2, 3, 9, and 10 have been stretched to nonbonding distances; this stretch distortion is also consistent with the arachno electron count. Finally, one can view the molecule as a 10-vertex $(CH_3)_3C_3B_7H_8$ system that is isoelectronic with $B_{10}H_{14}$ and bridged by an exopolyhedral $HC(CH_3)$ group, as mentioned earlier.

The acid–base chemistry of $(CH_3)_4C_4B_7H_9$ is most remarkable (*13*). On treatment with sodium hydride in THF the proton attached to the bridgehead carbon is removed to give a $(CH_3)_4C_4B_7H_8^-$ anion, the framework geometry of which is significantly changed from the neu-

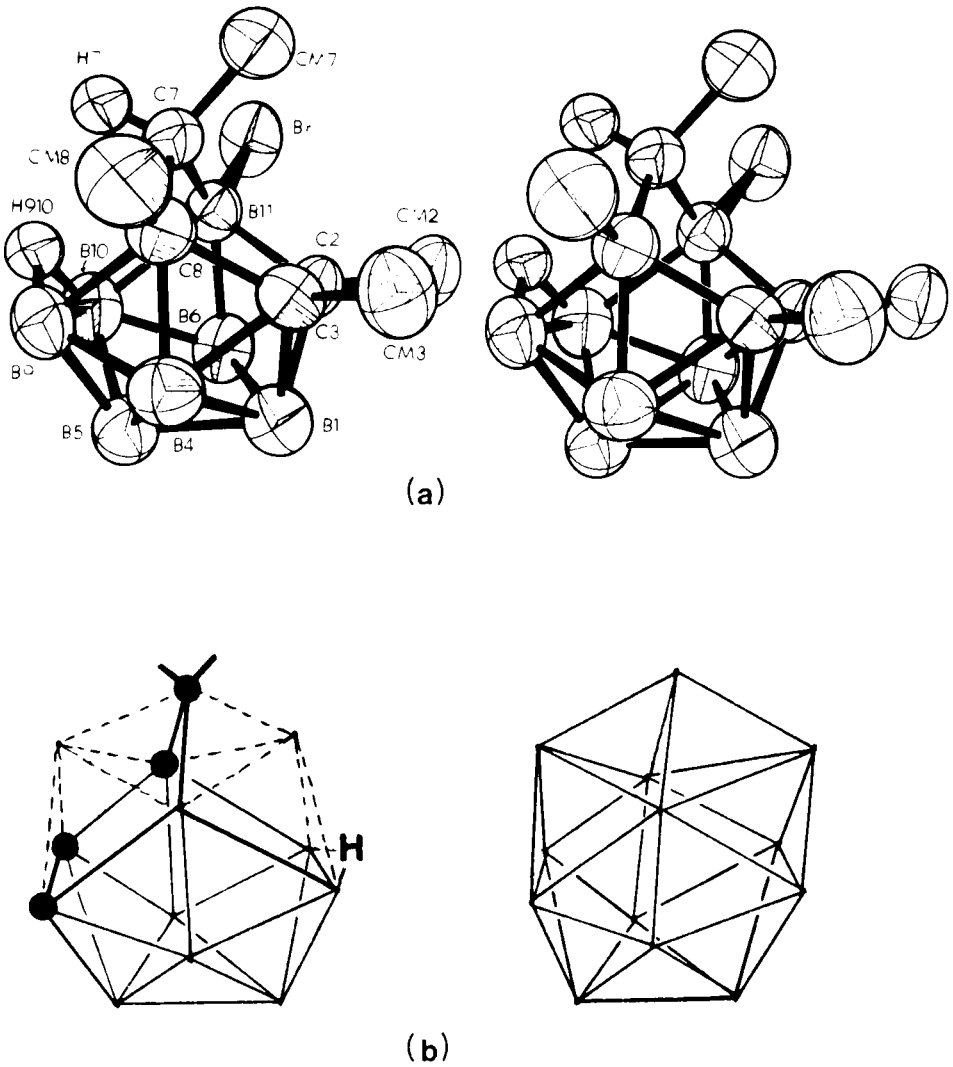

FIG. 20. (a) Stereoview of the structure of 11-Br-$(CH_3)_4C_4B_7H_8$ (*13*). (b) Same structure represented as an arachno fragment (left) of a closo 13-vertex polyhedron (right) (*13*). Reprinted from *J. Am. Chem. Soc.* **103,** 2675. Copyright 1981 American Chemical Society.

tral species, as indicated by the ^{11}B and ^{1}H spectra; reprotonation of the anion yields a neutral $(CH_3)_4C_4B_7H_9$ product that is different from both the original compound and the anion.

$$(CH_3)_4C_4B_7H_9 \xrightarrow[-H_2]{NaH} Na^+[(CH_3)_4C_4B_7H_8]^- \xrightarrow{HCl} (CH_3)_4C_4B_7H_9$$

Isomer I — Isomer II

A proposed mechanism for these interconversions is given in Fig. 21. That the proton removed is H(7) rather than the bridging hydrogen, H(910), is not surprising; deprotonation of the dicarbon species $(CH_3)_2C_2B_7H_{11}$ occurs similarly (*66*), and indications in general are that bridging CH protons in carboranes are more acidic than BHB bridges.

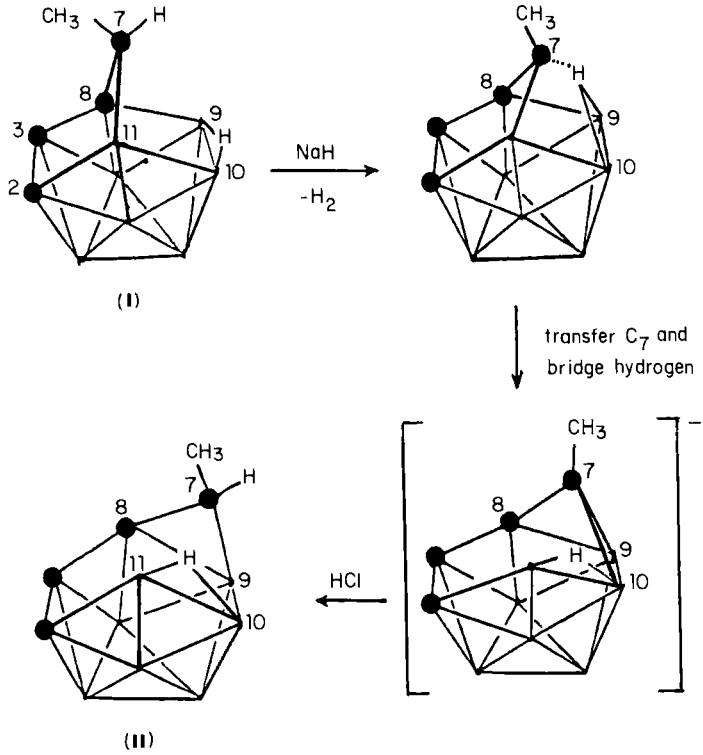

FIG. 21. Proposed scheme for conversion of $(CH_3)_4C_4B_7H_9$, isomer **I**, to **II** via deprotonation to $(CH_3)_4C_4B_7H_8^-$ and reprotonation (*13*). The structure of **I** is established; the others shown are based on NMR evidence. Reprinted from *J. Am. Chem. Soc.* **103**, 2675. Copyright 1981 American Chemical Society.

The structures shown in Fig. 21 for the anion and for isomer **II** have been proposed from NMR evidence combined with certain intuitive ideas about carborane rearrangements. First, removal of the CH proton from **I** obviously creates coordinative unsaturation at C(7), which can be relieved by movement of that atom into bonding interaction with B(9) and B(10); this, however, would induce the bridging hydrogen to move to a new location, very probably the B(10)—B(11) edge on the open face, as in the anion structure depicted. On reprotonation of the anion, reversion to the original structure (**I**) does *not* occur, evidently because that would entail a higher activation energy than does the conversion to **II** as shown. If the proposed geometry of **II** is correct, as is strongly indicated by the NMR spectra, it can be seen that only minor rearrangement [i.e., severing the C(7)—B(10) link and addition of a proton to C(7)] is required to convert the anion to **II**; re-formation of isomer **I**, in contrast, would require somewhat more atomic movement (including the relocation of the BHB bridge).

These processes represent, insofar as this author is aware, the first instance of carborane skeletal rearrangements induced by manipulation of protons under mild conditions. It can be assumed that other examples will be found, and this kind of stereochemistry is likely to prove quite general among carbon-rich carborane systems.

A scheme for the synthesis of $(CH_3)_4C_4B_7H_9$ (Fig. 21, **I**) from $(CH_3)_4C_4B_8H_8$ is presented in Fig. 22. The structure depicted for $(CH_3)_4C_4B_8H_8$ is that of isomer **B** (see Fig. 16), but clearly the same

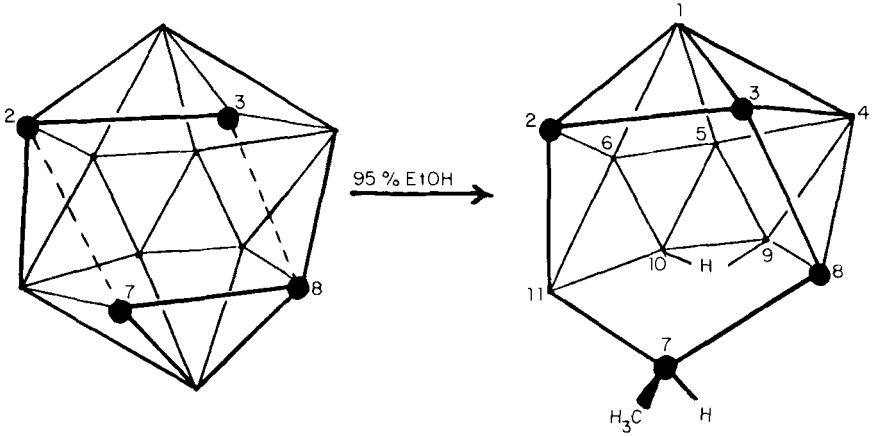

FIG. 22. Proposed scheme for conversion of $(CH_3)_4C_4B_8H_8$ to $(CH_3)_4C_4B_7H_9$ via removal of an apex BH and addition of hydrogen to C(7) (*13*). Reprinted from *J. Am. Chem. Soc.* **103**, 2675. Copyright 1981 American Chemical Society.

conversion could be drawn starting with isomer **A**. As shown, an apex BH unit is removed, atom C(7) picks up a hydrogen and moves into a bridging position [retaining its bonds to C(8) and B(11)], and a second hydrogen enters the open face as a BHB bridge between B(9) and B(10) (*13*). The attack of ethanol on B(12) is taken as evidence that this site and its equivalent, B(1), are the most electrophilic vertices in $(CH_3)_4C_4B_8H_8$; this correlates nicely with the fact that these are the only two boron atoms adjacent to more than one carbon. The well-known base degradation of 1,2-$C_2B_{10}H_{12}$ to $C_2B_9H_{12}^-$ (*21*) follows a similar pattern, in that the boron removed is vicinal to both carbon atoms and is, again, the most electrophilic site in the cage. [However, the observed bromination of $(CH_3)_4C_4B_7H_9$ at B(11), described previously, is somewhat surprising; electrophilic halogenation of the $C_2B_{10}H_{12}$ isomers usually takes place at boron atoms distant from carbon (*21*).]

V. Tetracarbon Metallacarboranes

The introduction of metals into carbon-rich carborane frameworks might be expected to produce some unusual stereochemistry, and this has amply been borne out by experience. When viewed against the known metallacarboranes based on one- and two-carbon systems (especially those derived from the $C_2B_{10}H_{12}$ isomers), the chemistry of the carbon-rich metal complexes is so different as to be almost beyond comparison; here one is well advised to "throw out the book." The basic reason for this dichotomy is that in the C_4 system the carbon atoms play a more distinctive stereochemical role and exhibit a clearly "non-boron" character.

A. Synthetic Routes

Four main pathways to four-carbon metallacarboranes have been described, namely, (1) oxidative fusion of dicarbon metallacarboranes, (2) direct insertion of metals into neutral C_4 carboranes, (3) metal insertion into C_4 carborane anions, and (4) thermal rearrangement. Of these routes, the first has no parallel in the synthesis of two-carbon metallacarboranes; methods 2, 3, and 4 are reminiscent of well-known procedures in the C_2-metallacarborane area, although for the most part the similarity is in concept only and does not hold in detail.

B. Oxidative Fusion of Dicarbon Metallacarboranes

1. Conversion of Two CoC_2B_3 Units to a $Co_2C_4B_6$ Cage

The face-to-face fusion of pyramidal $R_2C_2B_4H_4^{2-}$ ligands via metal complexation was described in Section IV,A. Metallacarborane analogs in which the apex is occupied by a metal can also undergo fusion, as shown by the conversion of 1,2,3-(η^5-C_5H_5)$CoR_2C_2B_3H_4^-$ (R = H or CH_3) ions to dicobalt, tetracarbon species (*91*).

$$2(C_5H_5)CoR_2C_2B_3H_4^- \xrightarrow[-2e^-,\ -H_2]{[O]} (C_5H_5)_2Co_2R_4C_4B_6H_6$$

R = CH_3, 1 isomer; H, 3 isomers

When R = CH_3, only one isomer of the $Co_2C_4B_6$ system is obtained, the structure of which (*76*) is shown in Fig. 23 and also in Fig. 7, type 4.

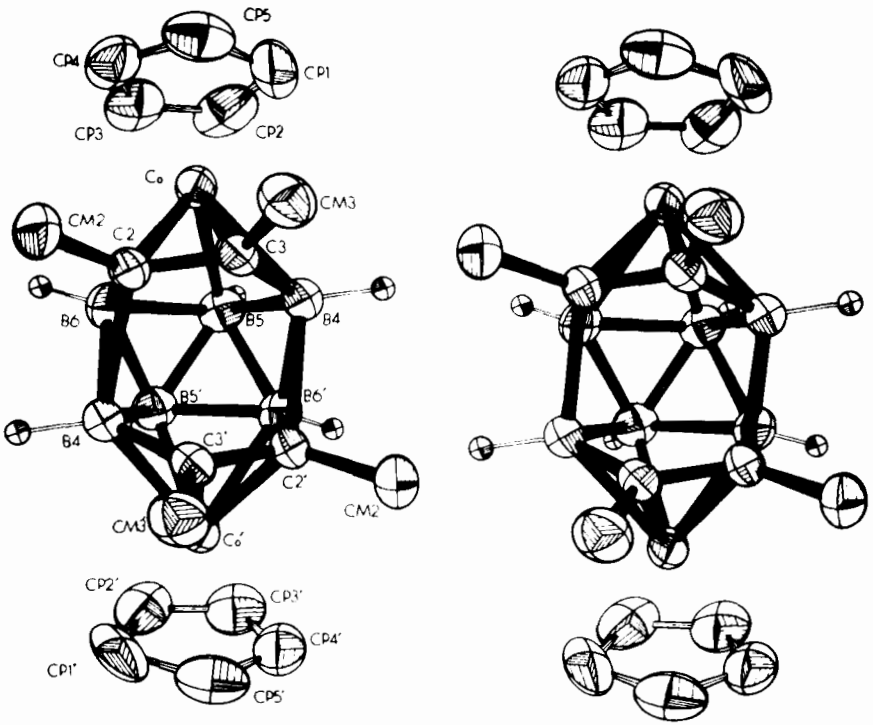

FIG. 23. Stereoview of (η^5-C_5H_5)$_2Co_2(CH_3)_4C_4B_6H_6$, isomer V (*76*). Reprinted from *Inorg. Chem.* **18**, 1936. Copyright 1979 American Chemical Society.

This complex is isoelectronic with $(CH_3)_4C_4B_8H_8$, and its cage geometry is similar except that in the dicobalt species the carbon–carbon distance across the center of the open face is distinctly nonbonding [2.791(5) Å], whereas, in the solid form (Fig. 16, **A**) of the carborane, it is bonding [1.515(5) Å] (*27*). This comparison provides a neat illustration of the electronic effects on cage structure induced by replacement of BH with $Co(C_5H_5)$ units at the apices. Evidently the metal–carbon bonding is relatively localized, tying up electron density at the expense of the central C—C interaction; in $(CH_3)_4C_4B_8H_8$ (Fig. 12) electron delocalization is more uniform and icosahedral geometry is more closely approached. [Of course, as we have seen in Section IV,B, the energy difference between the **A** and **B** forms, which, respectively, have bonded and nonbonded central carbon–carbon interactions, is quite small and leads to an **A** $\rightleftarrows$ **B** equilibrium in solution. Moreover, as noted previously, mere replacement of the four CH_3 groups in $(CH_3)_4C_4B_8H_8$ by C_2H_5 units is sufficient to reverse the situation and favor the **B** structure in the solid state (*87*).]

The structure of the dicobalt complex (Fig. 23) clearly resembles two CoC_2B_3 pyramidal units fused along the boron–boron edges and no doubt reflects a fusion process related to the formation of the $R_4C_4B_8H_8$ carboranes from $R_2C_2B_4H_4^{2-}$ pyramidal ligands (see previous discussion). When the starting material is the parent cobaltacarborane 1,2,3-$(\eta^5\text{-}C_5H_5)CoC_2B_3H_5$, not one but three $(C_5H_5)_2Co_2C_4B_6H_{10}$ isomers are obtained (*91*). One of these (designated isomer **V**) has a cage structure

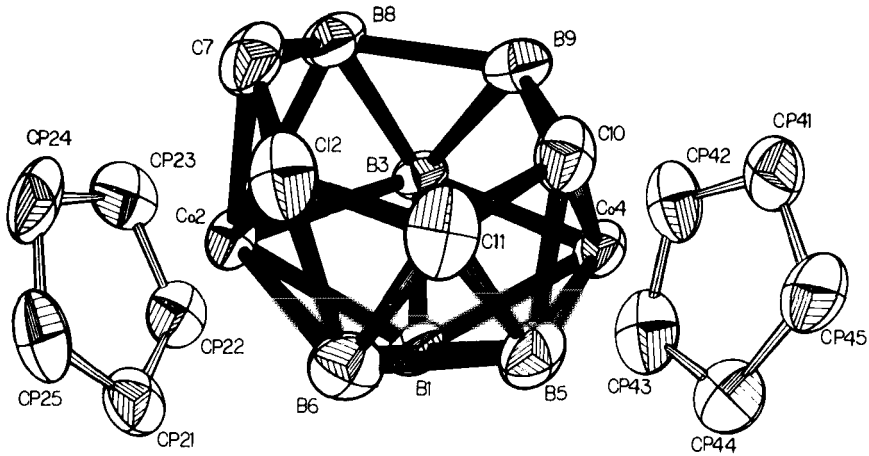

FIG. 24. Structure of $(\eta^5\text{-}C_5H_5)_2Co_2C_4B_6H_{10}$, isomer **VII** (*91*). Reprinted from *J. Am. Chem. Soc.* **100**, 5045. Copyright 1978 American Chemical Society.

analogous to that of $(C_5H_5)_2Co_2(CH_3)_4C_4B_6H_6$ in Fig. 23. A second isomer has the geometry depicted in Fig. 24, and the third, which has not yet been confirmed by X-ray data, is proposed to have pseudoicosahedral geometry. In the last instance, the high symmetry evident in both the ^{11}B- and ^1H-NMR spectra points rather strongly to this structure.

Figure 25 presents a mechanistic scheme (*76*) that accounts for all three isomers and indicates pathways for their interconversions. Species **I**, **II**, and **III** are proposed intermediates that have not been isolated, although tentative NMR evidence has been obtained for the quadruple-decker complex **I**. The formation of **I** would be analogous to the synthesis of $[(CH_3)_2C_2B_4H_4]_2CoH$ from $(CH_3)_2C_2B_4H_5^-$ and $CoCl_2$ in THF as described previously. To date, all efforts to characterize the quadruple-decker (**I**) have been unsuccessful, although an isomer of that species (in which one of the "end" cobalts is proposed to occupy an

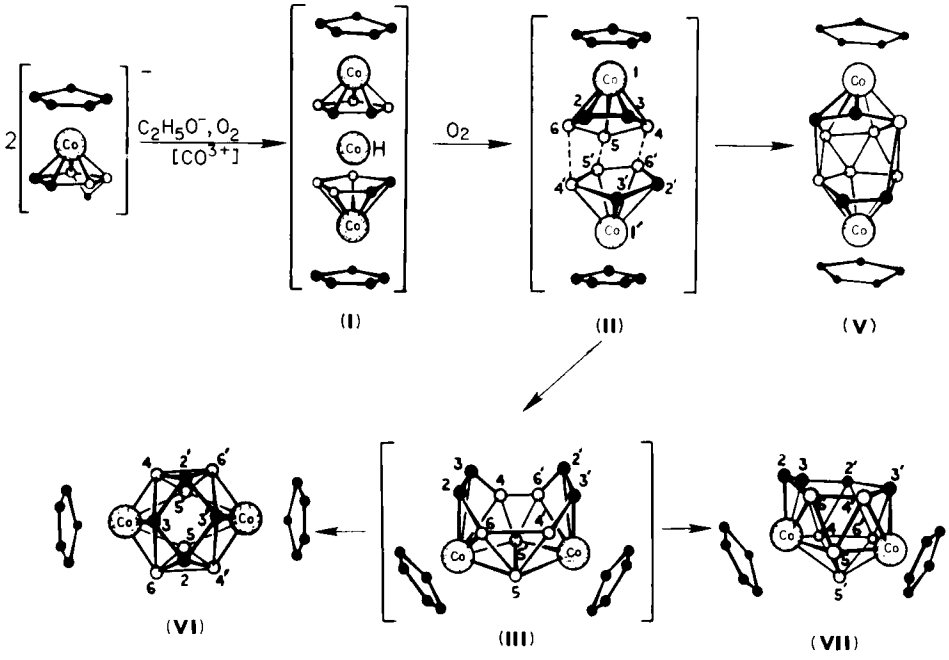

FIG. 25. Proposed scheme for formation of the three known isomers of $(\eta^5\text{-}C_5H_5)_2Co_2C_4B_6H_{10}$. Structures of **V** and **VII** are crystallographically established, and that of **VI** is postulated from NMR data; bracketed structures are possible intermediates (*76*). ○, BH; ●, CH. Reprinted from *Inorg. Chem.* **18**, 1936. Copyright 1979 American Chemical Society.

equatorial rather than an apical vertex) has been isolated (*54*). As shown, the three isomeric $(C_5H_5)_2Co_2C_4B_6H_{10}$ products **V**, **VI**, and **VII** are all postulated to originate from a common intermediate, **II**. Despite the dissimilarity of the three isomers, the atomic movements in **II** and **III** required to interchange them are relatively small.

Of the three isomers, **V**, **VI**, and **VII**, the "expected" geometry for a 28-electron 12-vertex (nido) system is represented by **VII** (Fig. 7, type 5), which is a fragment of a 13-vertex closo polyhedron. Indeed, for the analogous monocobalt system $(\eta^5\text{-}C_5H_5)Co(CH_3)_4C_4B_7H_7$, this type-5 geometry is thermodynamically favored, as demonstrated by a thermal isomerization study (see Section V,E). Presumably, **VII** is the preferred structural arrangement for the $Co_2C_4B_6$ system also, though this has not been proved. Why, then, in the fusion of the dimethyl complex $(\eta^5\text{-}C_5H_5)Co(CH_3)_2C_2B_3H_4^-$, is only one isomer (**V**) of $(\eta^5\text{-}C_5H_5)_2Co_2(CH_3)_4C_4B_6H_6$ obtained? Our reasoning is that the steric bulk of the methyl groups inhibits the close approach of C—CH_3 units in **III** (Fig. 25), as required for generation of **VII** and **VI**; the formation of **V** requires no such interaction, so that **V** is kinetically stabilized.

2. *Conversion of $[(CH_3)_2C_2B_4H_4]CoH[(CH_3)_2C_2B_3H_5]$ to $(\eta^5\text{-}C_5H_5)Co(CH_3)_4C_4B_7H_7$ (Isomer I)*

An apparent example of the oxidative fusion of C_2B_4 and C_2B_3 ligands involves the treatment of the sandwich complex $[(CH_3)_2C_2B_4H_4]CoH[(CH_3)_2C_2B_3H_5]$ with NaH or *n*-butyllithium to remove the metal-bound proton, followed by reaction of the resulting anion with $CoCl_2$ and NaC_5H_5 (*51*). The main product, $(\eta^5\text{-}C_5H_5)Co(CH_3)_4C_4B_7H_7$ (isomer **I**), has the open-cage structure depicted in Fig. 7, type 4, and it is identical to the species obtained on direct insertion of $Co(C_5H_5)$ into neutral $(CH_3)_4C_4B_8H_8$ (see following discussion). One assumes that the $[(CH_3)_2C_2B_4H_4]Co[(CH_3)_2C_2B_3H_5]^-$ anion undergoes fusion to generate a C_4B_7 carborane cage, into which cobalt is inserted to give the observed CoC_4B_7 product. However, this complex is isolated in only 14% yield, and other products are also formed, so that this reaction is not as clear-cut an example of fusion as are those involving the $[R_2C_2B_4H_4]_2MX_x$ species described previously.

C. Metal Insertion into Neutral C_4 Carboranes

Treatment of $(CH_3)_4C_4B_8H_8$ in solution with neutral metal reagents, at elevated temperature or under ultraviolet light, affords a variety of metallacarborane products (*50, 51*).

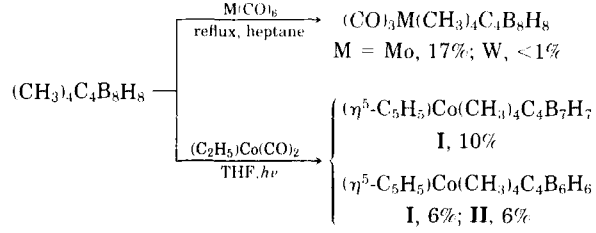

Because $(CH_3)_4C_4B_8H_8$ is fluxional and lacks a single, well-defined open face (see previous discussion), there is little steric control in such reactions; it is difficult to predict a priori the cage structures of the products, aside from the general rule in metallacarborane chemistry that metal atoms usually enter the cage in proximity to carbon atoms. The molybdenum complex (*50*) is a formal $(2n + 2)$-electron system corresponding to a 13-vertex closo polyhedron, but NMR data tell us only that the molecule lacks symmetry (no spectra are available for the tungsten species).

The cobalt reaction (*51*), however, is reasonably well defined in terms of product structures and a plausible pathway can be envisioned for their formation (Fig. 26). The major product, $(\eta^5\text{-}C_5H_5)Co(CH_3)_4C_4B_7H_7$, isomer **I**, has the type-4 structure (Fig. 7), which is directly analogous to that of $(\eta^5\text{-}C_5H_5)_2Co_2(CH_3)_4C_4B_6H_6$ (**V**), with one $Co(C_5H_5)$ unit replaced by BH. X-Ray structure determinations on both $(C_5H_5)Co(CH_3)_4C_4B_7H_7$ (*89*) and its 12-ethoxy derivative (*77*) reveal an open geometry with nonbonded C—C distances (~2.8 Å) across the open face; this is precisely like the dicobalt $Co_2C_4B_6$ (**V**) structure and different from $(CH_3)_4C_4B_8H_8$, which has a central C—C bond, as discussed earlier. Hence replacement of even one apex BH by $Co(C_5H_5)$ is sufficient to rupture the central C—C link and open the cage; the effect clearly cannot be a steric one and must be electronic in nature.

As shown in Fig. 26, the CoC_4B_7 product can be envisioned to form via displacement of an apex BH unit in the carborane reagent by $Co(C_5H_5)$. The other two characterized products in this reaction, both 11-vertex CoC_4B_6 systems, are assumed to form by loss of boron from the CoC_4B_7 species (*51*), as is also depicted in Fig. 26. The structures shown for these compounds were originally postulated from NMR data, which in both cases indicate mirror symmetry, but there was no unequivocal way to identify which was which. As it happens, X-ray diffraction studies of both compounds (*60*) have confirmed the proposed cage geometries (Fig. 27). These compounds are 11-vertex, 26-electron $(2n + 4)$ systems, which, as expected, adopt clear nido structures,

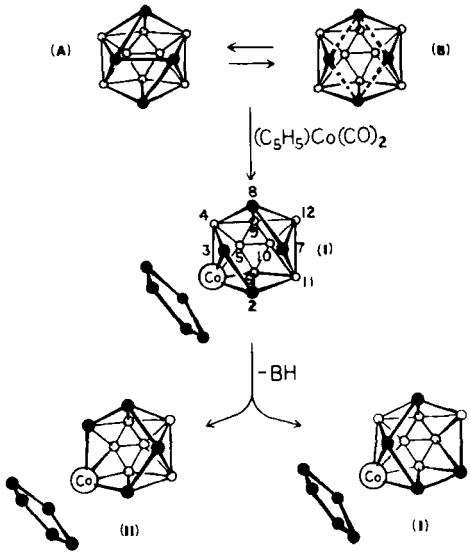

FIG. 26. Proposed scheme for formation of $(\eta^5\text{-}C_5H_5)Co(CH_3)_4C_4B_7H_7$, isomer **I**, from $(CH_3)_4C_4B_8H_8$ (**A** and **B**), and its degradation to $(\eta^5\text{-}C_5H_5)Co(CH_3)_4C_4B_6H_6$, **I** and **II** (*51*). ○, BH; ●, CH, CCH_3. Reprinted from *Inorg. Chem.* **18**, 2174. Copyright 1979 American Chemical Society.

based on removal of one vertex from an icosahedron. Unlike the 12-vertex nido systems, in which a variety of kinetically stabilized cage structures is observed, the icosahedral fragment is clearly the dominant geometry for 11-vertex, 26-electron cages.

The formation of the two CoC_4B_6 isomers from the CoC_4B_7 system as shown has not been directly established, but it does provide a straightforward explanation of their origin. Thus removal of B(11)—H from $(\eta^5\text{-}C_5H_5)Co(CH_3)_4C_4B_7H_7$, followed by movement of C(7)—CH_3 into the vacated position, yields $(\eta^5\text{-}C_5H_5)Co(CH_3)_4C_4B_6H_6$, (Fig. 26, **I**); removal of B(4)—H with similar migration of C(4)—CH_3, forms **II**. It should be noted that in both structures all four skeletal carbons occupy low-coordinate vertices on the open rim. This reflects a general trend that was mentioned in Section II and that is further discussed later in the chapter.

D. METAL INSERTION INTO $R_4C_4B_8H_8^{2-}$ DIANIONS

1. Cobalt Complexes

The reaction of transition-metal reagents with $R_4C_4B_8H_8^{2-}$ dianions furnishes another route to carbon-rich metallacarboranes. As we

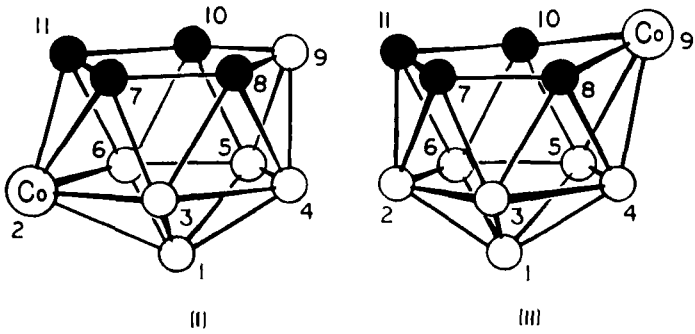

FIG. 27. Established cage geometries of $(\eta^5\text{-}C_5H_5)Co(CH_3)_4C_4B_6H_6$, isomers **I** and **II** (*60*). Reprinted from *Inorg. Chem.* **20**, 3858. Copyright 1981 American Chemical Society.

described earlier, the abundance of isomers generated from $(CH_3)_4C_4B_8H_8^{2-}$ under mild conditions strongly suggests that the dianion is fluxional in THF solution and that metal attack can occur on several isomeric forms of the substrate. The dianion is usually generated by reaction of neutral $R_4C_4B_8H_8$ (R = CH_3 or C_2H_5) with sodium naphthaleneide in cold THF, which is subsequently allowed to reach room temperature. Treatment of $(CH_3)_4C_4B_8H_8^{2-}$ with $CoCl_2$ and $C_5H_5^-$ ion, followed by acidification with HCl, produces three isolable compounds in low yield (*51*).

$$(CH_3)_4C_4B_8H_8^{2-} \xrightarrow[NaC_5H_5]{CoCl_2} (\eta^5\text{-}C_5H_5)Co(CH_3)_4C_4B_8H_8 + (\eta^5\text{-}C_5H_5)Co(CH_3)_4C_4B_7H_7 \quad \text{isomer II}$$
$$+ \sigma\text{-}[(\eta^5\text{-}C_5H_5)Co(\eta^5\text{-}C_5H_4]^+\text{—}[(CH_3]_4C_4B_8H_8]^-$$

The last two products have been structurally established from X-ray studies (*30, 31*), and the geometry of the CoC_4B_8 species has been deduced from the known structure of an NiC_4B_8 system (*31*), which appears, from NMR evidence, to be analogous to the cobalt compound. A schematic diagram of the reaction, Fig. 28 (*51*), represents two isomers of $(CH_3)_4C_4B_8H_8^{2-}$ in equilibrium; a mechanism for the interconversion of such species was suggested earlier (see Fig. 19). The introduction of a $Co(C_5H_5)$ unit into the cage, as shown (Fig. 28), gives the 13-vertex CoC_4B_8 nido complex, which in turn can lose a BH unit to produce the observed isomer **II** of a CoC_4B_7 system. Again, no direct mechanistic evidence is available; the scheme illustrated here is based on the known product structures and reasonable inferences. Thus it is not difficult to envision the $CoC_4B_8 \rightarrow CoC_4B_7$ conversion as shown, because it involves only removal of a boron and slight movement of a framework carbon atom to form a C—C link across the open face.

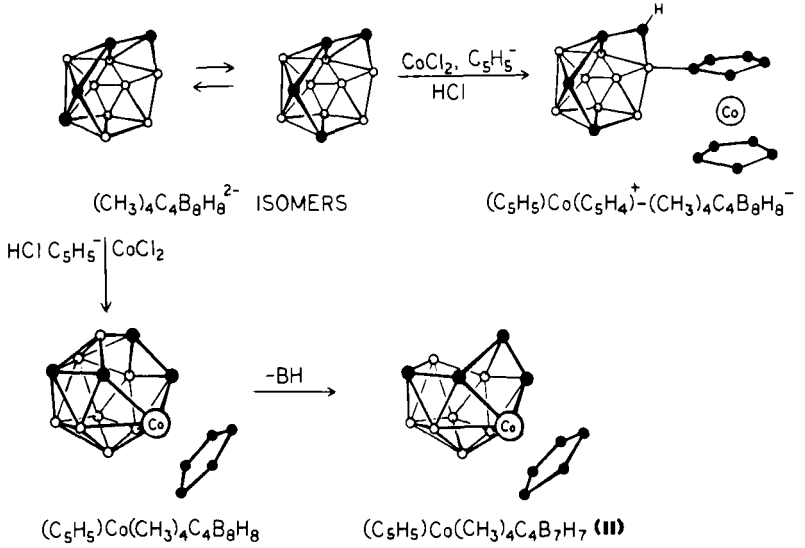

FIG. 28. Proposed scheme for reaction of $(CH_3)_4C_4B_8H_8^{2-}$ isomers with $CoCl_2$ and NaC_5H_5 in THF (*51*). The geometry depicted for $(C_5H_5)Co(CH_3)_4C_4B_8H_8$ is based on the known structure of an analogous nickel complex (see Fig. 29); the structures of the other products are established. Reprinted from *Inorg. Chem.* **18**, 2174. Copyright 1979 American Chemical Society.

The crystallographically determined structure of $(\eta^5\text{-}C_5H_5)Co(CH_3)_4C_4B_7H_7$ (**II**) (*31*), is unique and represents yet another form of nido geometry adopted by a 28-electron, 12-vertex system (Fig. 7, type 6). The central carbon–carbon bond in the framework is relatively long [1.567 (4) Å], indicating that the trans-cage bridging interaction across the open face is weak compared to normal bonds within the cage framework.

2. *Nickel Complexes*

Dichloro-1,2-bis(diphenylphosphino)ethanenickel(II) reacts with the $(CH_3)_4C_4B_8H_8^{2-}$ ion in THF to give at least five isolable nickelacarborane products, including two 12-vertex NiC_4B_7 and three 13-vertex NiC_4B_8 cage systems (*50*).

$$[(C_6H_5)_2PCH_2]_2NiCl_2 + Na_2[(CH_3)_4C_4B_8H_8] \xrightarrow[25°C]{THF} \xrightarrow{O_2} [(C_6H_5)_2PCH_2]_2Ni(CH_3)_4C_4B_7H_7 \text{ (two isomers)} + [(C_6H_5)_2PCH_2]_2Ni(CH_3)_4C_4B_8H_8 \text{ (three isomers)}$$

From ^{11}B- and ^1H-NMR observations it is evident that none of these complexes possesses a symmetry element. Because the $[(C_6H_5)_2PCH_2]_2$-

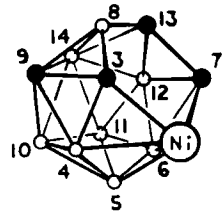

FIG. 29. Crystallographically determined cage structure of $[(C_6H_5)_2PCH_2]_2Ni(CH_3)_4C_4B_8H_8$, isomer **I** (*31*). ○, BH; ●, CCH_3. Reprinted from *Inorg. Chem.* **19**, 2087. Copyright 1980 American Chemical Society.

Ni unit is a formal two-electron donor to cage bonding [equivalent to $Co(\eta^5\text{-}C_5H_5)$ and BH], all of these species are $(2n + 4)$-electron systems of the nido class. The NiC_4B_7 isomers are 12-vertex, 28-electron cages that could well extend still further the number of distinguishable structural types in that series (see Fig. 7), but no X-ray data are available as yet. However, one of the NiC_4B_8 isomers has been characterized crystallographically (*31*), and its structure is shown in Fig. 29. This cage system can usefully be described as a 14-vertex closo polyhedron (bicapped hexagonal antiprism) from which one equatorial vertex has been removed; this geometry is clearly of the nido type and is in accord with the electron count. The well-defined five-membered open face contains three of the four carbon atoms in the cage, but this isomer is almost certainly not the thermodynamically most stable. This can be deduced from the absence of symmetry, the fact that the locations of B(8) and C(9) are reversed relative to the usual preference of carbon for low-coordinate vertices, the presence of a six-coordinate BH unit [B(14)], and the location of the metal on the open rim, where its orbital overlap with neighboring atoms would be less efficient than that of a nonrim metal atom. Thus we have yet another kinetically stabilized cage system.

The 13-vertex complex $(\eta^5\text{-}C_5H_5)Co(CH_3)_4C_4B_8H_8$ is isoelectronic with the nickel species in Fig. 29 and is believed to have the same cage geometry, although this has not been established.

3. *Iron Complexes*

The treatment of $(CH_3)_4C_4B_8H_8^{2-}$ salts with $FeCl_2$ and NaC_5H_5 in THF affords a rich harvest of isolable complexes, mostly in small yields to be sure, but air stable, characterizable, and structurally interesting (*50*).

$$(CH_3)_4C_4B_8H_8^{2-} \xrightarrow[FeCl_2]{NaC_5H_5} \xrightarrow{O_2} (\eta^5\text{-}C_5H_5)Fe(CH_3)_4C_4B_7H_8 + (\eta^5\text{-}C_5H_5)_2Fe_2(CH_3)_4C_4B_8H_8$$

I, II, III, IV

The 12-vertex FeC_4B_7 species has been characterized by X-ray diffraction (*50*), and the geometry Fig. 30, **5**) is of type 5 (Fig. 7), consisting of

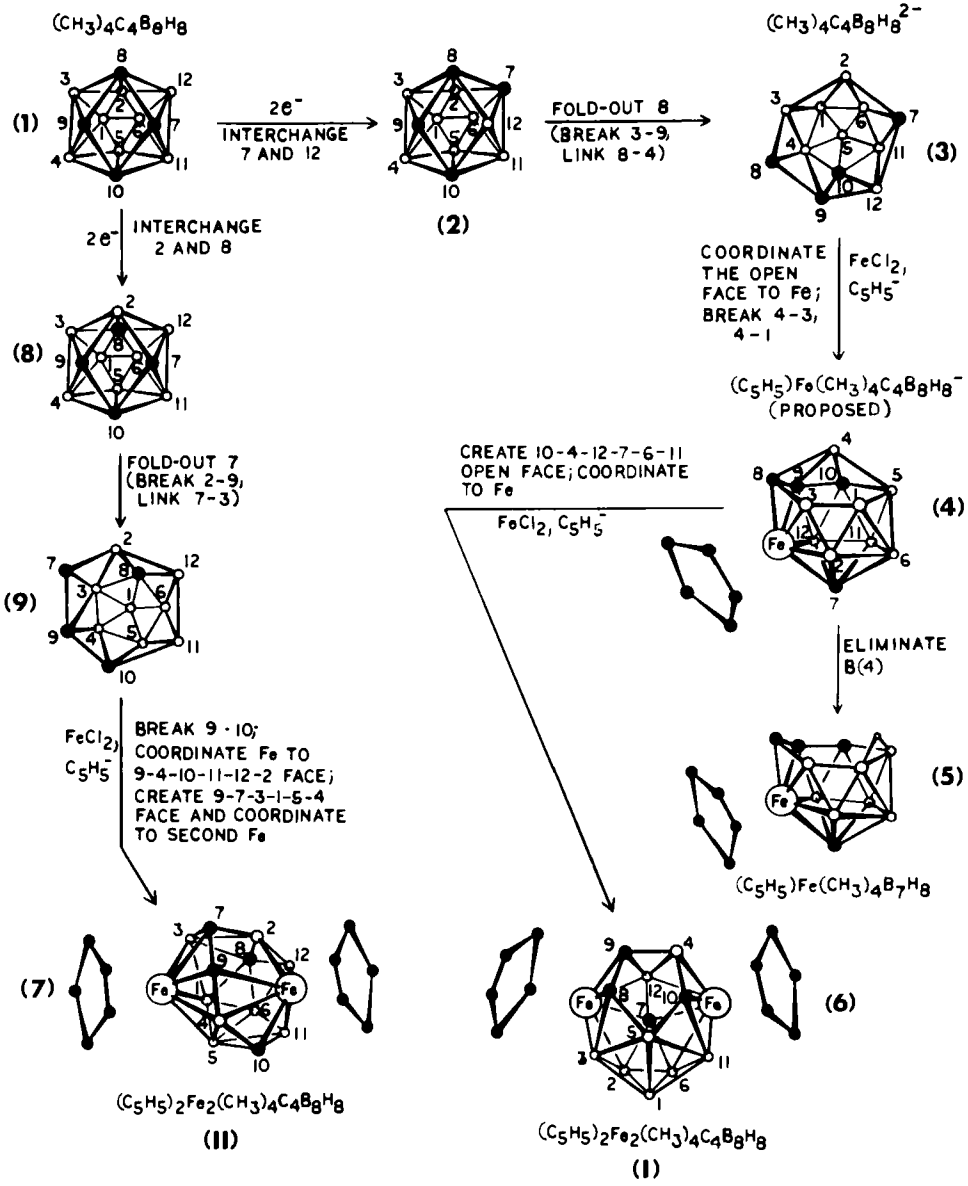

FIG. 30. Proposed sequence for formation of ferracarboranes from $(CH_3)_4C_4B_8H_8^{2-}$ isomers (*30*). ○, BH; ●, CH, CCH_3. Structures of products **5**, **6**, and **7** are established. The isomeric carborane species **2**, **3**, **8**, and **9** are proposed to form via pathways depicted in Figs. 18 and 19. Reprinted from *J. Am. Chem. Soc.* **101**, 4172. Copyright 1979 American Chemical Society.

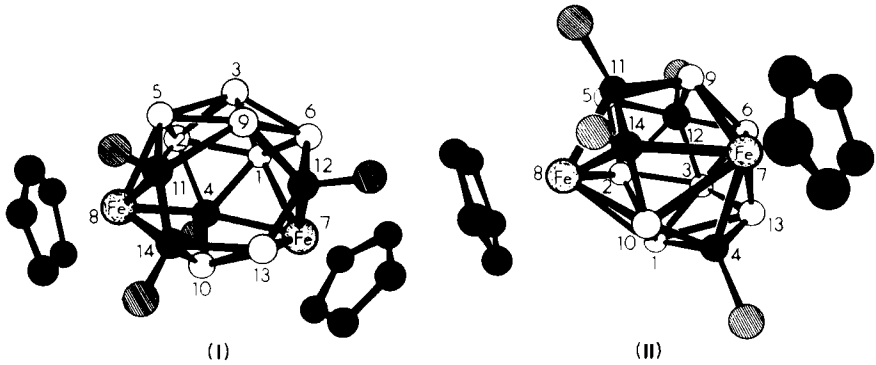

FIG. 31. Crystallographically determined structures of $(\eta^5\text{-}C_5H_5)_2Fe_2(CH_3)_4C_4B_8H_8$ isomers **I** and **II** (*57*). ○, BH; ●, C; ⊜, CH_3. Reprinted from *J. Am. Chem. Soc.* **99**, 4008. Copyright 1977 American Chemical Society.

a nido 12-vertex cage in conformity with the 28 ($2n$ + 4) skeletal electrons. The extra hydrogen atom is present in a B—H—B bridge on the open rim, as expected, but the structure has one peculiar feature: one of the skeletal carbon atoms [C(1)] is located in the apex, as far as possible from the open rim, and is not adjacent to any of the other carbons. Here again, the structure provides a clue to the mode of attack of the metal on the carborane anion substrate and further supports the idea that the $(CH_3)_4C_4B_8H_8^{2-}$ ion exists in more than one isomer in THF solution.

Figure 30 presents a mechanistic scheme that accounts for the observed geometry of $(C_5H_5)Fe(CH_3)_4C_4B_7H_8$ (**5**), as well as those of $(\eta^5\text{-}C_5H_5)_2Fe_2(CH_3)_4C_4B_8H_8$ isomers **I** and **II** (**6** and **7**, respectively, in Fig. 30). The latter two structures, determined from X-ray studies (*57*), are depicted in more detail in Fig. 31. These were among the first tetracarbon metallacarborane structures we studied, and they were astonishing at the time. Despite the closo electron count (14 vertices, 30 skeletal electrons), neither isomer has the expected closed polyhedral, bicapped square-antiprism geometry; instead, both are open-faced cages. Isomer **I** actually has a nido shape; it can be viewed as a 15-vertex closo cage with one vertex removed. That is, if one caps the open face (*56*), the resulting polyhedron has (idealized) D_{3h} symmetry, corresponding to the structure proposed by Brown and Lipscomb (*4*) for a hypothetical $B_{15}H_{15}^{2-}$ ion. In contrast, isomer **II** has a four-sided open face and bears no clear relationship to any standard polyhedron. (Indeed, if all 14 vertices were occupied by identical units there would still be no element of symmetry in the cage!)

Clearly, the structures of these 14-vertex isomers reflect their mechanism of formation from the carborane dianion. The scheme in Fig. 30 utilizes the proposed fluxional rearrangement of $(CH_3)_4C_4B_8H_8^{2-}$, as given earlier (see Fig. 19) to account for the observed ferracarborane products. It is significant that isomers **I** and **II** cannot be interconverted in a small number of steps (e.g., fewer than ten) by any simple mechanism such as diamond–square–diamond (dsd) (*47*); given that both species are obtained under mild conditions, it is obvious that they are produced independently in the reaction, together with other isomers of $(\eta^5\text{-}C_5H_5)_2Fe_2(CH_3)_4C_4B_8H_8$.

Thermal rearrangement of these 14-vertex species generates still other isomers, including, finally, the expected closo system, as described in Section V,E.

4. Chromium Complexes

Insertion of chromium into the $(C_2H_5)_4C_4B_8H_8^{2-}$ ion, utilizing $CrCl_3$ and NaC_5H_5 as reagents, forms two characterizable products, 12-vertex $(\eta^5\text{-}C_5H_5)Cr(C_2H_5)_4C_4B_7H_7$ and 13-vertex $(\eta^5\text{-}C_5H_5)Cr(C_2H_5)_4C_4B_8H_8$ (*61*). The structures of both species have been determined from X-ray crystal structure analyses (Fig. 32), and they provide further examples of "nonconformist" geometry wherein open faces seem to violate the electron-counting rules for clusters. Following the usual convention, $Cr(C_5H_5)$ is a formal (−1)-electron donor [having three fewer electrons than $Co(C_5H_5)$, a two-electron donor]; hence the two species are, respectively, 12-vertex, 25-electron and 13-vertex, 27-electron systems and are formal $(2n + 1)$-electron cages. The overall shapes of the two cages approach closo 12-and 13-vertex polyhedra, but the presence of an open face in each case is unmistakable; all transannular distances across these faces are clearly nonbinding. These structures can be rationalized as nido $(2n + 4)$-electron systems if the deficiency of three electrons is assumed to reside on chromium, which then becomes a 15-electron metal (*61*).

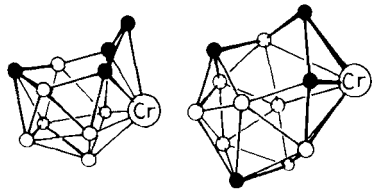

FIG. 32. Crystallographically determined cage geometries of $(\eta^5\text{-}C_5H_5)Cr(C_2H_5)_4C_4B_7H_7$ (left) and $(\eta^5\text{-}C_5H_5)Cr(C_2H_5)_4C_4B_8H_8$ (right) (*61*). ○, BH; ●, CC_2H_5.

E. Thermal Rearrangements

The numerous examples of unconventional, kinetically stabilized structures described up to this point underline the need for thermal-isomerization studies to determine the thermodynamically favored structures for these cage systems. Such studies are not trivial, because X-ray diffraction studies are usually required to establish the structures of the isomers formed; at this time only two rearrangements of tetracarbon metallacarboranes have been examined. However, in both cases some fundamental questions have been answered, and we can have confidence that the structural principles outlined in Section II do seem to hold with respect to thermodynamically preferred isomers, at least for iron and cobalt complexes.

1. The 14-Vertex $(\eta^5\text{-}C_5H_5)_2Fe_2(CH_3)_4C_4B_8H_8$ System

The unique, highly asymmetric cage structures of isomers **I** and **II** (Fig. 31) both rearrange at elevated temperature (*57*); **I** is converted to a new species, **V**, whereas **II** rearranges to another isomer (**VI**), which in turn is converted to **V**. Thus both **I** and **II** ultimately converge to the same product, **V** (Fig. 33). However, the structure of **V**, as determined crystallographically, is another open-faced cage, which in fact is closely related to its precursor **I**. Interchanging the BH and CCH_3 groups at vertices 3 and 11, respectively, *formally* converts **I** to **V** (this is not meant to imply an actual mechanism). What is the driving force for conversion of **I** to **V**? Because the overall shape of the $Fe_2C_4B_8$ cage is essentially unchanged, and because **V** actually has fewer carbons on the open face than **I**, it appears that *separation of the framework carbon atoms* is the dominant factor. This observation is in line with much previous evidence in dicarbon metallacarborane chemistry (*9, 11, 43, 64*), but the present carbon-rich systems present a much more complex stereochemical situation; there is more to consider here. Thus, when **V** itself is heated to still higher temperatures, further rearrangement takes place, yielding **VII**, as shown. This new species is believed to have a closo structure, depicted in Fig. 33, which is based on NMR evidence indicating twofold symmetry in the molecule (*57*). Although the arrangement shown, which has the carbon atoms in vertices 2, 4, 10, and 12, is only one of six possible isomers that are compatible with the NMR spectra, all six of these have at least one C—C bond, and four of them have two C—C interactions. For reasons discussed elsewhere (*57*), the 2,4,10,12-structure is preferred over the others, but this is a relatively minor point; the significant observation is that the conver-

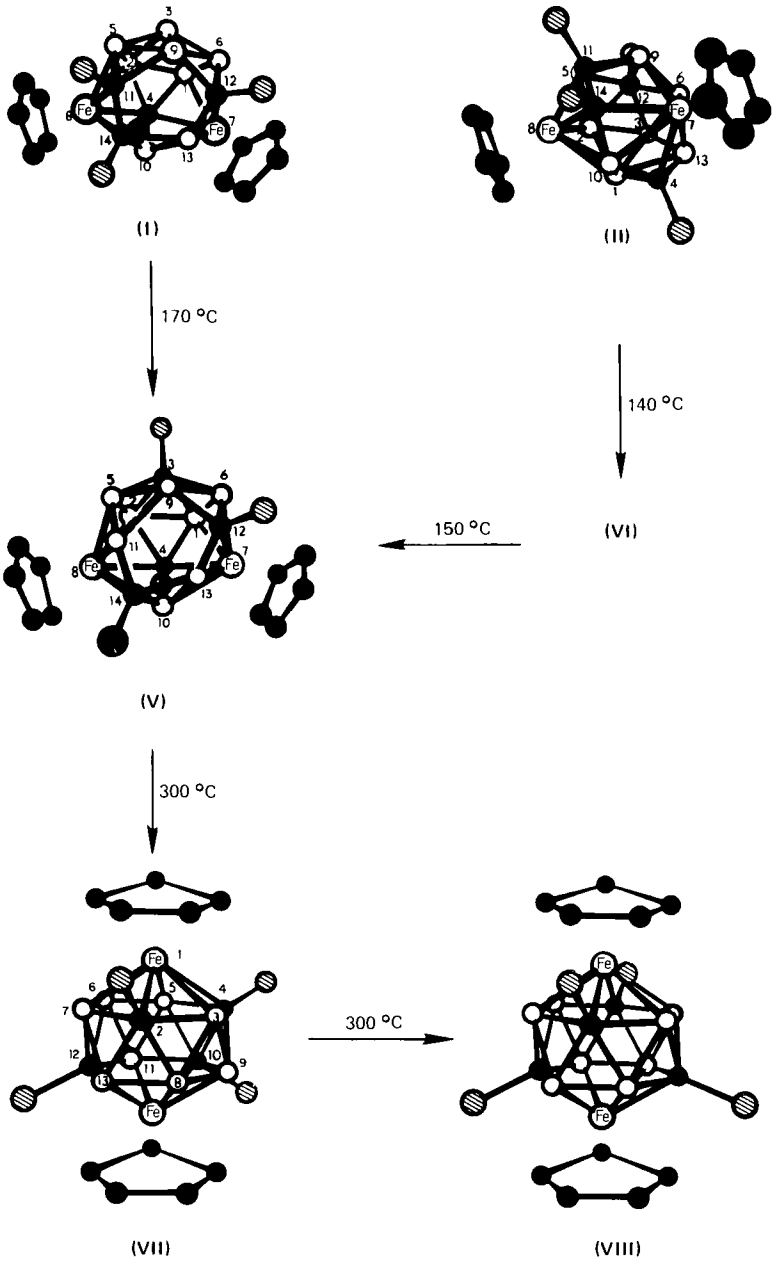

FIG. 33. Thermal rearrangement of $(\eta^5\text{-}C_5H_5)_2Fe_2(CH_3)_4C_4B_8H_8$, isomers **I** and **II**, to **V, VII,** and **VIII.** ○, BH; ●, C; ⊛, CH_3. All structures shown are crystallographically established except for **VII,** the geometry of which is postulated from NMR spectra (*57*). Reprinted from *J. Am. Chem. Soc.* **99,** 4016. Copyright 1977 American Chemical Society.

sion of **V** to **VII** involves movement of two carbon atoms toward each other, that is, to vicinal positions in the framework. Because this is contrary to the usual trend in carborane rearrangements, the lesson here must be that *the drive to achieve a closo structure is predominant.*

Continued heating at 300°C converts **VII** to the final product, isomer **VIII,** as shown (Fig. 33). The structure of **VIII** was virtually established from NMR spectra alone, which revealed the equivalence of all eight BH and all four CCH_3 units. The bicapped hexagonal-antiprism geometry with idealized D_{2d} cage symmetry was, however, established conclusively by X-ray diffraction (*73*) (Fig. 34). At this writing, this is the only crystallographically confirmed example of a 14-vertex closo system, although isomers of $(\eta^5\text{-}C_5H_5)_2Co_2C_2B_{10}H_{12}$ have been pro-

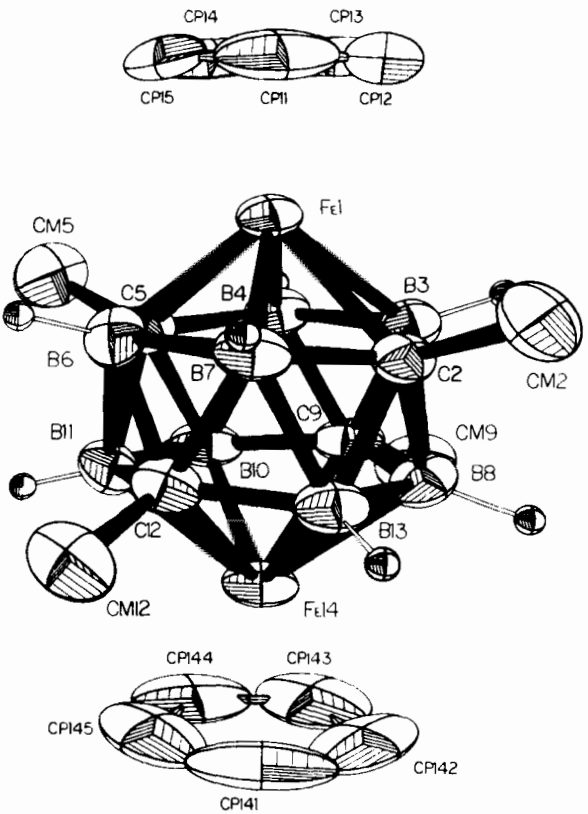

FIG. 34. Structure of $(\eta^5\text{-}C_5H_5)_2Fe_2(CH_3)_4C_4B_8H_8$ (isomer **VIII**), a 14-vertex closo polyhedron (bicapped hexagonal antiprism) (*73*). Reprinted from *Inorg. Chem.* **17,** 6. Copyright 1978 American Chemical Society.

posed to have similar structures, based on a 14-vertex closo polyhedron (*10*). The structure of **VIII** is, therefore, the preferred arrangement for the $Fe_2C_4B_8$ system and validates Wade's electron-counting rules for polyhedra of this size. If the observed rearrangement sequence in Fig. 33 can be taken to have general significance, it appears that the achievement of closo geometry (for $2n + 2$ systems) is dominant over separation of skeletal carbon atoms, which in turn is more important than placement of carbon in low-coordinate vertices. Time will tell, of course, whether these rules hold in a broader sense.

2. *The 12-Vertex* $(\eta^5\text{-}C_5H_5)Co(CH_3)_4C_4B_7H_7$ *System*

Three isomers of this $(2n + 4)$-electron complex are known, and, remarkably, all are of different structural classes, designated as types 4, 5, and 6 (Fig. 7). Thermal rearrangement of isomer **I**, which has the type-4 structure, at 140°C (*59*) gives isomer **III** (type 5), as illustrated in Fig. 35. This isomerization involves several trends: (1) adoption of a true nido geometry based on a fragment of a closo polyhedron; (2) retention of low-coordinate vertices on the rim by carbon; (3) migration of one of the carbon atoms to an isolated location on the open face; and (4) achievement of six-coordination (with respect to the cage) by the cobalt atom. The first trend is in accord with the basic ideas inherent in the closo–nido–arachno scheme described in Section II, and it also supports our intuitive feeling that the type-5 geometry is more compact and conducive to efficient delocalization of electrons than the type-4 structure of isomer **I**. (Recourse to intuition may not appeal to some, but until these systems can be handled in more definitive fashion by theorists, it can hardly be dispensed with.) Trend 2 appears to be unimportant here, because all carbons are in low-coordinate vertices in both isomers. Trend 3 illustrates the well-established tendency of cage carbon atoms to separate from each other, but it is notable here that *none of the carbons chooses to migrate away from the open face in order to achieve such separation.* This is interesting because it seems to contradict the observation of the $(\eta^5\text{-}C_5H_5)_2Fe_2(CH_3)_4C_4B_8H_8$ isomerization (**I** to **V**) discussed previously, where the conclusion was precisely the opposite. Either the two systems are sufficiently dissimilar that thermodynamic preferences of this sort are not truly comparable, or there is no low-energy pathway for migration of carbon away from the open face in the $(\eta^5\text{-}C_5H_5)Co(CH_3)_4C_4B_7H_7$ system. At present it is not possible to distinguish between these hypotheses.

Finally, as to the last point, the adoption of a high-coordinate vertex

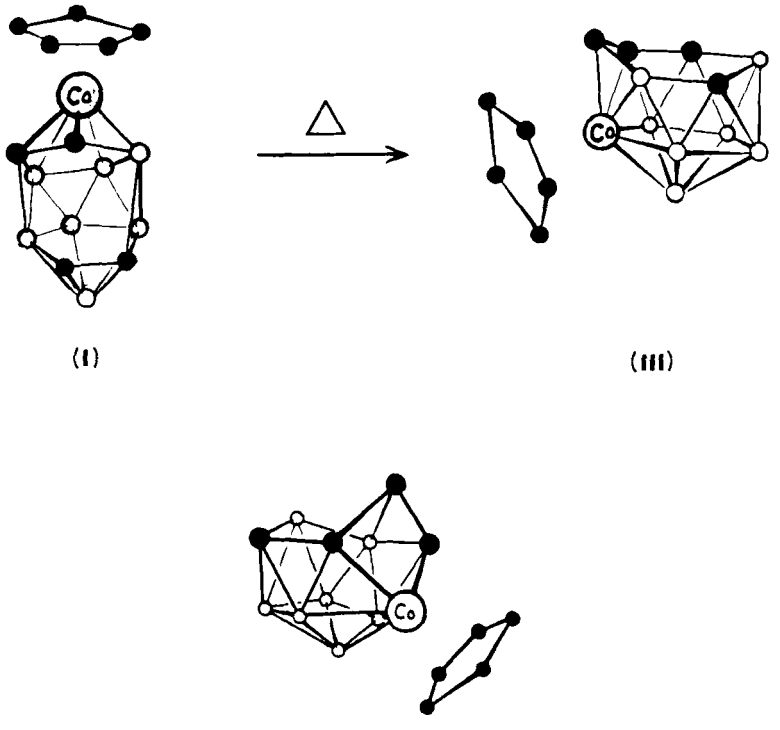

FIG. 35. Thermal rearrangement of $(\eta^5\text{-}C_5H_5)Co(CH_3)_4C_4B_7H_7$, isomer **I**, to **III** (*59*). Reprinted from *Inorg. Chem.* **20,** 1201. Copyright 1981 American Chemical Society. A third isomer, **II** (*31*), is shown below. Reprinted from *Inorg. Chem.* **19,** 2087. Copyright 1980 American Chemical Society. All three structures are established; that of **III** is evidently the thermodynamically preferred geometry.

by cobalt is in line with a general trend in cobaltacarborane and cobaltaborane chemistry; as a rule, iron and cobalt tend to maximize their coordination to the borane cage when the opportunity presents itself. It can be argued, in simple qualitative fashion, that the high-coordinate sites allow more efficient overlap between metal and framework orbitals. However, nickel and other electron-rich metals often exhibit the reverse trend, favoring low-coordinate cage vertices [for example, in the metallaboranes $(\eta^5\text{-}C_5H_5)_4M_4B_4H_4$, both of which are 8-vertex closo dodecahedra, the metal atoms occupy the high-coordinate vertices when M is cobalt (*74*), but low-coordinate vertices when M is nickel (*3*)].

VI. Partially Fused Polyhedra: Structures Related to the Tetracarbon Carboranes and Metallacarboranes

Carbon-rich carboranes, as defined for purposes of this chapter, are polyhedral borane cages containing three or more (usually four) carbon atoms. Ordinary bis(carboranyl) metal complexes of the type $(R_2C_2B_nH_m)_2M$ are excluded from this category because the individual MC_2B_n cage systems have only two carbons. However, there is an intermediate, borderline class of complexes in which the carborane ligands are linked by more than a common metal atom and which can be described as "partially fused." One might suspect that such species are related, somehow, to the oxidative fusion process described previously; such a relationship has already been found in at least one case.

A. $MFeC_4B_8$ "Wedged" Complexes (M = Co, Fe, Ge, Sn)

Reactions of the red iron complex $[(CH_3)_2C_2B_4H_4]_2FeH_2$ or its conjugate base anion with a variety of metal reagents result in the introduction of a second metal atom to give a wedged complex (*53, 58*).

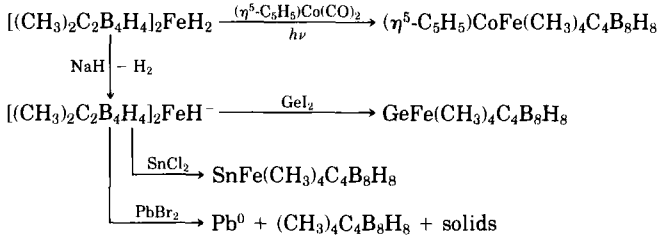

The cobalt–iron complex has been shown by X-ray crystallography (*55*) to have the structure depicted in Fig. 36a, wherein the cobalt displaces a BH unit into a wedging position. In the germanium–iron and tin–iron compounds, however, NMR evidence (*58*) suggests that the main-group metal occupies the wedging location (Fig. 36b). Such a structure has, in fact, been established for the diiron complex $[(CH_3)_2C_2B_4H_4]_2Fe_2 \cdot (OCH_3)_2C_2H_4$, which is described in Section IV,A (see Fig. 14). This latter compound, on exposure to O_2 or $FeCl_3$, undergoes rapid oxidative fusion to give $(CH_3)_4C_4B_8H_8$, but the three wedged, dimetallic species just listed are air stable and thus far have not shown any propensity to fuse.

In both of the established structures of wedged-type complexes (Figs. 14 and 36a), the bond distances from the wedging atom to the car-

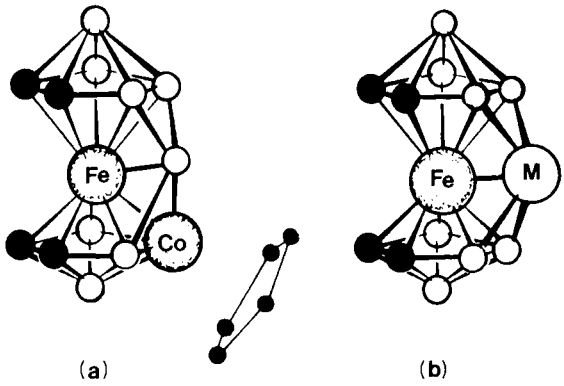

FIG. 36. (a) Established structure of $(\eta^5\text{-}C_5H_5)CoFe(CH_3)_4C_4B_8H_8$ (*55*). (b) Proposed structure of $MFe(CH_3)_4C_4B_8H_8$ (M = Ge, Sn) (*58*). Reprinted from *Inorg. Chem.* **16**, 3094. Copyright 1977 American Chemical Society. ○, BH; ●, CCH_3.

borane ligands are relatively long, although still well within bonding range. The chemistry of the wedged species has scarcely been examined as yet but should prove interesting; the wedging metal (or boron) atoms occupy comparatively exposed sites and are likely to be highly reactive toward attacking reagents. The almost instantaneous oxidation of $[R_2C_2B_4H_4]_2Fe_2L_2$ (L = THF or $\frac{1}{2}$DME) to form $R_4C_4B_8H_8$, noted earlier, is in line with this idea.

B. A Metallacarborane with a Fluxional Interligand B—B Linkage

The complex (*14*) to be described here is structurally unique in boron chemistry, although it is related to other known species. Treatment of a THF solution of $Na^+(CH_3)_2C_2B_4H_5^-$ with $CoCl_2$ and $Li^+C_5(CH_3)_5^-$ forms, as expected, the *closo*-cobaltacarboranes 1,2,3-$[C_5(CH_3)_5]$-$Co(CH_3)_2C_2B_4H_4$ and 1,7,2,3-$[C_5(CH_3)_5]_2Co_2(CH_3)_2C_2B_3H_3$ (the latter compound is a triple-decker sandwich), in analogy with the corresponding $C_5H_5^-$ reaction (*25*). However, with $C_5(CH_3)_5^-$ an additional product, *having no known $C_5H_5^-$ counterpart,* is also obtained in a yield of a few percent. An X-ray crystal-structure determination on this complex (*14*), $[\eta^5\text{-}C_5(CH_3)_5]_2Co_3(CH_3)_4C_4B_8H_7$, revealed that it consists of two CoC_2B_4 cages coordinated to a common cobalt atom, thereby forming two closo 8-vertex $Co_2C_2B_4$ polyhedra. The extraordinary feature, however, is that one boron atom on each cage lacks a terminal hydrogen, and these borons are directly linked to each other [bond distance 1.758(5) Å]. This structure is shown in Fig. 37.

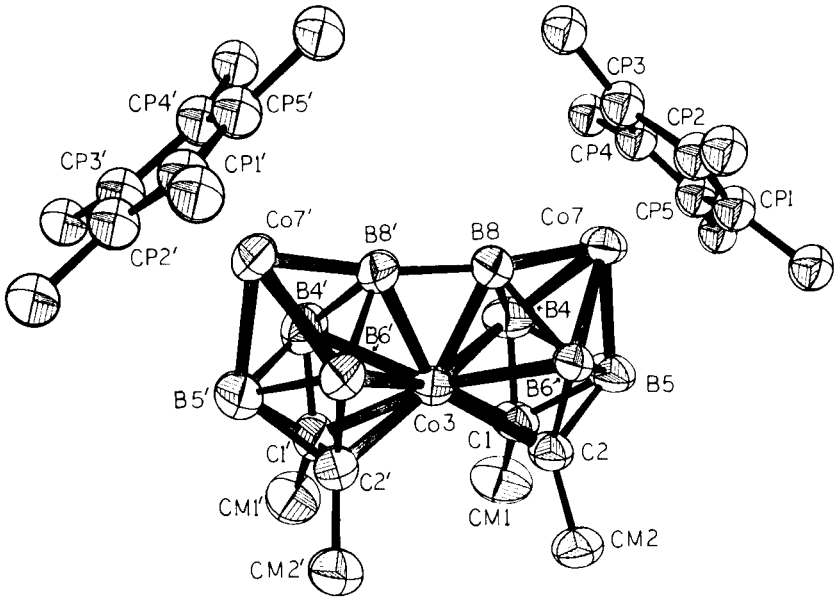

FIG. 37. Structure of $[\eta^5\text{-}C_5(CH_3)_5]_2Co_3(CH_3)_4C_4B_8H_7$ (*14*). Reprinted from *J. Am. Chem. Soc.* **103,** 1399. Copyright 1981 American Chemical Society.

The molecule possesses one nonterminal hydrogen atom that was not found in the X-ray study but that is presumed from indirect X-ray evidence to be located, in the solid state, in a pocket between the two cages, as suggested schematically in Fig. 38a. In $CDCl_3$ or C_6D_6 solution the interpolyhedral B—B bond is cleaved, thereby opening two sites available for terminal hydrogen bonding; the extra hydrogen atom apparently flips back and forth between these two boron atoms, as shown in Fig. 38b. A symmetrical B—H—B bridged arrangement (Fig. 38c) is evidently excluded both in the solid and solution states as a static structure, but it may well represent a transition state for the interchange shown in Fig. 38b. These conclusions are based on detailed ^{11}B- and ^1H-NMR studies, which have been described elsewhere (*14*).

Although this species is presently unique [there is no other example of a biscarboranyl *commo*-metallacarborane with a direct bond between the ligands], it may represent an early stage in the oxidative ligand-fusion process. This particular compound is air stable and has not exhibited any tendency to fuse, which is perhaps explained by the presence of the bulky $C_5(CH_3)_5$ ligands. Conceivably, however, somewhat similar interligand linkage may occur during the actual fusion of complexes such as $[R_2C_2B_4H_4]_2FeH_2$.

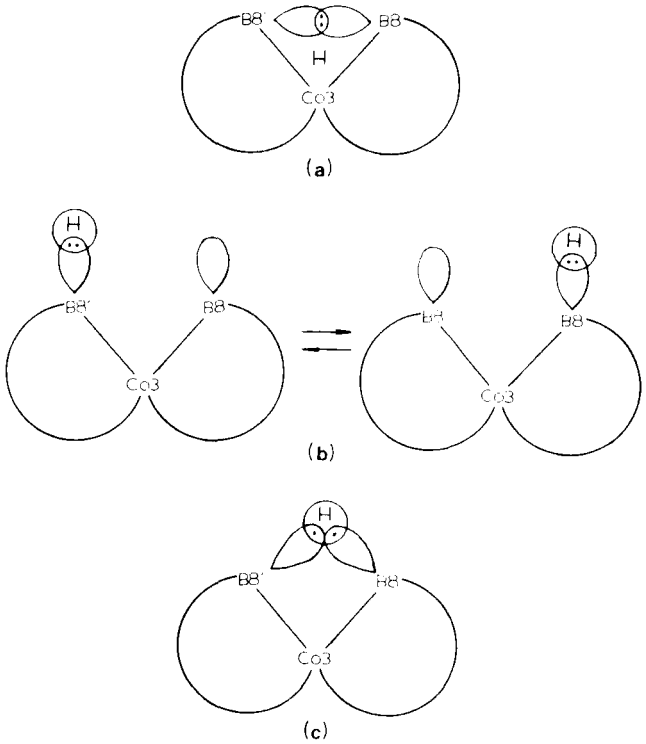

FIG. 38. Proposed sites for location of the fluxional hydrogen atom in the linked-cage tricobalt complex shown in Fig. 37. (a) Hydrogen in the vicinity of the central cobalt [Co(3)], with a direct B(8)—B(8′) link (solid-state structure). (b) Hydrogen exchanged between terminal positions on B(8) and B(8′) (proposed solution structure). (c) Three-center interligand B—H—B bridge. There is no evidence for structure (c), but it may exist as a transient during the tautomerism shown in (b) (*14*). Reprinted from *J. Am. Chem. Soc.* **103,** 1399. Copyright 1981 American Chemical Society.

VII. Structural Trends in Carbon-Rich Carborane Frameworks

Given the wide variety of geometric forms exhibited by the known four-carbon carborane and metallacarborane cage systems, there is every reason to believe many more novel structures will be encountered. This extraordinarily complex stereochemistry can be traced to several factors: (1) the importance of local bonding effects in systems with high heteroatom content; (2) the fact that most of these species were obtained under mild conditions that preclude rearrangement, allowing kinetic stabilization of unusual bonding patterns; and (3) the

presence of $2n + 4$ or $2n + 6$ skeletal electrons in most of the systems, leading (as predicted by Wade's rules) to open-cage geometries.

At this writing, over two dozen compounds in this class have been characterized by X-ray diffraction. These species, discussed in earlier sections, contain zero to two metal atoms per cage, and the metals represented are iron, cobalt, and nickel. Is anything to be gained by examining this somewhat random collection of molecules for structural trends? In a rigorous sense, probably not; on the other hand, clues to important principles of structure and bonding have often been first noted on a purely empirical plane, supported only later by careful theoretical analysis. This is particularly so in boron chemistry, where, for example, Stock's classifications of boranes into B_nH_{n+4} and B_nH_{n+6} groups (*83*) long preceded even the determination of molecular structures, let alone the development of bonding principles.

Two obvious patterns to be noted involve the carbon and metal locations, particularly with respect to the open faces. Figure 39 depicts in schematic fashion the open-face arrangements in the established four-carbon carborane and metallacarborane structures [the only closo framework, that of $(C_5H_5)_2Fe_2(CH_3)_4C_4B_8H_8$, isomer **VIII** (Fig. 34), lacks an open face and is omitted]. A conspicuous feature of these diagrams is the presence of three or four carbon atoms in most cases; indeed, 90% of the skeletal carbons in the structures under discussion occupy locations on an open rim. In the *nonmetal* species (Fig. 39a–d), *all* carbon atoms are on the rim.

In part, the tendency of carbon to occupy open-face vertices simply reflects a well-known rule that carbon prefers low-coordinate situations in borane clusters. Thus, although the skeletal coordination of carbon in the entire group of crystal structures ranges from two to five, nearly two-thirds of these carbons are four-coordinate with respect to the cage. In addition, one can expect the bonding around an open rim to be somewhat more localized than in the remainder of the cage. Both low coordination and localized electron distribution are favorable for carbon, a highly electronegative element that tends to adopt hydrocarbon-like bonding modes as far as possible (note, for example, the several structures in which a former framework carbon atom has been converted to an —RCH— bridging group via acquisition of hydrogen).

How does carbon manage to adopt low-coordinate rim locations so much of the time, given our assumption that extensive cage rearrangement is unlikely under the conditions of synthesis for most of these species? A likely explanation is that open faces are created merely by stretching particular edges of a polyhedral cage to nonbonding distances; this can be accomplished with relatively little atomic move-

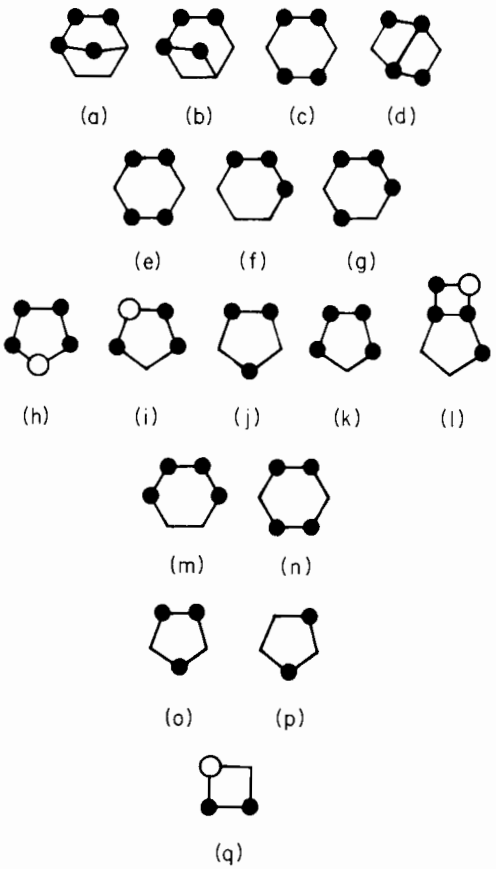

FIG. 39. Observed open-face geometries in structurally established C_4 carboranes and metallacarboranes. Systems: (a)–(d), nonmetal; (e)–(l), one-metal; (m)–(q), two-metal. Each diagram depicts the pattern of occupancy of vertices on the open face(s) by carbon, boron, and metal atoms. ●, Carbon; ∠, boron; ○, metal. Deviations from planarity of the open faces are ignored, as are bridging hydrogens and all atoms not located on open faces. (a) $(CH_3)_4C_4B_7H_8Br$ (Fig. 20). (b) $(CH_3)_4C_4B_8H_9^-$ (Fig. 17). (c) $(C_2H_5)_4C_4B_8H_8$ (*87*). (d) $(CH_3)_4C_4B_8H_8$ (Fig. 12) and $(C_5H_5)Fe(C_5H_4)$—$(CH_3)_4C_4B_8H_7$ (Fig. 13). (e) $(C_5H_5)Co(CH_3)_4C_4B_7H_7$, isomer **I** (Fig. 26) and $(C_5H_5)Co(C_6H_5)_4C_4B_3H_3$ (Fig. 9). (f) $(C_5H_5)Fe(CH_3)_4C_4B_7H_8$ (Fig. 30, **5**). (g) $(C_5H_5)Co(CH_3)_4C_4B_7H_7$, isomer **III** (Fig. 35) and $(C_5H_5)Cr(C_2H_5)_4C_4B_7H_7$ (Fig. 32). (h) $(C_5H_5)Co(CH_3)_4C_4B_6H_6$, isomer **II** (Fig. 27). (i) $[(C_6H_5)_2PCH_2]_2Ni(CH_3)_4C_4B_8H_8$ (Fig. 29). (j) $(C_5H_5)Cr(C_2H_5)_4C_4B_8H_8$ (Fig. 32). (k) $(C_5H_5)Co(CH_3)_4C_4B_6H_6$, isomer **I** (Fig. 27). (l) $(C_5H_5)Co(CH_3)_4C_4B_7H_7$, isomer **II** (Figs. 28 and 35). (m) $(C_5H_5)_2Co_2C_4B_6H_{10}$, isomer **VII** (Fig. 24). (n) $(C_5H_5)_2Co_2(CH_3)_4C_4B_6H_6$, isomer **V** (Fig. 23). (o) $(C_5H_5)_2Fe_2(CH_3)_4C_4B_8H_8$, isomer **I** (Fig. 31). (p) $(C_5H_5)_2Fe_2$-$(CH_3)_4C_4B_8H_8$, isomer **V** (Fig. 33). (q) $(C_5H_5)_2Fe_2(CH_3)_4C_4B_8H_8$, isomer **II** (Fig. 31).

ment and is clearly, in general, a low-energy process [the fluxional $R_4C_4B_8H_8$ carboranes (Section IV,B) provide an excellent illustration of this point]. Hence, in most C_4 carborane and metallacarborane cage systems, the skeletal carbons can be placed in low-coordinate and/or open-rim locations without actual migration of atoms on the polyhedral surface. Indeed, in the 14-vertex $(C_5H_5)_2Fe_2(CH_3)_4C_4B_8H_8$ complexes **I**, **II**, and **V** (Fig. 33) this is achieved by appropriate edge-stretching *despite* the fact that the $2n + 2$ framework electrons favor closo polyhedral geometry.

The placement of metal atoms requires little discussion. With one exception, all metals in this particular group of clusters are five- or six-coordinate; only in $(C_5H_5)Co(CH_3)_4C_4B_6H_6$, isomer **II** (Fig. 27), is the metal atom adjacent to as few as four skeletal atoms. This observation is consistent with a general pattern in metallacarborane structures (*22*), particularly those in which iron and cobalt are involved. Metal atoms tend to locate adjacent to carbon; each metal in these structures has at least two neighboring carbon atoms in the framework. In part, this merely reflects the high molar density of carbon in these C_4 clusters; in addition, however, metal insertion into open carborane cages almost inevitably takes place at the open face, and, as we have noted, such faces are usually rich in carbon.

VIII. Concluding Observations

The hypothetical experiment mentioned in Section I, in which boron atoms in a polyhedral $C_2B_{10}H_{12}$ carborane are successively replaced by carbon until one has $C_{12}H_{12}$, is of course well beyond the current state of the art in synthetic boron chemistry; for that matter, even theoretical predictions of the various intermediate structures are not presently feasible on any rigorous basis. What *has* happened, however, is that a particular stage in this series, $C_4B_8H_{12}$, has been fortuitously obtained in the form of tetraalkyl derivatives and studied extensively. Thus we have, basically, a picture of the consequences of replacing *some* of the boron in a 12-vertex polyhedron with carbon, and it is a complex picture indeed, particularly when the metallacarborane complexes are included.

As the carbon content of the cage is further increased, it would be reasonable to expect the main structural trends observed in the four-carbon systems to be extended; thus in a $R_6C_6B_6H_6$ polyhedron at least some of the framework carbon atoms should adopt hydrocarbon-like, localized, four-coordinate bonding modes. A particularly interesting

question is whether such cages would exhibit isomerism and fluxional behavior akin to that of the C_4B_8 systems described in this chapter. No carboranes having more than four skeletal carbon atoms have been characterized [although evidence for six- and eight-carbon species has been reported (*12*)], and for the foreseeable future it will be up to the synthetic chemist to resolve such questions.

ACKNOWLEDGMENTS

It is a pleasure to note the generous support of the Office of Naval Research and the National Science Foundation for the work at the University of Virginia described in this chapter, as well as the efforts of the many co-workers who are named in the references. I am grateful to T. Leon Venable for reading the manuscript and offering many helpful suggestions.

REFERENCES

1. Berger, H. O., Noeth, H., and Wrackmeyer, B., *Chem. Ber.* **112,** 2884 (1979).
2. Binger, P., *Tetrahedron Lett.* p. 2675 (1966).
3. Bowser, J. R., Bonny A., Pipal, J. R., and Gimes, R. N., *J. Am. Chem. Soc.* **101,** 6229 (1979).
4. Brown, L. D., and Lipscomb, W. N., *Inorg. Chem.* **16,** 2989 (1977).
5. Camp, R. N., Marynick, D. S., Graham, G. D., and Lipscomb, W. N., *J. Am. Chem. Soc.* **100,** 6781 (1978).
6. Chamberland, B. L., and Muetterties, E. L., *Inorg. Chem.* **3,** 1450 (1964).
7. Churchill, M. R., and DeBoer, B. G., *Inorg. Chem.* **12,** 2674 (1973).
8. Dixon, D. A., Kleier, D. A., Halgren, T. A., Hall, J. H., and Lipscomb, W. N., *J. Am. Chem. Soc.* **99,** 6226 (1977).
9. Dustin, D. F., Evans, W. J., Jones, C. R., Wiersema, R. J., Gong, H., Chan, S., and Hawthorne, M. F., *J. Am. Chem. Soc.* **96,** 3085 (1974).
10. Evans, W. J., and Hawthorne, M. F., *J. Chem. Soc., Chem. Commun.* p. 38 (1974).
11. Evans, W. J., Jones, C. J., Stibr, B., and Hawthorne, M. F., *J. Organomet. Chem.* **60,** C27 (1973).
12. Fehlner, T. P., *J. Am. Chem. Soc.* **102,** 3424 (1980).
13. Finster, D. C., and Grimes, R. N., *J. Am. Chem. Soc.* **103,** 2675 (1981).
14. Finster, D. C., Sinn, E., and Grimes, R. N., *J. Am. Chem. Soc.* **103,** 1399 (1981).
15. Franz, D. A., and Grimes, R. N., *J. Am. Chem. Soc.* **93,** 387 (1971).
16. Freyberg, D. P., Weiss, R., Sinn, E., and Grimes, R. N., *Inorg. Chem.* **16,** 1847 (1977).
17. Greenwood, N. N., and Thomas, B. S., "The Chemistry of Boron." Permagon, Oxford, 1973.
18. Grimes, R. N., *Acc. Chem. Res.* **11,** 420 (1978).
19. Grimes, R. N., *Acc. Chem. Res.* **16,** 22 (1983).
20. Grimes, R. N., *Ann. N.Y. Acad. Sci.* **239,** 180 (1974).
21. Grimes, R. N., "Carboranes." Academic Press, New York, 1970.
22. Grimes, R. N., *in* "Comprehensive Organometallic Chemistry" (G. Wilkinson, F. G. A. Stone, and E. Abel, eds.), Vol. 1, Chapter 5.5. Pergamon, Oxford, 1982.

23. Grimes, R. N., *Coord. Chem. Rev.* **28,** 47 (1979).
24. Grimes, R. N., ed., "Metal Interactions with Boron Clusters." Plenum, New York, 1982.
25. Grimes, R. N., Beer, D. C., Sneddon, L. G., Miller, V. R., and Weiss, R., *Inorg. Chem.* **13,** 1138 (1974).
26. Grimes, R. N., and Bramlett, C. L., *J. Am. Chem. Soc.* **89,** 2557 (1967).
27. Grimes, R. N., Maxwell, W. M., Maynard, R. B., and Sinn, E., *Inorg. Chem.* **19,** 2981 (1980).
28. Grimes, R. N., Maynard, R. B., Sinn, E., and Long, G. J., *Abstr. Pap., 182nd Natl. Meet., Am. Chem. Soc.* Abstract INOR-10 (1981); see also Maynard, R. B., and Grimes, R. N., *J. Am. Chem. Soc.* **104,** 5983 (1982).
29. Grimes, R. N., Maynard, R. B., Sinn, E., Brewer, G., and Long, G. J., *J. Am. Chem. Soc.* **104,** 5987 (1982).
30. Grimes, R. N., Pipal, J. R., and Sinn, E., *J. Am. Chem. Soc.* **101,** 4172 (1979).
31. Grimes, R. N., Sinn, E., and Pipal, J. R., *Inorg. Chem.* **19,** 2087 (1980).
32. Hawthorne, M. F., Pilling, R. L., and Stokely, P. F., *J. Am. Chem. Soc.* **87,** 1893 (1965).
33. Herberich, G. E., Hengesbach, J., Kolle, U., Huttner, G., and Frank, A., *Angew. Chem., Int. Ed. Engl.* **15,** 433 (1976).
34. Herberich, G. E., Hengesbach, J., Kolle, U., and Oschmann, W., *Angew. Chem., Int. Ed. Engl.* **16,** 42 (1977).
35. Herberich, G. E., Hessner, B., Beswetherick, S., Howard, J. A. K., and Woodward, P., *J. Organomet. Chem.* **192,** 421 (1980).
36. Herberich, G. E., Hessner, B., Huttner, G., and Zsolnai, L., *Angew. Chem.* **93,** 471 (1981).
37. Hosmane, N. S., and Grimes, R. N., *Inorg. Chem.* **18,** 2886 (1979).
38. Hosmane, N. S., and Grimes, R. N., *Inorg. Chem.* **18,** 3294 (1979).
39. Hosmane, N. S., and Grimes, R. N., *Inorg. Chem.* **19,** 3482 (1980).
40. Howard, J. W., and Grimes, R. N. *Inorg. Chem.* **11,** 263 (1972).
41. Janousek, Z., Hermanek, S., Plesek, J., and Stibr, B., *Collect. Czech. Chem. Commun.* **39,** 2363 (1974).
42. Kaczmarczyk, A., Dobrott, R. D., and Lipscomb, W. N., *Proc. Natl. Acad. Sci. U. S. A.* **48,** 729 (1962).
43. Kaloustian, M. K., Wiersema, R. J., and Hawthorne, M. F., *J. Am. Chem. Soc.* **94,** 6679 (1972).
44. King, R. B., and Rouvray, D. H., *J. Am. Chem. Soc.* **99,** 24 (1977).
45. Lipscomb, W. N., "Boron Hydrides." Benjamin, New York, 1963.
46. Lipscomb, W. N., *Inorg. Chem.* **18,** 2328 (1979).
47. Lipscomb, W. N., *Science* **153,** 373 (1966).
48. Maddres, P. S., Modinos, A., Timms, P. L., and Woodward, P., *J. Chem. Soc., Dalton Trans.* p. 1272 (1975).
49. Marynick, D. S., and Lipscomb, W. N., *J. Am. Chem. Soc.* **94,** 8699 (1972).
50. Maxwell, W. M., Bryan, R. F., and Grimes, R. N., *J. Am. Chem. Soc.* **99,** 4008 (1977).
51. Maxwell, W. M., and Grimes, R. N., *Inorg. Chem.* **18,** 2174 (1979).
52. Maxwell, W. M., Miller, V. R., and Grimes, R. N., *Inorg. Chem.* **15,** 1343 (1976).
53. Maxwell, W. M., Miller, V. R., and Grimes, R. N., *J. Am. Chem. Soc.* **96,** 7116 (1974).
54. Maxwell, W. M., Miller, V. R., and Grimes, R. N., *J. Am. Chem. Soc.* **98,** 4818 (1976).
55. Maxwell, W. M., Sinn, E., and Grimes, R. N., *J. Am. Chem. Soc.* **98,** 3490 (1976).
56. Maxwell, W. M., Sinn, E., and Grimes, R. N., *J. Chem. Soc., Chem. Commun.* p. 390 (1976).

57. Maxwell, W. M., Weiss, R., Sinn, E., and Grimes, R. N., *J. Am. Chem. Soc.* **99,** 4016 (1977).
58. Maxwell, W. M., Wong, K.-S., and Grimes, R. N., *Inorg. Chem.* **16,** 3094 (1977).
59. Maynard, R. B., Sinn, E., and Grimes, R. N., *Inorg. Chem.* **20,** 1201 (1981).
60. Maynard, R. B., Sinn, E., and Grimes, R. N., *Inorg. Chem.* **20,** 3858 (1981).
61. Maynard, R. B., Wang, Z., Sinn, E., and Grimes, R. N., *Inorg. Chem.* **22,** in press (1983).
62. Middaugh, R. L., and Farha, F., Jr., *J. Am. Chem. Soc.* **88,** 4147 (1966).
63. Miller, V. R., and Grimes, R. N., *Inorg. Chem.* **11,** 862 (1972).
64. Miller, V. R., and Grimes, R. N., *J. Am. Chem. Soc.* **97,** 4213 (1975).
65. Mingos, D. M. P., *Nature (London), Phys. Sci.* **236,** 99 (1972).
66. Muetterties, E. L., ed., "Boron Hydride Chemistry." Academic Press, New York, 1975.
67. Onak, T. P., "Organoborane Chemistry." Academic Press, New York, 1975.
68. Onak, T. P., Drake, R. P., and Dunks, G. B., *Inorg. Chem.* **3,** 1686 (1964).
69. Onak, T. P., and Dunks, G. B., *Inorg. Chem.* **5,** 439 (1966).
70. Onak, T. P., and Wong, G. T. F., *J. Am. Chem. Soc.* **92,** 5226 (1970).
71. O'Neill, M. E., and Wade, K., *in* "Metal Interactions with Boron Clusters" (R. N. Grimes, ed.) Chapter 1. Plenum, New York, 1982.
72. Pasinski, J. P., and Beaudet, R. A., *J. Chem. Phys.* **61,** 683 (1974).
73. Pipal, J. R., and Grimes, R. N., *Inorg. Chem.* **17,** 6 (1978).
74. Pipal, J. R., and Grimes, R. N., *Inorg. Chem.* **18,** 257 (1979).
75. Pipal, J. R., and Grimes, R. N., *Inorg. Chem.* **18,** 263 (1979).
76. Pipal, J. R., and Grimes, R. N., *Inorg. Chem.* **18,** 1936 (1979).
77. Pipal, J. R., and Grimes, R. N., *J. Am. Chem. Soc.* **100,** 3083 (1978).
78. Plesek, J., and Hermanek, S., *Chem. Ind. (London)* p. 890 (1972).
79. Rudolph, R. W. *Acc. Chem. Res.* **9,** 446 (1976).
80. Siebert, W., *Adv. Organomet. Chem.* **18,** 301 (1980).
81. Siebert, W., and Bochmann, M., *Angew. Chem., Int. Ed. Engl.* **16,** 468 (1977).
82. Siebert, W., and El-Essawi, M. E., *Chem. Ber.* **112,** 1480 (1979).
83. Stock, A., "Hydrides of Boron and Silicon." Cornell Univ. Press, Ithaca, New York, 1933.
84. Thompson, M. L., and Grimes, R. N., *J. Am. Chem. Soc.* **93,** 6677 (1971).
85. Timms, P. L., *Acc. Chem. Res.* **6,** 118 (1973).
86. Tolpin, E. I., and Lipscomb, W. N., *Inorg. Chem.* **12,** 2257 (1973).
87. Venable, T. L., Maynard, R. B., Sinn, E., and Grimes, R. N., to be submitted for publication.
88. Wade, K., *Adv. Inorg. Chem. Radiochem.* **18,** 1 (1976).
89. Welch, A. J., private communication.
90. Williams, R. E., *Adv. Inorg. Chem. Radiochem.* **18,** 67 (1976).
91. Wong, K.-S., Bowser, J. R., Pipal, J. R., and Grimes, R. N., *J. Am. Chem. Soc.* **100,** 5045 (1978).
92. Zimmerman, G. J., Hall, L. W., and Sneddon, L. G., *Inorg. Chem.* **19,** 3642 (1980).
93. Zimmerman, G. J., and Sneddon, L. G., *Inorg. Chem.* **19,** 3650 (1980).

FLUORINATED HYPOFLUORITES AND HYPOCHLORITES

JEAN'NE M. SHREEVE

Department of Chemistry, University of Idaho, Moscow, Idaho

I. Introduction

The richness of the exciting field of fluorinated hypofluorites and hypochlorites is due in very large part to the imaginative work by Ruff and Lustig. Dudley (*92*) had suggested that $AgOSF_5$ and $AgOSO_2F$ were active intermediates in the AgF(I,II) catalytic fluorination of OSF_4 and SO_3 to give SF_5OF and FSO_2OF, respectively. Because

Copyright © 1983 by Academic Press, Inc.
All rights of reproduction in any form reserved.
ISBN 0-12-023626-5

$CsOSF_5$ had been reported (*278*), a study of the fluorination of thionyl fluoride and thionyl tetrafluoride in the presence of CsF was undertaken (*237*). For the first time, SF_5OF could be consistently isolated in yields greater than 95%! The existence of the trifluoromethoxides of alkali metals as stable entities was demonstrated by Redwood and Willis (*46, 221, 222*). Ruff, Pitochelli, and Lustig proceeded to demonstrate the alkali-metal (K, Rb, or Cs) fluorides catalyzed addition of fluorine across the carbon–oxygen double bond in perfluorocarbonyl compounds to form fluoroxy compounds in nearly quantitative yields (*238*). In 1968 Fox and co-workers extended this method to the essentially quantitative preparation of the first perfluoroalkyl hypochlorite, CF_3OCl, by simply substituting ClF for F_2 in reaction with COF_2 in the presence of CsF. In that paper they also announced i-C_3F_7OCl and SF_5OCl (*124*). The flood gates were open and much beautiful work was about to commence.

This is not meant to detract in any way from the excellent contributions of the Cady school at the University of Washington and of Prager and Thompson at the 3M Co., for it was their elegant work that invented, characterized, and studied a very large number of the fluoroxy compounds and hypofluorites known today (*175*).

A brief summary of the history of catalytic fluorination has been published (*175, 311*). Cady and co-workers have devoted considerable effort in attempting to understand the role played by silver fluoride(I,II) in the fluorination of COF_2 to CF_3OF and CF_3OOCF_3. They concluded that (1) catalysts active at lower temperatures are generally the more ionic salts; (2) catalysts active at −78°C mostly catalyze the formation of CF_3OF; (3) catalysts that are initially active at 25–150°C cause the production of relatively high yields of CF_3OOCF_3; and (4) the percentage of CF_3OF in the product apparently increases with reaction temperature when the same catalyst is used (*149*).

Although there are many variations, the three main methods of preparing the alkali-metal fluorides for their catalytic role are thermal dehydration accompanied by mechanical powdering, heating under vacuum, and the formation of a salt, which is subsequently decomposed, for example, the reaction with hexafluoroacetone in acetonitrile. Using ^{85}Kr, Winfield and co-workers (*164*) have studied the surface areas of CsF, TlF, and RbF as a function of the pretreatment method used and have shown that the surface areas of CsF and TlF are increased markedly by any of these methods, with the surface of CsF being particularly enhanced by hexafluoroacetone. The surface area of RbF was less sensitive to pretreatment. That TlF shows little or no catalytic activity although its surface area can be greatly enhanced

indicates that surface area is not the sole factor involved. In a review of the utilization of ^{18}F-labeled inorganic compounds (*315*), it was shown that there is a correlation between ^{18}F exchange and catalytic ability; for example, exchange between $CF_3C(O)^{18}F$, $F^{18}FCO$, or $SF_3{}^{18}F$ and alkali-metal fluorides varies in the order Cs > Rb > K > Na > Li. CsF is the best catalyst whereas NaF and LiF have little or no catalytic activity. However, this correlation breaks down for ionic fluorides other than those of the alkali metals; for example, TlF, Hg_2F_2, HgF_2, and LaF_3 readily undergo ^{18}F exchange with $SF_3{}^{18}F$ but are not catalysts for the chlorofluorination of SF_4. Although much light has been shed on the subject of catalytic fluorination, there is still work to be done before complete predictability will be possible.

The present chapter is an effort to update the most recent accessible review on fluoroxy compounds and hypofluorites (*175*). No attempt has been made to cover the literature that was available prior to 1971 (except when needed for completeness) because this period was adequately handled earlier (*9, 16, 53, 135, 175, 200, 312*). Fluoroxy compounds used strictly as fluorinating agents are included in Section VI (*18, 19, 130, 160*). Although the hypochlorites of group VIa (*16*) and fluorinated compounds that contain positive chlorine have been reviewed more recently (*244*), the entire history of fluorinated hypochlorites has now been covered.

Suitable nomenclature for OCl-containing molecules presents little difficulty, with hypochlorite being a perfectly utilitarian term. However, for OF-containing molecules the situation is less straightforward. Therefore, the system used previously has been retained, that is, for perfluoroacyl and for inorganic OF compounds the term hypofluorite will be used. For perfluoroalkyl OF compounds the term fluoroxy is more suitable.

II. Hypofluorous Acid

At the time of our last hypofluorite review (*175*), hypofluorous acid had just been synthesized and isolated by passing fluorine over cold water (*283*). Earlier, infrared bands were assigned to HOF, which was formed by photolysis of a mixture of F_2 and H_2O that was frozen into a solid N_2 matrix at 14–20 K (*204*). Appelman (*9*) has described his historic synthesis as a result of a very simple experiment, whereby a drop of water was placed in a Kel-F tube with about 100 torr of fluorine gas, with the subsequent observation of a small HOF peak at mass 36, seen as a shoulder of the F_2 peak at mass 38 in a time-of-flight mass spectrometer.

At low temperature HOF is a white solid that melts at −117°C to a pale yellow liquid. The compound boils below room temperature (~HF) and has a vapor pressure of less than one torr at −79°C. Based on microwave studies, the O—H bond distance is 0.96(4) Å, the O—F bond distance 1.442 Å, and the HOF bond angle 97° (*152*). This is the smallest known oxygen bond angle. Appelman (*134*) rationalized this fact based on NMR studies of the molecule, which showed the fluorine to have a charge of about −0.5 e and the hydrogen to have a charge of about +0.5 e. Thus the smaller bond angle is a result of the electrostatic attraction between the ends of the molecule. This precludes the assignment of a +1 valence to fluorine except as a formalism. Matrix isolation (*121*) and gas-phase IR (*12*) spectral studies on relatively pure HOF gave fundamental bands at 886.0, 1359.0, and 3537.1 and 889.0, 1354.8, and 3578.5 cm^{-1}, respectively. The gas-phase spectrum of the deuterated molecule has also been recorded. A normal coordinate analysis of HOF and DOF is available (*205, 240*).

Photoionization (*37*) and photoelectron (*38*) studies are in close agreement for the first ionization potential of HOF at 12.70 eV. Ab initio LCAO MO SCF calculations gave 13.97, 14.94, and 17.16 eV for the first three ionization potentials (*153*). A value of -22.8 ± 1 kcal mol^{-1} was found for the standard heat of formation of the molecule, and the proton affinity of OF is 5.8 eV (*37*). The total electric dipole moment of HOF is $\mu = |2.23 \pm 0.1$ OD| (*228*). The calculated value is somewhat higher (*126*).

As is to be expected for such an interesting three-atom system, HOF has been the subject of a very large number of theoretical studies. These include (1) establishment of general harmonic ab initio and semiempirical force fields (*42, 45, 202, 273*); (2) vibrational frequencies from anharmonic ab inito/empirical potential-energy functions (*44*); (3) calculation of magnetic shielding and susceptibility (*328*); (4) analytical potentials (*201*); and (5) molecular orbital theory of the hydrogen bond in $HOF–H_2O$ and $(HOF)_2$ (*79*).

Despite the strong tendency of HOF to decompose to HF and O_2 at room temperature, in Kel-F or Teflon apparatus and at pressures of about 100 torr the compound has a half-life of about 30 min. It sometimes decomposes explosively. Although its chemistry has not been studied exhaustively, HOF has been shown to act only as an oxygenating or as a hydroxylating agent, that is, as a donor of atomic oxygen or of its conjugate acid, OH^+.

Hypofluorous acid mimics the behavior of F_2 in many of its reactions; for example, in weakly acidic solutions the water is oxidized primarily to H_2O_2, whereas in alkaline solutions O_2 is the main oxygen product.

In addition, only in alkaline solutions is bromate oxidized to perbromate. It may well be that HOF is the reactive species when fluorine is employed in aqueous systems (*9*). However, this may be an oversimplification, because although F_2 produces OF_2 from neutral, acidic, or basic media, interaction of HOF with water has never been noted to produce OF_2.

^{18}O-Tracer studies show that the reactions of $H^{18}OF$ with H_2O and with aqueous HSO_4^- and $Cr(NH_3)_5N_3^{2+}$ lead to transfer of oxygen with formation of $HO^{18}OH$, $O_3SO^{18}OH^-$, and $Cr(NH_3)_5N^{18}O^{2+}$, respectively (*13*). It is interesting to note that in reactions of F_2 and HOF with aqueous $HClO_4$ solutions containing various complexes of Cr(III), in no case was the chromium oxidized (*294*). The readiness with which HOF transfers an oxygen atom to reducing substrates is consistent with NMR studies that indicate the HOF molecule to be polarized $HO^{\delta+}—F^{\delta-}$ (*134*).

A variety of aromatic compounds, for example, ϕR [R = H, CH_3, $(CH_3)_3C$, CH_3O, NO_2, F, or Cl], p-$(CH_3)_2C_6H_4$, and naphthalene, undergo hydroxylation with HOF to form phenols (*11*). With octaethylporphyrin, HOF gives a new system—a prophyrin *N*-oxide—and possibly the *N*,*N*′-dioxide (*43*). Alkenes result in α-fluoro alcohols as the major products, whereas acetylenes gave mixtures of aldehydes, ketones, and acyl fluorides, which very likely are formed by tautomerization of the α-fluoro enol products formed initially (*185*). Although the expected Markownikoff addition products are usually found, on occasion anti-Markownikoff products are also formed. The reaction of ethynylbenzene with HOF gave 30% of the antiproduct and none of the Markownikoff. Hydrogen fluoride, which is a difficultly removed contaminant, may be part of the explanation. Mechanisms have been suggested.

III. Monofluoroxy Compounds or Monohypofluorites

A. OF Bonded to Carbon

1. Fluoroxyperfluoroalkanes (R_fOF)

Although the older methods of catalytic fluorination, over a AgF(I,II) catalyst at elevated temperatures (*52*), or the direct fluorination of partially fluorinated alcohols or salts (*217, 218*) are still of synthetic value, the most efficient and highest yielding route to these fluoroxy compounds is the fluorination of perfluoroalkyl ketones and

perfluoroacyl fluorides in the presence of an alkali-metal fluoride (*173, 238*). Nitrosyl fluoride has been used effectiely as a catalyst in place of MF (*317*). A discussion of the relative merits of various catalysts that have been employed can be found in Section I.

The first example of the production of fluoroxyperfluoroalkane via electrochemical fluorination (by bubbling COF_2/He through purified AHF in an electrolytic cell at 7°C to give 73 parts CF_3OF, 17 CF_3OOCF_3, and 10 CF_4) has been described by Abe *et al.* (*1*). Rozen has reported the *in situ* synthesis of CF_3CF_2OF (*218, 291*) to form a stable oxidizing solution at −78°C via Scheme 1 (*230, 232*). The suggested

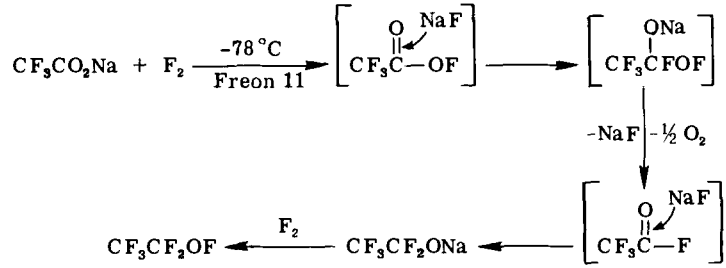

SCHEME 1

fluoroxy compound is not isolated, but its existence is supported by the synthesis of perfluoroalkyl ethers, for example,

$$C_6H_5CH{=}CHC_6H_5 + CF_3CF_2OF \xrightarrow[\text{Freon 11}]{-78°C} C_6H_5CHFCH(OCF_2CF_3)C_6H_5$$

cis	DL-erythro (38%)	DL-threo (7%)
trans	DL-erythro (<5%)	DL-threo (28%)

When treated with some stilbenes it produces stereospecific (syn addition) and regiospecific adducts.

A convenient procedure for the rapid synthesis of ^{18}F-labeled CF_3OF with $NiF_2 \cdot CsF$ as catalyst is available. The preparation requires a fluorine-passivated Ni target and anhydrous conditions (*203*).

The number of new fluoroxyperfluoroalkanes that appeared during the 1970s was very limited. Standard methods were used. DesMarteau

$$CF_3C(O)N{=}C(CF_3)_2 + 5F_2 \xrightarrow[-60°C]{KF} CF_3CF(OF)NFCF(CF_3)_2 \quad 27\%$$

$$CF_3C(O)NFCF(CF_3)_2 + 3F_2 \xrightarrow[-78°C]{KF} CF_3CF(OF)NFCF(CF_3)_2 \quad 40\%$$

$\nu_{OF} = 902\ cm^{-1}$
$\phi_{OF} = +164$ (*213*)

observed that when $(CF_3)_3COOSO_2F$ was subjected to fluorination at −55°C in the presence of CsF, $(CF_3)_3COF$ (*218*) as well as $(CF_3)_3$ COOF was formed (*327*). The former fluoroxy compound was also formed essentially quantitatively when F_2/N_2 was passed through a 50:50 mixture of $(CF_3)_3CONa$ and NaF at −23°C (*295*). Perhaps the first example of a fluoroxy compound with an ether linkage has appeared (*245*).

$$CF_3OCF_2C(O)F + F_2 \xrightarrow[25°C]{CsF} CF_3OCF_2CF_2OF$$

$\nu_{OF} = 895\ cm^{-1}$

$\phi_{OF} = +138.8$

Most of the literature dealing with fluoroxyperfluoroalkanes pertains to electrophilic fluorination applications (Section VI). However, some other studies, usually involving CF_3OF, have appeared.

Structural studies of CF_3OF which include IR and Raman spectra (*128, 166, 168, 274, 275, 309, 314*), microwave spectra (*49*), and electron diffraction (*84*), suggest C_s symmetry. From Stark-effect measurements, CF_3OF has been shown to have a small dipole moment (~0.3 D). The computed dipole moment agrees well with this value. In addition, the HOMO is found to be largely an O—F π^* orbital, and the O—F bond is also found to be the least ionic and weakest bond in the molecule (*206*). Using a Bendix time-of-flight mass spectrometer equipped with a Kel-F inlet system, a molecular ion (0.2 relative intensity) was observed for CF_3OF. The base peak was CF_3^+ (*140*). Calculations of the unimolecular decomposition of CF_3OF have appeared (*56, 72*). Kinetic studies of the formation of CF_3OOCF_3 from CF_3OF and COF_2 (*75*), the photochemical gas-phase fluorination of COF_2 between 15 and 80°C (*172*), thermal reactions between CF_3OF and NO_2 (*76*), and the behavior of mixtures of CF_3OF, CO, O_2, and CO_2 exposed to 366-nm radiation at 35–55°C (*40*) have been reported. In studying the kinetics of the decomposition to COF_2 and CF_3OF, a bond energy of 44.5 ± 0.8 kcal mol^{-1} was determined for CF_3O—F (*150*). This is in good agreement with the previous value of 43.5 ± 0.5 kcal mol^{-1} (*74*). The reactions of CF_3OF with CH_4, $CHCl_3$, CHF_2Cl, CH_3F, CH_2F_2, CH_2Cl_2, and CH_2FCl were studied from 25 to 100°C and at 3–30 mm. CF_3OF reacted with the dihalomethanes by a branched-chain mechanism (*289*).

It is interesting to compare the products obtained when CF_3OF or $(CF_3)_3COF$ is treated with hexafluorobenzene (*296*). Addition occurs more readily with the latter fluoroxy compound. But if the C_6F_6 and

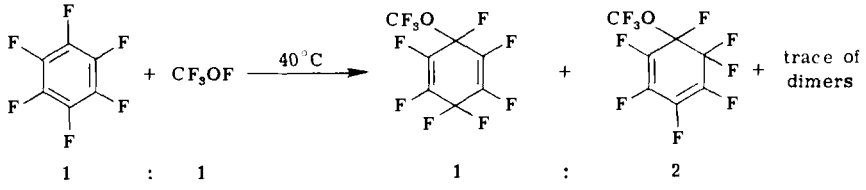

$(CF_3)_3COF$ are equimolar, the products are $C_6F_7[OC(CF_3)_3]$ (60%) and

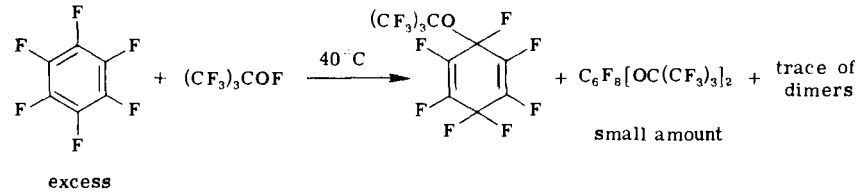

$C_6F_8[OC(CF_3)_3]_2$ (30%), plus dimers and a trace of the trifluoroxy adduct $C_6F_9[OC(CF_3)_3]_3$. The reaction between octafluorotoluene and CF_3OF occurred only after 8 h at 100°C to give mainly CF_3OOCF_3 and perfluoromethylmethoxycyclohexadiene, with perfluoromethylmethoxycyclohexene and dimer in smaller amounts.

At −62°C, addition of $(CF_3)_3COF$ to $CF_3CF{=}CF_2$ gave perfluoro-*n*-propyl perfluoro-*t*-butyl ether in greater than 95% yield, suggesting an electrophilic attack by the O—F group. Analogously, the reaction with perfluoro-3,6-dioxy-5-methyl-*n*-non-1-ene gives greater than 95% addition of the perfluoro-*t*-butoxy group to the unsaturated terminal carbon atom (*295*).

Under photolytic conditions at −20°C, $(CF_3)_3COF$ undergoes a one-electron reduction in the presence of perfluorocycloolefins (C_5F_8 or C_6F_{10}) to give a mixture of products including $(CF_3)_3COOC(CF_3)_3$ (major) and simple adducts $C_5F_9OC(CF_3)_3$ or $C_6F_{11}OC(CF_3)_3$ as well as $(CF_3)_2CO$, CF_4, C_5F_{10} or C_6F_{12}, and smaller amounts of vicinal $C_5F_8[OC(CF_3)_3]_2$ or $C_6F_{10}[OC(CF_3)_3]_2$. Similar conditions with CF_3OF and C_5F_8 or C_6F_{10} result in $C_5F_9OCF_3$ (83%) or $C_6F_{11}OCF_3$ (~100%). In the case of C_5F_8, small amounts of $(C_5F_8OCF_3)_2$ and $(C_5F_9)_2$ are formed (*297*). Surprisingly, although the reaction with CF_3OF was run with that reagent in twofold excess, no evidence was found for CF_3OOCF_3.

Fluoroxytrifluoromethane was found to be useful as a polymerization initiator for perfluoro-2-butyne (*59*). Radicals of the type $(CF_3O)_3S$ and $(CF_3O)_2SF$ have been detected via ESR spectra during the photolysis of CF_3OF and peroxides containing dissolved OCS, F_2SS, CS_2, Cl_2CS, or F_2CS (*199*). Similarly, with SF_4, radicals of the type CF_3OSF_4

are observed (*196*). An intense ESR spectrum observed in the UV-irradiated solid Kr/CF_3OF at 10 K is attributed to the linear radical KrFKr having a Σ_u ground state (*41*). Emission spectral measurements were made on diatomic xenon halides formed by the interaction of Xe with CF_3OF (*306*).

2. *Fluoroacyl Hypofluorites* [$R_fC(O)OF$]

Just as Cady *et al.* (*52, 117*) have demonstrated that the presence of water is necessary to form $CF_3C(O)OF$ from trifluoroacetic acid and fluorine, Rozen has shown that, when $CF_3C(O)ONa$ is not strictly anhydrous, the main oxidant formed when the latter in Freon 11 is treated with fluorine at −78°C is $CF_3C(O)OF$ (*230*). Although Rozen did not isolate the hypofluorite, its reaction with *trans*-$C_6H_5CH{=}CHC_6H_5$ gave DL-*threo*-$C_6H_5CHFCH(OC(O)CF_3)C_6H_5$.

Using elemental fluorine diluted with nitrogen at −78°C with $CF_3C(O)ONa$ in an inert solvent (usually CCl_3F) to generate CF_3CF_2OF (if anhydrous) and $CF_3C(O)OF$ (if damp), Rozen and coworkers have produced α-fluoroketones (*181, 230, 234, 235*). They suggested that the fluoroxy fluorine in $CF_3C(O)OF$ is more electrophilic in character than that in CF_3OF, based on the respective reaction products of diphenylacetylene. The 1-fluoro-2-trifluoroacetoxy compounds formed with stilbenes are readily hydrolyzed to the corresponding α-fluorohydrins (*231*).

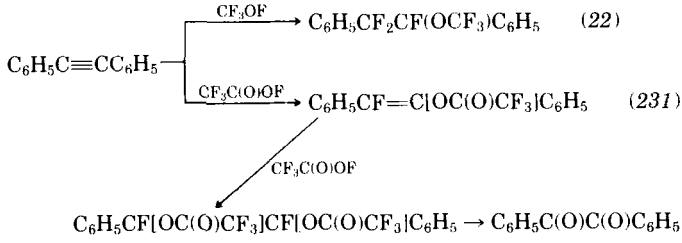

For completeness it should be mentioned that the first nonfluorinated acyl hypofluorite, CH_3CO_2F (50–80%), was claimed to have been generated *in situ* by bubbling F_2/N_2 through suspensions of sodium fluoride, acetate, or trifluoroacetate in acetic acid/Freon 11 (1:9) at −78°C. Although it has not been isolated, the reaction products with $C_6H_5CH{=}CHC_6H_5$ are *threo*-$C_6H_5CH(OC(O)CH_3)CHFC_6H_5$ (45%) and *erythro*- (7%) (*233*).

B. Inorganic Hypofluorites

1. Group Va Hypofluorites

Nitryl Hypofluorite or Fluorine Nitrate (O_2NOF). This is the only known hypofluorite in which an OF group is bonded to nitrogen (see Table I). Its high-yield synthesis results from the reaction of fluorine with HNO_3 or any alkali-metal nitrate (*51, 62, 239, 307, 316*). It has not been possible to reproduce others that have been reported (*62*). The kinetics of the unimolecular thermal decomposition reactions of O_2NOF have been studied at 120, 130, and 140°C, at pressures from approximately 0.5 to 10–20 torr (*48*). The heat of formation of gaseous O_2NOF has once again been determined with the value at 2.5 ± 0.5 kcal mol^{-1} (*223*).

Although long ago low-precision electron-diffraction studies pointed to a nonplanar structure for O_2NOF, in which the N—O—F group is perpendicular to the ONO_2 plane (*212*), the geometry continues to be discussed. Coplanarity is favored, based primarily on analogy with the planar structures well established for the related molecules $HONO_2$ and CH_3ONO_2 (*15, 47, 73, 91, 136, 186*). However, perhaps now the definitive work has appeared from two different laboratories, using Raman polarization measurements to show that O_2NOF and other halogen nitrates are indeed nonplanar (*67, 270*).

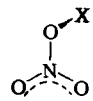

2. Group VIa Hypofluorites

a. Pentafluorosulfur Hypofluorite (SF_5OF). The preparation of this compound exemplifies the beauty of the Lustig and Ruff method for synthesis of hypofluorites through the use of alkali-metal fluorides (*237*). Based on the fact that it is possible to prepare a material having the composition $CsOSF_5$ (*66, 278*), they were able to demonstrate that thionyl fluoride or thionyl tetrafluoride could be catalytically fluorinated to SF_5OF in the presence of CsF in yields greater than 95% (*237*). This is in sharp contrast to yields obtained via the AgF(I,II)-catalyzed fluorination of SOF_2 (*93, 94*).

The addition of SF_5OF to olefins (*175, 216*) occurs readily to give only one product, which contains the components SF_5 and F. Penta-

$$SF_5OF \begin{cases} + CHCl{=}CHCl \xrightarrow{-183 \text{ to } 25^\circ C} SF_5OCHClCHClF \quad 81\% \\ + CH_2CCl_2 \xrightarrow{-183 \text{ to } 25^\circ C} SF_5OCH_2CCl_2F \quad 71\% \\ + CHBrCHBr \xrightarrow{23^\circ C} SF_5OCHBrCHBrF \quad 15\% \end{cases}$$

fluorosulfur hypofluorite is much more reactive than SeF_5OF (Table I). For EPR studies of the radical ClF_4, SF_5OF was photolyzed with Cl_2 or HCl (*197*). When SF_5OF was photolyzed in the presence of SO_2 and OSF_2, EPR spectra showed FSO_2 and OSF_3, respectively (*198*). Because of its facile synthesis, some use has been made of SF_5OF in electrophilic fluorination applications. These are included in Section VI.

b. Fluorosulfuryl Hypofluorite or Fluorine Fluorosulfate (FSO₂OF). The standard synthesis of FSO_2OF is the fluorination of sulfur trioxide in the presence of AgF(I,II) at 200°C in a flow reactor to give yields of approximately 60% (*95, 175*). Photolysis of SO_3–F_2 mixtures in Pyrex result in $S_2O_6F_2$ and FSO_2OF (*116*). A rather novel route to produce pure FSO_2OF has been described by Christe *et al.* (*69*). Little additional chemistry has appeared in recent years. This may reflect the treacherous nature of this material (Table I). However, one further olefin insertion and one chlorine abstraction reaction have been reported (*54*).

$$NF_4SbF_6 + CsSO_3F \xrightarrow[-78^\circ C]{AHF} NF_4SO_3F \xrightarrow[10^\circ C]{-AHF} NF_3 + FSO_2OF \quad \sim 100\%$$

$$CHCl{=}CCl_2 + FSO_2OF \xrightarrow{-78^\circ C} CHClFCCl_2OSO_2F \quad 70\%$$

$$CHCl_3 + FSO_2OF \xrightarrow{-78^\circ C} CHCl_2OSO_2F \quad 80\%$$

Experimental kinetic studies of the thermal reactions between FSO_2OF and N_2F_4 (*308*) or CO (*304*) or CO and O_2 (*305*) and a theoretical calculation on the unimolecular decomposition of FSO_2OF (*55*) are in the literature. Raman and IR spectral data suggest C_s symmetry (*219*).

c. Pentafluoroselenium Hypofluorite (SeF₅OF). The initial synthesis of SeF_5OF occurred in low yield (14%) via the reaction of SeO_2 and

TABLE I

INORGANIC HYPOFLUORITES

Compound	Melting point (°C)	Boiling point (°C)	ν_{OF} cm^{-1}	ϕ_{OF}	Comments	References
ON_2OF			927		Shock sensitive	(*67, 186*)
FSO_2OF	−158.5	−31.3	878	249	Unpredictable, explosive	(*93, 95*)
SF_5OF	−86.0	−55.1	935	189	Thermally stable to ~200°C	(*93, 94, 182*)
SeF_5OF	−55	−30	920	177.5	Store at low temperature	(*191, 263, 265*)
O_3ClOF	−167.3	−15.9	885	219.4	Shock sensitive	(*2, 71, 229*)
OIF_4OF	−33.1	28.4	890	202 (trans) 176 (cis)	Slow decomposition in Teflon or stainless steel	(*68, 70*)

F_2/N_2 in the presence of AgF(I,II) at 100°C (*191*). Later, Cady and Smith showed the yield could be tripled if KF and $SeOF_2$ were allowed to form $KSeOF_3$, which was then subjected to fluorination (*277*). Subsequently, Seppelt demonstrated that when $KSeOF_3$ was treated with fluorine an insoluble salt $KSeOF_5$ was formed (*261*). The latter can be further fluorinated to F_5SeOF. Seppelt has shown also that, if $Hg(OSeF_5)_2$ is used in place of the potassium salt, much higher yields of SeF_5OF are obtained, with smaller quantities of SeF_6 present as a contaminant (*265*). The vibrational spectra of F_5SeOF have been assigned (Table I) (*263*).

$$\underset{100\ \text{mmol}}{Hg(OSeF_5)_2} + \underset{260\ \text{mmol}}{F_2} \xrightarrow[14\ \text{h}]{25°C} \underset{74\%}{SeF_5OF}$$

Few synthetic reactions with SeF_5OF have been attempted. It is not as reactive as SF_5OF. However, with *c*-C_5F_8, SF_4, and $COSeF_5OC_5F_9$, SeF_5OSF_5, and $SeF_5OC(O)F$ are obtained, respectively. The first two occur at 25°C on long standing, whereas with CO the reaction goes to completion after 12 h at 65°C (*277*).

3. *Group VIIa Hypofluorites*

a. Perchloryl Hypofluorite or Fluorine Perchlorate (O$_3$ClOF). The classic synthetic routes to O_3ClOF are similar to those for O_2NOF, for

example, bubbling elemental fluorine through 70% perchloric acid (*229*) or direct combination of fluorine with metal perchlorates (*175*). A new and convenient synthesis has been discovered (*71*). The thermal decomposition of O_3ClOF has been studied at 65–100°C and found to give ClO_2F, ClF, and O_2 (Table I). The amount of ClF formed increased with temperature (*176*). Vibrational spectral studies have been carried out (*2*).

$$NF_4SbF_6 + CsClO_4 \xrightarrow[-78°C]{AHF} CsSbF_6\downarrow + NF_4ClO_4$$

$$NF_4ClO_4 \xrightarrow{25°C} NF_3 + O_3ClOF \quad (\sim 100\%)$$

$$C_3F_6 + O_3ClOF \xrightarrow[12\ h]{-45°C} CF_3CF_2CF_2OClO_3\ (50\%) + CF_3CF(OClO_3)CF_3\ (24\%)$$

$$C_2F_4 + O_3ClOF \xrightarrow{-45°C} CF_3CF_2OClO_3\ (68\%)$$

$$CF_3I + O_3ClOF \xrightarrow{-45°C} CF_3OClO_3\ (8\%)$$

Very little reaction chemistry has been attempted with O_3ClOF; there are only a few references to remote (*290*) or unpublished work (*169*). However, Schack and Christe (*246*) have examined reactions with olefins and with CF_3I. The formation of both isomers with C_3F_6 is in sharp contrast to the exclusive Markownikoff-type additions observed for $ClOClO_3$ and $BrOClO_3$ reactions, which give 100% of $CF_3CFXCF_2OClO_3$ (*251*). This would suggest that the F—O bond in $FOClO_3$ is not strongly polarized in either direction, and it certainly does not support a significant positive charge on fluorine. Steric effects could account for the somewhat larger yield of the *n*-propyl isomer. The reaction with CF_3I is more difficult to control than with olefins. The yield of CF_3OClO_3 was much smaller than when $ClOClO_4$ was used as the source of perchlorate.

b. cis- *and* trans-*Iodine(VII) Oxytetrafluoride Hypofluorite* (*OIF_4OF*). The synthesis of OIF_4OF, the first iodine-containing hypofluorite, was one of the most elegant pieces of hypofluorite work during this period. A metathetical reaction between NF_4SbF_6 and $CsBrO_4$ in AHF gave only $FBrO_2$ and O_2. However, when $CsIO_4$ was substituted, the reaction was thought to proceed via the following (*68, 70*).

$$CsIO_4 + 4\,HF \rightleftharpoons CsIF_4O_2 + 2\,H_2O$$

$$NF_4SbF_6 + CsIF_4O_2 \xrightarrow[-78°C]{HF} CsSbF_6\downarrow + HOIF_4O + NF_4HF_2$$

$$NF_3 + \textit{cis–trans}\text{-}OIF_4OF \xleftarrow{-30 \text{ to } 25°C}$$

81%

Fluorination reactions of $CsIO_4$ with ClF_5, BrF_5, ClF_3, or F_2 did not result in pure $CsIF_4O_2$, so they were less attractive reagents. Alkaline hydrolysis occurred according to

$$OIF_4OF + 6OH^- \rightarrow IO_4^- + 5F^- + 0.5O_2 + 3H_2O$$

Physical properties have been determined for the cis–trans mixture. OIF_4OF is colorless as a gas, pale yellow as a liquid, and white in the solid state. Vapor pressures may be obtained from the equation $\log P_{mm} = 7.62925 - 1432.0/T$ K over the temperature range −45.3 to 0°C. It is marginally stable at 25°C and can be handled in well-passivated metal and Teflon gear without rapid decomposition. When a sample was heated in a stainless steel cylinder to 120°C for 388 h, IF_5 and O_2 were formed. Addition across the double bond in C_2F_4 resulted only in COF_2, CF_3CFO, and C_2F_6. It has no Lewis-acid or -base properties, reacting with neither CsF nor SbF_5. The IR spectra of the gas and of the neon-matrix-isolated solid and the Raman spectra of liquid and solid $FOIF_4O$ have been recorded (Table I). The highest mass fragment in the mass spectrum has been assigned to IF_4O^+ (70 eV). The hypofluorite is much more stable than the corresponding hypochlorite.

trans

cis

C. Rubidium and Cesium Fluoroxysulfates

In one of the most exciting breakthroughs in hypofluorite chemistry, Appleman *et al.* identified Fichter's (*97*) *vergängliches Oxidationsmittel* in the form of its rubidium and cesium salts as the fluoroxysulfate ion, SO_4F^- (*10*). Fluorine (as a 20% mixture in nitrogen) was passed into a 1–2 *M* solution of Rb_2SO_4 or Cs_2SO_4 held at approximately 0°C

to give a yellowish-white precipitate of $RbSO_4F$ or $CsSO_4F$. These compounds are the first known examples of ionic hypofluorites.

The solid salts, which only lose oxidizing power slowly at 25°C, detonate mildly at 100°C. Aqueous solutions decompose gradually with the formation of O_2, H_2O_2 and HSO_5^-. Using $H_2{}^{18}O$, it was found that each product contained one atom of ^{18}O (*293*). At 15°C in 0.01 *M* $HClO_4$, the first-order rate constant $k = 3.6 \times 10^{-4}$ s^{-1}, $\Delta H^{\ddagger} = 16.8 \pm 0.4$ kcal mol^{-1} and $\Delta S^{\dagger} = -15.7 \pm 1.5$ cal mol^{-1} deg^{-1}. Mechanisms for decomposition of aqueous solutions of and oxidations by SO_4F^- have been postulated (*292, 293*).

$$MSO_4F \xrightarrow{100°C} MSO_3F + \tfrac{1}{2}O_2$$

Both salts in acetonitrile (more stable than in H_2O) give singlet resonance bands in their respective ^{19}F-NMR spectra at $\phi + 132.3$, compared to $\phi + 37.5$ for KSO_3F. The O—F stretching frequency in the IR and Raman spectra is assigned to a band at 830 cm^{-1} (*10*). The fluoroxysulfate anion in $RbSO_4F$ has distorted tetrahedral coordination, with each central sulfur atom bound to four oxygens (*118*). The S—O—F bond angle is 107.8°. Each Rb cation is coordinated to nine oxygen atoms and two fluorine atoms.

Aqueous solutions of the fluorooxysulfate salts are very powerfully oxidizing. Chloride, bromide, and iodide are oxidized first to the free halogens and then to higher states. In addition, V(IV) → V(V); Ce(III) → Ce(IV); Co(II) → Co(III); Mn(II) → Mn(III) → Mn(VII) (*10*). The heat of reaction of $CsSO_4F$ with aqueous HI has been determined by solution calorimetry. The standard heat of formation is -1004.9 ± 1.6 kJ mol^{-1} (*282*).

The fluoroxysulfate ion fluorinates aromatic compounds in acetonitrile at room temperature. Reaction of $CsSO_4F$ with PhOR (R = H, CH_3, C_4H_9, or $C_2H_5CHCH_3$) in CH_3CN with a BF_3 catalyst gave a mixture of 2-FC_6H_4OR and 4-FC_6H_4OR (70–80%), the product ratio being dependent on the size of OR (*280*). Under similar conditions benzene gave fluorobenzene (30–35%), and naphthalene gave a mixture of 1- and 2-fluoronaphthalene in the ratio 5:1 (38–42%) (*281*). Phenanthrene and pyrene as well as phenol, anisole, biphenyl, and toluene (*141*) have been fluorinated without the use of a catalyst. The major product with toluene was benzyl fluoride. Because of their relative stability and ease of preparation, storage, and use, these fluoroxysulfate salts appear to have a considerable potential as synthetic reagents for organic chemistry.

IV. Bisfluoroxy Compounds or Bishypofluorites

A. OF Bonded to Carbon

The use of alkali-metal-fluoride-catalyzed fluorination of appropriate oxygen-containing species enhances the ease of syntheses and the yields of bisfluoroxy compounds. However, Prager and Thompson have been remarkably successful in the preparation of several mono- and bisfluoroxy compounds, particularly via the mild fluorination of fluoroalkyl alcohols or ketones and sodium salts of perfluorocarboxylic acids or of hexafluoroacetone hydrate (*175*).

$$FOCF_2CF_2CF_2OF \xrightarrow[RH]{\Delta \text{ or}} CF_4 + 2\,COF_2$$

$$FC(O)(CF_2)_xC(O)F + 2F_2 \xrightarrow[-78°]{CsF} FO(CF_2)_{x+2}OF \quad (x = 2, 3)$$

$$FC(O)OOC(O)F + 2F_2 \xrightarrow[-95°C]{KF} \underset{95\%}{FOCF_2OOCF_2OF}$$

In 1966 Prager (*217*) reported the first bisfluoroxy compound, $FO(CF_2)_3OF$, which was obtained in a 2% yield by the direct fluorination of 1-hydroxy-3-trichloroacetoxypropane. Although it is stable at room temperature when pure, it is decomposed by heat or by chemical initiators, including hydrocarbons. This decomposition appears to occur in a manner analogous to that of monofunctional primary compounds having more than one carbon atom. Almost simultaneously, Lustig and co-workers (*173, 174, 238*) demonstrated the marked advantage of the low-temperature alkali-metal-fluoride-catalyzed fluorination of perfluoroalkyl acid fluorides or of bisfluorocarbonyl peroxide to produce bisfluoroxy compounds in high yield and a state of high purity. At 25°C in the presence of CsF, CO_2 was converted essentially quantitatively to the first geminal bisfluoroxy compound, $CF_2(OF)_2$ (*57, 137, 173*). This product was also obtained in somewhat smaller yields via the direct fluorination of sodium trifluoroacetate (2%) or of sodium oxalate (1–15%) (*165, 291*). In addition, in the former case, a second geminal bisfluoroxy compound, $CF_3CF(OF)_2$ (55%), was isolated. This compound was found as a product in the fluorination of the monosodium salt of perfluoroacetone hydrate in 3% yield, whereas $(CF_3)_2C(OF)_2$ occurred in 5% yield (*291*).

$$NaOC(CF_3)_2OH + F_2/N_2 \xrightarrow[\text{temp.}]{\text{reduced}} (CF_3)_2C(OF)_2 + CF_3CF(OF)_2 + \text{others}$$

Based on an earlier report by Cady and Cauble (*58*) of the CsF-catalyzed fluorination of FC(O)OF to $CF_2(OF)_2$, DesMarteau and Sekiya (*259, 260*) reasoned that this route might prove to be a general one to $R_fCF(OF)_2$. They cleverly demonstrated that, at reduced temperatures in the presence of CsF, acidic hydrogens of perfluorocarboxylic acids react very readily with fluorine to form the acyl hypofluorite, which is then further catalytically fluorinated *in situ* to give geminal bisfluoroxy molecules.

$$R_fCO_2H + F_2 \xrightarrow[-78 \text{ or } -111^\circ C]{CsF} [R_fC(O)OF] \xrightarrow[F_2]{fast} [R_fCF(OF)_2]$$

$R_f = CF_3(84\text{–}100\%); C_2F_5(96\%); C_3F_7(92\%); ClCF_2(100\%)$

The thermal stability of the $R_fCF(OF)_2$ compounds decreases with increasing number of carbons, with the greatest change from two to three carbons. When $R_f = CF_3$, the parent compound is 98% recovered; when $R_f = C_2F_5$, 35% recovered; and when $R_f = C_3F_7$, 22% recovered after 8 h in Pyrex glass at 53°C. $ClCF_2CF(OF)_2$ was too explosive to measure. On the other hand, $CF_2(OF)_2$ is recovered 100% unchanged after 6 h at 150°C and 40% unchanged after 3 h at 250°C (*175*). All of the geminal bisfluoroxyalkanes are strong oxidizers and explosive and must be handled with care. The greatest tendency toward explosive decomposition was at higher pressures in the gas phase. The known bisfluoroxy compounds are given in Table II.

$$R_fCF(OF)_2 \xrightarrow{53^\circ C} R_fF + COF_2 + O_2$$

Very little chemistry of these bisfluoroxy compounds has been explored, primarily, with the exception of $CF_2(OF)_2$, because of their instability and, in the case of geminal compounds, the inconvenient low-yield syntheses that were available. However, the very stable and easily synthesized $CF_2(OF)_2$ has received some attention. Much of the early reaction chemistry has already been reviewed (*175*).

Although it has been demonstrated that $CF_2(OF)_2$ does not yield $CF_2(ONF_2)_2$ (*138*) with N_2F_4 in strict analogy with CF_3OF (*127*), the desired product as well as the monoether hypofluorite has been produced in a slightly different way (*215*). Fluorinated amines and peroxy compounds have been prepared by the $F_2C(OF)_2$ oxidation of the adduct of KCN with $(F_2N)_2C{=}NF$ in a borosilicate pressure vessel (*285, 286*).

$$KF + HNF_2 \xrightarrow[-126 \text{ to } -80^\circ C]{F_2C(OF)_2} F_2C(ONF_2)_2 + F_2C(ONF_2)OF$$

$$CF_2(OF)_2 + KCN{:}\ (F_2N)_2C{=}NF \rightarrow$$
$$(F_2N)_2CF_2,\ CF_3OOC(O)F,\ CF_3OOOCF_3,\ CF_3OOCF_2OF,\ \text{etc.}$$

TABLE II

BISFLUOROXY COMPOUNDS

Compound	Boiling point (°C)	$\nu_{O-F}(cm^{-1})$	ϕ_{OF}	Comments	References
$FO(CF_2)_3OF$	—	886	146.0	Stable at 25°C when pure	(*217*)
$FO(CF_2)_4OF$	−119 (mp)	886	146.7	Stable at 25°C when pure	(*173*)
$FO(CF_2)_5OF$	−102.9 (mp)	890	146.9	Stable at 25°C when pure	(*173*)
$FOCF_2OOCF_2OF$	—	939	158.6	Stable at 25°C when pure	(*174*)
$CF_2(OF)_2$	−64	916, 933	159.2	$\Delta H_f^0 = -134.9 \pm 3$ kcal mol^{-1}	(*115, 190*)
$CF_3CF(OF)_2$	−35	895	150.0	Greater stability than C_2F_5OF	(*58, 291*)
$(CF_3)_2C(OF)_2$	—	888	148.0	Extreme tendency to explode	(*291*)
$CF_3CF_2CF(OF)_2$	~0	885	154.3	Decreasing stability with increasing chain length	(*260*)
$CF_3CF_2CF_2CF(OF)_2$	~40	870	153.8		(*260*)
$ClCF_2CF(OF)_2$	—	881	150.1	Very explosive	(*260*)
$SeF_4(OF)_2$	12.9	917	179.0	Stable at 22°C	(*276*)

In the presence of CsF and COF_2, $CF_2(OF)_2$ gave trifluoromethyl(fluoroformyl) peroxide, bistrifluoromethyl trioxide, and fluoroxytrifluoromethane (*8*). However, when $CF_2(OF)_2$ was treated with a mixture of $CsOCF_3$ and CsF at −78 to −5°C (10 h), small amounts of CF_3OOOCF_3 (20%) and $CF_3OOOCF_2OOCF_3$ were isolated as well as O_2 and large amounts of CF_3OF (*85*). When both $CF_2(OF)_2$ and COF_2 were reactants, substantial quantities of $CF_3OOC(O)F$ formed.

Not too surprisingly, $CF_2(OF)_2$ has found an interesting role in thermal and photopolymerizations with hexafluorobenzene, in which copolymers of molecular weight about 2500 have been formed in addition to two new perfluoroethers (*299*). Similar reactions have been studied with hexafluorobicyclo[2.2.0]hexa-2,5-diene (*298*), perfluorobicyclo[2.2.0]hexene oxides (*300*), pentafluoropyridine (*301*), and octafluoronaphthalene (*302*). Use of $CF_2(OF)_2$ in electrophilic fluorinations is discussed in Section VI.

B. OF Bonded to Selenium

The only known bishypofluorite which does not contain carbon is $SeF_4(OF)_2$ (*276*). The reaction of $KSeO_2F$ with fluorine at reduced temperatures gave *trans*-$FOSeF_4OF$ in about 16% yield. It is a stable gas at room temperature and obeys the vapor-pressure curve $\log P_{mm} = -1386/T + 7.726$ over the range 241–286 K. Some of its spectral data are in Table II. It undergoes alkaline hydrolysis to release oxygen and form SeO_4^{2-}.

$$KSeO_2F + 3F_2 \xrightarrow{-78°C} FOSeF_4OF + SeF_5OF + SeF_6 + O_2$$

V. Hypochlorites

A. Polyfluoroalkyl and Pentafluorosulfur Hypochlorites (R_fOCl and SF_5OCl)

1. Preparation and Characterization

The methods of preparation of R_fOCl and of SF_5OCl are essentially identical with those used for the analogous fluoroxy compounds and hypofluorites, using chlorine monofluoride in place of elemental fluorine. Some examples are as follows.

a. Chlorofluorination in the Presence of MF.

$$\begin{matrix} R_f' \\ Rf \end{matrix}\!\!>\!C{=}O + ClF \xrightarrow[-20\,°C]{MF} \begin{matrix} R_f' \\ F \\ R_f \end{matrix}\!\!>\!COCl \qquad (123\text{–}125, 249, 324)$$

R_f = F, CF_3, F, CF_2Cl

R_f' = F, CF_3, CF_3, CF_3

yield > 99% 91% 99%

M = Cs or, less often, K or Rb

$$FC(O)(CF_2)_3C(O)F + 2ClF \xrightarrow[-20°C]{CsF} ClO(CF_2)_5OCl \qquad (125)$$

$$OSF_4 + ClF \xrightarrow[-20°]{MF\ (M = K, Cs)} \underset{>95\%}{SF_5OCl} \qquad (125, 254)$$

Also, using FNO, both fluorinations with fluorine and chlorofluorination with ClF occur probably via the formation of an α-fluorinated nitrite (*317*).

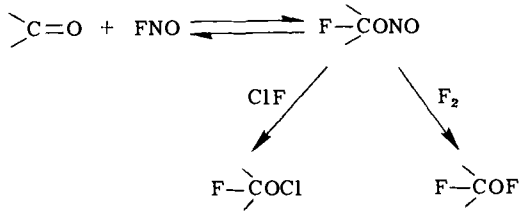

b. Chlorofluorination in the Presence of a Lewis Acid.

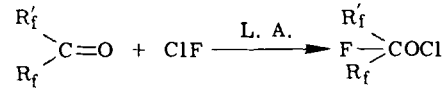

Lewis acid = HF, BF_3, AsF_5, ≠ PF_5 (*318*)

It is interesting to note that Lewis acids do not catalyze fluorine addition to form fluoroxy compounds.

c. Fluoroalcohols with Positive Chlorine-Containing Molecules.

$$R_fOH + ClF \xrightarrow{25°C} R_fOCl$$

R_f = $(CF_3)_3C$, $(CF_3)_2CH$, $CH_3C(CF_3)_2$, and CF_3CH_2 (*324*)

The reactions of ClF with the esters $CF_3(CH_3)CHOS(O)CF_3$ at −78°C and $(CF_3)_2C(CH_3)OS(O)CF_3$ at 25°C formed $CF_3(CH_3)CFOCl$ and $(CF_3)_2CCH_3OCl$, respectively (*177*).

The attempted preparation of *t*-butyl hypochlorite resulted in a sharp detonation. Although no explosion occurred, reactions with CH_3OH or perfluoropinacol gave none of the hypochlorites sought (*324*). The use of Cl_2O as a source of positive chlorine was successful with COF_2 to give CF_3OCl (*125*).

Fokin *et al.* (*114*) have used $ClOSO_2F$ as the source of positive chlorine in reaction with rather long-chain polyfluoroalcohols.

$$R_fCH_2OH + FSO_2OCl \xrightarrow[25–46\%]{-HSO_3F} R_fCH_2OCl$$

R_f = $H(CF_2)_2$, $H(CF_2)_4$, $H(CF_2)_6$, O_2NCF_2

Perfluoroalkyl hypochlorites and SF_5OCl are more stable thermally than the alkyl hypochlorites. For example, CF_3OCl decomposes slowly at 150°C, and the others have decreasing stability (*125*, *324*). When

thermal decomposition does occur, the general reaction is, for example,

$$CF_3OCl > (CF_3)_3COCl \sim CH_3C(CF_3)_2OCl \sim (CF_3)_2CHOCl \sim CF_3CH_2OCl > C_2F_5OCl \sim i\text{-}C_3F_7OCl > SF_5OCl$$

$$(CF_3)_3COCl \xrightarrow{\Delta} (CF_3)_2CO + Cl_2 + CF_3Cl + C_2F_6$$

and

$$i\text{-}C_3F_7OCl \xrightarrow{\Delta} CF_3C(O)F + CF_3Cl + (CF_3)_2CO + ClF$$

It is also interesting to note that although these hydrogen-containing fluorohypochlorites are stable to spontaneous decomposition, at least to 80°C, the analogous fluoroxy compounds either are not isolable or have only a very fleeting existence at low temperature. On the other hand, the fluorinated species are much more susceptible to hydrolysis than their alkyl analogs. A qualitative ordering of hydrolytic stabilities shows $(CF_3)_3COCl$ to be the least stable: $(CF_3)_3COCl < CH_3C(CF_3)_2OCl \sim (CF_3)_2CHOCl < CF_3CH_2OCl \ll (CH_3)_3COCl$.

In situ generation of partially fluorinated hypochlorites has been used considerably by J. C. Martin and co-workers in the preparation of S(IV) compounds. This preparative method, because it does not result in the synthesis and isolation of new hypochlorites, will be covered in Section V.A.2.*b*.

Vibrational spectral studies and normal coordinate analysis of CF_3OCl have been carried out (*166*, *309*). The low-frequency Raman spectrum of CF_3OCl (l) was recorded below 300 cm^{-1}, and the CF_3 torsional modes were observed (*128*). Also, the vibrational spectra for SF_5OCl have been analyzed (*87*). The low-pressure pyrolysis and UV photolysis of CF_3OCl have been studied to obtain information on the initial decomposition steps. The decomposition products of CF_3OCl were trapped at 8 K in an argon matrix, and the only detectable product was COF_2, identified by IR (*63*). Later, matrix-IR (*274*) and Raman (*275*) studies have identified COF_2, CF_3OOCF_3, CF_3OF, ClF, and COFCl. The photochemical decomposition of CF_3OCl at 2537 Å was investigated between 20 and 30°C and total pressures between 45 and 450 torr. The only products formed were CF_3OOCF_3 and Cl_2. When the decomposition was induced by chlorine atoms at 3650 Å, the same products were observed (*88*). The kinetics of the photochemical reaction between CF_3OCl and CO (*89*), and CF_3OCl and CF_2CCl_2 have been examined (*90*).

2. *Reactions*

There are many strong attributes that favor fluorohypochlorite reaction chemistry compared to that of the analogous fluoroxy compounds, at least to the synthesis chemist, including higher product yields with concomitantly fewer side products, less harsh conditions, and shorter reaction times. The other side of the coin is their lower thermal and hydrolytic stabilities. Throughout Section V.A.2 these comparisons will be made so that the reader can draw his own conclusions.

a. Oxidative Displacement and Oxidative Addition. Advantage was taken of either the hydrolytic instability of SF_5OCl or the positive character of the chlorine in CF_3OCl or SF_5OCl to prepare the first perfluorinated alcohol, CF_3OH, or pentafluoroorthosulfuric acid, $HOSF_5 \cdot CF_3OH$ decomposes slowly at $-20°C$, whereas SF_5OH begins

$$R_fOCl + HCl \xrightarrow{T} R_fOH + Cl_2$$

$R_f = CF_3$, $T = -120°C$ (*157, 267*)
$R_f = SF_5$, $T = -95°C$ (*266*)

to lose HF at $-60°C$. Fluoroxy compounds react very slowly with water or acid solution (*217*).

With boron trichloride the chlorine is oxidatively displaced to give the first perfluoroalkyl borate esters. The thermal stability of the products is a function of the number of fluorine atoms attached to the α-

$$3R_fOCl + BCl_3 \xrightarrow{T} B(OR_f)_3 + 3Cl_2$$

$R_f = CF_3$, $i\text{-}C_3F_7$, $t\text{-}C_4F_9$
$T = -20°C$, $-20°C$, $25°C$

carbon; thus $(CF_3O)_3B$ decomposes to $3F_2CO$ and BF_3 rapidly at 25°C, but $[(CF_3)_3CO]_3B$ is stable. The borates with fluorine atoms on the α-carbon can be stabilized by complexing with trimethylamine by blocking the α-fluoride shift (*319*). A similar displacement occurs with $PClF_4$ and PCl_2F_3. These perfluorobutoxyphosphoranes can be stored at 25°C, with the only decomposition being a very slow reorganization

$$t\text{-}C_4F_9OCl + PClF_4 \xrightarrow{25°C} t\text{-}C_4F_9OPF_4 + Cl_2 \quad (\sim 100\%)$$

$$2t\text{-}C_4F_9OCl + PCl_2F_3 \xrightarrow{25°C} (t\text{-}C_4F_9O)_2PF_3 + 2Cl_2 \quad (\sim 100\%)$$

of t-$C_4F_9OPF_4$ to PF_5 and $(t\text{-}C_4F_9O)_2PF_3$ (*325*). This compound is also obtained, but in lower yield (15%), in an oxidative addition reaction between PF_3 and $(CF_3)_3COCl$ at 0°C (*189*). At 0°C, $(CF_3)_3COCl$ gave essentially quantitative yields of $P[OC(CF_3)_3]_3$ and $P[OC(CF_3)_3]_5$ with PCl_3 and PCl_5, respectively. $P[OC(CF_3)_3]_5$ hydrolyzes readily to $OP[OC(CF_3)_3]_3$. The latter molecule could not be obtained from $OPCl_3$ + $(CF_3)_3COCl$. Analogous reactions between trifluoromethyl hypochlorite and PCl_3, PCl_5, and $OPCl_3$ result primarily in fluorination products (*189*). However, with $OPCl_3$, mass spectral data indicate the existence of such species as $OP(OCF_3)_3$, $OP(OCF_3)_2Cl$, and $OP(OCF_3)Cl_2$, which on standing give white solids and volatile materials such as COF_2 and OPF_3, which would be expected by analogy with the instability of the perfluoroalkyl borate esters with fluorine atoms on the α-carbon (*319*).

Oxidative addition reactions of CF_3OCl and $(CF_3)_3COCl$ with compounds in which the coordination number of the central atom is increased by the addition of two CF_3O or two $(CF_3)_3CO$ groups have provided a route to many new sulfuranes. A comparative study of the reactions of $(CF_3)_3COCl$ and CF_3OCl indicates that the vast difference in behavior of these two hypochlorites can be attributed in large degree to the fact that CF_3OCl is more stable, most of its reactions requiring photolysis, which suggests a free-radical mechanism. $(CF_3)_3COCl$ is less stable to thermolysis, hydrolysis, photolysis, and insertion reactions. Reactions of $(CF_3)_3COCl$ are carried out normally at 0°C. If photolytic conditions are employed, the $(CF_3)_3CO\cdot$ radical readily decomposes to the stable $(CF_3)_2CO$. It is not possible to carry out reactions of $(CF_3)_3COCl$ under rigorous conditions [e.g., photolysis of neat CF_3OCl (or SF_5OCl)] because of its overall lower stability (*188*). The high yields (>90%) [compare 25% yield from $SF_5OF \xrightarrow{h\nu} SF_5OOSF_5 + F_2$ (*80*)]

$$CF_3OCl(SF_5OCl) \xrightarrow{h\nu} CF_3OOCF_3(SF_5OOSF_5) + Cl_2 \qquad (249, 254, 274)$$

make this an attractive route to these two peroxides, but it is only applicable to hypochlorite precursors that do not contain fluorine on the α-carbon where, for example,

$$C_2F_5OCl \xrightarrow[25°C]{h\nu} CF_3Cl + COF_2$$

but for $(CF_3)_3COCl$ at low temperature,

$$(CF_3)_3COCl \xrightarrow[-78°C]{h\nu/\text{quartz}} \underset{30\%}{(CF_3)_3COOC(CF_3)_3}$$

and

$$CH_3C(CF_3)_2OCl \xrightarrow[25°C]{h\nu} CH_3C(CF_3)_2OOC(CF_3)_2CH_3 \qquad (80)$$

The products of the oxidative addition reactions of CF_3OCl and $(CF_3)_3COCl$ differ markedly (*188*), and, in fact, in all reactions attempted the only point of agreement is that neither can be caused to react with $(CF_3)_2SF_2$ under the conditions tried. In Table III some of the reactions are summarized. Although Gombler (*122*) had reported the synthesis of the first stable perfluoroalkyl-containing compound in which three-coordinate sulfur(IV) is bonded to sulfur (II), $CF_3S(O)SCF_3$, **A** (Table III) is the first sulfurane in which four-coordinate sulfur(IV) is bonded to sulfur(II). Although CF_3OCl adds 2 mol of CF_3O to each sulfur of $\overline{SCF_2SCF_2}$, under all conditions tried only 2 mol of $(CF_3)_3CO$ added to one sulfur in the ring **B**. X-Ray studies (*255*) of **B** show that both ring atoms occupy equatorial positions with the C—S—C angle of 77.4(6)° much reduced from the 120° required for the

TABLE III

REACTIONS OF CF_3OCl AND $(CF_3)_3COCl$

Reagent	CF_3OCl		$(CF_3)_3COCl$	
CF_3SCF_3	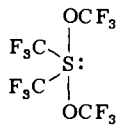 65%	(*154*, *155*)	No reaction	
CF_3SSCF_3	CF_3SF_3, COF_2, Cl_2 CF_3Cl (tr), SF_4 (tr)		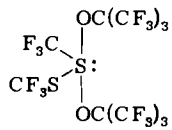 **(A)**	(*187*)
SF_4	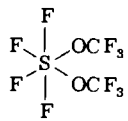 90–95%	(*156*)	No reaction	

TABLE III (*Continued*)

Reagent	CF_3OCl		$(CF_3)_3COCl$	
$C_6F_5SSC_6F_5$			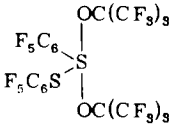	(*187*)
$CF_3S(O)CF_3$	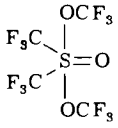 86%	(*155*)	No reaction	
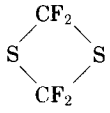	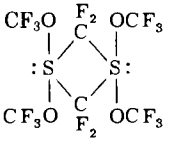 50%	(*154*, *155*)	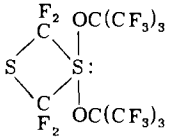 (**B**) 95%	(*188*, *285*)
SCl_2	COF_2, Cl_2, $SF_4(OCF_3)_2$	(*188*)	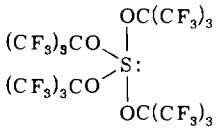 (**C**) 95%	(*188*)
CF_3SCl	CF_3Cl, COF_2, SF_4, Cl_2, CF_3SF_3	(*188*)	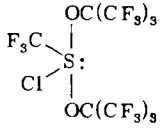 (**D**)	(*188*, *195*)
$CF_3S(O)Cl$	COF_2, Cl_2, $SOClF$, $SOCl_2$, CF_3SO_2Cl, CF_4, CF_3Cl	(*188*)	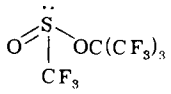 95%	(*188*)

ideal trigonal–bipyramidal structure. The axial positions are occupied by $(CF_3)_3CO$ groups that are bent over the ring away from the sulfur electron pair, precluding the oxidative addition of additional $(CF_3)_3CO$ groups to the second sulfur.

With either CCl_3SCl, SCl_2, S_2Cl_2, or CS_2, at 0°C $(CF_3)_3COCl$ oxidatively adds to sulfur, displacing all other ligands to give the hydrolytically stable $S[OC(CF_3)_3]_4$ (**C**, Table III). The behavior of $(CF_3)_3COCl$ toward CF_3SCl or CCl_3SCl is considerably different. As already noted with CCl_3SCl, **C** is obtained, but with CF_3SCl oxidative addition occurs at sulfur with no C—S or S—Cl bond breaking to give **D**, which is quite a different type of chlorosulfurane, with three different ligands. In none of these cases was chlorine also introduced in the oxidative addition reactions.

Alcohols of the type hexafluoro-2-phenyl-2-propanol are converted to hypochlorites by chlorination of a suspension of the alkoxide in anhydrous $CFCl_3$ at −78°C. This can be treated with sulfides in CH_2Cl_2 at −78°C to prepare the alkoxysulfonium chloride, which reacts further with the alkoxide to give a sulfurane (*14, 122, 178, 179, 211*). The more convenient route is the treatment of an ether solution of the alkoxide from reaction of the alcohol with potassium metal and, for example, diphenyl sulfide with chlorine at −78°C.

$$(C_6H_5)_2S + C_6H_5(CF_3)_2COK \xrightarrow[\text{ether}\ -78\,^\circ C]{Cl_2} \begin{matrix} H_5C_6 & OC(CF_3)_2C_6H_5 \\ & \diagdown\ \diagup \\ & S: \\ & \diagup\ \diagdown \\ H_5C_6 & OC(CF_3)_2C_6H_5 \end{matrix}$$

Just as the fluorohypochlorites can be photolyzed neat to form peroxides, so they can combine with other free radicals.

$$2CF_3OCl(SF_5OCl) + N_2F_4 \xrightarrow{h\nu} \underset{71\%}{CF_3ONF_2}(\underset{14\%}{SF_5ONF_2}) \qquad (249, 254)$$

$$SF_5OCl + (FC(O)O)_2 \xrightarrow{h\nu} SF_5OC(O)F + SF_5OOC(O)F \qquad (16)$$

Oxidative addition or insertion reactions where the units R_fO and Cl add to the central atom of the reactant are known and, in some cases, well studied. With CO or SO_2, perfluoroalkyl and pentafluorosulfur chloroformates or perfluorochlorosulfates are easily formed. $CF_3OC(O)Cl$ and $SF_5OC(O)Cl$ have also been synthesized using photolysis at 25°C (*249, 254*). Insertion of sulfur dioxide into the O—Cl bond occurred readily.

$$R_fOCl + CO \xrightarrow[25°C]{} R_fOC(O)Cl \quad \sim 100\%$$

R = CF_3, C_2F_5, *i*-C_3F_7, $(CF_3)_3C$, SF_5, $(CH_3)_2CH$, $(CF_3)_2C(CH_3)$, CF_3CH_2 (*322–324, 326*)

$$R_fOCl + SO_2 \xrightarrow{-20°C} R_fOSO_2Cl \quad \sim 50\%$$

R_f = CF_3, C_2F_5, *i*-C_3F_7, $(CF_3)_3C$, $(CF_3)_2CH$, $(CF_3)_2C(CH_3)$, CF_3CH_2 (*320–322, 324*)

Again it should be noted that although CF_3OF will react under photolytic conditions with CO to form the fluoroformate $CF_3OC(O)F$ (*17*), the chloroformate could be formed at 25°C. Similarly, the chlorosulfates were obtained at −20°C, but CF_3OSO_2F from CF_3OF and SO_2 required 180°C (*303*).

Both CF_3OCl and $(CF_3)_3COCl$ react with mercury to give COF_2 and HgClF (*188*) and $(CF_3)_3COHgCl$ (*195*), respectively. The latter is a useful precursor for the introduction of $(CF_3)_3CO$ into a variety of compounds with labile halogen; for example, although CF_3SCl would not react with $(CF_3)_3COH$ neat or in the presence of $(C_2H_5)_3N$, with the mercurial derivative ester formation proceeded smoothly (90% yield).

b. Addition to Unsaturated Systems. Perfluoroalkyl, polyfluoroalkyl, and pentafluorosulfur hypochlorites add readily and, in most cases, nearly quantitatively to unsubstituted and halogen-substituted terminal olefins (*7, 180*). With a few exceptions (e.g., $CF_2{=}CFCl$, $CF_3CF{=}CF_2$ and $CF_3OCH{=}CH_2$) the direction of addition to unsymmetric olefins is such that in the resulting ether the chlorine atom of the hypochlorite is bonded to the olefinic carbon with the greatest electron density. In cases where the difference in electron density be-

$$R_fOCl + \diagdown C{=}C \diagup \xrightarrow[\text{to } -45°C]{-111} R_fOC{-}CCl$$

R_f	$\diagdown C{=}C \diagup$
CF_3	$CF_2{=}CF_2$, $CH_2{=}CH_2$, $CH_2{=}CHCl$, $CF_2{=}CH_2$
i-C_3F_7	$CF_2{=}CF_2$
$(CF_3)_3C$	$CF_2{=}CF_2$, $CH_2{=}CH_2$
$(CF_3)_2CH$	$CF_2{=}CF_2$
SF_5	$CF_2{=}CF_2$, $CH_2{=}CH_2$
$H(CF_2)_4CH_2$	$CF_2{=}CF_2$
$H(CF_2)_6CH_2$	$CF_2{=}CF_2$
$O_2NCF_2CH_2$	$CF_2{=}CF_2$
$H(CF_2)_4CH_2$	$CH_2{=}CHC_5H_{11}$
$H(CF_2)_2CH_2$	$CF_2{=}CFCF_3$ (acid catalyst)

tween the two carbon atoms of the olefin is small, significant amounts of each isomer are found.

$$CF_3CF{=}CF_2 + CF_3OCl \xrightarrow{0°C} \underset{7}{CF_3CFClCF_2OCF_3} + \underset{3}{CF_3CF(OCF_3)CF_2Cl} \quad (194)$$

$$CF_3OCH{=}CH_2 + CF_3OCl \xrightarrow{-111°C} (CF_3O)_2CHCH_2Cl + CF_3OCHClCH_2OCF_3 \quad (7)$$

$$CF_2{=}CFCl + CF_3OCl \xrightarrow{-80°C} \underset{2.5}{CF_3OCFClCF_2Cl} + \underset{3}{CF_3OCF_2CFCl_2} \quad (180)$$

The highly fluorinated ethers are very stable compounds, for example when C_2F_4 is the substrate. They undergo essentially no change when held at 400°C or more for over 1 week or in contact with KOH pellets at 25°C. The less highly fluorinated ethers such as CF_3OCH_2-CH_2Cl, which have chlorine and hydrogen bonded to vicinal carbon atoms, readily undergo dehydrohalogenation to give fluoroolefins which can be further treated with more hypochlorite. Attempts to add CF_3OCl to either perfluoro-2-butene or perfluoro-2-butyne were unsuccessful up to 150°C (decomposition point of CF_3OCl) (*7*).

In the reaction of perfluoro-2-azabut-1-ene with CF_3OCl or CF_3OF, the latter acts strictly as a fluorinating agent $\xrightarrow{250\text{–}300°C}$ $CF_3(C_2F_5)NF$, whereas CF_3OCl plays a chlorofluorinating role $\xrightarrow{-196 \text{ to } 25°C}$ $CF_3(C_2F_5)NCl$ (*193*). The presence of an acid catalyst causes addition to trifluoromethyl isocyanate, heptafluorobutyronitrile, and bistrifluoromethyl ketene to occur (*113*, *114*).

$$H(CF_2)_4CH_2OCl \begin{cases} + CF_3NCO & \xrightarrow[H^+]{70\text{–}75°C} CF_3NClC(O)OCH_2(CF_2)_4H \\ + C_3F_7CN & \xrightarrow[H^+]{110\text{–}115°C} C_3F_7C(=NCl)OCH_2(CF_2)_4H \\ + (CF_3)_2CCO & \xrightarrow{H^+} (CF_3)_2CClC(O)OCH_2(CF_2)_4H \end{cases}$$

B. Polyfluoroacyl and Polyfluoroalkanesulfonyl Hypochlorites [$R_fC(O)OCl$ and R_fSO_2OCl]

Chlorine derivatives of varying stabilities of several strong fluorinated acids have been synthesized. Although several perfluoroacyl hypofluorites and FSO_2OCl are known and are discussed in this chapter, only very recently have the polyfluoroacyl and polyfluoroalkanesulfonyl hypochlorites been described.

1. *Preparation and Characterization*

The synthesis involves a metathesis reaction between a polyfluorocarboxylic acid or its sodium salt and a readily available source of positive chlorine.

$$R_fCO_2M + ClX \xrightarrow{T} R_fC(O)OCl + MX$$

$R_f = CF_3, C_2F_5, C_3F_7, HCF_2, ClCF_2, -CF_2-$; X = F; M = H, Na

T = −111 to −78°C yields ~80–90% *(86, 287)*

$R_f = CF_3, ClCF_2$; X = OSO_2F; M = H, Na

T = −78 to −45°C yields ~90% *(242)*

$$R_fSO_3H + ClF \xrightarrow{-78°C} R_fSO_2OCl + HF \quad (86, 148)$$

$R_f = CF_3, C_4F_9$ 80–100%

DesMarteau preferred the sodium carboxylate precursor because of fewer separation problems (*287*). Where a volatile acyl hypochlorite is formed, Schack has preferred the use of $ClOSO_2F$ with the carboxylic acid rather than ClF because HSO_3F is less volatile than HF. When salts are used, $ClOSO_2F$ has been claimed to be superior to ClF in chlorinating anionic species (*242*).

$$R_fC(O)OCl \xrightarrow{22°C} R_fCl + CO_2$$

$$CF_3SO_2OCl \xrightarrow{22°C} CF_3Cl + SO_3$$

All of the polyfluoroacyl hypochlorites are thermally unstable at 22°C and are explosive. If samples are warmed in a closed system so that the partial pressure of the hypochlorite exceeds 20–50 torr, they explode without fail (*287*). CF_3SO_2OCl slowly decomposes at 22°C, but no comment has been found about its explosiveness. The decomposition in each case proceeds as expected. At low pressure (< 10 torr) in glass, their complete decomposition requires several hours. The relative order of stability at 22°C is $CF_3CO_2Cl > C_2F_5CO_2Cl > C_3F_7CO_2Cl > ClCF_2CO_2Cl > HCF_2CO_2Cl \gg CF_2(CF_2CO_2Cl)_2$. $CF_3C(O)OCl$ and $CF_3C(O)OF$ are about equally stable thermally. The Raman spectrum of CF_3SO_2OCl, which suggests C_1 symmetry, has been analyzed (*148*). Infrared and Raman spectra of most of these hypochlorites have been recorded.

2. *Reactions*

The reaction chemistry of these hypochlorites is typical of compounds that contain positive chlorine.

a. Oxidative Displacement and Oxidative Addition. A very powerful route to trifluoromethanesulfonate esters is now available via reactions of R_fSO_2OCl with alkyl or haloalkyl halides. In the case of monohaloalkanes the yields in general are high, but low yields result with dihaloalkanes. It has not been possible to form tri- and tetrasubstituted compounds. All of the esters are colorless, stable compounds at 22°C and higher (*147*). However, when alkyl chlorides are employed multisubstitution occurs readily, that is, $CH_2Cl_2 \rightarrow (CF_3SO_3)_2CH_2$ (45%) + $CF_3SO_3CH_2Cl$ (35%); $(CH_2Cl)_2 \rightarrow (CF_3SO_3CH_2)_2$ (50%) + $CF_3SO_3CH_2CH_2Cl$ (50%); $(ClCH_2)_2CH_2 \rightarrow$ explosion at −55°C; and $HCCl_3 \rightarrow [(CF_3SO_3)_3CH]$ (unstable above 0°C) (*145*). In some cases, in which CF_3SO_2OCl is too vigorous, CF_3SO_2OBr, which is a milder but less stable reagent, has been used.

$$CF_3SO_2OCl + RX \xrightarrow{-111 \text{ to } 22^\circ C} XCl + CF_3SO_2OR$$

RX = CF_3Br (95%), C_2F_5Br (58%), C_3F_7Br (65%), CCl_2F_2 (82%), CBr_2F_2 (44%), CCl_3F (63%), $(CF_2Br)_2$ (62%), $CF_3SO_3CF_2Br$ (30%), *e*-$CF_3CO_2CHFCHFCl$ (80%), *t*-$CF_3CO_2CHFCHFCl$ (90%), *e*$CF_3SO_3CHFCHFBr$ (~100%) (*144, 147*)

$$2CF_3SO_2OCl + Br_2 \xrightarrow{-60, -20^\circ C} 2CF_3SO_2OBr + Cl_2 \quad (148)$$

With small molecules such as CO and SO_2, insertion into the O—Cl occurs at low temperature

$$R_fC(O)OCl + CO \xrightarrow{-111 \text{ to } -75^\circ C} R_fC(O)OC(O)Cl \xrightarrow{22^\circ C} R_fC(O)Cl + CO_2$$

$R_f = CF_3, C_3F_7$ (*86, 287*)

and

$$CF_3C(O)OCl + SO_2 \xrightarrow{-111 \text{ to } -15^\circ C} CF_3C(O)OSO_2Cl$$

b. Addition to Unsaturated Systems. Reactions of CF_3SO_2OCl and $CF_3C(O)OCl$ provide a second useful route to esters. Both Schack (*242*) and DesMarteau (*144, 146, 288*) have demonstrated the relative ease with which these two types of hypochlorites saturate olefinic double bonds. It should be noted that in every case the addition reactions were

$$R_fC(O)OCl + \diagdown C{=}C \diagup \xrightarrow{\text{Low temp.}} R_fC(O)OCCCl \quad (64, 242, 288)$$

R	C=C
CF_3	$CF_2{=}CF_2$ (54%); $CF_2{=}CH_2$ (94%); $CF_2{=}CFCl$ (65%)
CF_3	$CF_2{=}CCl_2$ (81%); $CH_2{=}CH_2$ (33%); *cis*-CFH=CFH (*e*-64%); *trans*-CFH=CFH (*t*-65%); $CF_3CF{=}CF_2$ (84%)
CF_2Cl	$CF_2{=}CF_2$ (42%); $CF_2{=}CH_2$ (93%); $CF_3CF{=}CF_2$ (74%)
C_2F_5	$CF_2{=}CF_2$ (65%); $CF_2{=}CH_2$ (80%)
n-C_3F_7	$CF_2{=}CF_2$ (66%); $CF_2{=}CH_2$ (80%)
HCF_2	$CF_2{=}CF_2$ (<1%); $CF_2{=}CH_2$ (95%)

regiospecific, suggesting concerted polar addition. Invariably, the positive chlorine is found at the most electronegative carbon. The addition of $CF_3C(O)OCl$ to *cis*- and *trans*-CFH=CFH gives a single different diastereomer, erythro and threo, respectively. Therefore, the reactions are stereospecific.

The behavior of CF_3SO_2OCl exactly mimics that of the polyfluoroacyl compounds, with addition occurring at low temperature to give only one structural isomer in each case (*144, 146*). Also, *cis*- and *trans*-CHF=CHF form a single, different diastereomer.

All of the new esters are stable in glass at 22°C, and all have good thermal stability at considerably higher temperatures, with the majority of the carboxylates approximately being 100% recovered after 10 h at 200°C. Most of the trifluoromethanesulfonates show no decomposition to at least 100°C. The carboxylate esters with α-fluorine in the carbalkoxy group are readily decomposed to acid fluorides by fluoride ion (KF but not NaF).

C. Fluorosulfuryl Hypochlorite (Chlorine Fluorosulfate) (FSO_2OCl)

1. Preparation and Characterization

Fluorosulfuryl hypochlorite was invented by Cady and Gilbreath via the extended thermal reaction of chlorine with peroxydisulfuryl difluoride (*120*). Later workers have demonstrated that ClF and SO_3 will react to form the yellow FSO_2OCl, essentially quantitatively after a slow warm-up to 25 from −196°C (*129, 252*). The Raman spectrum (*219*) of liquid FSO_2OCl and the IR spectra of the gas and solid (*65, 313*) have been assigned. C_s symmetry is suggested.

2. Reactions

One of the more useful reactions of FSO_2OCl, now that it can be synthesized by a route that does not require $S_2O_6F_2$, is to subject it to UV radiation to provide an alternate synthesis of $S_2O_6F_2$. A somewhat novel use is to spray a mixture of FSO_2OCl and H_2O_2 containing 20% H_2O and 1% NaOH on the bottom of a vessel at −78° to leave a gas stream that contains approximately 40% singlet O_2 (*214*).

$$ClOSO_2F \xrightarrow[\substack{2\text{–}4\ h\\ 25°C}]{h\nu} \underset{94\text{–}97\%}{FSO_2OOSO_2F} + Cl_2 \qquad (243)$$

As has been cited previously, FSO_2OCl is a valuable alternate source of positive chlorine for use as a precursor of other hypochlorites (*64, 114, 242*).

a. Oxidative Displacement and Oxidative Additions. Fluorosulfuryl hypochlorite reacted predictably with small molecules,

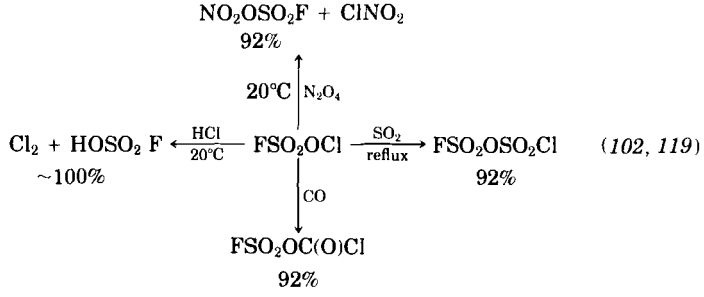

(*102, 119*)

However, with ozone the previously known ClO_2OSO_2F and oxygen resulted (*241*).

This reactive molecule is insensitive to naked flame and mechanical effects, but at approximately 20°C it reacts explosively with H_2O and $(CH_3)_2CO$, induces combustion of C_6H_6 and C_6H_{12}, and reacts vigorously with chlorocarbons and polyfluorinated lubricants (*111*). However, at −100°C it reacts with an excess of C_6H_6 to give C_6Cl_6 in 80% yield (*100, 104*). A similar behavior has been noted with 1,3,5-$Cl_3C_6H_3$ at −25°C (*108*). The chlorination reaction is substantially slowed when a nitro group is introduced into the aromatic ring. At 25°C, 1,3,5-trinitrobenzene does not react at all with $ClOSO_2F$.

$$O_2NC_6H_5 + FSO_2OCl \xrightarrow{-10 \text{ to } 25°C} \underset{60\%}{O_2NC_6Cl_5} + \underset{x = 1, 2, 3, 4}{O_2NC_6H_xCl_{5-x}}$$

The complex of FSO_2OCl with SbF_5 has more chlorinating activity than FSO_2OCl alone. At 20°C this reagent chlorinates pentafluorobenzene and 4,4′-dihydroperfluorobiphenyl to pentafluorochlorobenzene and 4,4′-dichloroperfluorobiphenyl in 95 and 60% yields, respectively (*103, 108*). The reactive species has been claimed to be $Cl(FSO_2OSbF_5)$. The latter reacts with C_6F_6 to give $C_6F_6Cl^+$. However, FSO_2OCl, unaided by SbF_5, will substitute the nitroso group by chlorine in perfluoronitrosoalkanes. Other nitro derivatives have been realized by using salts of nitro compounds with FSO_2OCl (*111*). In two very nice

$$ClOSO_2F \xrightarrow{O_2NCF_2CF_2NO} [O_2NCF_2CF_2\overset{+}{N}(O)Cl \cdot OSO_2F] \xrightarrow{-ONOSO_2F} O_2NCF_2CF_2Cl$$

reactions, Schack and co-workers have used FSO_2OCl to prepare $ClOClO_3$ and SeF_5Cl from appropriate salts.

$$RC(NO_2)_2M + FSO_2OCl \xrightarrow[-30 \text{ to } 0°C]{CCl_2FCClF_2} RC(NO_2)_2Cl$$

$$R = NO_2, CN; M = K, Na$$

$$MClO_4 + FSO_2OCl \xrightarrow{-45°C} MSO_3F + ClOClO_3 \qquad (250)$$

$$M = Cs, NO_2$$

$$CsSeF_5 + FSO_2OCl \xrightarrow{25°C} CsOSO_2F + SeF_5Cl \qquad (253)$$

Fokin and co-workers have synthesized perfluoroacyl fluorosulfates from perfluoroacyl chlorides in the presence of fluorosulfuric acid at

$$R_fC(O)Cl + FSO_2OCl \xrightarrow[20°C]{HSO_3F} R_fC(O)OSO_2F + Cl_2$$

$$R_f = CF_3, C_3F_7, C_8F_{17}$$

20°C (*105*). Perfluoroalkyl halides R_fX (R_f = C_{1-10} perfluoroalkyl; X = Cl, Br, I) result from treating the perfluorocarboxylic acid or its salt with FSO_2OCl (*247, 248*). It is likely that the corresponding acyl hypochlorite is the unstable intermediate.

$$R_fC(O)OM + FSO_2OX \xrightarrow{25-50°C} R_fCl + CO_2 + NaOSO_2F$$

M = H, Na, Ag, or $CF_3C{=}O$; X = Cl, Br; R_f = CF_3 (90%), $ClCF_2$ (85%), CF_3CF_2 (79%), C_7F_{15} (78%), $CF_2CF_2CF_2$ (86%)

Additionally, both the Soviet and the Rocketdyne workers have demonstrated that FSO_2OCl is an excellent reagent for substitution halo-

gen atoms in haloalkanes, halofluorocarbons, and various esters and polyfluoroethers. Reactions of chlorofluorocarbon ethers that can be readily obtained from addition of hypochlorites to perfluoroolefins (*7, 180*) with FSO_2OCl proceed very slowly (2 or 3 weeks, 110–140°C) when 10–20 mol % bromine is added, but in high yield (*245*). Pure FSO_2OCl does not produce appreciable reaction under the same conditions, which suggests the reactive reagent is FSO_2OBr generated *in situ*.

$$RCH_2Cl + FSO_2OCl \xrightarrow{-30°C} RCH_2OSO_2F + Cl_2$$

$$R = Cl, CH_2Cl, COOC_4H_9, COOC_2H_5 \qquad (105)$$

$$HCCl_2CCl_2H + FSO_2OCl \rightarrow HCCl_2CClHOSO_2F \xrightarrow{FSO_2OCl} Cl_2CHCH(OSO_2F)_2 + (FSO_2OCHCl)_2 \qquad (108)$$

3 : 1

$$R_fOCF_2CF_2Cl + FSO_2OCl \xrightarrow{Br_2} R_fOCF_2CF_2OSO_2F + Cl_2$$

$$R_f = CF_3\ (90\%),\ SF_5\ (71\%)$$

It has been claimed that the following reactions did not proceed, even at elevated temperatures, without excess fluorosulfuric acid (*110, 112*).

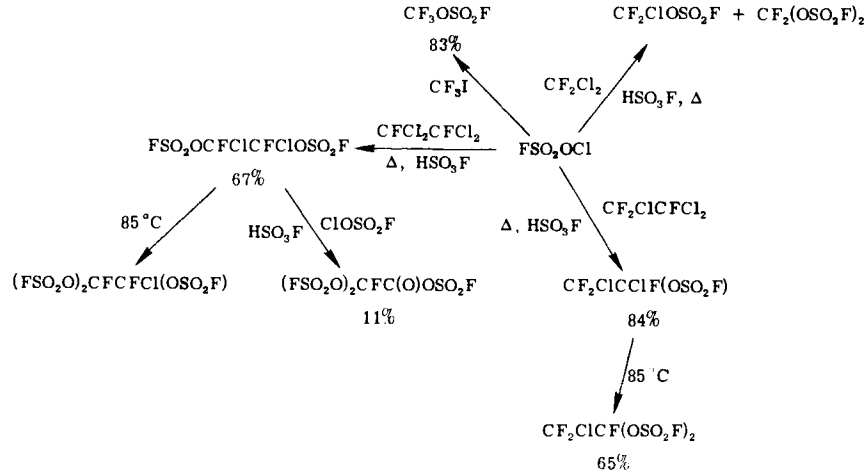

On the other hand, under strictly anhydrous conditions the displacement of halogen from halofluorocarbons by fluorosulfate has been carried out in high yields, with reactivity decreasing I > Br > Cl and with no intentional addition of fluorosulfuric acid (*248*). Under the condi-

TABLE IV

REACTIONS OF $ClOSO_2F$ AND $ClOSO_2F/Br_2$

Reactant	Temperature (°C)	Product (%)
$ClCF_2CF_2Cl$[a]	130	$ClCF_2CF_2OSO_2F$ (90)
$ClCF_2CF_2Cl$[b]	140	$ClCF_2CF_2OSO_2F$ (89) $FSO_2OCF_2CF_2OSO_2F$ (6)
$CF_3CFClCF_2Cl$[b]	25	$CF_3CFClCF_2OSO_2F$ (76)
$CF_3CFBrCF_2Br$[a]	25	$CF_3CFBrCF_2OSO_2F$ (70)
n-$C_7F_{15}I$[a]	25	n-$C_7F_{15}OSO_2F$ (85)
CF_3CF_2Cl[b]	130	$CF_3CF_2OSO_2F$ (22)
$ClCF_2CF_2OSO_2F$[b]	140	$FSO_2OCF_2CF_2OSO_2F$ (31)
CF_3CF_2Br[a]	25	$CF_3CF_2OSO_2F$ (96)
$BrCF_2CF_2Br$[a]	25	$BrCF_2CF_2OSO_2F$ (40)
$BrCF_2CF_2Br$[a]	65	$FSO_2OCF_2CF_2OSO_2F$ (64)
i-C_3F_7I[a]	−45	$[(i\text{-}C_3F_7)_2I]^+[I(SO_3F_4)]^-$ (~100)

[a] With $ClOSO_2F$.
[b] $ClOSO_2F/Br_2$.

tions used, it was demonstrated that (1) iodides reacted regardless of being primary or secondary; (2) only primary bromides or chlorides reacted; (3) the reactivity of FSO_2OCl was enhanced by the addition of catalytic amounts of bromine, but not sufficiently to cause reaction with secondary bromides or chlorides; and (4) several primary chlorides were unreactive, that is, C_2F_5Cl, $C_7F_{15}Cl$, $CF_3CFClCF_3$, $CF_3CFClCF_2Cl$, $ClCF_2CF_2OSO_2F$, and $CF_3CFClCF_2OSO_2F$ (Table IV).

The iodide reactions are particularly interesting, with $-OSO_2F$ first oxidatively adding to iodine, followed by slow elimination of $IOSO_2F$ in the n-heptyl case (*248*). It has been demonstrated that the combination of fluorosulfonation of a fluorocarbon halide with FSO_2OCl, conversion

$$Cl_2 + i\text{-}C_3F_7I(OSO_2F)_2 \xleftarrow[-45°C]{i\text{-}C_3F_7I} FSO_2OCl \xrightarrow[-45°C]{n\text{-}C_7F_{15}I} n\text{-}C_7F_{15}I(OSO_2F)_2 + Cl_2$$

$$\downarrow 101°C \qquad\qquad \text{slow} \downarrow 25°C$$

melts, stable, ionic $\qquad\qquad n\text{-}C_7F_{15}OSO_2F + IOSO_2F$

of the fluorosulfate to an alkali-metal perfluorocarboxylate with an alkali metal hydroxide, and subsequent further reaction of the perfluorocarboxylate with FSO_2OCl provide a route to a high-yield, chain-shortening reaction.

b. Addition to Unsaturated Systems. At temperatures between −20 and 20°C, FSO_2OCl adds with ease to hexafluorobenzene, with the products obtained dependent upon the stoichiometry used (*109*). Additions to olefins, with the exception of $CF_2{=}CFCl$, from which two isomers were obtained, were according to Markownikoff's rule and in high yield (90–95%) (*102, 106–108, 120, 194*). Reactivity of FSO_2OCl with olefins in increasing order of vigor is $CF_2{=}CF_2 < CFCl{=}CFCl \simeq CF_2{=}CF_2Cl > CF_3CF{=}CF_2 < (CF_3)_2C{=}CF_2$ (*107*). Bistrifluoromethyl ketene reacted easily at −70°C (*106*). Complete saturation occurs with acetylene in Freon 113 at −25°C to give $Cl_2CHCH(OSO_2F)_2$ (>90% yield) and $(FSO_2OCHCl)_2$ (5–7%). The former compound has high thermal and hydrolytic stability. However, with propyne and 2,2-dimethyl-3-pentyne, product decomposition results below 25°C (*108*).

$$C_6F_6 + FSO_2OCl \xrightarrow{\text{Freon 113}} \underset{\text{bp (°C): 60 (30 torr)}}{C_6F_6Cl(OSO_2F)} + \underset{\text{70 (1 torr)}}{C_6F_6Cl_2(OSO_2F)_2} + \underset{\text{110 (1 torr)}}{C_6F_6Cl_3(OSO_2F)_3}$$

$$FSO_2OCl + \diagup\!\!\diagdown C{=}C \diagup\!\!\diagdown \rightarrow FSO_2O\overset{|}{\underset{|}{C}}\!-\!\overset{|}{\underset{|}{C}}Cl$$

$\diagup\!\!\diagdown C{=}C \diagup\!\!\diagdown$ = $CF_3CF{=}CF_2$, C_2F_3Cl, $C_2F_2Cl_2$, C_2F_4, C_2Cl_4, $CF_2{=}C(CF_3)_2$, C_2HCl_3 (slow decomposition)

With nitriles the products obtained are a function of the stoichiometry of the reaction (*108*).

$$\underset{1:1}{R_fCN + FSO_2OCl} \xrightarrow{-45 \text{ to } -35°C} R_fC(=NCl)OSO_2F$$

R_f = CF_3OCF_2 (79%), n-C_3F_7 (89%), n-C_4F_9 (61%), CF_2NO_2 (90%)

$$\underset{1:2}{R_fCN + 2FSO_2OCl} \rightarrow R_fC(=NCl)OSO_2F + R_fC(O)OSO_2F + S_2O_5F_2$$

R_f = n-C_3F_7, n-C_4F_9

The products found can be rationalized as follows.

$$R_fCN \xrightarrow{FSO_2OCl} R_fC(=NCl)OSO_2F \xrightarrow{FSO_2OCl}$$

$$[R_fC(OSO_2F)_2NCl_2] \xrightarrow{FSO_2OCl} R_fC(O)OSO_2F + S_2O_5F_2 + [NCl_3]$$

When FSO_2OCl is treated with the sodium salt of dinitroacetonitrile, the yield of the chloro derivative is reduced because monoaddition at the nitrile function occurs as well (*111*).

$$FSO_2OCl \begin{cases} + \quad CF_3NCO \xrightarrow[25°C]{-78\text{ to}} CF_3N(Cl)C(O)OSO_2F \quad (279) \\ \qquad\qquad\qquad\qquad\qquad\qquad 96\% \\ + \; CF_3C(O)NCO \xrightarrow{25°C} CF_3C(O)N(Cl)C(O)OSO_2F \\ \qquad\qquad\qquad\qquad\qquad\qquad \sim 90\% \\ + \; (NF_2)_2C{=}NF \xrightarrow{-78°C} ClFNC(NF_2)_2OSO_2F \quad (98, 101) \\ \qquad\qquad\qquad\qquad\qquad\qquad 76\% \\ + \; C_2F_5N{=}CF_2 \xrightarrow{-78°C} C_2F_5N(Cl)CF_2OSO_2F \quad (193) \end{cases}$$

In the majority of cases with molecules that contain carbon–nitrogen double bonds, saturation with FSO_2OCl occurs with ease. However, with $(CF_3)_2C{=}NF$, fluorine abstraction was found. With ClNSO, sulfur–nitrogen bond breaking occurs with concomitant formation of thionyl fluorosulfate (*167*).

$$(CF_3)_2C{=}NF + FSO_2OCl \xrightarrow[-78\text{ to }20°C]{N_2} \underset{74\%}{(CF_3)_2C{=}NOSO_2F} \quad (99)$$

D. Pentafluoroselenium Hypochlorite (SeF_5OCl)

Because $OSeF_4$ is unstable, SeF_5OCl cannot be obtained in a manner analogous to that for SF_5OCl. However, chlorine monofluoride reacts readily with $Hg(OSeF_5)_2$ to form the thermally stable but easily hydrolyzed straw-yellow SeF_5OCl. It melts at −115°C and boils at 31.5°C. With H_2O, SeF_5OH and Cl_2O have been found. The IR and Raman spectra of SeF_5OCl have been assigned (*263*), and the ^{19}F-NMR spectrum has been reported (*262, 265*).

$$Hg(OSeF_5)_2 + ClF \xrightarrow{25°C} \underset{93\%}{SeF_5OCl} + HgF_2 \quad (265)$$

Although SeF_5OCl should be a useful precursor to new compounds that contain the SeF_5O group, little reaction chemistry has been reported. However, it has been demonstrated that compounds with iodine(I) and iodine(III) are possible but of low stability (*265*). Dibromomethane gives $CH_2(OSeF_5)_2$ with SeF_5OCl (*139*).

$$SeF_5OCl \begin{cases} + \; ICl \xrightarrow{CCl_3F} \underset{\text{brown}}{SeF_5OI} + Cl_2 \\ + \; ICl_3 \xrightarrow{CCl_3F} \underset{\text{orange–red}}{(SeF_5O)_3I} + 3Cl_2 \end{cases}$$

E. Pentafluorotellurium Hypochlorite (TeF_5OCl)

The essentially quantitative preparation of TeF_5OCl was realized via the reaction of chlorine monofluoride with $Hg(OTeF_5)_2$ at 25°C. The yellow liquid (mp −121°C; bp 38.1°C) is hydrolyzed easily to Cl_2O and TeF_5OH (*269*). The gas-phase IR and liquid Raman spectra of TeF_5OCl have been assigned (*263*), and the ^{19}F-NMR spectrum has been discussed (*262*).

The greater stability of hexavalent tellurium permits the formation of stable iodine derivatives. Also, the reaction of bromine with TeF_5OCl gives the stable, red TeF_5OBr (*264*).

$$ICl_3 + 3TeF_5OCl \rightarrow \underset{\text{orange}}{I(OTeF_5)_3} + 3Cl_2$$

$$I(OTeF_5)_3 + I_2 \leftarrow \underset{\text{brown}}{3IOTeF_5}$$

F. *cis*- and *trans*-Tetrafluorotellurium Bishypochlorite [$TeF_4(OCl)_2$]

A mixture of *cis*- and *trans*-$F_4Te(OH)_2$ is obtained when TeF_5OH and $Te(OH)_6$ are melted together. This mixture, when treated with ClF, gave the first bishypochlorites. When these bishypochlorites were treated with elemental bromine, the rather unstable red liquid *cis*- and *trans*-$TeF_4(OBr)_2$ formed (*268*).

yellow liquids

G. *cis*- and *trans*-Iodine(VII) Oxytetrafluoride Hypochlorite (OIF_4OCl)

Demonstrating the usefulness of FSO_2OCl as a source of positive chlorine, Christe and co-workers were able to synthesize the first iodine hypochlorite:

$$CsIF_4O_2 + FSO_2OCl \xrightarrow{-78°C} CsOSO_2F + OIF_4OCl \qquad (70).$$

Because of its high reactivity and thermal instability, this orange liquid was not well characterized. However, based largely on its gas-

phase IR spectrum (ν_{OCl} = 763 cm^{-1}), which is similar to that of the more stable OIF_4OF, with stretching modes shifted to slightly lower frequencies, its existence is likely. Attempts to isolate fluorocarbon derivatives of OIF_4OCl by addition to C_2F_4 at 25°C resulted in products such as COF_2, CF_3COF, $ClCF_2OF$, C_2F_5Cl, and IF_5.

VI. Applications

A detailed discussion of the applications of R_fOF as versatile and useful electrophilic fluorinating reagents or as general reagents for C-fluorinations under free-radical conditions is beyond the scope of this chapter. The interested reader is urged to peruse reviews of the subject (*18, 19, 130, 160*). However, what follows are notes on the specific applications of primarily CF_3OF and also $CF_2(OF)_2$, SF_5OF, FSO_2OF, CF_3CF_2OF, $CF_3C(O)OF$, and other R_fOF species.

Cady and Allison (*4*) first demonstrated that CF_3OF, under photolytic conditions, adds essentially quantitatively to $C_2H_4 \rightarrow CF_3OC_2H_4F$ and, with benzene in CCl_3F at −78°C, gives C_6H_5F (65%) and $C_6H_5OCF_3$ (10%). The first workers to use CF_3OF as a fluorinating reagent under non-free-radical conditions were Shreeve and Ratcliffe, who demonstrated that CF_3OF smoothly fluorinated CF_3SCl to CF_3SF_3 (95–100%) at −78°C (*220*). Others have used CF_3OF to fluorinate organic sulfides oxidatively, but the claimed fluorosulfuranes and fluoropersulfuranes have not been isolated (*81, 82*). Cyclic difluorophosphoranes result from the respective cyclic phosphines (*60, 78, 83*). Stable alkoxyaryltrifluoroperiodanes have been synthesized from 2,5-$CH_3IC_6H_3C(CF_3)_2OH$ or 2-$IC_6H_4C(CH_3)_2OH$ with CF_3OF (*5, 6*).

Action may occur at carbon, for example, CF_3OF reacts with activated olefins to convert 3-methoxycholest-2-ene to 2α-fluorocholestanone (*24*); at aromatic rings, 2,6-dimethylphenol → 6-fluoro-2,6-dimethyl-2,4-cyclohexadienone (*3, 23, 142, 207*); at unactivated and deactivated unsaturated linkages of steroids (*21, 22, 61*); with photolysis, c-$C_6H_{12} \rightarrow c$-$C_6H_{11}F$ (44%) (*161*); and with fluorination of a wide variety of organic compounds, for example, $CH_3C(O)OH \rightarrow FCH_2C(O)OH$ and 4-$(C_6H_5CH_2CH_2)C_6H_4C(CH_3)_2NH_2 \rightarrow$ 4-$(C_6H_5CF_2CF_2)C_6H_4C(CH_3)_2NH_2$ [with CF_3OF, SF_5OF, or CF_3CF_2OF in the presence of a free-radical-producing initiator (*158, 159*)]. $(CF_3)_3COF$, $(CF_3)_2C(OF)C_2F_5$, SF_5OF, $CF_2(OF)_2$, and CF_3OF act as electrophilic fluorinating reagents in solution in the absence of radical initiators (*34*). With CF_3OF, 5-fluorouracil is prepared directly from uracil (*133, 192, 227*); 5-fluorocytosine and its nucleosides directly from cytosine, cytidine, etc. (*224, 226*); griseofulvin to its 5-fluoro derivative (*33*). Photofluorination of diaryl-

sulfones, for example, $4\text{-}O_2NC_6H_4SO_2C_6H_4NHC(O)CH_3\text{-}4$ + $CF_3OF \xrightarrow{h\nu} 4\text{-}O_2NC_6H_4SO_2C_6H_3FNHC(O)CH_3\text{-}3,4$ [which, when hydrolyzed → $4\text{-}O_2NC_6H_4SO_2C_6H_3FNH_2\text{-}3,4$, which is useful as poultry feed additives for treatment and prophylaxis of Marek's disease (*143*)]. CF_3OF is used in synthesis of *N*-fluoroamines, for example, $p\text{-}RC_6H_4CH{=}NR' \rightarrow p\text{-}RC_6H_4CF_2NFR'$ and the intermediates $p\text{-}RC_6H_4CF{=}NR'$ (*170*) and direct preparation of 2′-amino-2′-deoxy-5-fluorouridine (*271*). Tetrahydropyrimidine-2,4-diones react to form 6-oxygenated 5-fluoropyrimidinediones (*20*), and fluorination of naphthalene and anthracene derivatives (*209*) occurs with CF_3OF. CF_3OF adds across double bonds in *cis—trans*-stilbenes (*28*). With CF_3OF, SF_5OF, and $CF_2(OF)_2$, secondary sulfonamides react to form *N*-fluoro derivatives (*26, 35, 131, 132*). Schiff bases with CF_3OF in alcohol media react to form *N,N*-difluoroamines (*30*). Fluorination may occur at saturated carbons, for example, with adamantanes and steroids (*27, 31, 32*). Antidepressant properties have been claimed for trifluoromethoxy azepines or azepinones (*25, 162*).

With CF_3OF the following transformations occur: methyl acetyl glycyrrhetate → monofluoroderivative (*236*); phenanthrenes → fluorinated K-region ketones (*210*); D-lactal hexaacetate → 2-deoxy-2-fluorolactose (*50, 151*); 2,3-benzofuran in methanol → fluorinated methoxy adduct (*29*). Reaction also occurs with diazoketones, for example, $C_6H_5C(O)CHN_2 \rightarrow C_6H_5C(O)CHF_2$ (14%) + $C_6H_5C(O)CHF(OCF_3)$ (10%) (*171, 310*); with 2-aminothiols and thiolamino acids in HF(l) → aminoalkyl fluorides and fluoroaminoacids, for example, D-penicillamine → D-3-fluorovaline (*163*).

5-Fluorouracil derivatives have been reportedly obtained from cytosine derivatives by using FSO_2OF in aqueous solution (?) (*284*). With CF_3OF, [*carboxy*-^{14}C]orotic acid is fluorinated to [*carboxy*-^{14}C]-5-fluoroorotic acid (*272*); 2′,3′,5′- tri-*O*-acetyluridine to 5-fluorouridine, (*225*), and 2′-deoxyuridine to 5-fluoro-2′-deoxyuridine (*77*). Substituted uracils are fluorinated to 5-fluorouracil derivatives (*96*), and with 1,1-diphenylethylene a mixture of $(C_6H_5)_2C(OCF_3)CH_2F$, $(C_6H_5)_2C(CH{=}C(C_6H_5)_2)CH_2F$, $(C_6H_5)_2CHCH_2F$, $(C_6H_5)_2C{=}CHF$, and $(C_6H_5)_2C(OCF_3)CHF_2$ is obtained (*208*). CF_3OF also reacts with a protected 2-*C*-cyano-2-deoxyglycal and a protected 3-amino-3-deoxyglucal to give 2-deoxy-2-fluoropyranose derivatives (*39*); a trichloromethiazide (6-chloro-3-dichloromethyl-7-sulfamoyl-3,4-dihydro-2*H*-1,2,4-benzo[*e*]thiadiazine 1,1-dioxide) to form a 5-fluoroderivative (*36*); N-non-

substituted aziridines to give 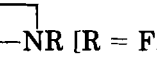 [R = F, C(O)F (*256, 257*)];

and N-substituted aziridines via ring opening and 1,3-addition of F on N and OCF_3 on C (*256*, *258*). α-Fluorocarbonyl compounds $R_2CFC(O)R'$ (R = H, alkyl, cycloalkyl, aryl, optionally substituted by halogen or alkoxy; R′ = H, alkyl, haloalkyl, cycloalkyl, silyl, OH, alkoxy, aryloxy, amino, and *S*-heterocycle; RR′ = diradical) result from conversion of carbonyl compounds $R_2CHC(O)R'$ to their silyl enol ethers, following by fluorination with CF_3OF (CCl_3F, −70°C) (*183*, *184*).

ACKNOWLEDGMENTS

We gratefully acknowledge the support of the National Science Foundation (CHE-8100156) and the donors to the Petroleum Research Fund, administered by the American Chemical Society. Gratitude is expressed to Barbara Crabtree and Margaret Kelnhofer for expert typing. Maryfrances Shreeve was particularly helpful in organizing the references.

REFERENCES

1. Abe, T., Nagase, S., Baba, H., and Kodaira, K., U.S. Patent 3,687,825 (1972); *Chem. Abstr.* **77**, 164024b (1972).
2. Agahigian, H., Gray, A. P., and Vickers, G. D., *Can. J. Chem.* **40**, 157 (1962).
3. Airey, J., Barton, D. H. R., Ganguly, A. K., Hesse, R. H., and Pechet, M. M., *An. Quim.* **70**, 871 (1974); *Chem. Abstr.* **83**, 163090g (1975).
4. Allison, J. A. C., and Cady, G. H., *J. Am. Chem. Soc.* **81**, 1089 (1959).
5. Amey, R. L., and Martin, J. C., *J. Am. Chem. Soc.* **100**, 300 (1978).
6. Amey, R. L., and Martin, J. C., *J. Am. Chem. Soc.* **101**, 5294 (1979).
7. Anderson, L. R., Young, D. E., Gould, D. E., Juurik-Hogan, R., Nuechterlein, D., and Fox, W. B., *J. Org. Chem.* **35**, 3730 (1970).
8. Anderson, L. R., and Fox, W. B., *Inorg. Chem.* **9**, 2182 (1970).
9. Appelman, E. H., *Acc. Chem. Res.* **6**, 113 (1973).
10. Appelman, E. H., Basile, L. J., and Thompson, R. C., *J. Am. Chem. Soc.* **101**, 3384 (1979).
11. Appelman, E. H., Bonnett, R., and Mateen, B., *Tetrahedron* **33**, 2119 (1977).
12. Appelman, E. H., and Kim, H., *J. Chem. Phys.* **58**, 3272 (1972).
13. Appelman, E. H., Thompson, R. C., and Engelkemeir, A. G., *Inorg. Chem.* **18**, 909 (1979).
14. Arhart, R. J., and Martin, J. C., *J. Am. Chem. Soc.* **94**, 4997 (1972).
15. Arvia, A. J., Cafferata, L. F. R., and Schumacher, H. J., *Chem. Ber.* **96**, 1187 (1963).
16. Aubke, F., and DesMarteau, D. D., *Fluorine Chem. Rev.* **8**, 73 (1977).
17. Aymonino, P. J., *J. Chem. Soc., Chem. Commun.* p. 241 (1965).
18. Barton, D. H. R., *Pure Appl. Chem.* **21**, 285 (1970).
19. Barton, D. H. R., *Pure Appl. Chem.* **49**, 1241 (1977).
20. Barton, D. H. R., Bubb, W. A., Hesse, R. H., and Pechet, M. M., *J. Chem. Soc., Perkin Trans. 1* p. 2095 (1974).
21. Barton, D. H. R., Danks, L. J., Ganguly, A. K., Hesse, R. H., Tarzia, G., and Pechet, M. M., *J. Chem. Soc., Chem. Commun.* p. 227 (1969).

22. Barton, D. H. R., Danks, L. J., Ganguly, A. K., Hesse, R. H., Tarzia, G., and Pechet, M. M., *J. Chem. Soc., Perkin Trans. 1* p. 101 (1976).
23. Barton, D. H. R., Ganguly, A. K., Hesse, R. H., Loo, S. N., and Pechet, M. M., *J. Chem. Soc., Chem. Commun.* p. 806 (1968).
24. Barton, D. H. R., Godinho, L. S., Hesse, R. H., and Pechet, M. M., *J. Chem. Soc., Chem. Commun.* p. 804 (1968).
25. Barton, D. H. R., and Hesse, R. H., *Ger. Offen.* **2,440,592** (1975); *Chem. Abstr.* **82,** 156138e (1975).
26. Barton, D. H. R., and Hesse, R. H., U.S. Patent 3,917,688 (1975); *Chem. Abstr.* **84,** 30714n (1976).
27. Barton, D. H. R., and Hesse, R. H., U.S. Patent 4,036,864 (1977); *Chem. Abstr.* **87,** 201887q (1977).
28. Barton, D. H. R., Hesse, R. H., Jackman, G. P., Ogunkoya, L., and Pechet, M. M., *J. Chem. Soc., Perkin Trans. 1* p. 739 (1974).
29. Barton, D. H. R., Hesse, R. H., Jackman, G. P., and Pechet, M. M., *J. Chem. Soc., Perkin Trans. 1* p. 2604 (1977).
30. Barton, D. H. R., Hesse, R. H., Klose, T. R., and Pechet, M. M., *J. Chem. Soc., Chem. Commun.* p. 97 (1975).
31. Barton, D. H. R., Hesse, R. H., Markwell, R. E., Pechet, M. M., and Rozen, S., *J. Am. Chem. Soc.* **98,** 3036 (1976).
32. Barton, D. H. R., Hesse, R. H., Markwell, R. E., Pechet, M. M., and Toh, H. T., *J. Am. Chem. Soc.* **98,** 3034 (1976).
33. Barton, D. H. R., Hesse, R. H., Ogunkoya, L., Westcott, N. D., and Pechet, M. M., *J. Chem. Soc., Perkin Trans. 1* p. 2889 (1972).
34. Barton, D. H. R., Hesse, R. H., Pechet, M. M., Tarzia, G., Toh, H. T., and Westcott, N. D., *J. Chem. Soc., Chem. Commun.* p. 122 (1972).
35. Barton, D. H. R., Hesse, R. H., Pechet, M. M., and Toh, H. T., *J. Chem. Soc., Perkin Trans. 1* p. 732 (1974).
36. Barton, D. H. R., Hesse, R. H., Pechet, M. M., and Toh, H. T., *J. Chem. Soc., Perkin Trans. 1* p. 712 (1980).
37. Berkowitz, J., Appelman, E. H., and Chupka, W. A., *J. Chem. Phys.* **58,** 1950 (1973).
38. Berkowitz, J., Dehmer, J. L., and Appelman, E. H., *Chem. Phys. Lett.* **19,** 334 (1973).
39. Bischofberger, K., Hall, R. H., Jordaan, A., and Woolard, G. R., *S. Afr. J. Chem.* **33,** 92 (1980); *Chem. Abstr.* **94,** 121825x (1981).
40. Blesa, M. A., and Aymonino, P. J., *Z. Phys. Chem.* **80,** 129 (1972).
41. Boate, A. R., Morton, J. R., and Preston, K. F., *Chem. Phys. Lett.* **54,** 579 (1978).
42. Bobkova, V. A., and Solomonik, V. G., *Zh. Prikl. Spektrosk.* **26,** 169 (1977); *Chem. Abstr.* **86,** 147927s (1977).
43. Bonnett, R., Ridge, R. J., and Appelman, E. J., *J. Chem. Soc., Chem. Commun.* p. 310 (1978).
44. Botschwina, P., *Chem. Phys.* **40,** 33 (1979).
45. Botschwina, P., Meyer, W., and Semkow, A. M., *Chem. Phys.* **15,** 25 (1976).
46. Bradley, D. C., Redwood, M. E., and Willis, C. J., *J. Chem. Soc., Proc.* p. 416 (1964).
47. Braendle, K., Schmeisser, M., and Luettke, W., *Chem. Ber.* **93,** 2300 (1960).
48. Bruna, P. J., and Sicre, J. E., *An. Asoc. Quim. Argent.* **59,** 205 (1971); *Chem. Abstr.* **76,** 63971g (1972).
49. Buckley, P., and Weber, J. P., *Can. J. Chem.* **52,** 942 (1974).
50. Butchard, C. G., and Kent, P. W., *Tetrahedron* **35,** 2551 (1979).

51. Cady, G. H., *J. Am. Chem. Soc.* **56,** 2635 (1934).
52. Cady, G. H., and Kellogg, K. B., *J. Am. Chem. Soc.* **75,** 2501 (1953).
53. Cady, G. H., *Int. Congr. Pure Appl. Chem., 17th, 1959.* Vol. 1, p. 205 (1960).
54. Cafferata, L. F. R., and Sicre, J. E., *Inorg. Chem.* **13,** 242 (1974).
55. Castro, E. A., and Jubert, A. H., *React. Kinet. Catal. Lett.* **9,** 53 (1978); *Chem. Abstr.* **90,** 44463r (1979).
56. Castro, E. A., and Jubert, A. H., *Rev. Roum. Chem.* **25,** 75 (1980); *Chem. Abstr.* **92,** 221601y (1980).
57. Cauble, R. L., and Cady, G. H., *J. Am. Chem. Soc.* **89,** 1962 (1967).
58. Cauble, R. L., and Cady, G. H., *J. Am. Chem. Soc.* **89,** 5161 (1967).
59. Chandrasekaran, S., U.S. Patent 3,684,786 (1972); *Chem. Abstr.* **77,** 140762q (1972).
60. Chang, L. L., Denney, D. Z., Denney, D. B., and Hsu, Y. F., *Phosphorus* **4,** 265 (1974).
61. Chavis, C., and Mousseron-Canet, M., *Bull. Soc. Chim. Fr.* p. 632 (1971).
62. Christe, K. O., *Z. Anorg. Allg. Chem.* **413,** 177 (1975).
63. Christe, K. O., and Pilipovich, D., *J. Am. Chem. Soc.* **93,** 51 (1971).
64. Christe, K. O., and Schack, C. J., U.S. Patent 4,216,338 (1980); *Chem. Abstr.* **93,** 204090j (1980).
65. Christe, K. O., Schack, C. J., and Curtis, E. C., *Spectrochim. Acta, Part A* **26,** 2367 (1970).
66. Christe, K. O., Schack, C. J., Pilipovich, D., Curtis, E. C., and Sawodny, W., *Inorg. Chem.* **12,** 620 (1973).
67. Christe, K. O., Schack, C. J., and Wilson, R. D., *Inorg. Chem.* **13,** 2811 (1974).
68. Christe, K. O., and Wilson, R. D., *Inorg. Nucl. Chem. Lett.* **15,** 375 (1979).
69. Christe, K. O., Wilson, R. D., and Schack, C. J., *Inorg. Chem.* **19,** 3046 (1980).
70. Christe, K. O., Wilson, R. D., and Schack, C. J., *Inorg. Chem.* **20,** 2104 (1981).
71. Christe, K. O., Wilson, W. W., and Wilson, R. D., *Inorg. Chem.* **19,** 1494 (1980).
72. Cobos, C. J., and Jubert, A. H., *React. Kinet. Catal. Lett.* **11,** 313 (1979).
73. Cox, A. P., and Riveros, J. M., *J. Chem. Phys.* **42,** 3106 (1965).
74. Czarnowski, J., Castellano, E., and Schumacher, H. J., *Chem. Commun.* p. 1255 (1968).
75. Czarnowski, J., and Schumacher, H. J., *Z. Phys. Chem.* **73,** 68 (1970).
76. Czarnowski, J., and Schumacher, H. J., *Z. Phys. Chem.* **78,** 234 (1972).
77. Dawson, W. H., and Dunlap, R. B., *J. Labelled Compd. Radiopharm.* **16,** 335 (1979).
78. De'Ath, N. J., Denney, D. B., Denney, D. Z., and Hsu, Y. F., *J. Am. Chem. Soc.* **98,** 768 (1976).
79. Del Bene, J. E., *J. Chem. Phys.* **57,** 1899 (1972).
80. De Marco, R. A., and Shreeve, J. M., *Adv. Inorg. Chem. Radiochem.* **16,** 109–176 (1974).
81. Denney, D. B., Denney, D. Z., and Hsu, Y. F., *J. Am. Chem. Soc.* **95,** 4064 (1973).
82. Denney, D. B., Denney, D. Z., and Hsu, Y. F., *J. Am. Chem. Soc.* **95,** 8191 (1973).
83. Denney, D. B., Denney, D. Z., and Hsu, Y. F., *Phosphorus* **4,** 213 (1974).
84. Deodati, F. P., and Bartell, L. S., *J. Mol. Struct.* **8,** 395 (1971).
85. DesMarteau, D. D., *Inorg. Chem.* **9,** 2179 (1970).
86. DesMarteau, D. D., *J. Am. Chem. Soc.* **100,** 340 (1978); Johri, K. K., and DesMarteau, D. D., *J. Org. Chem.* **46,** 5081 (1981).
87. DesMarteau, D. D., and Hammaker, R. M., *Isr. J. Chem.* **17,** 103 (1978).
88. Dicelio, L., and Schumacher, H. J., *An. Asoc. Quim. Argent.* **66,** 283 (1978).
89. Dicelio, L., and Schumacher, H. J., *Z. Phys. Chem.* **100,** 55 (1976).

90. Dicelio, L., and Schumacher, H. J., *J. Photochem.* **11,** 1 (1979).
91. Dixon, W. B., and Wilson, E. B., Jr., *J. Chem. Phys.* **35,** 191 (1961).
92. Dudley, F. B., *J. Chem. Soc.* p. 3407 (1963).
93. Dudley, F. B., Cady, G. H., and Eggers, D. F., *J. Am. Chem. Soc.* **78,** 290 (1956).
94. Dudley, F. B., Cady, G. H., and Eggers, D. F., Jr., *J. Am. Chem. Soc.* **78,** 1553 (1956).
95. Dudley, F. B., Shoolery, J. N., and Cady, G. H., *J. Am. Chem. Soc.* **78,** 568 (1956).
96. Ferrer Internacional S. A., Spanish Patent 458,886 (1978); *Chem. Abstr.* **89,** 197596r (1978).
97. Fichter, F., and Humpert, K., *Helv. Chim. Acta* **9,** 602 (1926).
98. Fokin, A. V., Gukov, A. M., Studnev, Yu. N., Komarov, V. A., and Uzun, A. T., *Izv. Akad. Nauk SSSR, Ser. Khim.* p. 422 (1977).
99. Fokin, A. V., Gukov, A. M., Studnev, Yu. N., Komarov, V. A., Krotovich, I. N., and Uzun, A. T., *Izv. Akad. Nauk SSSR, Ser. Khim.* p. 2221 (1977).
100. Fokin, A. V., Gukov, A. M., Studnev, Yu. N., Komarov, V. A., Krotovich, I. N., and Uzun, A. T., *Izv. Akad. Nauk SSSR, Ser. Khim.* p. 2222 (1977).
101. Fokin, A. V., Komarov, V. A., Uzun, A. T., Studnev, Yu. N., Gukov, A. M., and Shirokov, S. V., *Izv. Akad. Nauk SSSR, Ser. Khim.* p. 659 (1975).
102. Fokin, A. V., Nikolaeva, A. D., Studnev, Yu. N., Rapkin, A. N., Proshin, N. A., and Kuznetsova, L. D., *Izv. Akad. Nauk SSSR, Ser. Khim.* p. 915 (1975).
103. Fokin, A. V., Studnev, Yu. N., Krotovich, I. N., Furin, G. G., and Yakobson, G. G., *Izv. Akad. Nauk SSSR, Ser. Khim.* p. 927 (1981).
104. Fokin, A. V., Studnev, Yu. N., Krotovich, I. N., Kuznetsova, L. D., and Gukov, A. M., *Izv. Akad. Nauk SSSR, Ser. Khim.* p. 2388 (1977).
105. Fokin, A. V., Studnev, Yu. N., Krotovich, I. N., Kuznetsova, L. D., and Verenikin, O. V., *Izv. Akad. Nauk SSSR, Ser. Khim.* p. 748 (1979).
106. Fokin, A. V., Studnev, Yu. N., Kuznetsova, L. D., and Krotovich, I. N., *Izv. Akad. Nauk SSSR, Ser. Khim.* p. 559 (1978).
107. Fokin, A. V., Studnev, Yu. N., Kuznetsova, L. D., and Rud, V. L., *Izv. Akad. Nauk SSSR, Ser. Khim.* p. 441 (1974).
108. Fokin, A. V., Studnev, Yu. N., and Rapkin, A. I., *J. Fluorine Chem.* **18,** 553 (1981).
109. Fokin, A. V., Studnev, Yu. N., Rapkin, A. I., Krotovich, I. N., Kuznetsova, L. D., and Komarov, V. A., *Izv. Akad. Nauk SSSR, Ser. Khim.* p. 928 (1976).
110. Fokin, A. V., Studnev, Yu. N., Rapkin, A. I., and Kuznetsova, L. D., *Izv. Akad. Nauk SSSR, Ser. Khim.* p. 1817 (1974).
111. Fokin, A. V., Studnev, Yu. N., Rapkin, A. I., Kuznetsova, L. D., and Komarov, V. A., *Izv. Akad. Nauk SSSR, Ser. Khim.* p. 472 (1976).
112. Fokin, A. V., Studnev, Yu. N., Rapkin, A. I., Kuznetsova, L. D., Verenikin, O. V., and Krotovich, I. N., *Izv. Akad. Nauk SSSR, Ser. Khim.* p. 2259 (1976).
113. Fokin, A. V., Studnev, Yu. N., Rapkin, A. I., and Pasevina, K. I., *Izv. Akad. Nauk SSSR, Ser. Khim.* p. 2623 (1980).
114. Fokin, A. V., Studnev, Yu. N., Rapkin, A. I., Pasevina, K. I., Potarina, T. M., and Verenikin, O. V., *Izv. Akad. Nauk SSSR, Ser. Khim.* p. 2369 (1980).
115. Foss, G. D., and Pitt, D. A., *J. Phys. Chem.* **72,** 3512 (1968).
116. Gambaruto, M., Sicre, J. E., and Schumacher, H. J. *J. Fluorine Chem.* **5,** 175 (1975).
117. Gard, G. L., and Cady, G. H., *Inorg. Chem.* **4,** 594 (1965).
118. Gebert, E., Appelman, E. H., and Reis, A. H., Jr., *Inorg. Chem.* **18,** 2465 (1979).
119. Gilbreath, W. P., Ph.D. Thesis, University of Washington, Seattle (1962).
120. Gilbreath, W. P., and Cady, G. H., *Inorg. Chem.* **2,** 496 (1963).

121. Goleb, J. A., Claassen, H. H., Studier, M. H., and Appelman, E. H., *Spectrochim. Acta, Part A* **28,** 65 (1972).
122. Gombler, W., *Angew. Chem., Int. Ed. Engl.* **16,** 723 (1977).
123. Gould, D. E., Anderson, L. R., Fox, W. B., and Young, D. E., *Ger. Offen.* **1,928,539** (1969); *Chem. Abstr.* **72,** 54743z (1970).
124. Gould, D. E., Anderson, L. R., Young, D. E., and Fox, W. B., *J. Chem. Soc., Chem. Commun.* p. 1564 (1968).
125. Gould, D. E., Anderson, L. R., Young, D. E., and Fox, W. B., *J. Am. Chem. Soc.* **91,** 1310 (1969).
126. Ha, T.-K., *J. Mol. Struct.* **18,** 486 (1973).
127. Hale, W. H., Jr., and Williamson, S. M., *Inorg. Chem.* **4,** 1342 (1965); Shreeve, J. M., Duncan, L. C., and Cady, G. H., *ibid.* p. 1516.
128. Hammaker, R. M., Fateley, W. G., Manocha, A. S., DesMarteau, D. D., Streusand, B. J., and Durig, J. R., *J. Raman Spectrosc.* **9,** 181 (1980).
129. Hardin, C. V., Ratcliffe, C. T., Anderson, L. R., and Fox, W. B., *Inorg. Chem.* **9,** 1938 (1970).
130. Hesse, R. H., *Isr. J. Chem.* **17,** 60 (1978).
131. Hesse, R. H., and Barton, D. H. R., *Ger. Offen.* **2,332,430** (1974); *Chem. Abstr.* **80,** 108209r (1974).
132. Hesse, R. H., and Barton, D. H. R., *Ger. Offen.* **2,332,506** (1974); *Chem. Abstr.* **80,** 132210e (1974).
133. Hesse, R. H., Barton, D. H. R., Toh, H. T., and Pechet, M. M., *J. Org. Chem.* **37,** 329 (1972).
134. Hindman, J. C., Svirmickas, A., and Appelman, E. H., *J. Chem. Phys.* **57,** 4542 (1972).
135. Hoffman, C. J., *Chem. Rev.* **64,** 91 (1964).
136. Hohorst, F. A., and DesMarteau, D. D., *Inorg. Chem.* **13,** 715 (1974).
137. Hohorst, F. A., and Shreeve, J. M., *J. Am. Chem. Soc.* **89,** 1809 (1967).
138. Hohorst, F. A., and Shreeve, J. M., *Inorg. Chem.* **7,** 624 (1968).
139. Huppmann, P., Lentz, D., and Seppelt, K., *Z. Anorg. Allg. Chem.* **472,** 26 (1981).
140. Huston, J. L., and Studier, M. H., *J. Fluorine Chem.* **13,** 235 (1979).
141. Ip, D. P., Arthur, C. D., Winans, R. E., and Appelman, E. H., *J. Am. Chem. Soc.* **103,** 1964 (1981).
142. Ishikawa, N., and Kitazume, T., *Yuki Gosei Kagaku Kyokaishi* **34,** 173 (1976); *Chem. Abstr.* **85,** 32536a (1976).
143. Jensen, N. P., Kollonitsch, J., and Shen, T.-Y., U.S. Patent 3,775,444 (1973); *Chem. Abstr.* **80,** 36835s (1974).
144. Katsuhara, Y., and DesMarteau, D. D., *J. Am. Chem. Soc.* **101,** 1039 (1979).
145. Katsuhara, Y., and DesMarteau, D. D., *J. Fluorine Chem.* **16,** 257 (1980).
146. Katsuhara, Y., and DesMarteau, D. D., *J. Org. Chem.* **45,** 2441 (1980).
147. Katsuhara, Y., and DesMarteau, D. D., *J. Am. Chem. Soc.* **102,** 2681 (1980).
148. Katsuhara, Y., Hammaker, R. M., and DesMarteau, D. D., *Inorg. Chem.* **19,** 607, (1980).
149. Kennedy, R. C., and Cady, G. H., *J. Fluorine Chem.* **3,** 41 (1973–1974).
150. Kennedy, R. C., and Levy, J. B., *J. Phys. Chem.* **76,** 3480 (1972).
151. Kent, P. W., and Dimitrijevich, S. D., *J. Fluorine Chem.* **10,** 455 (1977).
152. Kim, H., Pearson, E. F., and Appelman, E. H., *J. Chem. Phys.* **56,** 1 (1972).
153. Kim, H., and Sabin, J. R., *Chem. Phys. Lett.* **20,** 215 (1973).
154. Kitazume, T., and Shreeve, J. M., *J. Am. Chem. Soc.* **99,** 4194 (1977).
155. Kitazume, T., and Shreeve, J. M., *Inorg. Chem.* **17,** 2173 (1978).

156. Kitazume, T., and Shreeve, J. M., *J. Am. Chem. Soc.* **100,** 492 (1978) (SF_4 + CF_3OF → $SF_4(OCF_3)_2$ (8%); Duncan, L. C., and Cady, G. H., *Inorg. Chem.* **3,** 850 (1964)).
157. Kloeter, G., and Seppelt, K., *J. Am. Chem. Soc.* **101,** 347 (1979).
158. Kollonitsch, J., *Ger. Offen.* **2,136,008** (1972); *Chem. Abstr.* **76,** 154488w (1972).
159. Kollonitsch, J., U.S. Patent 4,030,994 (1977); *Chem. Abstr.* **87,** 83904t (1977).
160. Kollonitsch, J., *Isr. J. Chem.* **17,** 53 (1978).
161. Kollonitsch, J., Barash, L., and Doldouras, G. A., *J. Am. Chem. Soc.* **92,** 7494 (1970).
162. Kollonitsch, J., and Doldouras, G. A., U.S. Patent 3,859,276 (1975); *Chem. Abstr.* **82,** 140199q (1975).
163. Kollonitsch, J., Marburg, S., and Perkins, L. M., *J. Org. Chem.* **41,** 3107 (1976).
164. Kolta, G. A., Webb, G., and Winfield, J. M., *J. Fluorine Chem.* **14,** 331 (1979).
165. Kroon, J. L., U.S. Patent 3,394,163 (1968); *Chem. Abstr.* **69,** 76606x (1968).
166. Kuo, J. C., DesMarteau, D. D., Fateley, W. G., Hammaker, R. M., Marsden, C. J., and Witt, J. D., *J. Raman Spectrosc.* **9,** 230 (1980).
167. Kuta, G. S., and Noftle, R. E., *Int. J. Sulfur Chem.* **8,** 335 (1973).
168. Langemann, R. T., Jones, E. A., and Woltz, P. J. H., *J. Chem. Phys.* **20,** 1768 (1952).
169. Lawless, E. W., and Smith, I. C., "Inorganic High-Energy Oxidizers," pp. 164–165. Dekker, New York, 1968; Lawless, E. W., and Rowatt, R. J., *Prepr. Pap.—Am. Chem. Soc., Div. Fuel Chem.* **12,** 108 (1968).
170. Leroy, J., Dudragne, F., Adenis, J. C., and Michaud, C., *Tetrahedron Lett.* p. 2771 (1973).
171. Leroy, J., and Wakselman, C., *J. Chem. Soc., Perkin Trans. 1* p. 1224 (1978).
172. Lopez, M. I., Castellano, E., and Schumacher, H. J., *J. Photochem.* **3,** 97 (1974).
173. Lustig, M., Pitochelli, A. R., and Ruff, J. K., *J. Am. Chem. Soc.* **89,** 2841 (1967).
174. Lustig, M., and Ruff, J. K., *J. Chem. Soc., Chem. Commun.* p. 870 (1967).
175. Lustig, M., and Shreeve, J. M., *Adv. Fluorine Chem.* **7,** 175–198 (1973).
176. Macheteau, Y., and Gillardeau, J., *Bull. Soc. Chim. Fr.* p. 1819 (1969).
177. Majid, A., and Shreeve, J. M., *Inorg. Chem.* **13,** 2710 (1974).
178. Martin, J. C., and Arhart, R. J., *J. Am. Chem. Soc.* **93,** 2339 (1971).
179. Martin, J. C., and Arhart, R. J., *J. Am. Chem. Soc.* **93,** 2341 (1971).
180. Maya, W., Schack, C. J., Wilson, R. D., and Muirhead, J. S., *Tetrahedron Lett.* p. 3247 (1969).
181. Menachem, Y., and Rozen, S., *J. Chem. Soc., Chem. Commun.* p. 479 (1979).
182. Merrill, C. I., and Cady, G. H., *J. Am. Chem. Soc.* **83,** 298 (1961).
183. Middleton, W. J., U.S. Patent 4,215,044 (1980); *Chem. Abstr.* **93,** 220474t (1980).
184. Middleton, W. J., and Bingham, E. M., *J. Am. Chem. Soc.* **102,** 4845 (1980).
185. Migliorese, K. G., Appelman, E. H., and Tsangaris, M. N., *J. Org. Chem.* **44,** 1711 (1979).
186. Miller, R. H., Bernitt, D. L., and Hisatsume, I. C., *Spectrochim. Acta, Part A* **23,** 223 (1967).
187. Mir, Q.-C., Babb, D. P., and Shreeve, J. M., *J. Am. Chem. Soc.* **101,** 3961 (1979).
188. Mir, Q.-C., Laurence, K. A., Shreeve, R. W., Babb, D. P., and Shreeve, J. M., *J. Am. Chem. Soc.* **101,** 5949 (1979).
189. Mir, Q.-C., Shreeve, R. W., and Shreeve, J. M., *Phosphorus Sulfur* **8,** 331 (1980).
190. Mitchell, R. W., and Merritt, J. A., *J. Mol. Spectrosc.* **24,** 128 (1967).
191. Mitra, G., and Cady, G. H., *J. Am. Chem. Soc.* **81,** 2646 (1959).
192. Miyashita, O., Matsumura, K., Shimazu, H., and Hashimoto, N., Jpn. Kokai 77 118,480 (1977); *Chem. Abstr.* **88,** 105397e (1978).

193. Moldavskii, D. D., Temchenko, V. G., and Antipenko, G. L., *J. Org. Chem. USSR (Engl. Transl.)* **7,** 44 (1971).
194. Moldavskii, D. D., Temchenko, V. G., Slesareva, V. I., and Antipenko, G. L., *J. Org. Chem. USSR (Engl. Transl.)* **9,** 694 (1973).
195. Morse, S. D., Laurence, K. A., Sprenger, G. H., and Shreeve, J. M., *J. Fluorine Chem.* **11,** 327 (1978).
196. Morton, J. R., and Preston, K. F., *Chem. Phys. Lett.* **18,** 98 (1973).
197. Morton, J. R., and Preston, K. F., *J. Chem. Phys.* **58,** 3112 (1973).
198. Morton, J. R., and Preston, K. F., *J. Chem. Phys.* **58,** 2657 (1973).
199. Morton, J. R., and Preston, K. F., *J. Phys. Chem.* **77,** 2645 (1973).
200. Mukhametshin, F. M., *Usp. Khim.* **49,** 1260 (1980); *Chem. Abstr.* **93,** 203434m (1980).
201. Murrell, J. N., Carter, S., Mills, I. M., and Guest, M. F., *Mol. Phys.* **37,** 1199 (1979).
202. Namasivayam, R., and Mayilavelan, S., *Z. Naturforsch. A* **34,** 716 (1979).
203. Neirinckx, R. D., Lambrecht, R. M., and Wolf, A. P., *Int. J. Appl. Radiat. Isot.* **29,** 323 (1978).
204. Noble, P. N., and Pimental, G. C., *Spectrochim. Acta, Part A* **24,** 797 (1968).
205. Ogilvie, J. F., *Can. J. Spectrosc.* **19,** 171 (1974).
206. Olsen, J. F., *J. Fluorine Chem.* **9,** 471 (1977).
207. Patrick, T. B., Cantrell, G. L., and Chang, C.-Y., *J. Am. Chem. Soc.* **101,** 7434 (1979).
208. Patrick, T. B., Cantrell, G. L., and Inga, S. M., *J. Org. Chem.* **45,** 1409 (1980).
209. Patrick, T. B., and Hayward, E. C., *J. Org. Chem.* **39,** 2120 (1974).
210. Patrick, T. B., LeFaivre, M. H., and Koertge, T. E., *J. Org. Chem.* **41,** 3413 (1976).
211. Paul, I. C., Martin, J. C., and Perozzi, E. F., *J. Am. Chem. Soc.* **93,** 6674 (1971).
212. Pauling, L., and Brockway, L. O., *J. Am. Chem. Soc.* **59,** 13 (1937).
213. Peterman, K. E., and Shreeve, J. M., *Inorg. Chem.* **13,** 2705 (1974).
214. Pilipovich, D., Goldberg, I. B., and Wagner, R. I., U.S. Patent 4,102,950 (1978); *Chem. Abstr.* **90,** 25547e (1979).
215. Pilipovich, D., and Warner, M. G., U.S. Patent 3,663,588 (1972); *Chem. Abstr.* **77,** 100747g (1972).
216. Place, R. D., and Williamson, S. M., *J. Am. Chem. Soc.* **90,** 2550 (1968).
217. Prager, J. H., *J. Org. Chem.* **31,** 392 (1966).
218. Prager, J. H., and Thompson, P. G., *J. Am. Chem. Soc.* **87,** 230 (1965).
219. Qureshi, A. M., Levchuk, L. E., and Aubke, F., *Can. J. Chem.* **49,** 2544 (1971).
220. Ratcliffe, C. T., and Shreeve, J. M., *J. Am. Chem. Soc.* **90,** 5403 (1968).
221. Redwood, M. E., and Willis, C. J., *Can. J. Chem.* **43,** 1893 (1965).
222. Redwood, M. E., and Willis, C. J., *Can. J. Chem.* **45,** 389 (1967).
223. Rewick, R. T., Anderson, R., and MacLaren, R. O., *J. Chem. Eng. Data* **17,** 409 (1972).
224. Robins, M. J., MacCoss, M., Naik, S. R., and Ramani, G., *J. Am. Chem. Soc.* **98,** 7381 (1976).
225. Robins, M. J., MacCoss, M., and Naik, S. R., *Nucleic Acid Chem.* **2,** 895 (1978).
226. Robins, M. J., and Naik, S. R., *J. Chem. Soc., Chem. Commun.* p. 18 (1972).
227. Robins, M. J., Ramani, G., and MacCoss, M., *Can. J. Chem.* **53,** 1302 (1975).
228. Rock, S. L., Pearson, E. F., Appelman, E. H., Norris, C. L., and Flygare, W. H., *J. Chem. Phys.* **59,** 3940 (1973).
229. Rohrback, G. H., and Cady, G. H., *J. Am. Chem. Soc.* **69,** 677 (1947).
230. Rozen, S., and Lerman, O., *J. Am. Chem. Soc.* **101,** 2782 (1979).

231. Rozen, S., and Lerman, O., *J. Org. Chem.* **45,** 672 (1980).
232. Rozen, S., and Lerman, O., *J. Org. Chem.* **45,** 4122 (1980).
233. Rozen, S., Lerman, O., and Kol, M., *J. Chem. Soc., Chem. Commun.* p. 443 (1981).
234. Rozen, S., and Menahem, Y., *Tetrahedron Lett.* p. 725 (1979).
235. Rozen, S., and Menahem, Y., *J. Fluorine Chem.* **16,** 19 (1980).
236. Rozen, S., Shahak, I., and Bergmann, E. D., *J. Org. Chem.* **40,** 2966 (1975).
237. Ruff, J. K., and Lustig, M., *Inorg. Chem.* **3,** 1422 (1964); Ruff, J. K., *Inorg. Synth.* **11,** 131 (1968).
238. Ruff, J. K., Pitochelli, A. R., and Lustig, M., *J. Am. Chem. Soc.* **88,** 4531 (1966).
239. Ruff, O., and Kwasnik, W., *Angew. Chem.* **48,** 238 (1935).
240. Sanyal, N. K., Gangull, A. K., and Dixit, L., *Curr. Sci.* **43,** 240 (1974); *Chem. Abstr.* **81,** 7837j (1974).
241. Schack, C. J., and Christe, K. O., *Inorg. Chem.* **13,** 2378 (1974).
242. Schack, C. J., and Christe, K. O., *J. Fluorine Chem.* **12,** 325 (1978).
243. Schack, C. J., and Christe, K. O., *Inorg. Nucl. Chem. Lett.* **14,** 293 (1978).
244. Schack, C. J., and Christe, K. O., *Isr. J. Chem.* **17,** 20 (1978).
245. Schack, C. J., and Christe, K. O., *J. Fluorine Chem.* **14,** 519 (1979).
246. Schack, C. J., and Christe, K. O., *Inorg. Chem.* **18,** 2619 (1979).
247. Schack, C. J., and Christe, K. O., U.S. Patent 4,222,968 (1980); *Chem. Abstr.* **94,** 65096w (1981).
248. Schack, C. J., and Christe, K. O., *J. Fluorine Chem.* **16,** 63 (1980).
249. Schack, C. J., and Maya, W., *J. Am. Chem. Soc.* **91,** 2902 (1969).
250. Schack, C. J., and Pilipovich, D., *Inorg. Chem.* **9,** 1387 (1970).
251. Schack, C. J., Pilipovich, D., and Hon, J. F., *Inorg. Chem.* **12,** 897 (1973).
252. Schack, C. J., and Wilson, R. D., *Inorg. Chem.* **9,** 311 (1970).
253. Schack, C. J., Wilson, R. D., and Hon, J. F., *Inorg. Chem.* **11,** 208 (1972).
254. Schack, C. J., Wilson, R. D., Muirhead, J. S., and Cohz, S. N., *J. Am. Chem. Soc.* **91,** 2907 (1969).
255. Schomburg, D., Mir, Q.-C., and Shreeve, J. M., *J. Am. Chem. Soc.* **103,** 406 (1981).
256. Seguin, M., Adenis, J. C., and Michaud, C., *J. Fluorine Chem.* **16,** 506 (1980).
257. Seguin, M., Adenis, J. C., Michaud, C., and Basselier, J. J., *J. Fluorine Chem.* **15,** 37 (1980).
258. Seguin, M., Adenis, J. C., Michaud, C., and Basselier, J. J., *J. Fluorine Chem.* **15,** 201 (1980).
259. Sekiya, A., and DesMarteau, D. D., *Inorg. Nucl. Chem. Lett.* **15,** 203 (1979).
260. Sekiya, A., and DesMarteau, D. D., *Inorg. Chem.* **19,** 1328 (1980).
261. Seppelt, K., *Chem. Ber.* **105,** 2431 (1972).
262. Seppelt, K., *Z. Anorg. Allg. Chem.* **399,** 65 (1973).
263. Seppelt, K., *Z. Anorg. Allg. Chem.* **399,** 87 (1973).
264. Seppelt, K., *Chem. Ber.* **106,** 1920 (1973).
265. Seppelt, K., *Chem. Ber.* **106,** 157 (1973).
266. Seppelt, K., *Angew. Chem., Int. Ed. Engl.* **16,** 44 (1976).
267. Seppelt, K., *Angew. Chem., Int. Ed. Engl.* **16,** 322 (1977).
268. Seppelt, K., Klöter, G., Potter, B., Lentz, D., and Pritzkow, H., *J. Fluorine Chem.* **16,** 587 (1980).
269. Seppelt, K., and Nothe, D., *Inorg. Chem.* **12,** 2727 (1973).
270. Shamir, J., Yellin, D., and Claassen, H. H., *Isr. J. Chem.* **12,** 1015 (1974).
271. Sharma, R. A., Bohek, M., and Bloch, A., *J. Med. Chem.* **17,** 466 (1974).
272. Silverman, R. B., and Kapili, L. V., *J. Labelled Compd. Radiopharm.* **16,** 361 (1979).

273. Singh, H. S., Pandey, A. N., Singh, B. P., and Sanyal, N. K., *Indian J. Pure Appl. Phys.* **11**, 17 (1973); *Chem. Abstr.* **79**, 59416z (1973).
274. Smardzewski, R. R., and Fox, W. B., *J. Phys. Chem.* **79**, 219 (1975).
275. Smardzewski, R. R., and Fox, W. B., *J. Fluorine Chem.* **6**, 417 (1976).
276. Smith, J. E., and Cady, G. H., *Inorg. Chem.* **9**, 1293 (1970).
277. Smith, J. E., and Cady, G. H., *Inorg. Chem.* **9**, 1442 (1970).
278. Smith, W. C., and Engelhardt, V. A., *J. Am. Chem. Soc.* **82**, 3838 (1960).
279. Sprenger, G. H., Wright, K. J., and Shreeve, J. M., *Inorg. Chem.* **12**, 2890 (1973).
280. Stavber, S., and Zupan, M., *J. Chem. Soc., Chem. Commun.* pp. 148, 795 (1981).
281. Stavber, S., and Zupan, M., *J. Fluorine Chem.* **17**, 597 (1981).
282. Steele, W. V., O'Hare, P. A. G., and Appelman, E. H., *Inorg. Chem.* **20**, 1022 (1981).
283. Studier, M. H., and Appelman, E. H., *J. Am. Chem. Soc.* **93**, 2349 (1971).
284. Suzuki, N., Wakabayashi, M., Sowa, T., Misaki, S., and Ishii, S., Jpn. Kokai 77 108,990 (1977); *Chem. Abstr.* **88**, 121665w (1978).
285. Talbott, R. L., U.S. Patent 3,541,128 (1970); *Chem. Abstr.* **74**, 31548s (1971).
286. Talbott, R. L., U.S. Patent 3,585,218 (1971); *Chem. Abstr.* **75**, 76161x (1971).
287. Tari, I., and DesMarteau, D. D., *Inorg. Chem.* **18**, 3205 (1979).
288. Tari, I., and DesMarteau, D. D., *J. Org. Chem.* **45**, 1214 (1980).
289. Teitelboim, M. A., Shoikhet, A. A., Kaplunov, M. G., and Vedeneev, V. I., *Kinet. Katal.* **22**, 298, 564, 852 (1981); *Chem. Abstr.* **95**, 96532k, 68722d, 186330x (1981).
290. Titov, Yu. A., Reshetova, I. G., and Akhrem, A. A., *Reakts. Metody Issled. Org. Soedin.* **15**, 7 (1966); *Chem. Abstr.* **66**, 28115c (1967).
291. Thompson, P. G., and Prager, J. H., *J. Am. Chem. Soc.* **89**, 2263 (1967).
292. Thompson, R. C., and Appelman, E. H., *Inorg. Chem.* **20**, 2114 (1981).
293. Thompson, R. C., and Appelman, E. H., *Inorg. Chem.* **19**, 3248 (1980).
294. Thompson, R. C., Appelman, E. H., and Sullivan, J. C., *Inorg. Chem.* **16**, 2921 (1977).
295. Toy, M. S., and Stringham, R. S., *J. Fluorine Chem.* **5**, 25 (1975).
296. Toy, M. S., and Stringham, R. S., *J. Fluorine Chem.* **5**, 31 (1975).
297. Toy, M. S., and Stringham, R. S., *J. Fluorine Chem.* **5**, 481 (1975).
298. Toy, M. S., and Stringham, R. S., *J. Fluorine Chem.* **13**, 23 (1979).
299. Toy, M. S., and Stringham, R. S., *J. Polym. Sci., Polym. Chem. Ed.* **16**, 2781 (1978); *Polym. Prepr., Am. Chem. Soc., Div. Polym. Chem.* **19**, 534 (1978).
300. Toy, M. S., and Stringham, R. S., *J. Org. Chem.* **44**, 2813 (1979).
301. Toy, M. S., and Stringham, R. S., *J. Polym. Sci., Polym. Lett. Ed.* **17**, 561 (1979).
302. Toy, M. S., and Stringham, R. S., *J. Polym. Sci., Polym. Lett. Ed.* **18**, 229 (1980).
303. VanMeter, W. P., and Cady, G. H., *J. Am. Chem. Soc.* **82**, 6005 (1960).
304. Vasini, E., and Schumacher, H. J., *Z. Phys. Chem. (Wiesbaden)* [N.S.] **94**, 39 (1975).
305. Vasini, E., and Schumacher, H. J., *Z. Phys. Chem. (Wiesbaden)* [N.S.] **104**, 219 (1977).
306. Velazco, J. E., and Setser, D. W., *J. Chem. Phys.* **62**, 1990 (1975).
307. Viscido, L., Sicre, J. E., and Schumacher, H. J., *Z. Phys. Chem. (Wiesbaden)* [N.S.] **32**, 182 (1962).
308. von Ellenrieder, G., Castellano, E., and Schumacher, H. J., *Z. Phys. Chem. (Wiesbaden)* [N.S.] **57**, 19 (1968).
309. Wahi, P. K., and Patel, N. O., *Can. J. Spectrosc.* **25**, 70 (1980).
310. Wakselman, C., and Leroy, J., *J. Chem. Soc., Chem. Commun.* p. 611 (1976).
311. Wechsberg, M., and Cady, G. H., *J. Am. Chem. Soc.* **91**, 4432 (1969).
312. Williamson, S. M., *in* "Preparative Inorganic Reactions" (W. L. Jolly, ed.), Vol. 1, p. 239. Wiley (Interscience), New York, 1964.

313. Wilson, W. W., Winfield, J. M., and Aubke, F., *J. Fluorine Chem.* **7,** 245 (1976).
314. Wilt, P. M., and Jones, E. A., *J. Inorg. Nucl. Chem.* **29,** 2108 (1967); **30,** 2933 (1968).
315. Winfield, J. M., *J. Fluorine Chem.* **16,** 1 (1980), and references therein.
316. Yost, D. M., and Beerbower, A., *J. Am. Chem. Soc.* **57,** 782 (1935).
317. Young, D. E., Anderson, L. R., and Fox, W. B., *Inorg. Nucl. Chem. Lett.* **6,** 341 (1970).
318. Young, D. E., Anderson, L. R., and Fox, W. B., *Inorg. Chem.* **9,** 2602 (1970).
319. Young, D. E., Anderson, L. R., and Fox, W. B., *Inorg. Chem.* **10,** 2810 (1971).
320. Young, D. E., Anderson, L. R., and Fox, W. B., U.S. Patent 3,681,423 (1972); *Chem. Abstr.* **77,** 151465v (1972).
321. Young, D. E., Anderson, L. R., and Fox, W. B., U.S. Patent 3,654,335 (1972); *Chem. Abstr.* **77,** 4893f (1972).
322. Young, D. E., Anderson, L. R., Gould, D. E., and Fox, W. B., *Tetrahedron Lett.* p. 723 (1969).
323. Young, D. E., Anderson, L. R., Gould, D. E., and Fox, W. B., U.S. Patent 3,732,274 (1973); *Chem. Abstr.* **79,** 31510b (1973).
324. Young, D. E., Anderson, L. R., Gould, D. E., and Fox, W. B., *J. Am. Chem. Soc.* **92,** 2313 (1970).
325. Young, D. E., and Fox, W. B., *Inorg. Nucl. Chem. Lett.* **7,** 1033 (1971).
326. Young, D. E., Gould, D. E., Anderson, L. R., and Fox, W. B., U.S. Patent 3,627,799 (1971); *Chem. Abstr.* **76,** 58966e (1972).
327. Yu, S.-L., and DesMarteau, D. D., *Inorg. Chem.* **17,** 2484 (1978).
328. Zaucer, M., Pumpernik, D., Hladnik, M., and Azman, A., *Z. Naturforsch. A* **31A,** 1727 (1976).

ADVANCES IN INORGANIC CHEMISTRY AND RADIOCHEMISTRY, VOL. 26

THE CHEMISTRY OF THE HALOGEN AZIDES

K. DEHNICKE

Fachbereich Chemie der Universität Marburg, Marburg, Federal Republic of Germany

I. Introduction

Although more than 80 yr have passed since the discovery of iodine azide by A. Hantzsch and M. Schümann (*59*), and the other halogen azides have been known for a long time [chlorine azide: 1908 by F. Raschig (*115*); bromine azide: 1925 by D. A. Spencer (*126*); fluorine azide: 1942 by J. F. Haller (*58*)], it is only in recent years that these azides have found use in preparative chemistry. Increasing knowledge of the properties has brought about a better understanding of the reaction pathways and improvement in the synthesis of the halogen azides and has facilitated their application in synthetic chemistry. In the field of organic chemistry, the work of A. Hassner *et al.* has shown the importance of iodine azide and bromine azide in olefinic addition, as the reaction products undergo numerous subsequent reactions. These topics were reviewed in 1971 (*76*). In inorganic chemistry, chlorine azide and iodine azide are predominant. The preferred type of reaction is the substitution of a halide ligand or an organic group by the azide

Copyright © 1983 by Academic Press, Inc.
All rights of reproduction in any form reserved.
ISBN 0-12-023626-5

group; however, oxidative additions and, for iodine azide, donor–acceptor complexes are also known. A summary of the properties of halogen azides was published in 1967 (*20*), followed in 1979 by a review of the development of iodine azide chemistry (*21*).

II. Preparation and Modes of Formation

A. Fluorine Azide

Fluorine azide is best prepared from dry hydrazoic acid and fluorine in the gas phase (*2, 58*).

$$4HN_3 + 2F_2 \rightarrow 3FN_3 + N_2 + NH_4F$$

Decomposition reactions of the fluorine azide are avoided when the reactants are diluted with N_2 (*54*). [FN_3 is also formed as an intermediate product in the synthesis of N_2F_2 from fluorine and solid sodium azide, moistened with traces of water (*119*) and diluted with CaF_2 to avoid local rise in temperature (*111*).] At 35 to 45°C the reaction mixture yields N_2F_2, NF_3, and N_2, as well as FN_3 (*110*). For papers reviewing N—F compounds see (*17, 109*).

B. Chlorine Azide

According to F. Raschig (*115*), chlorine azide is formed upon acidification of aqueous solutions of alkali hypochlorite and sodium azide with boric acid or acetic acid.

$$N_3^- + ClO^- + 2H^+ \rightarrow ClN_3 + H_2O$$

Because in this reaction chlorine azide is produced in high concentrations locally, explosions can occur. Later, Frierson *et al.* (*52*) obtained ether solutions of ClN_3 by passing gaseous chlorine through a suspension of silver azide in ether. For preparative purposes, the most convenient method is the reaction of chlorine gas, diluted with nitrogen, with an aqueous solution of sodium azide (*22*).

$$N_3^- + Cl_2 \xrightarrow[H_2O]{0°C} ClN_3 + Cl^-$$

After being dried with phosphorus pentoxide, the resulting chlorine azide can be used directly for further reactions (*8*). The process re-

quires careful avoidance of pressure variations, as otherwise explosions are inevitable (*8*).

Apart from NF_2Cl, chlorine azide is also formed in the reaction of fluorine with a mixture of sodium chloride and sodium azide (*1*). Possibly ClN_3 exists in aqueous solutions of $NaN_3/FeCl_3/H_2O_2$, which are applied in radical addition of Cl· and N_3· to olefinic double bonds (*81*); (see Section IV,A). The complex C_6H_5—I(Cl)N_3, accessible by a reaction of $C_6H_5I(OAc)_2$ with trimethylsilyl azide and acetyl chloride in several steps, can be interpreted as an adduct of chlorine azide, which however decomposes, even at 0°C. It is also used for the addition of ClN_3 to olefinic double bonds (*141*) (see Section IV, A).

C. Bromine Azide

Bromine azide was first prepared by D. A. Spencer (*126*), by passing a stream of bromine diluted with nitrogen over dry sodium azide. It is obtained as an orange-red and very explosive fluid.

$$NaN_3 + Br_2(g) \rightarrow NaBr + BrN_3$$

Even today this is the best method of preparing pure bromine azide; however, the slow reaction rate necessitates a long zone of contact. Caution is necessary, as violent explosions are apt to occur wherever liquid bromine comes into contact with powdered sodium azide (*37*)!

Solutions of bromine azide in hexane, carbon tetrachloride, and other inert solvents are obtained from silver azide and bromine when the suspension contains some dry sodium sulfate, to avoid decomposition of the BrN_3 by traces of water (*37*). For preparative purposes, solutions of bromine azide in dichloromethane or pentane can be prepared by addition of bromine to an agitated two-phase system held at 0°C, the aqueous phase of which consists of sodium azide and 30% HCl (*60*). It can be assumed that the hydrazoic acid formed here primarily is brominated.

$$HN_3 + Br_2 \rightarrow BrN_3 + HBr$$

D. Iodine Azide

Iodine azide has been known since 1900, from a paper by A. Hantzsch and M. Schümann (*59*), who obtained IN_3 in an ether suspension of silver azide with iodine.

$$AgN_3 + I_2 \rightarrow AgI + IN_3$$

The ether solutions are very unstable, especially when they contain traces of water. Higher stability is achieved by dry solutions of iodine azide in carbon tetrachloride, dichloromethane, benzene, and similar solvents. They are prepared from an excess of moist silver azide, which can be handled without risk, and iodine, in the presence of a drying agent like sodium sulfate (*23*). Evaporation of solutions in solvents with high vapor pressure, like CH_2Cl_2 and $CFCl_3$, yields pure iodine azide as golden, sublimable crystals (*21, 23*). For many preparative purposes it is convenient to use solutions in acetonitrile and other polar solvents, like pyridine or dimethylformamide; these are produced by heterogenous reaction of suspensions of NaN_3 with iodine chloride (*76*).

$$NaN_3 + ICl \xrightarrow{CH_3CN} NaCl + IN_3$$

III. Properties

A. Handling of the Halogen Azides and Chemical Properties

The gaseous halogen azides are very hazardous to handle—it is advisable to dilute them with an inert gas. Explosions can occur upon sudden variations of pressure (*20*). Appropriate use of gaseous chlorine azide in preparative operations has been described by Brauer (*8*). Especially dangerous are the pure halogen azides in the condensed phases. Thus fluorine azide inevitably explodes on attempting to evaporate the condensate (*58*), whereas the controlled thermal cleavage in the diluted gas phase results in N_2F_2 (*58, 110, 111, 119*).

$$2FN_3 \rightarrow N_2F_2 + 2N_2$$

On the other hand, dilute solutions of bromine azide and iodine azide in dichloromethane, hexane, and other nonpolar solvents can be handled safely and used for preparative purposes (*23, 37, 60*); the same is true for solutions of iodine azide in acetonitrile (*76*). Only in water does chlorine azide dissolve without decomposition, whereas bromine azide and iodine azide slowly dissociate to the elements. Anhydrous solutions in nonpolar solvents are more stable; for example, iodine azide solutions can be kept in the dark at 0°C for several days. Pentane slowly reacts with chlorine azide, undergoing substitution (*52*).

$$C_5H_{12} + ClN_3 \rightarrow C_5H_{11}Cl + HN_3$$

Contact with strong reducing agents like sodium, zinc, magnesium, or white phosphorus causes violent explosions (*52, 59, 126*).

In an aqueous, alkaline medium the halogen azides are hydrolyzed, forming hypochlorite (*59, 115*).

$$XN_3 + 2OH^- \rightarrow XO^- + N_3^- + H_2O$$
$$X = Cl, Br, I$$

The reaction with arsenite is suitable for titrimetric analysis (*57*).

$$XN_3 + AsO_3^{3-} + 2OH^- \rightarrow N_3^- + X^- + AsO_4^{3-} + H_2O$$

Because the redox potential of iodine azide is similar to that of iodine, an iodometric titration is equally possible (*21*).

$$IN_3 + 2S_2O_3^{2-} \rightarrow I^- + N_3^- + S_4O_6^{2-}$$

Therefore, iodine azide can be used as a mild oxidizing agent for the formation of S—S bonds (*12*).

$$2Na[4\text{-}NO_2C_6H_4S] + IN_3 \rightarrow (4\text{-}NO_2C_6H_4)_2S_2 + NaI + NaN_3$$

The toxicity of the halogen azides has not yet been investigated, but it can be supposed that they are at least as toxic as the halogens and hydrazoic acid, respectively. Chlorine azide smells somewhat like dichlorine monoxide or nitrogen trichloride, whereas the odor of the other halogen azides resembles rather that of the free halogens.

B. Physical Properties

1. Thermodynamic and Kinetic Data

Some physical data of the halogen azides are listed in Table I. Most physical investigations have been carried out on chlorine azide. The determination of the heat of decomposition (Table I) refers to the reaction

$$XN_3(g) \rightarrow \tfrac{3}{2}N_2(g) + \tfrac{1}{2}X_2(g)$$
$$X = Cl, Br$$

which was carried out calorimetrically as well as mass spectroscopically (*45*). The overall activation energy for BrN_3 is approximately

TABLE I

PROPERTIES OF HALOGEN AZIDES

Azide	Melting point (°C)	Boiling (sublimation) point (°C/Torr)	Heat of decomposition ΔH°_{293} (kcal mol^{-1})	Maximum flame temperature (K)
FN_3	−154 (*58*)	−82/760[a] (*58*)		
ClN_3	−100 (*52*)	15/760 (*52*)	−93.2 (±1.5) (*44, 107*)	3380 (20 Torr) (*107*)
BrN_3	−45 (*126*)	—	−92.0 (±2.0) (*45*)	4013 (20 Torr) (*45*)
IN_3	Solid	~20/760 (*23*)		

[a] Could only be determined as condensation temperature.

15–18 kcal mol^{-1} (*45*). In the thermal decomposition of ClN_3 in a flow reactor between 600 and 850 K under isothermal conditions, NCl was found by mass spectroscopy (*18*). The study of the kinetics of the reaction of Cl atoms with ClN_3 at pressures near 1 Torr in a discharge-flow reactor coupled with a quadrupole mass spectrometer gave the rate constant for the initial step

$$Cl + ClN_3 \rightarrow N_3 + Cl_2$$

as $k_1 = 2.3 \times 10^{-11} \exp(-1100/RT)$ cm^3 mol^{-1} sec^{-1} between 300 and 675 K (*18*). The kinetics of chemiluminescent reactions of the gaseous azide radical produced in the same rapid reaction have been studied (*14*). The rate constants of the following reactions of N_3 and NCl free radicals have also been determined, using a simulation technique (*68*).

$$Cl + N_3 \rightarrow NCl + N_2$$
$$N_3 + N_3 \rightarrow 3N_2$$
$$NCl + NCl \rightarrow N_2 + Cl_2$$

Critical quenching pressures P_C and velocities of the flame front D_L near detonation limits have been measured in capillary tubes of radius r for gaseous ClN_3; P_C has been found to be proportional to $1/r$ for $r >$ 0.25 mm (*105*). General characteristics of the decomposition flame of ClN_3 (*108*) and detonation velocities of ClN_3 in cylindrical tubes (*106*) have also been given. The explosion of chlorine azide produces a continuous spectrum, extending from the ultraviolet to the red, with a maximum intensity at 500–550 nm (*112*); the emission of blue light can be seen at all pressures above 0.1 Torr (*113*).

The very high rate of explosion of chlorine azide allows it to be used in gas lasers mixed with various gases, to transform its chemical en-

ergy into laser radiation (*117*). Thus, HF lasing has been produced by a Xe flash-lamp initiation of an explosion in ClN_3–NF_3–H_2 (1 : 1 : 2; 12–24 Torr) and ClN_3–SF_6–H_2 (24 : 19 : 57) mixtures (*67*). Also, ClN_3 serves as a Cl source to produce HCl laser action from H_2–ClN_3 gas mixtures containing less than 20 mol % ClN_3 (*118*). The sequence of reactions that lead to population inversion is as follows (*118*).

$$\begin{aligned} ClN_3 + h\nu &\rightarrow Cl + N_3 \\ Cl + H_2 &\rightarrow HCl + H \\ H + ClN_3 &\rightarrow HCl^* + N_3 \end{aligned}$$

2. Microwave Spectrum and Structure of Chlorine Azide

The structure determination of ClN_3 was carried out by R. L. Cook and M. C. L. Gerry on the basis of the microwave spectrum (*19*).

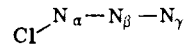

The bond distances (pm) and angles are

$Cl—N_\alpha$	174.5(5)	$Cl—N_\alpha—N_\beta$	108°40′ (30)
$N_\alpha—N_\beta$	125.2(10)	$N_\alpha—N_\beta—N_\gamma$	171°56′ (30)
$N_\beta—N_\gamma$	113.3(10)		

All atoms are coplanar; the deviation from the linearity of the NNN axis is surprising, but it can be explained by slight Cl=N double bonding **(III)** (*19*). The molecular structure can be described by **I** rather than by **II**.

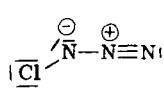

(I)

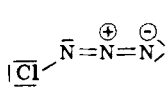

(II)

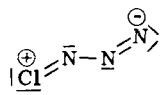

(III)

Values for the Cl quadrupole coupling constants have been obtained for all isotopic species, and for the most abundant, $^{35}Cl^{14}N_3$, they were transformed into the principal field gradient axis system. The values obtained were consistent with the proposed structure (*19*).

3. Vibrational Spectra

Information about the vibrational spectroscopy of the halogen azides XN_3 exists in the form of IR spectra in an Ar matrix for X = F, Cl, and Br (*80*), in solution for ClN_3 (*70*), and for IN_3 in solution (*23*), in the

TABLE II

VIBRATIONAL SPECTRA OF THE HALOGEN AZIDES[a]

Azide	Reference	Conditions	νN—X	$\nu_{as}N_3$	ν_sN_3	δN_3	$2 \times \nu_sN_3$	$\nu_sN_3 + \nu_{as}N_3$
FN_3	(*80*)	IR, Ar matrix	869	2034	1086	503, 654		
ClN_3	(*79*, *80*)	IR, Ar matrix	721 (^{37}Cl) 724 (^{35}Cl)	2060, 2072	1144	520		
	(*70*)	CH_2Cl_2 solution	719	2070	1134	518, 539		
BrN_3	(*80*)	IR, Ar matrix	687	2053, 2070	1160	530		
IN_3	(*21*)	IR, gas phase, 10 Torr IN_3/750 Torr N_2		2055, 2065	1170, 1180		2325	3190
	(*23*)	IR, benzene solution	338	2058	1176	578		3242
	(*23*)	IR, solid, Nujol	338	2045	1240	580, 648	2460	3242
	(*48*)	Raman (6471 Å) CH_2Cl_2, liq. N_2	410	2052	1207	583, 628		
	(*48*)	IR, CH_2Cl_2 143K	400	2050	1222	595, 623		

[a] All data in cm^{-1}.

gas phase (*21*), as the low-temperature matrix spectrum in CH_2Cl_2 (*48*), as well as in the solid state (*23*). The Raman spectrum of iodine azide could only be measured in a CH_2Cl_2 matrix due to its decomposition in the laser beam (6741 Å). The results are given in Table II. The spectra correspond to the molecular symmetry C_s, this also being found for ClN_3 from the microwave spectrum (*19*). In the series of the halogen azides from FN_3 to IN_3, the I—N stretching vibration appears shifted to surprisingly long wavelengths. This fact can be explained by the high polarity of the I—N bond according to $I^+—N^-$ (*23*), as well as by coupling with the in-plane bending vibration of the N_3 group (*3*). This interpretation is supported by the electron spectra of the halogen azides (see Section III,B,4), as well as by the chemical reactions of iodine azide (see Section IV). Therefore, among the halogen azides, iodine azide is the only species the halogen atom of which has acceptor qualities (see Section IV,B,3). Nevertheless, even the Cl atom in the ClN_3 molecule, according to LCAO–SCF–MO calculations, exhibits a weak positive charge (*72*), which corresponds to the values of the Cl quadrupole coupling constants (*19*).

4. *Ultraviolet–Visible Spectra*

The UV spectra have been measured in the gas phase for ClN_3 (*15*) and in a hexane solution in the case of ClN_3, BrN_3, and IN_3 (*38*). All halogen azides exhibit three absorption bands (Table III), one of which lies in the visible range of the spectrum and corresponds to an electron

TABLE III

UV–VISIBLE SPECTRA OF THE HALOGEN AZIDES ClN_3, BrN_3, AND IN_3

Azide	Solvent	λ_{max} (nm)	ε (l mol^{-1} cm^{-1})	Half width (nm)	Assignment	Reference
ClN_3	(Gas)	210–220	~2000			(*15*)
		249	455 ± 70			(*15*)
ClN_3	Hexane	211	815	13	$sp_x \rightarrow \pi_y^*$	(*38*)
		252	240	25	$\pi_y \rightarrow \pi_x^*$	(*38*)
		380	8	40	*a*	(*38*)
BrN_3	Hexane	235	366	30	$sp_x \rightarrow \pi_y^*$	(*38*)
		289	106	32	$\pi_y \rightarrow \pi_x^*$	(*38*)
	CCl_4	420	32	75	*a*	(*38*)
IN_3	Hexane	209	870	11	$sp_x \rightarrow \pi_y^*$	(*38*)
		243	615	26	$\pi_y \rightarrow \pi_x^*$	(*38*)
		350	40	60	*a*	(*38*)

[a] See text for assignment.

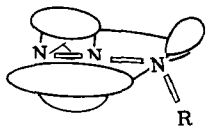

FIG. 1. Schematic representation of the bonding π orbitals of covalent azides according to Müller (*89*).

transition of the halogen components. The weak intensity of this band in chlorine azide (380 nm) is supported by its pale yellow-green color. In the case of bromine azide (red-brown) this band is at 420 nm, very near to the absorption maximum of Br_2 [417 nm (*38*)], whereas the absorption maxima of Cl_2 [332 nm (*114*)] and I_2 [517 nm (*9*)] clearly differ from the characteristic values of the halogen azides. In the case of IN_3 (gold colored) this band (341 nm) lies at shorter wavelengths than that of I_2. On the other hand, the opposite is true of chlorine azide and Cl_2.

In the UV, the halogen azides each show two band maxima, which, according to their position and the extinction values, correspond to other covalent monomeric azides, for example, alkyl azides [~285 and ~215 nm (*134*)]. In compliance with the bonding of these azides, which can be described by two N—N σ bonds, one localized π bond N_β—N_γ, one delocalized π bond N_α—N_β—N_γ, and two more lone electron pairs at the N_α atom and the N_γ atom (Fig. 1), these bands have been assigned by W. D. Clossen and H. B. Gray (*16*) to transitions of the electrons in the two highest occupied orbitals π_y and sp_x to the antibonding π^* orbitals (Fig. 2). In the free azide ion these transitions are degenerate, so that only one band is observed (*134*). In the series IN_3–BrN_3–ClN_3, the energy difference of these bands is the smallest in iodine azide (Δ = 34 nm), which is in agreement with a high polarity of the $I^{\delta+}$—$N^{\delta-}$ bond. Thus, IN_3 is in an intermediate position between the covalent alkyl azides and the azide ion, whereas BrN_3, probably due to its weak electronegativity, most closely resembles the alkyl azides (Δ = 54 nm). In chlorine azide this difference becomes smaller (Δ = 41 nm), an explanation being a reversal of the polarity according to $Cl^{\delta-}$—$N_3^{\delta+}$ (*38*), which was deduced from IR data some time ago (*20*). Ab initio calculations (Section II,B,3), however, indicate a charge distribution $Cl^{\delta+}$—$N_3^{\delta-}$ (*72*), which corresponds to nuclear quadrupole moment measurements (*19*). On the other hand, the ^{15}N-NMR spectrum (Section II,B,6) has also been interpreted; it suggests electron suction to the Cl atom (*85*). This question must probably remain unanswered until exact measurements of the electron distribution can be

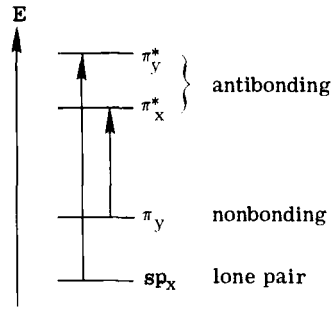

FIG. 2. Energy-level diagram of electron transitions of covalent azides according to Closson and Gray (*16*).

obtained. However, it is certainly not possible to derive a polarity $Cl^{\delta+}—N_3^{\delta-}$ from chemical reactions, as suggested occasionally (*13*, *72*), because reversal of this polarity is quite common here (see Section III,B).

5. *Photochemical Decomposition*

By UV irradiation of an argon matrix containing the halogen azides FN_3, ClN_3, and BrN_3, D. E. Milligan and M. E. Jacox obtained FN, ClN and BrN (*79*, *80*), the stretching vibrations of which were measured by IR. They are given in Table IV, together with the stretching-force constants, and are supplemented by information about IN, which was produced by glow discharge from the elements (*82*). The course of the force-constant values is as expected, showing maximum π bonding in NF. This species is isoelectronic with the O_2 molecule (f = 11.4 N cm^{-1}); however, its bonding should rather be compared with that of the O_2^- ion (KO_2, f = 6.2 N cm^{-1}) (*136*). So a correct description is provided by the following formulation.

$$\langle \overset{\ominus}{N}=\overset{\oplus}{F} \rangle \leftrightarrow \langle N-\overline{F} |$$

TABLE IV

IR ABSORPTIONS AND FORCE CONSTANTS FOR THE HALOIMIDO SPECIES XN

	NF (*80*)	NCl (*80*)	NBr (*80*)	^{14}NI (*82*)	^{15}NI (*82*)
ν (cm^{-1})	1115	819	689	590	573
f(N—X) (N cm^{-1})	5.9	4.9	3.35	2.58	—

TABLE V

^{15}N-NMR SPECTRUM OF ClN_3[a]

	N_α	N_β[b]	N_γ
δ (ppm)	−269.556	−120.207	−110.582
J (Hz)	24.0	7.8	

[a] At −80°C in CH_2Cl_2 solution (*85*).

[b] The isotope shift of the β N atom is 0.12 ppm (α ^{14}N, γ ^{14}N), 0.07 ppm (γ ^{14}N), and 0.02 ppm (α ^{14}N).

6. *^{15}N-NMR Spectra*

A ^{15}N-NMR spectrum is known only in the case of chlorine azide (*85*). It was measured on a sample with 50% abundance of ^{15}N for the β N atom and with 90% abundance for the α and γ N atoms in dichloromethane at −80°C (Table V). The values of the chemical shift refer to $^{15}NO_3^-$ in D_2O, externally. Noteworthy is the change in the order of the signals N_β—N_γ—N_α to N_γ—N_β—N_α, in agreement with the smallest shielding of the N_γ atoms, as observed in the case of covalent azides, for example, HN_3 and RN_3 (*85*). It can be explained by the electronegativity of the Cl atom and the resulting electron displacement toward the Cl atom (*85*).

7. *Photoelectron Spectra*

The helium [He(I)] photoelectron spectra of ClN_3 and BrN_3 have been recorded and the results compared with ab initio and semiempirical calculations (*53*). The spectra provide an interesting investigation into how the orbitals of a linear pseudohalide grouping are perturbed by an off-axis halogen atom. An important conclusion is that bending the linear 16-valence electron ion N_3^- removes the π degeneracies and stabilizes the out-of-plane orbital (a″) more than the in-plane orbital (a′). This is in contrast to the HN_3 molecule, in which the a′ orbital is preferentially stabilized, because this orbital has the required symmetry to interact with the H 1s atomic orbital. The net result is a substantial splitting of the π-bonding N_3 orbitals, the extent of the perturbation depending upon the nature of the halogen (*53*).

8. *Magnetic Susceptibility*

The determination of the magnetic susceptibility of chlorine azide, dissolved in carbon tetrachloride, shows at 20°C a weak paramagnetism of $\chi_{mol} = 16.5 \times 10^{-6}$ emu (*74*).

IV. Applications in Synthetic Chemistry

A. Organic Chemistry

The use of halogen azides, especially bromine azide and iodine azide, in synthetic organic chemistry mainly originates from work of A. Hassner *et al.*, who found a method of adding halogen azides to olefinic double bonds. A review of this work was published in 1971 (*76*); for a summary in Japanese see Ota and Yoshida (*102*). In this chapter only the most essential aspects of their investigations can be mentioned and some selected new work cited.

The addition of halogen azides to olefinic double bonds can occur both ionically and radically, depending on the polarity of the solvent among other things (*76, 116*). By addition of styrene, it is possible to obtain, for example, both regioisomeric azides, from which vinyl azides can be produced (*76*), which in their turn serve in the synthesis of azirines (*64, 66, 125*).

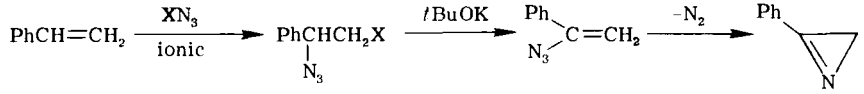

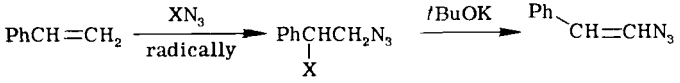

In this way, the first synthesis of a 2-vinylazirine was accomplished by the reaction of iodine azide with diphenyl butadiene and basic cleavage of HN_3, from the primary diazide (*61*).

In the ionic addition of iodine azide to olefins, an intermediate formation of a halogenium ion complex was proved (*51, 62*).

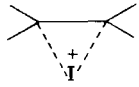

The tendency to homolytic cleavage increases in the sequence $IN_3 < BrN_3 < ClN_3$ (*76*), which is in accordance with the electronic spectra of halogen azides (*38*) as well as the IR spectra (*20–23, 48, 80*).

The radical addition of chlorine azide, which was produced *in situ* in the system $H_2O_2/FeCl_3/NaN_3$ in the presence of an olefin, can be described by the following sequence of reactions.

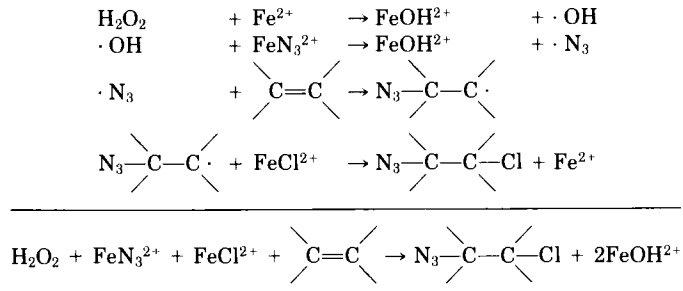

It is interesting that the easily decomposable $PhI(Cl)N_3$, which can be seen as an adduct of chlorine azide with iodobenzene, reacts differently from chlorine azide itself; for example although the stereoisomeric *cis*- and *trans*-2-chloro-1-azido-1-phenylcyclohexene are formed by treating phenyl-1-cyclohexene with ClN_3, the reagent $PhI(Cl)N_3$ yields the stereoisomeric mixture 1-chloro-2-azido-1-phenylcyclohexane (*141*).

Some new results are as follows. The reaction of iodine azide with cyclopentadiene in acetonitrile produces 2,4-diazidocyclopenten-1,2 (*122*), the addition of iodine azide to *trans*-1-azido-4-iodocyclooctene, 1-(4-iodocyclooctyl)-5-methyltetrazole and 5-azidocyclooctene (*63*). The synthesis of vicinal iodoazides can be carried out by using phase-transfer reagents in the system H_2O, $NaN_3/CHCl_3$, and I_2 in the presence of cyclohexene (*140*). The synthesis of *C*-silyl-substituted aziridine can be effected by the reaction (*43*)

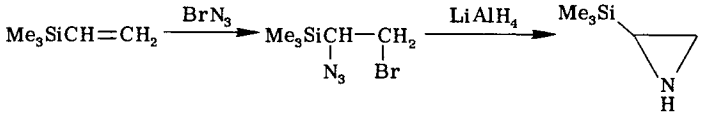

An easy synthesis of 2-bromo-Δ^1-unsaturated 3-ketosteroids has been carried out by addition of BrN_3, for example, to 5α-cholest-1-en-3-one, leading to 2-bromo-5α-cholest-1-en-3 one (*69*). A new synthetic route to 9,10-iminophenantrene was found by sequential treatment of phenanthrene with BrN_3 and $LiAlH_4$ (*40*). The addition of IN_3 to 3-*t*-butylcyclohexene and 3-methoxycyclohexene has been studied with respect to stereochemical addition (*11*), and general aspects of the addition of IN_3 to alkenes have also been published (*10*). The synthesis of 3-azidoindolenines by treatment of indoles with IN_3 or BrN_3 have been described (*132*), as well as the reaction of benzo[*b*]furan and 1-oxylindoles with IN_3 (*131*). Other authors have dealt with the reaction of IN_3 with vinyl sulfones (*133*), with tryptophols and *N*-acyl-

tryptamines (*65*), and with the reactions of IN_3 and BrN_3 with triacetylgalactal in the presence of mercury acetate, forming azidogalactopyranose (*7*).

B. Inorganic Chemistry

Most preparative applications in inorganic chemistry are based on iodine azide and chlorine azide; some reviews on this subject have already appeared (*20, 21, 49*). On the other hand, only two examples are known of the use of FN_3, which, in view of electronegativities, would better be called "azidium fluoride" (see Section III,B, concerning ClN_3).

The synthesis of NF_3 has been described as being achieved by passing FN_3 into liquid NOF or ClF_3, in a tubular Ni reactor at -70 to $-60°C$ (*55*). In a similar way, $ClNF_2$ can be obtained by reaction of FN_3 with excess chlorine at -85 to $-50°C$ (*56*).

$$4FN_3 + Cl_2 \rightarrow 2ClNF_2 + 5N_2$$

The reasons for the few examples of application of bromine azide in inorganic chemistry are, on the one hand, the difficult preparation of BrN_3 that is free of traces of bromine and, on the other, the fact that its behavior in reactions is of no advantage compared to ClN_3 and IN_3.

1. Substitution Reactions

a. Reactions with Element Halides. The dominating type of reaction of halogen azides in inorganic chemistry is the substitution of a halide ligand X (X = Cl, Br, or I) by the azide group.

$$M^{\delta+}—X^{\delta-} + X^{\delta+}—N_3^{\delta-} \rightarrow M—N_3 + X_2$$

These types of reactions proceed more rapidly the more polar the M—X bond and the more polar the X—N_3 bond of the halogen azide. Therefore, iodine azide exhibits the highest reactivity in the series Cl—$N_3 \leqq BrN_3 \ll IN_3$. Thus tungsten hexachloride reacts with chlorine azide in CCl_4 suspension within several hours, whereas the same reaction takes only a few seconds when iodine azide is used (*34, 99*).

$$WCl_6 + ClN_3 \rightarrow WCl_5N_3 + Cl_2$$

$$WCl_6 + IN_3 \rightarrow WCl_5N_3 + ICl$$

Chlorine azide also reacts extremely quickly when the metal halide is a Lewis acid; examples are the reactions with molybdenum pentachloride (*34*) and antimony pentachloride (*94*).

$$MoCl_5 + ClN_3 \rightarrow MoCl_5N_3 + \tfrac{1}{2}Cl_2$$

$$SbCl_5 + ClN_3 \rightarrow SbCl_4N_3 + Cl_2$$

Presumably, a donor–acceptor complex (**I**) is formed here primarily, which makes the halogen atom of the halogen azide positive so that charge compensation Cl^+/Cl^- and cleavage of the Cl_2 are effected in a secondary step (*20*). In favor of this mechanism is the large electron

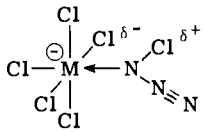

(I)

density of the N_α atoms, as concluded for ClN_3 from the structure (*19*) and the ^{15}N-NMR spectrum (*85*), the latter proving that the N_γ atom of ClN_3 has the lowest electron density, so that it cannot be considered for a donor function. This concept is also in agreement with all structural data, according to which only the N_α atom of covalent azides is capable of donor activities (*89*). Finally, it must be pointed out that halides of low polarity, for example, CCl_4, $SiCl_4$, and $GeCl_4$, do not react with chlorine azide. Table VI contains the results of reactions of halogen azides with element halides. Most of the azido halogeno complexes obtainable in this way are explosive as solids; nevertheless, some of them can be structurally investigated. They show very clearly the tendency to associate via the N_α atom.

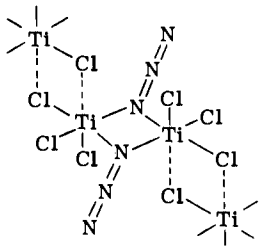

$[TiCl_3N_3]_\infty$ (*138*)

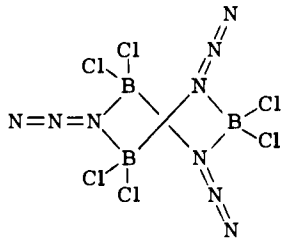

$[BCl_2N_3]_3$ (*90*)

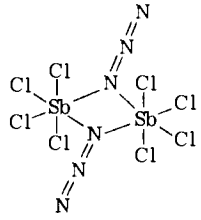

$[SbCl_4N_3]_2$ (*91*)

The use of iodine azide also allows the synthesis of metal bromide azides and iodide azides, as well as the preparation of halogeno azido complexes.

$$TiBr_4 + 2IN_3 \rightarrow TiBr_2(N_3)_2 + 2IBr \quad (75)$$

$$MoBr_4 + IN_3 \rightarrow MoBr_3N_3 + IBr \quad (29)$$

$$AlI_3 + IN_3 \rightarrow AlI_2N_3 + I_2 \quad (30)$$

$$PPh_4[NbCl_6] + IN_3 \rightarrow PPh_4[NbCl_5N_3] + ICl \quad (42)$$

Many of these azido complexes are highly energetic starting substances for the formation of nitrido halides, which are produced in high purity in thermal dissociation reactions in inert solvents like CCl_4.

$$TiCl_3N_3 \rightarrow [TiNCl]_x + N_2 + Cl_2 \quad (22)$$

$$VOCl_2N_3 \rightarrow [VON]_x + N_2 + Cl_2 \quad (22)$$

$$MoCl_5N_3 \rightarrow \tfrac{1}{4}[MoNCl_3]_4 + N_2 + Cl_2 \quad (34, 127)$$

$$MoBr_3N_3 \rightarrow MoNBr_3 + N_2 \quad (29)$$

$$ReCl_4N_3 \rightarrow ReNCl_3 + N_2 + \tfrac{1}{2}Cl_2 \quad (28)$$

A review article on the occurrence of transition metal–nitrogen multiple bonds in the products has appeared in 1981 (*35*). Table VII summarizes the results of secondary products of the metal azides with preparative importance.

The thermolysis of the trimeric azidodichloroboron has been known for a long time. It leads to hexachloroborazine by migration of a Cl ligand from boron to nitrogen (*92, 103*). A similar mechanism can be assumed in the decomposition of vanadium tetrachloride azide, obtained from VCl_4 and chlorine azide (*130*).

$$VCl_4N_3 \rightarrow Cl_3V{\equiv}N{-}Cl + N_2$$

TABLE VI

SUBSTITUTION REACTIONS OF THE HALOGEN AZIDES WITH METAL HALIDES AND WITH ORGANOMETALLIC COMPOUNDS

Starting materials	Reagent	Solvent	Reaction products	Color	Remarks	Reference	Crystal structure
BCl_3	ClN_3	—	$[BCl_2N_3]_3$	White	*abd*	(*104*)	(*90*)
BBr_3	BrN_3	—	$[BBr_2N_3]_3$	White	*abd*	(*104*)	
BI_3	IN_3	CH_2Cl_2	$[BI_2N_3]_n$	Yellow	*abcd*	(*31*)	
AlI_3	IN_3	C_6H_6	$[AlI_2N_3]_n$	Yellow	*ceg*	(*30*)	
GaI_3	IN_3	C_6H_6 suspension	$[GaI_2N_3]_n$	Yellow	*ceg*	(*30*)	
$SnCl_4$	ClN_3	—	$[SnCl_3N_3]_n$	White	*abe*	(*22*)	
$SbCl_5$	ClN_3	—	$[SbCl_4N_3]_2$	White-yellow	*abe*	(*94*)	(*91*)
$TiCl_4$	ClN_3	—	$[TiCl_3N_3]_n$	Yellow	*abe*	(*22*)	(*138*)
$TiBr_4$	IN_3	CCl_4	$[TiBr_2(N_3)_2]_n$	Orange-red	*abe*	(*75*)	
TiI_4	IN_3	C_6H_6	$[TiI_3N_3]_n$	Black	*abce*	(*75*)	
$ZrCl_4$	IN_3	CCl_4 suspension	$[ZrCl_3N_3]_n$	White	*abe*	(*46*)	
VCl_4	ClN_3	CCl_4	$[VCl_4N_3]_n$	Black-brown	*ab*	(*130*)	
VCl_4	NaN_3/Cl_2	—	$[Cl_3V{\equiv}N{-}Cl]_2$	Red	*bde*	(*50*)	(*129*)
VCl_4	IN_3	CCl_4	$[Cl_3V{\equiv}N{-}I]_2$	Black	*bce*	(*27*)	(*4*)
$VOCl_3$	ClN_3	—	$VOCl_2N_3$	Orange	*abe*	(*22*)	
$NbCl_5$, $TaCl_5$	ClN_3	CCl_4 suspension	$[MCl_4N_3]_2$	White	*abe*	(*128*)	(*128*) M = Ta
$CrCl_3$	IN_3	CCl_4 suspension	$[CrCl_2N_3]_n$	Violet	*ae*	(*47*)	
CrO_2Cl_2	ClN_3	—	CrO_2ClN_3	Dark green	*abe*	(*34*)	
$MoCl_5$	ClN_3	CCl_4 suspension	$MoCl_5N_3$	Red	*abd*	(*34*)	
$MoCl_5N_3$	ClN_3	CCl_4	$MoCl_4(N_3)_2$	Black	*ab*	(*34*)	
$MoCl_5$	IN_3	CCl_4 suspension	$[MoNCl_4]_2$	Brown	*be*	(*78*)	
$MoBr_4$	IN_3	CCl_4 suspension	$[MoBr_3N_3]_n$	Black-brown	*abe*	(*29*)	
MoI_3	IN_3	CCl_4 suspension	MoI_2N_3	Black	*bch*	(*75*)	

WCl_6	ClN_3	CCl_4	WCl_5N_3	Red	[abd]	(*34*)	
WCl_6	IN_3	CCl_4 (0°C)	$[WNCl_4]_n$	Brown	[be]	(*120*)	
WCl_6	IN_3	CCl_4 (20°C)	$[WNCl_3]_n$	Ocre	[be]	(*99*)	
WBr_6	BrN_3, IN_3	CH_2Br_2	$[WNBr_3]_n$	Black-brown	[be]	(*121*)	
$ReCl_5$	ClN_3	CCl_4 suspension (0°C)	$ReCl_4N_3$	Black	[ab]	(*28*)	
UCl_6	ClN_3	CH_2Cl_2	UCl_5N_3, $UCl_4(N_3)_2$	Black	[ab]	(*71*)	
$PPh_4[NbCl_6]$	IN_3	CH_2Cl_2	$PPh_4[NbCl_5N_3]$	Orange	[f]	(*42*)	(*90*)
$PPh_4[NbBr_6]$	IN_3	CH_2Cl_2	$PPh_4[NbBr_5N_3]$	Maroon	[f]	(*96*)	
$PPh_4[TaCl_6]$	IN_3	CH_2Cl_2	$PPh_4[TaCl_5N_3]$	White	[f]	(*42*)	
$PPh_4[TaBr_6]$	IN_3	CH_2Cl_2	$PPh_4[TaBr_5N_3]$	Yellow	[f]	(*96*)	
AlR_3 (R = Me, Et)	ClN_3	C_6H_6	$[AlR_2N_3]_3$	Colorless	Liquid[b,c,d]	(*36, 86, 87*)	
$AlClEt_2$	ClN_3	C_6H_6	$[AlClEtN_3]_3$	White	[bcd]	(*73*)	
GaR_3 (R = Me, Et)	ClN_3	C_6H_6	$[GaR_2N_3]_3$	Colorless	Liquid[d]	(*87, 88*)	
$InEt_3$	ClN_3	C_6H_6	$[InEt_2N_3]_2$	White	[bcd]	(*87*)	
$TlEt_3$	ClN_3	C_6H_6	$[TlEt_2]N_3$	White	[eh]	(*87*)	
ZnR_2 (R = Me, Et,Ph)	ClN_3	Hexane	$[ZnRN_3]_n$	White	[abce]	(*36, 83*)	
CdR_2 (R = Me, Et)	ClN_3		$[CdRN_3]_n$	White	[abce]	(*36, 84*)	
$CdEt(OEt)$	ClN_3	Hexane	$[Cd(OEt)N_3]_4$	White	[be]	(*84*)	
HgR_2 (R = Me, Et, *i*Pr, *c*Pr, *n*Pr, *n*Bu, Ph)	ClN_3	CCl_4, C_6H_6	R—Hg—N_3	White	[a](R = Me)[d]	(*33, 36, 124*)	

[a] Explosive.
[b] Sensitive to moisture.
[c] Sensitive to oxygen.
[d] Soluble in nonpolar solvents.
[e] Soluble in polar solvents like $POCl_3$, pyridine, etc.
[f] Soluble in CH_2Cl_2.
[g] Soluble in benzene in the presence of AlI_3.
[h] N_3 group ionic.

TABLE VII

SECONDARY PRODUCTS OF THE AZIDO COMPLEXES WITH PREPARATIVE IMPORTANCE

Starting materials	Conditions	Products	Remarks†	Reference	Crystal structure
$[BCl_2N_3]_3$	(200°C, pressure)	$[ClBNCl]_3$	*b*	(*103*)	(*92*)
$[BI_2N_3]_n$	CH_2Cl_2 (20°C)	$[IBNI]_n$, BN	*bc*	(*31*)	
$[SbCl_4N_3]_2$	CCl_4, boiling	$C(N_3)_3^+ SbCl_6^-$	*ab*	(*95*)	(*93*)
$[TiCl_3N_3]_n$	CCl_4 (20°C)	TiNCl	Polymeric *b*	(*22*)	
$VOCl_2N_3$	CCl_4 (20°C)	VON	Polymeric *b*	(*22*)	(*137*)
VCl_4N_3	CCl_4 (20°C)	$[Cl_3V{\equiv}N{-}Cl]_2$	*b*	(*130*)	(*129*)
$MoCl_5N_3$	CCl_4, boiling	$[MoNCl_3]_4$	*b*	(*34*)	(*127*)
$MoBr_3N_3$	CCl_4, boiling	$[MoNBr_3]_n$	*b*	(*29*)	
WCl_5N_3	CCl_4, boiling	$[WNCl_3]_n$	*b*	(*99*)	
UCl_5N_3	CCl_4 (20°C)	$C(N_3)_3^+ UCl_6^-$	*ab*	(*71*)	
UCl_5N_3	CH_2Cl_2 (20°C)	NH_4UCl_6		(*71*)	
$PPh_4[NbCl_5N_3]$	PPh_3, CH_2Cl_2 (20°C)	$PPh_4[NbCl_5(NPPh_3)]$	*f*	(*42*)	
$PPh_4[NbBr_5N_3]$	PPh_3, CH_2Cl_2 (20°C)	$PPh_4[NbBr_5(NPPh_3)]$	*f*	(*96*)	
$PPh_4[NbCl_5N_3]$	$AsPh_3$, CH_2Cl_2, $h\nu$ (65°C)	$PPh_4[NbCl_5(NAsPh_3)]$	*f*	(*96*)	
$PPh_4[TaCl_5N_3]$	PPh_3, CH_2Cl_2, $h\nu$ (65°C)	$PPh_4[TaCl_5(NPPh_3)]$	*f*	(*42*)	
$PPh_4[TaBr_5N_3]$	PPh_3, CH_2Cl_2, $h\nu$ (65°C)	$PPh_4[TaBr_5(NPPh_3)]$	*f*	(*96*)	

† See Table VI for footnotes.

On the other hand, the preservation of an I—N bond is observed in the reaction of vanadium tetrachloride with iodine azide (*27*).

$$VCl_4 + 2IN_3 \rightarrow Cl_3V{\equiv}N{-}I + 2.5N_2 + ICl$$

The compounds can be visualized as nitrene complexes; their crystal structures reveal a linear $V^{-}{\equiv}N^{+}{-}X$ axis (X = Cl, I) and a very short VN bond length of 165 pm (*4, 101, 129*). The N—I compound undergoes halogen exchange with chlorine or bromine (*27*).

$$Cl_3VNI + X_2 \rightarrow Cl_3VNX + IX$$

$$X = Cl, Br$$

A review article about nitrene complexes of transition metals was published in 1980 (*100*).

A noteworthy reaction takes place with molybdenum pentachloride and iodine azide at 0°C in a CCl_4 solution (*78*).

$$2MoCl_5 + 2IN_3 \rightarrow [MoNCl_4]_2 + 2ICl + 2N_2$$

The nitride chloride contains molybdenum(V) and is characterized by a direct N—N bond. Upon heating it releases chlorine and changes to $MoNCl_3$ (*78*). Some transition-metal azide complexes are capable of undergoing the Staudinger reaction with triphenylphosphine or triphenylarsine.

$$[MCl_4N_3]_2 + 2PPh_3 \rightarrow [MCl_4(NPPh_3)]_2 + 2N_2 \qquad (5, 6)$$

$$M = Nb, Ta$$

$$PPh_4[MCl_5N_3] + PPh_3 \rightarrow PPh_4[MCl_5(NPPh_3)] + N_2 \qquad (42)$$

$$M = Nb, Ta$$

$$PPh_4[NbCl_5N_3] + AsPh_3 \rightarrow PPh_4[NbCl_5(NAsPh_3] + N_2 \qquad (96)$$

In other cases, reactions with the solvent were observed. Thus, for example, the azide complexes $[SbCl_4N_3]_2$ (*95*), UCl_5N_3 (*71*), and $[ZrCl_3N_3]_\infty$ (*46*) react with carbon tetrachloride to form the triazido carbenium cation.

$$3SbCl_4N_3 + CCl_4 \rightarrow C(N_3)_3[SbCl_6] + 2SbCl_5$$

$[WNCl_3 \cdot 0.5HN_3]_4$ is produced in the reaction of excess iodine azide with tungsten hexachloride in dichloromethane solution, the hydrazoic

acid being formed with participation of the solvent. The tungsten atoms in the $[WNCl_3 \cdot 0.5HN_3]_4$ molecule are placed at the corners of a square, the edges of which are formed by linear W≡N—W bridges of alternating WN bond lengths. The HN_3 molecules are coordinated by the N_α atoms to two diametrical tungsten atoms, and the two remaining tungsten atoms coordinate via chloro bridges to form ribbons (*135*).

b. Reactions with Organometallic Compounds. Substitution reactions in metal organic compounds have so far been exclusively carried out with chlorine azide (see Table VI). The reactions take place according to the pattern

$$MR_n + ClN_3 \rightarrow MR_{n-1}N_3 + RCl$$

In contrast to the metal halide azides, in general the metal organic azides are not explosive. Exceptions to this are the monomeric organomercury azides R—Hg—N_3, which can explode upon extended heating, probably as a consequence of ligand exchange by which mercury diazide is formed. The dialkyl metal azides of aluminum (*36, 86, 87*) and gallium (*87, 88*) are colorless liquids that occur as trimeric molecules like $[R_2MN_3]_3$, in which the N_α atoms of the azide ligands link the metal atoms to planar six-membered rings (symmetry D_{3h}). On the other hand, diethyl indium azide is dimeric (*87*). The dialkylaluminum azides react very violently with water (*36, 86, 87*), whereas diethylgallium azide is affected only by concentrated sulfuric acid (*88*). The alkyl and aryl azides of zinc and cadmium form polymeric solids (*36, 83, 84*), whereas the same compounds of mercury

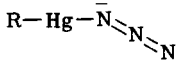

(*33*, *124*)

are molecular with local symmetry C_s and diethylthallium azide is ionic. Its cation

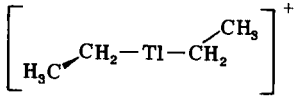

which is isosteric with diethylmercury, is only of symmetry C_2 on account of the absence of free rotation of the ethyl groups (*87*).

c. Reactions with Metal Carbonyls. The reactions of the halogen azides with metal carbonyls lead to products that vary greatly, depending on the metal carbonyl used as well as on the halogen azide (Table VIII). All reactions have in common the partial or complete substitution of carbonyl ligands and the occurrence of redox reactions.

Iron pentacarbonyl reacts even at −40 to −20°C in pentane solution with all halogen azides XN_3 (X = Cl, Br, I), yielding the yellow (X = Cl) or brown (X = Br, I) dicarbonyl azide halides (*25, 77*).

$$Fe(CO)_5 + XN_3 \rightarrow Fe(CO)_2XN_3 + 3CO$$

The compounds are high-spin complexes. $Fe(CO)_2ClN_3$ was investigated magnetically and was found to be surprisingly strongly paramagnetic (μ_{eff} = 5.29 BM, θ = 0°) (*77*). The thermolysis in vacuum at 90–100°C results in mixed azide halides, free of carbonyl, for X = Cl or Br (*77*).

$$Fe(CO)_2XN_3 \rightarrow FeXN_3 + 2CO$$

The metal carbonyls of manganese and cobalt react with iodine azide in dichloromethane, yielding diazides in very high purity (*25*).

$$Mn_2(CO)_{10} + 4IN_3 \rightarrow 2Mn(N_3)_2 + 10CO + 2I_2$$

On the other hand, the reaction of nickel tetracarbonyl yields only a mixture of $Ni(N_3)_2$ and NiI_2 (*25*).

Chlorine azide reacts with the hexacarbonyls of molybdenum and tungsten in carbon tetrachloride, forming the explosive metal dicarbonyl diazides (*77*). These compounds are polymeric, with chloro bridges and via the N_α atoms of the azido groups. Upon attempting to obtain the azide chlorides free of CO by thermal degradation, the products regularly explode (*77*). In contrast, the reaction with iodine azide leads to the highly explosive dicarbonyl diazides (*25*).

$$M(CO)_6 + ClN_3 \rightarrow M(CO)_2ClN_3 + 4CO$$

$$M(CO)_6 + 2IN_3 \rightarrow M(CO)_2(N_3)_2 + I_2 + 4CO$$

$$M = Mo, W$$

Finally, the reactions of iodine azide with dirhenium decacarbonyl and triosmium dodecacarbonyl, suspended in pentane, lead to the car-

TABLE VIII

REACTIONS OF METAL CARBONYLS WITH HALOGEN AZIDES

Starting materials	Reagent	Solvent	Reaction products	Color	Remarks†	Reference
$Mo(CO)_6$	ClN_3	CCl_4	$[Mo(CO)_2ClN_3]_n$	Brown	[ab]	(77)
$Mo(CO)_6$	IN_3	Pentane (−50°C)	$[Mo(CO)_2(N_3)_2]_n$	Brown	[ab]	(25)
$W(CO)_6$	ClN_3	CCl_4	$[W(CO)_2ClN_3]_n$	Brown	[ab]	(77)
$W(CO)_6$	IN_3	Pentane (−50°C)	$[W(CO)_2(N_3)_2]_n$	Brown	[ab]	(25)
$Mn_2(CO)_{10}$	IN_3	CH_2Cl_2	$Mn(N_3)_2$	Ocre	[ab]	(25)
$Re_2(CO)_{10}$	IN_3	Pentane suspension (−25°C)	$[Re(CO)_4NCO]_2$	Ocre	[j]	(25)
$Fe(CO)_5$	ClN_3	Pentane (−20°C)	$[Fe(CO)_2ClN_3]_n$	Yellow	(μ_{eff} = 5.29 BM)[b,j]	(77)
$Fe(CO)_5$	BrN_3	Pentane (−20°C)	$[Fe(CO)_2BrN_3]_n$	Brown	[bj]	(77)
$Fe(CO)_5$	IN_3	Pentane (−20°C)	$[Fe(CO)_2IN_3]_n$	Dark brown	[bj]	(25)
$Co_2(CO)_8$	IN_3	CH_2Cl_2	$Co(N_3)_2$	Grey-green	[ab]	(25)
$Os_3(CO)_{12}$	IN_3	CH_2Cl_2	$[Os(CO)_2NCO]_n$	Yellow-brown		(25)
$Ni(CO)_4$	IN_3	Pentane (−25°C)	$Ni(N_3)_2$, NiI_2	Black	[ab]	(25)

† See Table VI for footnotes [a] and [b].

[j] Light sensitive.

bonyl cyanates by dissociation of nitrogen and migration of a CO group (*25*).

$$Re_2(CO)_{10} + 2IN_3 \rightarrow [Re(CO)_4(NCO)]_2 + 2N_2 + I_2$$

$$Os_3(CO)_{12} + 3IN_3 \rightarrow 3Os(CO)_2(NCO) + 3N_2 + 1.5I_2 + 3CO$$

The rhenium complex is dimeric, with the nitrogen atoms of the cyanate groups acting as bridging atoms; there are no structural data available about the osmium compound.

2. Oxidative Addition Reactions

In analogy with the halogens, the halogen azides are capable of some oxidative additions. This has been examined in some examples (Table IX). The addition of halogen azides XN_3 (X = Cl, Br, I) to tin(II) chloride exclusively yields tin(IV) diazide dichloride as an almost insoluble white precipitate (*39*) yet the reaction probably proceeds via primary

$$2SnCl_2 + 2XN_3 \rightarrow SnCl_2(N_3)_2 + \text{“}SnCl_2X_2\text{”}$$

addition of an XN_3 molecule with subsequent X/N_3 ligand exchange. $SnCl_2(N_3)_2$ is interlinked by the N_α atoms of the azide bridges (*39, 139*), so that there is no further exchange of ligands in this species. The direct addition of iodine azide to tin(II) chloride has been proved in the presence of tetramethylammonium chloride, because the octahedrally coordinated tin does not allow a secondary ligand exchange (*39*).

$$SnCl_2 + IN_3 + 2NMe_4Cl \rightarrow (NMe_4)_2[SnCl_4IN_3]$$

The oxidative addition of chlorine azide to phosphorus trichloride results in a very explosive, white azide of unknown structure, which reacts with more phosphorus trichloride, undergoing N_2 elimination according to a Staudinger reaction (*98*).

$$PCl_3 + ClN_3 \rightarrow PCl_4N_3$$

$$PCl_4N_3 + PCl_3 \rightarrow [Cl_3PNPCl_3]Cl + N_2$$

The reaction of bromine azide with antimony tribromide in bromine solution leads to the explosive, probably dimeric tetrabromo antimony azide (*32*).

$$SbBr_3 + BrN_3 \rightarrow SbBr_4N_3$$

TABLE IX

OXIDATIVE ADDITION REACTIONS OF THE HALOGEN AZIDES

Starting materials	Reagent	Solvent	Reaction products	Color	Remarks†	Reference
$SnCl_2$	ClN_3,BrN_3,IN_3	CCl_4 suspension	$SnCl_2(N_3)_2$	White	[ab]	(*39*)
NMe_4Cl, $NMe_4[SnCl_3]$	IN_3	CH_2Cl_2 suspension	$(NMe_4)_2[SnCl_4IN_3]$	Orange		(*39*)
PCl_3	ClN_3	—	PCl_4N_3	White	[abi]	(*32*)
$SbBr_3$	BrN_3	Br_2	$SbBr_4N_3$	Red-brown	[ab]	(*32*)
SbR_3	IN_3	CH_2Cl_2 (−20°C)	SbR_3IN_3	White (R = CH_3, C_6H_5)		(*26*)
Hg	IN_3	CH_2Cl_2 suspension (20°C)	$HgIN_3$	Yellow	[a]	(*24*)

† See Table VI for footnotes [a] and [b].

[i] Rapid decomposition, forming $[Cl_3PNPCl_3]Cl$ (*98*).

whereas trimethylantimony and triphenylantimony react with iodine azide to form the nonexplosive monomeric triorganoantimony azide iodides (*26*).

$$R_3Sb + IN_3 \rightarrow R_3SbIN_3$$

According to ^{121}Sb Mössbauer spectroscopy, methyl and phenyl groups, respectively, are coordinated equatorially, whereas I and N_3 are placed in the axial positions of the trigonal bipyramid (*26*).

The only metal that has been brought into reaction with iodine azide in a satisfactory way is mercury (*24*). It reacts in dichloromethane to

$$Hg + IN_3 \rightarrow HgIN_3$$

form mercury azide iodide: sodium, magnesium, zinc, and also white phosphorus cause violent explosions without a solvent and yield only mixtures of the halides and the azides when the reaction is moderated by a solvent (*52, 59, 115*).

3. Donor–Acceptor Complexes of Iodine Azide

Within the series of the halogen azides only the iodine atom in iodine azide has sufficient positive charge to act as an acceptor component with Lewis bases. Donor–acceptor complexes can be isolated when halide or pseudohalide ions in their tetramethylammonium salts, dissolved in dichloromethane, react with iodine azide, and when the solvent is evaporated (Table X) (*41*). On the other hand, the reaction of

$$IN_3 + X^- \rightarrow [X{-}I{-}N_3]^-$$

iodine azide with thiocyanate ions resulted in a spontaneous decomposition of iodine azide to the elements (*41*). Free of solvent, the complexes of iodine azide containing NMe_4^+ cations are colored, explosive solids, the IR spectra of which indicate a linear X—I—N_α axis. The use of the larger tetraphenylphosphonium cation yields complexes that are no longer explosive and, on account of the hydrophobic character of the phenyl groups, are no longer hygroscopic in the crystalline state (*97*). The addition of IN_3 to X^- ions causes an increase of polarity in the I—N bond, which is expressed by the longwave shift of the asymmetric N_3 stretching vibration of iodine azide from 2045 to approximately 2000 cm^{-1}, as well as by the longwave shift of both N—I—N stretching vibrations in the $[N_3{-}I{-}N_3]^-$ complex from 338 cm^{-1} in the iodine azide molecule to 285 and 269 cm^{-1} (species A and B) (*97*).

TABLE X

DONOR–ACCEPTOR COMPLEXES OF IODINE AZIDE[a]

Compound	Symmetry of the anion	Color	Remarks	ν N—X (cm^{-1})	Reference
$NMe_4[F—I—N_3]$	C_s	Yellow	[b]	403	(*41*)
$NMe_4[Cl—I—N_3]$	C_s	Orange	[b]	333	(*41*)
$NMe_4[Br—I—N_3]$	C_s	Orange-red	[b]	260	(*41*)
$NMe_4[I—I—N_3]$	C_s	Dark violet	[b]		(*41*)
$NMe_4[N_3—I—N_3]$	C_2	Orange-red	[b]	250, 237	(*41*, *97*)
$PPh_4[N_3—I—N_3]$	C_2	Orange		285, 269	(*97*)
$NMe_4[OCN—I—N_3]$	C_1	Ocre	[b]		(*41*)
$NMe_4[NC—I—N_3]$	C_s	Orange	[b]	260	(*41*)
$NMe_4[N_3—I—NC—I—N_3]$	C_1	Orange	[b]	258	(*41*)

[a] All complexes were prepared in CH_2Cl_2 solution.
[b] Explosive.

A crystal structure investigation has been carried out on $PPh_4[I(N_3)_2]$. It confirms spectroscopic data, which are in favor of an interaction of the lone electron pairs at the iodine atom with the lone pairs of the N_α atoms in the azide groups (dihedral angle 123°) (*97*). It

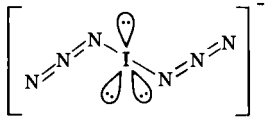

is noteworthy that the azido groups, exhibiting a NNN bond angle of 157°, significantly deviate from the expected linearity; however, this may be a consequence of disorder, though covalent azides with NNN bond angles as small as 160° are known (*89*).

Stable, crystalline donor–acceptor complexes of IN_3 with pyridine, α,α'-dipyridyle, urotropine, and other nitrogen-containing donors have been isolated (*24*). In these complexes, $C_5H_5N(IN_3)$, $(C_5H_4N)_2(IN_3)_2$, and $(CH_2)_6N_4(IN_3)_2$, the iodine azide is coordinated via linear bridges $N^+—I^-—N_3$. The α,α'-dipyridyle–diiodine azide complex was characterized by X-ray methods; one of the IN_3 molecules is almost coplanar with the pyridyle ring to which it is bonded, whereas the other one is nearly perpendicular to the second pyridyle ring; the dihedral angle of the pyridyle rings is 63.4° (*142*).

REFERENCES

1. Austin, T. A., and Mason, R. W., *Inorg. Chem.* **2,** 646 (1963).
2. Bauer, S. H., *J. Am. Chem. Soc.* **69,** 3104 (1947).
3. Becher, H.-J., personal communication (1978).
4. Beindorf, G., Strähle, J., Liebelt, W., and Weller, F., *Z. Naturforsch., B: Anorg. Chem., Org. Chem.* **35B,** 153 (1980).
5. Bezler, H., and Strähle, J., *Z. Naturforsch., B: Anorg. Chem., Org. Chem.* **34B,** 1199 (1979).
6. Bezler, H., Dissertation, Universität Tübingen (1980).
7. Bovin, N. V., Zurabyan, S. E., and Khorlin, A. Ya., *Bioorg. Khim.* **5,** 1257 (1979).
8. Brauer, G., "Handbuch der präparativen anorganischen Chemie," 3rd ed., Vol. 1, p. 463. Enke, Stuttgart 1975.
9. Buckles, R., and Mills, J., *J. Am. Chem. Soc.* **75,** 552 (1953).
10. Cambie, R. C., Hayward, R. C., Rutledge, P. S., Smith-Palmer, T., Swedlund, B. E., and Woodgate, P. D., *J. Chem. Soc., Perkin Trans. 1* p. 180 (1979).
11. Cambie, R. C., Rutledge, P. S., Smith-Palmer, T., and Woodgate, P. D., *J. Chem. Soc., Trans. Perkin 1* p. 997 (1978).
12. Chandri, T. A., *Pak. J. Sci. Ind. Res.* **19,** 1 (1976).
13. Christe, K. O., and Schack, C. J., *Inorg. Chem.* **20,** 2566 (1981).
14. Clark, T. C., and Clyne, M. A. A., *Trans. Faraday Soc.* **66,** 877 (1970).
15. Clark, T. C., and Clyne, M. A. A., *Trans. Faraday Soc.* **65,** 2994 (1969).
16. Closson, W. D., and Gray, H. B., *J. Am. Chem. Soc.* **85,** 290 (1963).
17. Colburn, C. B., *Endeavour* **24,** 138 (1965).
18. Combourieu, J., Le Bras, G., Poulet, G., and Jourdin, J. L., *Symp. (Int.) Combust. [Proc.]* **16,** 863 (1976).
19. Cook, R. L., and Gerry, M. C. L., *J. Chem. Phys.* **53,** 2525 (1970).
20. Dehnicke, K., *Angew. Chem.* **79,** 253 (1967); *Angew. Chem., Int. Ed. Engl.* **6,** 240 (1967).
21. Dehnicke, K., *Angew. Chem.* **91,** 527 (1979); *Angew. Chem., Int. Ed. Engl.* **18,** 507 (1979).
22. Dehnicke, K., *J. Inorg. Nucl. Chem.* **27,** 809 (1965).
23. Dehnicke, K., *Angew. Chem.* **88,** 612 (1976); *Angew. Chem., Int. Ed. Engl.* **15,** 553 (1976).
24. Dehnicke, K., and Dörner, H. D., unpublished results.
25. Dehnicke, K., and Dübgen, R., *Z. Anorg. Allg. Chem.* **444,** 61 (1978).
26. Dehnicke, K., Fleck, K., Schmidt, K., and Pebler, J., *Z. Anorg. Allg. Chem.* **451,** 109 (1979).
27. Dehnicke, K., and Liebelt, W., *Z. Anorg. Chem.* **453,** 9 (1979).
28. Dehnicke, K., Liese, W., and Köhler, P., *Z. Naturforsch., B: Anorg. Chem., Org. Chem.* **32B,** 1487 (1977).
29. Dehnicke, K., and Krüger, N., *Z. Naturforsch., B: Anorg. Chem., Org. Chem.* **33B,** 1242 (1978).
30. Dehnicke, K., and Krüger, N., *Z. Anorg. Allg. Chem.* **444,** 71 (1978).
31. Dehnicke, K., Krüger, N., and Siebert, W., *Z. Anorg. Allg. Chem.* **444,** 71 (1978).
32. Dehnicke, K., and Müller, U., unpublished results.
33. Dehnicke, K., and Seybold, D., *J. Organomet. Chem.* **11,** 227 (1968).
34. Dehnicke, K., and Strähle, J., *Z. Anorg. Allg. Chem.* **339,** 171 (1965).
35. Dehnicke, K., and Strähle, J., *Angew. Chem.* **93,** 451 (1981); *Angew. Chem., Int. Ed. Engl.* **20,** 413 (1981).

36. Dehnicke, K., Strähle, J., Seybold, D., and Müller, J., *J. Organomet. Chem.* **6,** 298 (1966).
37. Dehnicke, K., and Ruschke, P., unpublished results.
38. Dehnicke, K., and Ruschke, P., *Z. Naturforsch., B: Anorg. Chem., Org. Chem.* **33B,** 750 (1978).
39. Dehnicke, K., and Ruschke, P., *Z. Anorg. Allg. Chem.* **444,** 54 (1978).
40. Denis, J. N., and Krief, A., *Tetrahedron* **35,** 2901 (1979).
41. Dübgen, R., and Dehnicke, K., *Naturwissenschaften* **65,** 535 (1978).
42. Dübgen, R., Müller, U., Weller, F., and Dehnicke, K., *Z. Anorg. Allg. Chem.* **471,** 89 (1980).
43. Duboudin, F., and Laporte, O., *J. Organomet. Chem.* **156,** C25 (1978).
44. Dupre, G., Paillard, C., and Combourieu, J., *Dyn. Mass Spectrom.* **4,** 233 (1976).
45. Dupre, G., Paillard, C., and Combourieu, J., *C.R. Hebd. Seances Acad. Sci., Ser. C* **273,** 445 (1971).
46. Dyck, W. M., and Dehnicke, K., *Z. Anorg. Allg. Chem.* **482,** 113 (1981).
47. Dyck, W, M., and Dehnicke, K., unpublished results.
48. Engelhardt, U., Feuerhahn, M., and Minkwitz, R., *Z. Anorg. Allg. Chem.* **440,** 210 (1978).
49. Engelhardt, U., and Jander, J., *in* "Developments in Inorganic Nitrogen Chemistry" (C. B. Colburn, ed.), Vol. 2, p. 70. Elsevier, Amsterdam, 1973.
50. Fernández, V., and Dehnicke, K., *Naturwissenschaften* **62,** 181 (1975).
51. Fowler, F. W., Hassner, A., and Levy, L. A., *J. Am. Chem. Soc.* **89,** 2077 (1967).
52. Frierson, W. F., Kronrad, J., and Browne, A. W., *J. Am. Chem. Soc.* **65,** 1696 (1943).
53. Frost, D. C., McDonald, C. B., McDowell, C. A., and Westwood, N. P. C., *Chem. Phys.* **47,** 111 (1980).
54. Gipstein, E., and Maller, J. F., *Appl. Spectrosc.* **20,** 417 (1966).
55. Gordon, J., and Sukornick, B., U.S. Publ. Patent Appl. B 111,130 (1976).
56. Gordon, J., and Sukornick, B., U.S. Patent 3,969,486 (1976).
57. Gutmann, A., *Ber. Dtsch. Chem. Ges.* **57,** 1956 (1924).
58. Haller, J. F., Dissertation, Cornell University, Ithaca, New York (1942).
59. Hantzsch, A., and Schümann, M., *Ber. Dtsch. Chem. Ges.* **33,** 522 (1900).
60. Hassner, A., and Boerwinkle, F., *J. Am. Chem. Soc.* **90,** 216 (1968).
61. Hassner, A., and Keogh, J., *Tetrahedron Lett.* p. 1575 (1975).
62. Hassner, A., and Levy, L. A., *J. Am. Chem. Soc.* **87,** 4203 (1965).
63. Hayward, R. C., and Whitham, G. H., *J. Chem. Soc., Perkin Trans. 1* p. 2267 (1975).
64. Horner, L., Christbaum, A., and Gross, A., *Chem. Ber.* **96,** 399 (1963).
65. Ikeda, M., Ohno, K., Katsura, M., Chun, M. W., and Tamura, Y., *J. Chem. Soc., Perkin Trans. 1* p. 3061 (1979).
66. Isomura, K., Okada, M., and Taniguchi, H., *Tetrahedron Lett.* p. 4073 (1969).
67. Jensen, R. J., and Rice, W. W., Jr., U.S. Patent 3,662,280 (1972); *Chem. Abstr.* **77,** 41277 (1973).
68. Jourdain, J. L., Le Bras, G., Poulet, G., and Combourieu, J., *Combust. Flame* **34,** 13 (1979).
69. Kocor, M., and Gumulka, M., *Rocz. Chem.* **51,** 297 (1977).
70. Kolitsch, W., Dissertation, Universität Marburg (1974).
71. Kolitsch, W., and Müller, U., *Z. Anorg. Allg. Chem.* **410,** 21 (1974).
72. Kosmus, W., Nachbaur, E., and Faegri, K., Jr., *J. Chem. Soc., Faraday Trans. 2* p. 802 (1976).
73. Krieg, V., and Weidlein, J., *Z. Anorg. Allg. Chem.* **368,** 44 (1969).
74. Krogmann, K., Hausen, H. D., and Dehnicke, K., unpublished results (1967).

75. Krüger, N., and Dehnicke, K., *Chem.-Ztg.* **106,** 187 (1982).
76. L'abbé, G., and Hassner, A., *Angew. Chem.* **83,** 103 (1971); *Angew. Chem., Int. Ed. Engl.* **10,** 98 (1971).
77. Lange, G., and Dehnicke, K., *Z. Anorg. Allg. Chem.* **344,** 167 (1966).
78. Liebelt, W., and Dehnicke, K., *Z. Naturforsch., B: Anorg. Chem., Org. Chem.* **34B,** 7 (1979).
79. Milligan, D. E., *J. Chem. Phys.* **35,** 372 (1961).
80. Milligan, D. E., and Jacox, M. E., *J. Chem. Phys.* **40,** 2461 (1964).
81. Minisci, F., Galli, R., and Cecere, M., *Gazz. Chim. Ital.* **94,** 67 (1964).
82. Minkwitz, R., and Froben, F. W., *Chem. Phys. Lett.* **39,** 473 (1976).
83. Müller, H., and Dehnicke, K., *J. Organomet. Chem.* **10,** P1 (1967).
84. Müller, H., and Dehnicke, K., *Bol. Soc. Chil. Quim.* **19,** 17 (1972).
85. Müller, J., *Z. Naturforsch., B: Anorg. Chem., Org. Chem.* **33B,** 993 (1978).
86. Müller, J., and Dehnicke, K., *Z. Anorg. Allg. Chem.* **348,** 261 (1966).
87. Müller, J., and Dehnicke, K., *J. Organomet. Chem.* **12,** 37 (1968).
88. Müller, J., and Dehnicke, K., *J. Organomet. Chem.* **7,** P1 (1967).
89. Müller, U., *Struct. Bonding (Berlin)* **14,** 141 (1973).
90. Müller, U., *Z. Anorg. Allg. Chem.* **382,** 110 (1971).
91. Müller, U., *Z. Anorg. Allg. Chem.* **388,** 207 (1972).
92. Müller, U., *Acta Crystallogr., Sect. B* **B27,** 1997 (1971).
93. Müller, U., and Bärnighausen, H., *Acta Crystallogr., Sect. B* **B26,** 1671 (1970).
94. Müller, U., and Dehnicke, K., *Z. Anorg. Allg. Chem.* **350,** 113 (1967).
95. Müller, U., and Dehnicke, K., *Angew. Chem.* **78,** 825 (1966); *Angew. Chem., Int. Ed. Engl.* **5,** 841 (1966).
96. Müller, U., Dübgen, R., and Dehnicke, K., *Z. Anorg. Allg. Chem.* **473,** 115 (1981).
97. Müller, U., Dübgen, R., and Dehnicke, K., *Z. Anorg. Allg. Chem.* **463,** 7 (1980).
98. Müller, U., and Schmock, F., *Z. Naturforsch., B: Anorg. Chem., Org. Chem.* **35B,** 1529 (1980).
99. Musterle, W., Strähle, J., Liebelt, W., and Dehnicke, K., *Z. Naturforsch., B: Anorg. Chem., Org. Chem.* **34B,** 942 (1979).
100. Nugent, W. A., and Haymore, B. L., *Coord. Chem. Rev.* **31,** 123 (1980).
101. Oberhammer, H., and Strähle, J., *Z. Naturforsch.*, **30A,** 296 (1975).
102. Ota, H., and Yoshida, M., *Yuki Gosei Kagaku Kyokaishi* **28,** 453, (1970).
103. Paetzold, P. I., *Z. Anorg. Allg. Chem.* **326,** 47 (1963).
104. Paetzold, P. I., Gayoso, M., and Dehnicke, K., *Chem. Ber.* **98,** 1173, (1965).
105. Paillard, C., Dupre, G., and Combourieu, J., *J. Chim. Phys. Phys. Chim. Biol.* **71,** 175 (1974).
106. Paillard, C., Dupre, G., and Combourieu, J., *J. Chim. Phys. Phys. Chim. Biol.* **70,** 811 (1973).
107. Paillard, C., Moreau, R., and Combourieu, J., *C.R. Hebd. Seances Acad. Sci., Ser. C* **264,** 1721 (1967).
108. Paillard, C., Moreau, R., Combourieu, J., and Laffitte, P., *C.R. Hebd. Seances Acad. Sci., Ser. C* **264,** 832 (1967).
109. Pankratov, A. V., *Usp. Khim.* **32,** 336 (1963).
110. Pankratov, A. V., and Sokolov, O. M., *Russ. J. Inorg. Chem. (Engl. Transl.)* **11,** 801, (1966).
111. Pankratov, A. V., Sokolov, O. M., and Savenkova, N. I., *Russ. J. Inorg. Chem. (Engl. Transl.)* **9,** 1095 (1964).
112. Pannetier, G., *C.R. Hebd. Seances Acad. Sci.* **233,** 168 (1951).
113. Pannetier, G., and Lecamp, M., *Bull. Soc. Chim. Fr.* p. 1068 (1954).

114. Popov, A., and Mannion, J., *J. Am. Chem. Soc.* **74,** 222 (1952).
115. Raschig, F., *Ber. Dtsch. Chem. Ges.* **41,** 4194 (1908).
116. Reichardt, C., "Solvent Effects in Organic Chemistry," Vol. 3. Verlag Chemie, Weinheim and New York, 1979.
117. Rice, W. W., Jr., *U.S. At. E. C.* **LA-4689** (1971); *Chem. Abstr.* **76,** 40,003 (1972).
118. Rice, W. W., Jr., and Jensen, R. J., *J. Phys. Chem.* **76,** 805 (1972).
119. Roesky, H. W., Glemser, O., and Bormann, D., *Angew. Chem.* **76,** 713 (1964); *Angew. Chem., Int. Ed. Engl.* **3,** 701 (1964); *Chem. Ber.* **99,** 1589 (1966).
120. Ruschke, P., Dissertation, Universität Marburg (1980).
121. Ruschke, P., and Dehnicke, K., *Z. Naturforsch., B: Anorg. Chem., Org. Chem.* **35B,** 1589 (1980).
122. Sasaki, T., Kanematsu, K., and Yukimoto, Y., *Chem. Lett.* p. 1005 (1972).
123. Seybold, D., and Dehnicke, K., *J. Organomet. Chem.* **11,** 1 (1968).
124. Shihada, A.-F., and Dehnicke, K., *J. Organomet. Chem.* **26,** 157 (1971).
125. Smolinsky, G., and Pryde, C. A., *J. Org. Chem.* **33,** 2411 (1968).
126. Spencer, D. A., *J. Chem. Soc.* **127,** 216 (1925).
127. Strähle, J., *Z. Anorg. Allg. Chem.* **375,** 238 (1970); **380,** 96 (1971).
128. Strähle, J., *Z. Anorg. Allg. Chem.* **405,** 139 (1974).
129. Strähle, J., and Bärnighausen, H., *Z. Anorg. Allg. Chem.* **357,** 325 (1968).
130. Strähle, J., and Dehnicke, K., *Z. Anorg. Allg. Chem.* **338,** 287 (1965).
131. Tamura, Y., Chun, M. W., Kwon, S., and Bayomi, S. M., *Chem. Pharm. Bull.* **26,** 3315 (1978).
132. Tamura, Y., Chun, M. W., Nishida, H., Kwon, S., and Ikeda, M., *Chem. Pharm. Bull.* **26,** 2866 (1978).
133. Tamura, Y., Haruta, J., Bayomi, S. M., Chun, M. W., Kwon, S., and Ikeda, M., *Chem. Pharm. Bull.* **26,** 784 (1978).
134. Treinin, A., *in* "The Chemistry of the Azido Group (S. Patai, ed.), p. 11ff. Wiley (Interscience), 1971.
135. Walker, I., Strähle, J., Ruschke, P., and Dehnicke, K., *Z. Anorg. Allg. Chem.* **487,** 26 (1982).
136. Weidlein, J., Müller, U., and Dehnicke, K., "Schwingungsspektroskopie," p. 27. Thieme, Stuttgart, 1982.
137. Weishaupt, M., and Strähle, J., *Z. Anorg. Allg. Chem.* **429,** 261 (1977).
138. Wellern, H. O., and Müller, U., *Chem. Ber.* **109,** 3039 (1976).
139. Wiberg, N., and Schmid, K. H., *Chem. Ber.* **100,** 748 (1967).
140. Woodgate, P. D., Lee, H. H., Rutledge, P. S., and Cambie, R. C., *Synthesis* p. 462 (1977).
141. Zbiral, E., and Ehrenfreund, J., *Tetrahedron* **27,** 4125 (1971).
142. Dörner, H., Dehnicke, K., Massa, W., and Schmidt, R., *Z. Naturforsch., B: Anorg. Chem., Org. Chem.* (in press).

GASEOUS CHLORIDE COMPLEXES CONTAINING HALOGEN BRIDGES

HARALD SCHÄFER

Universität Münster, Münster, Westphalia, Federal Republic of Germany

I. Introduction

Several authors have already reviewed gaseous halide complexes from different points of view. Particular mention must be made of the following: Novikov and Gavryuchenkov (*78*), *Complex halides in vapors at high temperatures* (1967); Büchler and Berkowitz-Mattuck (*20*), *Gaseous ternary compounds of the alkali metals* (1967); Hastie (*50*), Section in *High Temperature Vapors* (1975); Schäfer (*110*), *Gasförmige*

Copyright © 1983 by Academic Press, Inc.
All rights of reproduction in any form reserved.
ISBN 0-12-023626-5

Chloridkomplexe mit Halogenbrücken; Homöokomplexe und Heterokomplexe (1976); see also (*106–108, 111–113*); Emmenegger (*37*), *Stability of gaseous complexes between two- and three-valent metal halides* (1977); Øye and Gruen (*83*), *Metal halide-group III halide vapor complexes with emphasis on aluminum chloride* (1979); Papatheodorou (*91*), *Spectroscopy, structure and bonding of high-temperature metal halide vapor complexes* (1980).

This chapter deals particularly with publications that have appeared in recent years, especially on the chloride complexes that have been investigated most frequently and above all on systematic thermodynamics in relation to coordination relationships. This allows a critical assessment of data and useful estimates for systems that have not as yet been investigated. In addition, an account is given of practical experience in the use of such complexes.

II. General Review

By determining molecular weights by Dumas' method, Sainte-Claire Deville and Troost (*103*) found as early as 1857 that the gaseous chlorides of aluminum and of trivalent iron were present as dimers. Almost 100 yr later mass-spectrometric investigations by Ionov (*55*) showed the vapors of the alkali halides to contain a more or less large proportion of the dimers. In addition, a very small proportion is present as still larger aggregates (*38, 156*). We now know that most chlorides form gaseous dimers in addition to monomers, though often to only a small degree (*110, 117*).

The simplest types of gaseous complexes are mixed dimers [Eq. (1)], many of which have been detected qualitatively (*13*).

$$0.5\ A_2Cl_{2n}(g) + 0.5\ B_2Cl_{2m}(g) = ABCl_{(n+m)}(g)$$

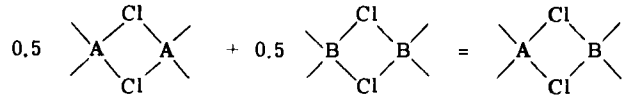

(1)

This reaction, first formulated by Novikov (*78*), takes place without change in the coordination numbers (C.N.) of A and B. It is therefore to be expected that ΔH for such reactions should lie close to 0 kcal. For alkali-free complexes this does in fact prove to be the case, $\Delta H_1^0 = 0 \pm 3$ kcal (*110*). The reaction entropy is also close to 0 cal/K; $\Delta S_1^0 = 0 \pm 2$ cal/K. For alkali-containing complexes, on the other hand, ΔH_1^0 is

significantly negative, but it is yet always capable of being estimated with a useful degree of accuracy (Section IV).

Because dimerization enthalpies are known for some 50 chlorides (*110*), it follows from a consideration of the possible combinations of them that stabilities can be predicted for the expected 1225 complexes of this type (Eq. 1). In addition, there are numerous other types of complexes the stability of which is also predictable on the basis of coordination relationships (Section V). It must be borne in mind that gaseous halide complexes may be significant in all equilibrium systems containing two or more gaseous chlorides (halides).

Most investigations have been concerned with chloride systems, and discussion of these therefore predominates here. In addition, however, extensive mass-spectrometric studies have been made on the formation of complexes by alkali fluorides (*148*). Other coordinatively unsaturated fluorides are as a rule of low volatility and, as a result, little suited for complex formation (or as yet not investigated). Also, little work has been done with bromides and iodides (Section V,B,5).

Good complex-forming species are those that are relatively quite volatile and with saturated vapors that contain appreciable concentrations of dimer. This leads to three groups of complex-forming compounds: alkali chlorides (Section IV), trichlorides ($AlCl_3$, $GaCl_3$, $InCl_3$, $FeCl_3$), (Section V), and uranium(V) chloride (Section VI). Other complexes will not be dealt with here, but see Binnewies and Schäfer (*13, 15*).

III. Methods for the Study of Thermodynamic Properties

Equilibria that are established in the reaction of, for example Al_2Cl_6 (g) with a solid or, in exceptional cases, a liquid component, (e.g., MCl, MCl_2, or MCl_3) are studied by the following methods: entrainment methods (see, e.g., *32, 165*); spectrophotometry (see, e.g., *82, 86*); mass spectrometry with double cells (see, e.g., *10, 123*); total-pressure measurements, in certain cases without a solid phase (see, e.g., *79*); labeling with radioactive isotopes and measurement of the activity in the gaseous phase (*94*); distillation at a predetermined pressure and analysis of the condensate (*80, 158*); quenching methods (see, e.g., *165*); and chemical transport in a temperature gradient (*136, 140*). The last two methods are particularly suitable for obtaining supplementary information.

A method that always permits the detection of several complexes in the presence of one another and therefore permits the measurement of

a specific complex in frequently occurring mixtures is mass spectrometry (with double cells); see, for example, $Pd_2Al_2Cl_{10}$ (*40*), $CoAl_3Cl_{11}$ (*124*). In favorable cases [$CuCl_2/GaCl_3$ (*35*)] spectrophotometry also allows the direct determination of two complexes in the presence of one another. As a rule, however, all of the methods apart from mass spectrometry give only the overall effect, which may then be divided among the various complexes by calculation. Clearly, this is meaningful only if the accuracy of measurement is high and there is a wide variation in the conditions of measurement. If the second phase is liquid, it is without exception necessary to have information or to make assumptions on the activity of the components in the melt.

IV. Complexes Formed by Alkali Halides

A. Thermodynamic Considerations

Numerous combinations ACl/MCl_n (A = alkali) have now been investigated. Frequently, however, only qualitative or relatively inexact results are obtained for complex formation from the monomers (e.g., ΔH with error limits of ± 5 kcal or more). We therefore restrict ourselves to a critical selection of the published material.

Complex formation is represented as in Eq. (1) with the combination of the dimers [dimerization enthalpy according to (*110*)]. Equation (2) may then be written for alkali-containing complexes as

$$0.5A_2Cl_2(g) + 0.5M_2Cl_{2n}(g) = AMCl_{(n+1)}(g) \tag{2}$$

$$\Delta H^0(AMCl_{n+1}) = 0.5\Delta H^0(A_2Cl_2) + 0.5\Delta H(M_2Cl_{2n}) + Y$$

The quantity Y equals zero for alkali-free compounds [Eq. (1)], but it is an important (negative) quantity for those containing alkali. If Eq. (2) is considered in terms of the Pauling derivation of electronegativities, Y will include the difference in electronegativities of A and M. This effect is, however, reduced by the bridging Cl atoms. It is therefore understandable that the influence of Y operates to a significant extent only for complexes containing alkalis (Table I).

In the series $LiCl–CsCl/MCl_x$ it will be recognized that Y for a particular MCl_x (M = Sc, Al, Ga) varies parallel with the difference in electronegativity (*122, 143*). It is unknown at present if it is possible to have a single systematic treatment of the Y values for all MCl_x species because of the uncertainty in the values of Y and also of the electronegativities. For complexes formed by two alkali chlorides, reference may

TABLE I

FORMATION OF GASEOUS COMPLEXES FROM THE DIMERS ACCORDING TO EQ. (2)[a]

	A				
	Li	Na	K	Rb	Cs
$AMgCl_3$		5.7 (*143*)			
$AScCl_4$	7.8 (*141*)	9.9 (*166*)	11.2 (*167*)	10.8 (*168*)	11.4 (*142*)
$AAlCl_4$	11.6 (*69*)	12.2 (*69*)	18.3 (*69*)		
$AFeCl_4$		8.8 (*102*)			
$AGaCl_4$	9.7 (*122*)		16.6 (*122*)		$\geqq$ 18.4 (*122*)

[a] Values for $-Y$ are given in kilocalories.

be made to Schäfer (*110*), who also has given ΔG^0 values for the formation of $ALnCl_4$ complexes.

The larger A_2MCl_{n+2} and $A_2M_2Cl_{2n+2}$ complexes must also be discussed in addition to $AMCl_{n+1}$ (A = alkali). As far as is known at present, the simplest complexes $AMCl_{n+1}$ predominate, as a rule. It is nevertheless advisable to test this relationship from case to case.

In addition to $AMCl_{n+1}$, the following are examples of some of the complexes detected qualitatively: A_2AgCl_3, AAg_2Cl_3 (*160*); $NaCu_2Cl_3$ (*44*); $Na_2Zn_2Cl_6$ (*16*); A_2GaCl_5, $A_2Ga_2Cl_8$ (*122*); and Na_2ScCl_5 and $Na_2Sc_2Cl_8$ (*166*). Analogous complexes are known for fluorides [e.g., Na_2BeF_4, $Na_2Be_2F_6$, and $Na_2Al_2F_8$ (*150*)]. Measured values of ΔH^0 are available for the dimerization of some chloride complexes:

$$2NaMgCl_3(g) = Na_2Mg_2Cl_6(g) \qquad (3)$$
$$\Delta H^0(298) = -44.8 \text{ kcal } (143)$$

$$2LiScCl_4(g)\ \ Li_2Sc_2Cl_8(g) \qquad (4)$$
$$\Delta H^0(298) = -39.1 \text{ kcal } (141);\ \Delta S^0(298) = -33.9 \text{ cal/K}$$

$$2KGaCl_4(g) = K_2Ga_2Cl_8(g) \qquad (5)$$
$$\Delta H^0(298) = -34.4 \text{ kcal } (122)$$

B. STRUCTURES

Structural determinations by electron diffraction are possible so far only for the simplest complexes present in relatively high concentration.

Considering the $AMCl_4$ molecule, A may be situated at an apex, an edge, or a face of the MCl_4 tetrahedron. As a rule, A, corresponding with Eq. (1), is found at the tetrahedral edge (C_{2v} symmetry). Bonding

of A to the relatively rigid MCl_4 tetrahedron is, however, only loose, so that A may possibly also occupy to a small extent other positions (with fluctuation), of $KAlCl_4$ (*49, 153*). In the extreme case of $CsAlCl_4$, Cs is even found on a face of the $AlCl_4$ tetrahedron (C_{3v} symmetry) (*96*). It is possible that the special stability (the large value for $-Y$) of $CsGaCl_4$ depends on this fact (Table I). Various structures may also be envisaged for larger molecules where M is always surrounded tetrahedrally by Cl.

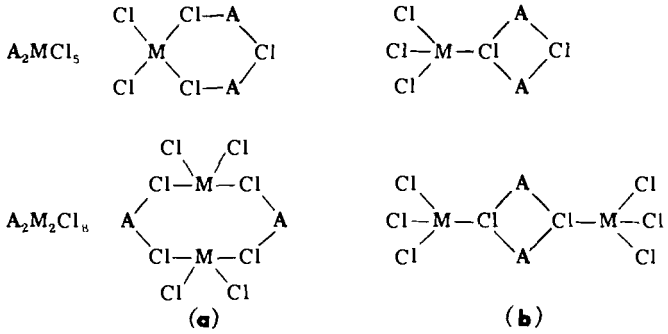

Structure **a**, with the larger ring, has been proposed for fluorides by Sholts and Siderov (*148*). Our mass-spectrometric observations on the fragmentation of $K_2Ga_2Cl_8$, which produces the K_2Cl^+ fragment, however, indicate structure **b** (*122*). This may be seen in relation to the special stability of alkali chloride dimers.

V. Trichlorides LCl_3 [L = Al, Ga, In, Fe(III), Sc] as Complex-Forming Species

Aluminum chloride is a specially suitable compound for complex formation. The first such investigation was by W. Fischer, who in 1949 detected the existence of $NaAlCl_4$ by the entrainment method (*39*). Dewing's work in 1970 on the complexes of dichlorides with $AlCl_3$ and $FeCl_3$ (*32*) gave an important further impulse to the subject.

A. MCl/LCl_3

Complexes containing alkali (M = alkali) have been dealt with already in Section IV. There are qualitative observations on the following: $AlCl_3$ complexes with CuCl (*14, 119*), AgCl (*119*), and InCl (*101*);

$GaCl_3$ complexes with GaCl (*22, 118*); $InCl_3$ complexes with CuCl (*14*), InCl (*118*), InCl, and TlCl (*22*); and $FeCl_3$ complexes with AgCl (*57*). Quantitative mass spectroscopy of the complicated $CuCl/AlCl_3$ (*137*) system lead to the conclusion that Cu_3AlCl_6 and $Cu_2Al_2Cl_8$, and not $CuAlCl_4$ (*66*), are the actual gaseous complexes.

$$3CuCl(s) + 0.5\ Al_2Cl_6(g) = Cu_3AlCl_6(g) \quad (6)$$

$$\Delta H^0(590) = 19.0 \text{ kcal}; \Delta S^0(590) = 20.3 \text{ cal/K}$$

$$2CuCl(s) + Al_2Cl_6(g) = Cu_2Al_2Cl_8(g) \quad (7)$$

$$\Delta H^0(590) = 5.9 \text{ kcal}; \Delta S^0(590) = 5.3 \text{ cal/K}$$

With $Cu_4Cl_4(g)$ these data may be combined to give

$$Cu_4Cl_4(g) + Cu_2Al_2Cl_8(g) = 2Cu_3AlCl_6(g) \quad (8)$$

$$\Delta H^0 = -2.5 \text{ kcal}; \Delta S^0 = 2.0 \text{ cal/K}$$

As expected, these values lie close to zero. It might be supposed that the complexes would have the same cubic structure as that postulated for Cu_4Cl_4 (*137*). Because, however, this would lead to an unusual coordination of Al[C.N.(Al) = 5], a ring structure with C.N.(Al) = 4 is probably more likely. Recently a ring structure for Cu_4Cl_4 has also been shown to be likely (*74*).

One may suppose that all $CuCl/LCl_3$ and $AgCl/LCl_3$ complexes would have structures like those found for $CuCl/AlCl_3$. On the other hand, we assume that LCl_3 forms "normal" complexes with GaCl, InCl and TlCl and that ΔH for their formation from the dimers is close to zero (Eq. 1). A small amount of Tl_2InCl_5 has been observed mass spectroscopically in addition to $TlInCl_4$ (*14*).

B. MCl_2/LCl_3

The complexes formed from dichlorides and aluminum trichloride are by far the most fully studied and are therefore given prominence here. Complexes formed with $GaCl_3$, $InCl_3$, $FeCl_3$, and $ScCl_3$ will, however, also be dealt with.

The following types of compounds have been observed so far with L = Al:

$MAlCl_5$	MAl_2Cl_8	MAl_3Cl_{11}	MAl_4Cl_{14}
	$M_2Al_2Cl_{10}$		
	$M_3Al_2Cl_{12}$		

In the medium-temperature range (~400–600°C) the type encountered most frequently over solid MCl_2 is MAl_2Cl_8. With increasing temperature $MAlCl_5$ and $MCl_2(g)$ become increasingly significant. Complexes richer in $AlCl_3$ occur at lower temperatures (and higher Al_2Cl_6 pressure) in addition to MAl_2Cl_8, and also in special cases. It is shown, however, in Section B,1, that the particular formula type predominating depends also on the relative stability of the coexisting solid phase $MCl_2(s)$. Complexes of the type $M_2Al_2Cl_{10}$ are observed mass spectroscopically with M = Pd (*40*) or Be (*100*) as is $M_3Al_2Cl_{12}$ with M = Be (*100*). Here the close relationship to the structures of the solid dichlorides is already apparent (see Sections B,1 and 3).

1. Complex Type and the Coordination of M

It is clear from Eqs. (9) and (10) that a greater stability of MCl_2 leads to formation of complexes richer in $AlCl_3$.

$$MCl_2(s) + MAl_2Cl_8(g) = 2MAlCl_5(g) \quad (9)$$

$$MCl_2(s) + 2MAl_3Cl_{11}(g) = 3MAl_2Cl_8(g) \quad (10)$$

TABLE II

COMPLEX TYPE AND COORDINATION OF M IN $MCl_2(s)$ AND IN THE COMPLEX[a]

	Gaseous complex present				
	$MAlCl_5$	MAl_2Cl_8	MAl_3Cl_{11}	MAl_4Cl_{14} (+ MAl_3Cl_{11})	Al_2Cl_6
	Hg	Be to Cd (Table III)	Ti, V	Eu	Mo
C.N. in $MCl_2(s)$	2(+2+2)	4, 4(+2), or 6	6 + M − M[b]	7(+2)	4 + M − M[c]
C.N. of M in the complex	3	4 or 6	6	6	—

[a] C.N., Coordination number. The Cl ligands in parentheses have only a small influence because of their greater distance from M. It can be seen that $HgAlCl_6$ is relatively more stable because of the greater coordination number compared to that of $HgCl_2(s)$. With $EuAl_4Cl_{14}$ or $EuAl_3Cl_{11}$, for example, the reverse relationship holds.

[b] Magnetic measurements indicate the presence of M—M bonds and thus greater stability.

[c] $MoCl_2$ has the structure $[Mo_6Cl_8]Cl_2Cl_{4/2}$ with relatively strong M—M bonds and therefore forms no $AlCl_3$ complexes; the $AlCl_3$-rich compound Al_2Cl_6 is present in addition to $MoCl_2$.

The coordination relationships serve as a measure of the stability of $MCl_2(s)$ (*126*) rather than the sublimation enthalpies, which are strongly influenced by the bond distances and angles in $MCl_2(g)$.

2. Complexes of the Type $MLCl_5$

a. Qualitative Observations of $MLCl_5$. $AlCl_3$ complexes with M(II) = Fe (*11*); Mn, Co, Ni, Mg, Sn, Pb (*12*); Pd (*40*); and Hg (*79*). $GaCl_3$ complexes with M(II) = Ge (*114*). $InCl_3$ complexes with M(II) = Be (?), Sn, and Zn (*13*). $FeCl_3$ complexes with M(II) = Be (?) (*13*). $ScCl_3$ complexes with M(II) = Ca, Sr, and Ba (*169*).

b. Thermodynamic Investigations. $CuAlCl_5$ is observed in small concentrations at relatively low temperatures in addition to $CuAl_2Cl_8$ (*165*). $HgAlCl_5$ is found mass spectroscopically to be the only complex. Equation (11) is valid for combination of the dimers (*126*); [for the dimerization enthalpy see Schäfer (*110*)].

$$0.5Hg_2Cl_4(g) + 0.5Al_2Cl_6(g) = HgAlCl_5(g) \qquad (11)$$

$$\Delta H^0(298) = 1.2 \text{ kcal}; \Delta S^0(298) = -2 \text{ cal/K}$$

Values of ΔH^0 of 0.4, 1.0, and 0.4 kcal were found mass spectroscopically for Eq. (12) with M = Mn, Co, or Ni (*12*), taking an estimated ΔS^0 value of 0 cal/K.

$$0.5M_2Cl_4(g) + 0.5Al_2Cl_6(g) = MAlCl_5(g) \qquad (12)$$

When M = Cr, ΔH^0 = 7 kcal, which may indicate the presence of a Cr—Cr bond in Cr_2Cl_4. Analysis of systems containing $MLCl_5$ and ML_2Cl_8 leads to Eqs. (14)–(18).

The literature gives mostly thermodynamic values for

$$MCl_2(s) + LCl_3(g) = MLCl_5(g) \qquad (13)$$

These, with $\Delta H^0(MCl_2, \text{subl. } T)$ (*7*), $\Delta C_p(g)$ = 3 cal/K, and the dimerization enthalpies (*110*) then yield the ΔH^0 values shown in Eqs. (14)–(18), with an uncertainty of about ±3 kcal.

$$0.5Cu_2Cl_4(g) + 0.5Ga_2Cl_6(g) = CuGaCl_5(g) \qquad (14)$$

$$\Delta H^0(298) = +0.3 \text{ kcal } (35)$$

$$0.5Cu_2Cl_4(g) + 0.5In_2Cl_6(g) = CuInCl_5(g) \qquad (15)$$

$$\Delta H^0(298) = -1.2 \text{ kcal } (36)$$

$$0.5Co_2Cl_4(g) + 0.5In_2Cl_6(g) = CoInCl_5(g) \quad (16)$$

$$\Delta H^0(298) = +1.3 \text{ kcal } (34) -2.1 \text{ kcal } (62)$$

$$0.5Ni_2Cl_4(g) + 0.5In_2Cl_6(g) = NiInCl_5(g) \quad (17)$$

$$\Delta H^0(298) = -4.9 \text{ kcal } (33)$$

The value of ΔH^0 for Eq. (18) with M = Mg, Ca, or Mn is known only approximately (*36*).

$$0.5M_2Cl_4(g) + 0.5In_2Cl_6(g) = MInCl_5(g) \quad (18)$$

$$\Delta H^0(298) = (-2.5) \text{ kcal}$$

Measurements of the total pressure (*23*) or preliminary mass spectroscopic measurements (*14*) lead to

$$0.5Zn_2Cl_4(g) + 0.5In_2Cl_6(g) = ZnInCl_5(g) \quad (19)$$

$$\Delta H^0(298) = +3.7 \text{ kcal } (23), +2.8 \text{ kcal } (14)$$

Equations (20)–(21) also result from mass spectrometric measurements.

$$0.5Sn_2Cl_4(g) + 0.5In_2Cl_6(g) = SnInCl_5(g) \quad (20)$$

$$\Delta H^0(298) = +0.9 \text{ kcal } (14)$$

$$0.5Mg_2Cl_4(g) + 0.5Sc_2Cl_6(g) = MgScCl_5(g) \quad (21)$$

$$\Delta H^0(298) = -0.7 \text{ kcal}; \Delta S^0(298) = +2.0 \text{ cal/K } (169)$$

Combination of trimers to form complexes also fits into this scheme:

$$\tfrac{2}{3}Mg_3Cl_6(g) + \tfrac{1}{3}Sc_3Cl_9(g) = Mg_2ScCl_7(g) \quad (22)$$

$$\Delta H^0(298) = -0.1 \text{ kcal } (169)$$

$$\tfrac{1}{3}Mg_3Cl_6(g) + \tfrac{2}{3}Sc_3Cl_9(g) = MgSc_2Cl_8(g) \quad (23)$$

$$\Delta H^0(298) = -2.5 \text{ kcal } (169)$$

Over all it seems reasonable to maintain that one is justified in formulating the reaction equations in such a way that the coordination numbers of the atoms remain unchanged. In this case ΔH^0 is zero (kcal) within the limits of error of the measurements. For $CoInCl_5$ and LCl_3 (L = Al, Ga, In) this constancy of C.N. also corresponds with indications based on the spectra (*91*). The entropy change of such reactions is also close to zero. The value of ΔS^0 would be weakly positive if

symmetry numbers alone were decisive for ΔS^0, but this is not yet apparent from the experiments.

c. Estimation of ΔH *Values According to Hastie (50).* For the sake of completeness the following methods may be mentioned.

i. Additivity of bonding increments. On the basis of bonding enthalpies D in the monomers AX and BX_3 (X = halogen) and in their dimers A_2X_2 and B_2X_6, D(bridge) $\cong$ 0.6 ($\pm$0.04) $\cdot$ D(terminal). From this it follows that

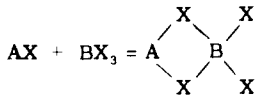

(24)

$$\Delta H \cong [D(\text{A—X}) + 3D(\text{B—X})] - [2 \cdot 0.6D(\text{A—X}) + 2 \cdot 0.6D(\text{B—X}) + 2D(\text{B—X})]$$
$$\cong -0.2[D(\text{A—X}) + D(\text{B—X})]$$

Because of the large contribution of D(A—X) and D(B—X), the result depends largely on the magnitude and reliability of these values and of the numerical factor.

ii. Ionic model. If we take

$$A_2X_2 + B_2X_6 = 2ABX_4 \tag{25}$$

as an example, the balance of the cation–cation repulsion potentials ΔU may be used as a measure of the relative values for ΔH.

$$\Delta U = [6/(r_A + r_B)] - (\tfrac{1}{2}r_A + \tfrac{8}{2}r_B)$$

Graphical representation of the experimental values of ΔH as a function of ΔU enables rough estimates of unknown values of ΔH to be made. These methods (*i, ii*) do not of course lead to the minimum accuracy of $\pm \leq 3$ kcal, which is necessary in these systems for thermodynamic purposes.

3. *Complexes of the Type* ML_2Cl_8

a. Qualitative Observations with Ml_2Cl_8. $AlCl_3$ complexes with M(II) = Be (*100, 146*); Mg, Cr, Mn, Co (*12*); Ca, Ba, Pb (*119*); Cr (*65, 129*); Cr, Co, Pd (*10*); Fe (*11*); Fe, Co, Ni, Cu, Pd, Pt (*119*); Mn, Fe, Co, Ni, Cu, Pd (*134*); Zn, Cd, Pb (*32*); Ti (*18*); Pd (*40*); and Sm (*93*). $GaCl_3$ complexes with M(II) = Co, Ni (*119*); Ca, Cr, Co, Cu, and Pd (*140*).

$InCl_3$ complexes with M(II) = Be (*13*). $FeCl_3$ complexes with M(II) = Be (*13*); Fe, Cu (*119*); and Fe (*11*).

b. Thermodynamic Investigations with ML_2Cl_8. $AlCl_3$ complexes with M(II) = Mg, Ca, Mn, Co, Ni (*32*); Co (*31, 88, 163*); Ni (*67*); Pd (*75, 86*); Pt (*85*); Cr (*2, 132*); Cu (*37, 159, 165*); Co, Ni, Cu (*136*); Be, Fe, Zn, Cd, Pt (*125*); and Fe (*91*). $GaCl_3$ complexes with M(II) = Co (*4, 37*) and Cu (*35, 159*). $InCl_3$ complexes with M(II) = Co (*34, 62*); Mg, Ca, Mn (*36*); Ni (*33*); and Be (*14*). $FeCl_3$ complexes with M(II) = Mn, Co, Ni, Cd (*32*); Mg, Ca, Sr, and Ba (*37*). $ScCl_3$ complexes with M(II) = Mg (*169*).

c. Bonding Relationships and Thermodynamic Models. In 1970 Dewing (*32*) wrote with reference to the relatively small differences in ΔH^0 from equilibrium measurements on the reactions

$$MCl_{2(s)} + 2AlCl_{3(g)} = MAl_2Cl_{8(g)} \qquad (26)$$

$$M = Mg, Ca, Mn, Co, Ni$$

> The stabilities of the complexes are obviously quite unrelated to the vapor pressures of the dichlorides themselves. This is best interpreted by implying that the bonding of the divalent ion in the complexes is very similar to that in the solid, so that the energy of forming the complexes from the solid is essentially constant and does not depend on the energy of separating the solid into individual gaseous molecules [p. 2174].

Like Hastie (Section V,B,2,*c*), Emmenegger (*37*) based his estimates on bond energies. For the combination of gas molecules he formulated the reactions as

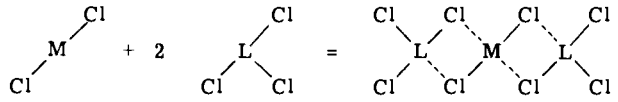

In Eq. (α) 2M—Cl bridges and 2L—Cl bridges are formed. The same is true for Eqs. (β) and (γ). From this it follows that

$$\Delta H^0_{(\alpha)} = \Delta H^0_{(\beta)} + \Delta H^0_{(\gamma)}$$

Starting from solid MCl_2, reaction with L_2Cl_6 leads to

$$MCl_{2(s)} + L_2Cl_{6(g)} = ML_2Cl_{8(g)} \qquad (27)$$

$$\Delta H^0_{(27)} = \Delta H^0_{(\beta)} + \Delta H^0 (MCl_2, \text{subl.})$$

The ΔH^0 values calculated by Emmenegger in this way (*37*) deviate by about 10 or more kcal from the experimental values, which indicates that such estimates are uncertain by several orders of magnitude for the complex concentrations. This relates clearly to the fact that the scheme does not take into consideration the change in the coordination of M. For the same reason the use of the same ΔH^0 for Eqs. (28) and (29) (*36*) is only a very rough approximation.

$$MCl_2(g) + LCl_3(g) = MLCl_5(g) \qquad (28)$$

$$MLCL_5(g) + LCl_3(g) = ML_2Cl_8(g) \qquad (29)$$

A somewhat better but still unsatisfactory estimate is obtained by assuming that $\Delta H^0_{(27)}$ corresponds roughly with the enthalpy of melting of the dichloride (or the tri- or tetrachloride) (*110*).

Very much better estimates for $\Delta H^0_{(27)}$ become possible if one starts from the coordination of M and Cl in the solid dichloride (Table III) (*125*). This contains the mean ΔH^0 values obtained by various authors (see *125*).

This systematic treatment of relative stabilities of the complexes [refer to Eq. (27)] may be understood on the basis that M in the complexes is coordinated by Cl (the same coordination number and a similar arrangement), as in solid MCl_2. The different values for various MCl_2 structures (Table III) are then attributable to different coordination of Cl in $MCl_2(s)$ and $MAl_2Cl_8(g)$. $\Delta H^0_{(27)}$ then becomes smaller the less firmly Cl is bound in the solid dichloride.

In the special case with C.N.(M) = 4 and C.N.(Cl) = 2, the coordination numbers in the solid dichloride are the same as in the gaseous complex. The small ΔH^0 values that still remain (7 kcal) may be attributed principly to the long-range order in the dichloride. Therefore, the ΔH^0 becomes close to zero if the long-range order is removed (or reduced) while the coordination numbers of M and Cl (or Br) remain unchanged [ΔH^0 for $MX_2(s) = \frac{1}{6}M_6X_{12}(g)$ according to Schäfer (*109*)]:

TABLE III

$\Delta H^0(298)$ AND $\Delta S^0(298)$ FOR THE REACTION $MCl_2(s) + Al_2Cl_6(g) = MAl_2Cl_8(g)$ AND THE COORDINATION IN THE SOLID DICHLORIDE

MCl_2	Coordination in $MCl_{2(J)}$	ΔH^0 (kcal)	ΔS^0 (cal/K)	Mean value ΔH^0 (kcal)	Mean value ΔS^0 (cal/K)
$BeCl_2$	$MCl_{4/2}$	(6.0)	—		
$ZnCl_2$	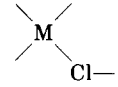	6.8	8.3	7 ± 1	8.5 ± 1
$PdCl_2$		7.0	9.4		
$PtCl_2$		7.9	7.8		
$CrCl_2$	$MCl_{4(+2)/2(+1)}$ 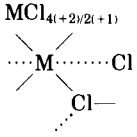	9.0	10.7	9 ± 0.5	11.5 ± 1
$CuCl_2$		9.1	12.4		
$MgCl_2$		14.7?	15.7?		
$CaCl_2$	$MCl_{6/3}$	10.4	7.7		
$MnCl_2$	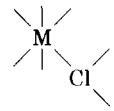	12.8	12.9	12 ± 2	11 ± 3
$FeCl_2$		12.5	13.2		
$CoCl_2$		11.0	11.5		
$NiCl_2$		12.3	9.6		
$CdCl_2$		10.9	8.8		

$$\tfrac{1}{6}Pd_6Cl_{12}(g) + Al_2Cl_6(g) = PdAl_2Cl_8(g) \qquad (30)$$

$$\Delta H^0(298) = -2 \text{ kcal}$$

$$\tfrac{1}{6}Pd_6Br_{12}(g) + Al_2Br_6(g) = PdAl_2Br_8(g) \qquad (31)$$

$$\Delta H^0(298) = -1.2 \text{ kcal}$$

$$\tfrac{1}{6}Pt_6Cl_{12}(g) + Al_2Cl_6(g) = PtAl_2Cl_8(g) \qquad (32)$$

$$\Delta H^0(298) = -1.1 \text{ kcal}$$

Formation and reaction enthalpies are different. Consequently, in general it is not possible to establish a correlation with the structure of only one of the reaction partners. It can, however, be done—as in the present case—if in the reaction the structure (C.N.) of only one of the partners changes significantly. In contrast to this, the influence of the structure on sublimation enthalpies of the dichlorides is not so apparent.

d. Structures. Table III leads to the conclusion that M in the gaseous complexes is coordinated in the same way through Cl as in the solid dichlorides, although distortion of the coordination polyhedra is not excluded. This consideration is also borne out by the absorption spectra of the complexes (*91*). Until recently the interpretation of the spectrum of $CoAl_2Cl_8$ was uncertain [C.N. = 4 or 6 (?)], but measurements on the spectra of mixed halogen complexes of the type $CoAl_2Cl_nI_{8-n}$ (*68*) have now settled the question in favor of a distorted octahedral array round the cobalt atom.

It is noteworthy that compounds of the type MAl_2Cl_8 may also be obtained in a crystalline form at temperatures greater than 200°C. Roentgenographic structure determinations showed that $CuAl_2Cl_8$ (*121*) and $PdAl_2Cl_8$ (*68*) crystallize in a molecular lattice with C.N.(Cu) = 4 (+2) and C.N.(Pd) = 4 the coordination of M corresponding with that in the solid dichloride. $CoAl_2Cl_8$, which is isotypic with the compounds where M = V, Cr, Mn, Fe, Cd (*8*), Ni (*19*), or Ti (*18*), forms a coordination lattice in which Co is surrounded by a distorted octahedral and Al by a tetrahedral arrangement of Cl (*54*). Here then the rearrangement of the molecules from the gaseous to the crystal structure involves no deep-seated changes (*68*).

4. Transition from L = Al to Ga, In, Fe, or Sc in ML_2Cl_8

Starting from the most fully investigated $AlCl_3$ complexes, we may write

$$MAl_2Cl_8(g) + L_2Cl_6(g) = ML_2Cl_8(g) + Al_2Cl_6(g) \tag{33}$$

We must assume here that the coordinations of M and L (or Al) do not change. Therefore, $\Delta H^0_{(33)}$ is expected to be zero. This also implies that $\Delta H^0_{(34)}$ should be independent of whether L = Al or Ga, In, Fe, or Sc:

$$\underset{\Delta H^0_{(34)}}{MCl_2(s) + L_2Cl_6(g) = ML_2Cl_8(g)} \tag{34}$$

With M = Co, ΔH^0 values shown in Eqs. (35)–(38) were measured.

$$CoCl_2(s) + Al_2Cl_6(g) = CoAl_2Cl_8(g) \tag{35}$$

$\Delta H^0(298) = 11.0$ kcal; $\Delta S^0(298) = 11.5$ cal/K (*31, 32, 88, 163*)

$$CoCl_2(s) + Ga_2Cl_6(g) = CoGa_2Cl_8(g) \tag{36}$$

$\Delta H^0(298) \approx 10.9$ kcal; $\Delta S^0(298) = 9.6$ cal/K (*4*)

$$CoCl_2(s) + In_2Cl_6(g) = CoIn_2Cl_8(g) \quad (37)$$

$\Delta H^0(298) = 13.5$ kcal; $\Delta S^0(298) = 11.9$ cal/K (*33*); 11.9 kcal; 10.2 cal/K (*62*); 11.6 kcal; 10.0 cal/K (*35*)

$$CoCl_2(s) + Fe_2Cl_6(g) = CoFe_2Cl_8(g) \quad (38)$$

$\Delta H^0(298) = 17.7$ kcal; $\Delta S^0(298) = 16.4$ cal/K (*32*)

Bearing in mind the evident scatter in the measurements for Eq. (37), the measured values with L = Al, Ga, and In agree closely. The measured values for $CoCl_2/Fe_2Cl_6$ [Eq. (38)], which deviate from those for the related reactions, come from preliminary results; the discrepancy is due to the formation of mixed crystals (solid $CoCl_2$ with $FeCl_2$) arising from the decomposition of $FeCl_3$ (*116*). For further information on this problem see Schäfer (*116*).

For a given value of $P(Ga_2Cl_6, 293\ K) = 0.5$ atm, the dissociation $Ga_2Cl_6 = 2GaCl_3$ results in the value for $P(MGa_2Cl_8)$ passing through a maximum between 600 and 700 K:

$$MCl_2(s) + Ga_2Cl_6(g) = MGa_2Cl_8(g) \quad \text{endothermic} \quad (39)$$

$$MCl_2(s) + 2GaCl_3(g) = MGa_2Cl_8(g) \quad \text{exothermic} \quad (40)$$

With a further temperature increase, $MGaCl_5(g)$ [and $MCl_2(g)$] are formed endothermically:

$$MCl_2(s) + GaCl_3(g) = MGaCl_5(g) \quad \text{endothermic} \quad (41)$$

The temperature dependence of the solubility λ is a measure of the chemical transport of MCl_2 (*105*):

$$\lambda = \frac{\Sigma P(M)}{\Sigma P(Ga)} = \frac{P(MGa_2Cl_8 + MGaCl_5 + MCl_2)}{P(2Ga_2Cl_6 + GaCl_3 + 2MGa_2Cl_8 + MGaCl_5)}$$

The value of λ first rises with T [Eq. (39)] and then falls again [Eq. (40)], finally rising again [Eq. (41)]. Transport to the hotter zone [Eq. (40)] has been experimentally confirmed with M = Ca, Cr, Co, Cu and Pd (*140*). If Eq. (41) is superimposed on Eq. (40), formation of the maximum for λ is hindered. Comparison of the calculated λ/T curves with the results of transport experiments permits a check of the thermodynamic values, introduced with λ (*140*). For smaller $Al_2Cl_6/AlCl_3$

pressures the corresponding MAl_2Cl_8 maxima have been observed mass spectroscopically with M = Mg, Cr, Mn, and Co (*12*).

5. *Comparison of Chlorides with Bromides and Iodides*

If one starts with the assumption that the coordination of M and Al in MAl_2X_8 is the same with X = Cl, Br, or I, and if this also is valid for MX_2, almost equal values for ΔH^0 and ΔS^0 are expected for

$$MCl_2(s) + Al_2Cl_6(g) = MAl_2Cl_8(g) \quad (42)$$

$$MBr_2(s) + Al_2Br_6(g) = MAl_2Br_8(g) \quad (43)$$

$$MI_2(s) + Al_2I_6(g) = MAl_2I_8(g) \quad (44)$$

This is the case with M = Co (Table IV) (*75*). For M = Pd, on the other hand, the value of ΔH^0 increases in the order Cl < Br < I, which is clearly caused by the structures of the solid halides. The α-$PdCl_2$ structure consists of infinite, planar $PdCl_{4/2}$ chains with the Pd atom square-planar coordinated. The $PdBr_2$ structure is similarly made up of $PdBr_{4/2}$ chains, but these are corrugated with differing Pd—Br distances of 2.34 and 2.57 Å (*17*). In the structure of the stable β-form of PdI_2 (*162*) Pd has C.N. = 4(+1+1) [Pd—I = 2.61 Å (4×) and 3.29 or 3.49 Å]. The more distant I atoms increase coordination to octahedral. This increased coordination renders the removal of PdI_2 from the lattice in the process of forming the complex more difficult.

In the analogous MCl_2 systems (Table III), change in the coordination of M in the solid dichloride from C.N. = 4 to 4(+2) raises the ΔH^0 value by about 2 kcal. The behavior of the palladium halides fits almost qualitatively into this picture, although the effect of coordination

TABLE IV

THERMODYNAMIC DATA FOR THE REACTIONS
$MX_2(s) + Al_2X_6(g) = MAl_2X_8(g)$[a]

M	X	$\Delta H^0(298)$ (kcal)	$\Delta S^0(298)$ (cal/K)	References
Co	Cl	11.0	11.5	(*31, 32, 88, 163*)
Co	Br	10.3	10.2	(*92*)
Co	I	10.8	12.4	(*155*)
Pd	Cl	6.7	8.9	(*25, 75*)
Pd	Br	8.3	8.4	(*25, 75*)
Pd	I	(13)	(10)	(*75*)

[a] M = Co, Pd; X = Cl, Br, I (*75*).

on ΔH^0 is apparently greater for iodides than for chlorides. Further investigation of this problem is desirable.

6. *MAl_3Cl_{11} Complexes*

Three complexes are known in the $CoCl_2/Al_2Cl_6$ system, with $CoAl_2Cl_8$ predominating under the usual conditions:

$$CoCl_2(s) + 0.5Al_2Cl_6(g) = CoAlCl_5(g) \quad (45)$$

$\Delta H^0(298) = 34.9$ kcal; $\Delta S^0(298) = 29.2$ cal/K [values combined from (*7*, *12*, *117*)]

$$CoCl_2(s) + Al_2Cl_6(g) = CoAl_2Cl_8(g) \quad (46)$$

$\Delta H^0(298) = 11.0$ kcal; $\Delta S^0(298) = 11.5$ cal/K (values from Table III)

$$CoCl_2(s) + 1.5Al_2Cl_6(g) = CoAl_3Cl_{11}(g) \quad (47)$$

$\Delta H^0(298) = 2.9$ kcal; $\Delta S^0(298) = -4.8$ cal/K [values from Schäfer and Flörke (*124*)]

When M(II) = Ti or V, only the formula of type MAl_3Cl_{11} is found (*5*, *152*), which is understandable on the basis of Table II.

$$TiCl_2(s) + 1.5Al_2Cl_6(g) = TiAl_3Cl_{11}(g) \quad (48)$$

$\Delta H^0(600) = 9.2$ kcal; $\Delta S^0(600) = 5.95$ cal/K

$$VCl_2(s) + 1.5Al_2Cl_6(g) = VAl_3Cl_{11}(g) \quad (49)$$

$\Delta H^0(730) = 4.5$ kcal; $\Delta S^0(730) = -6.1$ cal/K

The values for the formation of VAl_3Cl_{11} show it to be somewhat less stable than $CoAl_3Cl_{11}$, which may be explained by the presence of V—V bonds in VCl_2 (see Section V,B,1). The values for $TiAl_3Cl_{11}$ formation (Eq. 48), particularly the entropy, do, however, leave some questions open.

Structures α, β, γ, and δ must be considered, δ with C.N.(M) = 4 being unlikely in view of the MCl_2 structures with C.N.(M) = 6. In fact the absorption spectrum of VAl_3Cl_{11} indicates that there is octahedral coordination of V(II) (*91*). Further $AlCl_3$-rich complexes are considered in Section V,D.

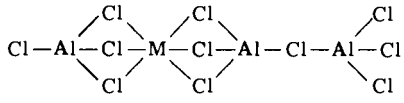

(α)

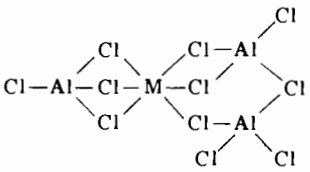

(β)

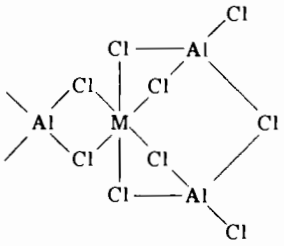

(γ)

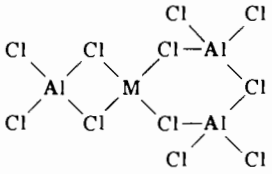

(δ)

C. MCl_3/LCl_3 ($MLCl_6$, ML_2Cl_9, ML_3Cl_{12})

1. Qualitative Observations

$AlCl_3$ complexes with M(III) = Cr (*3, 63, 64, 132*); Fe (*42, 77, 145*); Sc, Y, La (*119*); Ln (*157, 172*); Nd (*47*); Tb (*27, 94*); Ho, Er, Tb (*51*); Ho (*53*); Er (*9, 26, 27, 89, 91*); U (*99*); and Actinides (*173*). $GaCl_3$ complexes with M(III) = Er (*9, 89, 91*). $InCl_3$ complexes with M(III) = Er (*9, 89, 91*). $FeCl_3$ complexes with M(III) = Y (*119*) and Au (*48*).

2. Thermodynamic Investigations

$AlCl_3$ complexes with M(III) = Ti (*130, 152*); V (*5, 128*); Ti, V, Sc, Nd (*127*); Fe (*147*); Nd (*82*); Sm (*93*); Gd (*29*); Ho (*94*); Ga (*1*); In (*22*); and Bi (*60*). $GaCl_3$ complexes with M(III) = Nd (*41*) and In (*21*). $InCl_3$ complexes with M(III) = Ga (*21*). $FeCl_3$ complexes with M(III) = Gd (*29*). The following complexes have been described in these systems: $MLCl_6$, ML_2Cl_9, ML_3Cl_{12}, and ML_4Cl_{15}. At higher temperatures complexes poorer in LCl_3 predominate. Quantitative results are collected in Table V. For ML_4Cl_{15}, see also Section V,D.

TABLE V

COMPLEXES FROM MCl_3(s) AND nL_2Cl_6(g) (n = 0.5, 1.0, 1.5)

Type	Complex[a]	T (K)	$\Delta H^0(T)$ (kcal)	$\Delta S^0(T)$ (cal/K)	References
α	$TiAlCl_6$	298	19.6	24.1	(*127, 152*)
		298	22.7 ± 0.5	21.3 ± 3	(*127*)
	$VAlCl_6$	298	25.8	27.8	(*5, 127*)
		298	25.6 ± 0.5	23.0 ± 3	(*127*)
	$FeAlCl_6$	298	17.3	30.2	(*147, 156*)
	$ScAlCl_6$	298	39.6 ± 3	33.4 ± 3	(*127*)
	$NdAlCl_6$	298	37.5 ± 3	26.3 ± 3	(*127*)
	$NdGaCl_6$	298	34.9	28.2	(*41, 127*)
β	$AlAl_2Cl_9$	298	8.8	10.3	(*123, 156*)
	$TiAl_2Cl_9$	770	(−10.3)	(−22.8)	(*152*)
	VAl_2Cl_9	695	13.1	6.9	(*5*)
γ	$NdAl_3Cl_{12}$	815	10.6	+2.3	(*82*)
	$SmAl_3Cl_{12}$	700	6.7	−1.0	(*93*)
	$GdAl_3Cl_{12}$	750	8.1	+2.4	(*29*)
	$GdFe_3Cl_{12}$	800	(−12.7)[b]	(2.4)[b]	(*29*)

[a] M is equivalent to the first element in the formula.
[b] Preliminary values; estimated ΔS^0 (*29*).

a. Complexes of Type α (Table V). No systematic order is discernable in the ΔH^0 values for the formation of the gaseous $MLCl_6$ complexes from solid MCl_3 and gaseous L_2Cl_6 (Table V). If, however, the process is associated with the combination of the dimers, it would be expected that ΔH^0 would approximate zero (Table VI).

b. Complexes of Type β (Table V). The molecule Al_3Cl_9, which has been detected mass spectroscopically, is included in the series of MAl_2Cl_9 complexes (Table V). It is natural to postulate a ring structure with C.N. = 4 for all the metal atoms in the MAl_2Cl_9 complexes, and this is also in agreement with the spectra of VAl_3Cl_9 (and $VAlCl_6$) (*5, 91*). The general reaction will accordingly take place without change in the coordination numbers. Approximately equal thermodynamic values are to be expected for all of the M atoms, and ΔH^0 should be weakly negative because of the flexibility of the ring. With M = Al, $\Delta H_{50}{}^0(298) = -5.05$ kcal and $\Delta S_{50}{}^0(298) = -20.4$ cal/K (*123*). Results for the dimerization of VCl_3 are lacking for the corresponding evalua-

TABLE VI

COMBINATION OF DIMERS TO FORM COMPLEXES[a]

	$MLCl_6$					
	$ScAlCl_6$	$TiAlCl_6$	$FeAlCl_6$	$GaAlCl_6$	$InAlCl_6$	$GaInCl_6$
ΔH^0 (kcal)	+1.4	−0.6	0 (±0.5)	−0.65	−1.85 (±1.5)	−0.7
References	(*127*)	(*6, 7, 127*)	(*147*)	(*1*)	(*22*)	(*21*)

[a] $0.5M_2Cl_6(g) + 0.5L_2Cl_6(g) = MLCl_6(g)$; $\Delta H^0(298)$.

tion in the case of VAl_2Cl_9. The data for $TiAl_2Cl_9$ clearly do not agree (see later discussion).

$$0.5M_2Cl_6(g) + Al_2Cl_6(g) = MAl_2Cl_9(g) \quad (50)$$

Analogous considerations apply with tetrahedral coordination for all of the metals M, which should lead to data in approximate agreement:

$$MAlCl_6(g) + 0.5Al_2Cl_6(g) = MAl_2Cl_9(g) \quad (51)$$

M = Al: $\Delta H^0(298) = -5.05$ kcal; $\Delta S^0(298) = -20.4$ cal/K (*123*)

M = V: $\Delta H^0(695) = -11.1$ kcal; $\Delta S^0(695) = -17.5$ cal/K (*5*)

M = Ti: $\Delta H^0(770) = -31.50$ kcal; $\Delta S^0(770) = -41.3$ cal/K (*152*)

There is some measure of agreement in the values obtained for M = Al and V, but the values for M = Ti, which are subject to a small correction in the estimation of the main component $TiAlCl_6$ (*152*), deviate markedly. Chemical transport experiments also fail to confirm them (*130*).

c. Complexes of Type γ (Table V). Solid lanthanide chlorides $LnCl_3$ (with Ln = Nd, Sm, or Gd) all have the same UCl_3 structure with C.N. = 9. If Ln in the gaseous complexes is situated between the faces of $3AlCl_4$ tetrahedra, the C.N. will also equal 9. This is feasible with the distances and angles in $SmCl_3(s)$ and $AlCl_4^-$ (*93*). It may be concluded from this that formation of these complexes should occur with approximately similar (and small) values for ΔH^0 and ΔS^0. This is so within the limits of error in the measurements (Table V). In the complexes of the heavier lanthanides a coordination of six for Ln would be expected [corresponding to $CrAl_3Cl_{12}$ (*3*)], as in the solid trichlorides.

3. *Remarks on the Nature of the Bonding in $MLCl_6$*

If one starts from a model with ionic bonding, it would be expected that molecules α and β would have similar stabilities. The repulsion potential of the cations is indeed smaller in $MTiCl_6$ (8) than in Al_2Cl_6 (9). Yet, $MTiCl_6$ molecules have not so far been observed [e.g., no transport of $CoCl_2$ with $TiCl_4$ or $SiCl_4$ (*116*)]. From this it must be concluded that bonding is not purely ionic in nature but that donor–acceptor interaction in the sense of Scheme γ is of real significance (*116*). Structure δ with C.N.(Ti) = 5, which is also conceivable for $MTiCl_6$, is unfavorable, which also follows from the very low stability of Ti_2Cl_8 (*117*); note also the relationship between the dimerization enthalpy and coordination number (*110*).

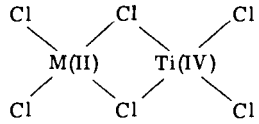

(α)

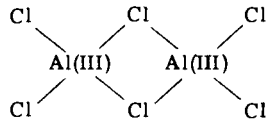

(β)

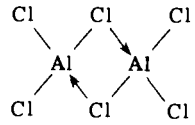

(γ)

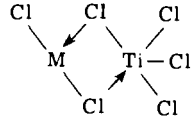

(δ)

D. Complexes Richer in $AlCl_3$

The normal $AlCl_3$ complexes that have been described are able to take up additional $AlCl_3$ (*115*) without change in the coordination

number of M:

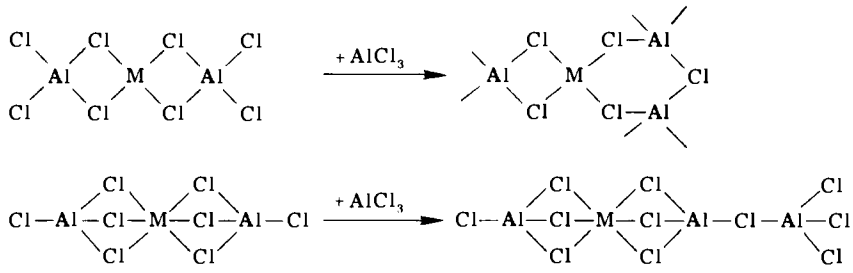

For further structural possibilities see Section V,B,6. One can expect that the energy balance for addition of $AlCl_3$ ($0.5Al_2Cl_6$) will be almost independent of the nature of M. There are direct mass-spectroscopic measurements for such systems only in the case of the equilibria

$$CoAl_2Cl_8(g) + 0.5Al_2Cl_6(g) = CoAl_3Cl_{11}(g) \quad (52)$$

$$\Delta H^0(298) = -7.7 \text{ kcal}; \Delta S^0(298) = -15.7 \text{ cal/K } (124)$$

$$Al_2Cl_6(g) + 0.5Al_2Cl_6(g) = Al_3Cl_9(g) \quad (53)$$

$$\Delta H^0(298) = -5.05 \text{ kcal}; \Delta S^0(298) = -20.4 \text{ cal/K } (123)$$

There are also measurements from which the existence of complexes richer in $AlCl_3$ and their thermodynamic data can be deduced by calculation from the overall composition of the equilibrium gas. This method naturally involves an increased uncertainty. Furthermore, the measurements may be falsified by the occurrence of gaseous oxyhalides (*120*). Table VII shows all the results so far available. Values shown in parentheses (Table VII) for M = Mg, Ca, and Mn, which are based on preliminary experiments (*32*), deviate much more markedly from these expected (cf. *115*); further measurements for resolution of this problem are desirable.

E. MCl_4/LCl_3 ($MLCl_7$, ML_2Cl_{10})

1. Qualitative Observations

$AlCl_3$ complexes with M(IV) = U (*45*); Th, U (*119*); and Zr (*161*). $InCl_3$ complexes with M(IV) = U (*13*).

TABLE VII

COMPARISON OF HOMOGENEOUS EQUILIBRIA[a]

Reaction	ΔH^0 (kcal)	ΔS^0 (cal/K)	References
$CoAl_2Cl_8(g) + 0.5Al_2Cl_6(g) = CoAl_3Cl_{11}(g)$	−7.7	−15.7	(*124*)
$CoAl_2Cl_8(g) + 0.5Al_2Cl_6(g) = CoAl_3Cl_{11}(g)$	−8.1	−13.1	(*32*)
$MgAl_2Cl_8(g) + 0.5Al_2Cl_6(g) = MgAl_3Cl_{11}(g)$	(−15.7)	(−22.9)	(*32*)
$CaAl_2Cl_8(g) + 0.5Al_2Cl_6(g) = CaAl_3Cl_{11}(g)$	(+0.3)	(−1.1)	(*32*)
$MnAl_2Cl_8(g) + 0.5Al_2Cl_6(g) = MnAl_3Cl_{11}(g)$	(−4.5)	(−6.7)	(*32*)
$EuAl_3Cl_{11}(g) + 0.5Al_2Cl_6(g) = EuAl_4Cl_{14}(g)$	−8.9	−14.2	(*151*)
$NdAl_3Cl_{12}(g) + 0.5Al_2Cl_6(g) = NdAl_4Cl_{15}(g)$	−10.0	−16.9	(*82*)
$NdGa_3Cl_{11}(g) + 0.5Ga_2Cl_6(g) = NdGa_4Cl_{15}(g)$	−12.2	−20.9	(*41*)
$VAlCl_6(g) + 0.5Al_2Cl_6(g) = VAl_2Cl_9(g)$	−11.9	−19.2	(*5*)

[a] Data corrected to 298K (*115*). Expected for addition of 1 $AlCl_3$ (represented as Al_2Cl_6): $\Delta H^0 = -8 \pm 3$ kcal; $\Delta S^0 = -16 \pm 4$ cal/K.

2. *Thermodynamic Investigations*

$AlCl_3$ complexes are known with M(IV) = U (*46*) and Zr (*127*). The following values have been measured.

$$ZrCl_4(s) + 0.5Al_2Cl_6(g) = ZrAlCl_7(g) \tag{54}$$

$$\Delta H^0(298) = 17.8 \text{ kcal}; \Delta S^0(298) = 26.6 \text{ cal/K } (127)$$

This leads (*127*) to

$$0.5Zr_2Cl_8(g) + 0.5Al_2Cl_6(g) = ZrAlCl_7(g) \tag{55}$$

$$\Delta H^0(298) = -0.9 \text{ kcal}; \Delta S^0(298) = 0 \text{ cal/K } (127)$$

These data support the view that the $ZrAlCl_7$ molecule contains a double Cl bridge, which is clearly the case for Zr_2Cl_8 also (C.N. = 5). It is not possible, however, a priori to exclude a triple Cl bridge (C.N. = 6) for $ZrAlCl_7$.

$$ZrCl_4(s) + Al_2Cl_6(g) = ZrAl_2Cl_{10}(g) \tag{56}$$

$$\Delta H^0(298) \cong 10.8 \text{ kcal}; \Delta S^0(298) \cong 11 \text{ cal/K } (127)$$

$$UCl_4(s) + Al_2Cl_6(g) = UAl_2Cl_{10}(g) \tag{57}$$

$$\Delta H^0(700) = 15.8 \text{ kcal}; \Delta S^0(700) = 15.3 \text{ cal/K } (46)$$

The different values for Eqs. (56) and (57) must be related to the different structures of $ZrCl_4$(s) and UCl_4(s) (C.N. = 6 or 8). In $ZrAl_2Cl_{10}$ and UAl_2Cl_{10}, Zr and U are probably octahedrally coordinated by Cl.

F. MCl_5/LCl_3 ($MAlCl_8$)

1. Qualitative Observations

$AlCl_3$ complexes with M(V) = U (*90*). $InCl_3$ complexes with M(V) = U (*13, 14*).

2. Thermodynamic Investigations

Measurements have been made for $AlCl_3$ complexes with M(V) = U (*46*) and Ta (*127*)

$$UCl_4(s) + 0.5Cl_2 + 0.5Al_2Cl_6(g) = UAlCl_8(g) \qquad (58)$$

From the values measured for Eq. (58) it was possible with data for $UCl_5(s) = UCl_4(s) + 0.5Cl_2$ (from *6*) to obtain ΔH^0 and ΔS^0 values for

$$UCl_5(s) + 0.5Al_2Cl_6(g) = UAlCl_8(g) \qquad (59)$$

$$\Delta H^0 = 19.1 \text{ kcal}; \Delta S^0 = 26.8 \text{ cal/K } (127)$$

These values are in close agreement with those for the corresponding reaction [Eq. (60)] with $TaCl_5$, which can be ascribed to similar M_2Cl_{10} molecular lattices for the two pentachlorides (*127*).

$$TaCl_5(s) + 0.5Al_2Cl_6(g) = TaAlCl_8(g) \qquad (60)$$

$$\Delta H^0(298) = 17.9 \text{ kcal}; \Delta S^0(298) = 28.4 \text{ cal/K}$$

It is found, as expected, that

$$0.5Ta_2Cl_{10}(g) + 0.5Al_2Cl_6(g) = TaAlCl_8(g) \qquad (61)$$

$$\Delta H^0 = +1.1 \text{ kcal}; \Delta S^0 = 0 \text{ cal/K } (127)$$

Uranium and tantalum atoms in the complexes are probably octahedrally coordinated by chlorine. Aluminum always has C.N. = 4.

VI. Complex Formation by UCl_5/U_2Cl_{10}

Gruen and McBeth (*46*) concluded from measurements on the reaction $UCl_4(s) + Cl_2$ that the dimer $U_2Cl_{10}(g)$ is formed. The existence of U_2Cl_{10} (as well as UCl_5) may also be detected mass spectroscopically at 423 K (*116*). Accordingly, U_2Cl_{10}/UCl_5 should be suitable for forming complexes. In the corresponding experiments thermal decomposition of U_2Cl_{10} to UCl_4 must be suppressed by addition of Cl_2. In fact, it was observed (*164*) that a small uranium content in chloride samples leads to an increased volatility for chlorides of Eu, Nd, Tb, and Am. Some experiments (*116*) showed that $CaCl_2$ and $CoCl_2$ were transported chemically with UCl_5/U_2Cl_{10} (773 → 673 K). Au_2Cl_6 could similarly be suitable for forming complexes.

VII. Practical Applications of Halide Complexes

Table VIII shows the elements the chlorides (bromides and iodides) of which form readily volatile complexes with the trichlorides (tribromides and triiodides) AlX_3, GaX_3, $InCl_3$, and FeX_3. It is essential throughout that the M content in the gas phase can be increased by powers of 10 over the saturation pressure of MX_n and that the complexes be labile, MX_n being rapidly available as required. In this section whenever AlX_3 (or LX_3) is referred to it is always as the gaseous equilibrium mixture $AlX_3 + Al_2X_6$ (or $LX_3 + L_2X_6$). Useful applications will now be summarized.

TABLE VIII

ELEMENTS OF WHICH THE CHLORIDES (BROMIDES, IODIDES) FORM VOLATILE COMPLEXES WITH THE TRICHLORIDES (BROMIDES, IODIDES) AlX_3, GaX_3, $InCl_3$ AND FeX_3

H																	He
Li	Be											B	C	N	O	F	Ne
Na	Mg											Al	Si	P	S	Cl	Ar
K	Ca	Sc	Ti	V	Cr	Mn	Fe	Co	Ni	Cu	Zn	Ga	Ge	As	Se	Br	Kr
Rb	Sr	Y	Zr	Nb	Mo	Tc	Ru	Rh	Pd	Ag	Cd	In	Sn	Sb	Te	I	Xe
Cs	Ba	*	Hf	Ta	W	Re	Os	Ir	Pt	Au	Hg	Tl	Pb	Bi	Po	At	Rn
Fr	Ra	†															

*La	Ce	Pr	Nd	Pm	Sm	Eu	Gd	Tb	Dy	Ho	Er	Tm	Yb	Lu
†Ac	Th	Pa	U	Np	Pu	Am	Cm	Bk	Cf	Es	Fm	Md	No	Lw

A. Halides

Preparation of halide crystals, for example, those of $CuCl_2$ (*179*), may be accomplished by chemical transport (*104*) with $AlCl_3$ in a temperature gradient is an example of preparation of oxide-free halides by transport with $AlCl_3$. Oxygen remains in the residue as AlOCl or, at higher temperatures, as Al_2O_3 (*134*).

Halide syntheses may be accomplished by reaction of oxides with $AlCl_3$ and removal of the halides by means of the $MCl/AlCl_3$ complexes (*91, 93*). Decomposition of Cu- and Fe-containing ores with Cl_2 results in appreciable votalization of Cu (as $CuFe_2Cl_8$) (*154*). If surface layers are formed during the reaction, which hinder its progress, attack is greatly accelerated if the solid reaction product (the surface layer) is removed to other parts of the reaction space by means of the gaseous complex (*134*):

$$Co + Br_2 + AlBr_3 \rightarrow CoBr_2 \text{ (134)}$$

$$Ni + Br_2 + AlBr_3 \rightarrow NiBr_2 \text{ (134)}$$

$$Pt + Br_2 + AlBr_3 \rightarrow PtBr_3 \text{ (144) [similarly, } PtCl_2 \text{ (144)]}$$

$$Cr + CrCl_3 + HCl + AlCl_3 \rightarrow CrCl_2 \text{ (65, 129) [similarly, } CrBr_2, CrI_2]$$

$$UCl_4 + Al + AlCl_3 \rightarrow UCl_3 \text{ (91)}$$

$$Ti + TiCl_3 + AlCl_3 \rightarrow Ti_7Cl_{16} \text{ (130, 131) [similarly, } Ti_7Br_{16} \text{ (130, 131)]}$$

$$PdI_2 + AlI_3 \rightarrow Pd_5AlI_2 \text{ (76)}$$

If surface films serve to protect from corrosion, removal of the surface film may result in considerably increased attack, for example, Monel + Cl_2 + $AlCl_3$ (*91*).

Difficultly volatile halides may be intercalated in graphite with $AlCl_3$ as carrier (transport agent) (*157*), UCl_5 and UCl_4 may be separated by transport with $AlCl_3$ + Cl_2 (*91*). Lanthanides (or actinides) may be separated by gas chromatography by volatilization of the chlorides in a $He/AlCl_3$ stream (*172, 173*). $CoCl_2$, $NiCl_2$, or $FeCl_2$ may be dehalogenated by transport in an $AlBr_3$ or AlI_3 atmosphere (*134*).

B. Metal Transport

The following reactions involving gaseous halide complexes are of interest and represent a development of van Arkel's classical work on the transport of metals with iodine (*104*) (T_1 is the lower temperature,

T_2 the higher, and the arrow gives the direction of transport in the temperature gradient):

$Cu + HCl + AlCl_3$:	Cu transport (400 → 600°C) (*138*)
$Ag + HCl + AlCl_3$:	Ag transport (450 → 700°C) (*138*)
$Au + I_2 + AlI_3$:	Au transport (300 → 350°C) (*138*)
$Ru + Cl_2 + AlCl_3$:	Ru transport (450 → 650°C) (*138*)
$Rh + Cl_2 + AlCl_3$:	Rh transport (600 → 800°C) (*138*)
$Pd + Cl_2 + FeCl_3$ ($AlCl_3$):	Pd transport (400 → 900°C) (*138*)
$Pd + I_2 + AlCl_3$:	Pd transport (375 → 600°C) (*134*)
$Ir + Cl_2 + AlCl_3$:	Ir transport (600 → 800°C) (*138*)
$Pt + Cl_2 + AlCl_3$ ($FeCl_3$):	Pt transport (600 → 800°C) (*138*)
$Co + GaX_3$ (X = Cl, I):	Co transport ($T_1 \rightarrow T_2$) (*133*)
$Ni + I_2 + InI_3$:	Ni transport ($T_1 \rightarrow T_2$) (*135*)
$Pd + I_2 + AlI_3$:	Pd_2Al (375 → 600°C) (*134, 138*)

In the decomposition of copper oxide-containing ores with carbon, NaCl, SiO_2, and a little water, HCl and Na_2SiO_3 are the primary products, and then $Cu_3Cl_{3(g)}$, $NaCu_2Cl_{3(g)}$, and $Na_2CuCl_{3(g)}$. These copper-containing molecules come into contact with carbon and are there reduced by H_2 to metal (*44*); this is the copper-segregation process (*50*). Formation of the relatively stable alkali metal complexes can be particularly useful if coupled with a subsequent reaction—here, reduction by hydrogen.

C. Oxide Transport

Aluminum trichloride cannot be used as a transport agent for oxides because of the great stability of Al_2O_3. With some limitations, however, $GaCl_3$ is suitable for this purpose. Transport leads, for example, to deposition of Fe_2O_3 in the hot zone:

$Fe_2O_3 + HCl + GaCl_3$:	Fe_2O_3 transport (327 → 427°C) (*139*)

Because of the similar ionic radii of Fe^{3+} and Ga^{3+}, a few percent of Ga atoms also go over into the solid phase.

D. Chalcogenides

For the transport of the spinel $CdCr_2(S_{1-x}Se_x)_4$ with $I_2 + AlCl_3$, see Pickardt *et al.*, (*97*); for that of $Mn_xHg_{1-x}Se$ and $Mn_xCd_{1-x}Se$ with $Cl_2 + AlCl_3$, see Pajaczkowska (*84*). Transport of chromium sulfides and selenides with $AlCl_3$ (*72, 73*) may require the additional presence of HCl (from the hydrolysis of $AlCl_3$). This is true for the synthesis of $Cu_xHg_{1-x}Cr_2Se_4$ from the elements in the presence of $AlCl_3$ (*81*) and for transport of $CrTe_3$ with $AlCl_3$ (*59*). Synthesis of $HgCr_2Se_4$, for example, from the elements is successful when $HgCl_2$ is added as a source of Cl_2 together with $AlCl_3$ to form the complex (*43, 119*).

E. Discharge Lamps

Discharge lamps in which, for example, Na atoms are to be excited in the plasma column, are charged with NaI. The Na content in the gas phase (quartz wall ~800°C) is increased by complex formation of NaI with $AlCl_3$ (*28, 71*). Other fillers for lamps where complex formation takes place are $CeI_3 + SmI_2 + CsI + NaI$ (*171*) and $ScI_3 + NaI$ (*58*). See also (*52, 170*).

F. Lasers

$AlCl_3$ complexes of suitable lanthanide chlorides have been tested in high-energy lasers (*27, 51–53, 56, 61*).

Acknowledgment

It is a pleasure for me to express my thanks to H. J. Emeléus for the translation of the German text into English.

References

1. I. L. Agafonov, L. G. Nikolaeva, and N. Kh. Agliulov, *Russ. J. Phys. Chem.* (*Engl. Transl.*) **48,** 623 (1974).
2. M. Aits and H. Schäfer, *Z. Anorg. Allg. Chem.* **408,** 37 (1974).
3. M. Aits and H. Schäfer, *J. Less-Common Met.* **57,** 219 (1978).
4. A. Anundskås, A. E. Mahgoub, and H. A. Øye, *Acta Chem. Scand. Ser. A* **30,** 193 (1976).
5. A. Anundskås and H. A. Øye, *J. Inorg. Nucl. Chem.* **37,** 1609 (1975).

6. I. Barin and O. Knacke, *Thermochem. Prop. Inorg. Subst., 1973* (1973).
7. I. Barin, O. Knacke, and O. Kubaschewski, *Thermochem. Prop. Inorg. Subst., 1977 Suppl.,* (1977).
8. R. F. Belt and H. Scott, *Inorg. Chem.* **3,** 1785 (1964).
9. R. W. Berg and G. N. Papatheodorou, *Inorg. Chim. Acta* **45,** L211 (1980).
10. M. Binnewies, *Z. Anorg. Allg. Chem.* **435,** 156 (1977).
11. M. Binnewies, *Z. Anorg. Allg. Chem.* **437,** 19 (1977).
12. M. Binnewies, *Z. Anorg. Allg. Chem.* **437,** 25 (1977).
13. M. Binnewies and H. Schäfer, *Z. Anorg. Allg. Chem.* **395,** 77 (1973).
14. M. Binnewies and H. Schäfer, *Z. Anorg. Allg. Chem.* **407,** 327 (1974).
15. M. Binnewies and H. Schäfer, *Z. Anorg. Allg. Chem.* **410,** 149 (1974).
16. H. Bloom, B. V. O'Grady, R. G. Anthony, and V. C. Reinsborough, *Aust. J. Chem.* **23,** 843 (1970).
17. K. Brodersen, G. Thiele, and H. Gaedcke, *Z. Anorg. Allg. Chem.* **348,** 162 (1966).
18. J. Brynestad, S. von Winbush, H. L. Yakel, and G. P. Smith, *Inorg. Nucl. Chem. Lett.* **6,** 889 (1970).
19. J. Brynestad, H. L. Yakel, and G. P. Smith, *Inorg. Chem.* **9,** 686 (1970).
20. A. Büchler and J. B. Berkowitz-Mattuck, *Adv. High Temp. Chem.* **1,** (1967).
21. I. T. Buraya, O. G. Polyachenok, and G. I. Novikov, *Zh. Fiz. Khim.* **48,** 1609 (1974); *Russ. J. Phys. Chem. (Engl. Transl.)* **48,** 952 (1974).
22. I. T. Buraya, O. G. Polyachenok, and G. I. Novikov, *Vestn. Akad. Nauk SSR, Ser. Khim. Nauk.* p. 53 (1975); *Chem. Abstr.* **84,** 80563 (1976).
23. I. T. Buraya, O. G. Polyachenok, O. N. Komshilova, and G. I. Novikov, *Izv. Vyssh. Uchebn. Zaved., Khim. Khim. Tekhnol.* **19,** 1797 (1976).
24. M. A. Capote, G. H. Kucera, and G. N. Papatheodorou, *Proc.—Electrochem. Soc.* **78-1** (1978).
25. M. A. Capote and G. N. Papatheodorou, *Inorg. Chem.* **17,** 3414 (1978).
26. W. T. Carnall, J. P. Hessler, H. R. Hoekstra, and C. W. Williams, *J. Chem. Phys.* **68,** 4304 (1978).
27. W. T. Carnall, J. P. Hessler, C. W. Williams, and H. R. Hoekstra, *J. Mol. Struct.* **46,** 269 (1978).
28. A. G. Chalmers, D. O. Wharmby, and F. L. Whittacker, *Light. Res. Technol.* **7,** 11 (1975).
29. M. Cosandey and F. P. Emmenegger, *J. Electrochem. Soc.* **126,** 1601 (1979).
30. S. J. Cyvin, B. N. Cyvin, and A. Snelson, *J. Phys. Chem.* **75,** 2609 (1971).
31. A. Dell'Anna and F. P. Emmenegger, *Helv. Chim. Acta* **58,** 1145 (1975).
32. E. W. Dewing, *Metall. Trans.* **1,** 2169 (1970).
33. F. Dienstbach and F. P. Emmenegger, *Inorg. Chem.* **16,** 2957 (1977).
34. F. Dienstbach and F. P. Emmenegger, *Helv. Chim. Acta* **60,** 166 (1977).
35. F. Dienstbach and F. P. Emmenegger, *Z. Anorg. Allg. Chem.* **436,** 127 (1977).
36. F. Dienstbach and F. P. Emmenegger, *J. Inorg. Nucl. Chem.* **40,** 1299 (1978).
37. F. P. Emmenegger, *Inorg. Chem.* **16,** 343 (1977).
38. D. H. Feather and A. W. Searcy, *High Temp. Sci.* **3,** 155 (1971).
39. W. Fischer, *Angew. Chem.* **61,** 336 (1949).
40. U. Flörke and H. Schäfer, *Z. Anorg. Allg. Chem.* **459,** 140 (1979).
41. T. Foosnaes (Mentor H. A. Øye), Dissertation, University of Trondheim (1979).
42. R. M. Fowler and S. S. Melford, *Inorg. Chem.* **15,** 473 (1976).
43. P. Gibart, *J. Cryst. Growth* **43,** 21 (1978).
44. P. Gross and M. C. Stuart, *Metall. Chem., Proc. Symp., 1971,* p. 499 (1972).
45. D. M. Gruen and R. L. McBeth, *Inorg. Nucl. Chem. Lett.* **4,** 299 (1968).

46. D. M. Gruen and R. L. McBeth, *Inorg. Chem.* **8,** 2625 (1969).
47. D. M. Gruen and H. A. Øye, *Inorg. Nucl. Chem. Lett.* **3,** 453 (1967).
48. J. P. Hager and R. B. Hill, *Metall. Trans.* **1,** 2723 (1970).
49. M. Hargittai and I. Hargittai, "The Molecular Geometries of Coordination Compounds in the Vapour Phase." Akad. Kiadó, Budapest, 1977.
50. J. W. Hastie, "High Temperature Vapors." Academic Press, New York, 1975.
51. J. P. Hessler, F. Wagner, C. W. Williams, and W. T. Carnall, Vortrag Amsterdam, 1976.
52. D. L. Hildenbrand and D. D. Cubicciotti, *Proc.—Electrochem. Soc.* **78-1** (1978).
53. H. R. Hoekstra, J. P. Hessler, C. W. Williams, and W. T. Carnall, *152nd Meet. Electrochem. Soc., 1977.*
54. J. A. Ibers, *Acta Crystallogr.* **15,** 967 (1962).
55. N. I. Ionov, *Dokl. Akad. Nauk SSSR* **59,** 467 (1948).
56. R. R. Jacobs, W. F. Krupke, J. P. Hessler, and C. W. Carnall, *Opt. Commun.* **21,** 395 (1977).
57. S. E. James and J. P. Hager, *Metall. Trans.* **9B,** 501 (1978).
58. W. M. Keeffe, *IES Trans.* p. 260 (1975).
59. K. O. Klepp and H. Ipser, *Monatsh. Chem.* **110,** 499 (1979).
60. E. S. Kotova, A. L. Kuzmenko, and G. I. Novikov, *Russ. J. Phys. Chem. (Engl. Transl.)* **46,** 1690 (1972).
61. W. F. Krupke, *Electron. Transition Lasers [Proc. Summer Colloq.], 2nd, 1975* p. 148 (1976).
62. G. H. Kucera and G. N. Papatheodorou, *J. Phys. Chem.* **83,** 3213 (1979).
63. K. Lascelles and H. Schäfer, *Angew. Chem.* **83,** 112 (1971); *Angew. Chem., Int. Ed. Engl.* **10,** 1728 (1971).
64. K. Lascelles and H. Schäfer, *Z. Anorg. Allg. Chem.* **382,** 249 (1971).
65. K. Lascelles, R. A. J. Shelton, and H. Schäfer, *J. Less-Common Metals* **29,** 109 (1972).
66. W. C. Laughlin and N. W. Gregory, *J. Phys. Chem.* **80,** 127 (1976).
67. W. Lenhard and H. Schäfer, *Z. Anorg. Allg. Chem.* **482,** 167 (1981).
68. W. Lenhard, H. Schäfer, H. U. Hürter, and B. Krebs, *Z. Anorg. Allg. Chem.* **482,** 19 (1981).
69. H. Linga, K. Motzfeldt, and H. A. Øye, *Ber. Bunsenges. Phys. Chem.* **82,** 568 (1978).
70. C. S. Liu and R. J. Zollweg, *J. Chem. Phys.* **60,** 2384 (1974).
71. R. Lorenz, *Light. Res. Technol.* **8,** 136 (1976).
72. H. D. Lutz and Cs. v. Lovász, *Angew. Chem.* **80,** 562 (1968).
73. H. D. Lutz, Cs. v. Lovász, K. H. Bertram, M. Sréckovié, and U. Brinker, *Monatsh. Chem.* **101,** 519 (1970).
74. T. P. Martin and H. Schaber, private communication. (1979).
75. H. B. Merker and H. Schäfer, *Z. Anorg. Allg. Chem.* **480,** 76 (1981).
76. H. B. Merker, H. Schäfer, and B. Krebs, *Z. Anorg. Allg. Chem.* **462,** 49 (1980).
77. T. N. Naumova, L. S. Zhevnina, R. V. Poponova, M. S. Chupakhin, and B. D. Stepin, *Russ. J. Inorg. Chem. (Engl. Transl.)* **24,** 13 (1979).
78. G. I. Novikov and F. G. Gavryuchenkov, *Russ. Chem. Rev. (Engl. Transl.)* **36,** 156 (1967).
79. G. I. Novikov and E. S. Kotova, *Zh. Fiz. Khim.* **47,** 483 (1973).
80. G. I. Novikov and O. G. Polyachenok, *Russ. J. Inorg. Chem. (Engl. Transl.)* **6,** 996 (1961)
81. I. Okańska-Kozlowska, M. Jelonek, and Z. Drzazga, *Z. Anorg. Allg. Chem.* **436,** 265 (1977).

82. H. A. Øye and D. M. Gruen, *J. Am. Chem. Soc.* **91,** 2229 (1969).
83. H. A. Øye and D. M. Gruen, *NBS Spec. Publ. (U.S.)* **561** (1979).
84. A. Pajaczkowska, *Mater. Res. Bull.* **15,** 1509 (1980).
85. G. N. Papatheodorou, *Inorg. Chem.* **12,** 1899 (1973).
86. G. N. Papatheodorou, *J. Phys. Chem.* **77,** 472 (1973).
87. G. N. Papatheodorou, *Inorg. Nucl. Chem. Lett.* **10,** 115 (1974).
88. G. N. Papatheodorou, *Z. Anorg. Allg. Chem.* **411,** 153 (1975).
89. G. N. Papatheodorou and R. W. Berg, *Chem. Phys. Lett.* **75,** 483 (1980).
90. G. N. Papatheodorou and D. A. Buttry, *Inorg. Nucl. Chem. Lett.* **15,** 51 (1979).
91. G. N. Papatheodorou, *Curr. Top. Mater. Sci.* (submitted) (1980).
92. G. N. Papatheodorou and G. H. Kucera, *Inorg. Chem.* **16,** 1006 (1977).
93. G. N. Papatheodorou and G. H. Kucera, *Inorg. Chem.* **18,** 385 (1979).
94. E. J. Peterson, J. A. Caird, J. P. Hessler, H. R. Hoekstra, and C. W. Williams, *J. Phys. Chem.* **83,** 2458 (1979).
95. E. J. Peterson, J. A. Caird, W. T. Carnall, J. P. Hessler, H. R. Hoekstra, and C. W. Williams, *Argonne Rep.* **1979,** *conf.* 790641. *Chem. Abstr.* **92,** 117350 (1980).
96. K. P. Petrov, V. A. Kulikov, V. V. Ugarov, and N. G. Rambidi, *Zh. Strukt. Khim.* **21,** 71 (1980); *Chem. Abstr.* **93,** 159515 (1980).
97. J. Pickardt, E. Riedel, and B. Reuter, *Z. Anorg. Allg. Chem.* **373,** 15 (1970).
98. O. G. Polyachenok and O. N. Komshilova, *Teplofiz. Vys. Temp.* **10,** 195 (1972); *Chem. Abstr.* **76,** 132322 (1972).
99. S. Poturay-Gutniak, *Nukleonika* **13,** 1157 (1968).
100. H. Rabeneck and H. Schäfer, *Z. Anorg. Allg. Chem.* **395,** 69 (1973).
101. P. L. Radloff and G. N. Papatheodorou, *J. Chem. Phys.* **72,** 992 (1980).
102. R. R. Richards and N. W. Gregory, *J. Phys. Chem.* **68,** 3089 (1964).
103. H. Sainte-Claire Deville and L. Troost, *C. R. Hebd. Seances Acad. Sci.* **45,** 821 (1857).
104. H. Schäfer, "Chemische Transportreaktionen." Weinheim, 1962; "Chemical Transport Reactions." Academic Press, New York, 1964.
105. H. Schäfer, *Z. Anorg. Allg. Chem.* **400,** 242 (1973).
106. H. Schäfer, *Proc. Conf. Chem. Vap. Deposition, Int. Conf., 5th, 1975* p. 3 (1975).
107. H. Schäfer, *J. Cryst. Growth* **31,** 31 (1975).
108. H. Schäfer, *Z. Anorg. Allg. Chem.* **414,** 151 (1975).
109. H. Schäfer, *Z. Anorg. Allg. Chem.* **415,** 217 (1975).
110. H. Schäfer, *Angew. Chem.* **88,** 775 (1976); *Angew. Chem., Int. Ed. Engl.* **15,** 713 (1976).
111. H. Schäfer, *Pure Appl. Chem.* **49,** 871 (1977).
112. H. Schäfer, *Z. Chem.* **19,** 362 (1979).
113. H. Schäfer, *NBS Spec. Publ. (U.S.)* **561** (1979).
114. H. Schäfer, *Z. Anorg. Allg. Chem.* **461,** 29 (1980).
115. H. Schäfer, *Z. Anorg. Allg. Chem.* **479,** 99 (1981).
116. H. Schäfer, *Z. Anorg. Allg. Chem.* **479,** 105 (1981).
117. H. Schäfer and M. Binnewies, *Z. Anorg. Allg. Chem.* **410,** 251 (1974).
118. H. Schäfer and M. Binnewies, *Rev. Chim. Miner.* **13,** 24 (1976).
119. H. Schäfer, M. Binnewies, W. Domke, and J. Karbinski, *Z. Anorg. Allg. Chem.* **403,** 116 (1974).
120. H. Schäfer, M. Binnewies, and U. Flörke, *Z. Anorg. Allg. Chem.* **427,** 31 (1981).
121. H. Schäfer, M. Binnewies, R. Laumanns, and H. Wächter, *Z. Anorg. Allg. Chem.* **461,** 31 (1980).

122. H. Schäfer and D. Boos, *Z. Anorg. Allg. Chem.* **477,** 35 (1981).
123. H. Schäfer and U. Flörke, *Z. Anorg. Allg. Chem.* **462,** 173 (1980).
124. H. Schäfer and U. Flörke, *Z. Anorg. Allg. Chem.* **469,** 172 (1980).
125. H. Schäfer and U. Flörke, *Z. Anorg. Allg. Chem.* **478,** 57 (1981).
126. H. Schäfer and U. Flörke, *Z. Anorg. Allg. Chem.* **479,** 84 (1981).
127. H. Schäfer and U. Flörke, *Z. Anorg. Allg. Chem.* **479,** 89 (1981).
128. H. Schäfer, U. Flörke, and M. Trenkel, *Z. Anorg. Allg. Chem.* **478,** 191 (1981).
129. H. Schäfer and R. Laumanns, *Z. Anorg. Allg. Chem.* **436,** 47 (1977).
130. H. Schäfer and R. Laumanns, *Z. Anorg. Allg. Chem.* **474,** 135 (1981).
131. H. Schäfer, R. Laumanns, B. Krebs, and G. Henkel, *Angew. Chem.* **91,** 343 (1979); *Angew. Chem. Int. Ed. Engl.* **18,** 325 (1979).
132. H. Schäfer and W. Lenhard, *Z. Anorg. Allg. Chem.* **482,** 163 (1981).
133. H. Schäfer and J. Nowitzki, *Z. Anorg. Allg. Chem.* **435,** 49 (1977).
134. H. Schäfer and J. Nowitzki, *J. Less-Common Metals* **61,** 47 (1978).
135. H. Schäfer and J. Nowitzki, *Z. Anorg. Allg. Chem.* **439,** 80 (1978).
136. H. Schäfer and J. Nowitzki, *Z. Anorg. Allg. Chem.* **457,** 13 (1979).
137. H. Schäfer and H. Rabeneck, *Z. Anorg. Allg. Chem.* **443,** 28 (1978).
138. H. Schäfer and M. Trenkel, *Z. Anorg. Allg. Chem.* **414,** 137 (1975).
139. H. Schäfer and M. Trenkel, *Z. Anorg. Allg. Chem.* **426,** 113 (1976).
140. H. Schäfer and M. Trenkel, *Z. Anorg. Allg. Chem.* **437,** 10 (1977).
141. H. Schäfer and K. Wagner, *Z. Anorg. Allg. Chem.* **450,** 88 (1979).
142. H. Schäfer and K. Wagner, *Z. Anorg. Allg. Chem.* **451,** 61 (1979).
143. H. Schäfer and K. Wagner, *Z. Anorg. Allg. Chem.* **452,** 89 (1979).
144. H. Schäfer, U. Wiese, C. Brendel, and J. Nowitzki, *J. Less-Common Metals* **76,** 63 (1980).
145. K. N. Semenenko, T. N. Naumova, L. N. Gorokhow, G. A. Semenova, and A. W. Novoselova, *Dokl. Akad. Nauk UdSSR* **154,** 169 (1964).
146. K. N. Semenenko, T. N. Naumova, L. N. Gorokhow, and A. W. Novoselova, *Dokl. Akad. Nauk UdSSR* **154,** 648 (1964).
147. C. F. Shieh and N. W. Gregory, *J. Phys. Chem.* **79,** 828 (1975).
148. V. B. Sholts and L. N. Sidorov, *Vestn. Mosk. Univ., Ser. 2: Khim.* **1972,** 371 (1972), and further publications of the Sidorov team.
149. E. Sibbing and H. Schäfer, *Z. Anorg. Allg. Chem.* **410,** 67 (1974).
150. L. N. Sidorov, *Mod. Prob. Phys. Chem.* **6,** 295 (1972) (in Russian).
151. M. Sørlie and H. A. Øye, *J. Inorg. Nucl. Chem.* **40,** 493 (1978).
152. M. Sørlie and H. A. Øye, *Inorg. Chem.* **17,** 2473 (1978).
153. V. P. Spiridonov, E. V. Erokhin, and B. I. Lutoshkin, *Vestn. Mosk, Univer., Ser. 2: Khim.* **26,** 296 (1971).
154. B. W. Spreckelmeyer, *Ger. Offen.* **2,216,807** (1972).
155. B. Stelthove and H. Schäfer, *Z. Anorg. Allg. Chem.* **451,** 25 (1979).
156. D. R. Stull and H. Prophet, "Janaf Thermochemical Tables, 2nd ed. NSRDS-NBS 37, Washington, D.C., 1971.
157. E. Stumpp and G. Nietfeld, *Z. Anorg. Allg. Chem.* **456,** 261 (1979).
158. Mien-tsêng Su and G. I. Novikov, *Russ. J. Inorg. Chem.* (*Engl. Transl.*) **11,** 270 (1966).
159. S. Sutakshuto (Mentor H. A. Øye), Dissertation, University of Trondheim (1976).
160. R. C. Svedberg (1966), cited in Büchler and Berkowitz-Mattuck (*20*).
161. D. R. Taylor and E. M. Larsen, *J. Inorg. Nucl. Chem.* **41,** 481 (1979).
162. G. Thiele, K. Brodersen, E. Kruse, and B. Holle, *Chem. Ber.* **101,** 2771 (1968).

163. P. J. Thistlethwaite and S. Ciach, *Inorg. Chem.* **14,** 1430 (1975).
164. S. S. Travnikov, A. V. Davydov, and B. F. Myasoedov, *Radiokhimiya* **21,** 579 (1979); *Chem. Abstr.* **91,** 150382 (1979).
165. H. Wächter and H. Schäfer, *Z. Anorg. Allg. Chem.* **471,** 38 (1980).
166. K. Wagner and H. Schäfer, *Z. Anorg. Allg. Chem.* **450,** 107 (1979).
167. K. Wagner and H. Schäfer, *Z. Anorg. Allg. Chem.* **450,** 115 (1979).
168. K. Wagner and H. Schäfer, *Z. Anorg. Allg. Chem.* **451,** 57 (1979).
169. K. Wagner and H. Schäfer, *Z. Anorg. Allg. Chem.* **452,** 83 (1979).
170. I. L. Wilson and L. P. Rehder, *152nd Meet. Electrochem. Soc. 1977,* p. 989 (1977).
171. R. J. Zollweg, C. S. Liu, C. Hirayama, and J. W. McNall, IES *Conf., 1974,* 249 (1974); *J. IES* p. 249 (1975).
172. T. S. Zvarova, *Radiochem. Radioanal. Lett.* **11,** 113 (1972).
173. T. S. Zvarova and I. Zvára, *J. Chromatogr.* **49,** 290 (1976).

ADVANCES IN INORGANIC CHEMISTRY AND RADIOCHEMISTRY, VOL. 26

ONE-DIMENSIONAL INORGANIC PLATINUM-CHAIN ELECTRICAL CONDUCTORS

JACK M. WILLIAMS

Chemistry Division, Argonne National Laboratory, Argonne, Illinois

I. Introduction

The decade of the 1970s has seen an enormous increase in studies of one-dimensional (1-D) electrical conductors, and during that period numerous summary articles and reviews of advances in the field have been published (*1–5*). A 1-D metal may be defined quite simply as one that exhibits metal-like properties in only one direction. For example, four-probe measurements of the electrical conductivity parallel to the Pt chain in 1-D conductors formed from the stacking of square-planar $[Pt(CN)_4]^{2-}$ groups, which comprises the basis of this review, frequently reveal values that are in excess of 10^5 over the conductivity perpendicular to the chain direction. The burgeoning field of studies of 1-D compounds is due to intrinsic scientific interest in unraveling the fundamental chemistry and physics of these unusual materials and, additionally, because of their possible practical uses. There is the likely probability that 1-D materials will find uses in electronic devices and even possibly that a high-temperature superconductor may eventually be discovered.

Copyright © 1983 by Academic Press, Inc.
All rights of reproduction in any form reserved.
ISBN 0-12-023626-5

Although 1-D Pt metal chain systems were first synthesized in the mid-1800s (*6, 7*) and described in detail by Levy (*8*) in 1912, it was not until the pioneering work of Krogmann (*9*) in the 1960s that it was fully realized that they were 1-D metals. Numerous reviews of the chemistry and physics (*3–5, 29*) of these intriguing materials were published in the 1970s. A general and up-to-date review of 1-D materials research was published in 1981 (*10*). The most comprehensive review prior to 1975 was that by Miller and Epstein (*5*). The latest and most complete review of the presently known low-dimensional materials has been published as a three-volume treatise (*1*). For this reason it was felt that an up-to-date and state-of-the-art overview, containing selected research highlights pertaining to Pt-chain metals, rather than a detailed tabulation of papers, was most appropriate.

Several classes of 1-D or "low-dimensional" metals are presently known, and they include polymers of the main-group elements [e.g., $(SN)_x$] (*11*), organic polymers such as polyacetylene [$(CH)_x$] (*12*), organic metals [e.g., TTF–TCNQ (*13*)], and superconducting $(TMTSF)_2X$ salts [TMTSF = tetramethyltetraselenafulvalene; X = PF_6^-, SbF_6^-, ClO_4^-, ReO_4^-, and AsF_6^- (*14*)], but they will not be included in this chapter. The main topic of this chapter will be 1-D metals in which the anisotropic metallic properties arise from partial oxidation of a chain of interacting Pt-metal atoms, resulting in very short intrachain metal–metal (M—M) distances (<3.0 Å). The specific focus will be on tetracyanoplatinate complexes formed by overlapping $5d_{z^2}$ orbitals (Fig. 1), because a comprehensive understanding of these partially

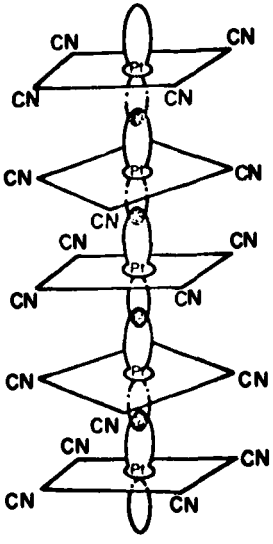

FIG. 1. Illustration of the stacking of square-planar $[Pt(CN)_4]^{X-}$ groups, showing the overlapping of Ptd_{z^2} orbitals.

oxidized (PO) or nonintegral oxidation-state (NIOS) materials has now been achieved (*1*). This chapter will not include such metal-chain systems as $NiPc(I)_x$ (Pc = phthalocyanine; $x \simeq 0.3$–0.4), because M—M distances greater than 3.0 Å are involved, electrical conduction arises primarily from intrachain ligand–ligand interactions, and because a review by Marks and Kalina was published in 1982 (*15*). Chain-forming Ir complexes such as $IrCl(CO)_3$ will not be discussed because a 1982 review of these systems is available (*16*).

The enormous progress that has been made since 1975 in understanding low-dimensional materials has been, in part, due to the in-depth collaborative research between chemists and physicists. Because the fields of chemistry and physics are so inextricably woven with respect to 1-D materials research, it is important that this chapter begin by defining certain terms and concepts related to the basic theories of 1-D conduction.

II. One-Dimensional Band Theory

The first discussion of metallic properties of PO Pt-chain compounds, in terms of a partially filled 1-D band in the chain direction, was given by Krogmann (*9*). In these systems overlap occurs principally between the d_{z^2} and p_z orbitals. The d_{xz}, d_{yz}, and $d_{x^2-y^2}$ orbitals of the metal atom apparently overlap only slightly. When the Pt-atom separations are less than or approximately equal to 3.0 Å, the overlap is substantial and results in the formation of a 1-D band in the chain direction. If the band is partially filled then 1-D metallic properties occur in the metal-atom chain direction. In the case of a system with a d^8 configuration, which must have an even electron count, the partial filling of a band can occur if overlap exists between the filled highest energy band and the empty lowest energy bands (Fig. 2a) or if there is electron removal from the top of the filled highest energy band (Fig. 2b); the latter is the case when partial oxidation of a d^8 ion occurs. A very comprehensive molecular orbital treatment of POTCP metals has been given by Whangbo and Hoffmann (*17*). Although this description (see previous discussion) provides a qualitative introduction to metallic conductivity in one dimension, a more quantitative basis is obtained using the tight-binding band approximation.

The tight-binding band approximation provides a simple theoretical basis for 1-D conduction. In this case we consider a 1-D lattice containing N equally spaced molecules [Fig. 3; see (*18*)] with a repeat distance c. Each isolated molecule has an orbital with energy E_0 that overlaps equivalent orbitals with each of its two surrounding neighbors. From

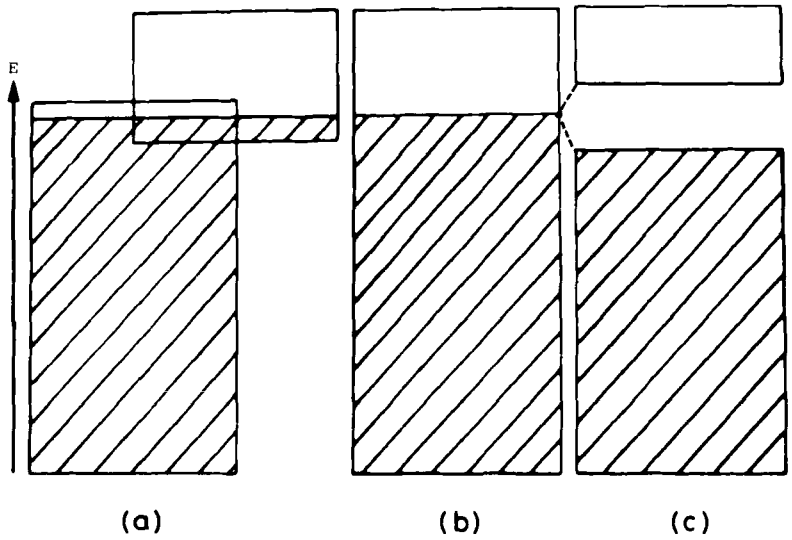

FIG. 2. Illustration of the band structure of a simple 1-D metal. (a) The overlap of full and empty bands. (b) A band that is partially filled. (c) The splitting of a band that is partially filled by a Peierls distortion. [Redrawn from Underhill and Watkins (2).]

tight-binding band theory the orbital energies in the delocalized 1-D array are given by

$$E_i(\mathbf{k}) = E_0 - w\cos(\mathbf{k}c) \equiv E_i(\mathbf{k}),$$

where the allowed values of the wavevector $\mathbf{k}$ and the energies E_i are quantized. As shown in Fig. 3a, the allowed energy levels are very closely spaced above and below that of the isolated molecule E_0, thereby giving the appearance of a continuum. The bandwidth $2W$ forms the boundary of the continuum and comprises N orbitals, which can contain $2N$ electrons. The nearest-neighbor transfer integral t is related to the bandwidth by $2W = 4t$. The density of states per unit energy per spin $D(E)$ (Fig. 3b) is derived from the fact that the wave vector $\mathbf{k}$ has N equally spaced values between $-\pi/c$ and $+\pi/c$.

It is now important to discuss *distortions* in molecular systems and the resulting effects on the total electronic energy of such an ensemble. The familiar Jahn–Teller theorem states that a nonlinear molecular system in a degenerate electronic state is unstable and will be distorted in a manner that will result in lower symmetry and a splitting in the degenerate state. The overall result is a decrease in the total electronic energy of the system.

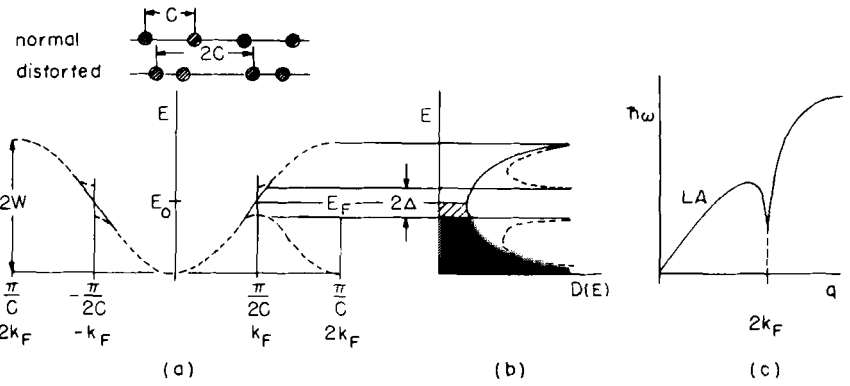

FIG. 3. Anomalies associated with a half-filled conduction band in a 1-D metal. (a) Formation of a band gap at $\mathbf{k}_F$ due to a Peierls distortion of the 1-D lattice. (b) Plot of the density of states per unit energy per spin. (c) A giant Kohn anomaly at $\mathbf{q} = 2\mathbf{k}_F$ in the LA branch of the phonon dispersion. [Adapted from Renker and Comés (*18*).]

In like fashion, Peierls (*19*) and Frohlich (*20*) have shown that a 1-D conductor is also inherently unstable with respect to a lattice distortion. A Peierls transition in an exactly half-filled band (Fig. 3a) causes a lattice distortion in which the molecules dimerize, and this results in the formation of a band gap at the Fermi wave vector $\mathbf{k} = \pi/2c$. It then follows that a Peierls transition in a metal-atom chain converts a 1-D metal into either a semiconductor or an insulator because of the opening of a band gap at the Fermi surface. For a semiconductor the band gap is twice the activation energy for conduction (Δ) and can be determined from electrical-conduction studies performed at variable temperatures. In passing it should be pointed out that the Peierls theory assumes $T = 0$ K, and in reality the band gap becomes temperature dependent at $T \gg 0$ K. At some finite temperature the band gap disappears and an undistorted metallic state exists. In a real 3-D crystalline system the occurrence of metal–insulator transitions occurs at $T \gg 0$ K and is the direct result of coupling between conduction-band electrons and the phonon mode at wave vector $2\mathbf{k}_F$. This in turn produces the *Kohn anomaly* (*21*), which is shown in Fig. 3c. Thus when the energy $\hbar\omega$ of the $2\mathbf{k}_F$ phonon $\equiv 0$, at some finite transition temperature, a static lattice distortion occurs.

It was Frohlich (*20*) who proposed that a distortion in a 1-D metal chain would result in formation of a charge-density wave (CDW) because of the production of a periodic potential by the lattice vibration occurring at $2\mathbf{k}_F$ [Fig. 4; see also (*22*)]. It was further pointed out that if at some point the CDW is not "pinned" in a crystal lattice, these waves

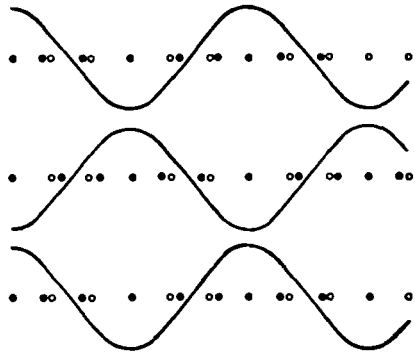

FIG. 4. Three-dimensional ordering caused by an electronic charge-density wave (CDW). For one wave, the relationship of the $2k_F$ lattice distortion and the CDW is shown. ○, Undistorted; ●, distorted lattice sites. [Redrawn from Toombs (*22*).]

produce a moving potential that might result in increased conductivity and, possibly, superconductivity (*20*). A practical consequence of this argument is that when a CDW does become pinned at some finite temperature a metal–insulator type transition occurs. Therefore it is obvious that a 1-D metal will remain metallic when the distortions due to electron–phonon coupling are overcome by the elastic restoring forces of the lattice. Consequently, the stronger the electron–phonon coupling, the higher the transition temperature to a nonconducting state. Thus the suppression of the Peierls transition in 1-D conductors is a practical problem that offers a considerable challenge with respect to the design and synthesis of new materials. We shall elaborate further on these points in Section IV, in which we discuss the physics associated specifically with 1-D Pt-chain metals.

It was not until 1949 that Mott (*23*) introduced the role of Coulombic repulsion between electrons in band theory. Then in 1964 Hubbard (*24*) proposed a model Hamiltonian that included the effective on-site Coulomb repulsion U and the nearest-neighbor transfer integral t. As a consequence, if $t \ll U$ and there is one electron per site, electron localization occurs and Coulomb repulsion is reduced, and the ground state is an antiferromagnetically coupled insulator or Mott–Hubbard insulator. In the case of $t \gg U$, the gain in energy stabilization from delocalization is greater than that due to electron–electron Coulomb repulsion, and the system should become metallic.

As mentioned previously, the search for high-temperature superconducting materials among 1-D systems has prompted a new look at this phenomenon. The BCS (*25*) theory of superconductivity has as its cor-

nerstone a phonon-driven electron-pairing mechanism. The transition temperature for superconductivity T_c can be predicted from the BCS theory by

$$T_c \simeq \frac{\omega_0}{k_B} \exp\left(\frac{-1}{D(\varepsilon_F)V}\right),$$

where k_B is the Boltzmann constant, ω_0 the lattice Debye frequency, $D(\varepsilon_F)$ the density of states at the Fermi surface, and V constitutes the effective electron–electron attraction. Instability will result at some point if V is increased in the hope of raising T_c. The present known maximum for T_c is approximately 25 K in certain metal-alloy systems. To avoid the instability problem, physicist W. A. Little (*26, 27*) proposed that ω_0 be increased instead by using the much higher frequency associated with an electronically polarizable exciton system. In the exciton model a 1-D spine (e.g., a 1-D metal chain) is surrounded by highly polarizable side groups, and electrons moving along the spine could pair up due to electron–exciton–electron interactions. Although very high T_cs are predicted using Little's theory, the problems associated with syntheses of such systems have not yet been surmounted. Still, refinements of Little's theory have resulted in confirmation of the basic principles, and the predictions appear valid (*28*).

Given this background it is now appropriate to consider in detail the chemistry of 1-D Pt-chain systems.

III. The Chemistry of One-Dimensional Partially Oxidized Tetracyanoplatinate (POTCP) Conductors

This chapter encompasses the presently known 1-D complexes formed by the stacking (Fig. 1) of square-planar tetracyanoplatinate (TCP), $[Pt(CN)_4$, (1)] groups. The large majority of 1-D Pt-chain complexes are TCP derivatives, and, to a much lesser extent, the bisoxalatoplatinates. However, because the latter 1-D salts have been extensively reviewed by Underhill *et al.* (*29*), they will not be discussed here.

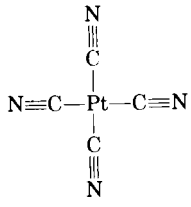

(1)

Complexes containing 1 have a d^8 electron configuration and tend to form square-planar complexes. Krogmann (*9*) and Underhill (*30*) were among the first to point out that the metals given in Table I all have accessible d^8 configurations and, therefore, because of the tendency to form square-planar ligand coordination complexes, could possibly form stacked, columnar structures. Ligands that promote or allow the interactions that favor stacked structures with d_{z^2} orbital overlap are CN^-, CO, Cl^-, and $(C_2O_4)^{2-}$. Although Pt, Ir, and Rh are all known to form 1-D complexes, those of Pt are by far the most predominant.

Although numerous $Pt^{2.0+}$ TCP salts are known to stack in a crystal in such a manner as to form Pt-atom chains, the Pt—Pt distances always exceed 3.0 Å [versus 2.78 Å (*31*) for Pt metal], and the complexes are not metallic. The presently known, and well-characterized, salts of $Pt^{2.0+}$ are given in Table II.

As indicated in Table II, the known TCP complexes of $Pt^{2.0+}$ have a wide range of colors, and their d_{M-M} separations are typically 0.3–0.8 Å longer than in Pt metal. They are nonmetallic in appearance and are electrical insulators because they possess a filled d_{z^2} band {e.g., the conductivity $\sim 5 \times 10^{-7}\ \Omega^{-1}\ cm^{-1}$ for $K_2[Pt(CN)_4] \cdot 3H_2O$}.

A. The Synthesis of One-Dimensional POTCP Metals

In order for metallic properties to arise it is necessary for partial oxidation ($Pt^{2.0} \rightarrow Pt^{2.0+x}$) to occur to form a salt with Pt in a NIOS. Salts of **1**, upon partial oxidation, form POTCP complexes containing $Pt^{2.0+x}$ ($x \cong 0.19$–0.4), which in the crystalline state always have *intra*-chain metal–metal distances (d_{M-M}) of less than 3.0 Å, as opposed to the d_{M-M} spacings given in Table II.

Partial oxidation of a $Pt^{2.0+}$ complex, with the resultant production of a NIOS $Pt^{2.0+x}$ salt with a partially filled band, may be accomplished (*46–49*) by (1) mixing solutions containing the desired $Pt^{2.0+}$ and $Pt^{4.0+}$ salt, (2) chemical oxidation in solution of the appropriate $Pt^{2.0+}$ salt using H_2O_2, or (3) electrolysis of a $Pt^{2.0+}$-containing solution (dc volt-

TABLE I

Metals Having Accessible d^8 Electron Configurations

Configuration	Metal (oxidation state)			
$3d^8$	Fe(0)	Co(+1)	Ni(+2)	Cu(+3)
$4d^8$	Ru(0)	Rh(+1)	Pd(+2)	Ag(+3)
$5d^8$	Os(0)	Ir(+1)	Pt(+2)	Au(+3)

age source and a potential of ~0.75–1.5 V). Method (3) is the preferred procedure at this time because crystal growth on the Pt electrodes is very rapid, namely, seconds or minutes, and well-formed single crystals are easily produced. POTCP complexes may also be grown in this same manner using Au electrodes, and no Au is incorporated in the final product (*50*). In many cases [e.g., $(FHF)^-$ salts (*51*)] method (3) is the only possible route because the appropriate $Pt^{4.0+}$ salt cannot be prepared. When method (1) is used the appropriate tetravalent TCP complex is synthesized by the addition of an excess of oxidant to the $Pt^{2.0+}$ starting material. In the future it may be possible to synthesize POTCP complexes using the $Pt(H_2O)_4^{2+}$ species (*52, 53*). It is important to point out that the success of all of these methods depends on the relative insolubility of the POTCP complex in aqueous solution. In turn, the POTCP salts may be crystallized from aqueous solution un-

TABLE II

THE WELL-CHARACTERIZED SALTS OF TETRACYANOPLATINATE (II)

Compound	Color	Crystal system	d_{Pt-Pt}(Å)[a]	References
$Sr[Pt(CN)_4] \cdot 3H_2O$	Violet	Monoclinic	3.09	(*32*)
$Mg[Pt(CN)_4] \cdot 7H_2O$	Red	Tetragonal	3.155	(*32, 33*)
$Ba[Pt(CN)_4] \cdot 2H_2O$	Dark Red	Orthorhombic	3.16	(*9*)
$Ba[Pt(CN)_4] \cdot 4H_2O$	Yellow-green	Monoclinic	3.321(3)	(*32, 34*)
$Er_2[Pt(CN)_4]_3 \cdot 21H_2O$	—	—	3.17	(*35*)
$Li_2[Pt(CN)_4] \cdot xH_2O$	—	—	3.18	(*36*)
$Dy_2[Pt(CN)_4]_3 \cdot 21H_2O$	—	Orthorhombic	3.18	(*35*)
$Tb_2[Pt(CN)_4]_3 \cdot 21H_2O$	—	—	3.18	(*35*)
$Y_2[Pt(CN)_4]_3 \cdot 21H_2O$	—	Orthorhombic	3.18	(*35*)
$KLi[Pt(CN)_4] \cdot 2H_2O$	—	—	3.20	(*37*)
$K_2Sr[Pt(CN)_4] \cdot 2H_2O$	Violet-red	Monoclinic	3.21	(*36*)
$KNa[Pt(CN)_4] \cdot 3H_2O$	—	Monoclinic	3.26(2)	(*38, 39*)
$(NH_4)_2[Pt(CN)_4] \cdot 2H_2O$	—	—	3.26	(*36*)
$K_2Sr[Pt(CN)_4] \cdot 6H_2O$	Yellow-green	Monoclinic	3.33	(*32*)
$Sm_2[Pt(CN)_4]_3 \cdot 18H_2O$	—	—	3.35	(*40*)
$Mg[Pt(CN)_4] \cdot 4.5H_2O$	Yellow	Triclinic	3.36	(*32*)
$Eu_2[Pt(CN)_4]_3 \cdot 18H_2O$	—	—	3.37	(*40*)
$Ca[Pt(CN)_4] \cdot 5H_2O$	Yellow	Orthorhombic	3.38	(*32*)
$Rb_2[Pt(CN)_4] \cdot 1.5H_2O$	Green	Monoclinic	3.421(2)	(*41*)
$K_2[Pt(CN)_4] \cdot 3H_2O$	—	Orthorhombic	3.478(1)	(*36, 42*)
$Cs_2[Pt(CN)_4] \cdot H_2O$	—	Hexagonal	3.545(1)	(*43, 44*)
$Sr[Pt(CN)_4] \cdot 5H_2O$	Colorless	Monoclinic	3.60	(*32*)
$Na_2[Pt(CN)_4] \cdot 3H_2O$	Colorless	Triclinic	3.71	(*45*)[b]

[a] Values in parentheses are estimated standard deviations of the distance given.

[b] Four independent spacings exist in this salt (3.65, 3.69, 3.75, and 3.75 Å).

der the appropriate conditions. A large number of POTCP complexes and their starting materials have been prepared (see Table III) and the syntheses independently checked (*46–49*).

B. Anion-Deficient and Cation-Deficient Complexes

We now turn to a discussion of the properties of the known POTCP complexes. A summary of the physical property data for all well-characterized POTCP complexes is given in Table III. From this tabulation it is apparent that a wide range of POTCP complexes have been well characterized. As shown in Table III there exist two basic types of POTCP complex as follows.

1. *Anion-Deficient (AD) Complexes.* In AD complexes PO of the Pt atom and partial filling of the d_{z^2} band are achieved by the formation of a compound that contains a nonstoichiometric number of anions (X). The general formula for these materials is $M_i[Pt(CN)_4]X_n \cdot jH_2O$ [where M is a monovalent cation, i an integer (1–3), n nonintegral and <1.0, and j has values of 0–3]. The molecular structures of AD salts vary significantly, as do the electrical properties, between the hydrated and anhydrous AD derivatives (see following discussion).

2. *Cation-Deficient (CD) Complexes.* In CD materials the nonstoichiometry occurs when the cation content is nonintegral. The general formula for these materials is $M_i[Pt(CN)_4] \cdot jH_2O$ [where i is nonintegral ($1 < i < 2$) and j always appears to be > 1].

The structural and electronic properties of 1-D POTCP metals are highly dependent on the nature of the species that constitute the crystal lattice. Before discussing the basic structural features of POTCP complexes it will be helpful if we first discuss the concept of the degree of partial oxidation (DPO) in these materials.

The Degree of Partial Oxidation of Pt in POTCP Complexes

A knowledge of the DPO of the metal atom in POTCP salts is critically important to the understanding of the associated solid-state properties. The DPO can be determined as follows.

1. By iodimetric titration of the POTCP complex in solution, the $Pt^{2.0}:Pt^{4.0}$ ratio may be determined.

2. By chemical analysis, the cation : anion mole ratio may be determined. This method is not without difficulty because in certain cases, for example, $(NH_4)_2(H_3O)_{0.17}[Pt(CN)_4]Cl_{0.42} \cdot 2.83H_2O$ [ACP(Cl)], the method yielded (before it was surmised that the complex contained

H_3O^+ due to crystallization from acid solution) DPO = 0.42, which was far too high for $d_{M-M} \simeq 2.92$ Å (*61, 62*). By comparison, the DPO (see Table III) for KCP(Br) is 0.3, and the d_{M-M}, which should be greater than that in ACP(Cl), is actually less (2.87 Å). This problem was clarified using method (3).

3. By the use of X-ray diffuse-scattering (XDS) techniques, the DPO may be determined. This method appears to be the most accurate for POTCP materials and can be used to understand the known "modulations" of the average structure, as determined by X-ray or neutron crystallography. For an introduction to the uses of XDS techniques, see Section III,D and (*77–79*).

Before discussing XDS "structural" studies of POTCP metals, we must first understand their basic structural types.

C. The Crystal and Molecular Structures of POTCP Metals

In order for us to understand the physical properties associated with POTCP materials, it is important that we begin with a description of some of their basic structural features and the variations produced when different cations and anions are introduced.

Given that a POTCP complex will always contain stacked $Pt(CN)_4^{2.0+x}$ groups, the basic molecular geometries that can be formed now appear somewhat predictable (*3*). There is obviously a certain "basic integrity" to the metal-atom chain in a POTCP salt, because the chain itself behaves in an *accordion*-like fashion upon partial oxidation, that is, the Pt—Pt distances vary over only a small range of approximately 0.2 Å for these materials (see Table III). The Pt—Pt distances and the DPO of the metal atom are now known to behave in a predictable manner (*80*). In general, as the DPO increases and the d_{M-M} decreases the conductivity of a POTCP salt increases.

1. Anion-Deficient POTCP Salts

a. Hydrated Derivatives. Krogmann and Hausen (*81*) were the first to report the crystal structure of the prototypical AD salt $K_2[Pt(CN)_4]Br_{0.3} \cdot 3H_2O$ ("KCP(Br)" or "KCP"). The structural description was slightly in error due to an incorrect distribution of the molecular contents of the unit cell, as pointed out from a neutron-diffraction study by Williams *et al.* (*82*), but the most important feature, the Pt-atom chain, was elucidated, thereby providing a structure of pivotal importance.

TABLE III

PARTIALLY OXIDIZED TETRACYANOPLATINATE METALS: CRYSTAL STRUCTURE AND CONDUCTIVITY DATA

Complex	Abbreviation	Space group[a]	Intrachain separation[b] d_{Pt-Pt} (Å) (T = 298K)	Conductivity[c] (ohm^{-1} cm^{-1})	Color
Pt metal			2.775[d]	9.4×10^4	Metallic
$K_2[Pt(CN)_4]Br_{0.30} \cdot 3H_2O$	KCP(Br)	$P4mm$[a,e]	2.89	4–1050	Bronze[f]
$K_2[Pt(CN)_4]Cl_{0.30} \cdot 3H_2O$	KCP(Cl)	$P4mm$[g]	2.87	~200	Bronze[f]
$K_2[Pt(CN)_4]Br_{0.15}Cl_{0.15} \cdot 3H_2O$	KCP(Br, Cl)	$P4mm$[h]	—	—	—
$Rb_2[Pt(CN)_4]Cl_{0.3} \cdot 3H_2O$	RbCP(Cl)	$P4mm$[i,j]	2.877(8) and 2.924(8) at T = 298K[i]; 2.885(6) and 2.862(6) at T = 110K[j]	10[k]	Bronze
$Cs_2[Pt(CN)_4]Cl_{0.3}$	CsCP(Cl)	$I4/mcm$[l]	2.859(2)	~200[m]	Bronze
$(NH_4)_2(H_3O)_{0.17}[Pt(CN)_4]Cl_{0.42} \cdot 2.83H_2O$	ACP(Cl)	$P4mm$[n]	2.910(5) and 2.930(5)	0.4[o]	Bronze
$Cs_2[Pt(CN)_4](N_3)_{0.25} \cdot 0.5H_2O$	CsCP(N_3)	$P\bar{4}b2$[p]	2.877(1)	40–270[q]	Reddish–copper
$Rb_3(H_3O_{0.x}[Pt(CN)_4]9O_3SO \cdot H \cdot OSO_3)_{0.49} \cdot (1 - x)H_2O$	RbCP(DSH)	$P\bar{1}$[r]	2.826(1)	[s]	Copper
$K_{1.75}[Pt(CN)_4] \cdot 1.5H_2O$	K(def)TCP	$P\bar{1}$[t]	2.965(1) and 2.961(1)	115–125[u,v]	Bronze

$Rb_{1.75}[Pt(CN)_4] \cdot xH_2O$	Rb(def)TCP	V^{w}	2.94[x]	1[v]	Bronze
$Cs_{1.75}[Pt(CN)_4] \cdot xH_2O$	Cs(def)TCP	V^{w}	2.88	~25[y]	Bronze
$K_2[Pt(CN)_4](FHF)_{0.30} \cdot 3H_2O$	$KCP(FHF)_{0.3}$	$P4mm^{z}$	2.918(1) and 2.928(1)	[s]	Reddish–bronze[aa]
$Rb_2[Pt(CN)_4](FHF)_{0.40}$	$RbCP(FHF)_{0.4}$	$I4/mcm^{bb}$	2.798(1)	1600[cc] 2300[dd]	Gold
$Rb_2[Pt(CN)_4](FHF)_{0.26} \cdot 1.7H_2O$	$RbCP(FHF)_{0.26}$	$C2/c^{w}$	2.89	[s]	Greenish–bronze[aa]
$Cs_2[Pt(CN)_4](FHF)_{0.39}$	$CsCP(FHF)_{0.4}$	$I4/mcm^{ee}$	2.833(1)	2000[cc] 1600[dd]	Reddish–gold[aa]
$Cs_2[Pt(CN)_4](FHF)_{0.23}$	$CsCP(FHF)_{0.23}$	$I4/mcm^{w}$	2.872(2)	250–350[w]	Reddish–bronze[aa]
$Cs_2[Pt(CN)_4]F_{0.19}$	CsCP(F)	$Immm^{w}$	2.866(1)	[s]	Reddish–gold[aa]
$[C(NH_2)_3]_2[Pt(CN)_4](FHF)_{0.26} \cdot xH_2O$	$GCP(FHF)_{0.26}$	[s]	2.90[ff]	[s]	Bronze
$[C(NH_2)_3]_2[Pt(CN)_4]Br_{0.25} \cdot H_2O$[gg]	GCP(Br)	$I4cm^{gg}$	2.908(2)	11[gg]	Bronze

[a] In space group $P4mm$ the Pt—Pt intrachain distances are not required to be equal, but they often appear so. When they have been determined to be different both distances are given.

[b] Values in parentheses are estimated standard deviations of the distances given.

[c] The range of literature values reported for room temperature four proble DC conductivities are given.

[d] (*31*). [e] (*3*). [f] (*5*). [g] (*54*). [h] (*55*). [i] (*56*). [j] (*57*). [k] (*58*). [l] (*59*). [m] (*60*). [n] (*61*). [o] (*62*). [p] (*63*). [q] (*64*). [r] (*3*), pp. 361–362. [s] (*107*). [t] (*65–67*). [u] (*68*). [v] (*69*).

[v'] The crystal class is monoclinic, but the space group is unknown. The lattice constants for the Cs salt[w] are a = 18.35(1) Å, b = 5.760(3) Å, c = 19.92(1) Å, β = 109.03(4)°; for the Rb salt[u] the lattice constants are a = 10.56(1) Å, b = 33.2(1) Å, c = 11.74(1) Å, β = 114.23(3)°.

[w] J. M. Williams, work in progress.

[x] (*70*). [y] (*71*). [z] (*72*). [aa] (*51*). [bb] (*73*). [cc] (*3*). [dd] (*74*). [ee] (*75*). [ff] (*3*), p. 357. [gg] (*76*).

In KCP(Br) and its isostructural "type-P" [P = primitive (*3*)] derivatives (see Table III, space group $P4mm$), DPO = 0.3, indicating that in the process of oxidation 0.3 electrons per Pt atom have been removed from the highest filled ($5d_{z^2}$) band. Therefore, 1.7 electrons per Pt atom remain in the band, and in the crystal (see Fig. 5) the $[Pt(CN)_4]^{1.7-}$ moieties stack to form linear, metal-atom chains that have *equal intra*atomic Pt—Pt spacings (d_{M-M} = 2.89 Å). The K^+ ions are situated in one-half of the unit cell, and the H_2O molecules, which are located in the other half, form a network of hydrogen bonds between the CN^- ligands and either the Br^- anion at the unit-cell center or the CN^- ligand from a TCP group on an adjacent chain. Adjacent TCP chains are separated by 9.89 Å, which accounts in part for the great anisotropy in the physical properties for KCP derivatives. Therefore, type-P salts are those in which the cations and water molecules do *not* occupy the same molecular plane as the $Pt(CN)_4$ groups. Isostructural halide (Br^-, Cl^-) derivatives of KCP are all nonstoichiometric, and the central portion of the unit cell is alternatively occupied by either a Br^- ion (at ½, ½, ½, labeled Br* in Fig. 5, 60% occupancy) or an H_2O molecule (at

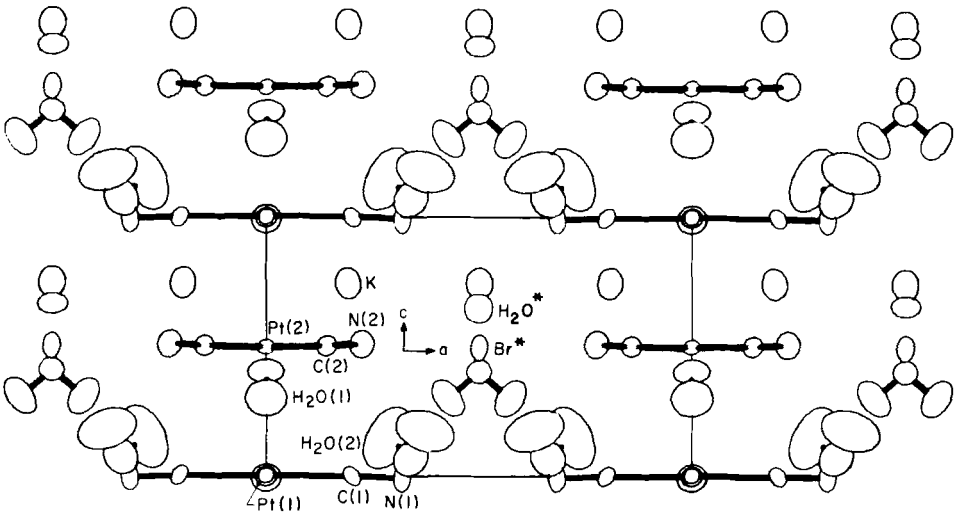

FIG. 5. Structure of the prototypical type-P complex $K_2[Pt(CN)_4]Br_{0.3} \cdot 3H_2O$ [KCP(Br)], shown as a *b*-axis half-cell projection. In type-P 1-D metals (*3*) the cations are interleaved *between* the $Pt(CN)_4$ groups. The independent atoms in the asymmetric unit are identified. The disordered Br^- and H_2O sites are labeled as Br* and H_2O*. The K^+ ions occupy one-half of the unit cell, and the H_2O molecules occupy the other half. Note that the Pt—Pt distances are all equal at 2.89 Å.

½, ½, 0.67, H_2O* in Fig. 5, 40% occupancy). Accompanying the very short intrachain Pt—Pt separation of 2.89 Å is an intrachain torsion angle of 45° between adjacent $[Pt(CN)_4]^{1.7-}$ groups, which apparently minimizes ligand stearic hindrance. Numerous structural studies of KCP(Br, Cl) have been reported (*54, 82, 83*), and the structural architecture of these prototypical salts is well understood.

A discussion of structure–property relationships in KCP analogs would be incomplete if it were not mentioned that these compounds undergo gradual transitions from an ambient-temperature conducting state [σ = 5–800 Ω^{-1} cm^{-1} (*84*)] to a low-temperature insulating state.

From variable-temperature Mössbauer and ESCA studies the electronic equivalence of the Pt atoms in KCP(Br) has been confirmed (*5*). In addition, classical crystallographic studies (*54, 82, 83*) have shown that the structure of KCP(Br) remains basically unchanged, even to liquid-He temperatures. The observation of a giant Kohn anomaly (*77, 85*) and a low-temperature 3-D superlattice (*77–79*) from various XDS and inelastic neutron-scattering studies provides ample evidence for a Peierls distortion and CDW formation in these materials. Therefore, in KCP(Br) the *average* crystallographic structure is invariant with temperature but is "modulated" by a CDW, and the room-temperature response of the $Pt(CN)_4$ groups is that a dynamic, sinusoidal displacement of each Pt atom along each chain occurs with no coherence between neighboring chains. The repeat period of 6.67 c', where c' is twice the d_{Pt-Pt} distance, is exactly that expected for a Peierls distortion. At 77 K and below, a 3-D ordering occurs, and the distortion becomes static. From neutron-scattering studies Lynn *et al.* (*86*) have shown that the sinusoidal Pt-chain distortion, due to the formation of a CDW by the d_{z^2} electrons, involves each atom of the $Pt(CN)_4^{1.7-}$ moiety that "rides" on the CDW. At liquid-He temperature the Pt atom displacement, due to the CDW, is only 0.025 Å from the perfectly equal spacing derived in a classical structure analysis (*86*). Therefore, the average crystallographic structure of KCP(Br) is constant but is modulated by a CDW, to which each $Pt(CN)_4^{1.7-}$ group responds.

Although $Rb_2[Pt(CN)_4]Cl_{0.3} \cdot 3H_2O$ [RbCP(Cl)] has been characterized by single-crystal neutron scattering and XDS (*56*) and appears to be isostructural with KCP(Br), only one halide site per unit cell has been identified. Another significant structural feature is that, although not required by the space-group symmetry, all intrachain Pt—Pt separations in KCP are equal. However, in RbCP(Cl) there is a definite *dimerization* of the linear Pt-atom chain (see Fig. 6). Compared to KCP(Br), it appears that the replacement of the K^+ ion by the larger Rb^+ ion results in lattice expansion along c, which in turn pro-

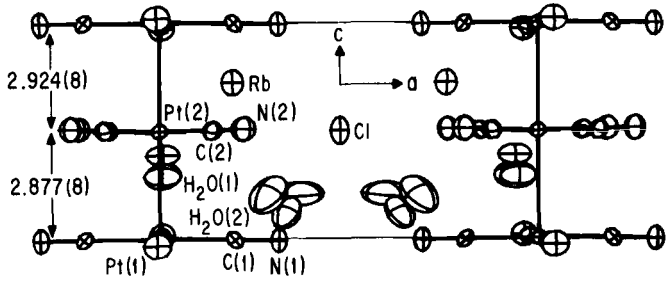

FIG. 6. Structure of $Rb_2[Pt(CN)_4]Cl_{0.3} \cdot 3.0H_2O$ at 298 K, showing the *unequal* Pt—Pt separations in the linear metal-atom chain. The average Pt—Pt distance in the dimerized chain is approximately 0.03 Å longer than in KCP(Br) (Fig. 5). Only one Cl^- site was identified (*56*).

duces larger Pt—Pt spacings in RbCP(Cl). It is therefore reasonable to expect that the electrical conductivity of RbCP(Cl) might be less than that of KCP(Br) due to the longer, dimerized Pt chain.

However, the question of how the electrical conductivity varies with structural changes and temperature in hydrated type-P POTCP salts affords surprising results, as explained here for RbCP(Cl). A low-temperature neutron-diffraction study (*57*) of this salt showed that the degree of dimerization *decreases* with temperature (see Fig. 7) which was unexpected because variable-temperature conductivity studies (*58*) established that the electrical conductivity along the Pt-atom chain also decreases with decreasing temperature in the sequence ACP(Cl) < RbCP(Cl) ≃ KCP(Br) (Fig. 8). Just the opposite results are expected, that is, that as chain dimerization and the associated electron localization decrease, the conductivity should rise. The explana-

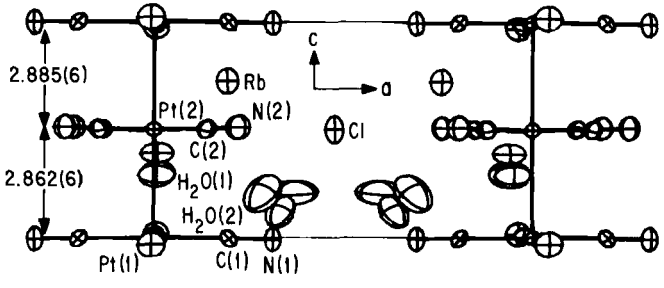

FIG. 7. Unit cell of $Rb_2[Pt(CN)_4]Cl_{0.3} \cdot 3H_2O$, derived from neutron-diffraction data collected at 110 K. Note that the degree of chain dimerization *decreases*, compared to the room-temperature structure (Fig. 6) and that the average Pt—Pt spacing decreases by approximately 0.02 Å at 110 K (see *57*).

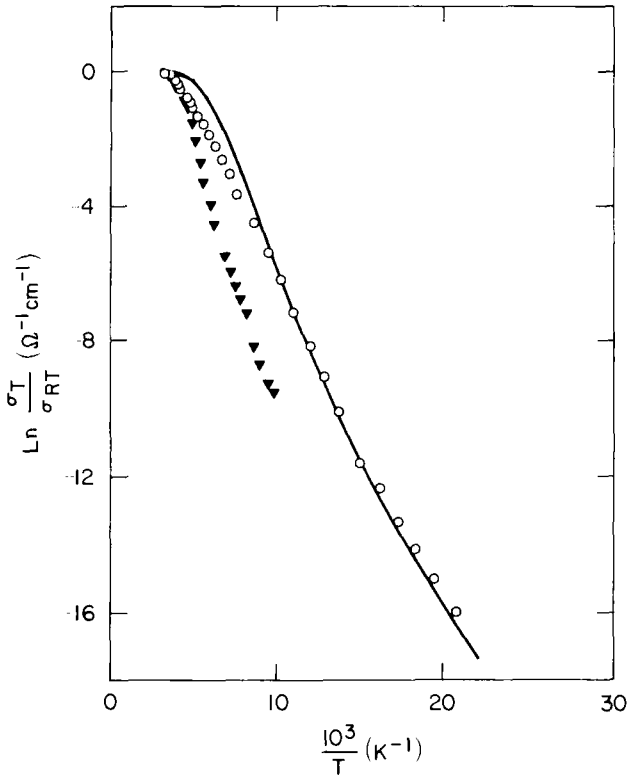

FIG. 8. Temperature dependence of the dc electrical conductivity along the Pt—Pt chain for three type-P isostructural compounds (space group *P4mm*): —, KCP(Br); ○, RbCP(Cl); ▼, ACP(Cl) (see *58*).

tion for this behavior does not lie in the degree of chain dimerization but rather in terms of *differing temperatures* at which there is coupling of the 1-D lattice distortions, or Peierls distortions, which in turn cause the Pt-atom chains to undergo a 3-D ordering transition at a temperature termed T_{3D} (*87*). It appears that there is always a decrease in conductivity in POTCP salts at T_{3D}. The means whereby T_{3D} may be derived and the T_{3D}s for POTCP materials are discussed in Section IV.

It is apparent that although KCP(Br) never undergoes chain dimerization at any temperature, some type-P salts exhibit this behavior, even if the d_{Pt-Pt} is almost that of KCP(Br). A summary of the structural results derived from numerous diffraction studies, in which monovalent cations of differing radius (r^+) have been substituted for K^+, is as follows (*59*).

1. For a given d_{Pt-Pt}, as r^+ increases the probability of dimerization increases.
2. For a given r^+, as d_{Pt-Pt} decreases the probability that dimerization will occur decreases.
3. For a given r^+ the d_{Pt-Pt} tends to depend on the DPO, and therefore the degree of chain dimerization may depend on the DPO.

b. Anhydrous Derivatives. Extensive synthetic studies of POTCP metals at Argonne National Laboratory in the late 1970s resulted in the discovery of a new class of salts, "type-I" (I = body-centered lattice), with markedly different structure–property relationships compared to the hydrated KCP-type derivatives. The most salient structural difference between the hydrated type-P and anhydrous type-I salts is that in the latter the M^+ cations occupy the same molecular plane as the square-planar $Pt(CN)_4$ groups, which maximizes M^+—$^-N{\equiv}C$ interactions. Examples of this class of material are $Cs_2[Pt(CN)_4]Cl_{0.3}$ [(*59*); see Fig. 9], $Cs[Pt(CN)_4](FHF)_{0.38}$ (*75*), $Cs[Pt(CN)_4](FHF)_{0.23}$ (*51*), $Rb_2[Pt(CN)_4](FHF)_{0.4}$ [(*73*); Fig. 10], and pseudo-body-centered $Cs_2[Pt(CN)_4](N_3)_{0.25} \cdot xH_2O$ (*63*). It appears that although the $(FHF)^-$ salts are strictly anhydrous, both $Cs_2[Pt(CN)_4]Cl_{0.3}$ and $Cs_2[Pt(CN)_4](N_3)_{0.25} \cdot xH_2O$ may be slightly hydrated. $Rb_2[Pt(CN)_4](FHF)_{0.4}$ is unique in that it contains the *shortest* Pt—Pt spacing (2.798 Å) and *highest* room-temperature electrical conductivity of any known POTCP salt (*73, 74*). However, all of these derivatives possess type-I molecular architecture, which markedly affects (improves!) the conduction behavior (see following discussion).

The results of variable-temperature electrical-conduction studies of a number of type-I salts have been reported (*60, 74*), and they are

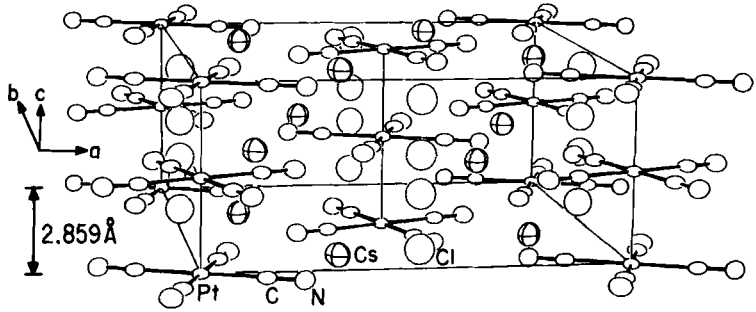

FIG. 9. Unit cell of the type-I 1-D metal, anhydrous $Cs_2[Pt(CN)_4]Cl_{0.3}$, [CsCP(Cl)]. Note that in type-I complexes the cation Cs^+ occupies the same molecular plane as the $Pt(CN)_4$ groups (see *59*).

compared with KCP(Br) in Fig. 11. Metallic conduction is exhibited by KCP(Br) at room temperature, but at low temperature it becomes semiconducting in nature. From Fig. 11 it is apparent that the conduction behavior of $Cs_2[Pt(CN)_4]Cl_{0.3}$ is intermediate between that of KCP(Br) and $Rb_2[Pt(CN)_4](FHF)_{0.4}$.

In all of the known POTCP salts it appears that the room-temperature conductivity $\sigma_\parallel$ is dominated by the *intra*chain Pt—Pt separation, but considerable differences in behavior arise at reduced temperature, depending on the structure type, nature of the cations and anions present, etc. *Inter*chain Pt—Pt distances vary somewhat, and it is noteworthy that in the type-I derivatives enhanced conductivity parallels reduced interchain spacings, {cf. 9.32 Å in $Cs_2[Pt(CN)_4]Cl_{0.3}$, 9.23 Å in $Cs_2[Pt(CN)_4](FHF)_{0.39}$, and 8.97 Å in $Rb_2[Pt(CN)_4](FHF)_{0.4}$}. However, this trend in reduced interchain separation also parallels a reduced intrachain Pt—Pt distance.

From Fig. 11 it is obvious that the decrease in conductivity in passing from room temperature to the lower-temperature semiconducting region is much less for the anhydrous type-I salts compared to the type-P salts. The activation energies in the semiconducting region are approximately 0.02 eV for the bifluoride salts with DPO $\cong$ 0.40 compared to approximately 0.07 eV for KCP(Br), for which DPO = 0.30 (*60*). As discussed in Section IV, the 3-D ordering temperature T_{3D} is a measure of Coulombic interchain coupling and depends to some degree on the presence of hydrogen bonding between $Pt(CN)_4$ groups. Therefore, it is not unexpected that T_{3D} is lowest for type-I salts, as will be shown later (see Fig. 15).

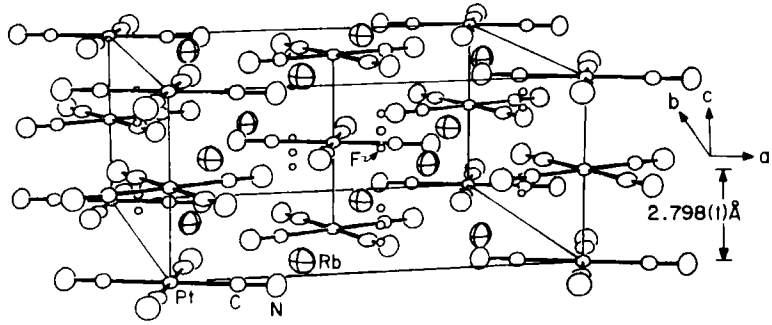

FIG. 10. Perspective view of the unit cell of type-I $Rb_2[Pt(CN)_4](FHF)_{0.4}$ [RbCP(FHF)$_{0.4}$]. The small circles are the partially filled F-atom positions. The Pt—Pt spacing is the *shortest* known for any POTCP 1-D metal (*73*). The corresponding Pt-chain conductivity is the *highest* (~2000 Ω^{-1} cm^{-1} at 298 K) for any known POTCP complex (see *60, 73*).

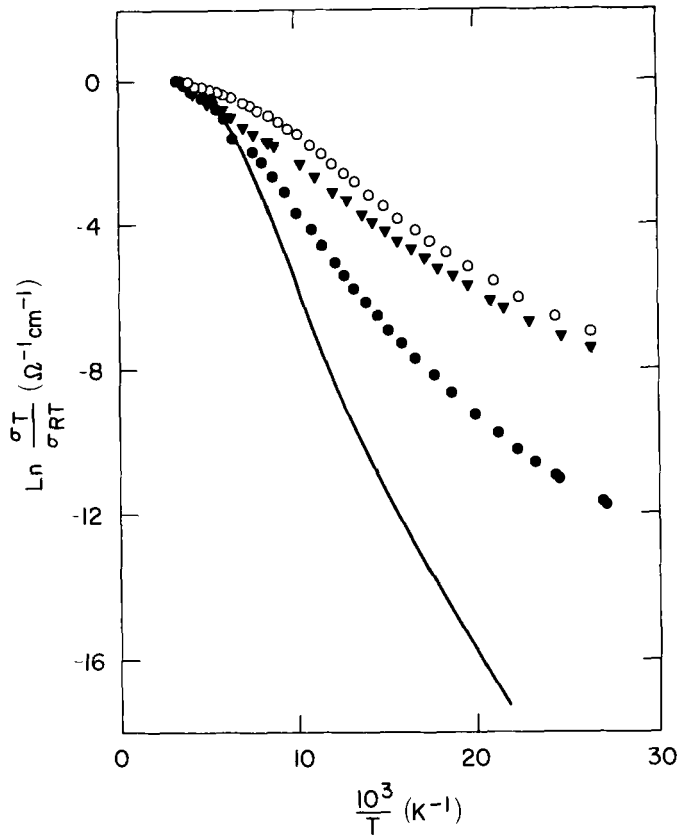

FIG. 11. Temperature dependence of the in-chain dc conductivity for three isostructural type-I compounds (space group *I4/mcm*): ○, $RbCP(FHF)_{0.4}$; ▼, $CsCP(FHF)_{0.4}$; ●, $CsCP(Cl)_{0.3}$ (see *60, 74*). The curve (—) is for type-P KCP(Br) and is shown for comparison purposes.

2. *Cation-Deficient POTCP Salts*

The CD complexes of POTCP metals are few in number compared to the AD derivatives, and only $K_{1.75}[Pt(CN)_4] \cdot 1.5H_2O$ [K(def)TCP, where K(def) = K deficient] has been well characterized (DPO = 0.25) by a variety of physical and theoretical studies [see (*65–67, 88*) and Table III]. A high-precision neutron-diffraction study (*66*) was used to locate all atoms in the structure, including hydrogen, and the derived crystal structure is shown in Fig. 12. The most unusual finding was that K(def)TCP contains the longest Pt—Pt separations (2.96 and 2.97 Å) and the only known bent atom chain in a POTCP salt. From these

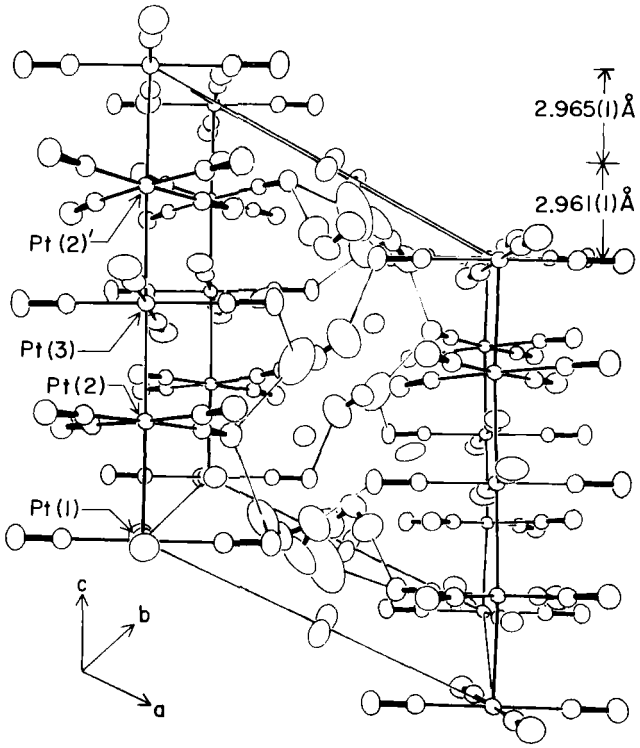

FIG. 12. Unit cell of triclinic $K_{1.75}[Pt(CN)_4] \cdot 1.5H_2O$ [Kdef(TCP)], derived from neutron-diffraction data showing the *non*linear Pt-atom chain [Pt(1)-Pt(2)-Pt(3) = 173.3°], which extends along *c*. Note that the Pt—Pt spacings, which are equal although not required by the space-group symmetry, are the longest for any known POTCP complex (see *65*, *66*).

results it appears that $d_{Pt-Pt} \simeq 3.0$ Å is the upper limit of the *intra*-chain Pt—Pt separation for POTCP formation. Another noteworthy finding was that, even though not required crystallographically as is also the case for KCP, the Pt—Pt separations are essentially equal. XDS studies (*70*) of K(def)TCP have been used to show that it possesses a superlattice structure that is *commensurate* with the Pt-atom chain (*c* axis of the crystal) with a repeat distance $8c'$ (c' = average d_{Pt-Pt}). In KCP derivatives in which DPO = 0.30, XDS studies reveal a superlattice that is *incommensurate* (6.67 c'). The wave vector derived from the XDS studies agrees very well with $2\mathbf{k}_F$ predicted from the chemical stoichiometry (*89*). This may be demonstrated as follows. A completely filled d_{z^2} band would contain a contribution of two electrons from each Pt atom, and the calculated Fermi wave vector would then

be $\mathbf{k}_F = (1.75/2)\pi/c'$. From the XDS study the derived wave vector $\mathbf{k} = 2\pi/8.1\ c'$ or $2\pi(1 - 1/8.1)/c'$, which is in essential agreement with that just predicted. In passing it should be noted that the *nature* (commensurate versus incommensurate) of the superlattice observed in POTCP metals may be an underlying factor in the conductivity trend K(def)TCP $\ll$ KCP(Br).

Three M(def)TCP salts (M = K^+, Rb^+, and Cs^+) have all been shown to be 1-D metals from optical-reflectance studies (*90*). Neutron-scattering studies (*88*) have shown the presence of a Kohn anomaly in K(def)TCP.

Although two independent electrical-conduction studies (*68, 69*) have established that the room-temperature values ($\sigma_\parallel \simeq 100\ \Omega^{-1}\ cm^{-1}$) are the same and also that the conduction *behavior* of K(def)TCP and KCP(Br) is different, the detailed interpretation of the data and the derived zero-temperature band gaps (Δ) and T_{3D}s, respectively, are at some variance. These results and the interpretation derived from an independent Raman scattering study (*91*) have been discussed in detail elsewhere (*92*).

Perhaps the most important finding from all of these studies is that the M(def)TCP salts have physical properties that are considerably different from those of KCP-type analogs, and each of these two sets appears to constitute a separate class. The source of the physical property differences is in part due to the finding that in POTCP materials the observed Peierls distortions are related to the DPO. In fact, an understanding of the relationships between the DPO and the physical parameters used to describe POTCP metals provides the basic information needed for unraveling the physics of these materials.

D. X-Ray Diffuse Scattering and Structural Modulation in POTCP Metals

A characteristic of all 1-D POTCP metals is the existence of a modulated structure (*89*). In the case of a TCP stack (see Fig. 1), this subtle structural feature is best described as a modulation of the *average* atomic positions, which arises from electron–phonon coupling, and it can provide basic information regarding the conduction-band properties of a material.

The prototypical POTCP complex $K_2[Pt(CN)_4]Br_{0.3} \cdot 3H_2O$ ["KCP(Br)" or "KCP"] exhibits both neutron and XDS, which led Comés and co-workers (*77*) to elucidate in detail this phenomenon in KCP(Br). The important concepts for a hypothetical case are illustrated in Fig. 13, in which we assume a 1-D lattice with a one-eighth

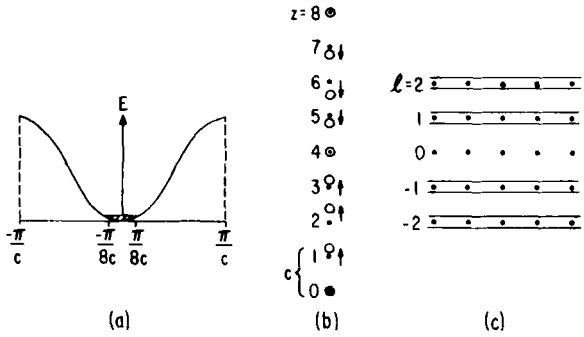

FIG. 13. (a) One-eighth filled band. (b) Sinusoidal lattice distortion with shifts of $\delta = \Delta\sin(2\pi z/8)$ and a period of 8c. (c) X-Ray diffuse-scattering diagram showing diffuse satellite planes around Bragg spots in reciprocal space.

filled band [the actual case for K(def)TCP, with DPO = 0.25]. The band gap is formed at $\mathbf{k}_F = \pi/8c$, which produces a lattice modulation of periodicity 8c. This results in sinusoidal distortions, namely, a CDW (see Fig. 4) along the metal chain. At high temperatures there is no phase correlation between the CDWs of parallel chains in a crystal, and this property may be observed using elastic XDS or neutron diffuse scattering as satellite planes of diffuse scattering in reciprocal space with wave vectors of $2\mathbf{k}_F$. When using X rays and a photographic film, the manifestation of the Peierls distortion (i.e., a CDW) is the presence of weak planes or lines (diffuse lines) about the layer line spots, which are due to normal Bragg scattering (*70*). For POTCP complexes the DPO can be calculated from the position of the diffuse scattering lines using the relationship

$$\text{DPO} = 2(1 - \mathbf{k}_F d_{\text{Pt}-\text{Pt}}/\pi),$$

where $d_{\text{Pt}-\text{Pt}}$ is the average *intra*chain Pt—Pt separation.

At some reduced temperature, referred to as the 3-D ordering temperature T_{3D}, the weak planes of scattering density coalesce into superlattice Bragg spots as a result of the 3-D ordering of the CDWs on *adjacent* metal-atom chains caused by *inter*chain Coulombic interactions. At T_{3D} the waves on adjacent chains have opposite phases (see Fig. 4). Thus η, the *inter*chain coupling parameter, is related to the three-dimensionality of the lattice.

One may differentiate between a dynamic [Kohn anomaly (*21*)] or static lattice distortion [Peierls distortion (PD) (*19*)] using inelastic neutron scattering. As stated previously the Kohn anomaly is a soft

phonon mode at wave vector $2\mathbf{k}_F$ that is the result of a dynamic periodic distortion that arises from electron–phonon interactions. When the temperature is decreased, the energy (frequency) of the $2\mathbf{k}_F$ mode approaches zero (see Fig. 3c), at which point the distortion becomes a static PD.

Because POTCP complexes always contain cations or anions in crystallographic disorder, it is important to point out that the diffuse scattering does not arise from chemical disorder–diffuse scattering. This has been established from the observation that the intensity of the planes of diffuse scattering increases at higher diffraction angles. This rules out disorder–diffuse scattering arising from long-range ordering of anions or cations in the crystal.

Although Comés *et al.* (*78, 93*) were the first to use XDS techniques to measure the $2\mathbf{k}_F$ superstructure lines of KCP(Br), the methods were later taken up by Schultz *et al.* (*70*), Carneiro *et al.* (*62*), and by Braude *et al.* (*94*). Table IV lists the POTCP metals studied that exhibit $2\mathbf{k}_F$ scattering and the DPOs derived from the scattering study compared

TABLE IV

$2\mathbf{k}_F$ VALUES (IN UNITS OF $2\pi/d_{Pt-Pt}$) DETERMINED BY DIFFUSE X-RAY SCATTERING AND CHEMICAL ANALYSIS AND COMPARED TO INTRACHAIN Pt—Pt DISTANCES

Compound	Abbreviation	d_{Pt-Pt} (Å)	$2\mathbf{k}_F$ (chemical)	$2\mathbf{k}_F$ (X-ray)
$K_2[Pt(CN)_4]Br_{0.30} \cdot 3H_2O$	KCP(Br)	2.89	1.70	1.67[a] 1.70[b]
$[C(NH_2)_3]_2[Pt(CN)_4]Br_{0.25} \cdot xH_2O$	GCP(Br)	2.908	1.77	1.75[c]
$K_{1.75}[Pt(CN)_4] \cdot 1.5H_2O$	K(def)TCP	2.965 2.961	1.75	1.76[c] 1.775
$Rb_{1.75}[Pt(CN)_4] \cdot xH_2O$	Rb(def)TCP	2.94	1.75	1.73[c]
$Cs_{1.75}[Pt(CN)_4] \cdot xH_2O$	Cs(def)TCP	2.88	1.75	1.72[c]
$(NH_4)_2(H_3O)_{0.17}[Pt(CN)_4]Cl_{0.42} \cdot 2.83H_2O$	ACP(Cl)	2.92	1.58[d]	1.75[e,f]
$Rb_3(H_3O)_{0.x}[Pt(CN)_4](O_3SO{\cdot}H{\cdot}OSO_3)_{0.49} \cdot (1 - x)H_2O$[g]	RbCP(DSH)	2.826	1.53[h]	1.68[f]
$Cs[Pt(CN)_4](FHF)_{0.39}$	CsCP(FHF)$_{0.4}$	2.833	1.61	1.60[f]

[a] (*78*). [b] (*95*). [c] (*70*).

[d] $2\mathbf{k}_F$ (chemical) was determined from the mole ratios of NH_4^+, Pt, and Cl, before (H_3O^+) was inserted in the formula.

[e] (*62*). [f] (*94*).

[g] The chemical formula given here is the "most likely" formula for RbCP(DSH), based on the crystal structure, probable chemical composition, and X-ray diffuse-scattering measurements (*107*).

[h] This value is for $x = 0$. If $x = 0.12$, then the chemical stoichiometry and the X-ray diffuse scattering are in agreement.

to those obtained from chemical analysis. It should be noted from Table IV that there is generally good agreement between $2\mathbf{k}_F$ as determined by XDS and chemical methods, except for ACP(Cl) and RbCP(DSH). This difference is explained (*62, 96*) by assuming that additional positive charge is present in the crystals as H_3O^+, which counterbalances part of the charge due to the anion, thus rendering inaccurate the determination of the DPO via the $Pt^{2.0+}$ and $Pt^{4.0+}$ ratio deduced from oxidation–reduction titrations. This was eventually understood as resulting from the crystallization of the POTCP complex from a highly acidic solution, which resulted in the incorporation of a hydrated proton species (or more than one species) in the crystal. Finally, the study of diffuse scattering from POTCP compounds has proven to be an invaluable aid in understanding their chemical composition and many related aspects (*1*).

Metal–Metal Bond Lengths and Correlations with DPO

The metal–metal bond lengths in POTCP complexes vary in a systematic manner with the DPO, and Williams (*80*) was the first to point

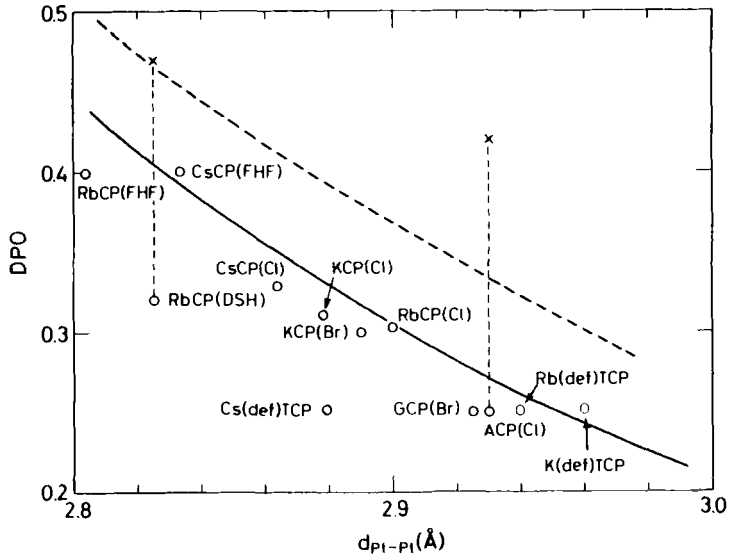

FIG. 14. Plot of the degree of partial oxidation (DPO) versus intrachain Pt—Pt bond lengths for POTCP metals (*80*). Curve (—) is derived using Pauling's formula for metallic resonance, curve (– –) is for no metallic resonance (see *97, 98*). Analysis: x, chemical; O, X-ray diffuse-scattering. The d_{Pt-Pt} spacing for RbCP(Cl) is the average value given in Table III.

out that d_{Pt-Pt} may be calculated from the DPO, and vice versa, using the concept of "metallic resonance" advanced by Pauling (*97*). As originally proposed by Pauling (*98*) $D(n) = D(1) - 0.60 \log_{10} n$, where for a metallic system $D(n)$ is the metallic bond distance for a bond of order n and the single-bond distance is $D(1)$. For POTCP compounds the equation becomes (*80*)

$$d_{Pt-Pt}\,(\text{Å}) = 2.59 - 0.60 \log_{10} \text{DPO},$$

and the derived DPO versus d_{Pt-Pt} values are shown in Fig. 14 for the compounds listed in Table IV. The case of "no metallic resonance" (*98*) is also indicated in Fig. 14. The obvious correlation between DPO and d_{Pt-Pt} suggests that other physical parameters related to these parameters and characterizing POTCP metals may show similar correlations. That this is certainly the case is discussed in the next section.

IV. The Physics of Anion-Deficient POTCP Metals

In Section II we introduced the physics relative to 1-D materials using the tight-binding electron approximation (*99, 100*). However, optical studies of KCP(Br) have shown that the electron-conduction behavior is best described by the free-electron approximation. Nielsen and Carneiro (*101*) have extended the original treatment by Horowitz *et al.* (*102*) of the free-electron case to anion deficient POTCP compounds.

In Table III there are 19 POTCP compounds, and it should be pointed out that the physics of 10 of them has been elucidated in detail in work by Carneiro (*103*) and Underhill *et al.* (*87*).

In order to show continuity in the equations describing the physics of AD POTCP compounds and also to show the interrelation between the structural, chemical, and physical properties of POTCP metals, the reader is reminded that d_{Pt-Pt} and DPO vary regularly and that both quantities are related (*87*) to the Fermi wave vector $\mathbf{k}_F$ namely, the degree of band filling) by

$$\text{DPO} = 2(1 - \mathbf{k}_F d_{Pt-Pt}/\pi). \tag{1}$$

In the intrachain direction the band structure is deduced from free-electron relationships so that the Fermi energy is

$$\varepsilon_F = (h\mathbf{k}_F)^2/4\pi m. \tag{2}$$

Because all of the POTCP compounds exhibit Peierls instabilities, at low temperature a band gap Δ arises where

$$\Delta = 4\frac{1 - \mathbf{k}_F d_{Pt-Pt}/\pi}{1 + \mathbf{k}_F d_{Pt-Pt}/\pi}\varepsilon_F e^{-1/\lambda}, \tag{3}$$

where λ, the dimensionless electron–phonon coupling constant, is given by

$$\lambda = g^2 N(\varepsilon_F)/\omega^0_{2\mathbf{k}_F}, \tag{4}$$

where g is the electrostatic energy gain per relative displacement of the Pt atoms, $N(\varepsilon_F)$ the electronic density of states at ε_F in the metallic phase, and $\omega^0_{2\mathbf{k}_F}$ a bare phonon frequency (*1*). The relationship between the temperature scale T_p of the Peierls instability and Δ is given by

$$T_p = \Delta/(1.77\mathbf{k}_F). \tag{5}$$

Now, from experimental studies using structure analysis, XDS, and dc-conductivity measurements, the values of d_{Pt-Pt}, $\mathbf{k}_F$, and Δ are obtained, and then λ and T_p are computed using Eqs. (3) and (5).

Next, the previously mentioned *inter*chain coupling parameter η, which is defined as the ratio of the bandwidth in the inter- and intrachain directions, allows us to determine the 3-D ordering temperature, which, from the theory of Horowitz *et al.* (*102*) provides

$$T_{3D} = T_p \exp\left(\frac{-2.5}{\eta}\frac{\mathbf{k}_B T_p}{\varepsilon_F}\right). \tag{6}$$

The value of T_{3D}, the 3-D ordering temperature, may be derived (*104*) from the maximum in the logarithmic derivative of the conductivity versus inverse temperature and then, from Eq. (6), η can be determined. For comparison, the *measured* parameters DPO, Δ, and T_{3D} are given in Fig. 15, and the derived *physical* parameters λ and η are shown in Fig. 16.

The most striking features of both Figs. 15 and 16 are the obvious correlations between observed and derived parameters, as shown in the form of rather smooth curves. By inspection it is obvious that the AD compounds are different from the CD derivatives. It is also noteworthy that two types of behavior are obvious from Figs. 15 and 16, that is, (1) there is a steady increase in the electron–phonon coupling λ when d_{Pt-Pt} increases upon going from $Rb_2[Pt(CN)_4](FHF)_{0.4}$ to

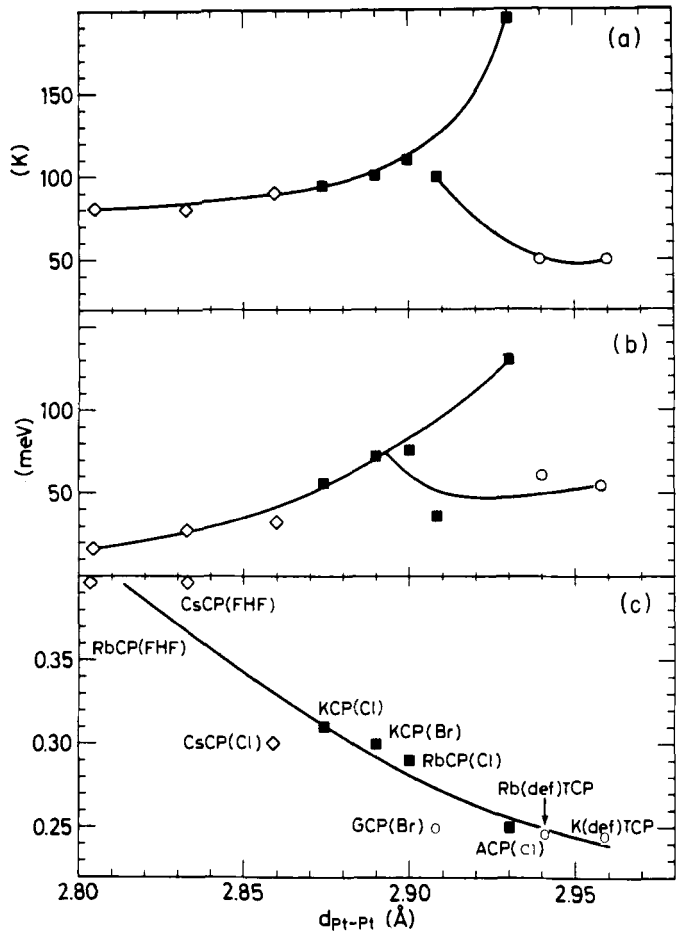

FIG. 15. Plot of the measured values for POTCP metals of the T_{3D} (three-dimensional ordering temperature) (a), △ (band gap) (b), DPO (degree of partial oxidation) (c), and versus d_{Pt-Pt} [intrachain Pt—Pt separation; see (*1*)]. Space groups: ■, *P*4mm; ◇, *I*4/mcm; ○, other.

$NH_4(H_3O)_{0.17}[Pt(CN)_4]Cl_{0.42} \cdot 2.83H_2O$, and (2) there are few exceptions in the regular behavior of AD POTCP compounds, whereas this is not the case for the CD POTCP derivatives, which do not follow the same curves given for the AD metals. Behavior type (1) is explained in terms of the dependence of DPO (and $\mathbf{k}_F$) upon d_{Pt-Pt}, because an increase in $\mathbf{k}_F$ results in a decrease in $\omega^0_{2\mathbf{k}_F}$, which in turn causes an increase in λ [see Eq. (4)]. On the other hand, the DPO versus d_{Pt-Pt} relation appears to "stabilize" ε_F and, therefore, $g^2N(\varepsilon_F)$. It is also noteworthy that in this same series of compounds the interchain coupling η in-

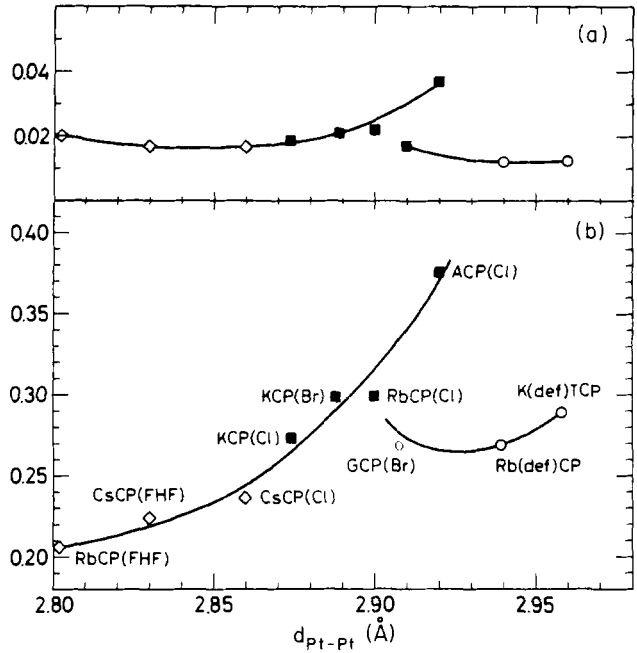

FIG. 16. Plot of the interchain coupling parameter η (a) and electron–phonon coupling constant λ (b), as deduced from experimental studies and plotted versus d_{Pt-Pt}. Space groups: ■, *P*4mm; ◇, *I*4/mcm; ○, other.

creases both for long and short d_{Pt-Pt}s in the presence of increased hydrogen-bonding interactions or more bulky cations. This is a nice demonstration of the effect of "talking between the chains," that is, increased Coulombic interchain coupling and increased electron hopping when the Pt-atom chains come closer together. Behavior type (2) is probably correlated with the more complicated crystal structures and hydrogen-bonding interactions exhibited by the CD salts compared to the AD derivatives.

V. Summary and Conclusions

Clearly, the decade of the 1970s has seen an enormous increase not only in the number of new Pt-chain electrical conductors, but also in the understanding of the chemistry and physics of these materials. A few generalizations are as follows.

1. Partially oxidized tetracyanoplatinate (POTCP) complexes that are hydrated form primitive (type-P) tetragonal lattices (*P4mm*), with the M^+ cations located in one-half of the unit cell and water molecules

in the other half. More importantly, the cations are always located between the planes of the $Pt(CN)_4$ groups. Compounds in this class include KCP(Br), KCP(Cl), RbCP(Cl), (NH_4)CP(Cl), and KCP(FHF).

2. POTCP complexes that are anhydrous form body-centered tetragonal lattices (*I4/mcm*) in which the cations occupy sites in the *same plane* as the $Pt(CN)_4$ groups (type-I). Some of these salts, {e.g., $Rb_2[Pt(CN)_4](FHF)_{0.4}$} have the shortest intra- and interchain Pt—Pt spacings and highest electrical conductivities of all known POTCP salts (*105*). Compounds in this class include CsCP(Cl), $RbCP(FHF)_{0.40}$, $CsCP(FHF)_{0.39}$, and $CsCP(N_3)_{0.25}$ (*106*).

3. Electrical conductivities parallel to the Pt–atom chain, $\sigma_\parallel$, in POTCP metals vary inversely with the *intra*chain Pt—Pt spacing d_{Pt-Pt}. The d_{Pt-Pt} spacings are most dependent on two factors. (1) The degree of partial oxidation (DPO) and d_{Pt-Pt} are inversely related, that is, the Pt-atom chain in a POTCP complex behaves in an accordion-like fashion, depending on the DPO. (2) In a series of isostructural compounds those containing the smaller alkali-metal cations have the shortest d_{Pt-Pt}. For example, RbCP(FHF) < CsCP(FHF) (type-I), and KCP(Br, Cl) < RbCP(Cl) (type-P). In addition, POTCP salts containing smaller cations have a higher tendency to be hydrated which tends to increase d_{Pt-Pt}. POTCP materials have metallic behavior near room temperature, with $\sigma_\parallel$ as high as approximately 2000 Ω^{-1} cm^{-1}, but they become semiconductors at low temperature.

4. POTCP metals have intrachain Pt—Pt spacings of 2.8–2.96 Å, that is, as short as in Pt metal itself (2.775 Å). The d_{Pt-Pt} spacing may be calculated from DPO (*80*).

5. The type-I anhydrous salts, with the shortest d_{Pt-Pt}, have the lowest three-dimensional ordering temperatures (T_{3D}). Therefore, they have the highest electrical conductivities down to the lowest temperatures. These properties are due in part to the absence of hydrogen-bonding interactions.

6. No Na^+ salts and no anhydrous Li^+ POTCP metals have been reported. The synthesis of a POTCP complex with Pt—Pt separations less than in Pt metal might be possible if anhydrous Li^+ or Na^+ derivatives can be prepared.

From the discussion in the text it is quite clear that the POTCP metals have been extensively characterized, and they are well understood because the chemistry and physics of these materials have been worked out hand-in-hand. It appears that new high-conducting Pt-chain metals with even lower semiconductor-transition temperatures than those now known will be developed in the near future.

ACKNOWLEDGMENTS

The author acknowledges the invaluable collaboration of the students and colleagues whose names appear in the cited articles, and he expresses his special thanks to Dr. Arthur J. Schultz, Professor Kim Carneiro, and Professor Allan E. Underhill. Work at Argonne National Laboratory was sponsored by the U. S. Department of Energy, Office of Basic Energy Sciences, Division of Materials Science, under Contract W-31-109-Eng-38. The author also thanks NATO (grants 1276 and 016-81), which made possible collaborative research with foreign scientists.

REFERENCES

1. Williams, J. M., Schultz, A. J., Underhill, A. E., and Carneiro, K., *in* "Extended Linear Chain Compounds" (J. S. Miller, ed.), Vol. I, p. 73. Plenum, New York, 1982. For a comprehensive summary of the known one-dimensional conductors of all types, see Vols. I–III of this treatise.
2. Underhill, A. E., and Watkins, D. M., *Chem. Soc. Rev.* **9,** No. 4, 429 (1980).
3. Williams, J. M., and Schultz, A. J., *NATO Conf. Ser.* [*Ser.*] *6* **1,** 337 (1979).
4. Stucky, G. D., Schultz, A. J., and Williams, J. M., *Annu. Rev. Mater. Sci.* **7,** 301 (1977).
5. Miller, J. S., and Epstein, A. J., *Prog. Inorg. Chem.* **20,** 1 (1976). This article is a comprehensive review of one-dimensional conductors through 1975.
6. Knop, W., and Schneidermann, G., *J. Prakt. Chem.* **37,** 462 (1846).
7. Döbereiner, J. W., *Pogg. Ann.* **28,** 180 (1833).
8. Levy, L. A., *J. Chem. Soc.* p. 1081 (1912).
9. Krogmann, K., *Angew. Chem., Int. Ed. Engl.* **8,** 35 (1969), and references therein.
10. Carneiro, K., ed., "The International Conference of Low-Dimensional Metals," Chemica Scripta Vol. 17, p. 1. Almqvist & Wiksell, Stockholm, 1981.
11. Labes, M. M., Love, P., and Nichols, L. F., *Chem. Rev.* **79,** 1 (1979).
12. Heeger, A. J., and MacDiarmid, A. G., *Chem. Scr.* **17,** 115 (1981).
13. Heeger, A. J., *in* "Highly Conducting One-Dimensional Solids" (J. T. Devreese, R. P. Evrard, and V. E. Van Doren, eds.), p. 69. Plenum, New York, 1979.
14. Bechgaard, K., Jacobsen, C. S., Mortensen, K., Pedersen, H. J., and Thorup, N., *Solid State Commun.* **33,** 1119 (1980).
15. Marks, T. J., and Kalina, D. W., *in* "Extended Linear Chain Compounds" (J. S. Miller, ed.), Vol. 1, p. 197. Plenum, New York, 1982.
16. Reis, A. H., Jr., *in* "Extended Linear Chain Compounds" (J. S. Miller, ed.), Vol. I, p. 157. Plenum, New York, 1982.
17. Whangbo, M.-H., and Hoffmann, R. J., *J. Am. Chem. Soc.* **100,** 6093 (1978).
18. Renker, B., and Comés, R., *in* "Low-Dimensional Cooperative Phenomena" (H. J. Keller, ed.), p. 236. Plenum, New York, 1975.
19. Peierls, R. E., *in* "Quantum Theory of Solids," p. 108. Oxford Univ. Press, London and New York, 1955.
20. Frohlich, H., *Proc. R. Soc. London, Ser. A* **223,** 296 (1954).
21. Kohn, W., *Phys. Rev. Lett.* **2,** 393 (1959).
22. Toombs, G. A., *Phys. Rep.* **40,** 181 (1978).
23. Mott, N. F., *Proc. Phys. Soc., London, Sect. A* **62,** 416 (1949).
24. Hubbard, J., *Proc. R. Soc. London, Ser. A* **281,** 401 (1964).
25. Bardeen, J., Cooper, L. N., and Schrieffer, J. R., *Phys. Rev.* **108,** 1175 (1957).

26. Little, W. A., *Phys. Rev. A* [2] **134,** 1416 (1964).
27. Little, W. A., *J. Polym. Sci., Part C* **29,** 17 (1970).
28. Davis, D., Gutfreund, H., and Little, W. A., *Phys. Rev. B: Solid State* [3] **13,** 4766 (1976). Also see Gutfreund, H., and Little, W. A., *in* "Highly Conducting One-Dimensional Solids" (J. T. Devreese, R. P. Evrard, and V. E. Van Doren, eds.), p. 305. Plenum, New York, 1979.
29. Underhill, A. E., Watkins, D. M., Williams, J. M., and Carneiro, K., *in* "Extended Linear Chain Compounds" (J. S. Miller, ed.), Vol. I, p. 119. Plenum, New York, 1982.
30. Underhill, A. E., *in* "Low-Dimensional Cooperative Phenomena" (H. J. Keller, ed.), p. 287. Plenum, New York, 1975.
31. "Handbook of Chemistry and Physics," 53rd ed., p. F-80. Chem. Rubber Publ. Co., Cleveland, Ohio, 1972–1973.
32. Krogmann, K., and Stephan, D., *Z. Anorg. Chem.* **362,** 290 (1968).
33. Bozorth, R. M., and Pauling, L., *Phys. Rev.* **39,** 537 (1932).
34. Maffly, R. L., Johnson, P. L., and Williams, J. M., *Acta Crystallogr., Sect. B* **33,** 884 (1977).
35. Daniels, W., Yersin, H., Philpsborn, H. V., and Gliemann, G., *Solid State Commun.* **30,** 353 (1979).
36. Moreau-Colin, M. C., *Bull. Soc. R. Sci. Liege* **34,** 778 (1965).
37. Holzapfel, W., Yersin, H., Gliemann, G., and Otto, H. H., *Ber. Bunsenges. Phys. Chem.* **82,** 207 (1978).
38. Johnson, P. L., Musselman, R. L., and Williams, J. M., *Acta Crystallogr., Sect. B* **33,** 3155 (1977).
39. Moreau-Colin, M. C., *Bull. Soc. Miner. Cristallogr.* **91,** 332 (1968).
40. Yersin, H., *J. Chem. Phys.* **68,** 4707 (1978).
41. Koch, T. R., Johnson, P. L., and Williams, J. M., *Inorg. Chem.* **16,** 640 (1977).
42. Washecheck, D. M., Peterson, S. W., Reis, A. H., Jr., and Williams, J. M., *Inorg. Chem.* **15,** 74 (1976).
43. Johnson, P. L., Koch, T. R., and Williams, J. M., *Acta Crystallogr., Sect. B* **33,** 1293 (1977).
44. Otto, H. H., Schultz, H., Thiemann, K. H., Yersin, H., and Gliemann, G., *Z. Naturforsch. B: Anorg. Chem., Org. Chem.* **32B,** 127 (1977).
45. Johnson, P. L., Koch, T. R., and Williams, J. M., *Acta Crystallogr., Sect. B* **33,** 1976 (1977).
46. Williams, J. M., *et al., Inorg. Synth.* **19,** 1–13 (1979).
47. Miller, J. S., *Inorg. Synth.* **19,** 13 (1979).
48. Williams, J. M., *et al., Inorg. Synth.* **20,** 20 (1980).
49. Williams, J. M., *et al., Inorg. Synth.* **21,** 141 (1982).
50. Williams, J. M., work in progress.
51. Williams, J. M., and Schultz, A. J., *Ann. N. Y. Acad. Sci.* **313,** 509 (1978).
52. Toftlund, H., *J. Chem. Soc., Chem. Commum.* p. 837 (1979).
53. Jones, S. A., Taylor, W. H., Holida, M. D., Sutton, L. J., and Williams, J. M., *Inorg. Synth.* **21,** 191 (1982).
54. Williams, J. M., Iwata, M., Peterson, S. W., Leslie, K. A., and Guggenheim, H. J., *Phys. Rev. Lett.* **34,** 1653 (1975).
55. Miller, J. S., and Weagley, R., *Inorg. Chem.* **16,** 2965 (1977).
56. Williams, J. M., Johnson, P. L., Schultz, A. J., and Coffey, C. C., *Inorg. Chem.* **17,** 834 (1978).
57. Brown, R. K., and Williams, J. M., *Inorg. Chem.* **18,** 1922 (1979).

58. Underhill, A. E., Watkins, D. M., and Wood, D. J., *J. Chem. Soc., Chem. Commun.* p. 805, (1976).
59. Brown, R. K., and Williams, J. M., *Inorg. Chem.* **17,** 2607 (1978).
60. Wood, D. J., Underhill, A. E., and Williams, J. M., *Solid State Commun.* **31,** 219 (1979).
61. Johnson, P. L., Schultz, A. J., Underhill, A. E., Watkins, D. M., Wood, D. J., and Williams, J. M., *Inorg. Chem.* **17,** 839 (1978).
62. Carneiro, K., Petersen, A. S., Underhill, A. E., Wood, D. J., Watkins, D. M., and MacKenzie, G. A., *Phys. Rev. B: Condens. Matter* [3] **19,** 6279 (1979).
63. Brown, R. K., Vidusek, D. A., and Williams, J. M., *Inorg. Chem.* **18,** 801 (1979).
64. Underhill, A. E., Coles, G. S. V., Williams, J. M., and Carneiro, K., *Phys. Rev. Lett.* **47,** 1220 (1981).
65. Keefer, K. D., Washecheck, D. M., Enright, N. P., and Williams, J. M., *J. Am. Chem. Soc.* **98,** 233 (1976).
66. Williams, J. M., Keefer, K. D., Washecheck, D. M., and Enright, N. P., *Inorg. Chem.* **15,** 2446 (1976).
67. Reis, A. H., Peterson, S. W., Washecheck, D. M., and Miller, J. S., *J. Am. Chem. Soc.* **98,** 234 (1976).
68. Epstein, A. J., and Miller, J. S., *Solid State Commun.* **29,** 345 (1979).
69. Carneiro, K., Jacobson, C. S., and Williams, J. M., *Solid State Commun.* **31,** 837 (1979).
70. Schultz, A. J., Stucky, G. D., Williams, J. M., Koch, T. R., and Maffly, R. L., *Solid State Commun.* **21,** 197 (1977).
71. Epstein, A. J., and Miller, J. S., *Bull. Am. Phys. Soc.* [2] **22,** 453 (1977); Carneiro, K., and Jacobsen, C., unpublished results.
72. Brown, R. K., Johnson, P. L., Lynch, T. L., and Williams, J. M., *Acta Crystallogr., Sect. B* **34,** 1965 (1978).
73. Schultz, A. J., Coffey, C. C., Lee, G. C., and Williams, J. M., *Inorg. Chem.* **16,** 2129 (1977).
74. Wood, D. J., Underhill, A. E., Schultz, A. J., and Williams, J. M., *Solid State Commun.* **30,** 501 (1979).
75. Schultz, A. J., Gerrity, D. P., and Williams, J. M., *Acta Crystallogr., Sect. B* **34,** 1673 (1978).
76. Although the space group was not determined unambiguously *I4cm* was used. See Stucky, G. D., Putnik, C., Kelber, J., Schaffman, M. J., Salamon, M. B., Pasquali, G., Schultz, A. J., Williams, J. M., Cornish, T. F., Washecheck, D. M., and Johnson, P. L., *Ann. N. Y. Acad. Sci.* **313,** 525 (1978).
77. For reviews and background on X-ray and neutron scattering studies see Comés, R., *in* "One-Dimensional Conductors" (H. G. Schuster, ed.), p. 32. Springer-Verlag, Berlin and New York, 1975; Renker, B., Pintschovious, L., Gläser, W., Rietschel, H., and Comés, R., *ibid.* p. 53; Renker, B., and Comés, R., *in* "Low-Dimensional Cooperative Phenomena" (H. J. Keller, ed.), p. 236. Plenum, New York, 1975.
78. Comés, R., Lambert, M., and Zeller, H. R., *Phys. Status Solidi B* **58,** 587 (1973).
79. Renker, B., Pintschovius, L., Gläser, W., Rietschel, H., Comés, R., Liebert, L., and Drexel, W., *Phys. Rev. Lett.* **32,** 836 (1974).
80. Williams, J. M., *Inorg. Nucl. Chem. Lett.* **12,** 651 (1976).
81. Krogmann, K., and Hausen, H. D., *Z. Anorg. Allg. Chem.* **358,** 67 (1968). A simultaneous study of KCP(Br) was carried out by A. Piccinin and J. Toussaint, *Bull. Soc. R. Sci. Liege* **36,** 122 (1967).

82. Williams, J. M., Petersen, J. L., Gerdes, H. M., and Peterson, S. W., *Phys. Rev. Lett.* **33,** 1079 (1974).
83. See the following articles and references therein: Heger, G., Deiseroth, H. J., and Schultz, H., *Acta Crystallogr., Sect. B* **34,** 725 (1978); Peters, C., and Eagen, C. F., *Inorg. Chem.* **15,** 782 (1976).
84. Miller, J. S., and Epstein, A. J., *Prog. Inorg. Chem.* **20,** 46 (1976).
85. Renker, B., Rietschel, H., Pintschovius, L., Gläser, W., Brüesch, P., Kuse, D., and Rice, M. J., *Phys. Rev. Lett.* **30,** 1144 (1973).
86. Lynn, J. W., Iizumi, M., Shirane, G., Werner, S. A., and Saillant, R. B., *Phys. Rev. B: Condens. Matter* [3] **12,** 1154 (1975).
87. Underhill, A. E., Wood, D. J., and Carneiro, K., *Synth. Met.* **1,** 395 (1979–1980).
88. Carneiro, K., Eckert, J., Shirane, G., and Williams, J. M., *Solid State Commun.* **20,** 333 (1976).
89. Williams, J. M., and Schultz, A. J., *in* "Modulated Structures—1979" (J. M. Cowley, J. B. Cohen, M. B. Salamon, and B. J. Wuensch, eds.), p. 187. Am. Inst. Phys., New York, 1979.
90. Musselman, R., and Williams, J. M., *J. Chem. Soc., Chem. Commun.* p. 186 (1977).
91. Steigmeier, E. F., Baeriswyl, D., Auderset, H., and Williams, J. M., *in* "Quasi One-Dimensional Conductors II" (S. Barisic *et al.*, eds.), p. 229. Springer-Verlag, Berlin and New York, 1979.
92. Williams, J. M., Schultz, A. J., Underhill, A. E., and Carneiro, K., *in* "Extended Linear Chain Compounds" (J. S. Miller, ed.), vol. I, p. 98. Plenum, New York, 1982.
93. Comés, R., Lambert, M., Launois, H., and Zeller, H. R., *Phys. Rev. B: Condens. Matter* [3] **8,** 571 (1973).
94. Braude, A., Lindegaard-Andersen, A., Carneiro, K., and Petersen, A. S., *Solid State Commun.* **33,** 365 (1980).
95. Renker, B., and Comés, R., unpublished results.
96. Williams, J. M., and Schultz, A. J., *NATO Conf. Ser.* [*Ser.*] *6* **1,** 361–363 (1979).
97. Pauling, J., "The Nature of the Chemical Bond and the Structure of Molecules and Crystals," pp. 398–404. Cornell Univ. Press, Ithaca, New York, 1960.
98. Pauling, L., *J. Am. Chem. Soc.* **69,** 542 (1947).
99. Kuse, D., and Zeller, H. R., *Phys. Rev. Lett.* **27,** 1060 (1971); Zeller, H. R., and Brüesch, P., *Phys. Status Solidi* **65,** 537 (1974).
100. Steigmeier, E., Loudon, R., Harbeke, G., Auderset, H., and Scheiber, G., *Solid State Commun.* **17,** 1447 (1975).
101. Nielsen, J. B., and Carneiro, K., *Lect. Notes Phys.* **96,** 238 (1979).
102. Horowitz, B., Gutfreund, H., and Weger, M., *Phys. Rev. B: Solid State* [3] **12,** 3174 (1975).
103. Carneiro, K., unpublished results.
104. Carneiro, K., *NATO Conf. Ser.* [*Ser.*] *6* **1,** 369 (1979).
105. The room temperature electrical conductivity of $RbCP(FHF)_{0.4}$ is $\sim 2000 \Omega^{-1}$ cm^{-1} and is the highest yet reported for a POTCP metal.
106. Both CsCP(Cl) and $CsCP(N_3)_{0.25}$ are not strictly anhydrous but do have type-I molecular structures.
107. Coles, G. S. V., Lindegaard-Andersen, A., Williams, J. M., Schultz, A. J., Brown, R. K., Besinger, R. E., Ferraro, J. R., Underhill, A. E., and Watkins, D. M., *Physica Scripta* **25,** 873 (1982).

ADVANCES IN INORGANIC CHEMISTRY AND RADIOCHEMISTRY, VOL. 26

TRANSITION-METAL ALKOXIDES

R. C. MEHROTRA

Department of Chemistry, University of Rajasthan, Jaipur, India

I. Introduction

After an early doubtful claim by Demarcay (*1*) in 1875, titanium tetraethoxide was synthesized in 1924 by Bischoff and Adkins (*2*), employing the reaction of titanium tetrachloride with sodium ethoxide in excess ethanol. This was followed by the classical work of Jennings, Wardlaw, and Way (*3*) in 1936, showing that the reaction of titanium tetrachloride with ethanol only resulted in a crystalline compound, $TiCl_2(OEt)_2 \cdot 2EtOH$. Thereafter, progress in the field of alkoxide chemistry of transition metals was slow until 1950, and the only alkoxides of transition metals that appear to have been reported until then

Copyright © 1983 by Academic Press, Inc.
All rights of reproduction in any form reserved.
ISBN 0-12-023626-5

were those of tungsten(V) (*4*), vanadyl(III) (*5*), tantalum(V) (*6*), chromium(III) (*7*), iron(III) (*7*), manganese(II) (*8*), and cobalt(III) (*8*).

With the publication of the work on zirconium ethoxide by Bradley and Wardlaw (*9*) in 1950, the knowledge of this interesting class of compounds has grown at a rapid pace, as evinced by the publication of a number of review articles on alkoxides of metals in general (*10*, *11*) and transition metals in particular (*12*). A survey of the rapidly growing literature (about 1200 references) up to 1975 in a recent book *Metal Alkoxides* (*13*) indicates that the alkoxide chemistry of the elements that are placed within the borders in the periodic table had already been studied in some detail by that time. A closer scrutiny reveals that among the transition elements the main focus of attention was on the earlier transition metals (particularly in the d^0 state), except for some work on alkoxides of $3d^{5-9}$ elements, which were investigated mainly from the points of view of their magnetochemistry and electronic spectra (*14*). In contrast to the soluble and volatile alkoxides of earlier transition metals, almost all of the alkoxides of later 3d elements, with the exception of iron(III) alkoxides (*15*) and chromium tetra-*t*-alkoxides (*16*), were found to be insoluble in organic solvents and nonvolatile. There appears to be a surge, particularly since publication of *Metal Alkoxides* (*13*), in research activity in a number of laboratories on the alkoxy derivatives of later transition metals [$3d^{5-9}$ (*17*), Mo, W, Re, Ru, Rh, Pd, and Pt], including the synthesis of a number of soluble and volatile bimetallic alkoxides of later 3d metals. Sterically demanding alcohols have also received special attention for enhancing the kinetic stability of transition-metal alkoxides in general.

Because the literature up to 1975 has already been reviewed (*13*), this chapter is in general limited to the progress made since then in the alkoxide chemistry of 3d, 4d, and 5d metals [4f (*18*) and 5f metals are also excluded], referring to the essential background literature relevant to new advances only.

H																He
Li	Be											B	C	N	O	F	Ne
Na	Mg											Al	Si	P	S	Cl	Ar
K	Ca	Sc	Ti	V	Cr	Mn	Fe	Co	Ni	Cu	Zn	Ga	Ge	As	Se	Br	Kr
Rb	Sr	Y	Zr	Nb	Mo	Tc	Ru	Rh	Rd	Ag	Cd	In	Sn	Sb	Te	I	Xe
Cs	Ba	*	Hf	Ta	W	Re	Os	Ir	Pt	Au	Hg	Tl	Pb	Bi	Po	At	Rn
Fr	Ra	†															

*La	Ce	Pr	Nd	Pm	Sm	Eu	Gd	Tb	Dy	Ho	Er	Tm	Yb	Lu
†Ac	Th	Pa	U	Np	Pu	Am	Cm	Bk	Cf	Es	Fm	Md	No	Lw

II. Alkoxy and Allied Derivatives of 3d Metals

A. Titanium

The most significant contribution in this area has been a detailed study (*19*) of titanium diphenoxide dichloride, which has been shown to have the same dimeric structure in solution as in the solid state (*20*). Interest in this compound was renewed by the observation (*21*) that the phenoxide ion can be η-bonded to a metal atom (Ru or Rh) through ring carbon atoms (*21*) rather than through the oxygen atom. Van Tamelen (*22*) reported that the reduction of various alkoxide complexes of titanium, including $Ti(OPh)_2Cl_2$, with sodium naphthalide or potassium under nitrogen gave appreciable quantities of ammonia via an intermediate for which the stoichiometry $Na_3Ti_4N_4(OR)_{10}$ has been

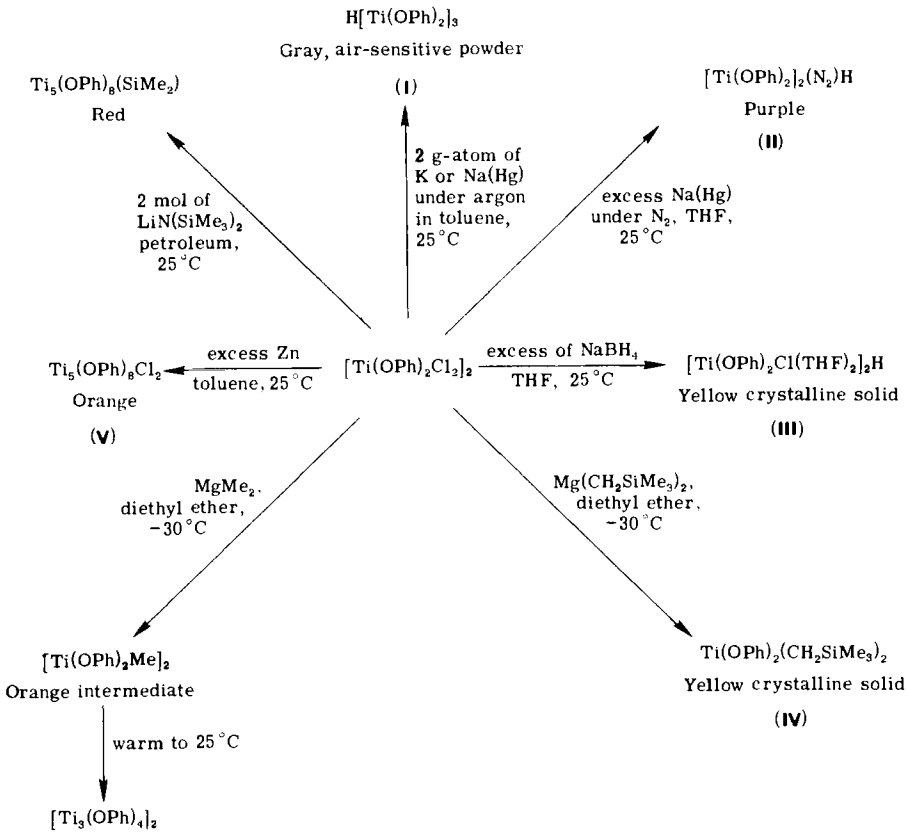

Scheme 1

proposed. Although the expectation of the workers (*19*)—to synthesize π-bonded products—was not fulfilled, the results of the reactions of $Ti(OPh)_2Cl_2$ with a number of reducing agents can be summarized, as shown in Scheme 1.

The following tentative structures have been suggested for some of the products in Scheme 1.

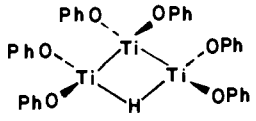

(I)

$H[Ti(OPh)_2]_3$(I)

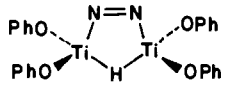

(II)

$[Ti(OPh)_2]_2(N_2)H$

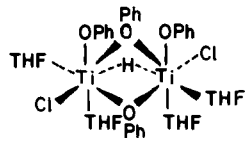

(III)

$[Ti(OPh)_2Cl(THF)_2]_2H$

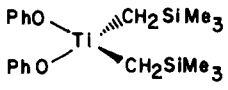

(IV)

$Ti(OPh)_2(CH_2SiMe_3)_2$

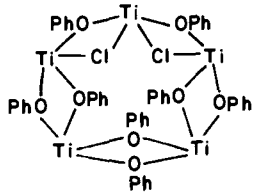

(V)

$Ti_5(OPh)_8Cl_2$

An interesting migration of one methyl group from aluminum to titanium, without reduction of titanium, has been reported (*23*) in the reactions of titanium complexes, $XTi(OR)_3$ [X = η^5-cyclopentadienyl (Cp); R = Et, *i*Pr] with aluminum trimethyl to give bimetallic complexes with alkoxy bridges:

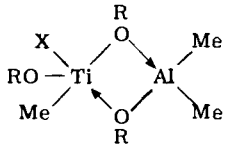

Following the preparation (*24*) of $Ti(OR_f)_4$ and $Zr(OR_f)_4$ by the reactions of anhydrous chlorides with 2,2,2-trifluoroethanol (R_fOH) in the presence of anhydrous ammonia, the preparation of $(Cp)Ti(OR_f)_3$ by the reaction of $(Cp)TiCl_3$ with $LiOR_f$, has been reported (*25*). The reaction of $(Cp)TiCl_3$ with R_fOH itself gave $(Cp)TiCl(OR_f)_2$, which on methylation with LiMe gave $(Cp)(Me)Ti(OR_f)_2$. Synthesis of a series of de-

rivatives $TiX_{4-n}(OR_f)_n$ (n = 2 or 3 for X = Cl; n = 1 or 2 for X = (O-*i*Pr) and their adducts with RCN (R = Me, Et) and R_fOH has been reported (*26*).

Following a study of the insertion reactions of $Ti(OR)_4$ (*27*) and $(Et_2N)Ti(OR)_3$ (*28*), complexes of the type $CpTi(OR)_{3-n}[N(Ph)COOR]_n$ (R = Et, *i*Pr, *t*Bu; n = 1, 2, or 3) have been synthesized (*29*) by reactions of $CpTi(OR)_3$ with PhNCO.

A number of mixed isocyanatotitanium derivatives, $Ti(O\text{-}iPr)_{4-n}(NCO)_n \cdot mX$ (n = 1, 2, 3, or 4; X = $MeCO_2$-*i*Pr or MeCN; m = 0, 1, or 2) were prepared (*30*) by the reactions of $Ti(O\text{-}iPr)_4$ with acetyl isocyanate or by the reactions of $Ti(O\text{-}iPr)_{4-n}Br_n$ with AgNCO in acetonitrile. Insertion reactions in these complexes were also studied with isopropanol, which yielded the corresponding carbamates. Similarly, the reactions of $M(OR)_4$ (M = Ti, Zr; R = Et, *i*Pr) with pyruvonitrile have been reported (*31*) to yield products of the type $M(OR)_{4-n}(CN)_n \cdot m$MeCOOR ($m$ = 0, 0.5, and 1 when n = 1, 2, and 3, respectively; m = 1.5 for Ti and 2 for Zr when n = 4). The reactions of metal tetracyanides with isopropanol were also found to yield $Ti(O\text{-}iPr)_2(CN)_2$*i*PrOH and $Zr_2(CN)_5(O\text{-}iPR)_32i$PrOH.

A variable-temperature NMR study (*32*) of titanium chelates (**I–IV**)

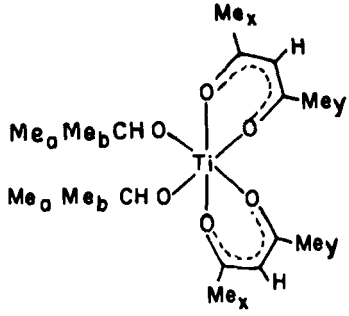

(I)

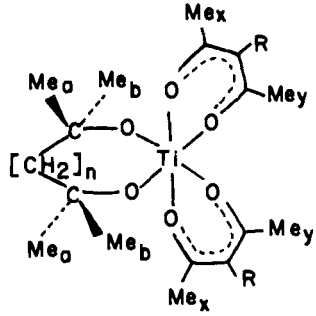

(II)-(IV)

(**II**), n = 1, R = H; (**III**), n = 0, R = H; (**IV**), n = 1, R = COMe

indicated that distereoisomerism is possible in the diisopropoxy compound (**I**), but the NMR spectrum indicates the presence of only the cis isomer, as reported previously by Bradley and Holloway (*33*) for titanium and by Saxena *et al.* for zirconium (*34*). For derivatives (**I**) to (**III**) a low-temperature NMR study showed anisochronous geminal methyl

groups (Me_a and Me_b) and acetylacetonatomethyls (Me_x and Me_y), indicating that metal-centered rearrangement is slow on the NMR time scale. Study of the 3-acetylpentane-2,4-dionato(triac) complex (**IV**) provided information on the problem of bond rupture versus twisting.

Continuing their earlier studies on similar compounds, Bickley and Serpone (*35*) have investigated the configurational rearrangements in *cis*-$Ti(acac)_2XY$ [acac = anion of 2,4-pentanedione, X = Cl or Br, and Y = iC_3H_7O or 2,6-$(iC_3H_7)_2C_6H_3O$]. When Y = O-iC_3H_7, the isopropyl methyl NMR resonance remains a sharp doublet even at −63°C, but diastereotopic splitting was observed when Y = 2,6-$(iC_3H_7)_2C_6H_3O$. It has been suggested on the basis of previous results (*36*) that rearrangements probably occur via twist processes.

Substitution of an OR group by a Cl ligand by the action of HCl on quasi-tetrahedral biscyclopentadienyltitanium complexes of the type (Cp)(Cp′)Ti(OR)(OR′) has been shown (*37*) to be a stereospecific process that occurs with retention of configuration at titanium. The ligand-exchange reactions of (Cp)(Cp′)Ti(OR)Cl with KCNS and of (Cp)(Cp′)Ti(OR)NCS with HBr at the chiral titanium atom have also been studied (*38*); both reactions are selective, but only the latter is stereospecific, involving retention at the titanium atom.

In a number of publications Paul and co-workers (*39*) have investigated the complexation reactions of a number of chloride alkoxides of titanium with ligands such as phthalimide, succinimide, α,α'-dipyridyl, 1,10-phenanthroline, acetonitrile, pyridines, triphenylarsine oxide, dimethylformamide, triphenylphosphine oxide and 2-, 3-, and 4-picoline *N*-oxides and hexamethylphosphoramide.

A number of titanium(IV) and zirconium(IV) complexes of Schiff bases and related ligands have been prepared by reactions with titanium and zirconium isopropoxides in different stoichiometric ratios. They have been characterized by Tandon and co-workers (*40*), using IR and NMR spectroscopy.

B. Vanadium

Phenylvanadyl complexes, $PhVO(O\text{-}iPr)_2$ and $PhVOCl(O\text{-}iPr)$, have been synthesized (*41*) by stirring $VO(O\text{-}iPr)_2Cl$ with PhLi and $VO(O\text{-}iPr)Cl_2$ with Ph_2Hg in pentane at −50 and −10°C, respectively. Similar attempts to prepare $PhVO(OCH_2CF_3)_2$ have, however, been reported to be unsuccessful.

The novel complexes $(Me_3SiO)_3V{=}NR$ (R = *t*-butyl or 1-adamantyl) have been synthesized (*42*) by the following reactions.

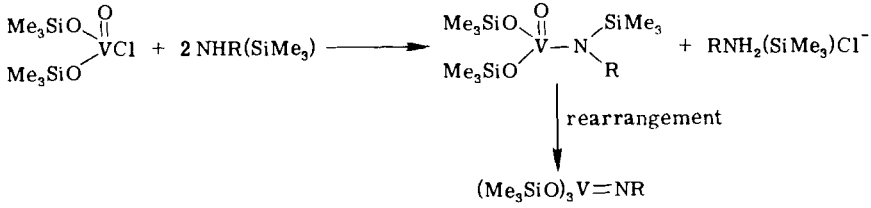

R = *t*-butyl or 1-adamantyl

The structure of the adamantyl derivatives has been determined by X-ray crystallography and is represented in Fig. 1; the V—N bond length is extremely short 1.614(2) Å and the V—N—C angle is nearly linear 175.8(2)°, indicating a considerable triple-bond character in V=NR.

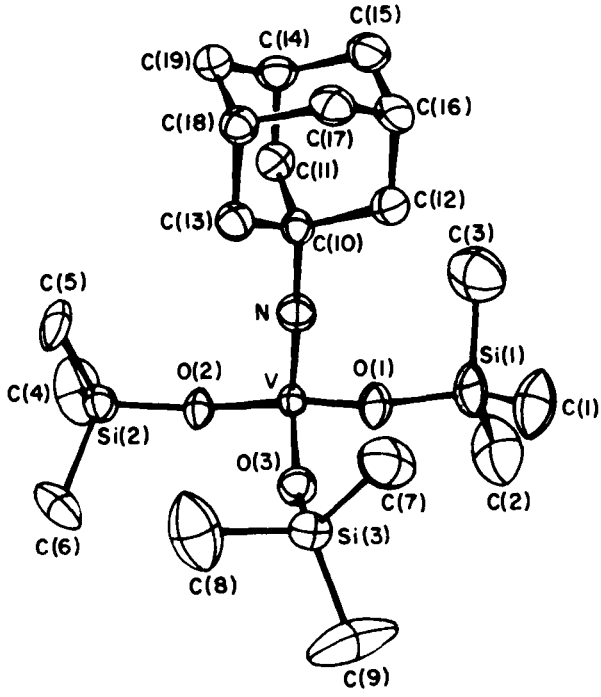

FIG. 1. Structure of $(Me_3SiO)_3V{=}N$(adamantyl).

C. Chromium

Although a number of novel routes involving rather inaccessible starting materials (*43*, *44*) have been employed, the literature on the synthesis of even simple alkoxides of chromium in its most common +3 oxidation state is full of contradictions, and even simple derivatives like $Cr(O\text{-}iPr)_3$ and $Cr(O\text{-}tBu)_3$ have not been described until recently. The claim (*7*) for the preparation of $Cr(OEt)_3$ by the simple metathetic reaction between $CrCl_3$ and NaOEt in ethanol could not be confirmed by Brown, Cunningham, and Glass (*45*), who had earlier described (*44*) the synthesis of $Cr(OMe)_3$ and $Cr(OEt)_3$ by photolytic decarboxylation of tricarbonylarenechromiums. These workers (*45*) were, however, able to confirm partially the preparation of the two alkoxides by photolysis of alcoholic solutions of ammonium chromate, which were reported in 1964 by von Hornduff and Kappler (*43*). However, attempts to prepare $Cr(O\text{-}iPr)_3$ and $Cr(O\text{-}tBu)_3$ by both of these methods resulted in products with very low carbon and hydrogen analyses, which was ascribed to the instability of these branched alkoxides (*45*). After attempting a number of routes, the best method reported for preparation of $Cr(OPh)_3$ was the irradiation of tricarbonylbenzenechromium in the presence of phenol under oxygen.

In a publication dealing with magnetism and electronic spectra of methoxides and ethoxides of later 3d metals, Adams *et al.* (*14*) used the more plausible (in view of the ease of separation of products) route employing metathesis between LiOMe and $CrCl_3$. $Cr(OEt)_3$ was, however, prepared by these workers also using the method of von Hornduff and Kappler (*43*).

The preparation of primary alkoxides of chromium(III) has been carried out (*46*) successfully using the simple reactions of the $CrCl_3 \cdot 3THF$ adduct (solubility of which in organic solvents provides a distinct advantage) with lithium alkoxides:

$$CrCl_3 \cdot 3THF + 3LiOR \xrightarrow[C_6H_6]{ROH} Cr(OR)_3 + 3LiCl$$

$$R = Me, Et, nBu$$

$Cr(O\text{-}iPr)_3$ and $Cr(O\text{-}tBu)_3$ could not be prepared by this method; instead, hydrolyzed products were obtained. These latter, branched alkoxides also could not be prepared by the alcoholysis or transesterification reactions of lower alkoxides, even under forcing conditions. $Cr(OPh)_3$ could, however, be synthesized by refluxing $Cr(OEt)_3$ with excess phenol in benzene, removing the ethanol azeotropically with the solvent. This $Cr(OPh)_3$ was found to undergo reaction with excess iso-

propanol (but not with *t*-butanol), and, on repeating the reaction a number of times, almost pure $Cr(O\text{-}iPr)_3$ could be prepared for the first time as a green, insoluble solid. Interestingly, it was finally possible to synthesize $Cr(O\text{-}tBu)_3$ by the simple reaction of $CrCl_3 \cdot 3THF$ with 3 mol of $LiO\text{-}tBu$ (avoiding excess of *t*-butanol) in THF:

$$CrCl_3 \cdot 3THF + 3LiO\text{-}tBu \xrightarrow{THF} Cr(O\text{-}tBu)_3 + 3LiCl$$

$Cr(O\text{-}tBu)_3$, obtained as a soluble product in this reaction, gave volatile $Cr(O\text{-}tBu)_4$, which could be distilled under reduced pressure. The spectrum of this distilled liquid shows bands at 13,870 and 15,700 cm^{-1} and a shoulder at 25,300 cm^{-1}, which can be understood on the basis of a distorted octahedral environment for chromium in $Cr(O\text{-}tBu)_4$, the special stability of which has been explained (*47*) on the basis of two singly occupied lower e_g shells in a tetrahedral environment for chromium. On treatment of $Cr(O\text{-}tBu)_4$ with methanol, ethanol, and isopropanol, $Cr(OMe)_3$, $Cr(OEt)_3$, and $Cr(O\text{-}iPr)_3$ were obtained.

The spectra of primary and secondary alkoxides of chromium(III) are similar and may be interpreted (*46*) on the basis of an octahedral environment for chromium (see Table I).

Primary alkoxides of chromium(III) do not appear to undergo alcoholysis reactions, even under forcing conditions with other (tertiary, secondary, as well as other primary) alcohols. This is rather unusual in view of the usually strong lability of the alkoxy groups exhibited in

TABLE I

ELECTRONIC VISIBLE SPECTRA OF SOME CHROMIUM(III) ALKOXIDES

Product	$^4A_{2g} \rightarrow {}^4T_{2g}$(10 Dq) ($cm^{-1}$)	$^4A_{2g} \rightarrow {}^4T_{1g}$ (cm^{-1})	B (cm^{-1})
$Cr(OMe)_3$[a]	17,610	24,150	612
$Cr(OEt)_3$[a]	17,000	23,470	600
$Cr(O\text{-}tBu)_3$[a]	17,060	23,700	610
$Cr(OPh)_3$	16,900	23,920	615
$Cr(OMe)_3$[b]	17,240	23,800	609
$Cr(OEt)_3$[b]	16,370	23,470	654
$Cr(O\text{-}iPr)_3$[b]	15,880	22,940	720
$Cr(OMe)_3$[c]	17,180	24,150	613
$Cr(O\text{-}iPr)_3$[c]	16,180	23,280	728

[a] Prepared from LiCl method.
[b] Prepared from $Cr(OPh)_3$.
[c] Prepared from $Cr(O\text{-}tBu)_4$.

alkoxides of most of the metals studied; the main factor hindering such facile interchange has generally been explained on the basis of steric requirements (*13*). The special inertness of Cr(III) primary alkoxides to alcoholysis may, therefore, be ascribed to the special stability of octahedral chromium(III) (with three singly occupied lower energy t_{2g} levels). The Jahn–Teller effect does not appear to be able to disturb the regularity of this octahedral species, which is consequently unable to react both by dissociative as well as associative mechanisms.

Although primary alkoxides of chromium(III) do not undergo alcoholysis reactions, $Cr(O\text{-}iPr)_3$ could be converted to $Cr(OMe)_3$ or $Cr(OEt)_3$ by refluxing with excess MeOH or EtOH. $Cr(O\text{-}iPr)_3$, however, does not undergo alcoholysis reactions with tertiary or other secondary alcohols, even under forcing conditions. As reported earlier, $Cr(O\text{-}t\text{Bu})_4$ on treatment with MeOH, EtOH, or *i*PrOH readily gives the corresponding Cr(III) alkoxides; this may be easily understood on the basis of greater stability and insolubility of the octahedral species.

In view of the general inertness of the primary alkoxides of chromium(III), a more detailed investigation of their substitution reactions has been carried out, and it has been shown that although these are inert to other simple alcohols they undergo interchange with chelating ligands such as ethanolamine (*46*), β-diketones (*46, 48*) and carboxylic acids (*46*). A wide variety of derivatives synthesized in such reactions has been characterized by detailed spectral and magnetochemical studies (*46*).

$$Cr(OEt)_3 + x HOCH_2CH_2NH_2 \xrightarrow{\text{benzene}} Cr(OEt)_{3-x}(OCH_2CH_2NH_2)_x + x EtOH$$

(These are slow reactions that give products insoluble in organic solvents.)

$$Cr(OR)_3 + x\beta\text{-dkH} \xrightarrow{\text{benzene}} Cr(OR)_{3-x}(\beta\text{-dk})_x + x ROH$$

$$Cr(OR)_3 + x R'COOH \xrightarrow{\text{benzene}} Cr(OR)_{3-x}(OOCR')_x + x ROH$$

R = Me, Et; β-dkH = acetylacetone, benzoylacetone, 2-theonyltrifluoroacetone; R′ = C_7H_{15}, $C_{13}H_{27}$, $C_{15}H_{31}$, $C_{21}H_{43}$; x = 1, 2, or 3

The reactions in the latter two cases (i.e., with β-diketones and carboxylic acids) are slow in the beginning, and the products $Cr(OR)_2(\beta\text{-dk})$ and $Cr(OR)_2(OOCR')$ are insoluble and polymeric; products $Cr(OR)(\beta\text{-dk})_2$ and $Cr(OR)(OOCR')_2$ are all soluble in organic solvents, in which

they depict dimeric behavior, probably with an octahedral configuration of the type

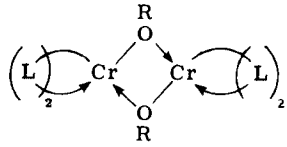

Only a few mixed methoxide 3-chloro- or 3-bromoacetylacetonates of chromium(III) could be prepared (*49*, *50*) by the reactions of the β-diketonates with methanol, but the derivatives of simple (unhalogenated) β-diketones could not be prepared by this method. The simple method of treating the alkoxides with β-diketones appears to have general applicability, and a wide variety of allied mixed derivatives could also be prepared by this route, as exemplified (*46*) by the reactions

$$Cr(OEt)_x(\beta\text{-dk})_{3-x} + x\beta\text{-dk'H} \longrightarrow Cr(\beta\text{-dk'})_x(\beta\text{-dk})_{3-x} + x\text{EtOH}$$

β-dk and β-dk' = acetylacetone or benzoylacetone; $x = 1, 2$

The physicochemical properties of a few β-diketonate derivatives of chromium(III) are listed in Table II.

TABLE II

ELECTRONIC VISIBLE SPECTRA OF ALKOXY β-DIKETONATES OF CHROMIUM(III)

Compound[a]	$^4A_{2g} \rightarrow {}^4T_{2g}(F)$ (cm^{-1})	$^4A_{2g} \rightarrow {}^4T_{1g}(F)$ (cm^{-1})	B (cm^{-1})	μ_{eff} (BM)[b]
$Cr(acac)_3$	17,825	23,981	594	3.88
$Cr(OEt)(acac)_2$	17,007	24,875	850	3.81
$Cr(OEt)_2(acac)$	17,067	23,585	604	3.78
$Cr(bza)_3$	17,452	22,833	491	3.85
$Cr(OEt)(bza)_2$	17,421	23,474	592	3.81
$Cr(OEt)_2(bza)$	17,064	23,809	609	3.79
$Cr(tta)_3$	17,182	23,640	596	3.84
$Cr(OEt)(tta)_2$	16,835	24,390	775	3.80
$Cr(OEt)_2(tta)$	16,234	23,753	811	3.77
$Cr(OMe)(acac)_2$	16,949	25,125	926	3.68
$Cr(O\text{-}i\text{Pr})(acac)_2$	16,780	23,100	529	—

[a] Abbreviations: acac, acetylacetone; bza, benzoylacetone; tta, 2-theonyltrifluoroacetone.

[b] BM, Bohr magneton.

Like the alkoxides of earlier transition elements, for example, titanium (*26, 29*), chromium(III) alkoxides (methoxide and ethoxide) have been shown to react exothermally with isocyanates in stoichiometric ratios in benzene, giving the insertion products as shown in the reaction (*51*)

$$Cr(OR)_3 + nR'NCO \longrightarrow (RO)_{3-n}Cr[N(R')COOR]_n$$

R = Me and Et; R′ = Ph and Naph; n = 1–3

All the insertion products are colored solids, sparingly soluble in common organic solvents, and highly sensitive to moisture; on hydrolysis they yield urethanes HN(R′)COOR.

A detailed physicochemical study of the compounds with the formulas $Cr_2(O\text{-}iPr)_6(NO)_2$, $Cr(O\text{-}iPr)_3(NO)L$ (L = ammonia, pyridine, or 2,4-lutidine), and $Cr(O\text{-}tBu)_3NO$ has been carried out (*52*). These products have been obtained (*53*) by the reactions of the monomeric compound $Cr(N\text{-}iPr_2)_3NO$ with alcohols in hydrocarbon solvents. The bulky and relatively nonacidic *t*-butanol reacts slowly to give a red solid $Cr(O\text{-}tBu)_3NO$, which has been shown (*54*) to be monomeric. The reaction of isopropanol under similar conditions, however, yields a brick-red crystalline dimeric compound $Cr_2(O\text{-}iPr)_6(NO)_2$, whereas less sterically demanding and more acidic methyl and ethyl alcohols react to give the polymeric alkoxides $[Cr(OR)_3]_n$.

The diamagnetic crystalline compound $Cr_2(O\text{-}iPr)_6(NO)_2$ is air sensitive. It is appreciably soluble and quite stable in organic solvents, in which it is dimeric. It is thermally quite stable and can be sublimed at 90–100°C (10^{-4} cm Hg). $Cr_2(O\text{-}iPr)_6(NO)_2$ shows a single IR band at 720 cm^{-1} due to NO.

In both $Cr(O\text{-}tBu)_3(NO)$ and $Cr_2(O\text{-}iPr)_6(NO)_2$ the metal atom appears either in a local trigonal–pyramidal or – bipyramidal ligand field that splits metal orbitals into three sets: a(d_{z2}), e(d_{x2-y2}, d_{xy}), and e(d_{xz}, d_{yz}). The latter e set is little involved in a metal–ligand σ bond and thus lies lowest in energy. The formal oxidation state of the metal is +2, and, irrespective of the formalism used to count valence electrons, the electronic ground-state configuration is (d_{xz}, d_{yz}).

On the basis of physicochemical properties (mol wt measurements, mass, IR, and NMR spectra), the structure of $Cr_2(O\text{-}iPr)_6(NO)_2$ could be represented schematically as in Fig. 2, in which each chromium atom is in a trigonal bipyramidal environment with a crystallographically imposed inversion center and a virtual C_{2h} symmetry. The σ_h plane contains the two chromium atoms, the two bridging oxygen atoms, and the two nitrosyl ligands.

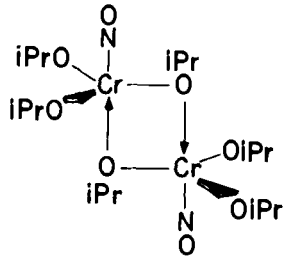

FIG. 2. Schematic representation of the molecular structure of $Cr_2(O\text{-}iPr)_6(NO)_2$.

The relatively low position of a single intense IR band at 1720 cm^{-1} for ν NO indicates a higher component of metal d → NO π^* bonding. The NMR spectrum of the derivative in toluene below 0°C shows two septets in the integral ratio of 2 : 1, which are assignable to the terminal and bridging methyne protons and three partially overlapping doublets assignable to the isopropyl methyl groups, indicating the diastereotopic nature of the methyl groups of the terminal O-*i*Pr ligand [cf. structure of $Mo_2(O\text{-}iPr)_6(NO)_2$ (*55*)]. These resonances broaden slowly as the temperature is raised and coalesce above 80°C to give a sharp doublet and septet indicative of rapid (NMR time scale) bridge ⇄ terminal O-*i*Pr ligand exchange.

The formation (*52*) of bimetallic $CrMo(O\text{-}iPr)_6(NO)_2$ in equilibrium with the simple moieties on mixing equimolecular amounts of $Cr_2(O\text{-}iPr)_6(NO)_2$ and $Mo_2(O\text{-}iPr)_6(NO)_2$ indicated that the interchange of O-*i*Pr groups is intramolecular. A study of variable temperature PMR spectra of the bridge ⇄ terminal equilibrium indicated the following threshold mechanism for the interchange process.

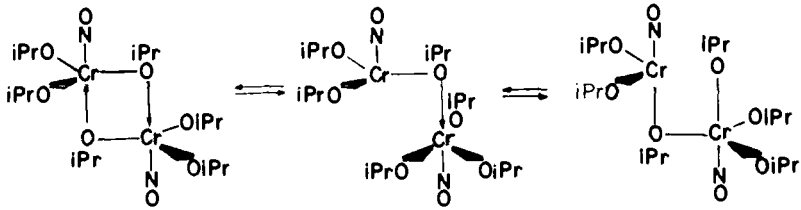

This mechanism involves the formation of reactive four-coordinate chromium species, $Cr(O\text{-}iPr)_3NO$, which should be stabilized compared to the dimer formed by the replacement of O-*i*Pr groups by the bulkier O-*t*Bu groups. Conversely, decreasing the ramification of the alkoxy ligands or increasing the size of the central metal atom should favor the formation of six-coordinated species.

Formation of a number of extremely oxygen-sensitive (some pyrophoric) alkoxides of chromium(II) by alcoholysis of $Cr[N(SiMe_3)_2]_2LL'$ (LL' = ether, THF, or py) has been described (*56*). Solubility of these alkoxides has been reported to be influenced by drying conditions. Thoroughly dried aliphatic products are quite insoluble and exhibit coordination-polymer characteristics. Alkoxides from sterically demanding alcohols and phenols (e.g., 2,6-di-*t*-butylphenol) are less associated and exhibit in general higher solubility; these latter products tend to form adducts with donor ligands.

Hydrocarbon solutions of chromocene have been shown (*57*) to react rapidly with alcohols (Me, Et, and *i*Pr) to give polymeric chromium(II) alkoxides $[Cr(OR)_2]_n$. The more sterically demanding and less acidic *t*-butanol and R'_3SiOH (R' = Me and Ph) react more slowly and lead to products of empirical formulas CpCrO-*t*Bu and $CpCrOSiR_3$, respectively. The *t*-butoxide complex, characterized by a number of physical techniques, including single-crystal X-ray crystallography, is dinuclear $Cp_2Cr_2(O\text{-}tBu)_2$ with a nonplanar $(Cr\text{-}\mu O)_2$ moiety and a Cr—Cr distance of 2.65(2) Å. The Patterson map is quite complex, as expected, with four unique chromium atoms per asymmetric unit. This prompted the investigators to examine the possibility of the existence of two essentially identical and crystallographically related molecules, only one of which is illustrated in Fig. 3. It is reactive toward a number of

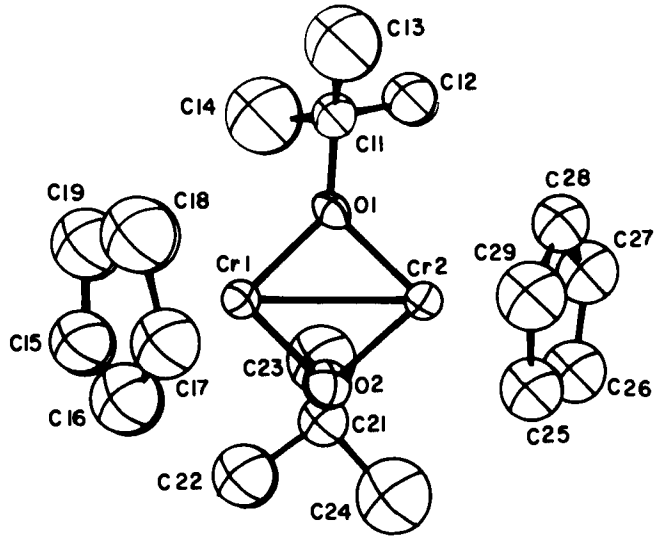

FIG. 3. X-Ray structural view of $Cp_2Cr_2(O\text{-}tBu)_2$.

small, unsaturatd molecules, including acetylenes, CO, CO_2, nitric oxide, and nitrous oxide. The reaction between CO_2 and $Cp_2Cr_2(O\text{-}t\text{Bu})_2$ in THF leads to chromocene and $Cr_2(O_2CO\text{-}t\text{Bu})_4(THF)_2$, which has been structurally characterized by single-crystal X-ray crystallography. $Cr_2(O_2CO\text{-}t\text{Bu})_4(THF)_2$ has the dichromium acetate structure with a Cr—Cr distance of 2.367(3) Å and axially coordinated THF molecules. The principal crystallographic data for $Cp_2Cr_2(O\text{-}t\text{Bu})_2$ are space group $P2_{1/n}$, a = 15.102(4), b = 18.712(4), c = 14.413(3) Å, β = 104.40(2)°, V = 3945(2) Å^3, and Z = 8. The principal crystallographic data for $Cr_2(O_2CO\text{-}t\text{Bu})_4(THF)_2$ are space group $P2_{1/c}$, a = 10.011(1), b = 9.852(2), c = 19.477(3) Å, β = 104.74(1)°, V = 1857(1) Å^3, and Z = 2.

D. Manganese

A series of air-sensitive alkoxides of manganese(II) also have been prepared (*58*) in a manner similar to those of chromium(II), by the alcoholysis of the adducts of $Mn[N(SiMe_3)_2]_2$:

$$Mn[N(SiMe_3)_2]_2 \cdot (L)_n + 2ROH \rightarrow Mn(OR)_2 + 2HN(SiMe_3)_2 + nL$$

L = tetrahydrofuran, pyridine, or *t*-butyl cyanide; n = 0, 1, or 2; R = Me, Et, *i*Pr, *n*Bu, *s*Bu, *t*Bu, 1-pentyl, 2-pentyl, neopentyl, 2-hexyl, triethylmethyl, 1-octyl, 1-nonyl, 1-decyl, 1-adamantyl, benzyl, 2,6-di-*t*-butylphenyl, 2,4,6-tri-*t*-butylphenyl, etc.

The products, characterized by elemental analyses, reflectance spectroscopy, and chemical behavior, range from amorphous coordination polymers and gelatinous fibers to (probably monomeric) crystals.

The manganese(II) alkoxides are all extremely air sensitive, especially when wet and incompletely dried. With traces of oxygen they all change their color, eventually becoming brown or black. Some of them are pyrophoric and burn (or explode) in oxygen.

Abel, Farrow, and Towle (*59*) have studied the reactions of bromopentacarbonylmanganese, $MnBr(CO)_5$, with a number of alcohols (Et, *i*Pr, *n*Bu) and triethylamine:

$$3MnBr(CO)_5 + 3ROH + 3NEt_3 \rightarrow [Mn(OR)(CO)_3]_3 + 6CO + 3NEt_3HBr$$

According to these workers other alcohols did not appear to undergo reactions (which is rather difficult to understand). However, taking advantage of trimethyltin as a leaving group (*60*) in metathetical reactions, they were earlier successful in synthesizing similar compounds

by the reactions

$$3MnBr(CO)_5 + 3Me_3Sn(OR) \rightarrow [Mn(OR)(CO)_3]_3 + 6CO + 3Me_3SnBr$$

$$R = Me, Et, nPr, iPr, nBu, C_6H_{11}, CH_2CH{=}CH_2, CH_2Ph$$

All the products were trimeric, except in the case of the benzyl (CH_2Ph) product, in which a tetrameric derivative, $[Mn(OCH_2Ph)(CO)_3]_4$, was the major component. This tetrameric product showed only three metal–carbonyl bands in the IR spectrum, whereas its NMR spectrum showed that all of the benzyl groups had identical environments. On the basis of these observations, the symmetrical structure shown in Fig. 4 was suggested for the tetrameric product.

The trimeric products, on the other hand, exhibited nine clearly defined Mn—CO stretching modes in their IR spectra, and ^1H- and ^{13}C-NMR sprectra showed two different types of alkyl group environments. These observations suggested (*61*) a remarkably unsymmetrical structure.

Phenyldimethylphosphine reacts with $(EtO)_3Mn_2(CO)_9$ to displace one carbonyl group producing $(EtO)_3Mn_3(CO)_8(PMe_2Ph)$, which also shows two different alkoxy-group environments and eight IR bands in the carbonyl stretching region. Its structure as determined by X-ray diffraction (*61*) is illustrated in Fig. 5a, and from this the structure of the parent trimeric alkoxotricarbonyls of manganese is deduced to be that given in Fig. 5b.

The structure in Fig. 5b is in accordance with the observations of two different types of alkoxyl groups and the large number of active CO

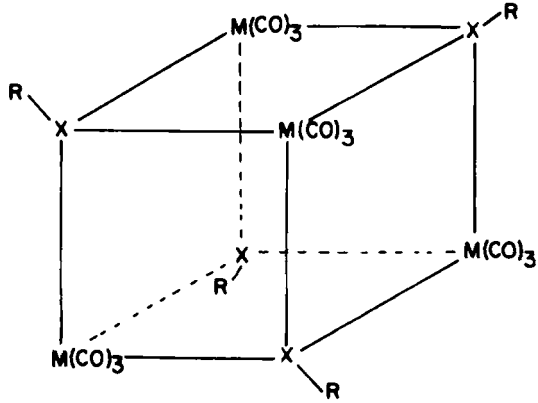

FIG. 4. Cube-shaped structure of the tetrameric alkoxo tricarbonyls of manganese.

stretching modes. The three manganese atoms form a scalene triangle in which only one of the sides (Mn^1—Mn^3) is construed as a metal–metal bond.

Interaction of $Mn_3(OEt)_3(CO)_9$ with phenol brings about (*59*) replacement of only one ethoxide group. Of the three alkoxide groups in the type of structure in Fig. 5b, the formally five-electron-donor face-bridging alkoxide groups have no nucleophilic character, but the edge-bridging oxygen atom formally still has one lone pair of electrons available for reaction.

Reactions of $Mn_3(CO)_9(\mu_3\text{-}OEt)_2(\mu_2\text{-}OEt)$ have been studied (*62*) with BX_3 (X = F, Cl, Br, I), and the halide complexes $Mn_3(CO)_9(\mu_3\text{-}OEt)_2(\mu_2\text{-}X)$ have been isolated; the Cl and Br products have also been prepared from the reactions of anhydrous HX. The crystal and molecular structures of $Mn_3(CO)_9(\mu\text{-}OEt)_2(\mu_2\text{-}X)$ (X = F, I) and $Mn_3(CO)_8(PMe_2Ph)(\mu_3\text{-}OEt)_2(\mu_2\text{-}OEt)$ have been determined by X-ray diffraction. The complexes have a similar structure, consisting of three manganese atoms at the corners of a scalene triangular cluster with two face-bridging OEt ligands and one edge-bridging X or OEt ligand. The remaining ligands are arranged symmetrically around the plane defined by manganese atoms.

Ultraviolet irradiation of fac-[$(\ddot{N}C)_2C{=}C(Cl)Mn(CO)_3(dppe)$] (dppe = $Ph_2PCH_2CH_2PPh_2$) with excess triisopropyl phosphate results in elimination of both isopropyl chloride and carbon monoxide to give an isopropoxymanganese complex [$(NC)_2C{=}CP(O)(OCHMe_2)_2Mn$

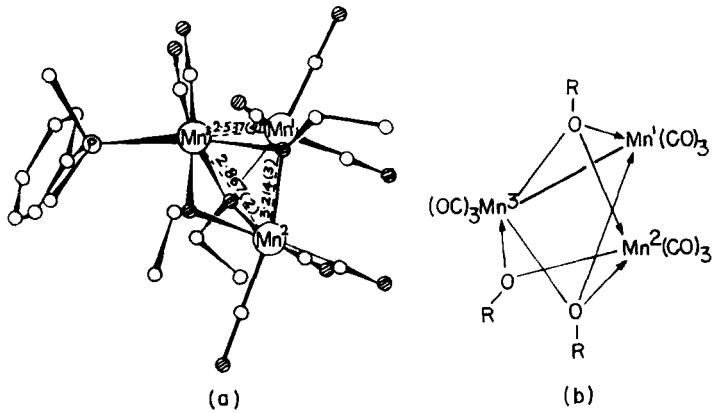

FIG. 5. (a) Structure of the complex $Mn_3(OEt)_3(CO)_8(PMe_2Ph)$. ○, C; ⊘, O. (b) Representation of the structure of $[Mn(OR)(CO)_3]_3$, showing the unique nature of each $Mn(CO)_3$ group and the noble gas formalism for each Mn atom.

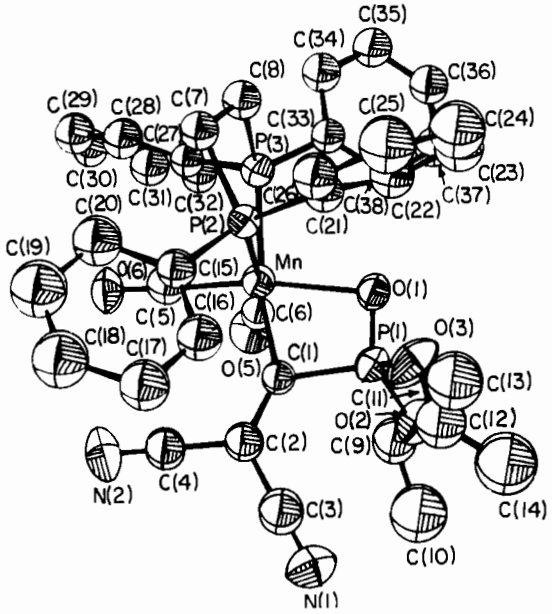

FIG. 6. Ortep drawing of the structure of $(NC)_2C{=}CP(O)(O\text{-}iPr)_2Mn(CO)_2(Ph_2PCH_2CH_2PPh_2)$.

$(CO)_2$(dppe)], the crystal structure of which has been determined by X rays (*63*) and is represented in Fig. 6.

E. IRON

A series of complexes of iron(II) aryloxides and alkoxides with 2,2′-bipyridine (L) with the formulas $Fe(OC_6H_4X)_2L_n$ and $Fe(OR)_2L_n$ have been prepared (*64*) by the reaction of diethylbis(2,2′-bipyridine)iron(II) with *p*-substituted phenols (X = H, Me, Ph, Cl, CN, NO_2) and alcohols (R = Me, Et, *i*Pr, H_2CPh). Interaction of these complexes with acyl and alkyl halides leads to the formation of corresponding esters and ethers. When treated with organic acetates, these complexes yield the corresponding acetates via an alkoxo exchange reaction.

F. COBALT

Alkoxy derivatives of cobalt appear to have received comparatively much less attention. Adams *et al.* (*14*) reported in 1966 the preparation for the first time of cobalt(II) methoxide by the reaction of anhydrous cobalt chloride with lithium methoxide in methanol. On the basis of

spectral and magnetic measurements an octahedral geometry was suggested for this compound. Kakos and Winter (*65*) in the following year prepared a series of derivatives Co(OMe)X (X = Cl, Br, or I) and examined their magnetic and spectral properties.

A detailed study of the alcoholates of cobalt(II) has been carried out (*66*). $CoCl_2$ dissolves in a number of alcohols, and from the clear blue solutions thus obtained alcoholates with the general formula $CoCl_2 \cdot 2ROH$ (R = Me, Et, *i*Pr, *n*Bu, *i*Bu and *s*Bu) and $CoCl_2 \cdot t$BuOH could be isolated by removing the excess alcohol under reduced pressure (1 mm) at 20–25°C, either from solution or from the crystallized alcoholate (after decanting the excess alcohol). Magnetic measurements and electronic spectra of the alcoholates suggest an octahedral environment for cobalt(II) in the methanolate complex and tetrahedral geometry for all other alcoholates.

Cobalt alkoxides have been synthesized (*67*) by the reactions of cobalt chloride with 2 mol of lithium alkoxide in the respective alcohol and benzene:

$$CoCl_2 + 2LiOR \xrightarrow[C_6H_6]{ROH} Co(OR)_2 + 2LiCl$$

R = Me, Et, or *i*Pr

The purple-colored alkoxides are insoluble in organic solvents and are nonvolatile.

Cobalt isopropoxide interchanges its alkoxy groups readily with primary alcohols at room temperature:

$$Co(O\text{-}i\text{Pr})_2 + \underset{\text{(excess)}}{2ROH} \rightarrow Co(OR)_2 + 2i\text{PrOH}$$

R = Me, *n*Bu

However, it does not react with other secondary and tertiary alcohols. Similarly, the primary alkoxides do not react with any alcohol, even under forcing conditions.

The visible spectra of cobalt(II) alkoxides show a multiple band with maximum in the range 18,235 ± 285 cm^{-1} and a shoulder on the higher frequency side at 20,170 ± 450 cm^{-1}. The observed spectra indicate an octahedral geometry for cobalt in these alkoxides.

G. Nickel

A number of alcoholate complexes of nickel chloride, $NiCl_2 \cdot x$ROH, have been described (*68*). The alcoholates of the primary alcohols ROH (R = CH_3, C_2H_5, C_4H_9, C_6H_{13}, and C_8H_{17}) have been prepared from

solutions of $NiCl_2$ in the respective alcohols. $NiCl_2$ is insoluble in secondary and tertiary alcohols, but their adducts were prepared by an alcohol-interchange technique:

$$NiCl_2 \cdot CH_3OH + R'OH \rightarrow NiCl_2 \cdot R'OH + CH_3OH$$

$$R' = i\text{-}C_3H_7,\ t\text{-}C_4H_9, \text{ or } t\text{-}C_5H_{11}$$

All of the monoalcoholates (primary, secondary, and tertiary) exhibit three bands in their electronic spectra at around 7500 ± 500 ($^3A_{2g} \rightarrow {}^3T_{2g}$), 12,500 ± 1000 [$^3A_{2g} \rightarrow {}^3T_{1g}(F)$], and 22,000 ± 500 cm^{-1} [$^3A_{2g} \rightarrow {}^3T_{1g}(P)$], indicating a pseudooctahedral geometry for the complexes.

Following the method of Adams *et al.* (*14*), a number of alkoxides of nickel(II) have been synthesized (*17, 69*) by the reactions of anhydrous nickel chloride with lithium alkoxides in 1:2 stoichiometric ratios:

$$NiCl_2 + 2LiOR \xrightarrow[1,4\text{-dioxane}]{ROH \text{ or}} Ni(OR)_2 + 2LiCl$$

$$R = CH_3,\ C_2H_5,\ n\text{-}C_3H_7,\ i\text{-}C_3H_7,\ s\text{-}C_4H_9,\ t\text{-}C_4H_9,\ t\text{-}C_5H_{11}, \text{ or } t\text{-}C_6H_{13}$$

As mentioned earlier, nickel chloride is soluble in primary alcohols (with the formation of adducts), whereas it is insoluble in secondary and tertiary alcohols. The reactions of nickel chloride suspended in the latter alcohols (and dioxane) with the corresponding lithium alkoxides are much slower and do not appear to proceed to completion easily. Because this might be due to insolubility of nickel chloride in secondary and teritary alcohols, addition of a little pyridine, which tends to solubilize nickel chloride, has been attempted and has been found to facilitate the reactions considerably. All of these alkoxides of nickel are nonvolatile, colored solids, which are insoluble in common organic solvents. The primary alkoxides are light green in color, whereas the secondary and tertiary alkoxides are blue to violet. The latter alkoxides are particularly sensitive to moisture, in the presence of which they are hydrolyzed with a sharp color change from violet (blue) to green. All of the secondary and tertiary alkoxides are unstable toward heat and tend to decompose at around 90–100°C.

The spectra and magnetic moments of these alkoxides also show interesting differences. The spectra of the primary alkoxides exhibit three well-defined spin-allowed bands at 8750 ± 250 (ν_1; $^3A_{2g} \rightarrow {}^3T_{2g}$), 14,810 ± 115 [$\nu_2$; $^3A_{2g} \rightarrow {}^3T_{1g}(F)$], and 24,980 ± 125 cm^{-1} [ν_3; $^3A_{2g} \rightarrow {}^3T_{1g}(P)$], which are characteristic of an octahedral environment for nickel in these primary alkoxides. On the other hand, the spectra of

secondary and tertiary alkoxides of nickel indicate a tetrahedral geometry with well-defined spin-allowed transitions at 7580 ± 100 (ν_2; $^3T_1 \rightarrow {}^3A_2$) and 15,850 ± 70 cm^{-1} [ν_3; $^3T_1 \rightarrow {}^3T_1(P)$].

The magnetic moments of the primary alkoxides of nickel(II) fall in the range 3.45 ± 0.04 BM (Bohr magnetons), and those of secondary as well as tertiary alkoxides are found in the range 3.65 ± 0.05 BM at room temperature; these observations also are in accord with their octahedral and tetrahedral configurations, respectively.

Like the primary alkoxides of chromium(III), the primary alkoxides of nickel also do not undergo alcoholysis reactions with other alcohols, even under forcing conditions. The secondary and tertiary alkoxides, however, undergo alcoholysis reactions with primary alcohols even at room temperature, but these also do not appear to react with other secondary and tertiary alcohols. Similar trends are observed in the transesterification reactions of the different alkoxides with alkyl esters.

It is interesting to observe that, although nickel methoxide does not undergo alcoholysis reactions, these undergo insertion reactions with phenyl and naphthyl isocyanates with evolution of heat (*70*):

$$Ni(OR)_2 + xR'NCO \rightarrow (RO)_{2-x}Ni[N(R')COOR]_x$$

R = Me and *i*Pr; R′ = Ph and Naph; x = 1, 2

Nickel alkoxides also undergo reactions with alkanolamines, β-diketones, and carboxylic acids, and interesting products have been obtained. The reactions with alkanolamines (*71*) in different stoichiometric ratios in benzene can be represented by the reactions

$$Ni(OR)_2 + n\text{Hetha} \rightarrow Ni(OR)_{2-n}(\text{etha})_n + n\text{ROH}$$

$$Ni(OR)_2 + H_2\text{etha}' \rightarrow Ni(\text{etha}') + 2\text{ROH}$$

R = Me or *i*Pr; etha = ethanolamine with n = 1 or 2; etha′ = di- or triethanolamine

Nickel alkoxides have been shown to interact slowly with β-diketones:

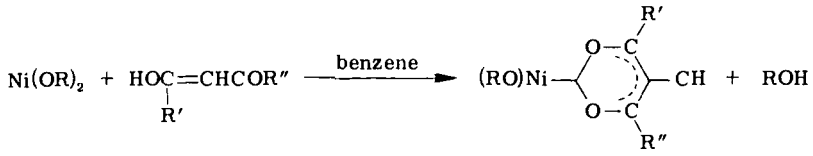

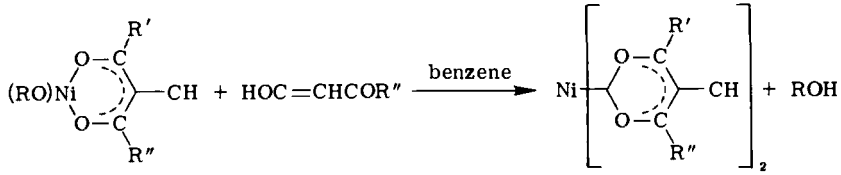

R = CH_3, i-C_3H_7; R′, R″ = CH_3, C_6H_5, CF_3, or C_4H_3S

It is interesting to record that the monoalkoxide mono-β-diketonates (even the methoxide) undergo alcoholysis reactions with other alcohols (primary, secondary, and tertiary), as illustrated by the following typical reactions.

$$Ni(O\text{-}iPr)(\beta\text{-dk}) + \underset{(excess)}{ROH} \xrightarrow{r.t.} Ni(OR)(\beta\text{-dk}) + iPrOH$$

R = Me or Et

$$Ni(OMe)(\beta\text{-dk}) + ROH \xrightarrow[reflux]{benzene} Ni(OR)(\beta\text{-dk}) + MeOH$$

R = Et, iPr, or tBu

$$Ni(O\text{-}iPr)(\beta\text{-dk}) + tBuOH \xrightarrow[reflux]{benzene} Ni(O\text{-}tBu)(\beta\text{-dk}) + iPrOH$$

The mixed alkoxide β-diketonates also undergo exchange reactions with other β-diketones, resulting in the synthesis of a variety of mixed β-diketonates:

$$Ni(OR)(\beta\text{-dk}) + H\beta\text{-dk}' \xrightarrow{benzene} Ni(\beta\text{-dk})(\beta\text{-dk}') + ROH$$

R = Me or iPr, and β-dk or β-dk′ = acac, bzac, dbzm, or tta

All of these products are colored solids and are soluble in benzene, from which they can all be recrystallized. All the bis-β-diketonate derivatives are trimeric. Among the monoalkoxide derivatives, the isopropoxide and tertiary butoxide mono-β-diketonates are trimeric, but the methoxide and ethoxide analogs are tetrameric.

Nickel bisacetylacetonate also forms monoadducts with a number of alcohols: $Ni(acac)_2 \cdot ROH$ (R = Me, Et, iPr, nBu, sBu or tAm). These alcoholates can be recrystallized from benzene, in which they show dimeric association.

On the basis of infrared, electronic reflectance, and electron-spin resonance spectra as well as magnetic measurements, all of these derivatives have been shown (*70, 72*) to have distorted octahedral structures.

The reactions of nickel alkoxides with carboxylic acids can also be represented (*73*) by the reactions

$$Ni(OR)_2 + nR'COOH \xrightarrow{\text{benzene}} Ni(OR)_{2-n}(OOCR')_n + nROH$$

$$R = CH_3 \text{ or } i\text{-}C_3H_7;\ R' = C_{13}H_{27},\ C_{15}H_{31},\ \text{or } C_{17}H_{35};\ n = 1 \text{ or } 2$$

The progress of the reaction can be conveniently followed by estimating the alcohol liberated in the reaction and collected azeotropically with benzene. The reactions are quite facile and can be completed in a short period. Unlike the parent alkoxides, all of the colored mono- as well as disubstituted products obtained are highly soluble in benzene and other organic solvents. Monomethoxide monocarboxylates do not undergo alcoholysis reactions. The isopropoxide analogs, on the other hand, undergo facile interchange with methanol or ethanol at ambient temperature, but the complete interchange of isopropoxide by tertiary butoxide groups, requires refluxing for a long time with continuous fractionation of isopropanol produced in the reaction.

All of these carboxylate derivatives are nonvolatile colored solids, soluble in benzene but insoluble in alcohols. All of the alkoxide monocarboxylate derivatives have been shown to be tetrameric, whereas the dicarboxylates are trimeric in refluxing benzene. The IR spectra of these derivatives appear to suggest a bidentate nature of the carboxylate moieties in them. Electron-reflectance spectra and magnetic measurements indicate an octahedral environment for nickel in all these derivatives.

H. Copper

The general applicability of the lithium alkoxides (cf. *14*, *74*) in the synthesis of copper(II) alkoxides has been shown (*75*):

$$CuCl_2 + 2LiOR \xrightarrow{ROH} Cu(OR)_2 + 2LiCl$$

$$R = \text{Me, Et, } i\text{Pr, } t\text{Bu}$$

Synthesis of a few more alkoxides of copper has been described (*67*) by the alcohol-interchange reactions

$$Cu(OR)_2 + \underset{\text{(excess)}}{2R'OH} \xrightarrow{\text{benzene}} Cu(OR')_2 + 2ROH$$

$$R = \text{Me, Et or } n\text{Bu};\ R' = \text{Me, Et, } i\text{Pr, } n\text{Bu, } s\text{Bu, } t\text{Bu, or } t\text{Am}$$

Alcohol-interchange reactions of copper(II) alkoxides reveal some novel features compared to those of alkoxides of chromium(III) (*17, 46*), cobalt(II) (*17, 66*), and nickel(II) (*17, 69*). Compared to the novel nature of alcoholysis reactions of these latter alkoxides, copper(II) alkoxides undergo facile alcohol-interchange reactions. Copper(II) alkoxides in this respect show resemblance to alkoxides of earlier transition metals like titanium and vanadium, which also undergo very facile alcoholysis reactions.

It has been observed that the primary alkoxides of copper(II) interchange their alkoxide groups quantitatively with tertiary, secondary, or other primary alcohols under refluxing conditions only, whereas the secondary and tertiary alkoxides undergo a more facile alcohol-interchange reaction with primary alcohols, even at room temperature with slight evolution of heat. It has been found that the secondary and tertiary alkoxides of copper(II) do not appear to undergo alcohol-interchange reactions with other secondary and tertiary alcohols. Although it is difficult to sort out the effects of various factors like thermodynamic and kinetic stabilities as well as the role of crystal field stability in different plausible geometries (apparently the main factor in alcoholysis trends of nickel alkoxides), the alcohol-interchange reactions of copper(II) alkoxides appear to be governed mainly by steric factors. As in a number of other metals, the alkoxy interchange reactions are sterically less hindered when esters are used in place of alcohols as reactants. For example, it has been reported (*67*) that copper(II) isopropoxide, which hardly undergoes interchange with *t*-butanol can be converted to *t*-butoxide by treating with *t*-butyl acetate:

$$Cu(O\text{-}i\text{Pr})_2 + 2CH_3COO\text{-}t\text{Bu} \rightleftharpoons Cu(O\text{-}t\text{Bu})_2 + 2CH_3COO\text{-}i\text{Pr}$$

The alcoholysis reactions of copper(II) alkoxides thus follow the following order of relative lability, which is similar to that already reported in the alkoxides of a number of earlier transition metals (*13*): primary alkoxides $\gg$ secondary alkoxides $\sim$ teritary alkoxides.

Brubaker and Wicholas (*74*) reported subnormal magnetic moments for $Cu(OMe)_2$ (1.12 BM) and $Cu(OEt)_2$ (1.18 BM) and suggested a highly polymeric structure for these with tetragonally distorted copper atoms. Adams *et al.* (*14, 76*) measured the magnetic susceptibility of $Cu(OMe)_2$ over the range 80–350 K. They favored a linear-chain model for polymeric $Cu(OMe)_2$ analogous to that of $CuCl_2$.

Singh (*67*) has measured the magnetic susceptibilities of typical primary, secondary, and tertiary alkoxides of copper and has found that (a) for $Cu(OBu)_2$ it increases from 0.64 at 88.5 to 1.18 at 298.7 K; (b) for $Cu(O\text{-}i\text{Pr})_2$ it increases from 0.98 at 88.0 to 1.50 at 297.1 K; and

(c) for $Cu(O\text{-}t\text{Am})_2$ it increases from 1.37 at 87.5 to 1.83 at 297 K. These data indicate the presence of antiferromagnetic exchange interaction, which, as expected, decreases with increasing ramification of the alkyl group. The J values calculated employing the Ising model also follow a trend in the same direction as shown from the following values of J.

$\lvert J\rvert Cu(O\text{-}n\text{Bu})_2$	$\lvert J\rvert Cu(O\text{-}i\text{Pr})_2$	$\lvert J\rvert Cu(O\text{-}t\text{Am})_2$
129 cm^{-1}	81 cm^{-1}	43 cm^{-1}

The visible spectra of $Cu(OMe)_2$, $Cu(OEt)_2$, and $Cu(O\text{-}n\text{Bu})_2$ are similar and show absorption bands at 15,500 ± 75 and 19,100 ± 300 cm^{-1}, which point to a distorted octahedral environment around copper. However, the spectra of branched alkoxides of copper, $Cu(O\text{-}i\text{Pr})_2$, $Cu(O\text{-}s\text{Bu})_2$, $Cu(O\text{-}t\text{Bu})_2$, and $Cu(O\text{-}t\text{Am})_2$, are characterized by a very broad absorption in the visible region at approximately 15,000 cm^{-1} that appears to tail in the near-infrared region. This band may be assigned to a $^2E_g \rightarrow {}^2T_{2g}$ transition, which would indicate a six-coordinated tetragonal geometry for copper in these branched alkoxides.

Copper(II) complexes with unsubstituted phenoxide groups have not been reported as yet, and it may be that these have not been isolated because they would be unstable toward reductive elimination to phenoxy radicals, which would then couple to give diphenoquinone or 1,4-phenylene ethers (*77*) in the presence of copper. In view of this, it is interesting to report that coordinated diphenoxo derivatives of copper(II) have been obtained by the reactions

$$CuCl_2(bipy) + 2NaOPh \xrightarrow{THF} \underset{\substack{\text{(brown complex}\\ \text{moderately soluble}\\ \text{in THF)}}}{Cu(OPh)_2(bipy)} + 2NaCl$$

$$CuCl_2(en) + 2Na(OPh)\cdot PhOH \xrightarrow{THF} \underset{\substack{\text{(green complex)}\\ \text{sparingly soluble}\\ \text{in THF)}}}{Cu(OPh)_2(en)\cdot PhOH} + 2NaCl$$

The bisphenoxo derivative of copper(II), $Cu(OPh)_2(en)_2 \cdot 2PhOH$ has been shown (*78*) by X-ray diffraction to be a centrosymmetric phenoxo-bridged dimer with terminal phenoxo and ethylenediamine groups and hydrogen bonded phenol molecules. The crystals are monoclinic (space group $P2_{1/n}$, and the unit cell has dimensions a = 19.000(3), b = 10.930(9), c = 8.968(5) Å, β = 89.90(2)°, V = 1862.4 $Å^3$, and Z = 4. The copper atoms are five-coordinate, and the coordination geometry is that of a distorted square pyramid. The Cu—Cu distance is 3.215 Å, and the compound has a nearly normal magnetic moment at room

temperature. The X-ray crystal structure of CuO-*t*Bu prepared by the reaction of CuCl with LiO-*t*Bu in THF showed it to be a tetrameric compound, $[CuO\text{-}tBu]_4$ (*79*). The crystals are triclinic (space group $P\bar{1}$) with $a = 11.890$, $b = 11.284(2)$, $c = 10.047(9)$ Å; $\alpha = 90.54(3)$, $\beta = 106.39(5)$, and $\gamma = 113.86(4)^\circ$; d(calculated) = 1.55 for $Z = 8$. Four of the formula units form a planar ring containing four Cu and four O atoms. The tertrameric units persist even in the vapor phase.

Treatment of Cu(O-*t*Bu) with di-*t*-butyl peroxide gave $Cu(O\text{-}tBu)_2$ as a yellow-green solid (*80*). Cu(O-*t*Bu) has been shown to be an excellent metalation reagent, as illustrated by the following facile reaction at room temperature.

$$\underset{80\ \text{mmol}}{PhC{\equiv}CH} + \underset{4\ \text{mmol}}{Cu(O\text{-}tBu)} \rightarrow \underset{97\%}{PhC{\equiv}CCu} + \underset{97\%}{tBuOH}$$

The coupling of 1,3-dinitrobenzene with aryl iodides by Cu(O-*t*Bu) and pyridine provides (*81*) a convenient route for 2,6-dinitrobiphenyls and is an improvement on the earlier methods (*82*).

Secondary and primary alkoxides and the phenoxide of copper(I) have been synthesized (*83*) by the heterogeneous reaction of alcohols with methylcopper(I). The reactions of copper(I) alkoxides with aryl halides yield alkyl aryl ethers under particularly mild conditions. Thermal decomposition of primary alkoxides of copper(I) generates intermediate alkoxy radicals, whereas that of secondary alkoxides appears to take place either by a free-radical mechanism or through an intermediate formation of copper(I) hydride.

Copper(I) alkoxides, $ROCu(PPh_3)_2$ (R = Et, $PhCH_2$), react with CO_2 to give products corresponding in composition to $ROCO_2Cu(PPh_3)_2$ (*84*). Hydrolysis or thermolysis of these (alkylcarbonato)copper(I) complexes gives a binuclear carbonatocopper(I) complex, $(Ph_3P)_2CuOCO_2\text{-}Cu(PPh_3)_2$.

Continuing their earlier investigations (*84a,b*) on the condensation of 5,5,5-trifluoro-4-hydroxy-4(trifluoromethyl)-2-pentanone (hexafluorodiacetone alcohol) with diamines in the presence of metal ions, Willis *et al.* (*84c*) have determined the structure of a dinuclear iminoalkoxy compound of copper(II).

III. Alkoxy and Allied Derivatives of 4d and 5d Metals

Except for some earlier work on alkoxy derivatives of zirconium, niobium, and tantalum, and a more recent surge in penetrating inves-

tigations of the alkoxy derivatives of molybdenum and tungsten, the chemistry of 4d and 5d metal alkoxides appears to have received comparatively little attention. These are, therefore, dealt with together, which is also convenient because pairs of these elements show more similarities in their chemistry compared to those of the corresponding 3d metals.

A. Zirconium and Hafnium

A series of *N*-methylaminoalkoxides of zirconium, $Zr(O\text{-}iPr)_{4-n}(OCHR'CH_2NR''R''')$ (R′ = R″ = H, R‴ = Me, R′ = H, R″ = R‴ = Me, R′ = R″ = R‴ = Me, n = 1–4), have been synthesized (*35*) by the reactions of $Zr(O\text{-}iPr)_4 \cdot iPrOH$ with aminoalcohols. Similar to zirconium isopropoxides (*86*), these aminoalkoxides, $Zr(OCHR'CH_2NR''R''')_4$, have also been shown to undergo insertion reactions with PhNCO to give products of the type $Zr(NPhCOOCHR'CH_2NR''R''')_4$.

A series of mixed derivatives of zirconium with possible coordination numbers 5, 6, 7, and 8 have been synthesized (*87*) by the reactions of zirconium isopropoxide with a number of aliphatic and aromatic hydroxy esters: $HOC_6H_{10}R$, HOCHPhR, and HOCMePhR (R = CH_2COOEt).

Conductometric titration of $ZrCl_4$ with KOPh in nitrobenzene indicates (*88*) the formation of a number of chloride phenoxides and a tetraphenoxide of zirconium.

The compounds $MCl(OC_6H_3tBu_2\text{-}2,6)_3$ (M = Zr, Hf) have been synthesized by the reactions of the metal tetrachlorides with $LiO(C_6H_3tBu_2\text{-}2,6)$ in diethyl ether (*88a*). The hafnium has been structurally characterized to show a sterically congested, mononuclear molecule in which several distortions of the aryloxo ligands have taken place.

B. Niobium and Tantalum

A detailed variable-temperature ^{13}C-NMR study of $Nb(OEt)_5$ and $Ti(OR)_4$ (R = Et, Pr, Bu, *i*Bu, *i*Pr, *t*Bu, neopentyl) has been carried out (*89*), and the data have been interpreted in terms of the degree of association and equilibria among the oligomeric entities.

A crystal and molecular structure study (*90*) of niobium pentamethoxide showed a structure with two conformers in the unit cell that is pronouncedly pseudo-body-centered and that contains two crystallographically different centrosymmetric dimeric molecules with different conformations. Both forms consist of two approximately octahedral

units with a shared edge, which are differentiated by a cis or trans arrangement of the equatorial methyl groups with respect to the equatorial plane.

A detailed study of the coordination ability of about 40 potential nitrogen-, oxygen-, phosphorus-, and sulfur-donor ligands has been made by Hubert-Pfalzgraf (*91*) and has been actually discussed in terms of frontier orbitals, pK_a values, charge distribution, and Gutmann's donor numbers (D_n) of the ligands.

A very interesting mixed $NbTa(OCH_3)_{10}$ has been isolated (*92*) as a crystalline compound, and it has been characterized by proton NMR, IR, and mass spectrometry. In solution it is in dynamic random equilibrium with the symmetric dimers $Nb_2(OCH_3)_{10}$ and $Ta_2(OCH_3)_{10}$:

NbX_5 and TaX_5 (X = Cl, Br) have been shown (*93*) to react with oxygen-donor ligands in anhydrous alcohol to yield halide alkoxide complexes of the type $M(OR)_3X_2L$ [M = Nb, Ta; R = Me, Et; X = Cl, Br; L = Ph_3PO, Ph_3AsO, Ph_2SO and $(Me_2N)_3PO$].

$M(OPh)_nBr_{5-n}$ (M = Nb, Ta) have been prepared (*94*) by stepwise phenolysis of MBr_5 in CCl_4.

Chelates of niobium and tantalum phenoxides and chloride phenoxides with benzoin (HL) with the formulas $M(OPh)_4L$, $MCl(OPh)_3L$ and $MCl_2(OPh)_2L$ have been prepared (*95*) by refluxing $M(OPh)_5$, $MCl_2(OPh)_3$, and $MCl_3(OPh)_2$ with benzoin in a 1:1 molar ratio in benzene.

Crystalline high-melting-point salts $[M(OPh)_4]SbCl_6$ have been synthesized (*96*) by the reactions of $M(OPh)_4Cl$ (M = Nb, Ta) with $SbCl_5$ in CH_2Cl_2.

A series of mixed alkoxide cyanides of niobium and tantalum, $M(OR)_{5-n}(CN)_n \cdot xCH_3COOR$ (M = Nb, Ta; R = Et, *i*Pr; n = 1–5, x = 0.5–2.5) have been prepared (*97*) by the reactions of the pentaalkoxides with pyruvonitrile in the required molar ratios in cyclohexane. The reactions of $Nb(CN)_5 \cdot 2CH_3COO$-*i*Pr and $Ta(CN)_5 \cdot 2.5CH_3COO$-*i*Pr with refluxing isopropanol yield products, $M(O\text{-}iPr)_2(CN)_3CH_3COO\text{-}iPr$, similar to those obtained in the reactions of $M(O\text{-}iPr)_5$ with CH_3COCN in 1:3 molar-ratio reactions.

A number of niobium(V) oxyalkoxide derivatives, $[NbO(OCH_2CF_3)_3 \cdot MeCN]_2$, $NbO(OCH_2CF_3)_2(OCH{=}CF_2)(CF_3CH_2OH)_{0.5}$, $[NbO(OEt)_3]_2$, $[NbOCl_2(OCH_3) \cdot CH_3OH]_2$, and $NbO(OCH_3)(OC_6H_4CHO)$, have been synthesized (*98*) by direct alkoxylation of niobium oxychloride. The molecular constitution of the solutions of $[NbO(OEt)_3]_2$ and $[NbO(OCH_2CF_3)_3 \cdot MeCN]_2$ in nonpolar solvents was tentatively interpreted as a dynamic equilibrium between various μ-alkoxo and μ-oxo isomers, the latter being favored by dilution. In polar media dimeric units are retained for $[NbO(OEt)_3]_2$, whereas the trifluoroethoxide derivative splits into monomeric species.

C. Molybdenum and Tungsten

1. *Higher Alkoxides and Halide Alkoxides of Molybdenum and Tungsten*

The preparation of $W(OPh)_6$ by the reaction of WCl_6 with PhOH has been reported (*99*). Hexamethoxides of molybdenum and tungsten as well as uranium have been synthesized (*99a*) by the reactions of their hexafluorides with excess of tetramethylsilicate; the last stage of the reaction is slow in the case of tungsten, yielding mainly $WF(OMe)_5$, which can be converted into $W(OMe)_6$ by treatment with a methanol solution of NaOMe.

Reactions of $MoOCl_4$ in CH_2Cl_2 with solid $NaOC(CF_3)_3$ have been investigated in different molar ratios, and derivatives $MoOCl[OC(CF_3)_3]_3$ and $MoO[OC(CF_3)_3]_4$ have been isolated (*100*). Both products are volatile and may be sublimed at temperatures as low as 60°C. The cell dimensions of $MoOCl[OC(CF_3)_3]_3$ are a = 6.82, b = 20.86, and c = 17.22 Å (primitive orthorhombic), and those for $MoO[OC(CF_3)_3]_4$ are a = 13.305, b = 13.946, and c = 13.570 Å (face-centered orthorhomic).

2. *Alkoxides of Molybdenum and Tungsten in 3- and 4-Oxidation States*

A series of alkoxides of molybdenum and tungsten with the general formulas $M(OR)_3$ and $M(OR)_4$ have been described. The derivatives $M(OR)_3$ are of special interest because they represent the first known examples in which association occurs not through alkoxy bridges but by the formation of metal–metal triple bonds (*101–104*).

a. Alkoxides of Molybdenum(III). Alkane solutions of $Mo_2(NMe_2)_6$ react (*102–104*) smoothly with the alcohols and silanols ROH [R = Me,

Et, *n*Pr, *i*Pr, *t*Bu, CH_2CMe_3, CMe_2Ph, $C(CF_3)_3$, $SiMe_3$, and $SiEt_3$] and pinacol, $Me_2C(OH)C(OH)Me_2$. The ease of alcoholysis decreases with the ramification of the alkyl group, so much so that even under refluxing conditions with Et_3COH partial substitution occurs yielding $Mo_2(NMe_2)_2(OCEt_3)_4$. Stripping the solvent in these reactions gives crude samples of $[Mo(OR)_3]_x$ compounds or their amine adducts. Dinuclear compounds $Mo_2(OR)_6$ (R = *i*Pr, CH_2CMe_3, *t*Bu, $SiMe_3$, and $SiEt_3$) and $Mo_2(O_2C_2Me_4)_3$ have been obtained by vacuum sublimation (100–160°C, 10^{-4} cm Hg). These $Mo_2(OR)_6$ compounds are crystalline solids that are soluble in alkanes, benzene, toluene, and THF, with the exception of R = CMe_2Ph and $C(CF_3)_3$ and the pinacolate derivative. Their colors, which vary from pale yellow to red, depending on the nature of the R group, arise from a tailing of strong UV absorption into the visible region of the spectrum: they show no λ_{max} in the visible region of the spectrum. The molecular weight of $Mo_2(O\text{-}tBu)_6$ in benzene corresponds to the dimeric formula. They are diamagnetic both in the solid state and in solution. In the mass spectrometer they show strong parent ions $Mo_2(OR)_6^+$ together with many other Mo_2-containing ions; indeed, the virtual absence of mononuclear ions is quite striking. ^1H- and ^{13}C-NMR spectra in the temperature range 90 to −90°C of the compounds in toluene-d_8 show one type of OR ligand. However, in the case of R = CH_2CMe_3 both proton and ^{13}C signals are lost in the baseline at low temperatures.

The structure of $Mo_2(OCH_2CMe_3)_6$ is shown in Fig. 7, and some of the important structural parameters are given in Table III. The structure is similar to those of $Mo_2(NMe_2)_6$ (*105*) and $Mo_2(CH_2SiMe_3)_6$

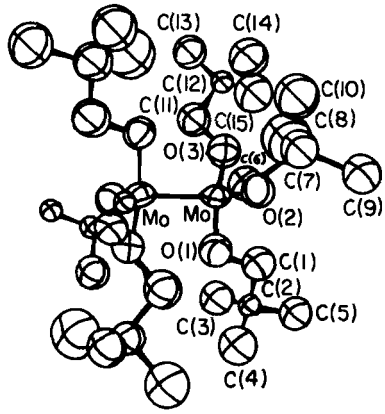

FIG. 7. Ortep stereoscopic view of the $Mo_2(OCH_2CMe_3)_6$ molecule.

(*106*). The central Mo_2X_6 moiety (X = O, N, C) virtually has D_{3d} symmetry, and the Mo—Mo distances are in the range 2.167–2.222 Å.

The bonding in $Mo_2(OCH_2CMe_3)_6$ and related $Mo_2(OR)_6$ compounds appears to involve four σ bonds (three to oxygen atoms and one to the other molybdenum atom), using approximately tetrahedral orbitals (may be sp^3, sd^3, or any intermediate combination) on each Mo atom. Then, taking the Mo—Mo σ bond as the z axis, two metal σ bonds can be formed employing d_{xz}, d_{yz}, and/or p_x, p_y orbitals on each atom. The Mo≡Mo bond so formed would readily account for the short Mo≡Mo distance (2.222 Å), which is about 1 Å less than that in a Mo—Mo bond, and the diamagnetic nature of the compound.

The importance of steric factors in determining the characteristics of this series of $Mo(OR)_3$ alkoxides can be demonstrated (*104*) by the fact that dimers $(RO)_3Mo{\equiv}Mo(OR)_3$ with Mo≡Mo bonds are formed only in the cases of highly ramified R groups. Even the neopentyl (H_2CCMe_3) derivative appears to be on the border. In hydrocarbon solvents $Mo_2(OCH_2CMe_3)_6$ undergoes a slow and irreversible reaction, leading to the formation of a brick-red precipitate, which appears to be a polymeric compound of the composition $[Mo(OCH_2CMe_3)_3]_n$. The reaction of $Mo_2(NMe_2)_6$ with EtOH yields a black compound that is highly soluble in hydrocarbons; analyses and molecular-weight determina-

TABLE III

INTERATOMIC DISTANCES AND ANGLES FOR MOLECULES IN FIGURE 7[a]

Molecule	Interatomic distance (Å)	Molecule	Interatomic distance (Å)
Mo—Mo′	2.222(2)	C(2)—C(5)	1.57(1)
Mo—O(1)	1.905(6)	C(6)—C(7)	1.57(1)
Mo—O(2)	1.867(6)	C(7)—C(8)	1.58(1)
Mo—O(3)	1.855(6)	C(7)—C(9)	1.54(1)
Molecule	**Bond angle (deg)**	**Molecule**	**Bond angle (deg)**
Mo′—Mo—O(1)	98.3(2)	C(3)—C(2)—C(4)	108.1(10)
Mo′—Mo—O(2)	105.5(2)	C(3)—C(2)—C(5)	111.0(10)
O(1)—Mo—O(2)	115.9(3)	C(6)—C(7)—C(8)	103.5(8)
Mo—O(1)—C(1)	114.5(7)	C(8)—C(7)—C(9)	109.0(8)
Mo—O(2)—C(6)	135.1(6)	C(8)—C(7)—C(10)	111.4(9)

[a] Primed atoms are symmetry related to the corresponding unprimed atoms.

tions indicate a tetrameric formula $[Mo(OEt)_3]_4$. In the mass spectrometer the ion of the highest mass corresponded to $[Mo_4(OEt)_{12}]^+$ although other multinuclear species, for example, $[Mo_3(OEt)_9]^+$ and $[Mo_2(OEt)_6]^+$, were very prominent and mononuclear moieties like $Mo(OEt)_5^+$ also were observed. This ethoxide is diamagnetic and gives a very complex ^{1}H-NMR spectrum due to overlapping of several ethyl resonances. In the ^{13}C-NMR spectrum in benzene-d_6, eight methylene carbon signals were observed in the intensity ratio 1 : 1 : 1 : 1 : 2 : 2 : 2 : 2, which appears to be consistent with the tetrameric formula. In contrast to this, the corresponding reaction of $Mo_2(NMe_2)_6$ with MeOH leads to a nonvolatile hydrocarbon-insoluble brown paramagnetic polymeric alkoxide $[Mo(OMe)_3]_n$. The IR spectrum of the methoxide indicates a predominance of the bridging OMe ligands, and the polymerization probably occurs by the formation of MoO_6 units [cf. $Cr(OMe)_3$ (*45*)]. A notable difference in the chemistry of Cr(III) and Mo(III) is that Cr(III) will, though somewhat reluctantly, form tetrahedral complexes as in the salts $LiCr(CH_2SiMe_3)_4$ (*107*) and $LiCr(O\text{-}t\text{Bu})_4$ (*108*), whereas molybdenum prefers to adopt a $L_3Mo{\equiv}MoL_3$ structure at the expense of forming a fourth Mo—L bond.

In trying to explain the slow polymerization of $Mo_2(OCH_2CMe_3)_6$, Chisholm *et al.* (*104*) have cited the "aging" phenomenon of $Al(O\text{-}i\text{Pr})_3$ (*109*). The latter has, however, been shown to involve a change from a tetrahedral to an octahedral aluminum atom (*110*), but the same may not be applicable in the case of molybdenum neopentyloxide, in which a reorganization of the following type has been suggested by Chisholm *et al.* (*104*).

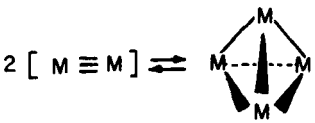

$Mo_2(O\text{-}i\text{Pr})_6$ reacts with Cl_2, Br_2, and I_2 in carbon tetrachloride solutions to yield tetrahalide products with the composition $Mo_2(O\text{-}i\text{Pr})_6X_4$, which are orange (X = Cl or Br) and brown (X = I) crystalline solids. X-Ray studies of the chloro and bromo compounds show that both of these contain contral $Mo_2O_6X_4$ units that have virtual D_{2h} symmetry (*111a*).

A black, air-sensitive hydrocarbon-soluble solid of empirical composition $MoF(O\text{-}t\text{Bu})_2$ is obtained (*111*) by the addition of PF_3 (2 equivalents) to a hydrocarbon solution of $(t\text{BuO})_3Mo{\equiv}Mo(O\text{-}t\text{Bu})_3$.

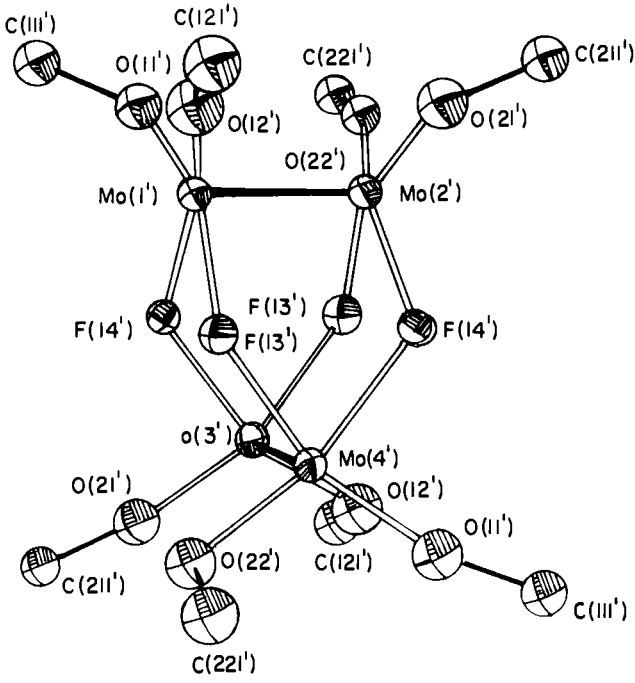

FIG. 8. Ortep view of the central $Mo_4(\mu\text{-}F)_4(OC)_8$ skeleton of the $Mo_4(\mu\text{-}F)_4(O\text{-}t\text{Bu})_8$ molecule.

The product is tetrameric with the structure $Mo_4(\mu\text{-}F)_4(O\text{-}t\text{Bu})_8$, which is shown in Fig. 8.

An interesting derivative with the suggested formulation $(t\text{BuO})_2(\text{Et})\text{Mo}{\equiv}\text{Mo}(O\text{-}t\text{Bu})_3$ has been synthesized (*112*) by the reaction of $Mo_2Et_2(NMe_2)_4$ [obtained (*113*) by the reaction of $Mo_2Cl_2(NMe_2)_4$ with LiEt] with *t*-butanol in benzene at room temperature:

$$Mo_2Et_2(NMe_2)_4 + \underset{\text{(excess)}}{4t\text{-BuOH}} \rightarrow \underset{\text{burgundy-red solid}}{Mo_2Et(O\text{-}t\text{Bu})_5} + 4NHMe_2 + C_2H_6$$

The alkylation of $Mo_2(O\text{-}i\text{Pr})_6$ with $LiCH_2SiMe_3$ in pentane results (*113a*) in a high (75%) yield of $Mo_2(CH_2SiMe_3)_6$. The corresponding reactions of $Mo_2(O\text{-}i\text{Pr})_8$ gives an almost equimolar mixture of $Mo_2(CH_2SiMe_3)_6$. The corresponding reaction of $Mo_2(O\text{-}i\text{Pr})_8$ gives an almost equimolar mixture of $Mo_2(CH_2SiMe_3)_6$ and $Mo(CH_2SiMe_3)_3(=CSiMe_3)$.

b. Alkoxides of Molybdenum(IV). A series of molybdenum(IV) alkoxides have been prepared (*114*) by the reaction

$$Mo(NMe_2)_4 + 4ROH \rightarrow M(OR)_4 + 4NHMe_2$$

R = Me, Et, *i*Pr, *t*Bu and CH_2CMe_3

The corresponding reactions involving trialkylsilanols R_3SiOH (R = Me and Et) yield an amine adduct:

$$Mo(NMe_2)_4 + 4R_3SiOH \rightarrow Mo(OSiR_3)_4 \cdot (HNMe_2)_2 + 2NMe_2H$$

The properties of the alkoxides depend upon the steric requirements of the alkoxy group, as illustrated by a few properties of these derivatives, which are given in Table IV.

Of all the derivatives given in Table IV, only $[Mo(O\text{-}iPr)_4]_2$ is diamagnetic. It is a fluxional molecule on the NMR time scale, and the low-temperature-limiting (^1H and ^{13}C)-NMR spectra correspond to a structure of the type $(iPrO)_3Mo(\mu\text{-}O\text{-}iPr)_2 \cdot Mo(O\text{-}iPr)_3$. X-Ray crystallography (*115*) has shown (Fig. 9) that the molecule has a rigorous crystallographic center of inversion and approximately C_{2h} symmetry, with the configuration of oxygen atoms around each molybdenum a slightly distorted trigonal bipyramid. The observed Mo—Mo distance of 2.523(1) Å could be explained on the basis of a double metal–metal bond or coupling of one pair of electrons through the bridge system.

The Mo—Mo distance in the oxide alkoxide derivative, $Mo_3(\mu_3\text{-}O)(\mu_3\text{-}OR)(\mu_2\text{-}OR)_3(OR)_6$ (R = $H_2C \cdot CMe_3$ or $HCMe_2$) has been shown (*115a*) to be 2.535 Å, which is comparable with Mo—Mo distance (2.524 Å) in $Zn_2Mo_3O_8$.

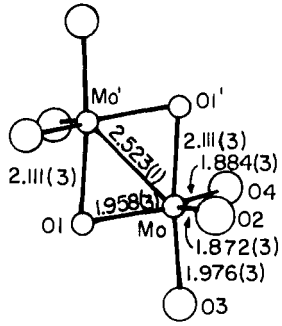

FIG. 9. Skeleton of the structure of $Mo_2(O\text{-}iPr)_8$, showing relevant internuclear distances and bond angles.

TABLE IV

CHARACTERIZATION DATA FOR ALKOXIDES AND TRIALKYLSILOXIDES OF MOLYBDENUM(IV)

Compound[a]	Color	Volatility[b] (°C, 10^{-4} torr)	UV–vis λ_{max}, [nm(ε)][c]	μ_{eff}[d] (BM) T = 313 K	Mol wt[e] (calc)	Mass-spectrum parent peak (m/e)
$Mo(O\text{-}tBu)_4$	Green–brown	70–75	600(40)	1.38	450 ± 20 (388)	388
$Mo(O\text{-}iPr)_4$	Blue	70–90	640(700)	Diamagnetic	600 ± 30 (332.28)	664
$Mo(OCH_2CMe_3)_4$	Blue-green	150–170	640(320)	0.70	740 ± 30 (444)	888
$Mo(OEt)_4$	Dark green	70–90	700(340)	0.31	860 ± 30 (276)	828
$Mo(OSiMe_3)_4 \cdot 2HNMe_2$	Yellow	100–120	955(2.0) 915(2.0) 390(35)	2.63	551 ± 20 (542)	542
$Mo(OSiEt_3)_4 \cdot 2HNMe_2$	Orange–brown	76 (dec.)	1185(10) 1150(10) 885(20) 730(30) 480(40)	2.20	(711.2)	620

[a] $Mo(OMe)_4$ is purple, nonvolatile, and insoluble in hydrocarbon solvents.
[b] May be sublimed readily at these temperatures.
[c] In cyclohexane.
[d] Determined in toluene by the Evans method.
[e] Determined cryoscopically in benzene.

The reactions of $Mo_2(O\text{-}tBu)_6$ (*115b*) and $Mo_2(O\text{-}iPr)_6$ (*115c*) with molecular oxygen yield derivatives with the formulas $MoO_2(OR)_6$. Only in the latter case could an intermediate product with the composition $Mo_6O_{10}(O\text{-}iPr)_{12}$ be isolated, and it has been shown to contain a serpentine chain of molybdenum atoms with both six- and five-coordinated molybdenums. The average oxidation state for molybdenum is 5.33, which leaves four electrons free for metal–metal bonding. These are apparently used to form two localized single Mo—Mo bonds with length 2.585 Å. An interesting feature not observed previously in metal-alkoxide structures is the presence of "semibridging" OR groups with an M · · · O distance of 2.88 Å, which is too long for a regular bridging bond but much too short to be viewed as nonbonding.

c. Alkoxides of Tungsten(III and IV). The reactions of $W_2(NMe_2)_6$ with alcohols lead to the formation of tungsten alkoxides (*101, 116*). The nature of the products, however, appears to be much more dependent, compared to those in the corresponding reactions of $Mo_2(NMe_2)_6$ (*103–105*), on the nature of the alcohol.

The reactions of $W_2(NMe_2)_6$ with *t*BuOH and Me_3SiOH yield (*116*) the crystalline compounds $W_2(O\text{-}tBu)_6$ and $W_2(OSiMe_3)_6(NHMe_2)_2$, re-

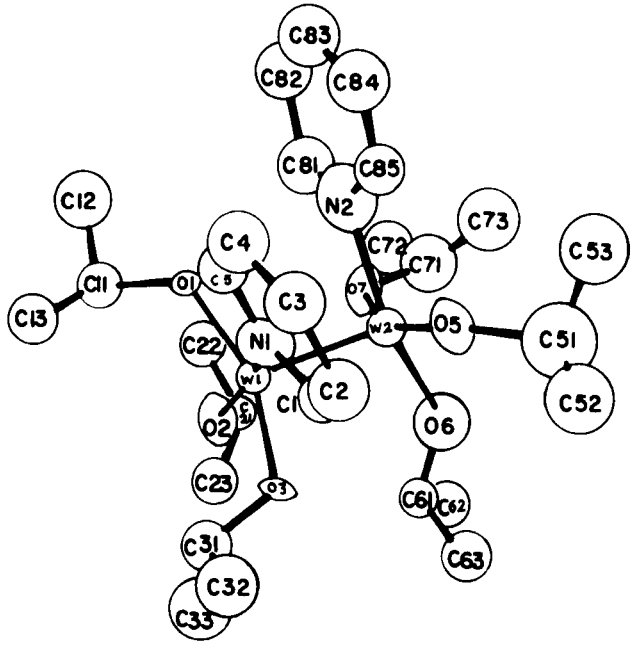

FIG. 10. Structure of the $W_2(O\text{-}iPr)_6 \cdot (py)_2$ molecule.

spectively. These tungsten compounds, unlike their molybdenum analogs, cannot be sublimed *in vacuo;* they are thermally unstable and the mode of their thermal decomposition *in vacuo* appears to be autocatalytic and not stoichiometric.

The reaction between $W_2(NMe_2)_6$ and the less bulky alcohols *i*PrOH and Me_3CCH_2OH leads to polynuclear products instead of the binuclear products $(RO)_3Mo{\equiv}Mo(OR)_3$ obtained in the corresponding reactions of $Mo_2(NMe_2)_6$. When the reaction of $W_2(NMe_2)_6$ with isopropanol is carried out in pyridine solution, a black, crystalline product, $W_2(O\text{-}iPr)_6(py)_2$, is obtained that has (Fig. 10) two $W(O\text{-}iPr)_3 \cdot py$ units linked by a $W{\equiv}W$ bond with a length of 2.332(1) Å. Low-temperature ^{13}C-NMR spectra support the conclusion that this structure is present in solution also.

A detailed study of the reaction of $W_2(NMe_2)_6$ with excess isopropanol has revealed a much more fascinating (*117, 118*) story, involving oxidation of tungsten from the +3 to the +4 state and the final formation of an interesting derivative $W_4(\mu\text{-}H)_2(O\text{-}iPr)_{14}$. Although the mechanism of the reaction has not been fully investigated, the initial step appears to be a normal alcoholysis reaction, common to all metal dimethylamides, leading to the formation of $W_2(O\text{-}iPr)_6$, which undergoes an oxidative addition of H and *i*PrO across the tungsten–tungsten triple bond to give a solvated $W_2(\mu\text{-}H)(O\text{-}iPr)_7$ species. Solvation again probably involves coordination of excess isopropanol, and evidence has been adduced that $W_4(\mu\text{-}H)_2(O\text{-}iPr)_{14}$ forms dinuclear fragments in the presence of donor molecules such as pyridine, dioxane, and isopropanol.

The compound $[W_2(\mu\text{-}H)(O\text{-}iPr)_7]_2$ has been investigated by IR, NMR, and mass spectroscopy and by a single-crystal X-ray study (see Fig. 11).

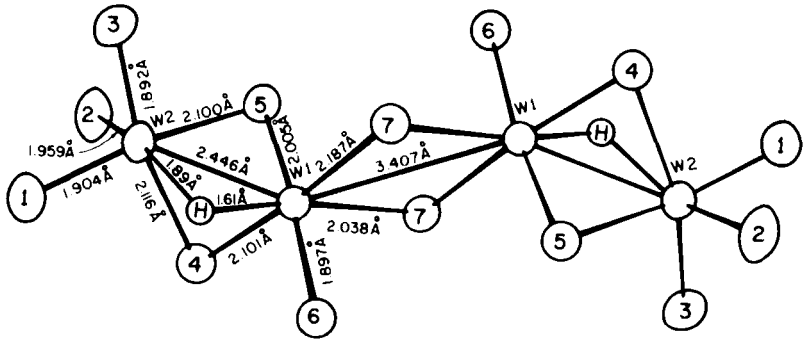

FIG. 11. A view of the $W_4(\mu\text{-}H)_2O_{14}$ skeleton, showing the bridging hydrogen atoms and emphasizing the essentially octahedral coordination of each tungsten atom.

Finally, the reactions of $W_2(NMe_2)_6$ with methanol and ethanol ($\geqslant$6 equivalents) in hydrocarbon solvents at ambient temperatures yield (*119*) dark green or brown crystals of empirical formula $W(OR)_4$. These compounds are diamagnetic, air sensitive, and hydrocarbon soluble. The structure of $[W(OEt)_4]_4$ as represented in Fig. 12 has a striking resemblance to that reported for $[Ti(OEt)_4]_4$, with the change that the presence of d^2 tungsten atoms brings them closer to each other than the d^0 titanium atoms in Fig. 12; Ti—Ti distances are shown (in parentheses) with W—W distances.

Cotton and Fang (*119a*) have carried out a calculation depicting that the lengthening of the two W—W bonds in the eight-electron cluster $W_4(OEt)_{16}$ results from a second-order Jahn–Teller distortion, caused by removal of two electrons from the C_{2h} rhombohedral M_4 geometry, thus accommodating ten cluster electrons in effectively five M—M bonds.

d. Adduct Formation and Other Reactions of $Mo_2(OR)_6$ and $W_2(OR)_6$. Red or purple crystalline adducts $Mo_2(OR)_6 \cdot 2NHMe_2$ have been isolated (*104*) by treating $Mo_2(OR)_6$ (R = Me_3Si and Me_3CCH_2) with dimethylamine, and it has been shown that in hydrocarbon solvents the following equilibrium lies well to the right when L = NH_3, $MeNH_2$, Me_2NH, Me_3N, or Me_2PhP.

$$Mo_2(OR)_6 + 2L \rightleftharpoons Mo_2(OR)_6L_2$$

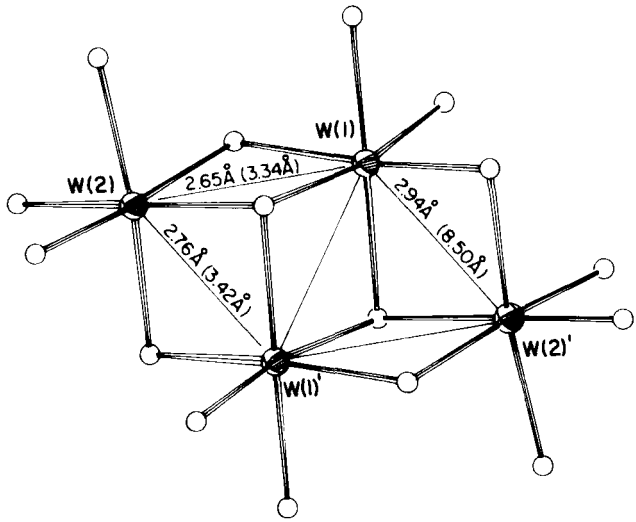

FIG. 12. Ortep view of the central W_4O_{16} unit of the $W_4(OEt)_{16}$ molecule.

In view of the fact that the related dialkylamides (*105*) and alkyls (*106*) Mo_2L_6 (L = NR_2, R) do not show this type of affinity for Lewis bases like ammonia, it was conjectured (*105*) that the exceptional behavior of some $Mo_2(OR)_6$ compounds could be due to the preferential ability of these alkoxy groups to form derivatives with alkoxy bridges, endowing the adduct with a structure of the type $L(RO)_2Mo(\mu\text{-}OR)_2Mo(OR)_2L$. However, determination (*120*) of crystal structure by X rays showed that the molecule $Mo_2(OSiMe_3)_6 \cdot 2NHMe_2$ has a nonbridged structure, $(Me_3SiO)_3(Me_2NH)Mo{\equiv}Mo(Me_2NH)(OSiMe_3)_3$, with an Mo≡Mo distance of 2.242(1) Å, a mean Mo—O distance (average of six) of 1.95 ± 0.02 Å, and a mean Mo—N distance (average of two) of 2.282 ± 0.004 Å (Fig. 13). The rotational conformation is intermediate between eclipsed and staggered, but closer to the latter. This structure, therefore, provides the first proven example of a molecule having two four-coordinated metal atoms triply bonded to each other, without any bridging groups (see Fig. 13).

In contrast to the adduct $Mo_2(OSiMe_3)_6 \cdot 2NMe_2H$, in which the original Mo≡Mo bond is retained and there is no bridging ligand, the reaction of a solution of $Mo_2(O\text{-}t\text{Bu})_6$ in hydrocarbon with CO at room temperature and 1-atm pressure appears to give an intermediate monocarbonyl adduct $Mo_2(O\text{-}t\text{Bu})_6(\mu CO)$, in which the CO ligand bridges a Mo=Mo double bond. The overall reaction can be represented as (*121*)

$$2Mo_2(O\text{-}t\text{Bu})_6 + 6CO \rightleftharpoons Mo(CO)_6 + 3Mo(O\text{-}t\text{Bu})_4 \quad . \quad . \quad . \qquad (1)$$

As mentioned previously, the reaction proceeds via slow and reversible formation of a bridged adduct, $Mo_2(O\text{-}t\text{Bu})_6(CO)$. Dark purple crystals of the compound could be isolated by exposing near-saturated alkane

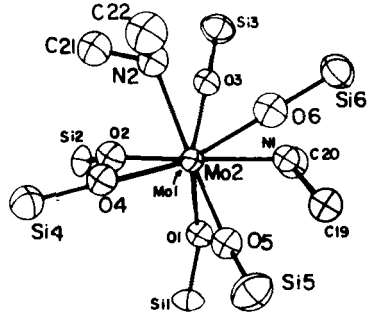

FIG. 13. Ortep view of the $Mo_2(OSi)_6(NC_2)_2$ portion of $Mo_2(OSiMe_3)_6(NHMe_2)_2$, looking directly down the Mo—Mo bond with Mo(1) eclipsed by Mo(2).

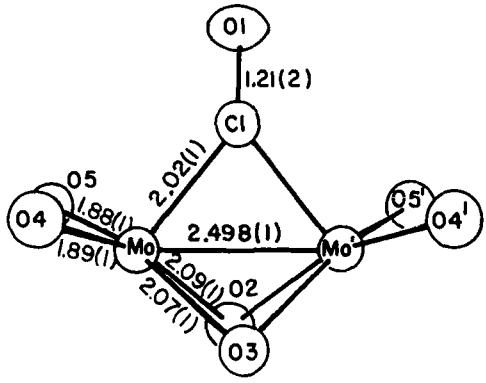

FIG. 14. A view of the $Mo_2O_6(CO)$ skeleton of the $Mo_2(O\text{-}t\text{Bu})_6(CO)$ molecule, with relevant internuclear distances.

solutions of $Mo_2(O\text{-}t\text{Bu})_6$ to two equivalents of CO at room temperature and then cooling the solution to about $-15°C$. $Mo_2(O\text{-}t\text{Bu})_6(CO)$ is thermally unstable, liberating CO and forming $Mo_2(O\text{-}t\text{Bu})_6$ when heated under vacuum:

$$Mo_2(O\text{-}t\text{Bu})_6 + CO \rightleftharpoons Mo_2(O\text{-}t\text{Bu})_6(CO) \quad . \quad . \quad . \qquad (2)$$

The structure of this interesting compound, as revealed by X-ray studies, is illustrated in Fig. 14.

TABLE V

PERTINENT STRUCTURAL DATA FOR THE $Mo(O\text{-}t\text{Bu})_2(CO)_2(py)_2$ MOLECULE[a]

Molecule	Bond distance (Å)	Molecule	Bond distance (Å)
Mo—C(1)	1.94	Mo—O(3)	1.94
Mo—C(2)	1.95	Mo—O(4)	1.95
C(1)—O(1)	1.16	Mo—N(1)	2.34
C(2)—O(2)	1.17	Mo—N(2)	2.36
Molecule	**Angle (deg)**	**Molecule**	**Angle (deg)**
C(1)—Mo—C(20	72	O(3)—Mo—O(4)	156
N(1)—Mo—N(2)	85	C(3)—O(3)—Mo	140
C(1)—Mo—N(1)	101	C(4)—O(4)—Mo	141
C(2)—Mo—N(2)	102	Mo—C(1)—O(1)	173
		Mo—C(2)—O(2)	174

[a] All distances and angles quoted are significant to ±1 in the last digit quoted.

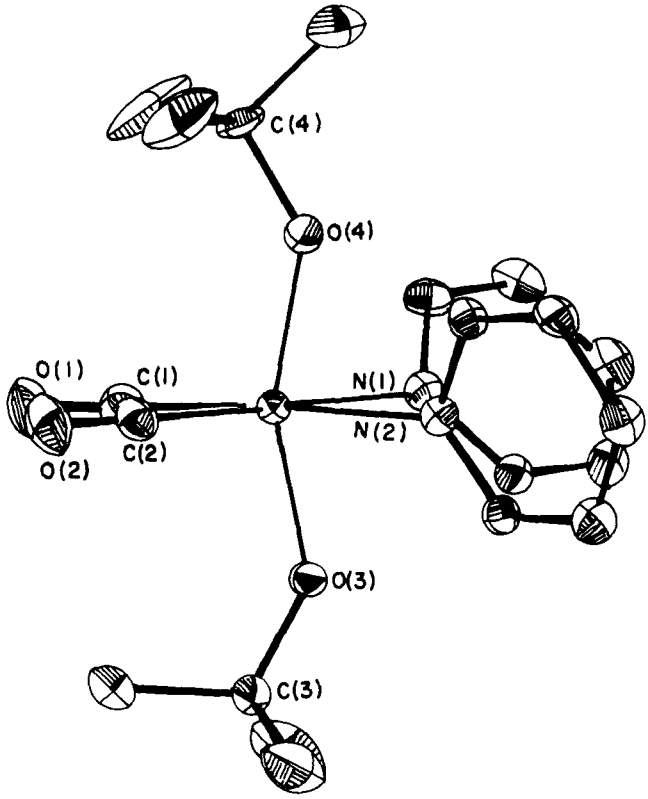

FIG. 15. Ortep view of the $Mo(O\text{-}tBu)_2(CO)_2(py)_2$ molecule, showing the atomic numbering scheme used in Table V.

In an attempt to trap alkoxide–carbonyl compounds of molybdenum in a reduced oxidation state in reaction (1), mild carbonylation (room temperature and 1-atm pressure of CO) of $Mo_2(O\text{-}tBu)_6$ was carried out (*122*) in a hexane–pyridine solvent mixture. The structure of a green, air-sensitive crystalline compound with the composition $Mo(O\text{-}tBu)_2(py)_2(CO)_2$ is represented in Fig. 15 (see also Table V).

Although analogous carboxylation of $(iPrO)_3M{\equiv}M(O\text{-}iPr)_3$ also yields $Mo(CO)_6$, the reaction probably follows a different stoichiometry from that indicated by reaction (1), because molybdenum(IV) isopropoxide $[Mo_2(O\text{-}iPr)_8]$ is binuclear, with a Mo=Mo double bond (*114*), and itself reacts with CO to give a black crystalline substance of empirical formula $Mo(O\text{-}iPr)_3CO$. The derivative is unstable in solution, slowly reacting to form $Mo(CO)_6$; in the presence of added CO this

reaction is fast. Although X-ray structural determination has not been possible so far, the molecule appears to be tetrameric.

In view of the known catalytic activity of molybdenum oxide compounds, the reactions of molybdenum alkoxides were studied with alkynes (*123*). $Mo_2(O\text{-}i\text{Pr})_6$ in hydrocarbon solutions reacts rapidly with alkynes RC_2R' (R = R′ = H; R = Me, R′ = H, R = R′ = Me) at room temperature, but products could not be identified with certainty. However, in the presence of added pyridine (>2 equivalents), crystalline solids with the composition $Mo_2(O\text{-}i\text{Pr})_6(py)_2(RC_2R')$ were isolated from a hexane solution. The crystal and molecular structures of the ethyne adduct are shown in Fig. 16.

The acetylene bridges the two molybdenum atoms in a crosswise manner. The C—C distance, 1.368(6) Å, is longer than in ethylene [1.337(3) Å] and is, in fact, among the longest known for $M_2(\mu\text{-}C_2R_2)$ compounds. The Mo—C distances are, however, short [2.09 Å (average)]. These values may be compared with C—C = 1.337(5) Å and Mo—C = 2.18 Å (average) associated with the $Mo_2(\mu\text{-}C_2H_2)$ unit in $Cp_2Mo_2(CO)_4(C_2H_2)$ (*124*). The compound $Mo_2(OCH_2CMe_3)_6(HNMe_2)_2$ reacts in hydrocarbon solvents with HC≡≡CH (1 equivalent) to give a similar derivative, $Mo_2(OCH_2CMe_3)_6(HNMe_2)_2(C_2H_2)$.

Hydrocarbon solutions of $Mo_2(OR)_6$ compounds (R = *i*Pr, *t*Bu) react with dimethylcyanamide, Me_2NCN, to give intensely purple solutions

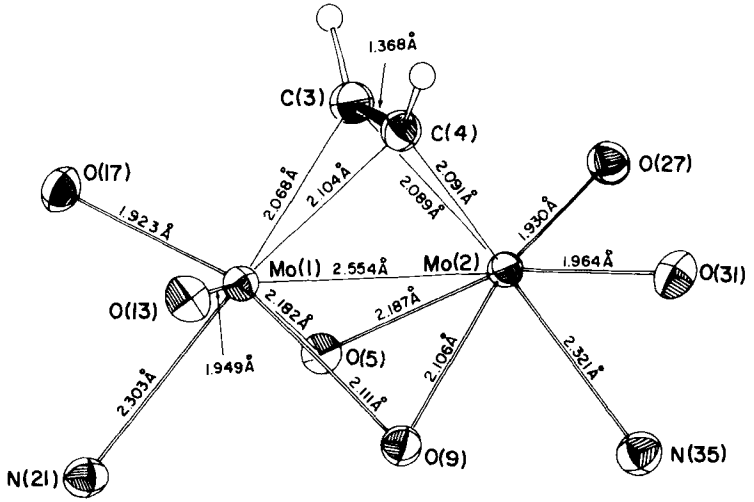

FIG. 16. Ortep view of the central skeleton of the $Mo_2(O\text{-}i\text{Pr})_6(py)_2(C_2H_2)$ molecule, showing the relevant internuclear distances.

from which dark, air- and moisture-sensitive crystals corresponding in analysis to $Mo_2(OR)_6 \cdot NCNMe_2$ are obtained (*125*). Formation of these adducts is reversible, and the Me_2NCN ligand is readily lost when these compounds are heated *in vacuo;* only $Mo_2(OR)_6$ compounds sublime. On the basis of IR and ^{1}H-NMR studies, it has been proposed that the ligand Me_2NCN acts as a four-electron donor and spans the Mo—Mo bond in a manner similar to that reported in the $Cp_2Mo_2(CO)_4 \cdot NCNMe_2$ derivative (*126*). The cyanamide ligand can be considered to form an N σ bond to one molybdenum atom and a CN π bond to the other. It has been further suggested that in the ground state (solid structure) the alkoxy groups are not eclipsed but adopt a partially staggered configuration similar to that in $Mo_2(OSiMe_3)_6 \cdot 2NHMe_2$ (*120*). The ground-state structure would, therefore, consist of two enantiomers, which are schematically represented in Fig. 17.

The reactions of $Mo_2(OR)_6$ compounds (R = *i*Pr, *t*Bu, and CH_2CMe_3) with nitric oxide yield (*55*) a novel type of yellow crystalline nitrosyl complex with the empirical formula $Mo(OR)_3NO$. These derivatives show NO stretching frequencies at approximately 1640 cm^{-1}, and they are diamagnetic, dimeric, and fluxional in solution. The compound $[Mo(O\text{-}iPr)_3NO]_2$ crystallizes in space group $P\bar{1}$ with $Z = 2$ and unit-cell dimensions $a = 10.828(1)$, $b = 15.848(2)$, $c = 9.885(2)$ Å, $\alpha = 90.21(2)$, $\beta = 115.93(2)$, $\gamma = 82.42(1)°$, and $V = 1509.4(5)$ Å^3. There are two crystallographically independent molecules, one centered on the origin, the other at $\frac{1}{2}$, $\frac{1}{2}$, $\frac{1}{2}$, that are essentially identical in structure. Each molybdenum atom is five-coordinated in a trigonal bipyramidal

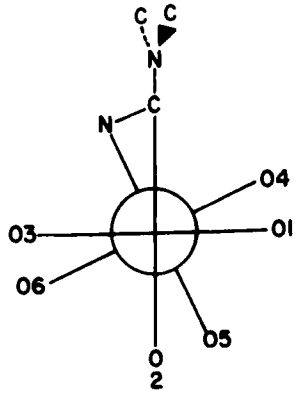

FIG. 17. Schematic representation of the proposed ground-state structure of the $Mo_2(O\text{-}iPr)_6 \cdot NCNMe_2$ molecule, viewed down the Mo—Mo bond.

manner and attains only a 14-valence-shell electron configuration. The nitrosyl ligands occupy terminal axial positions, and the two bridging O-*i*Pr groups form short bonds in equatorial positions and long bonds in axial positions that are trans to the NO ligands. The Mo—N—O units are essentially linear (178°), and the bond lengths therein are 1.754(7) Å for Mo—N and 1.19(1) Å for N—O. The Mo · · · Mo separation of 3.335(2) Å precludes metal-to-metal bonding; the Mo≡Mo bonds of $Mo_2(OR)_6$ derivatives are thus cleaved by the addition of two NO ligands. The electronic structure in these new nitrosyl metal complexes can be formulated so that the highest filled MO is the e level responsible for Mo to NO π bonding; it is made up of metal d_{xz}, d_{yz}, and NO π^* orbitals. It would be interesting, in view of this, to investigate the possibility of the existence of other similar $MX_3(NO)L$ molecules.

An adduct of the type just discussed of tungsten(III) with composition $W(O\text{-}t\text{Bu})_3(NO)(C_5H_5N)$ has been isolated (*127*) by the direct reaction between $W_2(O\text{-}t\text{Bu})_6$ and NO (2 equivalents) in pyridine as solvent. The compound exists in a slightly distorted trigonal bipyramidal structure (Fig. 18), with the axial positions occupied by nitrosyl and pyridine ligands. The tungsten atom is displaced 0.34 Å toward the nitrosyl ligand from the equatorial plane of the three alkoxy oxygen atoms. The nitrosyl ligand is coordinated linearly, and the W—N(1) bond is quite short [1.732(8) Å], which is indicative of some multiple-

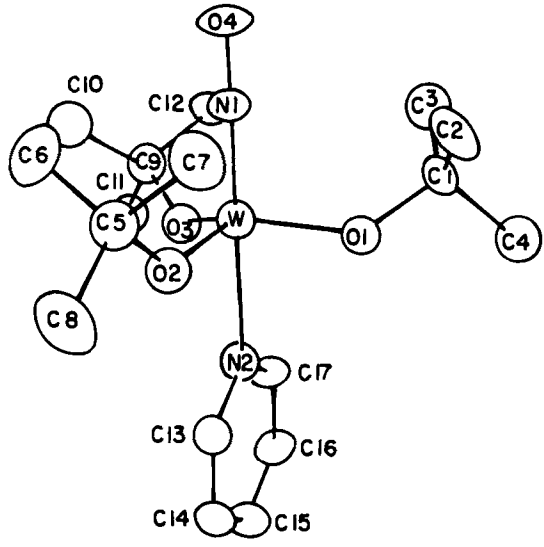

FIG. 18. Ortep view of the $W(O\text{-}t\text{Bu})_3(NO)(C_5H_5N)$ molecule.

bond character, whereas the tungsten–pyridine bond is considerably longer, W—N(2) = 2.323(7) Å. The W—O distances are in the expected range, that is, 1.876–1.898 Å.

Pyridine as well as similar adducts with other donor ligands (NH_3 and NMe_3) have also been isolated as soluble products by the addition of the ligands to the insoluble products, $W(O\text{-}tBu)_3NO$, obtained by the reaction between $W_2(O\text{-}tBu)_6$ and nitric oxide (2 equivalents) in hydrocarbon solvents.

$Mo_2(OR)_6$ compounds (R = Me_3Si, iPr, tBu, and Me_3CCH_2) react (*128*) readily and reversibly both in solution and in the solid state with CO_2 (>2 equivalents) to give insertion products according to the equation

$$Mo_2(OR)_6 + 2CO_2 \rightleftharpoons Mo_2(OR)_4(O_2COR)_2$$

The products are moisture- and oxygen-sensitive cream-colored solids that are diamagnetic. These are quite stable in the solid state at room temperature, but decarboxylation and sublimation occur simultaneously at 90°C under 10^{-4} cm Hg, yielding $Mo_2(OR)_6$. The physicochemical properties suggested a structure of the type

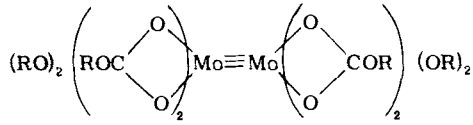

which has been confirmed by the structure shown in Fig. 19, revealed by X-ray crystallography. Using the SCF-X_α scattered-wave method, the ground-state electronic structures of $(HO)_3Mo{\equiv}Mo(OH)_3$ and related molecules (*129*) have been calculated. The $\pi(e_u)$ and $\sigma(a_{1g})$ orbitals, which have large amounts of metal character, have been identified as the orbitals primarily responsible for Mo—Mo bonding. Using the transition-state technique to allow for relaxation effects, the photoelectron spectra have been calculated for $Mo_2(OH)_6$ and have been (after applying a constant downshift to correct for inductive effects) found to compare very well for the experimental spectra exhibited by $Mo_2(OCH_2C(CH_3)_3]_6$.

D. Rhenium

With the exception of a volatile brown hexamethoxide (*99a*) and the triple-alkoxo-bridged carbonyl anions (*130*) $[(CO)_3Re(\mu\text{-}OR)_3Re$-

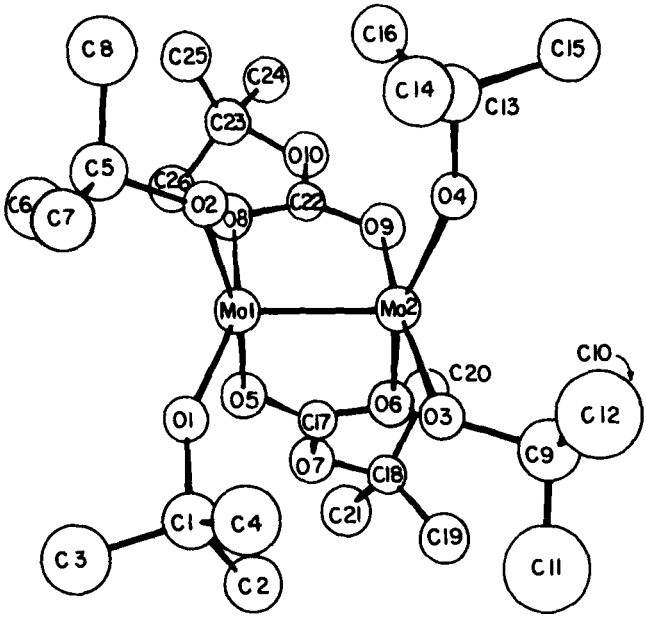

FIG. 19. Ortep drawing of the $Mo_2(O_2COCMe_3)_2(OCMe_3)_4$ molecule.

$(CO)_3]^-$ (R = Et, *i*Pr), other alkoxo species of rhenium have only one alkoxo group and contain either tertiary phosphine ligands (*131*), as in $ReO(OEt)Cl_2(PPh_3)_3$, or methyl and acetate groups in the insoluble $[ReMe(OMe)(O_2CMe)]_n$ (*132*).

Interaction (*133, 134*) of $ReOCl_4$ with methanol in the presence of amines gives the unusual alkoxo compound $(MeO)_2(O)Re(\mu\text{-}O)(\mu\text{-}OMe)_2ReO(OMe)_2$ (**I**), whereas LiO-*t*Bu gives $ReO(O\text{-}tBu)_4$ (**II**), and LiO-*i*Pr gives an unusual dimeric species, $Li[ReO(O\text{-}iPr)_5]LiCl(THF)_2$ (**III**). The interaction with phenol in the presence of trimethylphosphine leads to the compound *trans*-$(Me_3P)_2Re(OPh)_4$ (**IV**), whereas with lithium bis(trimethylsilylamide) a unique tetracoordinate rhenium(V) compound $ReO[N(SiMe_3)_3]_3$ is obtained.

The crystal structures of **I** (Fig. 20), **II**, and **IV** have been determined by X-ray crystallography. Compound **I** is monoclinic, space group $P2_{1/n}$, a = 12.142(1), b = 15.369(1), c = 7.311(1) Å, β = 90.22(1)°, and Z = 4. Compound **II** is triclinic, space group $P\bar{1}$, a = 14.602(5), b = 13.363(3), c = 9.244(6) Å, α = 98.39(4), β = 102.35(5), γ = 68.71(2)°, and Z = 1. Compound **IV** is monoclinic, space group $P2_{1/c}$, a = 10.079(2), b = 10.527(3), c = 14.443(3) Å, β = 97.28(2)°, and Z = 2.

The reaction of trimethylsilyl perrhenate, $Me_3SiOReO_3$, with excess

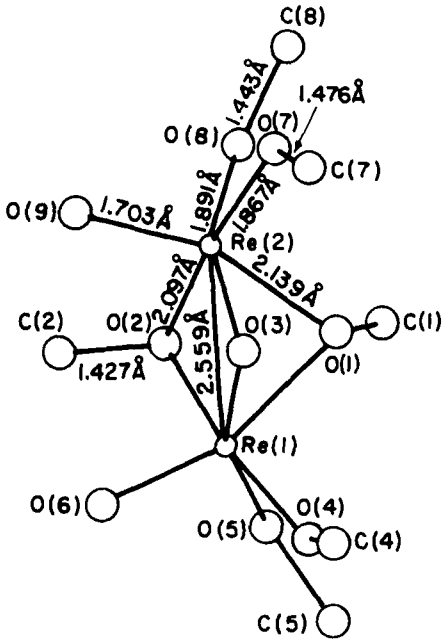

FIG. 20. Molecular structure of $Re_2O_3(OMe)_6$, showing typical internuclear distances.

butyltrimethylsilylamine in hexane gives (*135*) a yellow derivative, $Me_3SiORe(N\text{-}tBu)_3$ (mp 36–38°C):

$$Me_3SiOReO_3 + 3tBuNHSiMe_3 \rightarrow Me_3SiORe(N\text{-}tBu)_3 + 3Me_3SiOH$$

When an insufficient amount of $tBuNHSiMe_3$ is used in this reaction, a yellow, low-melting-point solid is obtained that corresponds in analysis to $Re_3(N\text{-}tBu)_4O_5(OSiMe_3)_2$, which has been characterized by X-ray crystal-structure study to have a configuration of the type

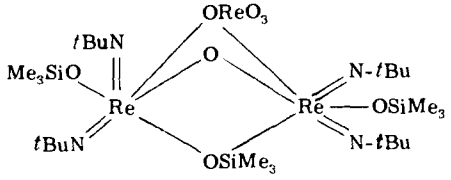

The trirhenium-cluster alkoxide $Re_3Cl_3(O\text{-}tBu)_6$ has also been synthesized (*136*).

E. Ruthenium and Rhodium

The interaction of dihydridotetrakis(triphenylphosphine)ruthenium(II) with phenol gives a neutral complex, $RuH(C_6H_5O)(PPh_3)_3$, which may also be obtained with an additional molecule of phenol hydrogen-bonded to the oxygen atom of the phenoxo ligand. The $C_6H_5O^-$ ligand can be considered to be bound as an η^6-phenoxo or, probably more realistically, as an η^5-oxacyclohexadienyl ligand. The π-bonded nature of the phenoxide ion is confirmed by IR, NMR, and X-ray structural data (*21*). A complex of the composition $Rh(OPh)(PPh_3)_3$ (*137*), obtained by the action of phenol on $RhMe(PPh_3)_3$ or $RhPh(PPh_3)_3$, has also been shown to be a π-phenoxo complex.

The crystal structure (Fig. 21) of $Rh(ArO\text{-}\eta^5)(PPh_3)_2$ (Ar = 2,6-tBu$_2$-4MeC_6H_2), obtained by the reaction of ArOH on $Rh[N(SiMe_3)_2](PPh_3)_2$ in toluene at 20°C has been shown (*138*) to involve π-bonded phenoxo ligands with (a) C(2)—C(6) in the same plane [average C—C = 1.38(2) Å], (b) C(1)—O = 1.28 Å, and (c) Rh—C(2) and Rh—C(6) bond lengths in the range 2.19–2.65 Å. The structure of the corresponding titanium complex, $Ti(\eta\text{-}C_5H_5)_2OAr$, by contrast, was depicted as the O-bonded phenoxo ligand.

F. Platinum and Palladium

Transition-metal d^8 complexes containing metal–oxygen bonds have been reported to play an important role as intermediates in synthetic reactions, particularly in some catalytic processes, for example, hydration of nitriles and oxidation of ethylene and alcohols. Until fairly recently, few nonionic hydroxo- or alkoxoplatinum(II) complexes were known. Complexes originally formulated as $Pt(GePh_3)(OR)(PEt_3)_2$ (R = H, Me, Et, *i*Pr) (*139*) are now known to be $Pt(Ph)[Ge(OR)Ph_2](PEt_3)_2$, following a single-crystal X-ray study (*140*) of the hydroxo derivative. Although some nonbridging hydroxo complexes of $5d^8$ and $6d^8$ metals such as Ru^0, Os^0, Rh^I, Ir^I, Pd^{II}, and Pt^{II} had been isolated, only two alkoxo complexes of these soft metals were known until 1976 (*141*); they are Pt(cyclohexenyl)$(Ph_2PCH_2CH_2PPh_2)$ (*142*) and $[Ir(NO)(OR)(PPh_3)_2]^+$ (R = Et or *n*-Pr) (*143*). A series of mononuclear methoxo complexes, *cis*- and *trans*-$[MR(OMe)(PPh_3)_2]$ (M = Pd or Pt; R = C_6H_5, $CH{=}CCl_2$, $CCl{=}CCl_2$), have been synthesized by metathesis of $MRCl(PPh_3)_2$ with NaOMe. The stability of the M—OR bond appears to be influenced markedly by the identity of the metal (Pt > Pd) and the nature of the trans ligand R. In contrast to mononuclear platinum and palladium complexes, the reaction of NiR-

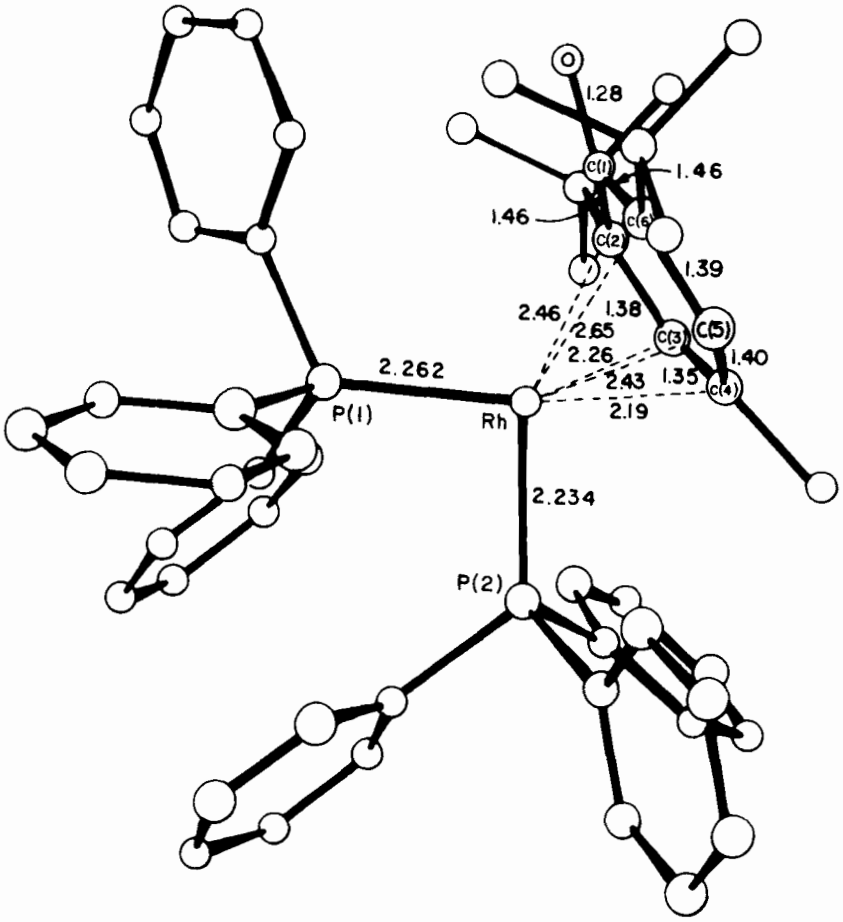

FIG. 21. Perspective view of the molecular structure of [Rh(OAr-η^5)(PPh_3)$_2$], showing selected bond lengths.

(Cl)(PPh_3)$_2$ (R = C_6F_5, CCl=CCl_2) with NaOMe gives red, crystalline μ-methoxo complexes, [NiR(μ-OMe)(PPh_3)]$_2$, with dissociation of 1 mol of PPh_3 (*144*).

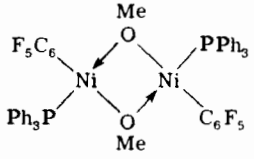

Cyclohexene–platinum(0) complexes can be prepared as shown here:

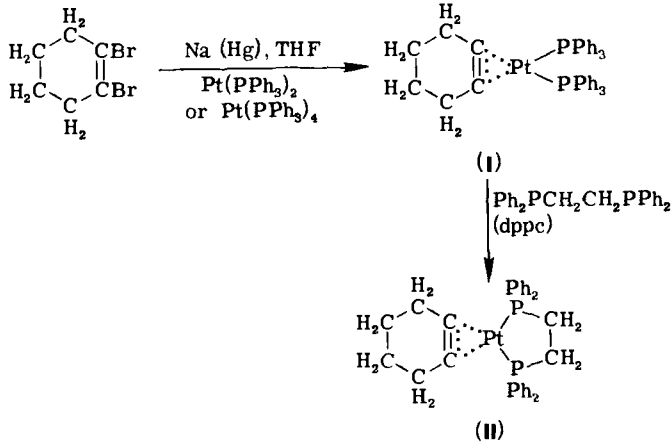

Compounds **I** and **II** are protonated by water and primary alcohols (*145*), yielding thermally stable crystals of σ-alkoxoplatinum(II) complexes, for example, $Pt(OCH_3)(C_6H_9)$(dppe). The complexes react readily with CO, bringing about insertion between platinum–oxygen bonds, yielding, for example, $Pt(CO_2CH_3)(C_6H_9)$(dppe).

The first moisture-stable mixed methoxy- and chlorobridged dinuclear platinum(II) (*145a*) palladium(II) (*145b*) complexes, $M_2(\mu\text{—Cl})=(\mu\text{—OMe})(t\text{-}Bu_2PCMe_2CH_2)_2$ (M = Pt, Pd), have been isolated by the reactions of the corresponding chloro-bridged dinuclear complexes, $M_2(\mu\text{—Cl})_2(t\text{-}Bu_2PCMe_2CH_2)_2$, suspended in methanol with an equimolar amount of NaOH at 40°C. The corresponding reaction of (COD)$PtCl_2$ (COD=1,5-cyclooctadiene) with 2 equivalents of NaOH in aqueous methanol has been reported (*145c*) to yield the methoxy-bridged dinuclear complex $[Pt(\mu\text{—}OCH_3)(C_8H_{12}OCH_3)]_2$. The methoxy bridges in this last complex are cleared by tertiary phosphines (L) to yield mononuclear methoxy complexes, $(C_8H_{12}OCH_3)Pt(OCH_3)L$.

In order to elucidate the factors governing the stability and nature of σ Pt—OR bonds,a series of square-planar complexes, *cis*- and *trans*-$Pt(OMe)(R)L_2$ (R = CH_2CN, CF_3, CH_2CF_3; L_2 = $2PPh_3$, diphosphene), have been prepared as colorless products in high yields by metathesis of $PtCl(R)L_2$ or $[Pt(R)L_2]BF_4$ with NaOMe, slightly above room temperatures in an anhydrous benzene–methanol mixture. The success in preparing these complexes seems to be related to the nature of the alkyl ligand R; a more electronegative R will increase the effective positive charge on the platinum, and consequently the electron density

on the OCH_3 group will decrease, increasing the covalency of the Pt—OCH_3 bond. These complexes can be converted to the corresponding hydroxo derivatives by hydrolysis with water. The platinum–oxygen bonds in these complexes undergo facile insertion of CO, COS, CS_2, and SO_2 (*146*).

IV. Alkoxides of Transition Metals with Sterically Hindered and Unsaturated Alcohols

Ever since the pronounced effects of the branching of alkyl groups on the properties of alkoxides of a number of metals, [e.g., titanium, zirconium (*147*), and aluminum (*148*)] were demonstrated (*13*), the preparation of sterically hindered alkoxides of metals has been attracting the attention of the investigators (see *56, 58, 149*).

In view of their sterically demanding and highly symmetrical nature, alkoxides of metals containing adamantyl groups could be expected to exhibit some unusual features. Bochmann *et al.* (*150*) have described the synthesis and properties of 1-adamantoxides, 2-adamantoxides, and 1-adamantylmethoxides of a number of transition metals

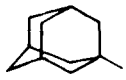

1-adamantyl

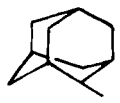

2-adamantyl

[i.e., Ti(IV), V(IV), Nb(IV and V), Cr(III and IV), Mo(IV), Mn(II), Fe(III), Co(II)] by the reaction

$$Ti(O\text{-}iPr)_4 + 4ROH \xrightarrow[\text{refluxing}]{\text{benzene}} Ti(OR)_4 + 4iPrOH$$

$$V(NEt_2)_4 + 4ROH \xrightarrow[\text{r. t., (12–18 h)}]{\text{diethyl ether}} V(OR)_4 + 4NHEt_2$$

$$Nb(NEt_2)_4 + 4(1\text{-ado})H \xrightarrow[\text{r. t.}]{\text{diethyl ether}} Nb(1\text{-ado})_4 + 4NHEt_2$$

$$Nb(NEt_2)_4 + (1\text{-ado})H \xrightarrow[\text{refluxing}]{\text{diethyl ether}} Nb(1\text{-ado})_5$$

$$Nb(NEt_2)_4 + (2\text{-ado})H \xrightarrow[\text{r. t.}]{\text{diethyl ether}} Nb(2\text{-ado})_5$$

$$Nb(NEt_2)_4 + 4(1\text{-admeo})H \rightarrow Nb(1\text{-admeo})_4 \cdot 0.5NEt_2H + 3.5NHEt_2$$

$$Cr(N\text{-}iPr_2)_3 + 3(1\text{-ado})H \xrightarrow[\text{r. t.}]{\text{diethyl ether}} Cr(1\text{-ado})_3 + 3NH\text{-}iPr_2$$

$$Cr[N(SiMe_3)_2]_3 + (1\text{-ado})H \xrightarrow{\text{boiling toluene}} \text{no reaction}$$

$$Cr(NEt_2)_4 + 4(1\text{-ado})H \xrightarrow[40\text{–}60^\circ C]{\text{pet. ether}} Cr(1\text{-ado})_4 + 4NHEt_2$$

$$Mo(NMe_2)_4 + 4(1\text{-ado})H \xrightarrow[\text{r. t.}]{\text{diethyl ether}} Mo(1\text{-ado})_4 \cdot (NHMe_2) + 3NHMe_2$$

$$\begin{matrix} Mn[N(SiMe_3)_2]_2 \\ \text{or} \\ 2(1\text{-admeo})H \end{matrix} + 2(1\text{-ado})H \xrightarrow[\text{diethyl ether}]{\text{light pet.}} \begin{matrix} Mn(1\text{-ado})_2 \\ \text{or} \\ Mn(1\text{-admeo})_2 \end{matrix} + 2NH(SiMe_3)_2$$

$$Fe[N(SiMe_3)_2]_3 + 3(1\text{-ado})H \xrightarrow[\text{refluxing}]{\text{benzene}} Fe(1\text{-ado})_3 + 3NH(SiMe_3)_2$$

$$\begin{matrix} Co[N(SiMe_3)_2]_2 \\ \text{or} \\ 2(1\text{-admeo})H \end{matrix} + 2(1\text{-ado})H \xrightarrow{\text{benzene}} \begin{matrix} Co(1\text{-ado})_2 \\ \text{or} \\ Co(1\text{-admeo})_2 \end{matrix} + 2NH(SiMe_3)_2$$

(1-ado)H = 1-adamantyl alcohol, (1-admeo)H = 1-adamantylmethanol; RO = (1-ado), (2-ado), or (1-admeo)

The alkoxides of tetra- and pentavalent metals are polymeric or monomeric crystalline solids, but those of di- and trivalent metals are polymeric materials. As expected, adamantylmethoxides show characteristics that are somewhat distinct from the adamantoxides; for example, $Ti(1\text{-ado})_4$ and $Ti(2\text{-ado})_4$ are white, crystalline solids with melting points above 350°C and are only moderately soluble in organic solvents, but $Ti(1\text{-admeo})_4$ has a lower melting point, is considerably more soluble in diethyl ether and benzene, and is much more sensitive to hydrolysis.

An X-ray crystallographic study of $Mo(1\text{-ado})_4(NHMe_2)$ confirms a trigonal bipyramidal structure of the complex, with the amine and one alkoxo group in the axial positions (see Fig. 22). The axial Mo—O distance [1.963(2) Å] is approximately 0.06 Å longer than the equatorial distances [1.888(3)–1.916(2) Å], and Mo—N bond length is 2.321(3) Å. The compound crystallizes in triclinic space group $P1$, with $a = 13.500(1)$, $b = 13.168(2)$, $c = 11.646(1)$ Å, $\alpha = 91.034(10)$, $\beta = 103.835(8)$, $\gamma = 70.842(10)^\circ$, and $Z = 2$. The structure in Fig. 22 has been solved by Patterson and Fourier methods and refined by least squares to $R = 0.041$, using 5267 observed diffractometer data.

It may not be out of place to mention here the syntheses (*151*) of per-

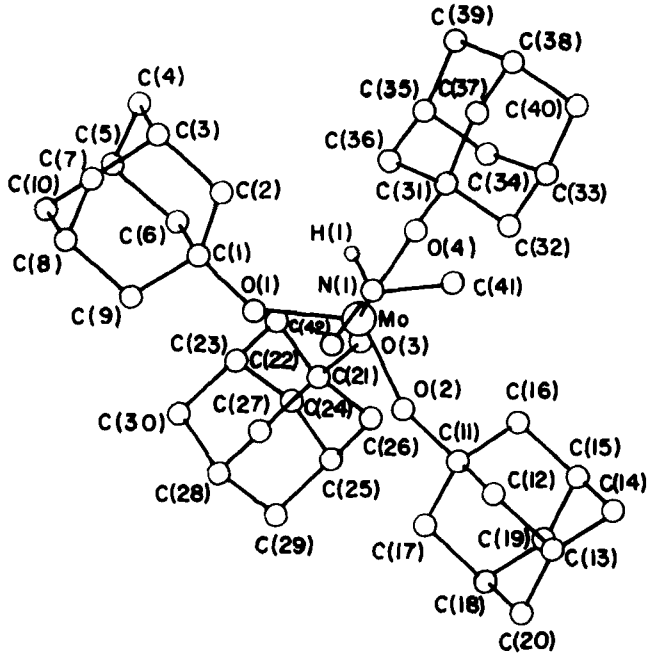

FIG. 22. Structure of $Mo(1\text{-ado})_4(NHMe_2)$, showing the atom-numbering system.

1-adamantylmethyls of Ti, V, Cr, Mn, and Zr by the reactions of $Ti(O\text{-}i\text{Pr})_4$, $V(O\text{-}i\text{Pr})_4$, $Cr(O\text{-}t\text{Bu})_4$, $MnBr_2$, and $ZrCl_4$ with Li(1-adamantylmethyl) in light petroleum or diethyl ether. The special stability of these peralkyls and their ease of formation can also be understood on the basis of the inertness of the adamantene cage toward structural rearrangements.

In a later publication (*152*) the synthesis and properties of bis(*t*-butyl)methoxides of chromium(III and IV), manganese(II), iron(III), cobalt(II), and copper(I) were described. Bis(*t*-butyl)methanol appears to be sterically even more demanding than 1- or 2-adamantanols; for example, it does not react even in boiling toluene with some first-row transition metal dialkylamides, notably the tris and tetrakis compounds $V(NEt_2)_4$, $Cr[N(SiMe_3)_2]_3$, or $Cr(NEt_2)_4$, although it does react with some bis derivatives, such as $Mn[N(SiMe_3)_2]_2$. The tris and tetrakis alkoxides have, therefore, been obtained from the metal halide and lithium bis(*t*-butyl)methoxide. Scheme 2 represents the reactions studied.

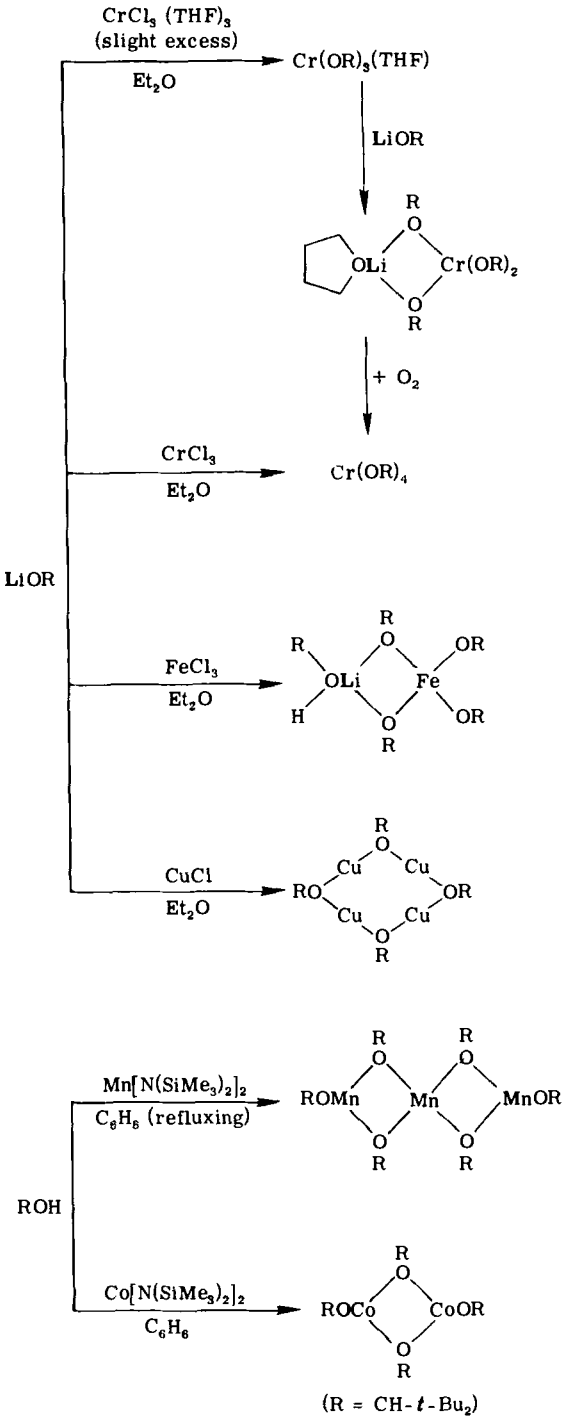

Royal-blue air-sensitive crystals. Soluble in organic solvents; monomeric. μ_{eff} = 3.2 BM. Dimeric in solid (broad band at 555 cm^{-1}).

Blue or intensely green crystals. Monomeric in benzene; readily oxidized by O_2 or CuCl to $Cr(OR)_4$.

Blue-green crystals stable in air. Absence of absorption in 450–700-cm^{-1} range indicates monomeric nature in solid state.

Air-sensitive yellow crystals; structure similar to $LiCr(OR)_4(THF)$.

Very air-sensitive pale yellow crystals. Decomposes slowly at r.t., particularly in light. More stable than $[CuOMe]_n$ and less stable than Cu(O-*t*Bu).

Pale pink crystals. Air sensitive. Readily soluble in nonpolar solvents; trimeric in benzene. Suggested 3-coordinated structure for terminal metal atoms similar to Mn dialkyls (*153*).

Air sensitive; deep blue; soluble in nonpolar solvents. Dimeric in benzene (cryoscopy). Electronic spectrum in diethyl ether suggests 4-coordinate Co because of coordination of solvent molecules.

SCHEME 2

Electron paramagnetic resonance and electron absorption spectral data of the derivatives in Scheme 2 are given in Table VI. Furthermore, the crystal and molecular structures of the complexes $LiCr(OCH\text{-}tBu_2)_4 \cdot THF$ (**I**), $Cr(OCH\text{-}tBu_2)_4$ (**II**), and $LiFe(OCH\text{-}tBu_2)_4 \cdot tBu_2CHOH$ (**III**) have been determined by X-ray crystallographic studies and are depicted in Figs. 23–25.

Compound **I** (Fig. 23) is triclinic, space group $P1$, with $a = 19.986(2)$, $b = 11.618(2)$, $c = 11.390(1)$ Å, $\alpha = 117.61(1)$, $\beta = 76.45(1)$, $\gamma = 93.11(1)°$, and $Z = 2$. Compound **II** (Fig. 24) is monoclinic, space group $C_{1/c}$, with $a = 20.249(3)$, $b = 10.748(1)$, $c = 20.275(2)$ Å, $\beta = 116.68(1)°$, and $Z = 4$. Compound **III** (Fig. 25) is monoclinic, space group $P2_{1/n}$, with $a = 18.308(3)$, $b = 22.505(4)$, $c = 11.979(5)$ Å, $\beta = 94.20(1)°$, and $Z = 4$. The structures were determined using data measured on an automatic diffractometer and were refined by least squares to R values of 0.068 (3396 observed data), 0.067 (2057 data), and 0.061 (4879 data) for **I**, **II**, and **III**, respectively. All structures contain a distorted, tetrahedrally coordinated chromium or iron atom; and in **I** and **III** the lithium ion is incorporated into the Mo_4 coordination sphere, bridging two of the four alkoxo oxygen atoms. The transition-metal geometries are discussed in terms of steric and electronic factors.

Among the new alkoxides of transition metals described are the alkenoxides (*154*) [namely, cinnamoxides (*155*), crotyloxides (*156*), methylbutenoxide (*157*), 3-pentene-2-oxides (*158*) and 4-pentene-2-oxides (*159*)], and β-methalloxides (*160*) of titanium, niobium, and tanta-

TABLE VI

ELECTRON PARAMAGNETIC RESONANCE AND ELECTRONIC ABSORPTION SPECTRA OF BIS(t-BUTYL)METHOXIDES

Compound	ESR	Electronic absorption[a] (λ, nm)
$Cr(OCH\text{-}tBu_2)_3 \cdot THF$	—	700
$LiCr(OCH\text{-}tBu_2)_4$	$g \approx 3.22$ $g \approx 2.0$[b]	690
$Cr(OCH\text{-}tBu_2)_4$		716, 567
$Mn(OCH\text{-}tBu_2)_2$	$g \approx 1.9585$[a]	Absorption rising to charge-transfer band at 300
$LiFe(OCH\text{-}tBu_2)_4 \cdot Bu_2CHOH$	$g_x = 4.067, 21.3$ $g_y = 6.93$ $g_z = 5.54, 1.65(3)$[b]	Absorption rising to charge-transfer band at 260
$Co(OCH\text{-}tBu_2)_2$	—	653, 597, 513, 434

[a] In light petroleum, 25°C.
[b] In light petroleum, −160°C.

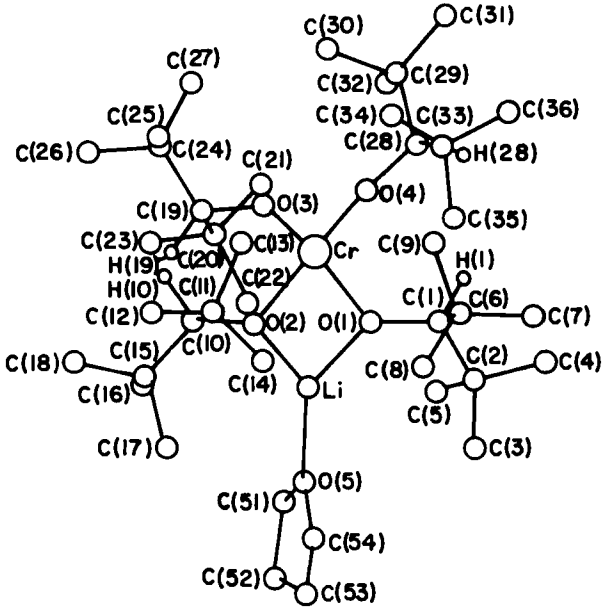

FIG. 23. Structure of $LiCr[OCH(CMe_3)_2]_4 \cdot C_4H_8O$, showing the atom-numbering system and omitting methyl hydrogens.

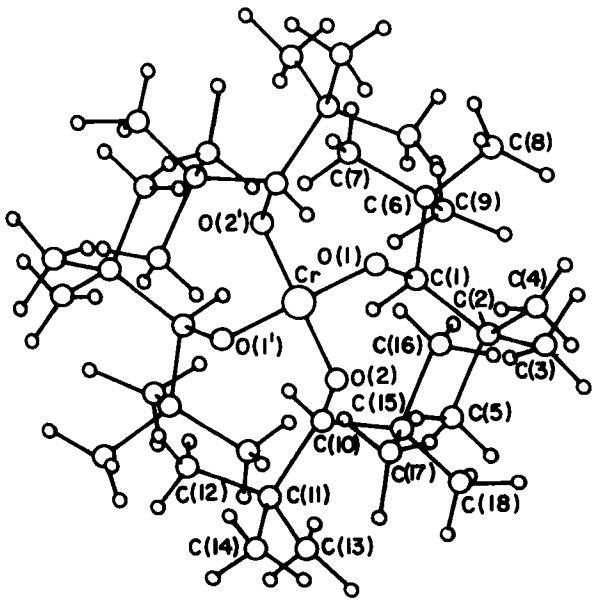

FIG. 24. Structure of $Cr[OCH(CMe_3)_2]_4$, showing the atom-numbering scheme in the asymmetric units. The smallest circles without numbers represent hydrogen atoms.

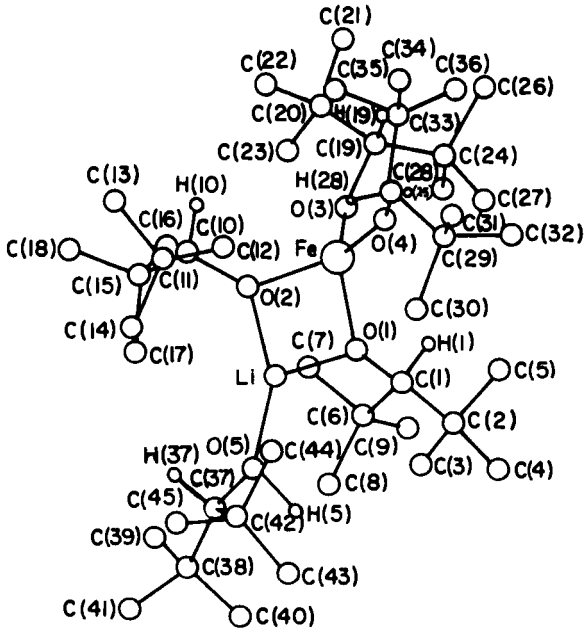

FIG. 25. Structure of $LIFe(OCH\text{-}tBu_2)_4 \cdot tBu_2CHOH$, showing the atom-numbering system and omitting methyl hydrogens.

lum. These alkoxides were generally prepared by the reaction of ethoxides or isopropoxides with the alkenols in benzene, removing the ethanol or isopropanol azeotropically with benzene.

V. Bimetallic Alkoxides of Transition Metals

A large number of bimetallic alkoxides incorporating atoms of two metals within the same molecule were synthesized during the late 1920s by Meerwein and Bersin (*161*), who considered these as "alkoxo salts" similar to hydroxo salts formed by the neutralization of alkali hydroxide with less basic (amphoteric) hydroxides of metals like beryllium, zinc, and aluminum. Isolation of stable volatile derivatives like $NaZr_2(OR)_9$ [not the $Na_2Zr(OR)_6$ expected for an alkoxo salt formulation] by Bartley and Wardlaw (*162*) gave a new orientation to the field. Detailed investigations by Mehrotra and co-workers (*163*), beginning in the late 1960s, particularly on tetraisopropoxyaluminates of a number of metals with the formulation (a) $M[Al(O\text{-}iPr)_4]_n$ (M = Li, Na, K, Rb, Cs, Be, Mg, Ca, Sr, Ba, Zn, Cd, Ga, In, Sc, lanthanides, Th, Sn,

etc.), (b) $(i\text{PrO})_2\text{M}[\text{Al}(\text{O-}i\text{Pr})_4]_2$ (M = Zr or Hf), and (c) $(i\text{PrO})_3\text{M}[\text{Al}(\text{O-}i\text{Pr})_4]_2$ (M = Nb or Ta), have shown that the formation of such bimetallic alkoxides could be more easily understood on the basis of a "coordination model" in which alkoxy ligands (OR) bridge atoms of different elements rather than atoms of the same element. The preparation and properties of interesting bimetallic derivatives with the structures

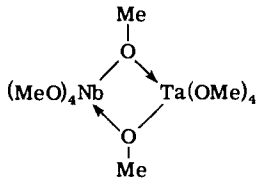

(92) and

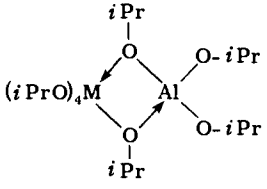

(163)

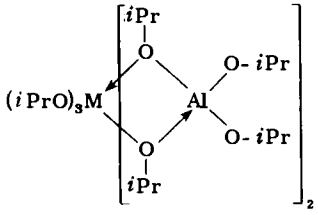

(M = Nb or Ta)

(163)

(where M = Nb or Ta) confirm this point of view. Because the literature on bimetallic (earlier termed "double") alkoxides up to 1975 has already been covered (*13, 17, 164, 165*), the following account deals mainly with advances made in these directions since then.

Bimetallic isopropoxides (*166*) and ethoxides (*167*) of niobium and tantalum with magnesium, calcium, strontium, and barium have been synthesized by the reactions of alkaline-earth metals with niobium and tantalum alkoxides in the respective alcohol (*92, 163*).

$$\text{M} + 2\text{M}'(\text{OR})_5 + 2\text{ROH} \xrightarrow[\text{HgCl}_2]{\text{ROH}} \text{M}[\text{M}'(\text{OR})_6]_2 + \text{H}_2\uparrow$$

(M = Mg, Ca, Sr, Ba; M′ = Nb, Ta, and R = Et or *i*Pr)

All of these bimetallic isopropoxides are colorless solids, and the corresponding ethoxides are viscous liquids, except the barium derivatives (which are foamy solids). Their identity as single entities and not mixtures of the component alkoxides is established by the simple ob-

servation that these bimetallic derivatives are volatile (vapor pressure ~1 mm in the temperature range 170–230°C) and soluble in organic solvents like benzene and parent alcohols, whereas the simple alkoxides of alkaline-earth metals are all nonvolatile and insoluble in organic solvents. Comparatively, the solubility of the bimetallic ethoxides is generally higher than that of the corresponding ethoxides. The volatility of these derivatives appears to indicate their covalent character, which is substantiated by their low molar conductances in organic solvents. Based on these observations and their monomeric nature in organic solvents, the following type of simple structure has been assigned to the derivatives

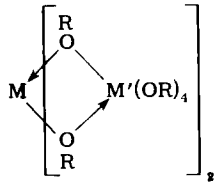

Reactions of bimetallic ethoxide with excess *n*- and *t*-butanol in benzene (with the help of which the ethanol liberated in the reactions was continuously azeotroped out) can be represented by

$$M[Nb(OEt)_6]_2 \xrightarrow{n\text{-BuOH}} M[Nb(O\text{-}nBu)_6]_2 + 12EtOH\uparrow$$
(I) (II)

$$M[Nb(OEt)_6]_2 \xrightarrow{t\text{BuOH}} M[Nb(OEt)_3(O\text{-}tBu)_3]_2 + 6EtOH\uparrow$$
(I) (III)

On the basis of PMR spectra, the following types of structures have been suggested for derivatives **I** and **III**.

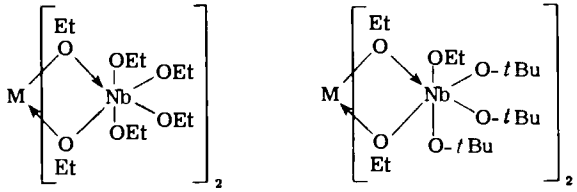

Bimetallic isopropoxides of alkaline-earth metals with hafnium were synthesized (*168*) by the reactions

$$M + 4Hf(O\text{-}iPr)_4 \cdot iPrOH \xrightarrow[\substack{HgCl_2\\(catalyst)}]{iPrOH} M[Hf_2(O\text{-}iPr)_9]_2 + H_2\uparrow$$

These products, like the zirconium analogs (*169, 170*), are white, crystalline solids that can be volatilized unchanged under reduced pressure. These are soluble in common organic solvents, in which their molecular weights correspond to their formula weights.

Following the earlier work (*13*) on similar derivatives of lighter alkali metals, apparently covalent (volatile and yielding nonconducting solutions in organic solvents) derivatives with the formulas $M[Al(O\text{-}iPr)_4]$, $M[Zr_2(O\text{-}iPr)_9]$, $M[Hf_2(O\text{-}iPr)_9]$, $M[Nb(O\text{-}iPr)_6]$, and $M[Ta(O\text{-}iPr)_6]$ (M = Rb or Cs) have been described (*171*).

Following a more detailed study (*172*) of volatile bimetallic isopropoxides of aluminum with alkaline-earth metals, bimetallic isopropoxides of chromium(III) and iron(III), $M[Al(O\text{-}iPr)_4]_3$ (M = Fe or Cr), and manganese(II), cobalt(II), nickel(II), and copper(II), $M[Al(O\text{-}iPr)_4]_2$ (M = Mn, Co, Ni, or Cu), have been synthesized (*173*) by the reactions

$$CrCl_3 \cdot 3THF + 3K[Al(O\text{-}iPr)_4] \rightarrow Cr[Al(O\text{-}iPr)_4]_3 + 3KCl\downarrow + 3THF$$

$$FeCl_3 + 3K[Al(O\text{-}iPr)_4] \rightarrow Fe[Al(O\text{-}iPr)_4]_3 + 3KCl\downarrow$$

$$MCl_2 + 2K[Al(O\text{-}iPr)_4] \rightarrow M[Al(O\text{-}iPr)_4]_2 + 2KCl\downarrow$$

$$M = Mn, Co, Ni, \text{ or } Cu$$

All of these bimetallic isopropoxides are colored liquids that are miscible with common organic solvents. They can all be purified by distillation under reduced pressure. Ebullioscopic determination of their molecular weights in benzene showed that they are monomeric. A study of chemical reactions of these products with hydroxy reagents like alcohols and β-diketones has not only yielded new products but has also thrown light on their structural features, which have been corroborated by study of their magnetic and spectroscopic properties (*17, 67*). In some cases the geometry of the molecule appears to be affected by the ramification of the alkyl group. For example, $Ni[Al(OMe)_4]_2$ shows an electronic spectrum characteristic of an octahedral geometry, whereas $Ni[Al(OEt)_4]_2$ and $Ni[Al(O\text{-}iPr)_4]_2$ show increasing proportions of tetrahedral nickel species in equilibrium with the octahedral form. Furthermore, the effect of steric factors on this equilibrium can be discerned in a finer difference, that is, the spectrum of $Ni[Al(OEt)_4]_2$ in ethanol shows a complete shift to the octahedral species, whereas, in the case of $Ni[Al(O\text{-}iPr)_4]_2$ in isopropanol, this shift appears to be only partial. For this latter derivative a stronger donor molecule like pyridine is required to change the equilibrium fully to the octahedral species. These structural features can be illustrated as follows.

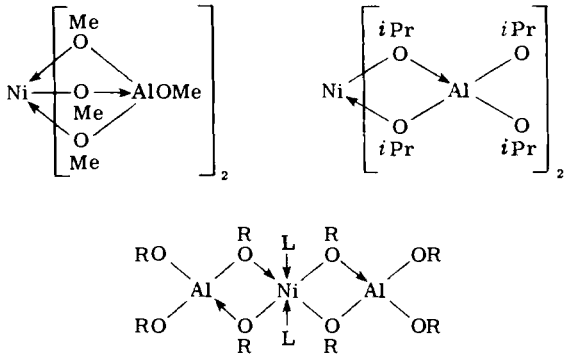

The octahedral nature of $Ni[Al(OEt)_4]_2$ has been corroborated by a study of the spectral properties of the compounds $M[Al(OR)_4]_2$ (M = Co, Ni, Cu; and R = Me, Et, *n*Pr and *n*Bu) by Stumpp and Hillebrand (*174*).

In view of the interesting properties of these bimetallic alkoxides, it is expected that there would be a rapid development of research into these compounds, particularly later 4d and 5d elements, the alkoxide chemistry of which has just begun to be explored during the last few years.

References

1. Demarcay, E., *C. R. Hebd. Seances Acad. Sci.* **80,** 51 (1875).
2. Bischoff, F., and Adkins, H., *J. Am. Chem. Soc.* **46,** 256 (1924).
3. Jennings, J. S., Wardlaw, W., and Way, W. J. R., *J. Chem. Soc.* p. 637 (1936).
4. Fischer, A., *Z. Anorg. Allg. Chem.* **81,** 170 (1913).
5. Prandtl, W., and Hess, L., *Z. Anorg. Allg. Chem.* **82,** 103 (1913).
6. Funk, H., and Niederlander, K., *Ber. Dtsch. Chem. Ges. B* **62,** 1688 (1929).
7. Thiessen, P. A., and Koerner, O., *Z. Anorg. Allg. Chem.* **180,** 65 (1929); **181,** 285 (1929).
8. Kandelaki, B. S., *Colloid J. USSR* (*Engl. Transl.*) **3,** 483 (1937); *Chem. Abstr.* **32,** 6227 (1938).
9. Bradley, D. C., and Wardlaw, W., *Nature* (*London*) **165,** 75 (1950).
10. Bradley, D. C., *Prog. Inorg. Chem.* **2,** 303 (1960); *Adv. Inorg. Chem. Radiochem.* **15,** 259 (1972).
11. Mehrotra, R. C., *Inorg. Chim. Acta Rev.* **1,** 99 (1967).
12. Bradley, D. C., and Fischer, K. J., *MTP Int. Rev. Sci. Gen. Chem. Transition Met.* **5,** 65 (1972).
13. Bradley, D. C., Mehrotra, R. C., and Gaur, D. P., "Metal Alkoxides." Academic Press, New York, 1978.

14. Adams, R. W., Bishop, E., Martin, R. L., and Winter, G., *Aust. J. Chem.* **19,** 207 (1966).
15. Sharma, P. P., and Mehrotra, R. C., *Indian J. Chem.* **5,** 456 (1967); *J. Indian Chem. Soc.* **45,** 736 (1968); **46,** 123 (1969).
16. Basi, J. S., and Bradley, D. C., *Proc. Chem. Soc., London* p. 305 (1963).
17. Mehrotra, R. C., *Coord. Chem.* **21,** 113 (1981).
18. Mehrotra, R. C., Batwara, J. M., and Kapoor, P. N., *Coord. Chem. Rev.* **31,** 67 (1980).
19. Flamini, A., Cole-Hamilton, D. J., and Wilkinson, G., *J. Chem. Soc., Dalton Trans.* p. 454 (1978).
20. Watenpaugh, K., and Caughlan, C. N., *Inorg. Chem.* **5,** 1782 (1966).
21. Cole-Hamilton, D. J., Young, R. J., and Wilkinson, G., *J. Chem. Soc., Dalton Trans.* p. 1995 (1976).
22. Van Tamelen, E. E., *Acc. Chem. Res.* **3,** 361 (1970).
23. Blandy, C., Sadani, M. T., and Gervais, D., *Synth. React. Inorg. Met.-Org. Chem.* **8,** 381 (1978).
24. Kapoor, P. N., and Mehrotra, R. C., *Chem. Ind. (London)* p. 1034 (1966).
25. Basso-Bert, M., and Gervais, D., *J. Organomet. Chem.* **165,** 209 (1979).
26. Basso-Bert, M., and Gervais, D., *Inorg. Chim. Acta* **34,** 191 (1979).
27. Meth-Cohn, O., Thorpe, D., and Twitchett, H. J., *J. Chem. Soc. C* p. 132 (1970).
28. Choukroun, R., and Gervais, D., *Synth. React. Inorg. Met.-Org. Chem.* **8,** 137 (1978).
29. Parashar, G. K., Bharara, P. C., and Mehrotra, R. C., *Z. Naturforsch. B: Anorg. Chem., Org. Chem.* **34B,** 109 (1979).
30. Gorsi, B. L., Kapoor, P. N., and Mehrotra, R. C., *Indian J. Chem.* **13,** 1200 (1975).
31. Gorsi, B. L., and Mehrotra, R. C., *J. Indian Chem. Soc.* **55,** 321 (1978).
32. Baggett, N., Poolton, D. S. P., and Jennings, W. B., *J. Chem. Soc., Chem. Commun.* p. 239 (1975).
33. Bradley, D. C., and Holloway, C. E., *J. Chem. Soc. A* p. 282 (1969).
34. Saxena, U. B., Rai, A. K., Mathur, V. K., Mehrotra, R. C., and Radford, D., *J. Chem. Soc. A* p. 904 (1970).
35. Bickley, D. G., and Serpone, N., *Inorg. Chim. Acta* **40,** 213 (1980).
36. Bickley, D. G., and Serpone, N., *Inorg. Chem.* **15,** 948 (1976); *Inorg. Chim. Acta* **28,** 169 (1978); **32,** 217 (1979); **38,** 177 (1980).
37. Besancon, J., Top, S., Tirouflet, J., Dusausoy, J., Lecomte, C., and Protas, J., *J. Chem. Soc., Chem. Commun.* p. 325 (1976).
38. Besancon, J., Camboli, D., and Tirouflect, J., *J. Organomet. Chem.* **186,** C15 (1980).
39. Paul, R. C., *et al., Indian J. Chem.*, **14A,** 776 (1976); **15A,** 653 (1977); **16A,** 630 (1978); *Inorg. Nucl. Chem. Lett.* **13,** 665 (1977).
40. Tandon, J. P., and co-workers, *Indian J. Chem.* **18,** 360 (1979); **19,** 376, 378 (1980); *Synth. React. Inorg. Met.-Org. Chem.* **9,** 519 (1979); *J. Inorg. Nucl. Chem.* **42,** 463, 1267 (1980); *J. Prakt. Chem.* **322,** 161, 508 (1980).
41. Choukroun, R. C., and Sabo, B., *J. Organomet. Chem.* **182,** 221 (1979).
42. Nugent, W. A., and Harlow, R. L., *J. Chem. Soc., Chem. Commun.* p. 342 (1979).
43. von Hornduff, G., and Kappler, E., *J. Prakt. Chem.* **23,** 54 (1964).
44. Brown, D. A., Cunningham, D., and Glass, W. K., *J. Chem. Soc., Chem. Commun.* p. 306 (1966).
45. Brown, D. A., Cunningham, D., and Glass, W. K., *J. Chem. Soc. A* p. 1563 (1968).
46. Mahendra, K. N., Ph.D. Thesis, Delhi University, Delhi (1979).

47. Alyea, E. C., Basi, J. S., Bradley, D. C., and Chisholm, M. H., *J. Chem. Soc. A* p. 772 (1971).
48. Mahendra, K. N., Parashar, G. K., and Mehrotra, R. C., *Synth. React. Inorg. Met.-Org. Chem.* **9,** 213 (1979).
49. Kasuga, K., Itou, J., and Yamamoto, Y., *Bull. Chem. Soc. Jpn.* **47,** 1026 (1976).
50. Estes, E. D., Scaringe, R. P., Hatfield, W. E., and Hodgson, D. J., *Inorg. Chem.* **15,** 1179 (1976); **16,** 1605 (1977).
51. Mahendra, K. N., Bharara, P. C., and Mehrotra, R. C., *Inorg. Chim. Acta* **25,** L5 (1977).
52. Bradley, D. C., Newing, C. W., Chisholm, M. H., Kelly, R. L., Haitko, D. A., Little, D., Cotton, F. A., and Fanwick, P. E., *Inorg. Chem.* **19,** 3010 (1980).
53. Bradley, D. C., Hursthouse, M. B., Newing, C. W., and Welch, A. J., *J. Chem. Soc., Chem. Commun.* p. 567 (1972).
54. Bradley, D. C., and Vuru, G., private communication as quoted in B. P. Bananwal, Ph.D. Thesis, Delhi University, Delhi (1979).
55. Chisholm, M. H., Cotton, F. A., Extine, M. W., and Kelly, R. L., *J. Am. Chem. Soc.* **100,** 3354 (1978).
56. Horvath, B., and Horvath, E. G., *Z. Anorg. Allg. Chem.* **457,** 51 (1979).
57. Chisholm, M. H., Cotton, F. A., Extine, M. W., and Redeout, D. C., *Inorg. Chem.* **18,** 120 (1979).
58. Horvath, B., Moseler, R., and Horvath, E. G., *Z. Anorg. Allg. Chem.* **449,** 41 (1979).
59. Abel, E. W., Farrow, G., and Towle, I. D. H., *J. Chem. Soc., Dalton Trans.* p. 71 (1979).
60. Abel, E. W., *Ann. N. Y. Acad. Sci.* **239,** 306 (1974).
61. Abel, E. W., Towle, I. D. H., Cameron, T. S., and Cordes, R. E., *J. Chem. Soc., Chem. Commun.* p. 285 (1977).
62. Abel, E. W., Towle, I. D. H., Cameron, G. S., and Cordes, R. E., *J. Chem. Soc., Dalton Trans.* p. 1943 (1979).
63. Newton, M. G., Pantaleo, N. S., King, R. B., and Diefenbach, S. P., *J. Chem. Soc., Chem. Commun.* p. 55 (1979).
64. Komiya, S., Tane-ichi, S., Yamamoto, A., and Yamamoto, T., *Bull. Chem. Soc. Jpn.* **53,** 673 (1980).
65. Kakos, G. A., and Winter, G., *Aust. J. Chem.* **20,** 2343 (1967).
66. Singh, J. V., Jain, N. C., and Mehrotra, R. C., *Z. Naturforsch.* **356,** 1555 (1980).
67. Singh, J. V., Ph.D. Thesis, Delhi University, Delhi (1980).
68. Baranwal, B. P., and Mehrotra, R. C., *Z. Anorg. Allg. Chem.* **443,** 284 (1978).
69. Baranwal, B. P., Ph.D. Thesis, Delhi University, Delhi (1979).
70. Mehrotra, R. C., Bharara, P. C., and Baranwal, B. P., *Indian J. Chem.*, **15A,** 458 (1977).
71. Baranwal, B. P., Bharara, P. C., and Mehrotra, R. C., *Trans. Met. Chem.* **2,** 204 (1977).
72. Baranwal, B. P., and Mehrotra, R. C., *Trans. Met. Chem.* **3,** 220 (1978).
73. Baranwal, B. P., Parashar, G. K., and Mehrotra, R. C., *Z. Naturforsch.* **34b,** 459 (1979).
74. Brubaker, C. M., and Wicholas, M., *J. Inorg. Nucl. Chem.* **27,** 59 (1965).
75. Mehrotra, R. C., and Singh, J. V., *Z. Anorg. Allg. Chem.* **477,** 235 (1981).
76. Adams, R. W., Barraclough, C. G., Martin, R. L., and Winter, G., *Aust. J. Chem.* **20,** 235 (1967).
77. Calderazzo, F., and Dell'Amico, G., *J. Chem. Soc., Dalton Trans.* p. 1238 (1979).

78. Calderazzo, F., Marchetti, F., Dell'Amico, G., Pelizzi, G., and Colligiani, A., *J. Chem. Soc., Dalton Trans.* p. 1419 (1980).
79. Greiser, T., and Weiss, E., *Chem. Ber.* **109,** 3142 (1976).
80. Tsuda, T., Hashimoto, T., and Saegusa, T., *J. Am. Chem. Soc.* **94,** 658 (1972).
81. Cornforth, J., Sierakowoski, A. F., and Wallace, T. W., *J. Chem. Soc., Chem. Commun.* p. 294 (1979).
82. Fanta, P. E., *Synthesis* p. 9 (1974).
83. Whitesides, G. M., Sadowski, J. S., and Lilburn, J., *J. Am. Chem. Soc.* **96,** 2829 (1976).
84. Yamamoto, T., Kubota, M., and Yamamoto, A., *Bull. Chem. Soc. Jpn.* **53,** 680 (1980).
84a. Martin, J. W. L., and Willis, C. J., *Canad. J. Chem.* **55,** 2459 (1977).
84b. Martin, J. W. L., Payne, N. C., and Willis, C. J., *Inorg. Chem.* **17,** 8478 (1978).
84c. Barber, D. L., Loeb, S. J., Martin, J. W. L., Payne, N. C., and Willis, C. J., *Inorg. Chem.*, **20,** 272 (1981).
85. Bharara, P. C., Gupta, V. D., and Mehrotra, R. C., *Synth. React. Inorg. Met.-Org. Chem.* **7,** 537 (1977).
86. Mehrotra, R. C., Gupta, V. D., and Bharara, P. C., *Indian J. Chem.* **13,** 156 (1975).
87. Pal, M., and Kapoor, R. N., *Inorg. Chim. Acta* **40,** 99 (1980).
88. Malhotra, K. C., Mehrotra, G., and Chaudhry, S. C., *Natl. Acad. Sci. Lett. (India)* **3,** 21 (1980).
88a. Chamberlain L., Huffman, J. C., Keddington, J., and Rothwell, I. P., *J. Chem. Soc., Chem. Commun.* p. 805 (1982).
89. Holloway, C. E., *J. Chem. Soc., Dalton Trans.* p. 1050 (1976).
90. Pinkerton, A. A., Schwarzenbach, D., Hubert-Pfalzgraf, L. G., and Riess, J. G., *Inorg. Chem.* **15,** 1196 (1976); Riess, J. G., Hubert-Pfalzgraf, L. G., and Liliane, G., *Chimia* **30,** 481 (1976).
91. Hubert-Pfalzgraf, L. G., *Inorg. Chim. Acta* **12,** 229 (1975).
92. Hubert-Pfalzgraf, L. G., and Riess, J. G., *Inorg. Chem.* **14,** 2854 (1975).
93. Behzadi, K., and Thompson, A., *J. Less-Common Met.* **56,** 9 (1977).
94. Schoenherr, M., and Koellner, J., *Z. Chem.* **18,** 36 (1978).
95. Malhotra, K. C., Banerjee, U. K., and Chaudhary, S. C., *Indian J. Chem.*, **16A,** 987 (1978).
96. Malhotra, K. C., Banerjee, U. K., and Chaudhary, S. C., *Curr. Sci.* **48,** 816 (1979).
97. Gorsi, B. L., Kapoor, P. N., and Mehrotra, R. C., *Indian J. Chem.*, **14A,** 406 (1976).
98. Hubert-Pfalzgraf, L. G., and Riess, J. G., *Inorg. Chim. Acta* **41,** 111 (1980).
99. Basikhin, Yu. Y., Rodinore, P. P., Sysoera, N. P., and Lel'kin, K. P., *Khim. Prom-st., Ser.: Reakt. Osobo Chist. Veshchestva* **2,** 11 (1979); *Chem. Abstr.* **91,** 185833u (1979).
99a. Jacob, E., *Angew. Chem. Int. Ed. Engl.*, **21,** 143 (1982).
100. Johnson, D. A., Taylor, J. C., and Wangh, A. B., *Inorg. Nucl. Chem. Lett.* **15,** 205 (1979).
101. Chisholm, M. H., and Extine, M., *J. Am. Chem. Soc.* **97,** 5625 (1975).
102. Chisholm, M. H., Extine, M., and Reichert, W. W., *Adv. Chem. Ser.* **150,** (1976).
103. Chisholm, M. H., Reichert, W. W., Cotton, F. A., and Murillo, C. A., *J. Am. Chem. Soc.* **99,** 1652 (1977).
104. Chisholm, M. H., Cotton, F. A., Murillo, C. A., and Reichert, W. W., *Inorg. Chem.* **16,** 1801 (1977).
105. Chisholm, M. H., Cotton, F. A., Frenz, B. A., Reichert, W. W., Shrive, L. W., and Stults, B. R., *J. Am. Chem. Soc.* **98,** 4469 (1976).

106. Mowat, W., and Wilkinson, G., *J. Chem. Soc., Dalton Trans.* p. 1120 (1973).
107. Mowat, W., Shortland, A. J., Hill, N. J., and Wilkinson, G., *J. Chem. Soc., Dalton Trans.* p. 770 (1973).
108. Alyea, E. C., Basi, J. S., Bradley, D. C., and Chisholm, M. H., *J. Chem. Soc., Chem. Commun.* p. 495 (1968).
109. Mehrotra, R. C., *J. Indian Chem. Soc.* **31,** 85 (1954).
110. Bradley, D. C., *Nature (London)* **182,** 1221 (1958).
111. Chisholm, M. H., Huffman, J. C., and Kelly, R. L., *J. Am. Chem. Soc.* **101,** 7100 (1979).
111a. Chisholm, M. H., Kirkpatrick, C. C., and Huffman, J. C., *Inorg. Chem.* **20,** 871 (1981).
112. Chisholm, M. H., Haitko, D. A., and Murillo, C. A., *J. Am. Chem. Soc.* **100,** 6262 (1978).
113. Chisholm, M. H., Cotton, F. A., Extine, M. W., Millar, M., and Stults, B. R., *Inorg. Chem.* **16,** 320 (1977).
113a. Chamberlain, L., Keddington, J., and Rothwell, I. P., *Organometallics* **1,** 1098 (1982).
114. Chisholm, M. H., Reichert, W. W., and Thornton, P., *J. Am. Chem. Soc.* **100,** 2744 (1978).
115. Chisholm, M. H., Cotton, F. A., Extine, M. W., and Reichert, W. W., *Inorg. Chem.* **17,** 2944 (1978).
115a. Chisholm, M. H., Folting, K., Huffman, J. C., Kirkpatrick, C. C., *J. Am. Chem. Soc.* **103,** 5967 (1981).
115b. Chisholm, M. H., Folting, K., Huffman, J. C., Kirkpatrick, C. C., and Ratermann, A. L., *J. Am. Chem. Soc.* **103,** 1305 (1981).
115c. Chisholm, M. H., Huffman, J. C., and Kirkpatrick, C. C., *J. Chem. Soc., Chem. Commun.* p. 189 (1982).
116. Akiyama, M., Chisholm, M. H., Cotton, F. A., Extine, M. W., Haitko, D. A., Little, D., and Fanwick, P. E., *Inorg. Chem.* **18,** 2266 (1979).
117. Akiyama, M., Little, D., Chisholm, M. H., Haitko, D. A., Cotton, F. A., and Extine, M. W., *J. Am. Chem. Soc.* **101,** 2504 (1979).
118. Akiyama, M., Chisholm, M. H., Cotton, F. A., Extine, M. W., Haitko, D. A., Leonelli, J., and Little, D., *J. Am. Chem. Soc.* **103,** 779 (1981).
119. Chisholm, M. H., Huffman, J. C., and Leonelli, J., *J. Chem. Soc., Chem. Commun.* **270** (1981); Chisholm, M. H., Huffman, J. C., Kirkpatrick, C. C., Leonelli, J., and Folting, K., *J. Am. Chem. Soc.* **103,** 6093 (1981).
119a. Cotton, F. A., and Fang, A., *J. Am. Chem. Soc.* **104,** 113 (1982).
120. Chisholm, M. H., Cotton, F. A., Extine, M. W., and Reichert, W. W., *J. Am. Chem. Soc.* **100,** 153 (1978).
121. Chisholm, M. H., Kelly, R. L., Cotton, F. A., and Extine, M. W., *J. Am. Chem. Soc.* **100,** 2256 (1978); **101,** 7645 (1979).
122. Chisholm, M. H., Huffman, J. C., and Kelly, R. L., *J. Am. Chem. Soc.* **101,** 7615 (1979).
123. Chisholm, M. H., Huffman, J. C., and Rothwell, I. P., *J. Am. Chem. Soc.* **103,** 4245 (1981).
124. Bailey, W. I., Chisholm, M. H. Cotton, F. A., and Rankel, L. A., *J. Am. Chem. Soc.* **100,** 5764 (1978).
125. Chisholm, M. H., and Kelly, R. L., *Inorg. Chem.* **18,** 2321 (1979).
126. Chisholm, M. H., Cotton, F. A., Extine, M. W., and Rankel, L. A., *J. Am. Chem. Soc.* **100,** 807 (1978).

127. Chisholm, M. H., Cotton, F. A., Extine, M. W., and Kelly, R. L., *Inorg. Chem.* **18,** 116 (1979).
128. Chisholm, M. H., Cotton, F. A., Extine, M. W., and Reichert, W. W., *J. Am. Chem. Soc.* **100,** 1727 (1978).
129. Cotton, F. A., Stanley, G. G., Kalbacher, B., Green, J. C., Seddon, E., and Chisholm, M. H., *Proc. Natl. Acad. Sci. U.S.A.* **74,** 3109 (1977).
130. Ginsberg, A. P., and Hawkes, M. J., *J. Am. Chem. Soc.* **90,** 5930 (1968).
131. Johnson, N. P., Lock, C. J. L., and Wilkinson, G., *J. Chem. Soc.* p. 1054 (1964).
132. Jones, R. A., and Wilkinson, G., *J. Chem. Soc., Dalton Trans.* p. 1063 (1978).
133. Edword, P. G., Wilkinson, G., Hursthouse, M. B., and Abdul Malik, K. M., *J. Chem. Soc., Chem. Commun.* p. 1158 (1979).
134. Edward, P. G., Wilkinson, G., Hursthouse, M. B., and Abdul Malik, K. M., *J. Chem. Soc., Dalton Trans.* p. 2467 (1980).
135. Nugent, W. A., and Harlow, R. L., *J. Chem. Soc., Chem. Commun.* p. 1105 (1979).
136. Wilkinson, G., private communication.
137. Keim, W., *J. Organomet. Chem.* **14,** 179 (1968).
138. Cetinkaya, B., Hitchcock, P. B., Lappert, M. F., Torroni, S., Atwood, J. L., Hunter, W. E., and Zaworotko, M. J., *J. Organomet. Chem.* **188,** 31 (1980).
139. Cross, R. J., and Glockling, F., *J. Chem. Soc.* p. 5422 (1965).
140. Gee, R. J. D., and Powell, H. M., *J. Chem. Soc. A* p. 1956 (1971).
141. Yoshida, T., Okano, T., and Otsuka, S., *J. Chem. Soc., Dalton Trans.* p. 993 (1976).
142. Bennett, M. A., Robertson, G. B., Whimp, P. O., and Yoshida, T., *J. Am. Chem. Soc.* **95,** 3028 (1973).
143. Reed, C. A., and Roper, W. R., *J. Chem. Soc., Dalton Trans.* p. 1014 (1973).
144. Klein, H. F., and Karsh, H. H., *Chem. Ber.* **106,** 1433 (1973).
145. Bennett, M. A., and Yoshida, T., *J. Am. Chem. Soc.* **100,** 1750 (1978).
145a. Clark, H. C., and Goel, A. B., *J. Organometal. Chem.* **178,** C27 (1979).
145b. Goel, A. B., and Goel, S., *Transition Met. Chem.* **5,** 378 (1980).
145c. Goel, A. B., Goel, S., and Vanderveer, D. G., *Inorg. Chim. Acta.* **54,** L169 (1981).
146. Michelin, R. A., Napote, M., and Ros, R., *J. Organomet. Chem.* **175,** 239 (1979).
147. Bradley, D. C., Mehrotra, R. C., and Wardlaw, W., *J. Chem. Soc.* pp. 2027, 4204, 5020 (1952); Mehrotra, R. C., *J. Indian Chem. Soc.* **31,** 904 (1954).
148. Mehrotra, R. C., *J. Indian Chem. Soc.* **30,** 585 (1953).
149. Cetinkaya, B., Gumrucku, I., Lappert, M. F., Atwood, J. L., Rodgers, R. D., and Zawortko, M. J., *J. Am. Chem. Soc.* **102,** 2088 (1980).
150. Bochmann, M., Wilkinson, G., Young, G. B., Hursthouse, M. B., and Abdul Malik, K. M., *J. Chem. Soc., Dalton Trans.* p. 901 (1980).
151. Bochmann, M., Wilkinson, G., and Young, G. B., *J. Chem. Soc., Dalton Trans.* p. 1879 (1980).
152. Bochmann, M., Wilkinson, G., Young, G. B., Hursthouse, M. B., and Abdul Malik, K. M., *J. Chem. Soc., Dalton Trans.* p. 1863 (1980).
153. Anderson, R. A., Carmono Guzman, Gibson, J. F., and Wilkinson, G., *J. Chem. Soc., Dalton Trans.* p. 2204 (1976).
154. Goel, S. C., Ph.D. Thesis, University of Delhi, Delhi (1979).
155. Goel, S. C., Mehrotra, S. K., and Mehrotra, R. C., *Synth. React. Inorg. Met.-Org. Chem.* **7,** 519 (1977).
156. Goel, S. C., and Mehrotra, R. C., *Z. Anorg. Allg. Chem.* **440,** 281 (1978).
157. Goel, S. C., Singh, V. K., and Mehrotra, R. C., *Z. Anorg. Allg. Chem.* **447,** 253 (1978).

158. Goel, S. C., Singh,V. K., and Mehrotra, R. C., *Synth. React. Inorg. Met.-Org. Chem.* **9,** 459 (1979).
159. Goel, S. C., and Mehrotra, R. C., *Synth. React. Inorg. Met.-Org. Chem.* **11,** 35 (1981).
160. Goel, S. C., and Mehrotra, R. C., *Indian J. Chem.* **20A,** 440 (1981).
161. Meerwein, H., and Bersin, T., *Justus Leibigs Ann. Chem.* **476,** 113 (1929).
162. Bartley, W. G., and Wardlaw, W., *J. Chem. Soc.* p. 421 (1958).
163. Govil, S., Kapoor, P. N., and Mehrotra, R. C., *Inorg. Chim. Acta* **15,** 43 (1975).
164. Mehrotra, R. C., *Proc. Indian Natl. Sci. Acad.* **42,** 1 (1976).
165. Mehrotra, R. C., and Singh, J. V., *J. Indian Chem. Soc.* **54,** 109 (1977).
166. Govil, S., Kapoor, P. N., and Mehrotra, R. C., *J. Inorg. Nucl. Chem.* **38,** 172 (1976).
167. Goel, S., Goel, A. B., and Mehrotra, R. C., *Synth. React. Inorg. Met.-Org. Chem.* **6,** 251 (1976).
168. Govil, S., and Mehrotra, R. C., *Indian J. Chem.,* **14A,** 138 (1976).
169. Goel, S., Ph.D. Thesis, University of Rajasthan, Jaipur (1975).
170. Govil, S., and Mehrotra, R. C., *Aust. J. Chem.* **28,** 2125 (1975).
171. Mehrotra, R. C., Sharma, C. K., and Goel, S., *Indian J. Chem.,* **14A,** 878 (1976).
172. Mehrotra, R. C., Goel, S., Goel, A. B., King, R. B., and Nainan, K. C., *Inorg. Chim. Acta* **29,** 131 (1978).
173. Singh, J. V., Jain, N. C., and Mehrotra, R. C., *Synth. React. Inorg. Met.-Org. Chem.* **9,** 79 (1979).
174. Stumpp, E., and Hillebrand, U., *Z. Naturforsch.* **34b,** 262 (1979).

ADVANCES IN INORGANIC CHEMISTRY AND RADIOCHEMISTRY, VOL. 26

TRANSITION-METAL THIONITROSYL AND RELATED COMPLEXES

H. W. ROESKY and K. K. PANDEY

Anorganisch-Chemisches Institut der Universität Göttingen, Göttingen, Federal Republic of Germany

I. Introduction

Nitrosyl complexes of transition metals have created considerable interest for many years. Attempts have been made to understand the

Copyright © 1983 by Academic Press, Inc.
All rights of reproduction in any form reserved.
ISBN 0-12-023626-5

nature of the bond formed between metal ions and the nitrosyl group (*21, 36, 41*). However, similar molecules containing the isoelectronic thionitrosyl ligand (NS) have only been discovered since 1974 (*17*). One of the reasons for the relatively late development of the chemistry of transition-metal thionitrosyl complexes is undoubtedly the instability of NS compared to NO and the present lack of reagents that can be utilized to introduce the thionitrosyl group into the transition-metal complexes.

The presence of the thionitrosyl monomer NS was observed for the first time by Fowler and Bakker in 1932, while studying the band spectrum of emitted light after passing an electric discharge through a mixture of nitrogen and sulfur vapor (*22*). A review article by Glemser and Mews (*23*) has described the preparation and physical properties of ionic compounds of composition $NS^+MF_6^-$ (M = As, Sb) and $NS^+BF_4^-$, as well as covalent compounds like NSF, NSF_3, and NSCl. Herberhold has reported metal complexes with thionitrosyl ligands (*28*).

A. The Thionitrosyl Radical

The thionitrosyl radical with one unpaired electron, unlike its homolog NO, polymerizes so readily that it is not possible to isolate it as a monomer, solid, or liquid, and even in the gas phase ·NS has only a transient existence (*27*). Like NO, it can also exist as NS^+ or NS^-, respectively, by losing or gaining an electron (*19, 45*), and, therefore, most of its properties should be approximately similar to those of NO. It has a low ionization potential (*44*) of 9.85 eV and a high dipole moment (*14*), 1.83 ± 0.03 D. It is a paramagnetic molecule having a doublet $^2\pi_{1/2}$ ground state with the lowest excited state, $^2\pi_{3/2}$, lying about 223 cm^{-1} above the ground-state level. A large number of papers related to the microwave spectrum of NS have appeared in the literature (*20, 35, 55*), and the excited valence states $B^2\pi$, $A^2\Delta$, $G^2\Sigma^-$, $H^2\pi$, and $I^2\Sigma^+$ have been identified in addition to the ground state $X^2\pi$. The vibration frequency of the gaseous NS molecule is 1204.1 cm^{-1} (*16, 65*). The ESR spectrum of the NS radical has also been studied (*15, 69*); it consists of three triplets. The g factor is consistent with the value expected for a molecule in a $^2\pi_{3/2}$ state in the lowest rotational level with $J = \frac{3}{2}$.

B. Bonding Modes in Metal Complexes

It is evident that NS can be stabilized by coordination to many transition metals, and well over 50 thionitrosyl complexes have been re-

ported. Although the majority of metal thionitrosyl complexes contain terminal NS ligands, there are a few examples of bridging thionitrosyl groups. Similar to nitrosyl complexes, there are three principal bonding modes in thionitrosyl complexes:

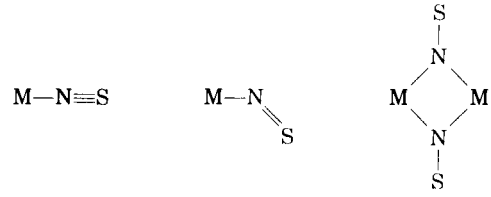

(a) (b) (c)

In case **a** the thionitrosyl ligand can be represented as coordinated "NS^+" and in **b** as coordinated "NS^-."

Because of the isoelectronic nature of NO and NS, there has been considerable interest in the comparative bonding properties of these ligands. The molecular orbitals for NO and NS are compared in Fig. 1 (*59*). The 7σ donor orbital of NS is at higher energy than the 5σ donor orbital of NO, whereas the 3π (π^*) acceptor level of NS is at lower energy than the 2π (π^*) acceptor level of NO. There is weaker $p\pi$–$p\pi$

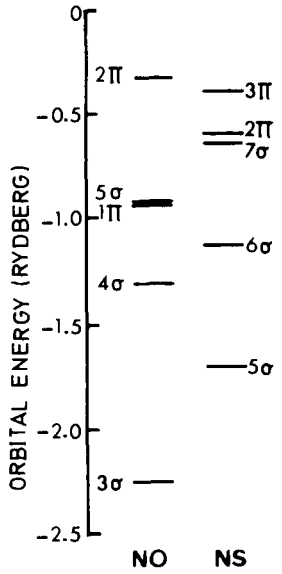

FIG. 1. Molecular orbital diagrams for NO and NS ground-state configurations: (NO) $1\sigma^2$, $2\sigma^2$, $3\sigma^2$, $4\sigma^2$, $1\pi^4$, $5\sigma^2$, $2\pi^1$; (NS) $1\sigma^2$, $2\sigma^2$, $3\sigma^2$, $4\sigma^2$, $1\pi^4$, $5\sigma^2$, $6\sigma^2$, $7\sigma^2$, $2\pi^4$, $3\pi^1$.

bonding for sulfur compared to oxygen. It should also be mentioned that the 7σ level of NS is significantly antibonding in character. These results lead one to expect that M—NS bonds should be stronger than M—NO bonds. Comparison of the spectroscopic properties and the electronic structures of M—NX complexes have indicated that NS is a better σ-donor and π-acceptor ligand than NO.

There has been no comprehensive review of transition-metal thionitrosyl complexes; only a brief introduction has appeared in the literature (*18, 23, 28, 42*). The objectives of this account are (1) to illustrate the currently available synthetic routes to metal thionitrosyl complexes and (2) to give a brief review of the physicochemical properties of these new classes of complexes. Because many metal nitrosyls have been used as reagents in organic synthesis and as homogeneous catalysts in industrial reactions, it is anticipated that some metal thionitrosyls may well find similar uses in the future.

II. Preparation of Thionitrosyl Complexes

In general, metal nitrosyl complexes are readily available by reactions of metal salts or metal complexes with NO gas. In view of the instability of NS, this approach could not be applied to the synthesis of metal thionitrosyl complexes.

As yet, there is no general synthetic route to metal thionitrosyl complexes. However there are a few limited preparative methods known which are discussed here.

1. Reactions of nitride complexes with elemental sulfur or with sulfur halides
2. Reaction of trithiazyltrichloride [$(NSCl)_3$] with transition-metal complexes
3. Elimination of fluoride from NSF metal complexes
4. Generation of NS^+ salts and its reaction with metal complexes

A. Chromium

In a preliminary communication, Kolthammer and Legzdins (*24, 38*) reported that $Na[(\eta^5\text{-}C_5H_5)Cr(CO)_3]$ was found to react with trithiazyltrichloride in tetrahydrofuran (THF) to yield the first organometallic thionitrosyl complex $(\eta^5\text{-}C_5H_5)Cr(CO)_2(NS)$ by the reaction

$$Na[(\eta^5\text{-}C_5H_5)Cr(CO)_3] + \tfrac{1}{3}(NSCl)_3 \xrightarrow{THF} (\eta^5\text{-}C_5H_5)Cr(CO)_2(NS) + CO + NaCl$$

Herberhold and Haumaier (*29*) showed that the reaction of $NS^+PF_6^-$, obtained *in situ* from $(NSCl)_3$ and $AgPF_6$ (1 : 3), with benzene tricarbonyl chromium in acetonitrile solution yields the cationic thionitrosyl complex $[Cr(NS)(NCMe)_5](PF_6)_2$. In the presence of *t*-butyl isocyanide and zinc powder this complex is reduced to $[Cr(NS)(CNCMe_3)_5]PF_6$.

B. Thionitrosoamine Complexes

The unstable dimethyl(thionitroso)amine, prepared from dimethylhydrazine and elemental sulfur, reacts in THF with $(CO)_5Cr \cdot THF$ to yield the 1 : 1 complex:

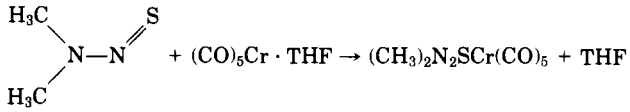

The structure was investigated by X-ray analysis. The dimethyl(thionitroso)amine ligand coordinates via the sulfur atom to the metal atom. The Cr—C bond distance [184.6(2) pm] of the CO group in the trans position to the sulfur atom is shortened in comparison to the average value of the remaining CO ligands [190.3(5)] (*58*):

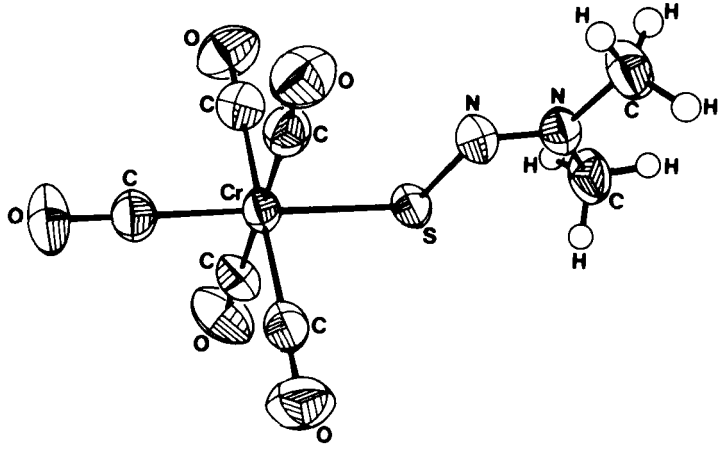

C. Molybdenum

The complexes $Mo(NS)(S_2CNR_2)_3$ [R_2 = Me_2, Et_2, or $(CH_2)_4$] (*11, 12*) were prepared by treating the dioxo complex $MoO_2(S_2CNR_2)_3$ with trimethylsilylazide in acetonitrile under reflux. This reaction proceeds

via intermediate formation of a nitrido complex and, subsequently, the nitrido complex $MoN(S_2CNR_2)_3$ reacts with elemental sulfur in refluxing acetonitrile to give the appropriate thionitrosyl complex.

$$MoN(S_2CNR_2)_3 + \tfrac{1}{8}S_8 \xrightarrow[\text{reflux}]{CH_3CN} Mo(NS)(S_2CNR_2)_3$$

D. Rhenium

Reactions of S_2Cl_2 with $ReNCl_2(PRPh_2)$ (R = Ph or *n*-Pr) yield the thionitrosyl complexes $Re(NS)Cl_3(PRPh_2)_2$ (*12*). The complexes $ReNX_2(PR_3)_3$ (PR_3 = PMe_2Ph, PEt_2Ph, or $PMePh_2$; X = Cl or Br) react with half an equivalent of S_2Cl_2 to give the complexes of composition $Re(NS)ClX(PR_3)_3$. Reaction of the nitrido complex $ReNCl_2(PR_3)_3$ with an excess of S_2Cl_2 or SCl_2 affords the derivatives $Re(NS)Cl_3(PR_3)_2$. Similarly, the reaction of S_2Cl_2 with $[ReNCl(dppe)_2]Cl$ (dppe = $Ph_2PCH_2CH_2PPh_2$) results in the formation of $[Re(NS)Cl(dppe)_2]Cl$. In the IR spectra of these rhenium complexes, a single strong peak observed in the region 1167–1185 cm^{-1} confirms the presence of the NS^+ cation. The $[Re(CO)_5NS]^{2+}$ cation is prepared from the reaction of $Re(CO)_5Br$ and $NS^+SbF_6^-$ and also by elimination of a fluoride ion of $[Re(CO)_5(NSF)]^+$, by means of AsF_5 (*43*).

E. Ruthenium

The ruthenium thionitrosyl complexes $Ru(NS)Cl_3L_2$ (L = PPh_3, $AsPh_3$) are prepared by the reaction of $RuCl_3 \cdot H_2O$ with $(NSCl)_3$ in THF in the presence of triphenylphosphine or triphenylarsine (*51*). Reaction of $RuCl_2(PPh_3)_3$ with $NSCl(THF)_x$ results in the formation of the dithionitrosyl complex, which, on recrystallization with different solvents, gives solvated complexes of composition $Ru(NS)_2Cl_2(PPh_3)_2 \cdot X$ (X = CH_2Cl_2, $CHCl_3$, or $CHBr_3$). The IR spectra of these complexes show absorption bands at 1300 cm^{-1}, which suggest the presence of a coordinated NS^+ ligand, and at 1120 cm^{-1}, due to coordination of an NS^- ligand (*33*). An X-ray crystal-structure analysis of the analogous nitrosyl complex $Ru(NO)Cl_3(PPh_3)_2$ showed the Ru—NO system is essentially linear with angle Ru—N—O equal to 180° (*26*). It is therefore extremely likely that thionitrosyl analogs have a linear RuNS group.

F. Osmium

Green thionitrosyl complexes of osmium have been reported as a result of reactions of $OsNX_3L_2$ [X = Cl or Br, L = $AsPh_3$, PMe_2Ph or $\frac{1}{2}$ (2,2'bipyridyl)] with half an equivalent of S_2Cl_2. Addition of pyridine (py) to a methylene chloride solution of the product formed by reaction of $(Bu_4N)OsNCl_4$ with S_2Cl_2, gives $Os(NS)Cl_3(py)_2$. The osmium thionitrosyl complexes of composition $Os(NS)Cl_3L_2$ (L = PPh_3 or $AsPh_3$) are obtained by the reaction of $(NSCl)_3$ in THF with $OsCl_3$ in the presence of PPh_3 or $AsPh_3$, respectively (*12, 51*).

G. Cobalt

Reaction of $(NSCl)_3$ in THF with $CoH[P(OPh)_3]_4$ results in the formation of the five-coordinated air-sensitive intermediate thionitrosyl complex $Co(NS)Cl_2[P(OPh)_3]_2$ (ν_{NS} = 1113 cm^{-1}) (*66*), which, on reaction with air or oxygen, is converted to the thionitro complex $Co(NSO)Cl_2[P(OPh)_3]_2$. The IR spectrum of the thionitro complex exhibits absorption bands at 1540 and 990 cm^{-1}, which are assigned to ν_{NO} and ν_{NS}, respectively, of the NSO group.

H. Rhodium

Trithiazyltrichloride reacts with $Rh(CO)Cl(PPh_3)_2$ to yield the green complex $[Rh(CO)(NS)Cl_2(PPh_3)]_2$ (*34, 53*), which is also prepared by treating $RhH(CO)(PPh_3)_3$ with a solution of trithiazyltrichloride in THF.

$$2Rh(CO)Cl(PPh_3)_2 + \tfrac{2}{3}(NSCl)_3 \xrightarrow{THF} [Rh(CO)(NS)Cl_2(PPh_3)]_2 + 2PPh_3$$

The reactions of $[Rh(CO)(NS)Cl_2(PPh_3)]_2$ with (L = PPh_3 or $AsPh_3$) result in the formation of red-brown complexes of composition $Rh(CO)(NS)Cl_2L_2$. The products of these reactions strongly depend on the refluxing time. Similarly, the reaction of $NSCl(THF)_x$ with $Rh(CO)Cl(AsPh_3)_2$ results in the formation of a yellow-green complex $[Rh(CO)(NS)Cl_2(AsPh_3)]_2$, which reacts with $AsPh_3$ to give $Rh(CO)(NS)Cl_2(AsPh_3)_2$ (*54*).

The IR spectrum of $Rh(CO)(NS)(PPh_3)_2$ shows absorption bands at 1970 cm^{-1} (due to ν_{CO}) and at 1122 cm^{-1} (due to ν_{NS}). $Rh(NS)(PPh_3)_3$ is also obtained by treating $NSCl(THF)_x$ with $RhCl(PPh_3)_3$ in the pres-

ence of PPh_3 and zinc. Its IR spectrum shows an absorption band at 1100 cm^{-1}, due to ν_{NS}. $(NSCl)_3$ reacts with $RhX(PPh_3)_3$ (X = Cl or Br) and with $RhH(PPh_3)_4$ to yield the brown complex $[Rh(NS)ClX(PPh_3)]_2$, which on reaction with triphenylphosphine or triphenylarsine results in the formation of the complex $Rh(NS)ClX(PPh_3)_2$ and $Rh(NS)ClX(PPh_3)(AsPh_3)$. These pentacoordinated complexes are also obtained by the reaction of $(NSCl)_3$ with $RhCl_3 \cdot 3H_2O$ in the presence of L. The IR spectra of the complexes $Rh(NS)Cl_2L_2$ and $Rh(NS)ClBr(PPh_3)_2$ show absorption bands in the range 1118–1120 cm^{-1}, due to ν_{NS} (*46, 53, 54, 56*).

I. Iridium

Reaction of $(NSCl)_3$ in THF separately with $Ir(CO)Cl(PPh_3)_2$ and $IrH(CO)(PPh_3)_3$ yields the brown complex $Ir(CO)(NS)Cl_2(PPh_3)_2$. The reaction of $Ir(CO)Cl(PPh_3)_2$ with $(NSCl)_3$ in THF in an oxygen atmosphere affords a bright green complex of composition $Ir(CO)(NSO)Cl_2(PPh_3)_2$ with 40% yield (*46*). The same compound is also obtained when $Ir(CO)Cl(O_2)(PPh_3)_2$ is treated with $NSCl(THF)_x$. This indicates that the Vaska complex in solution takes up oxygen from the atmosphere to form the oxygen-containing complex, which, on reaction with $(NSCl)_3$, forms the NSO iridium complex. Covalent and ionic (*2–4, 6, 57, 60, 61*) derivatives containing the NSO group are well known. The gas-phase reaction of NH_3 with thionyl chloride has long been known (*6, 60*) to produce thionylimide and ammonium chloride. The IR (*67*), microwave (*37*), ultraviolet (*1*), and photoelectronic spectra (*68*) of HNSO have been reported. The IR spectrum of $Ir(CO)(NSO)Cl_2(PPh_3)_2$ exhibits absorption bands at 2060 cm^{-1}, due to ν_{CO}, and three bands at 1160, 1060, and 565 cm^{-1}, which are attributed to the $\nu_{as}(NSO)$, $\nu_{sym}(NSO)$ stretching modes and $\delta(NSO)$ of the NSO ligand, respectively. These frequencies are comparable to the asymmetric and symmetric stretching and bending modes of coordinated SO_2, which is isoelectronic with the NSO^- group.

J. Platinum

The major product of the reaction of $Pt(PPh_3)_4$ and $S_4N_4H_4$ in acetone has been determined to be $(Ph_3P)_2Pt(OSNH)_2$ from single-crystal X-ray diffraction data. $(Ph_3P)_2Pt(OSNH)_2$ exists as a square-planar complex with a cis arrangement of ligands. Each triphenylphosphine ligand is trans to an OSNH, which is coordinated to platinum via oxygen (*8–10, 30*). The structure shows some divergence between the

two HNSO ligands, particularly O—S bond lengths 126(1) and 134(2) pm and Pt—O—S angles 138.1(10) and 129.5(9)°. Better agreement is shown by S—N bond lengths 148(2) and 145(2) pm, and O—S—N angles 121.9(12) and 122.0(9)°. The S—O and S—N distances are shorter than those determined by microwave spectroscopy (*37*) for *cis*-thionylimide [S—O 145.1(5), S—N 151.2(5) pm]. The possibility that the ligands are also arranged in the thiazyl *S*-hydroxide form cannot be eliminated. The thiazyl *S*-hydroxide HOSN has been reported (*68*).

$Pt(OSNH)_2S_2N_2H_2$ has been prepared by the reaction of an aqueous solution of K_2PtCl_4 with $S_4N_4H_4$ in acetone (*9*). The absorption spectrum in DMF of $Pt(OSNH)_2S_2N_2H_2$ shows three absorption bands at 450, 310, and 300 nm, possibly due to electronic transitions $^1A_{1g} \rightarrow {}^1A_{2g}$, $^1A_{1g} \rightarrow {}^1B_{2g}$, and $^1A_{1g} \rightarrow {}^1E_g$, respectively. These three transitions are typical of square-planar d^8 configurations. The proposed structure is

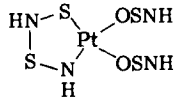

K. Metal Complexes with Thiazyl Fluoride and Thiazyl Trifluoride Ligands

The chemistry of these complexes has been reviewed by Glemser and Mews (*23*). Therefore, these complexes are mentioned here only briefly. They are prepared in liquid SO_2 by treating the metal complexes of $[M(SO_2)_x](AsF_6)_2$ (M = Co or Ni) and $[Re(CO)_5SO_2]AsF_6$ with NSF or $[M(SO_2)_x](AsF_6)_2$ (M = Mn, Fe, Co, Ni, or Cu), $AgAsF_6$, $[M(CO)_5SO_2]AsF_6$ (M = Mn or Re), and $[\eta^5\text{-}C_5H_5Fe(CO)_2SO_2]AsF_6$ with NSF_3.

The M^{2+} cations are able to coordinate to six NSF but only to four NSF_3 ligands. An interesting observation was made that in NSF as well as in NSF_3 complexes the N—S bond length is shorter than in the free ligands.

III. Reactions of Thionitrosyl Complexes

The reaction of $(\eta^5\text{-}C_5H_5)Cr(CO)_2(NS)$ with NOCl and $NOPF_6$ gives the nitrosyl complex $(\eta^5\text{-}C_5H_5)Cr(NO)_2Cl$ and the nitrosylthionitrosyl complex $[(\eta^5\text{-}C_5H_5)Cr(CO)(NO)(NS)]PF_6$, respectively (*25*).

$$(\eta^5\text{-}C_5H_5)Cr(CO)_2(NS) + NOPF_6 \xrightarrow{CH_3CN/CH_2Cl_2} [(\eta^5\text{-}C_5H_5)Cr(CO)(NO)(NS)]PF_6 + CO$$

This cationic nitrosylthionitrosyl complex exhibits a ν_{CO} at 2122 cm^{-1}, a ν_{NO} at 1790 cm^{-1}, and a ν_{NS} at 1243 cm^{-1}. $[(\eta^5\text{-}C_5H_5)Cr(CO)(NO)(NS)]PF_6$ undergoes nucleophilic attack by I^- to give $(\eta^5\text{-}C_5H_5)Cr(NO)_2I$. The thionitrosyl complex $(\eta^5\text{-}C_5H_5)Cr(CO)_2(NS)$ does not react with triphenylphosphine, although its nitrosyl analog reacts with triphenylphosphine to yield $(\eta^5\text{-}C_5H_5)Cr(CO)(PPh_3)(NO)$. $[Cr(NS)(CNCMe_3)_5]PF_6$ has also been reported to react with $NOPF_6$ or $AgPF_6$ to give $[Cr(NS)(CNCMe_3)_5](PF_6)_2$ (*29*).

$$[Cr(NS)(CNCMe_3)_5]PF_6 + NOPF_6 \rightarrow [Cr(NS)(CNCMe_3)_5](PF_6)_2 + NO$$

The IR spectra of $[Cr(NS)(CNCMe_3)_5](PF_6)_2$ includes absorptions at 2225 cm^{-1} (attributable to ν_{CN}) and 1220 cm^{-1} (attributable to ν_{NS}). The thionitrosyl stretching frequency occurs at higher energy than that exhibited by the $[Cr(NS)(CNCMe_3)_5]PF_6$ complex. This is consistent with a decrease in electron density at the metal center which manifests itself in less back donation from the metal d orbital to the NSπ^* orbitals (*64*).

The desulfurization of thionitrosyl complexes of molybdenum, rhenium, and osmium to the parent nitrido complexes have been observed by refluxing the complexes with n-Bu_3P in toluene or acetonitrile (*12*). The reaction of $Re(NS)Cl_2(PMe_2Ph)_3$ with KNCS or $Na(S_2CNMe_2)$ leads to $Re(NS)ClL(PMe_2Ph)_3$ [L = NCS or (S_2CNMe_2)].

$$Re(NS)Cl_2(PMe_2Ph)_3 \xrightarrow{KNCS} Re(NS)Cl(NCS)(PMe_2Ph)_3 + KCl$$

$$Re(NS)Cl_2(PMe_2Ph)_3 \xrightarrow{Na(S_2CNMe_2)} Re(NS)Cl(PMe_2Ph)_3(S_2CNMe_2) + NaCl$$

The cationic thionitrosyl complex $[Re(NS)Cl(dppe)_2]Cl$ also reacts with $FeCl_3$ or NH_4PF_6 with formation of the $FeCl_4^-$ or PF_6^- salt.

$$[Re(NS)Cl(dppe)_2]Cl \xrightarrow{FeCl_3} [Re(NS)Cl(dppe)]FeCl_4$$

$$[Re(NS)Cl(dppe)_2]Cl \xrightarrow{NH_4PF_6} [Re(NS)Cl(dppe)]PF_6 + NH_4Cl$$

The ruthenium dithionitrosyl complex $Ru(NS)_2Cl_2(PPh_3)_2 \cdot CH_2Cl_2$ was found to react with NOX (X = Cl or Br) to yield the nitrosyl thionitrosyl complexes $Ru(NO)(NS)ClX(PPh_3)_2$ (X = Cl or Br) at room temperature (25 ° C) whereas refluxing the reaction mixture with excess NOX or N_2O_3 led to formation of the nitrosyl complexes $Ru(NO)ClX_2(PPh_3)_2$ (X = Cl or Br) (*33*). The IR spectra of Ru(NO)(NS)-

$Cl(PPh_3)_2$ exhibits ν_{NO} at 1880 cm^{-1} and ν_{NS} at 1320 cm^{-1}. Reaction of $Ru(NS)_2Cl_2(PPh_3)_2CH_2Cl_2$ with H_2O affords $Ru(NS)(NSOH)Cl(PPh_3)_2$ and HCl.

$$Ru(NS)_2Cl_2(PPh_3)_2CH_2Cl_2 + H_2O \rightarrow Ru(NS)(NSOH)Cl(PPh_3)_2 + HCl$$

In the IR spectrum of the complex $Ru(NS)(NSOH)Cl(PPh_3)_2$ it was found that the band at 1330 cm^{-1} disappeared and a new band due to the coordinated NSOH group appeared, although the position of the band at 1120 cm^{-1} remained the same. Whether the thionylimide is bonded via oxygen or nitrogen to ruthenium is not known. Reactions of $Ru(NS)_2Cl_2(PPh_3)_2 \cdot CH_2Cl_2$ with X_2 (X_2 = Cl_2, Br_2, or I_2) result in the formation of charge-transfer complexes with the composition $Ru(NS)_2Cl_2(PPh_3)_2CH_2Cl_2 \cdot X_2$.

When nitrosyl halides NOX (X = Cl or Br) react with $Rh(CO)(NS)Cl_2L_2$ (L = PPh_3 or $AsPh_3$), the displacement of the thionitrosyl group and the formation of carbonylnitrosyl complexes of rhodium(III), $Rh(CO)(NO)ClXL_2$ (X = Cl or Br; L = PPh_3 or $AsPh_3$), (*54*) are observed. The mechanism of the reaction is not yet known. The complex $Rh(NS)(PPh_3)_3$ reacts with chlorine to give the pentacoordinated complex $Rh(NS)Cl_2(PPh_3)_2$ (*46*).

$$Rh(NS)(PPh_3)_3 + Cl_2 \rightarrow Rh(NS)Cl_2(PPh_3)_2 + PPh_3$$

Bridged Thionitrosyl Complexes

It was mentioned earlier that the thionitrosyl group (NS) can form metal–N(S)–metal bridge complexes. Reaction of trithiazyltrichloride in THF or CCl_4–$CHCl_3$ (1 : 1) with $Rh(NO)Cl_2(PPh_3)_2$ leads to the formation of a novel complex of composition $[Rh(\mu\text{-}NS)Cl_2(PPh_3)]_2$, which has been isolated as brown, shining crystals (*49, 50*). A plausible mechanism involves the prior formation of the six-coordinate intermediate sulfur monoxide complex $[Rh(NS)(SO)Cl_2(PPh_3)]_2$, ($\nu_{SO}$ = 1035 cm^{-1}), which reacts readily with triphenylphosphine to give $[Rh(\mu\text{-}NS)Cl_2PPh_3]_2$, $SPPh_3$, and $OPPh_3$. The formation of triphenylphosphine sulfide and triphenylphosphine oxide from $[Ir(S_2O_2)(dppe)_2]Cl$ with triphenylphosphine has been reported by Schmid and Ritter (*62, 63*).

Similar reactions of $NSCl(THF)_x$ with $Rh(NO)L_3$ (L = PPh_3 or $AsPh_3$), $Rh(NO)ClBr(PPh_3)_2$, $Rh(NO)Br_2(PPh_3)_2$, or $Rh(NO)Cl_2(AsPh_3)_2$ result in the formation of brown complexes with the composition $Rh(\mu\text{-}NS)X_2(MPh_3)_2$ (X = Cl or Br; M = P or As) (*46, 56*). All

these thionitrosyl bridged complexes are air stable, nonelectrolytic, diamagnetic solids. The IR spectra exhibit a slightly broad band at 840 cm^{-1}, which is attributed to the bridging thionitrosyl group. The absence of a band around 1630 cm^{-1} [due to ν_{NO} (*48*) and the appearance of a new band at 840 cm^{-1} indicate the replacement of the nitrosyl group by the thionitrosyl group.

In order to prove further the bridging nature of the NS group, the reactions of $[Rh(\mu\text{-}NS)X_2(MPh_3)]_2$ with PPh_3 and $AsPh_3$ have been carried out. These reactions result in the cleavage of the bridge and yield complexes of composition $Rh(NS)X_2(MPh_3)_2$.

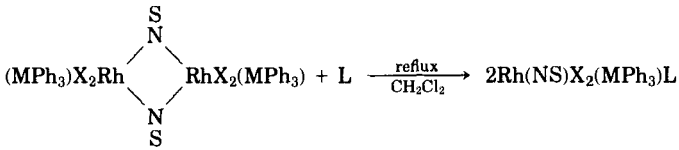

M = P	L = PPh_3
M = P	L = $AsPh_3$
M = As	L = PPh_3
M = As	L = $AsPh_3$

The IR spectra of the complexes $Rh(NS)X_2L_2$ show absorption bands around 1118–1120 cm^{-1} [due to terminal (NS)] and disappearance of the band at 840 cm^{-1}. This supports the view that the band at 840 cm^{-1} in the complexes $[Rh(\mu\text{-}NS)X_2L]_2$ is the characteristic band of a bridging thionitrosyl group.

Displacement of an NO group by NS is observed in iridium nitrosyl complexes, but, contrary to rhodium and iridium complexes, Ru(II) and Os(II) complexes of composition $M(NO)X_3(PPh_3)_2$ (M = Ru or Os; X = Cl or Br) do not react with $(NSCl)_3$ (*46*).

It is obvious from these reactions that the NO group is replaced by the NS group in those metal nitrosyl complexes in which ν_{NO} appears at relatively low frequencies.

IV. Properties of Thionitrosyl Complexes

The ligand NS might be expected to have bonding properties similar to those of NO. As in nitrosyl complexes the most readily accessible and sensitive technique for identifying metal thionitrosyl complexes is IR spectroscopy. A variety of other physical techniques has been applied to thionitrosyl complexes, but these have concentrated on comparing analogous nitrosyl and thionitrosyl systems.

A. Theoretical Studies

It has been shown previously that NS is a better σ donor and π acceptor than NO. Physical measurements have supported the conclusion that NS binds more strongly to an electron-rich metal than does NO. An investigation of the electronic structure of $(\eta^5\text{-}C_5H_5)Cr(CO)_2(NS)$ by photoelectron spectroscopy (*31*) and theoretical calculations has been reported by Lichtenberger and Fenske (*40*). Their study confirms the early predictions, based on molecular orbital theory, that the NS group is a slightly better σ donor than NO. The improved donor ability results from the additional charge on the nitrogen atom, both from the less electronegative sulfur atom and the improved π-acceptor ability of NS. As in the case of CO and CS (*28*), this also has an important influence on their chemical and physical properties.

B. IR Studies

Nitrosyl stretching-frequency modes in metal nitrosyl complexes have a characteristic intense absorption in the region between 1500 and 2000 cm^{-1}, depending on the type of bonding involved in the nitrosyl complexes. At present the frequency range for different modes in thionitrosyl complexes has been found to be between 840 and 1370 cm^{-1}. The NS stretching frequency in the linear M—NS structure generally appears at higher values (*26*), in the range between 1150 and 1370 cm^{-1}. The complexes that absorb in the region 1110–1130 cm^{-1} have been considered to involve bonding of the terminal bent type (Table I).

The IR spectrum of $(\eta^5\text{-}C_5H_5)Cr(CO)_2(NS)$ exhibits absorption bands at 2033 and 1962 cm^{-1} (due to ν_{CO}) and at 1180 cm^{-1} (due to ν_{NS}). The ν_{CO} bands of $(\eta^5\text{-}C_5H_5)Cr(CO)_2(NS)$ appear at higher frequencies than those of $(\eta^5\text{-}C_5H_5)Cr(CO)_2(NO)$. The IR spectrum of the green complex $[Rh(CO)(NS)Cl_2(PPh_3)]_2$ shows absorption bands at 2110, 1118, 340, and 260 cm^{-1} in addition to the characteristic bands of PPh_3. The bands at 2110 and 1118 cm^{-1} are characteristic stretching frequencies of terminal carbonyl and thionitrosyl groups. The band at 340 cm^{-1} is typical of ν_{RhCl}, whereas the band at 260 cm^{-1} could be due to either ν_{RhCl} or to bridging chlorine modes. The IR spectra of $Rh(CO)(NS)Cl_2L_2$ (L = PPh_3 or $AsPh_3$) exhibits absorption bands at ν_{CO} = 2105, ν_{NS} = 1120, and ν_{RhCl} = 330 cm^{-1}. According to the magnetic data these complexes are diamagnetic, suggesting rhodium to be present either in a +1 [$Rh(I)NS^+$] or a +3 [$Rh(III)NS^-$] oxidation state. The high frequency of ν_{CO} is also reasonable for a Rh(III) system.

TABLE I

IR DATA OF THIONITROSYL COMPLEXES

Complex	ν_{NS} (cm^{-1})	References	Complex	ν_{NS} (cm^{-1})	References
$(\eta^5\text{-}C_5H_5)Cr(CO)_2(NS)$	1180	(*38*)	$Ru(NO)(NS)ClBr(PPh_3)_2$	1320	(*33*)
	1150	(*29*)	$Ru(NS)(NSOH)Cl(PPh_3)_2$	1120	(*33*)
$[(\eta^5\text{-}C_5H_5)Cr(CO)(NO)(NS)]PF_6$	1243	(*25*)	$Os(NS)Cl_3(PPh_3)_2$	1294	(*51*)
$[Cr(NS)(CNCMe_3)_5]PF_6$	1135	(*29*)	$Os(NS)Cl_3(AsPh_3)_2$	1290	(*51*)
$[Cr(NS)(CNCMe_3)_5](PF_6)_2$	1220	(*29*)	$Os(NS)Cl_3(PMe_2Ph)_2$	1285	(*12*)
$[Cr(NS)(NCMe)_5](PF_6)_2$	1245	(*29*)	$Os(NS)Cl_3(bipy)$	1282	(*12*)
$Mo(NS)(S_2CNMe_2)_3$	—	(*12*)	$Os(NS)Cl_3(py)_2$	1284	(*12*)
$Mo(NS)(S_2CNEt_2)_3$	—	(*12*)	$Os(NS)ClBr_2(AsPh_3)_2$	1270	(*12*)
$Mo(NS)[S_2CN(CH_2)_4]_3$	—	(*12*)	$Os(NS)ClBr_2(bipy)$	1280	(*12*)
$Re(NS)Cl_2(PMe_2Ph)_3$	1180	(*12*)	$Co(NS)Cl_2[P(OPh)_3]_2$	1130	(*66*)
$Re(NS)Cl_2(PEt_2Ph)_3$	1167	(*12*)	$[Rh(CO)(NS)Cl_2(PPh_3)]_2$	1118	(*34*, *53*)
$Re(NS)Cl_2(PMePh_2)_3$	1172	(*12*)	$[Rh(CO)(NS)Cl_2(AsPh_3)]_2$	1120	(*54*)
$Re(NS)ClBr(PEt_2Ph)_3$	1168	(*12*)	$Rh(CO)(NS)Cl_2(PPh_3)_2$	1120	(*53*, *54*)
$Re(NS)Cl(SCN)(PMe_2Ph)_3$	1177	(*12*)	$Rh(CO)(NS)Cl_2(AsPh_3)_2$	1120	(*54*)
$Re(NS)Cl(S_2CNMe_2)(PMe_2Ph)_2$	1150	(*12*)	$Rh(CO)(NS)(PPh_3)_2$	1122	(*54*)
$[Re(NS)Cl(dppe)_2]PF_6$	1177	(*12*)	$Rh(NS)(PPh_3)_3$	1100	(*46*)
$[Re(NS)Cl(dppe)_2]Cl$	1185	(*12*)	$[Rh(NS)Cl_2(PPh_3)]_2$	1120	(*46*)
$[Re(NS)Cl(dppe)_2]FeCl_4$	1173	(*12*)	$Rh(NS)Cl_2(PPh_3)_2$	1120	(*50*, *53*)
$[Re(NS)Cl(dppe)_2]S_2CNEt_2$	1183	(*12*)	$Rh(NS)Cl_2(AsPh_3)_2$	1120	(*50*, *53*)
$Re(NS)Cl_3(PMe_2Ph)_2$	1228	(*12*)	$Rh(NS)Cl_2(PPh_3)(AsPh_3)$	1120	(*49*)
$Re(NS)Cl_3(PEt_2Ph)_2$	1230	(*12*)	$Rh(NS)ClBr(PPh_3)_2$	1120	(*49*)
$Re(NS)Cl_3(PMePh_2)_2$	1220	(*12*)	$Rh(NS)Br_2(PPh_3)_2$	1118	(*49*)
$Re(NS)Cl_3(PPh_3)_2$	1214	(*12*)	$Rh(NS)ClBr(PPh_3)(AsPh_3)$	1120	(*49*)
$Re(NS)Cl_3(Pn\text{-}PrPh_2)_2$	1226	(*12*)	$[Rh(\mu\text{-}NS)Cl_2(PPh_3)]_2$	840	(*50*)
$[Re(CO)_5(NS)](AsF_6)_2$	1371	(*43*)	$[Rh(\mu\text{-}NS)Cl_2(AsPh_3)]_2$	840	(*50*)
$Ru(NS)Cl_3(PPh_3)_2$	1297	(*51*)	$[Rh(\mu\text{-}NS)ClBr(PPh_3)]_2$	840	(*49*)
$Ru(NS)Cl_3(AsPh_3)_2$	1295	(*51*)	$[Rh(\mu\text{-}NS)Br_2(PPh_3)]_2$	840	(*49*)
$Ru(NS)_2Cl_2(PPh_3)_2 \cdot X$	1300	(*33*)	$Ir(CO)(NS)Cl_2(PPh_3)_2$	1115	(*46*)
($X = CH_2Cl_2$, $CHCl_3$, or $CHBr_3$)	1120		$Ir(NS)Cl_2(PPh_3)_2$	1115	(*46*)
$Ru(NO)(NS)Cl_2(PPh_3)_2$	1320	(*33*)	$Ni(NS)Cl(PPh_3)_2$	1186	(*47*)

TABLE II

COMPARISON OF CARBONYL STRETCHING FREQUENCIES IN NITROSYL AND THIONITROSYL COMPLEXES

Complex	X = O ν_{CO} (cm^{-1})	X = S ν_{CO} (cm^{-1})	References
$(\eta^5\text{-}C_5H_5)Cr(CO)_2(NX)$	2038, 1955	2033, 1962	(*38*)
$Rh(CO)(NX)Cl_2(PPh_3)_2$	2090	2105	(*54*)
$Ir(CO)(NX)Cl_2(PPh_3)_2$	2055	2050	(*39, 52*)

A comparison of the spectroscopic properties of the carbonyl complexes $(\eta^5\text{-}C_5H_5)Cr(CO)_2NX$, $Rh(CO)(NX)Cl_2(PPh_3)_2$, and $Ir(CO)(NX)Cl_2(PPh_3)_2$ (X = O or S; Table II) indicates that the NS ligand is more effective in removing electron density from the central metal atom than is the NO ligand.

C. NMR STUDIES

The ^{1}H-NMR spectrum of $(\eta^5\text{-}C_5H_5)Cr(CO)_2NS$ consists of a single sharp peak that occurs at a slightly lower field than the corresponding absorption due to the cyclopentadienyl protons of the nitrosyl analogs. Similarly, the ^{13}C-NMR chemical shifts of the cyclopentadienyl and carbonyl carbons are further downfield from Me_4Si for the complex $(\eta^5\text{-}C_5H_5)Cr(CO)_2(NS)$. The ^{1}H-NMR spectrum of $Mo(NS)(S_2CNMe_2)_3$ in nitrobenzene at room temperature shows a 1 : 2 : 3 triplet consisting of two overlapping doublets (due to the dithiocarbamate methyl groups).

The ^{1}H-NMR spectrum of $Re(NS)Cl_2(PMe_2Ph)_3$ consists of two triplets and a doublet in the tertiary phosphine alkyl group region, indicating a meridional configuration:

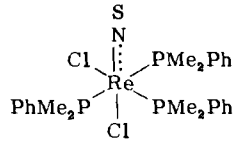

The ^{31}P-NMR spectra of $[ReCl(N)(dppe)_2]Cl$ and $[ReCl(NS)(dppe)_2]Cl$ both have a singlet at approximately 120 ppm, confirming that four phosphorus atoms lie in the plane, with the NS and Cl in a trans position.

D. Mass Spectral Data

In their attempt to gain further insight into the bonding of Cr—NX (X = O, S), Legzdins *et al.* (*24, 38*) investigated the low-resolution mass spectral data of $(\eta^5\text{-}C_5H_5)Cr(CO)_2(NX)$ complexes, and both types of complexes were observed to undergo similar fragmentations: $C_5H_5Cr(CO)_2(NX)^+$, $C_5H_5Cr(CO)(NX)^+$, $C_5H_5Cr(NX)^+$, $C_5H_5Cr^+$, and Cr^+. The $C_5H_5Cr(NS)^+$ ion is markedly more abundant in the mass spectrum of the thionitrosyl complex than is the corresponding ion in the spectrum of the nitrosyl complex. It was noted that carbonyls were lost in preference to the thionitrosyl group.

The mass spectrum of the complexes $Mo(NS)(S_2CNR_2)_3$ [$R_2 = Me_2$, Et_2, or $(CH_2)_4$] all show peaks attributable to the parent ions, together with those assigned to $[Mo(S_2CNR_2)_3]^+$ and $[MoS(S_2CNR_2)_2]^+$.

E. X-Ray Structural Determinations

The structures of $(\eta^5\text{-}C_5H_5)Cr(CO)_2(NS)$ (*24, 25*) and $Mo(NS)(S_2CNMe_2)_3$ (*12, 32*) have been determined by X-ray crystallography. In both complexes the thionitrosyl ligand coordinates essentially linearly to the metal via the nitrogen atom, with M—NS angles of 176.8(1) and 172.0(7)°, respectively, suggesting that the NS ligand is functioning as a three-electron donor. The molecular geometry of the chromium thionitrosyl complex is similar to that exhibited by the molecules $(\eta^5\text{-}C_5H_5)Mn(CO)_3$ (*7*) and $(\eta^5\text{-}C_5H_5)Cr(CO)_2(NO)$ (*5*), and the Cr—C(C_5H_5), Cr—C(O) and C—O bond lengths are comparable to those found in other cyclopentadienylchromium carbonyls (*64*). The structure of $Mo(NS)(S_2CNMe_2)_3$ is pentagonal bipyramidal, with a linear apical NS group. A comparison of the thionitrosyl complex $Mo(NS)(S_2CNMe_2)_3$ with the nitrosyl complex $Mo(NO)(S_2CN\text{-}t\text{-}Bu_2)_3$ (*13*) indicates that in both complexes the M—N distance and M—N—X (X = S, O) angle are equal, within the limits of experimental error (Table III).

TABLE III

Crystallographic Data for Thionitrosyl Complexes

Complex	M—NS (pm)	N—S (pm)	M—N (pm)	References
$(\eta^5\text{-}C_5H_5)Cr(CO)_2(NS)$	176.8(1)	155.1	169.4(3)	(*24, 25*)
$Mo(NS)(S_2CNMe_2)_3$	172.0(7)	159	173	(*32*)

F. Electronic Spectral Data

The electronic spectrum of $[Rh(CO)(NS)Cl_2(PPh_3)]_2$ shows bands at 15,300, 21,745, and 27,760 cm^{-1}. The spectra of the complexes $Rh(CO)(NX)Cl_2(PPh_3)_2$ (X = O or S) show bands at 25,000, 29,410, and 22,220, 27,200 cm^{-1}, respectively. The very high intensity of these bands suggests that they should be charge transfer and not d–d transition bands. All d–d transitions are masked by intense charge-transfer bands, and hence no d–d bands appeared in any of the spectra of these complexes.

V. Prospects

It is evident that the chemistry of thionitrosyl will continue to be a fertile area of research. One major difference between metal nitrosyl and thionitrosyl is the present scarcity of complexes containing multiple NS groups. It is probable that future research will show that these types of complexes will be difficult to obtain because of the destabilizing effect resulting from the strong acceptor capacity of the NS ligand. Finally, it is anticipated that the catalytic potential of these complexes will become an important research area. The availability of these complexes now makes possible a systematic study of the different modes of bonding of NS groups to transition metals. The following are some of the problems that will be investigated in the future.

1. The syntheses and reactions of thionitrosyl complexes of the other transition and nontransition metal ions
2. The reactions of electrophilic and nucleophilic reagents with the thionitrosyl group
3. Syntheses of complexes having two or more thionitrosyl groups in the molecule
4. Syntheses of complexes in which sulfur is end-on coordinated with the NS group
5. Conversion of the thionitrosyl group to nitride complexes by pulling sulfur out of the coordinated NS by metal ions such as Hg^{2+}, Hg^{+}, Pd^{2+}, Ag^{+}, Pb^{2+}, etc.
6. Reactions of the coordinated NS group with molecular oxygen or other oxidizing agents to convert NS to an oxygen- or nitrogen-bonded NSO^{-} ligand or to a thionitro () group

7. Reactions of molecular oxygen complexes with thionitrosyl chloride
8. Preparation of metal complexes with the ligands $R_2NN{=}S$, $RN{=}S{=}S$, $S{=}NN{=}S$, $RN{=}S$, NSe, and NTe

ACKNOWLEDGMENTS

We wish to thank the Deutsche Forschungsgemeinschaft for financial support. K. K. Pandey is also grateful to the Alexander von Humboldt Foundation for a fellowship.

REFERENCES

1. Allegretti, J. M., and Merer, A. J., *Can. J. Phys.* **50,** 404 (1972).
2. Armitage, D. A., and Brand, J. C., *J. Chem. Soc., Chem. Commun.* p. 1079 (1979).
3. Armitage, D. A., and Clark, M. J., *J. Organomet. Chem.* **24,** 629 (1970).
4. Armitage, D. A., and Sinden, A. W., *J. Organomet. Chem.* **44,** C43 (1972).
5. Atwood, J. L., Shakir, R., Malito, J. T., Herberhold, M., Kremnitz, W., Bernhagen, W. P. E., and Alt, H. G., *J. Organomet. Chem.* **165,** 65 (1979).
6. Becke-Goehring, M., Schwarz, R., and Spiess, W., *Z. Anorg. Allg. Chem.* **293,** 294 (1957). HOSN is only briefly stable at room temperature and forms red violet derivatives LiOSN and NaOSN.
7. Berndt, A. F., and Marsh, R. E., *Acta Crystallogr.* **16,** 118 (1963).
8. Bhattacharyya, A. A., McLean, J. A., and Turner, A. G., *Inorg. Chim. Acta* **34,** L199 (1979).
9. Bhattacharyya, A. A., and Turner, A. G., *Inorg. Chim. Acta* **53,** L89 (1981).
10. Bhattacharyya, A. A., Turner, A. G., Holt, E. M., and Alcock, N. W., *Inorg. Chim. Acta* **44,** L185 (1980).
11. Bishop, M. W., Chatt, J., and Dilworth, J. R., *J. Chem. Soc., Chem. Commun.* p. 780 (1975).
12. Bishop, M. W., Chatt, J., and Dilworth, J. R., *J. Chem. Soc., Dalton Trans.* p. 1 (1979).
13. Brennan, T. F., and Bernal, I., *Inorg. Chim. Acta* **7,** 283 (1973).
14. Byflett, R., Carrington, A., and Russell, D. K., *Mol. Phys.* **20,** 271 (1971).
15. Carrington, A., Howard, B. J., Levy, D. H., and Robertson, J. C., *Mol. Phys.* **15,** 187 (1968).
16. Chapman, D., Warn, R. J., Fitzgerald, A. D., and Yoffe, A. D., *Trans. Faraday Soc.* **60,** 294 (1964).
17. Chatt, J., and Dilworth, J. R., *J. Chem. Soc., Chem. Commun.* p. 508 (1974).
18. Cotton, F. A., and Wilkinson, G., "Advanced Inorganic Chemistry—A Comprehensive Text," 4th ed., p. 93.
19. Dressler, K., *Helv. Phys. Acta* **28,** 563 (1955).
20. Dyke, J. M., Morris, A., and Trickle, I. R., *J. Chem. Soc., Faraday Trans. 2* **73,** 147 (1977).
21. Enemark, J. H., and Feltham, R. D., *Coord. Chem. Rev.* **13,** 339 (1974).
22. Fowler, A., and Bakker, C. J., *Proc. R. Soc. London, Ser. A* **136,** 28 (1932).

23. Glemser, O., and Mews, R., *Angew. Chem.* **92,** 904 (1980): *Angew. Chem., Int. Ed. Engl.* **19,** 883 (1980).
24. Greenhough, T. S., Kolthammer, B. W. S., Legzdins, P., and Trotter, J., *J. Chem. Soc., Chem. Commun.* p. 1036 (1978).
25. Greenhough, T. S., Kolthammer, B. W. S., Legzdins, P., and Trotter, J., *Inorg. Chem.* **18,** 3548 (1979).
26. Haymore, B. L., and Ibers, J. A., *Inorg. Chem.* **14,** 3060 (1975).
27. Heal, H. G., *Adv. Inorg. Chem. Radiochem.* **15,** 375 (1972).
28. Herberhold, M., *Nachr. Chem., Tech. Lab.* **29,** 365 (1981).
29. Herberhold, M., and Haumaier, L., *Z. Naturforsch. B* **35B,** 1277 (1980).
30. Holt, E. M., Alcock, N. W., Bhattacharyya, A. A., and Turner, A. G., *Inorg. Chim. Acta* **47,** 255 (1981).
31. Hubbard, J. L., and Lichtenberger, D. L., *Inorg. Chem.* **19,** 1388 (1980).
32. Hursthouse, M. B., and Motevalli, M., *J. Chem. Soc., Dalton Trans.* p. 1362 (1979).
33. Jain, K. C., Pandey, K. K., and Agarwala, U. C., *Inorg. Chem.* (to be published).
34. Jain, K. C., Pandey, K. K., Katiyar, S. S., and Agarwala, U. C., *Proc. Int. Conf. Coord. Chem., 21st, 1980* p. 440 (1980).
35. Jenouvrier, A., and Daumont, D., *J. Mol. Spectrosc.* **61,** 313 (1976).
36. Johnson, B. F. G., and McCleverty, J. A., *Prog. Inorg. Chem.* **7,** 277 (1966).
37. Kirchoff, W. H., *J. Am. Chem. Soc.* **91,** 2437 (1969).
38. Kolthammer, B. W. S., and Legzdins, P., *J. Am. Chem. Soc.* **100,** 2247 (1978).
39. Kubota, M., and Phillips, D. A., *J. Am. Chem. Soc.* **97,** 5637 (1975).
40. Lichtenberger, D. L., and Fenske, R. F., *Inorg. Chem.* **15,** 2015 (1976).
41. McCleverty, J. A., *Chem. Rev.* **79,** 53 (1979).
42. Mews, R., *Adv. Inorg. Chem. Radiochem.* **19,** 223 (1976).
43. Mews, R., and Liu, C., *Angew. Chem.* **95,** 156 (1983).
44. O'Hare, P. A. G., *J. Chem. Phys.* **52,** 2992 (1970).
45. O'Hare, P. A. G., *J. Chem. Phys.* **54,** 4124 (1971).
46. Pandey, K. K., unpublished work.
47. Pandey, K. K., unpublished observations. Reaction of $NSCl(THF)_x$ with $NiCl_2(PPh_3)_2$ in the presence of sodiumborohydride affords $Ni(NS)Cl(PPh_3)_2$, whereas in the absence of sodiumborohydride the products are $NiCl_2$ and $SPPh_3$.
48. Pandey, K. K., and Agarwala, U. C., *J. Inorg. Nucl. Chem.* **42,** 293 (1980).
49. Pandey, K. K., and Agarwala, U. C., *Indian J. Chem.* **20**(1), 74 (1981).
50. Pandey, K. K., and Agarwala, U. C., *Inorg. Chem.* **20**(4), 1308 (1981).
51. Pandey, K. K., and Agarwala, U. C., *Z. Anorg. Allg. Chem.* **461,** 231 (1980).
52. Pandey, K. K., and Agarwala, U. C., *Indian J. Chem.* **20,** 240 (1981).
53. Pandey, K. K., Datta, S., and Agarwala, U. C., *Z. Anorg. Allg. Chem.* **468,** 228 (1980).
54. Pandey, K. K., Jain, K. C., and Agarwala, U. C., *Inorg. Chim. Acta* **48**(1), 23 (1981).
55. Raghuveer, K., and Narasimham, N. A., *J. Mol. Spectrosc.* **70,** 323 (1978).
56. Raju, D. K. M., M.Phil. Thesis, Indian Institute of Technology, Kanpur (1980).
57. Roesky, H. W., *Sulfur Org. Inorg. Chem.* **4,** 15 (1982).
58. Roesky, H. W., Emmert, R., Clegg, W., Isenberg, W., and Sheldrick, G. M., *Angew. Chem.* **93,** 623 (1981); *Angew. Chem., Int. Ed. Engl.* **20,** 591 (1981).
59. Salahub, D. R., and Messmer, R. P., *J. Chem. Phys.* **64,** 2039 (1976).
60. Schenk, P. W., *Chem. Ber.* **75,** 94 (1942).
61. Scherer, O. J., and Hornig, P., *Angew. Chem.* **78,** 776 (1966); *Angew. Chem., Int. Ed. Engl.* **5,** 729 (1966).
62. Schmid, G., and Ritter, G., *Chem. Ber.* **108,** 3008 (1975).

63. Schmid, G., and Ritter, G., *Angew. Chem.* **87,** 673 (1975); *Angew. Chem., Int. Ed. Engl.* **14,** 645 (1975).
64. Sneeden, R. P. A., "Organochronium Compounds." Academic Press, New York, 1975.
65. Teichman, R. A., and Nixon, R. E., *Inorg. Chem.* **15,** 1993 (1976).
66. Tiwari, R. D., Pandey, K. K., and Agarwala, U. C., *Inorg. Chem.* **21,** 845 (1982).
67. Toher, P. O., and Spratley, R. D., *Can. J. Chem.* **53,** 2311 (1975).
68. Toher, P. O., and Spratley, R. D., *Can. J. Chem.* **53,** 2318 (1975).
69. Uehara, H., and Morino, Y., *Mol. Phys.* **17,** 239 (1969).

INDEX

D

E

F

R

S

T